

*COMPARATIVE
PATHOPHYSIOLOGY
AND TOXICOLOGY OF
CYCLOOXYGENASES*

COMPARATIVE PATHOPHYSIOLOGY AND TOXICOLOGY OF CYCLOOXYGENASES

ZAHER A. RADI

Pfizer Worldwide Research and Development

Drug Safety Research and Development

Cambridge, Massachusetts



A JOHN WILEY & SONS, INC., PUBLICATION

Copyright © 2012 by John Wiley & Sons, Inc. All rights reserved.

Published by John Wiley & Sons, Inc., Hoboken, New Jersey.
Published simultaneously in Canada.

No part of this publication may be reproduced, stored in a retrieval system, or transmitted in any form or by any means, electronic, mechanical, photocopying, recording, scanning, or otherwise, except as permitted under Section 107 or 108 of the 1976 United States Copyright Act, without either the prior written permission of the Publisher, or authorization through payment of the appropriate per-copy fee to the Copyright Clearance Center, Inc., 222 Rosewood Drive, Danvers, MA 01923, (978) 750-8400, fax (978) 750-4470, or on the web at www.copyright.com. Requests to the Publisher for permission should be addressed to the Permissions Department, John Wiley & Sons, Inc., 111 River Street, Hoboken, NJ 07030, (201) 748-6011, fax (201) 748-6008, or online at <http://www.wiley.com/go/permission>.

Limit of Liability/Disclaimer of Warranty: While the publisher and author have used their best efforts in preparing this book, they make no representations or warranties with respect to the accuracy or completeness of the contents of this book and specifically disclaim any implied warranties of merchantability or fitness for a particular purpose. No warranty may be created or extended by sales representatives or written sales materials. The advice and strategies contained herein may not be suitable for your situation. You should consult with a professional where appropriate. Neither the publisher nor author shall be liable for any loss of profit or any other commercial damages, including but not limited to special, incidental, consequential, or other damages.

For general information on our other products and services or for technical support, please contact our Customer Care Department within the United States at (800) 762-2974, outside the United States at (317) 572-3993 or fax (317) 572-4002.

Wiley also publishes its books in a variety of electronic formats. Some content that appears in print may not be available in electronic formats. For more information about Wiley products, visit our web site at www.wiley.com.

Library of Congress Cataloging-in-Publication Data:

Radi, Zaher A.

Comparative pathophysiology and toxicology of cyclooxygenases / Zaher A. Radi.
p. cm.

Includes Bibliographical references and index.

ISBN 978-0-470-57754-7 (cloth)

1. Cyclooxygenases – Pathophysiology. 2. Cyclooxygenases–Toxicology. I. Title.

RM405.5.R33 2012

615.9'5137–dc23

2012002908

Printed in the United States of America

10 9 8 7 6 5 4 3 2 1

*This book is dedicated with love and appreciation to my father,
Dr. Ahmad Khalil Radi; my mother; my brothers; my sisters;
my wife, Rawan; and my kids, Ahmad, Waleed, Laith, and Lamees.*

CONTENTS

PREFACE	xi
INTRODUCTION: DISCOVERY OF CYCLOOXYGENASES AND HISTORICAL PERSPECTIVE	1
Aspirin	1
Prostaglandins	2
Cyclooxygenases	4
COX-2 Selective NSAIDs	7
References	8
CHAPTER 1 GASTROINTESTINAL TRACT	11
Introduction	11
Comparative COX-1 and COX-2 Expression in the GI Tract	13
Effects of ns-NSAIDs on the GI Tract	15
Effects of Arylpropionic Acid ns-NSAIDs on the GI Tract	17
Effects of Enolic Acid (Oxicam) ns-NSAIDs on the GI Tract	22
Effects of Acetic Acid Derivative ns-NSAIDs on the GI Tract	23
Effects of Aminonicotinic Acid Derivative ns-NSAIDs on the GI Tract	26
Effects of Pyrazolone Derivative ns-NSAIDs on the GI Tract	27
Effects of Salicylic Acid Derivative ns-NSAIDs on the GI Tract	28
Effects of Anthranilic Acid Derivative ns-NSAIDs on the GI Tract	30
Effects of COX-1 Inhibitors on the GI Tract	30
Effects of COX-2 s-NSAIDs on the GI Tract	31
Pathophysiology and Mechanisms of NSAID-Associated GI Toxicity	38
Role of Cyclooxygenase Potency	39
Species Differences in NSAID-Associated Susceptibility to GI Injury	39
GI Anatomical Differences	40
Enterohepatic Recirculation and NSAID Toxicity	41
Role of Xenobiotic Glucuronidation	42
Aging and Stress and NSAID GI Effects	43
Disruption of GI Physiological Mucosal Defense Mechanisms	44
GI Disequilibrium	45
Effects on Physiological GI Mucosal Cell Renewal Mechanisms After Mucosal Injury	46
Effects on Leukocyte Adhesion Molecules and Trafficking	49
Effects of GI Physiological Local pH, Gut Absorption, and Fasting	50
NSAID Topical Effect-Mediated Injury	51
Changes in GI Motility, Microcirculation, and Enterobacteria	52
Decreased Phosphatidylcholine Levels	53

viii CONTENTS

Impaired Drug Metabolism	54
Role of Toll-like Receptor (TLR)-4/MyD88 and Enteric Bacteria	54
Role of Uncoupling of Mitochondrial Oxidative Phosphorylation	56
Role of Peroxisome Proliferator-Activated Receptor γ	56
Role of Mitogen-Activated Protein Kinases	57
NSAID GI Injury-Associated Risk Factors	57
Conclusions	57
References	58

CHAPTER 2 BONE–TENDON–LIGAMENT SYSTEM

72

Introduction	72
Comparative Physiological and Anatomical Aspects of the Skeleton	72
Role of Prostaglandins in Skeleton Metabolism	78
The Process of Bone Healing and Potential Role of Prostaglandins	85
Inflammatory Response	85
Bone Resorption	88
Bone Formation	90
COX-1 and COX-2 Expression in Bone, Tendon, and Ligament During Repair and in Pathological Conditions	91
Effects of ns-NSAIDs on Bone Healing	96
Effects of COX-2 s-NSAIDs on Bone Healing	103
Effects of ns-NSAIDs on Ligament and Tendon Healing	112
Effects of COX-2 s-NSAIDs on Ligament and Tendon Healing	113
Conclusions	114
References	115

CHAPTER 3 RENAL SYSTEM

127

Introduction	127
Comparative Physiological, Developmental, and Anatomical Aspects of the Renal System	128
Role of Prostaglandins in the Renal System	140
COX-1 and COX-2 Expression in the Kidney	149
Effects of ns-NSAIDs on the Kidney	154
Effects of COX-2 s-NSAIDs on the Kidney	162
Potential Mechanisms of NSAID Effects on the Renal System	165
Conclusions	166
References	167

CHAPTER 4 CARDIOVASCULAR SYSTEM

180

Introduction	180
Comparative Physiological and Anatomical Aspects of the Cardiovascular System	181
The Heart	181
Cardiovascular Blood Flow	183
Cardiac Conduction System and Blood Pressure	183
Heart Rate	186
Renin–Angiotensin–Aldosterone in the Cardiovascular System	187
Natriuretic Peptides in the Cardiovascular System	188

Cardiovascular Research and Animal Models	189
Cardiovascular Atherosclerosis	191
COX-1 and COX-2 Expression in the Cardiovascular System	192
Pathophysiological Role of Prostaglandins in the Cardiovascular System	196
Effects of NSAIDs on the Cardiovascular System	201
Effects of COX-1 and COX-2 Inhibition on Myocardial Ischemia, Infarction, and Thrombosis	201
Effects of COX-1 and COX-2 Inhibition on Coronary Blood Flow and Blood Pressure	211
Effects of COX-1 and COX-2 Inhibition on Atherogenesis	215
Conclusions	216
References	216

CHAPTER 5 OCULAR SYSTEM 228

Introduction	228
Comparative Physiological and Anatomical Aspects of the Ocular System	228
Role of Prostaglandins in the Ocular System	238
COX-1 Expression in the Eye Under Normal and Pathological Conditions	245
COX-2 Expression in the Eye Under Normal and Pathological Conditions	248
Effects of COX-2 s-NSAIDs in Ophthalmology	253
Effects ns-NSAIDs in Ophthalmology	256
Conclusions	259
References	259

CHAPTER 6 RESPIRATORY SYSTEM 270

Introduction	270
Comparative Physiological and Anatomical Aspects of the Respiratory System	270
Role of Prostaglandins in the Respiratory System	275
COX-1 Expression in the Respiratory System Under Normal and Pathological Conditions	283
COX-2 Expression in the Respiratory System Under Normal and Pathological Conditions	288
Effects of COX-2 s-NSAIDs on the Respiratory System	295
Effects of ns-NSAIDs on the Respiratory System	299
Conclusions	300
References	301

CHAPTER 7 CURRENT RESEARCH STRATEGIES FOR DESIGNING SAFER NSAIDs 309

Nitric Oxide–Releasing NSAIDs	309
Hydrogen Sulfide–Releasing NSAIDs	311
NSAIDs Associated with Zwitterionic Phospholipids	311
Chiral NSAIDs	313
Trefoil Peptides	314
Novel Mechanism of Action NSIADs	314
mPGES-1 Inhibitors	316
References	316

INDEX 321

PREFACE

This book covers the hot topic of cyclooxygenases (COXs) and fills the gap in the discipline of pathophysiology and toxicology of prostanoids. Information on the comparative aspects in the field of prostanoids and COX inhibitors is relatively scant. COXs catalyze the conversion of arachidonic acid into prostaglandins, which play a significant role in the health and disease of many organ systems, including the gastrointestinal tract, skeletal, renal, cardiovascular, ocular, and respiratory systems. It is known that COX-1 is expressed constitutively and is found in most normal tissues, while COX-2 can be expressed at low levels in normal tissues and is induced strongly by proinflammatory mediators. Inhibitors of COX activity include (1) conventional nonselective nonsteroidal anti-inflammatory drugs and (2) COX-2 selective nonsteroidal anti-inflammatory drugs (COX-2 s-NSAIDs).

This comprehensive book covers the toxicology and pathophysiological role of COXs and the mechanisms of their toxicity after their inhibition in various body systems. The book will be of interest to toxicologic pathologists (e.g., Society of Toxicologic Pathologists, European Society of Toxicologic Pathologists, and American College of Veterinary Pathologists), toxicologists (Society of Toxicology and Academy of Toxicological Sciences), pharmacologists (American Society for Pharmacology and Experimental Therapeutics), and scientists and researchers (Inflammation Research Association) in both academia and the pharmaceutical industry working in the field of prostanoid research and drug development of COXs; or related inhibitors as therapeutic agents. There are at present no books that address the comparative aspects of COXs; hopefully, this book will fill that gap.

Inhibition of COX-1 often elicits gastrointestinal (GI) toxicity in animals and humans. Therefore, COX-2 s-NSAIDs medicines were developed to provide a selective COX-2 agent while minimizing the attendant COX-1-mediated GI toxicities. Various nonclinical species differ in their response to COX inhibition, and COX expression varies across various body systems and within each body system. For example, rats and dogs overpredict COX inhibition for renal effects such as renal handling of electrolytes in humans. COX inhibitors in various animal models are shown to have both beneficial and detrimental effects on the skeletal system, such as on healing of ligament or tendon tears in animal models; however, large clinical trials are lacking. There is a large gap in the literature regarding these comparative aspects of prostanoid research. The book addresses such differences in expression, pathophysiology, and toxicology across species.

The book begins with an introduction that details the discovery of COXs, includes a historical background, and explains how COXs were ultimately used as therapeutic agents. The book is designed to focus on the comparative aspects of COXs based on body systems. The first chapter covers the effects and

pathophysiology of COX inhibitors on the GI tract and mechanisms of toxicity. Subsequent chapters cover the pathophysiology of COX inhibition on bone, tendon, and ligament healing, COX inhibitors and renal system pathophysiology and mechanisms of toxicity, the pathophysiological role of COX inhibition in the ocular system, and COX inhibition in the respiratory and cardiovascular systems. The final chapter focuses on current research efforts to design COX inhibitors that are devoid of adverse side effects.

Zaher A. Radi

INTRODUCTION: DISCOVERY OF CYCLOOXYGENASES AND HISTORICAL PERSPECTIVE

ASPIRIN

The anti-inflammatory, antipyretic, and analgesic effects of medicinal plants have been recognized since ancient times in Egypt and Greece. Various herbal medicines, such as extracts of willow bark and leaves of myrtle, have been used for the relief of pain and swelling caused by inflammatory conditions. The ancient Greeks chewed the bark of willow trees to alleviate pain and fever. In 1543 B.C., about 3500 years ago, the Ebers Papyrus, an ancient Egyptian medical text, recommended the application of a decoction of the dried leaves of myrtle to the abdomen and back to expel rheumatic pains from the womb. Hippocrates, about 2400 years ago, recommended the juices of the poplar tree for treating eye diseases and those of the white willow tree (*Salix alba*) bark to relieve the pain of childbirth and to reduce fever. By the middle of the nineteenth century the active ingredient in these medicinal remedies was found to contain salicylates (Vane and Botting, 1998). Around A.D. 30, Aulus Cornelius Celsus described the four cardinal signs of inflammation as rubor (redness), calor (heat), dolor (pain), and tumor (swelling), and used extracts of willow leaves to relieve these signs of inflammation. In the second century A.D. and throughout Roman times, Dioscorides and Galen, Greek physicians, recommended willow bark to treat mild to moderate pain. In China and other parts of Asia, salicylate-containing plants were being applied therapeutically. The *Spiraea* plant species (called meadowsweet) had a long history of medicinal use by Native Americans. This plant contains methyl salicylate and other salicylates. The anti-inflammatory and analgesic effects of *Salix* and *Spiraea* species were known to the early inhabitants of North America and South Africa (Vane and Botting, 1998).

The era of salicylates started with a letter sent in 1758 by Reverend Edward Stone to the Royal Society in London in which he described “an account of the success of the bark of willow in the cure of agues” (Stone, 1763). Investigation of the therapeutically active substance in willow extract began early in the nineteenth century. In 1803, Wilkinson extracted the active substance from *Cortex salicis*

latifoliae, which was later found to contain high levels of tannin. In the early 1820s, Brugnateli, Fontana, and Buchner obtained therapeutically active substances of a less contaminated nature, and further purification was achieved by Buchner in 1828 at the University of Munich. Buchner removed the tannins and obtained a yellowish substance, which he called *salicin*, the Latin name for willow (Mahdi et al., 2006). In 1829, the pure crystalline form of salicin was obtained by Henri Leroux, a French pharmacist (Leroux, 1830; Vane and Botting, 1998). In 1833, Lowig prepared salicin from oil of wintergreen (*Gaultheria*) and meadowsweet (*Spiraea ulmaria*). In 1874, the commercial organic synthesis of salicylic acid was formulated by Kolbe and his colleagues and led to the founding of the Heyden Chemical Company (Vane and Botting, 2003). In 1876, Maclagan, a physician from Scotland, used salicin, the bitter principle of the common white willow, to reduce the fever, pain, and inflammation of rheumatic fever (Maclagan, 1876). By the middle of the nineteenth century, the active ingredient of these herbal medicines was found to be acetylsalicylic acid (aspirin). The name *aspirin* is derived from *A* = *acetyl* and *Spirsäure* = an old (German) name for salicylic acid.

Acetylsalicylic acid was synthesized by a chemistry professor, Charles Frederick von Gerhard, at Strasbourg, Germany in 1853 and the quest for the pharmaceutical development of similar remedies began. In 1895, Arthur Eichengru, director of the chemical research laboratories at the Bayer Company, assigned this task to Felix Hoffman one of his chemists. Hoffman also had personal reasons for wanting a more acceptable salicylic acid derivative. Hoffman's father had been taking salicylic acid for many years to treat his arthritis and had recently discovered that he could no longer take the drug without vomiting. Therefore, there was a need for a better tolerated salicylic acid derivative. Hoffman searched through the scientific literature and found a way of acetylating the hydroxyl group on the benzene ring of salicylic acid to form acetylsalicylic acid. After initial laboratory tests, Hoffman's father was given the drug; it was pronounced effective and later confirmed as such by a more impartial clinical trial. By 1899, the pharmaceutical manufacturing house of Frederick Bayer in Germany had named and released palatable acetylsalicylic acid (aspirin) onto the market (Vane and Botting, 1998). Thus, by the early twentieth century the antipyretic and anti-inflammatory therapeutic actions of aspirin were recognized. Similar several other antipyretic and anti-inflammatory drugs were discovered later [e.g., phenacetin, acetaminophen (paracetamol), phenylbutazone]. Because these drugs were clearly distinct from the glucocorticoids, all of them except acetaminophen were called *nonsteroidal anti-inflammatory drugs* (NSAIDs). However, endoscopic studies in 1938 found that long-term aspirin use was associated with gastric mucosa hyperemia, congestion, erosions, and ulcers (Douthwaite and Lintott, 1938).

PROSTAGLANDINS

In 1982, the presence of two distinct cyclooxygenase (COX) isoforms in brain tissue with differing sensitivities to indomethacin was suggested (Lysz and Needleman, 1982). However, COX enzymes were not purified and sequenced until 1988 (Merlie

et al., 1988; DeWitt et al., 1989). The early discovery of prostaglandins (PGs) took place before cyclooxygenases were discovered. Initially, a fatty acid with potent vasoactive properties was identified in human seminal fluid (Goldblatt, 1933; von Euler, 1935). In the 1930s, Ulf von Euler of Sweden named this fatty acid *prosta glandin*, thinking it originated from the prostate gland, and he suggested that PGs play a role in sperm transport (von Euler, 1935). In the 1960s, the structure of the first two PGs (named PGE and PGF because of their partition into ether and phosphate buffer, respectively) was established (Bergström et al., 1964). Furthermore, others also discovered in the 1970s a group of lipid mediators called PGs and their relationship to inflammation (Piper and Vane, 1969; Vane, 1971,2000). Hamberg et al. (1975) discovered rabbit aorta contracting substance (RCS), which provided the first clue to the relationship between aspirin and the PGs when it was found that aspirin blocked RCS released during anaphylaxis from isolated guinea pig lungs (Palmer et al., 1970). Shortly thereafter, it was found, using guinea pig lung homogenate, that acetylsalicylic acid and indomethacin (both nonselective nonsteroidal anti-inflammatory drugs), but not morphine or hydrocortisone, also blocked PG synthesis (Vane, 1971). Smith and Willis found that aspirin prevented the release of PGs from aggregating human platelets (Smith and Willis, 1971). Additionally, it was demonstrated that aspirin and indomethacin blocked PG release from the isolated perfused spleen of dogs (Ferreira et al., 1971). Collier and Flower also demonstrated that aspirin inhibited human seminal PGs (Collier and Flower, 1971). Today, 10 specific molecular groups of PGs exist, designated by the letters A through J. Among the PGs, the most widely distributed and best characterized are those derived from arachidonic acid (i.e., PGE₂, PGD₂, PGI₂ and PGF_{2α}). Eight types and subtypes of membrane PG receptors are conserved in mammals from mice to humans: the PGD receptor, DP; four subtypes of the PGE receptor, EP₁, EP₂, EP₃, and EP₄; the PGF receptor, FP; the PGI receptor, IP; and the thromboxane A receptor, TPA. They have different cell- and tissue-specific functions (Narumiya and Fitzgerald, 2001). PGs are known to have anti-inflammatory and antipyretic properties. For example, PGE₂ is a potent vasodilator that increases blood flow, increases vascular permeability, contributes to edema formation in inflammation, and sensitizes peripheral sensory nerve endings located at the site of inflammation (Williams and Peck, 1977; Bley et al., 1998). PGF_{2α} and PGE₂ play a role in the ovulation process, luteolysis, and pregnancy (Franczak et al., 2006). In 1999, Jakobsson et al. identified and characterized a novel human enzyme called microsomal PGE synthase-1 (mPGES-1), a member of the membrane-associated proteins involved in the eicosanoid and glutathione metabolism (MAPEG) superfamily with the ability to catalyze the conversion of PGH₂ to PGE₂. In addition, a cytosolic form of PGE synthase, termed cPGES-1, which also isomerizes PGH₂ to PGE₂, was also cloned (Tanioka et al., 2000). In 2002, another isoform of membrane-associated PGE synthase, termed mPGES-2, was identified (Tanikawa et al., 2002). These PG discoveries led to the identification of the COX enzyme, which led to the generation of PGs (Vane, 1971; Vane and Botting, 1998). Among the three PGE synthase enzymes, mPGES-1 has received much attention since it is inducible and linked functionally with COX-2 (Mancini et al., 2001).

CYCLOOXYGENASES

The most important lipid mediators are known as eicosanoids (Greek *eicosa* = 20, for 20-carbon fatty acid derivatives). The polyunsaturated fatty acid arachidonic acid (AA) is the precursor for the biosynthesis of eicosanoids. In mammalian cells, AA cannot be synthesized *de novo* and must be obtained either through diet or through conversion of linoleic acid by chain elongation to dihomo- γ -linolenic acid (Funk, 2001). The discovery of the importance of fatty acids and AA to health came from experiments in laboratory animals, where it was found that feeding a fat-free diet to rats led to growth retardation, reproductive disturbances, scaly skin, kidney lesions, and excessive water consumption (Burr and Burr, 1930). Arachidonic acid is found in mammalian cell membrane phospholipids. When the cell receives a stimulus (e.g., inflammation, trauma), the phospholipase A₂(PLA₂) enzyme is activated to release AA from membrane phospholipids. Prostaglandin H (PGH) synthases, also called cyclooxygenases (COXs), are membrane-bound enzymes whose main role is to catalyze the first two steps (cyclooxygenation and peroxidation) to transform AA into the intermediate cyclic endoperoxidase prostaglandin H₂(PGH₂) and prostaglandin G₂(PGG₂). In the first step, COX cyclizes and adds two molecules of O₂ to AA to form the cyclic hydroperoxide PGG₂. Therefore, the term *cyclooxygenase* originated from this first reaction involving the transformation of AA to PG via cyclization and oxygenation. In the second step, COX reduces PGG₂ to PGH₂. PGH₂ is highly unstable and serves as an intermediate precursor for a variety of prostanoids [e.g., thromboxane A₂(TXA₂), prostacyclin (PGI₂), PGD₂, PGE₂, PGF₂] with diverse biological actions (Funk, 2001) (Fig. I-1) (Radi, 2009). COX is present in the endoplasmic reticulum and nuclear membrane. The primary source of COX isolation and characterization originated from ovine seminal vesicles (Hemler et al., 1976; Miyamoto et al., 1976).

COX isoforms are called COX-1, COX-2, and COX-3. The COX-1 (constitutive) gene encodes a 2.8-kb message and is localized to the endoplasmic reticulum. It is expressed constitutively in most normal tissues throughout the body and is responsible for the synthesis of PGs in many cell types. High levels of COX-1 are present in monocytes, endothelial cells, platelets, and seminal vesicles (Smith and DeWitt, 1996). Therefore, COX-1 is considered as a “housekeeping” enzyme involved in normal physiological processes. COX-1 is inhibited by aspirin, resulting in irreversible acetylation of PGHS-1 and inhibition of platelet TXA₂ formation (Shimokawa and Smith, 1992). TXA₂ is involved in platelet aggregation and PGE₂ is involved in protecting the gastric mucosa. COX-2 (inducible) is localized to the endoplasmic reticulum and the nuclear membrane and is found in low amounts in healthy tissue, but is induced rapidly and strongly in inflamed and pathological tissues by proinflammatory mediators and cytokines (Radi, 2009). Cytokines (e.g., IL-1, IL-6, IL-8), immunomodulatory proteins [tumor necrosis factor alpha (TNF α), gamma interferon (IFN γ)], bacterial lipopolysaccharides (LPs), paramyxoviruses, and growth factors [epidermal growth factor (EGF), platelet-derived growth factor (PDGF)] can induce COX-2 expression in various cell types, including fibroblasts;

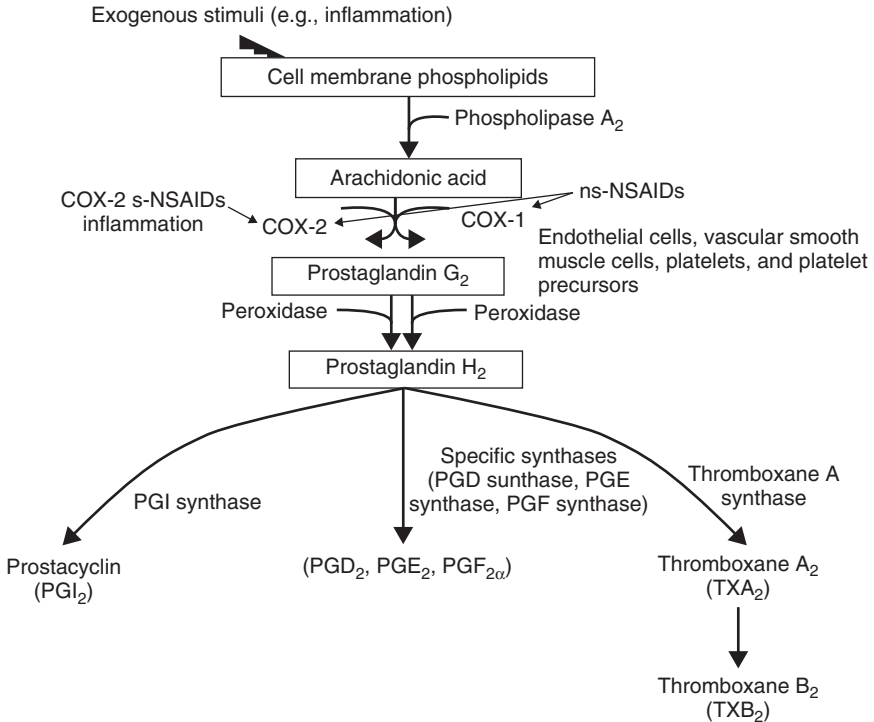


FIGURE I-1 Prostaglandin (PG) metabolism pathway. Arachidonic acid (AA) is found in mammalian cell membrane phospholipids. When the cell receives a stimuli (e.g., inflammation, trauma), the phospholipase A₂(PLA₂) enzyme is activated to release AA from membrane phospholipids. Prostaglandin H (PGH) synthases, also called cyclooxygenases (COXs), are membrane-bound enzymes whose main role is to catalyze the first two steps (cyclooxygenation and peroxidation) to transform AA into the intermediate cyclic endoperoxidase prostaglandin H₂(PGH₂) and prostaglandin G₂(PGG₂). In the first step, COX cyclizes and adds two molecules of O₂ to AA to form the cyclic hydroperoxide PGG₂. In the second step, COX reduces PGG₂ to PGH₂. PGH₂ is highly unstable and serves as the precursor intermediate for a variety of prostanoids [e.g., thromboxane A₂(TXA₂), prostacyclin (PGI₂), PGD₂, PGE₂, PGF₂]. [The final, definitive version of this figure was published in Z. A. Radi, *Toxicologic Pathology*, 37(1), 2009, pp. 34–46. Copyright © Sage Publications. All rights reserved.]

macrophages; epithelial, endothelial, and smooth muscle cells; synoviocytes; and osteoblasts (Morita, 2002; Radi et al., 2010).

Polyclonal antiserum against sheep seminal vesicle PGH synthase, which cross-reacts with human cyclooxygenase, was used to determine PGH synthase modulation by interleukin-1 (IL-1) cytokine in cultured human dermal fibroblast cells (Raz et al., 1988). It was demonstrated that IL-1 treatment resulted in dose–response curves for stimulation of PE₂ formation, increased cellular COX activity, and the increased synthetic rate of newly formed COX. The authors concluded that the IL-1 effect is mediated primarily, if not solely, via induction of

COX synthesis (Raz et al., 1988). Another experiment found that LPS stimulation of human monocytes resulted in increased COX enzyme activity without affecting phospholipase and thromboxane synthase activities. Additionally, a PG inhibitor, dexamethasone, completely blocked LPS-induced prostanoid release by inhibiting the activity of COX (Fu et al., 1990).

Both COX isoforms map to distinct chromosomes. In humans, COX-1 and COX-2 are localized on chromosomes 9 and 1, respectively (Funk et al., 1991; Tay et al., 1994). The COX isoforms differ in length, the COX-2 gene being smaller. The COX-1 gene is approximately 22 kb in length, contains 11 exons, and is transcribed as a 2.8-kb mRNA (Yokoyama and Tanabe, 1989; Funk et al., 1991). The COX-2 gene is approximately 8 kb in length, contains 10 exons and 9 introns, and is transcribed as 4.6-, 4-, and 2.8-kb mRNAs variants (Hla and Neilson, 1992). The amino acid sequences of COX-1 and COX-2 are about 80% identical. There are amino acid carboxyl (C) and N terminus differences between the two COX isoforms. COX-1 has a 17-amino acid hydrophobic leader sequence near its N terminus; COX-2, on the other hand, has an 18-amino acid residue located near its C terminus (Funk et al., 1991; Jones et al., 1993; Tay et al., 1994). COX-1 has 576 amino acids with a molecular mass of 70 kDa (Yokoyama et al., 1989; Funk et al., 1991). The human COX-2 cDNA encodes a polypeptide that contains 604 amino acids with a molecular mass of 70 kDa (Hla and Neilson, 1992; Jones et al., 1993). The COX-2 cDNA of several other species (e.g., rat, mouse, chicken, dog, sheep, rabbit, guinea pig, horse, mink, cow) was also cloned later. A number of sequence elements control the half-life of an mRNA, either by stimulating or inhibiting degradation. In mammalian cells, sequence elements rich in adenosine and uridine, called AU-rich elements (AREs), were identified by their ability to target host mRNAs toward rapid degradation (Barreau et al., 2006). COX-2 mRNA has multiple AUUUA instability sequences that mediate transcript rapid degradation (Barreau et al., 2006).

In 2002, a third COX enzyme, COX-3, although still controversial, was discovered. COX-3 is expressed primarily in the canine cerebral cortex (Chandrasekharan et al., 2002). COX-3 was suggested to represent a potential primary central mechanism for the action of acetaminophen. Functional studies have demonstrated that the dog COX-3 possesses glycosylation-dependent cyclooxygenase activity and is potently inhibited by some, but not all, NSAIDs. COX-3 in dogs is selectively inhibited by drugs such as acetaminophen, phenacetin, antipyrine, and dipyrrone (Chandrasekharan et al., 2002). The existence of human COX-3 and its relationship to analgesic drugs such as acetaminophen is yet to be determined. Database analysis of human COX-1 showed a frameshift induced by intron 1, possibly revealing COX-3 to be a virtual protein in humans. Western blot analysis of human aorta tissue using polyclonal antibodies directed against the first 13 amino acids of the predicted human and dog/mouse COX-3 detected a 65-kDa protein postulated to be human COX-3 (Schwab et al., 2003).

However, Schneider et al. (2005) confirmed that the spliced variant COX-1 protein is not detectable in human tissue and does not possess any catalytic activity in expression studies. Interestingly, the expression of intron 1 retaining COX-1 splice variants was studied in the human colon cancer cell line Caco-2 and

in human colonic tissue samples. The investigators observed an increase of the COX-3 transcript, but not of protein, in human colonic tissue. In addition, COX-3 was up-regulated in hypertonic conditions in a human colon cancer cell line, and transcript-specific degradation by RNA interference increases COX-1 and COX-2 mRNA. Thus, although the transcript is not translated, it may play a regulatory role in COX-mediated epithelial osmoregulation (Nurmi et al., 2005). COX-3 has also been cloned in the mouse and rat (Snipes et al., 2005; Kis et al., 2006).

Inhibitors of COX activity include (1) conventional nonselective nonsteroidal anti-inflammatory drugs (ns-NSAIDs) and (2) COX-2 selective nonsteroidal anti-inflammatory drugs (COX-2 s-NSAIDs). The antipyretic, analgesic, and anti-inflammatory properties of NSAIDs are due to blocking the transformation of AA into PGH₂ and subsequent PGs. Examples of NSAIDs include, but are not limited to, aspirin, ibuprofen, ketoprofen, piroxicam, naproxen, sulindac, fenoprofen, indomethacin, meclofenamate, and phenylbutazone (Radi and Khan, 2006). After the early introduction of aspirin, the 1940s saw the introduction of phenylbutazone, the fenamates appeared in the 1950s, indomethacin in the 1960s, the propionates in the 1970s, and the oxicams in the 1980s (Flower, 2003). The development of the first category of ns-NSAIDs began with phenylbutazone in 1946. Epidemiological studies revealed that inhibition of COX-1 often elicits gastrointestinal (GI) toxicity in animals and humans. Therefore, COX-2 s-NSAIDs were developed to provide a selective COX-2 agent while minimizing the attendant COX-1-mediated GI toxicities.

COX-2 SELECTIVE NSAIDS

In 1991, before the discovery of the COX-2 selective inhibitors, the Dupont Company reported the development of DuP697, a potent inhibitor of paw swelling in unestablished and established adjuvant arthritis in rats (Gans et al., 1990). DuP697 was a novel orally effective PG synthesis inhibitor with potent anti-inflammatory effects and reduced ulcerogenic properties (Gans et al., 1990). DuP697 showed activity in in vitro assays of COX using seminal vesicle or rat kidney preparations (known to contain predominantly COX-1), but was more effective against rat brain prostanoid synthesis (Flower, 2003). DuP697 served as a building block for the synthesis of COX-2 selective inhibitors and as the basic chemical model for the coxibs. In 1993, another COX-2 s-NSAID, NS-398 [*N*-(2-cyclohexyloxy-4-nitrophenyl)methane sulfonamide], was found to be associated with fewer gastric side effects (Futaki et al., 1993). The crystal structures of COX-1 and COX-2 were identified in 1994 and 1996, respectively (Picot et al., 1994). For the COX-1 crystal structure, attention was drawn to the importance of arginine 120 (which interacted with the carboxyl group of both substrate and inhibitors) and tyrosine 355 in determining the stereospecificity of NSAID binding (Picot et al., 1994; Kurumbail et al., 1996). For the COX-2 crystal structure, the structure of murine COX-2 and complexes with flurbiprofen, indomethacin, and SC-558 were determined at resolutions of 3 to 2.5 Å (Kurumbail et al., 1996). The identification of COX-2 s-NSAIDs was based on (1) cell lines with COX-1 and COX-2 activities, (2) isolated recombinant

COX enzymes, (3) cellular sources of COX-1 (platelets) and COX-2 (stimulated macrophages), (4) cell lines such as Chinese hamster ovary cells transfected with recombinant COX-1 or COX-2, and (5) whole blood assays in which PG levels were measured.

Thus, celecoxib (Celebrex) and rofecoxib (Vioxx), the first COX-2 s-NSAIDs inhibitors to reach the market, were based on DuP697 (Flower, 2003). Chemically, rofecoxib and celecoxib belonged to a diaryl-substituted class of compounds. Celecoxib is a sulfonamide-substituted 1,5-diaryl pyrazole compound, whereas rofecoxib is a methylsulfonylphenyl compound. Celecoxib and rofecoxib were approved in 1998 and 1999, respectively. Celecoxib exhibits anti-inflammatory, analgesic and antipyretic activities in animal models and was approved in the United States in December 1998 and in Europe (Sweden) in December 2000 for symptomatic relief in the treatment of osteoarthritis and rheumatoid arthritis in humans. In subsequent years, the U.S. Food and Drug Administration placed a boxed warning on all prescription NSAIDs.

REFERENCES

- Barreau C, Paillard L, Osborne HB. AU-rich elements and associated factors: Are there unifying principles? *Nucleic Acids Res* 2006;33:7138–7150.
- Bergström S, Danielsson H, Samuelsson B. The enzymatic formation of prostaglandin E2 from arachidonic acid. *Biochim Biophys Acta* 1964;90:207–210.
- Bley KR, Hunter JC, Eglen RM, Smith JA. The role of IP prostanoid receptors in inflammatory pain. *Trends Pharmacol Sci* 1998;19:141–147.
- Burr GO, Burr MM. On the nature and role of the fatty acids essential in nutrition. *J Biol Chem* 1930;86:587–621.
- Chandrasekharan NV, Dai H, Roos KL, Evanson NK, et al. COX-3, a cyclooxygenase-1 variant inhibited by acetaminophen and other analgesic/antipyretic drugs: cloning, structure, and expression. *Proc Natl Acad Sci USA* 2002;99:13926–13931.
- Collier JG, Flower RJ. Effect of aspirin on human seminal prostaglandins. *Lancet* 1971;2:852–853.
- DeWitt DL, el-Harith EA, Smith WL. Molecular cloning of prostaglandin G/H synthase. *Adv Prostaglandin Thromboxane Leukot Res* 1989;19:454–457.
- Douthwaite A, Lintott CA. Gastroscopic observations of the effect of aspirin and certain other substances on the stomach. *Lancet* 1938;2:1222.
- Ferreira SH, Moncada S, Vane Jr. Indomethacin and aspirin abolish prostaglandin release from the spleen. *Nat New Biol* 1971;231:237–239.
- Flower RJ. The development of COX-2 inhibitors. *Nat Rev Drug Discov* 2003;2:179–191.
- Franczak A, Kotwica G, Kurowicka B, Oponowicz A, et al. Expression of enzymes of cyclooxygenase pathway and secretion of prostaglandin E2 and F2alpha by porcine myometrium during luteolysis and early pregnancy. *Theriogenology* 2006;66:1049–1056.
- Fu JY, Masferrer JL, Seibert K, Raz A, et al. The induction and suppression of prostaglandin H2 synthase (cyclooxygenase) in human monocytes. *J Biol Chem* 1990;265:16737–16740.
- Funk CD. Prostaglandins and leukotrienes: advances in eicosanoid biology. *Science* 2001;294:1871–1875.
- Funk CD, Funk LB, Kennedy ME, Pong AS, et al. Human platelet/erythrocyte cell prostaglandin G/H synthase: cDNA cloning, expression, and gene chromosomal assignment. *FASEB J* 1991; 5:2304–2312.
- Futaki N, Arai I, Hamasaka Y, Takahashi S, et al. Selective inhibition of NS-398 on prostanoid production in inflamed tissue in rat carrageenan-air-pouch inflammation. *J Pharm Pharmacol* 1993;45: 753–755.

- Gans KR, Galbraith W, Roman RJ, Haber SB, et al. Anti-inflammatory and safety profile of DuP 697, a novel orally effective prostaglandin synthesis inhibitor. *J Pharmacol Exp Ther* 1990;254:180–187.
- Goldblatt MW. A depressor substance in seminal fluid. *J Soc Chem Ind (Lond)* 1933;52:1056–1057.
- Hamberg M, Svensson J, Samuelsson B. Thromboxanes: a new group of biologically active compounds derived from prostaglandin endoperoxides. *Proc Natl Acad Sci USA* 1975;72:2994–2998.
- Hemler M, Lands WE. Purification of the cyclooxygenase that forms prostaglandins: demonstration of two forms of iron in the holoenzyme. *J Biol Chem* 1976;251:5575–5579.
- Hla T, Neilson K. Human cyclooxygenase-2 cDNA. *Proc Natl Acad Sci USA* 1992;89:7384–7388.
- Jakobsson PJ, Thoren S, Morgenstern R, Samuelsson B. Identification of human prostaglandin E synthase: a microsomal, glutathione-dependent, inducible enzyme, constituting a potential novel drug target. *Proc Natl Acad Sci USA* 1999;96:7220–7225.
- Jones DA, Carlton DP, McIntyre TM, Zimmerman GA, et al. Molecular cloning of human prostaglandin endoperoxide synthase type II and demonstration of expression in response to cytokines. *J Biol Chem* 1993;268:9049–9054.
- Kis B, Snipes JA, Gaspar T, Lenzser G, et al. Cloning of cyclooxygenase-1b (putative COX-3) in mouse. *Inflamm Res* 2006;55:274–278.
- Kurumbail RG, Stevens AM, Gierse JK, McDonald JJ, et al. Structural basis for selective inhibition of cyclooxygenase-2 by anti-inflammatory agents. *Nature* 1996;384:644–648.
- Leroux H. Discovery of salicine. *J Chim Med* 1830;6:340–432.
- Lysz TW, Needleman P. Evidence for two distinct forms of fatty acid cyclooxygenase in brain. *J Neurochem* 1982;38:1111–1117.
- Maclagan TJ. The treatment of acute rheumatism by salicin. *Lancet* 1876;2:601–604.
- Mahdi JG, Mahdi AJ, Bowen ID. The historical analysis of aspirin discovery, its relation to the willow tree and antiproliferative and anticancer potential. *Cell Prolif* 2006;39:147–155.
- Mancini JA, Blood K, Guay J, Gordon R, et al. Cloning, expression, and up-regulation of inducible rat prostaglandin E synthase during lipopolysaccharide-induced pyresis and adjuvant-induced arthritis. *J Biol Chem* 2001;276:4469–4475.
- Merlie JP, Fagan D, Mudd J, Needleman P. Isolation and characterization of the complementary DNA for sheep seminal vesicle prostaglandin endoperoxide synthase (cyclooxygenase). *J Biol Chem* 1988;263:3550–3553.
- Miyamoto T, Ogino N, Yamamoto S, Hayaishi O. Purification of prostaglandin endoperoxide synthetase from bovine vesicular gland microsomes. *J Biol Chem* 1976;251:2629–2636.
- Morita I. Distinct functions of COX-1 and COX-2. *Prostaglandins Other Lipid Mediat* 2002;68–69:165–175.
- Narumiya, S, Fitzgerald, GA. Genetic and pharmacological analysis of prostanoid receptor function. *J Clin Invest* 2001;108:25–30.
- Nurmi JT, Puolakkainen PA, Rautonen NE. Intron 1 retaining cyclooxygenase 1 splice variant is induced by osmotic stress in human intestinal epithelial cells. *Prostaglandins Leukot Essent Fatty Acids* 2005;73:343–350.
- Palmer MA, Piper PJ, Vane Jr. The release of rabbit aorta contracting substance (RCS) from chopped lung and its antagonism by anti-inflammatory drugs. *Br J Pharmacol* 1970;40:581P–582P.
- Picot D, Loll PJ, Garavito RM. The x-ray crystal structure of the membrane protein prostaglandin H2 synthase-1. *Nature* 1994;367:243–249.
- Piper PJ, Vane Jr. Release of additional factors in anaphylaxis and its antagonism by anti-inflammatory drugs. *Nature* 1969;223:29–35.
- Radi ZA. Pathophysiology of cyclooxygenase inhibition in animal models. *Toxicol Pathol* 2009;37:34–46.
- Radi ZA, Khan NK. Effects of cyclooxygenase inhibition on the gastrointestinal tract. *Exp Toxicol Pathol* 2006;58:163–173.
- Radi ZA, Meyerholz DK, Ackermann MR. Pulmonary cyclooxygenase-1 (COX-1) and COX-2 cellular expression and distribution after respiratory syncytial virus and parainfluenza virus infection. *Viral Immunol* 2010;23:43–48.
- Raz A, Wyche A, Siegel N, Needleman P. Regulation of fibroblast cyclooxygenase synthesis by interleukin-1. *J Biol Chem* 1988;263:3022–3028.

- Schneider C, Boeglin WE, Brash AR. Human cyclo-oxygenase-1 and an alternative splice variant: contrasts in expression of mRNA, protein and catalytic activities. *Biochem J* 2005;385:57–64.
- Schwab JM, Beiter T, Linder JU, Laufer S, et al. COX-3: a virtual pain target in humans? *FASEB J* 2003;17:2174–2175.
- Shimokawa T, Smith WL. Prostaglandin endoperoxide synthase: the aspirin acetylation region. *J Biol Chem* 1992;267:12387–12392.
- Smith JB, Willis AL. Aspirin selectively inhibits prostaglandin production in human platelets. *Nat New Biol* 1971;231:235–237.
- Smith WL, Dewitt DL. Prostaglandin endoperoxide H synthases-1 and -2. *Adv Immunol* 1996;62:167–215.
- Snipes JA, Kis B, Shelness GS, Hewett JA, et al. Cloning and characterization of cyclooxygenase-1b (putative cyclooxygenase-3) in rat. *J Pharmacol Exp Ther* 2005;313:668–676.
- Stone E, Rev. An account of the success of the bark of the willow in the cure of agues. *Philos Trans* 1763;53:195–200.
- Tanikawa N, Ohmiya Y, Ohkubo H, Hashimoto K, et al. Identification and characterization of a novel type of membrane-associated prostaglandin E synthase. *Biochem Biophys Res Commun* 2002;291:884–889.
- Tanioka T, Nakatani Y, Semmyo N, et al. Molecular identification of cytosolic prostaglandin E2 synthase that is functionally coupled with cyclooxygenase-1 in immediate prostaglandin E2 biosynthesis. *J Biol Chem* 2000;275:32775–32782.
- Tay A, Squire JA, Goldberg H, Skorecki K. Assignment of the human prostaglandin- endoperoxide synthase 2 (PTGS2) gene to 1q25 by fluorescence in situ hybridization. *Genomics* 1994;23:718–719.
- Vane Jr. Inhibition of prostaglandin synthesis as a mechanism of action for aspirin-like drugs. *Nat New Biol* 1971;231:232–235.
- Vane JR. The fight against rheumatism: from willow bark to COX-1 sparing drugs. *J Physiol Pharmacol* 2000;51:573–586.
- Vane JR, Botting RM. Anti-inflammatory drugs and their mechanism of action. *Inflamm Res* 1998;47 Suppl 2:S78–S87.
- Vane JR, Botting RM. The mechanism of action of aspirin. *Thromb Res* 2003;110:255–258.
- von Euler US. A depressor substance in the vesicular gland. *J Physiol* 1935;84:21P.
- Williams TJ, Peck MJ. Role of prostaglandin-mediated vasodilatation in inflammation. *Nature* 1977;270:530–532.
- Yokoyama C, Tanabe T. Cloning of human gene encoding prostaglandin endoperoxide synthase and primary structure of the enzyme. *Biochem Biophys Res Commun* 1989;165:888–894.

GASTROINTESTINAL TRACT

INTRODUCTION

Rheumatoid arthritis (RA) is a chronic systemic inflammatory autoimmune disorder characterized by inflammation of synovial joints leading to progressive erosion of cartilage and bone. RA is associated with swelling, pain, and stiffness of multiple synovial joints, with an annual incidence of 31 per 100,000 women and 13 per 100,000 men. RA is more common in women than in men by a ratio of approximately 3 : 1 (Doan and Massarotti, 2005). Osteoarthritis (OA) is a common, age-related disorder of synovial joints that is pathologically characterized by irregularly distributed loss of cartilage more frequently in areas of increased load, sclerosis of subchondral bone, subchondral cysts, marginal osteophytes, increased metaphyseal blood flow, and variable synovial inflammation. Cyclooxygenase (COX) has two distinct membrane-anchored isoenzymes: a constitutively expressed (COX-1) and a highly induced (COX-2) isoenzyme. Following exogenous stimuli (i.e., inflammation), arachidonic acid is liberated by phospholipases. COX-1 and COX-2 are rate-limiting enzymes with COX and peroxidase activities that catalyze the conversion of arachidonic acid to prostaglandin (PG) endoperoxide (PGG₂) and prostanoids, which are then reduced to PGH₂ (Eling et al., 1990). PGH₂ is further metabolized to thromboxane A₂ (TXA₂), prostacyclin (PGI₂), PGD₂, PGF_{2α}, and PGE₂ (Fig. 1-1) (Dannenberg et al., 2001; Radi and Khan, 2006b; Radi, 2009). Prostanoids, including TXA₂ and PGI₂, help regulate vascular tone and thrombosis via COX activity. TXA₂ is a vasoconstrictor that is largely platelet derived and COX-1 dependent, and it promotes platelet adhesion and aggregation and smooth muscle cell proliferation. PGI₂ is an endothelial-derived vasodilator with antiaggregatory platelet functions but is both COX-1 and COX-2 dependent (Kearney et al., 2004).

The inhibitors of COX activity include nonselective nonsteroidal anti-inflammatory drugs (ns-NSAIDs) and COX-2 selective nonsteroidal anti-inflammatory drugs (s-NSAIDs). Nonselective NSAIDs, at therapeutic doses, inhibit both COX-1 and COX-2 (Fig. 1-1) (Dannenberg et al., 2001; Radi and Khan, 2006b; Radi, 2009). The analgesic and anti-inflammatory properties of NSAIDs are linked to COX-2 inhibition, while many of the gastrointestinal tract (GI) toxicities and side effects have been linked variably to COX-1 and/or COX-2 inhibition and, in some cases, directly to the secondary pharmacologic properties of

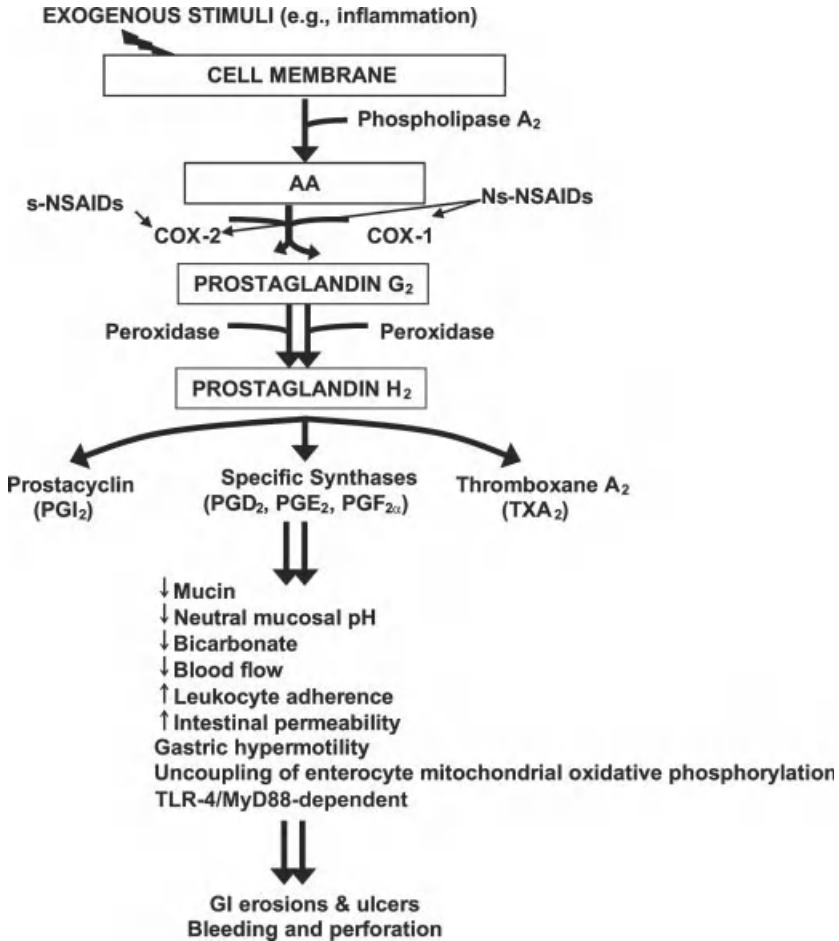


FIGURE 1-1 Pathophysiological role of prostaglandins (PGs) in the gastrointestinal (GI) tract and effects of ns-NSAIDs and COX-2 s-NSAIDs. Following an exogenous stimulus (e.g., inflammation), cell membrane phospholipid is liberated to arachidonic acid (AA) by phospholipase A₂. Both COX-1 and COX-2 catalyze the conversion of AA into various PGs. COX-1 is the predominant isoform in the normal GI tract (gastric fundus, corpus, antrum and/or pylorus, duodenum, jejunum, ileum, cecum, and colon), while COX-2 expression is up-regulated during inflammatory or neoplastic conditions. Nonselective NSAIDs (e.g., carprofen, etodolac, flunixin meglumine, ketoprofen, indomethacin, phenylbutazone) inhibit COX-1 and COX-2, while selective s-NSAIDs (e.g., celecoxib, firocoxib, rofecoxib, lumiracoxib, valdecoxib) spare COX-1 and inhibit only COX-2. Potential mechanisms of ns-NSAID-mediated GI toxicity include (1) increased intestinal epithelial permeability, (2) uncoupling of mitochondrial oxidative phosphorylation, (3) gastric hypermotility, (4) decreased epithelial cell secretion of bicarbonates, (5) decreased mucin secretion, (6) decreased blood flow, (7) decreased neutral pH of mucosa, (8) leukocyte infiltration, and (9) TLR-4/MyD88-dependent into the GI mucosa after injury. Loss of these GI protective mechanisms can lead to GI erosion, ulcers, bleeding, and perforation. (Reprinted from Z. A. Radi and N. K. Khan, *Effects of cyclooxygenase inhibition on the gastrointestinal tract*, *Experimental and Toxicologic Pathology*, 58, pp. 163–173. Copyright © 2006, with permission from Elsevier.)

the select drugs. COX-2 selective NSAIDs (i.e., celecoxib, deracoxib, etoricoxib, firocoxib, lumiracoxib, parecoxib, robenacoxib, rofecoxib, and valdecoxib) were developed to provide a drug that is selective for COX-2, which at therapeutic doses demonstrated therapeutic benefits comparable to those of conventional ns-NSAIDs without the attendant COX-1-mediated toxicities (Radi and Khan, 2006b). The first human-use COX-2 s-NSAIDs were celecoxib and rofecoxib, approved for the treatment of OA and RA. Later drug developments would produce deracoxib, etoricoxib, firocoxib, parecoxib, lumiracoxib, robenacoxib, and valdecoxib. The focus of this chapter is a detailed examination of the comparative expression of COX-1 and COX-2, the effects of COX-2 selective and nonselective NSAID inhibition on the GI system, and the pathophysiological mechanisms of such GI effects and toxicities.

COMPARATIVE COX-1 AND COX-2 EXPRESSION IN THE GI TRACT

GI expression of COX-1 and COX-2 in various species is summarized in Table 1-1 (Radi and Khan, 2006b; Radi, 2009). COX-1 (and not COX-2) is the predominant isoform in the normal GI tract (i.e., gastric fundus, corpus, antrum and/or pylorus, duodenum, jejunum, ileum, cecum, and colon) and is expressed normally in canine, humans, and nonhuman primates. The COX-2 isoform is nearly absent in these species, except in rats and for low levels in the large intestine (Kargman et al., 1996; Seibert et al., 1997; Koki et al., 2002a; Maziasz et al., 2003). Both COX-1 and COX-2 are present in the normal human gastric mucosa and colon (Jackson et al., 2000; Fornai et al., 2006).

COX-1 is found in the mucosal epithelium, vascular endothelium, neurones of myenteric ganglia, and in smooth muscle cells of the tunica muscularis. However, expression levels of COX-1 in the GI tract show wide intra-anatomical and interspecies variability. For example, both the gastric antrum and pyloric region of dogs contain 10-fold more COX-1 protein than is contained in the small intestine

TABLE 1-1 Comparative COX-1 and COX-2 Expression in the Gastrointestinal Tract

Location	COX-1					COX-2				
	Dog	Horse	Human	Monkey	Rat	Dog	Horse	Human	Monkey	Rat
Stomach fundus	×		×	×	×			×		×
Pyloric antrum	×		×	×	×			×		×
Duodenum	×		×	×	×					×
Jejunum	×	×	×	×	×		×			×
Ileum	×		×	×	×					×
Cecum	×		×	×	×					×
Colon	×		×	×	×	×		×	×	×

Source: Reprinted from Z. A. Radi and N. K. Khan, Effects of cyclooxygenase inhibition on the gastrointestinal tract, *Experimental and Toxicologic Pathology*, 58, pp. 163–173. Copyright © 2006, with permission from Elsevier.

(Seibert et al., 1997). In comparison, the nonhuman primate small intestine has five-fold more COX-1 protein than that in rodent or canine small intestine tissues, and rodents express less COX-1 in the GI tract than do nonhuman primates or humans (Kargman et al., 1996). In rats, weak COX-1 immunostaining is found in the stomach, small intestine, and colon (Burdan et al., 2008). In a rat model of colitis, both COX-1 and COX-2 were expressed in the normal colon and present in neurons of myenteric ganglia, while COX-2 was up-regulated in rats with colitis (Fornai et al., 2006). In rabbits, only COX-1 was detected in parietal cells, while both COX-1 and COX-2 were expressed in gastric glands, with the relative protein density of COX-1 being sixfold higher than that of COX-2 (Nandi et al., 2009). In humans, the highest and lowest areas of COX-1 expression are in the small intestine and gastric fundus/antrum, respectively (Kargman et al., 1996). Strong gastric parietal cell COX-1 and COX-2 immunoreactivity has been observed in the normal human gastric mucosa (Jackson et al., 2000). COX-2 up-regulation has been described within the mucosa in the presence of inflammation or ulcers. COX-1 and COX-2 immunostaining was increased at the rim of ulcers and in *Helicobacter pylori* gastritis, particularly at the mid-glandular zone and lamina propria inflammatory cells (Jackson et al., 2000). Some studies suggest that the predominant source of increased gastric PGE₂ in *H. pylori* infection in humans is probably COX-1 derived (Scheiman et al., 2003). In inflammatory bowel disease (IBD), COX-1 was localized in the crypt epithelium of the normal ileum and colon and its expression was unchanged. COX-2 expression, on the other hand, was undetectable in normal ileum or colon but was induced in apical epithelial cells of inflamed foci in IBD (Singer et al., 1998). In another study, COX-2 expression up-regulation occurred in neural cells of the myenteric plexus in patients with active IBD (Roberts et al., 2001).

COX-2 is normally absent (except in the colonic mucosa) in the intestinal tract in dogs, nonhuman primates, and humans (Koki et al., 2002a; Maziasz et al., 2003). In horses, COX-1 and COX-2 were expressed in nonischemic- and ischemic-injured jejunal mucosa tissues obtained 18 h after recovery, with ischemia causing significant up-regulation of both COX isoforms (Tomlinson et al., 2004). In rats, COX-2 is present at low levels in close association with macrophages in the region of gut-associated lymphoid tissue (Kargman et al., 1996). COX-2 expression was observed in the rat fundus and pylorus regions of the stomach, intestinal tract (jejunum, ileum, duodenum, cecum, colon, and rectum), and intestinal tract parasympathetic ganglia of the submucosa and muscularis (Haworth et al., 2005). The highest level of COX-2 expression was noted at the ileocecal junction in rats (Haworth et al., 2005). This ileal-side high level of COX-2 expression may explain the spontaneous ulceration and perforation of the distal ileum in COX-2 knockout (COX-2^{-/-}) rodents (Sigthorsson et al., 2002). There is site-dependent susceptibility to intestinal injury that is related to local prostanoid homeostasis. For example, the rat cecum is particularly sensitive to long-term, low-dose indomethacin administration (NygAard et al., 1995). COX-2 immunostaining was observed in the small intestine lamina propria in mice (Hull et al., 1999).

COX-2 can be induced in pathological conditions and in the inflamed GI mucosa, and its inhibition by NSAIDs has been hypothesized to delay the resolution of GI injury (Kishimoto et al., 1998). Increased COX-2 expression, observed

TABLE 1-2 Comparative Susceptibility to Toxicity and Location^a of Lesions in the Gastrointestinal Tract After COX Inhibition

GI injury	Interspecies differences
Relative susceptibility at therapeutic exposures	Rat > dog > monkey > human
Upper GI most common site	Human > monkey > dog > rat
Lower small intestine most common site	Rat > dog > monkey ^b > human

Source: Reprinted from Z. A. Radi and N. K. Khan, Effects of cyclooxygenase inhibition on the gastrointestinal tract, *Experimental and Toxicologic Pathology*, 58, pp. 163–173. Copyright © 2006, with permission from Elsevier.

^aLocation of injury similar for both ns-NSAIDs and s-NSAIDs, with the exception that injuries with s-NSAIDs occur at high exposure multiples.

^bInjury to lower GI tract uncommon in monkeys.

maximally at 24 h, has been observed in a rat model of ischemia/reperfusion–induced acute gastric mucosal injury (Kishimoto et al., 1998). COX-2 expression was increased in cultured rat gastric mucosal cells in vitro and after acid-induced gastric injury to rats in vivo (Sawaoka et al., 1997; Erickson et al., 1999; Sun et al., 2000). COX-2 may play a role in rodent postoperative ileus since intestinal manipulation induced COX-2 within resident muscularis macrophages, a discrete subpopulation of myenteric neurons and recruited monocytes (Schwarz et al., 2001). Additionally, COX-2 has been shown to be induced in various hyperplastic and neoplastic lesions of the GI tract, such as colon cancer, familial adenomatous polyposus (FAP), and sporadic adenomatous polyps in the colon (Soslow et al., 2000; Khan et al., 2001; Koki et al., 2002b). Up-regulation of COX-2 has been demonstrated within adenomas of the small and large intestine of multiple intestinal neoplasia (Min) mice (Hull et al., 1999). These observations support the use of NSAIDs in the treatment of epithelial cancer. In fact, a COX-2 s-NSAID, celecoxib, has been approved as adjunct therapy to the usual care (e.g., endoscopic surveillance, surgery) to reduce the number of adenomatous colorectal polyps in humans. In humans, gastric mucosal expression of COX-2 is increased in gastritis and gastric ulceration (Tatsuguchi et al., 2000; Bhandari et al., 2005).

In summary, COX-1 (and not COX-2) is the predominant isoform in the normal GI tract. There appears to be significant interspecies differences in both the level of COX-1 expression and the ratio of COX-1 and COX-2 expression in the GI tract. Both COX-1 expression and relative COX-1/COX-2 expression are highest in some animal species, including the dog and rat, compared with humans and nonhuman primates, which may partly explain the overt sensitivity of these species to subtherapeutic doses of ns-NSAIDs (Table 1-2) (Radi and Khan, 2006b; Radi, 2009).

EFFECTS OF ns-NSAIDS ON THE GI TRACT

Several ns-NSAID classes (Table 1-3) are used in human and veterinary medicine for their anti-inflammatory, analgesic, and antipyretic effects. In veterinary medicine, phenylbutazone, meclofenamic acid, meloxicam, carprofen, and

TABLE 1-3 Nonselective NSAID Major Classes

ns-NSAID class	Generic name	Trade name
Arylpropionic acid	Ibuprofen	Advil, Motrin, Nuprin
	Naproxen	Aleve, Naprosyn
	Ketoprofen	Orudis, Oruvail
	Carprofen	Rimadyl, Zenecarp, Novox
	Fenoprofen	Nalfon
	Flurbiprofen	Flurofen, Ansaid
Enolic acids	Piroxicam	Feldene
	Tenoxicam	Tilcotil
	Lornoxicam	Xefo
Acetic acids	Etodolac	Etogesic
	Indomethacin	Indocin
	Diclofenac	Cataflam, Voltarin
	Sulindac	Clinoril
	Nabumetne	Relfen
Aminonicotinic acids	Flunixin meglumine	Banamine
Pyrazoles	Phenylbutazone	Zolandin
Salicylic acids	Acetylsalicylic acid	Aspirin
Anthranilic acids	Meclofenamate	Ponstel, Arquel, Meclofen

etodolac are approved for use in dogs in the United States (Fox and Johnston, 1997; Budsberg et al., 1999); flunixin meglumine, meclofenamic acid, naproxen, and phenylbutazone are approved for horses (Kopcha and Ahl, 1989). Although the broad range of applications for ns-NSAID therapy makes it an attractive prescriptive choice, it has been partnered adversely with GI toxicity. Implications to humans have included nonulcer dyspepsia and serious GI-related side effects, such as gastric and duodenal ulcers, erosions, bleeding, perforation, esophagitis, and esophageal strictures (Lanza et al., 1983; Bjorkman, 1996; Mason, 1999; Schoenfeld et al., 1999; Scheiman, 2003). Similar to use in humans, chronic ns-NSAID use in dogs has also been associated with serious GI side effects, manifested as bleeding, ulceration, erosions, perforations, peritonitis, melena, anemia, anorexia, and abdominal pain (Ewing, 1972; Roudebush and Morse, 1981; Cosenza, 1984; Daehler, 1986; Stanton and Bright, 1989; Wallace et al., 1990; Ricketts et al., 1998; Reed, 2002). The incidence of GI ulceration is greatly increased in animals receiving ns-NSAIDs in combination with steroids; therefore, this combination should be avoided (Johnston and Budsberg, 1997; Reed, 2002).

To limit the potential for serious complications associated with NSAID use in veterinary medicine, clinicians should take the following precautions before prescribing NSAIDs: (1) verify that corticosteroids and other NSAIDs are not being given concurrently with the NSAID prescribed, (2) adhere to the dosages recommended, (3) advise clients of potential safety risks and their clinical signs,

and (4) avoid use in at-risk cases (Lascelles et al., 2005b). At-risk indications are (1) a history of GI ulceration, (2) geriatric patients (older animals have reduced clearance capacity and are more susceptible to NSAID GI toxicity), (3) the use of aspirin, (4) GI comorbidities (e.g., preexisting GI ulcer, *H. pylori* colonization, liver disease), and (5) clinical chemistry (e.g., indications of impaired hepatic function, hypoproteinemia) (Lascelles et al., 2005b). The comparative GI effects of various classes of ns-NSAIDs are detailed below.

Effects of Arylpropionic Acid ns-NSAIDs on the GI Tract

Arylpropionic acids represent the largest class of widely prescribed group of ns-NSAIDs, which include ibuprofen, naproxen, ketoprofen, carprofen, fenoprofen, and flurbiprofen (Table 1-3). These drugs are approved for use in the treatment of RA, OA, and ankylosing spondylitis.

Ibuprofen (Advil, Motrin, and Nuprin) is one of the most commonly used ns-NSAIDs and is supplied as tablets. It probably ranks after aspirin and paracetamol in nonprescription over-the-counter (OTC) drugs used in humans for the relief of symptoms of pain, inflammation, and fever (Rainsford, 2009). In dogs, ibuprofen has been used as an anti-inflammatory agent. However, dogs are much more sensitive than humans to the development of GI toxicity from ibuprofen administration. At therapeutic doses, adverse GI effects observed in dogs include vomiting, diarrhea, anorexia, abdominal pain, nausea, and GI bleeding. Dogs given 8 or 16 mg/kg per day of ibuprofen orally for 30 days showed no clinical signs of toxicity. However, postmortem examination revealed the presence of gastric ulcers or erosions, usually in the antrum or pylorus, less often in the fundic or cardiac regions of the stomach, and intestinal inflammation (Adams et al., 1969). No GI lesions were noted in a 4-mg/kg per day dose in this study in dogs. In another study, ibuprofen oral repeated dosing at 8 and 16 mg/kg per day (0.4- and 0.9-fold multiples of the human dose, respectively) for one month in dogs caused GI pathology comprised of bloody or discolored stools and intestinal ulceration and/or perforation (Hallesy et al., 1973). During 26-week repeat-dose toxicity in dogs given ibuprofen in a 16-mg/kg per day dose, clinical signs of GI toxicity characterized by frequent vomiting, diarrhea with occasional passage of fresh blood, and loss of weight were noted in week 8 of dosing (Adams et al., 1969). Dogs given 4- and 2-mg/kg per day doses had no evidence of GI toxicity. On the other hand, similar GI pathology was observed in rats only after six months of repeated dosing and at a higher oral dose of 180 mg/kg per day (9.7-fold multiples of the human dose) (Hallesy et al., 1973). The approximate LD₅₀ values for ibuprofen are 800 mg/kg orally and 320 mg/kg intraperitoneally in the mouse and 1600 mg/kg orally and 1300 mg/kg subcutaneously in the rat (Adams et al., 1969). The proportions of the dose recovered from the ligated stomach and ligated intestine of rats at various times after introduction of ¹⁴C-labeled ibuprofen were measured. Only 73% of the dose was recovered from the stomach and its contents 3 min after dosing, while no radioactivity was detected in plasma (Adams et al., 1969). Intestinal absorption of ibuprofen in rats was so rapid that by 3 min the plasma concentration of radioactivity was maximal (Adams et al., 1969). Thus, although

some absorption occurs in the stomach, the main site of ibuprofen absorption, at least in rats, is the intestine. Rats given ibuprofen for 26 weeks orally at 180 mg/kg per day grew normally but were anemic (had low erythrocyte counts, hemoglobin concentration, and hematocrits) by the final week of dosing, and a few rats had intestinal ulcers (Adams et al., 1969). Therefore, due to its narrow margin of safety, ibuprofen is generally not recommended for use or should be used with caution in dogs and also in cats or ferrets (Cathers et al., 2000). Ibuprofen toxicosis can occur in dogs and ferrets after accidental ingestion. When ibuprofen toxicosis is suspected, serum, urine, and liver samples can be used for toxicological analyses for ibuprofen by gas chromatography and mass spectrophotometry (Cathers et al., 2000). In laboratory animals, ibuprofen administration has been linked to vomiting, gastric irritation, and ulceration and duodenal and jejunal ulceration in rats, dogs, rabbits, and monkeys (Adams et al., 1969; Scherkl and Frey, 1987; Elliott et al., 1988; Godshalk et al., 1992; Arai et al., 1993). Pregnant female rabbits given 60 or 20 mg/kg per day of ibuprofen on days 1 to 29 of pregnancy grew less than controls and had stomach ulcers (Adams et al., 1969). Female rabbits receiving 7.5 mg/kg per day grew normally, but some had gastric ulcers or erosions (Adams et al., 1969). Thus, pregnant rabbits are highly sensitive to ibuprofen, and during pregnancy the intestinal tract, at least in rabbits, is more sensitive than that of nonpregnant animals (Adams et al., 1969). The route of ibuprofen administration affects the GI pathology observed. Little or no GI damage occurred when ibuprofen was given daily by oral administration to nonhuman primates at doses up to 300 mg/kg for 90 days. However, intravenous (IV) administration of ibuprofen to nonhuman primates over a 24-h period in four equal doses of 75 mg/kg at 6-h intervals resulted in gastric erosions or ulcers (Elliott et al., 1988). When given IV for 14 days at 100 and 200 mg/kg per day using the same 24-h dosing conditions described above, nonhuman primates showed gastric and/or duodenal ulcers (Elliott et al., 1988). In rats, acute single oral doses under 500 mg/kg of ibuprofen were free of GI pathological changes (Elliott et al., 1988). However, acute IV administration of ibuprofen at a dose of 270 mg/kg given in four equal doses of 67.5 mg/kg at 6-h intervals over a 24-h period resulted in gastric and intestinal (ileum and jejunum) ulcerations (Elliott et al., 1988). Therefore, the acute (24 h) IV route of ibuprofen administration in rats is more ulcerogenic than the oral route.

One factor that has been correlated with GI events with ns-NSAID use is the drug plasma elimination half-life ($t_{1/2}$). There is less gastric mucosal adaptation with NSAIDs that have long half-lives. For example, due to the short plasma $t_{1/2}$ of elimination of ibuprofen, approximately 2 h, and its rapid absorption, ibuprofen at doses of 200 and 800 mg/kg has low possibilities of serious GI events and complications (i.e., epigastric or abdominal pain, dyspepsia, flatulence, nausea, heartburn, diarrhea, constipation, vomiting) in humans (Rainsford, 2009). Another GI event that can be associated with ns-NSAID intake is chronic anemia. For example, daily treatment (800 mg three times daily) with ibuprofen has also been associated with significant fecal blood loss in healthy volunteers (Bowen et al., 2005). Several ns-NSAIDs, including ibuprofen, were compared for GI events in a large two-year epidemiological safety study involving 30,000 to 40,000 rheumatic patients in centers in Germany, Switzerland, and Austria, known as the Safety Profile of

Antirheumatics in Long-Term Administration (SPALA) (Rainsford, 2009). This SPALA study found ibuprofen to be associated with the lowest numbers of GI events. In another large-scale study, fewer GI events were observed in patients taking ibuprofen at doses up to 1200 mg daily for 7 days compared with aspirin and paracetamol (Rampal et al., 2002).

Similarly, naproxen (Aleve, Naprosyn), which has a variably longer half-life across species ($t_{1/2}$ is approximately 14 h in humans, 2 h in nonhuman primates, 35 h in dogs, 9 h in guinea pigs, and 5 h in rats), is used in humans and dogs for its anti-inflammatory, analgesic, and antipyretic properties (Hallesy et al., 1973; Rainsford, 2009). The long half-life of naproxen in dogs appears to be due to its extensive enterohepatic recirculation. With the exception of the dog, all species excreted naproxen and its metabolic transformation products predominantly in the urine. In dogs, naproxen is eliminated primarily through the bile and feces, whereas in other species, the primary route of elimination is through the kidneys (Runkel et al., 1972). Once in the blood after oral administration, naproxen is absorbed fully and rapidly in all species. Naproxen is indicated for temporary relief of fever and minor aches and pains due to backache, headache, and toothache in humans (Runkel et al., 1972; Rainsford, 2009). In dogs, naproxen has been shown to cause gastric ulceration and hemorrhage, melena, vomiting, abdominal pain, weakness, and hemorrhagic gastroenteropathy, including transmural pyloric perforation (Daehler, 1986; Stanton and Bright, 1989). Repeated oral administration of naproxen to dogs for one month at 15 mg/kg per day (1.3-fold multiple of human dose) and for three months at 5 mg/kg per day (0.4-fold multiples of human dose) caused GI pathology of bloody or discolored stools and intestinal ulceration and/or perforation (Hallesy et al., 1973). Additionally, mice and rats administered an acute oral dose of naproxen displayed bloody or discolored stools and intestinal ulceration and perforation (Rainsford et al., 2003). A single oral naproxen dose of 250 mg/kg to rats caused death in 6 to 8 days and abdominal adhesions, and small intestine necrotic foci were observed at necropsy (Elliott et al., 1988). Repeated oral administration of naproxen to rats for six months at 30 mg/kg (2.6-fold multiple of human dose) and for 22 months at 2, 10, and 30 mg/kg per day (0.2-, 0.9-, and 2.6-fold multiples of human dose, respectively) caused GI pathology of bloody or discolored stools and intestinal ulceration and/or perforation (Hallesy et al., 1973). Repeated oral administration of naproxen in nonhuman primates for six months at doses up to 120 mg/kg per day (10.4-fold multiples of human dose) was well tolerated with no adverse GI pathological toxicity (Hallesy et al., 1973). The pig closely resembles humans in respect to anatomy, physiological functions in the GI tract, and the histological and pathophysiological changes in the development of gastric ulcers induced by NSAIDs (Rainsford et al., 2003). Daily oral administration of naproxen to pigs at doses up to 45 mg/kg (3.9-fold multiples of human dose) for one year was well tolerated with no adverse GI pathology (Hallesy et al., 1973). In an experimental pig model using healthy Landrace males, naproxen induced gastroduodenal ulcers and erosions when given orally for 10 days at a dose of 100 or 150 mg/kg per day (Rainsford et al., 2003). In horses, naproxen has been used for the treatment of inflammatory conditions and pain from myositis and soft tissue injuries, and it has a reasonable margin of safety. However, adverse GI ulceration has been reported in

horses (Lees and Higgins, 1985). In humans, GI events associated with naproxen include GI erosions and ulcers, dyspepsia, upper abdominal pain, nausea, diarrhea, constipation, abdominal distension, and flatulence (Lohmander et al., 2005).

Ketoprofen (Orudis, Oruvail) has a $t_{1/2}$ of approximately 8.5 h and is used to treat RA in humans (Rainsford, 2009). It is used in dogs, cats, and horses to treat postsurgical and musculoskeletal pain, colic, synovitis, and OA. Its $t_{1/2}$ in dogs and cats is approximately 2 to 3 h and 2 h in horses. Ketoprofen was ulcerogenic when used in laboratory animal models (Rainsford, 1977) but to a lesser degree than other ns-NSAIDs (phenylbutazone and flunixin meglumine). Similarly, in horses, ketoprofen was less toxic than phenylbutazone and flunixin meglumine (MacAllister et al., 1993). Gastric-duodenal erosion and/or hemorrhage and ulceration of the glandular and nonglandular portions of the stomach were noted in dogs and horses, respectively (MacAllister et al., 1993; Forsyth et al., 1998). Similar ulceration was seen in a one-month oral toxicity study with ketoprofen in rats and dogs (Julou et al., 1976). In a study of Sprague–Dawley rats given a 10-mg/kg dose of ketoprofen subcutaneously that had undergone ovariectomy, many rats died or were euthanized within 3 to 7 days after surgery, due to clinical illness that was related to GI ulceration (Lamon et al., 2008). The safety profile of a reduced dosage of ketoprofen (0.25 mg/kg per day) was evaluated in a 30-day oral study in healthy beagle dogs. Mild to moderate gastric mucosal injuries, especially in the pyloric antrum, were observed in this study (Narita et al., 2006). Gastric lesions were observed in a long-term (up to 90 days) study after oral administration of various ns-NSAIDs (i.e., carprofen, etodolac, flunixin meglumine, and ketoprofen) in dogs (Luna et al., 2007). In addition, the bleeding time was significantly longer by day 7 in dogs treated with meloxicam, ketoprofen, and flunixin meglumine (Luna et al., 2007). Scaring in the pyloric antrum suggestive of ulceration healing was present in one of 12 monkeys following 12 months of ketoprofen treatment (Julou et al., 1976).

Interestingly, a study in hamster cheek pouch microcirculation showed that topically applied ketoprofen lysine salt significantly inhibited both the leukocyte adhesion and microvascular leakage induced by bradykinin (Daffonchio et al., 2002). A kallikrein-kinin cascade such as bradykinin has been shown to be involved in gastric ulcers (Sawant et al., 2001). Therefore, this study by Daffonchio et al. suggests that in addition to COX inhibition, ketoprofen may have an antagonistic effect on bradykinin, which may contribute to its ulcerogenic potential. In humans, ketoprofen is often used in a once-daily 200-mg sustained-release formulation to treat rheumatic diseases, especially in elderly patients. Long-term safety and prospective studies on 20,000 patients showed that ketoprofen is associated with a 28% rate of such GI events as peptic ulcers, bleeding, melena, and black stools (Le Loet 1989; Schattenkirchner, 1991). Most of these serious GI side effects occurred during the first three months of treatment.

Carprofen (Rimadyl, Zenecarp, Novox) is approved for use in dogs to treat pain and inflammation associated with OA and pain associated with soft tissue or orthopedic surgery. The $t_{1/2}$ in dogs is approximately 8 h and is highly variable in cats (20 ± 16 h). In dogs, biliary secretion predominates, and 70% of an IV dose of carprofen is excreted in the feces, while 8 to 15% of the dose is excreted

in the urine. In rats, fecal excretion due to biliary secretion varies from 60 to 75%, and urinary excretion accounts for 20 to 30% of an IV dose (Rubio et al., 1980). Therefore, excretion in dogs, rats, and cattle is mainly fecal after biliary secretion, whereas it is primarily urinary in horses. In dogs, most carprofen is metabolized by direct conjugation to an ester glucuronide followed by oxidation to phenol and further conjugation. These conjugated phenols are eliminated in the feces. Carprofen has produced GI lesions that are mild but of no clinical relevance or significance compared with placebos (Reimer et al., 1999). Typical adverse GI effects of this drug include vomiting, diarrhea, and change in appetite (Raekallio et al., 2006). A transient decrease in serum protein and albumin concentrations (concentrations were lower in treated dogs than in those that received placebo at 4 weeks, but not at 8 weeks) was observed after daily administration of carprofen in a two-month study in dogs (Raekallio et al., 2006). When administered orally daily in a 4-mg/kg dose, carprofen induced the lowest frequency of adverse GI effects compared with etodolac, flunixin meglumine, ketoprofen, and meloxicam in a 90-day study in dogs (Luna et al., 2007).

GI ulceration and bleeding are sometimes accompanied secondarily by anemia and hypoproteinemia, due to blood and protein loss (Adams et al., 1969; Lanas et al., 2003). In a 14-day safety study (according to the Rimadyl package insert) involving oral administration of 10 mg/lb twice daily (10 times the recommended total daily dose), two of eight dogs exhibited hypoproteinemia (hypoalbuminemia). Three incidents of black or bloody stool were observed in one dog. Five of eight dogs exhibited reddened areas of duodenal mucosa on gross pathological examination. Histological examination of these areas revealed no evidence of ulceration but did show minimal congestion of the lamina propria in two of the five dogs. In separate safety studies lasting 13 and 52 weeks, respectively, dogs were administered orally up to 11.4 mg/lb per day (5.7 times the recommended total daily dose of 2 mg/lb) of carprofen. In both studies the drug was well tolerated clinically by all the animals. No gross or histological changes were seen in any of the animals treated.

In cats, carprofen is an effective analgesic for soft tissue and orthopedic procedures and is approved in several countries (Australia, France, Germany, United Kingdom) for use at 4 mg/kg for daily subcutaneous or intravenous administration (Steagall et al., 2009). Carprofen was well tolerated, and no clinical or endoscopic adverse GI effects were seen in cats after its administration in clinical trials for up to 5 days (Möllenhoff et al., 2005; Steagall et al., 2009). Although carprofen is not used routinely in nonhuman primates for postoperative analgesia, a dose of 2.2 mg/kg carprofen intramuscularly, or a combination of 0.01 mg/kg buprenorphine and 2.2 mg/kg carprofen intramuscularly provided more reliable postoperative analgesia than did buprenorphine alone (Allison et al., 2007). Although carprofen has been used to treat mastitis in cattle, it is not generally recommended for use in large animals, due to its long $t_{1/2}$ (30 to 40 h).

Fenoprofen (Nalfon) has a relatively short, 3-h half-life. GI events are similar to those with naproxen or ibuprofen. In rats, single fenoprofen oral doses of 1000 to 1600 mg/kg resulted in death and small intestine necrosis and abdominal adhesions (Elliott et al., 1988). Flurbiprofen (Flurofen, Ansaid) caused abdominal adhesions

and small intestinal necrosis or ulceration in rats after either acute oral (at 80 and 125 mg/kg) or intraperitoneal (at 125, 320, and 500 mg/kg) administration (Elliott et al., 1988). Chronic administration in a three-month study in rats caused ulcerative gastritis in 4- and 8-mg/kg doses and 0.5-, 2-, and 4-mg/kg doses in another two-year study (Elliott et al., 1988).

Effects of Enolic Acid (Oxicam) ns-NSAIDs on the GI Tract

Piroxicam (Feldene) is one of few enolic acid derivatives (Table 1-3) that is absorbed completely after oral administration and that undergoes enterohepatic recirculation. Due to its antitumor activity, it is used in dogs and cats to treat some cancers, such as transitional cell carcinoma (TCC) and oral squamous cell carcinoma. The average estimated $t_{1/2}$ is approximately 40 h in dogs and 12 h in cats. Due to this long $t_{1/2}$ in dogs, the steady state is typically not reached for 7 to 12 days. GI irritation was seen in some dogs after bladder TCC treatment with piroxicam orally in a 0.3-mg/kg dose (Knapp et al., 1994). Gastric ulcers occurred in rats after once-daily piroxicam administration in doses of 2.7, 5.3, and 6.7 mg/kg, which are equieffective for indomethacin (10, 20, and 25 mg/kg) (Aguwa, 1985). Gastric ulcers were induced in rats after two oxicam oral dosing. However, the incidence of such lesions was higher for tenoxicam (Tilcotil) (10.2 mg/kg) than for diclofenac sodium (34 mg/kg, equivalent to 6.8 mg/kg tenoxicam) or piroxicam (6.2 mg/kg) (al-Ghamdi et al., 1991). Other subchronic 14- and 28-day studies in rats assessed the GI effects of equipotent doses of meloxicam (3.75 and 7.5 mg/kg) and piroxicam (5 and 10 mg/kg) in rats. Both drugs dose-dependently caused multiple gastric erosions and hemorrhage. Meloxicam led to greater gastric damage than with piroxicam on day 14, although these results were not significant (Villegas et al., 2002). In a dose-escalation study of piroxicam with oral doses ranging from 0.5 mg/kg every 48 h to 1.5 mg/kg every 48 h in dogs, a dose-limiting GI irritation or ulceration occurred in dogs that received 1.5 mg/kg, with a maximum tolerated dose of 1 mg/kg (Knapp et al., 1992). Lornoxicam (Xefo), a novel ns-NSAID compound in the same chemical class as piroxicam and tenoxicam, caused GI lesions in monkeys (Atzpodien et al., 1997). In the dose-range-finding study, animals were dosed orally for 6 weeks with 0.25, 0.5, 1, or 2 mg lornoxicam/kg per day. GI toxicity was observed in the 1- and 2-mg/kg per day dose groups only. Toxicity included mortality, diarrhea, prostration, decreased body weight gain and food consumption, fecal occult blood, anemia, hypoalbuminemia, GI erosions, and ulcerations (Atzpodien et al., 1997). A follow-up chronic study was conducted using dose levels of 0.125, 0.25, or 0.5 mg/kg per day for 52 weeks. The high-dose level was increased to 0.6 mg/kg/day from week 39 to week 52. Histopathological examination of the GI tract revealed erosions, ulcerations, and inflammation in both males and females at 0.5 or 0.6 mg/kg per day. Cinicopathological findings included decreased hematocrit and hypoproteinemia and hypoalbuminemia (Atzpodien et al., 1997).

In a clinical study in elderly patients with knee OA, piroxicam at a dose of 20 mg/day for 3 weeks resulted in elevation of the gastric mucosa endoscopic score in 78% of the subjects compared to the beginning of the study, and 22% of

the subjects developed ulcers. Mild dyspepsia symptoms after piroxicam administration were positive in 67% of subjects (Girawan et al., 2004). Significantly higher bleeding was found in a 28-day study in healthy male volunteers using a 20-mg piroxicam dose compared with a placebo. In addition, endoscopy scores were significantly higher with piroxicam than in the meloxicam group at a dose of 7.5 mg (Patoia et al., 1996). In another 28-day study in healthy volunteers, significant macroscopic gastric mucosal damage occurred within 24 h of 20-mg piroxicam administration; however, such GI damage resolved in most subjects by day 28 (Lipscomb et al., 1998).

Effects of Acetic Acid Derivative ns-NSAIDs on the GI Tract

Acetic acid derivatives include etodolac, indomethacin, diclofenac, sulindac, and nabumetone (Table 1-3). Etodolac (Etogesic) is approved for use in dogs with OA and has been studied in horses. Adverse reactions to etodolac in dogs include vomiting, soft or dark brown stool, and diarrhea with blood, as reported in a three-month oral toxicity study at a dose of 25 mg/kg, as well as gastric and small intestinal ulceration with associated weight loss, anorexia, anemia, and hypoproteinemia in a one-year chronic toxicity study at doses of 40 and 80 mg/kg (Budsberg et al., 1999). In a 28-day study in healthy dogs, etodolac was given orally once a day at an average dose of 12.8 mg/kg and gastroduodenal endoscopy was performed. Only minor gastric lesions were observed (Reimer et al., 1999). In an experimental study of the GI effects of etodolac in horses, jejunum was exposed to 2 h of ischemia during anesthesia, and then horses received etodolac at 23 mg/kg IV every 12 h. Tissue specimens were obtained from ischemic-injured and nonischemic jejunum immediately after ischemia and 18 h after recovery from ischemia. The investigators found that ischemic-injured tissue from horses treated with etodolac had significantly lower transepithelial electric resistance and retarded recovery of the jejunal mucosa barrier after 18 h of reperfusion (Tomlinson et al., 2004).

In rats, indomethacin (Indocin) caused gastric mucosal bleeding, cecal ulceration, and small intestine (jejunum and ileum) ulcers, perforations, and adhesions (Kent et al., 1969; Brodie et al., 1970; Schriver et al., 1975; Fang et al., 1977; Arai et al., 1993; Anthony et al., 1994; Sigthorsson et al., 1998; Campbell and Blikslager, 2000; Altinkaynak et al., 2003; Takeuchi et al., 2004), with gastric damage being significantly greater in arthritic rats than in normal rats (McCafferty et al., 1995). The half-life of indomethacin in plasma ranges from hours in rats to minutes in dogs and monkeys. There are significant species differences in the distribution and excretion of indomethacin (Yesair et al., 1970). In rats, plasma clearance of indomethacin by liver, although low, is 30 times the clearance rate by kidney, and the reabsorption of indomethacin from the intestine is extensive. Desmethylin-domethacin, the major metabolite, is cleared from plasma equally by liver and kidney and is not reabsorbed from the intestine of rats. In dogs, indomethacin is secreted in bile extensively and rapidly, and is eventually excreted in their feces as an unchanged drug and minimally metabolized to eschlorobenzoylindomethacin, which is excreted in urine. Nonhuman primates are similar to dogs in that the liver was more than 10 times as effective as the kidneys in clearing total radioactivity

from plasma. However, the primates differed from dogs in that the drug was maximally reabsorbed from the intestine (Yesair et al., 1970). In a six-month repeat oral daily dosing study in rats, indomethacin at doses of 2 and 4 mg/kg (0.7- and 1.3-fold multiples over human dose, respectively) caused GI pathology characterized by bloody or discolored stools and intestinal ulceration and/or perforation (Hallesy et al., 1973). Indomethacin increased the incidence and ulcer index of duodenal ulcers in arthritic rats on days 14 and 28 of arthritis (DiPasquale and Welaj, 1973). Additionally, the intestinal ulcerogenic response to indomethacin was markedly aggravated in arthritic rats, and the onset of the ulceration was much earlier in arthritic rats than in normal rats (Kato et al., 2007). GI hemorrhage and ulceration, potentially attributed to the extensive enterohepatic recirculation of indomethacin, were seen in dogs (Duggan et al., 1975) (Figs. 1-2 and 1-3). In a one-month repeat oral dosing study in dogs, indomethacin at 6 and 18 mg/kg per day (1.9- and 5.8-fold multiples over human dose) caused GI pathology of bloody or discolored stools and intestinal ulceration and/or perforation (Hallesy et al., 1973). In an experimental pig model for human GI disease, indomethacin was given orally for 10 days at a

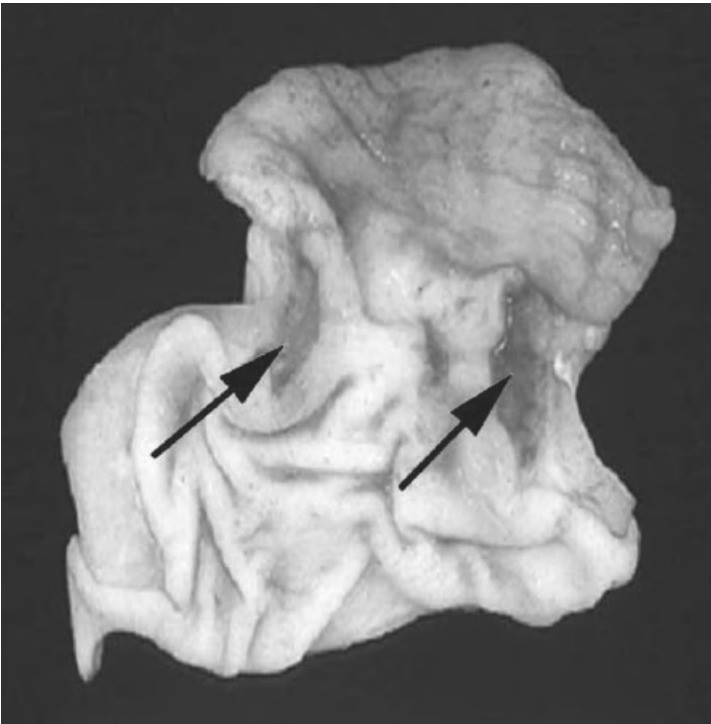


FIGURE 1-2 Severe indomethacin-induced gastric mucosal hemorrhage and ulceration at the gastroduodenal junction (arrows) in a dog. (Reprinted from Z. A. Radi and N. K. Khan, *Effects of cyclooxygenase inhibition on the gastrointestinal tract*, *Experimental and Toxicologic Pathology*, 58, pp. 163–173. Copyright © 2006, with permission from Elsevier.)

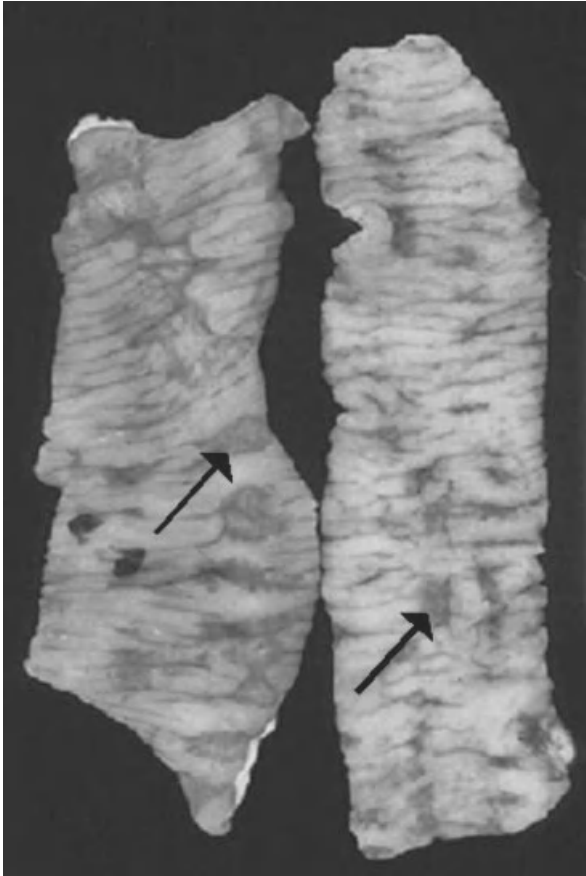


FIGURE 1-3 Indomethacin-induced small intestine mucosal ulceration (arrows) in a dog. Note the skip ulcerations typical of ns-NSAID-induced lesions in the small intestine in dogs. (Reprinted from Z. A. Radi and N. K. Khan, Effects of cyclooxygenase inhibition on the gastrointestinal tract, *Experimental and Toxicologic Pathology*, 58, pp. 163–173. Copyright © 2006, with permission from Elsevier.)

does of 10 or 20 mg/kg per day and GI effects were evaluated. Gastroduodenal ulcers and lesions occurred with indomethacin treatment at both doses. Additionally, indometacin produced focal ulcers in the cecum. The mucosal concentrations of indometacin in the gastric and intestinal mucosa correlated with mucosal injury (Rainsford et al., 2003). A 4-week toxicity study of indomethacin was conducted in nonhuman primates (marmoset) in which indomethacin was administered by oral route at dose levels of 2, 6, and 12 mg/kg per day. All animals given the daily 12-mg/kg dose and one animal given 6 mg/kg per day died during the dosing period and within 20 days. At 12 mg/kg per day, indomethacin induced severe GI toxicity, characterized by hemorrhage, ulcers, and necrosis with peritonitis (Oberto et al., 1990).

Diclofenac (Cataflam, Voltarin) has a rapid absorption, a short-half life of approximately 2 h, and is metabolized in the liver by CYP2C in humans. It is the most widely used NSAID in the world to treat RA, OA, and ankylosing spondylitis. The GI adverse effects of twice-daily administration of 75 mg of diclofenac were evaluated in one of the largest and longest individual-outcome randomized double-blind clinical studies of NSAID use in RA and OA patients. A total of 23,504 patients were randomized with mean treatment duration from 19.4 to 20.8 months (Combe et al., 2009). Significantly higher upper GI events (perforation, bleeding, obstruction, and ulcer) occurred with diclofenac than with 90- or 60-mg once-daily administration of etoricoxib (Combe et al., 2009). In rats, diclofenac acute (5 h) oral administration at 3.5, 7, and 15 mg/kg caused gastric ulcers. In rats treated with diclofenac at 15 mg/kg, pathological changes included longitudinal and diffuse gastric ulcers, particularly along the mucosal pleats, and thinning and inflammation of the intestinal wall with poor elasticity (Conforti et al., 1993).

Sulindac (Clinoril) is a prodrug whose anti-inflammatory activity (used to treat rheumatoid arthritis, osteoarthritis, ankylosing spondylitis, and acute gouty arthritis) resides in its sulfide metabolite. Sulindac is available in 200-mg tablets and undergoes two major biotransformations after oral administration. It is oxidized to the sulfone and then reversibly reduced to the sulfide. The sulfide is formed largely by the action of gut microflora on sulindac excreted in the bile. The half-life of the active sulfide is approximately 18 h. Sulindac can cause serious adverse GI events in humans, including inflammation, bleeding, ulceration, and perforation of the stomach, small intestine, or large intestine (according to a sulindac package insert).

Nabumetone (Relfen) exerts its pharmacological effects via its metabolite 6-methoxy-2-naphthylacetic acid (6-MNA) and is used to treat RA and OA. 6-MNA is not a biliary secretion and is inactivated in the liver, then conjugated before excretion. Because it is a nonacidic, prodrug formulation, fewer GI events were observed after nabumetone treatment than after treatment with other NSAIDs. GI events in humans included perforations, ulcers and bleeding, nausea, abdominal pain, and dyspepsia (Bannwarth, 2008). No gastric damage was observed in a 3-day study in rats in which nabumetone was orally dosed at 79 mg/kg and 6-MNA was given IV at 34 mg/kg (Melarange et al., 1992). The GI tolerability and pathology of nabumetone and etodolac were evaluated in an extensive nonclinical acute and chronic safety study (Spangler, 1993). In a single-dose study, etodolac caused a significant increase in both gastric and intestinal damage at 6, 24, 48, and 144 h after dosing. In contrast, no significant GI damage was noted with nabumetone. In the 28-day study, a significant increase in GI damage was noted with etodolac, but not with nabumetone, despite the higher dose employed [the nabumetone dose was five times the ID₂₅ (the dose that reduces inflammation by 25% in 50% of animals)] (Spangler, 1993).

Effects of Aminonicotinic Acid Derivative ns-NSAIDs on the GI Tract

Although not approved for use in cats, dogs, or food animals, flunixin meglumine (Banamine), an aminonicotinic acid derivative, is approved for use in nonhuman

primates and horses to control pain, colic, and endotoxic shock (Moore et al., 1981; Lees and Higgins, 1985; Kopcha and Ahl, 1989; Kallings et al., 1999). Renal excretion contributes significantly to flunixin meglumine in horses (Lees and Higgins, 1985). Flunixin meglumine can be administered to horses by IV, intramuscular, or oral routes at the recommended therapeutic dose of 1.1 mg/kg once a day for up to 5 days. Flunixin meglumine GI toxicity at recommended doses appears to be rare. Oral administration at three times the recommended dose for 10 days failed to elicit toxicity (Lees and Higgins, 1985). However, GI ulceration and erosion occurred in horses dosed 1.1 mg/kg IV every 8 h for 12 days (MacAllister et al., 1993). Tissue specimens were obtained from ischemic-injured and nonischemic jejunum immediately after ischemia and 18 h after recovery from ischemia. The investigators found that ischemic-injured tissue from horses treated with flunixin meglumine had significantly lower transepithelial electric resistance and retarded recovery of the jejunal mucosa barrier after 18 h of reperfusion (Campbell and Blikslager, 2000; Tomlinson et al., 2004). Additionally, this ns-NSAID was linked with GI ulceration and diarrhea in horses and dogs (Traub-Dargatz et al., 1988; Carrick et al., 1989; Vonderhaar and Salisbury, 1993; Luna et al., 2007). Flunixin meglumine has a significantly longer $t_{1/2}$ in cows (approximately 8 h) compared with horses (approximately 2 h) or dogs (approximately 4 h) and is used to treat bovine pneumonia at a dose of 2 mg/kg once a day for 3 to 5 days, as well as acute mastitis. No effects on the GI tract were noted when flunixin meglumine was given experimentally to calves (Kopcha and Ahl, 1989). In dogs, flunixin at 1 mg/kg for 3 days with 4-day intervals resulted in a significantly longer bleeding time and gastric lesions (Luna et al., 2007).

Effects of Pyrazolone Derivative ns-NSAIDs on the GI Tract

Phenylbutazone (Butazolidin), a pyrazolone derivative, is a widely studied pyrazolone ns-NSAID approved for use in dogs and horses to treat OA, osteoporotic conditions, and laminitis and studied experimentally in rats, cats, and food animals. Phenylbutazone metabolite is oxyphenylbutazone. When used in dogs, phenylbutazone was less toxic to this species than to humans but induced blood dyscrasia and GI injury (Watson et al., 1980; Conlon, 1988; Johnston and Budsberg, 1997). In horses, phenylbutazone has a $t_{1/2}$ that ranges from 3 to 10 h and has a narrow therapeutic index that may be related to lower plasma protein binding (Tobin et al., 1986). Absorption of phenylbutazone from the GI is influenced by the dose administered and the relationship of dosing to feeding. Access to hay can delay the time of peak plasma concentration to 18 h or longer (Tobin et al., 1986). GI-associated toxicity in horses includes gastric ulcers and erosions, edema of the small intestine, mucosal atrophy, duodenal erosions, erosions and ulcers of the large colon, and ulcerative colitis (Mackay et al., 1983; Traub et al., 1983; Collins and Tyler, 1985; Karcher et al., 1990; Meschter et al., 1990a,b). Phenylbutazone resulted in more severe GI toxicity in horses than did ketoprofen and flunixin meglumine, causing edema in the small intestine, erosions and ulcerations in the large intestine, and gastric ulceration at a dose of 4.4 mg/kg IV every 8 h for 12 days (MacAllister et al., 1993). In addition, hypoproteinemia and hypoalbuminemia secondary to

protein-losing enteropathy was seen in these horses. A 10-mg/kg dose of phenylbutazone once daily for 14 days is considered toxic and caused weight loss, diarrhea, and GI erosions and ulcerations (MacAllister, 1983). In laboratory animals such as dogs and rats, phenylbutazone caused GI pathology of blood or discolored stools and intestinal ulceration and/or perforation. In dogs, daily oral dosing at 200 mg/kg per day (32.3-fold multiples of human dose) for three months caused GI lesions. In rats, repeated oral dosing at 50, 100, and 200 mg/kg per day (8.1-, 16.1-, and 32.3-fold multiples of human dose) for six months caused GI lesions (Hallesy et al., 1973).

In ruminants, phenylbutazone is used to control arthritis and laminitis and is absorbed slowly following oral administration and cleared more slowly than that in horses and dogs. Although it protected calves against local dermal inflammation and systemic shock, it partially blocked rumen stasis in goats (Van Miert et al., 1977; Eyre et al., 1981). In rats, it caused gastric mucosal ulceration, bleeding, and hemorrhage and small intestine perforation and adhesions (Shriver et al., 1977; Mersereau and Hinchey, 1981; Takeuchi et al., 2004). These lesions are attributed to increased gastric contractions induced by the drug (Mersereau and Hinchey, 1981).

Effects of Salicylic Acid Derivative ns-NSAIDs on the GI Tract

Acetylsalicylic acid (aspirin) is still used widely due to its analgesic, antipyretic, and anti-inflammatory properties. Some salicylates, such as sulfasalazine, olsalazine, and mesalamine, are used to reduce inflammation associated with inflammatory bowel disease (IBD), such as Crohn's disease and ulcerative colitis [UC] (Radi et al., 2011). These IBD drugs cause splitting of the diazo bond by colonic bacteria to give sulfapyridine and 5-aminosalicylic acid (5-ASA), which is considered to be the active moiety that is delivered to the GI mucosa (Robinson, 1989). Emerging data suggest that 5-ASA treatment reverses an imbalance between the angiogenic factor VEGF and the antiangiogenic factors endostatin and angiostatin in an experimental UC rat model (Deng et al., 2009). The authors conclude that the effect of 5-ASA in UC may be caused by the down-regulation of expression of endostatin and angiostatin by modulation of matrix metalloproteinases-2 (MMP2) and MMP9 via inhibition of TNF α (Deng et al., 2009). Acetylsalicylic acid is rapidly absorbed mostly from the upper small intestine and undergoes rapid metabolism to the hydrolyzed active product, salicylic acid. Acetylsalicylic acid is the only salicylate that irreversibly inhibits cyclooxygenase by covalent acetylation of the enzyme. Salicylic acid is eliminated by hepatic conjugation with glucuronide and glycine and by renal excretion through glomerular filtration. The safety margin of aspirin is generally wide. The elimination half-life of salicylate varies significantly across species. The $t_{1/2}$ in cats is 27 to 45 h, 4.5 to 8.5 h in dogs, 1 h in horses, and 0.5 h in cows. Therefore, aspirin dosages range from 10 to 20 mg/kg orally every 2 to 3 days in cats, 10 to 20 mg/kg orally every 12 h in dogs, and 100 mg/kg orally every 12 h in cows (Langston and Clarke, 2002). Comparison of NSAID glucuronidation between several species indicated that it was most potent in monkeys, dogs, and humans. Cats were efficient in that respect because cats tend to be deficient in some

glucuronyl transferases enzymes that are important for glucuronidation (Magdalou et al., 1990). As a result, drugs that are excreted as glucuronide conjugates in other species, such as aspirin and paracetamol (acetaminophen), may have a prolonged half-life in cats, therefore increasing the risk of toxicity due to drug accumulation. Oral bioavailability of aspirin may vary due to differences in stomach content and pH (Conlon, 1988). A rise in pH increases the solubility of salicylates, and salicylate excretion depends on urinary pH; therefore, the short $t_{1/2}$ in horses is related to the basic urinary pH. Acetylsalicylic acid is poorly absorbed from the GI tract of horses after oral administration and disappears rapidly from the plasma. Although not approved for use in small animals, aspirin is most commonly used in dogs, but with associated GI complications, including mucosal erosions and hemorrhage in the pyloric antrum, cardia, and lesser curvature of the stomach (Conlon, 1988). These findings are not unusual, considering that aspirin and sodium salicylate are readily absorbed from the stomach and intestine of dogs and cats. Aspirin is rapidly deacetylated to salicylate, which is toxic to cells, affects mucosal barrier function, reduces cytosolic adenosine triphosphate, stimulates sodium transport and permeability, and increases proton dissipation from surface epithelial cells, resulting in microvascular damage, inflammation, hemorrhage, and gastric ulceration (Kauffman, 1989). In humans, aspirin use is associated with upper GI bleeding related to gastric hemorrhage and erosions distributed throughout the antrum of the stomach, especially more proximate to the body of the stomach with GI clinical manifestations of stomach upset, nausea, constipation, and diarrhea (Cryer, 2002).

Aspirin is available in a variety of preparations, such as plain, buffered, time-release, and enteric-coated. A potential strategy to combat the adverse GI effects from aspirin is administration of buffered or enteric-coated aspirin, which may prove less irritating to the dog stomach (Kauffman, 1989). Doses of 25 mg/kg of plain aspirin given at 8-h intervals for seven treatments resulted in gastric mucosal erosions in dogs, whereas there was minimal damage in dogs receiving buffered and enteric-coated preparations (Lipowitz et al., 1986). Misoprostol, a synthetic PGE₁ analog, has also been effective at decreasing endoscopically detectable mucosal gastric lesions (submucosal hemorrhage, erosion, or ulceration) in dogs given aspirin (Gullikson et al., 1987; Murtaugh et al., 1993; Johnston et al., 1995). In a dog repeat oral dosing study of aspirin at 60 mg/kg per day (onefold multiple of human dose) for three months, GI pathology of bloody or discolored stools, intestinal ulceration and/or perforation was seen (Hallesy et al., 1973). Aspirin given at 300 and 600 mg/kg per day for 4 days to Lewis rats with adjuvant-induced arthritis caused gastric mucosal bleeding and submucosal hemorrhage, which was seen at various time points of 24, 48, 72, and 96 h postdosing at necropsy (Shriver et al., 1975; Shriver et al., 1977). There are differences in the susceptibility of normal and arthritic rats to the gastric lesion-inducing properties of aspirin, with arthritic rats being more sensitive than normal rats. Oral administration of aspirin at doses of 10, 20 and 40 mg/kg caused dose-related increases in both the percentage of rats with gastric lesions and the severity of gastric lesion formation in both arthritic and nonarthritic rats. However, arthritic rats were less able to cope with the aspirin-induced insult to the gastric mucosal barrier (Katz et al., 1987).

Effects of Anthranilic Acid Derivative ns-NSAIDs on the GI Tract

Anthranilic acid derivatives include meclofenamate and mefenamic acid (Table 1-3). Meclofenamate (Ponstel, Arquel, Meclofen) is highly protein bound, metabolized by the liver, excreted in the urine and feces, and indicated to treat RA and OA in humans and musculoskeletal pain and inflammation in veterinary medicine (horses, dogs, cows). In a metaanalysis clinical study of dyspepsia, increased risk of dyspepsia was observed in meclofenamate users and NSAIDs (indomethacin, piroxicam) (Ofman et al., 2003). Dyspepsia in this study included any outcome terms, such as epigastric or upper abdominal pain/discomfort, but did not include nausea, vomiting, or heartburn. In humans, however, the most common GI event with meclofenamate is diarrhea. In cattle, oral administration of meclofenamic acid results in a biphasic pattern of absorption. Peak plasma concentration occurs at approximately 30 min and this is followed by a second peak at 4 to 6 h after dosing. The second peak is presumed to be due to enterohepatic recirculation (Aitken and Sanford, 1975). In horses, meclofenamic acid is absorbed rapidly and is effective in treating acute and chronic laminitis. It has a narrow therapeutic window and the onset of action is slow, requiring 2 to 4 days of dosing for clinical efficacy (Lees and Higgins, 1985). In rats, repeated oral dosing of mefenamic acid at 50 and 100 mg/kg per day (3.3- and 6.55-fold multiples of human dose) for 18 months caused GI pathology of bloody or discolored stool and intestinal ulceration and/or perforation (Hallesy et al., 1973). In nonhuman primates, repeated oral dosing of mefenamic acid at 400 and 600 mg/kg per day (26- and 39-fold multiples of human dose) for two years caused GI pathology similar to that described above in rats (Hallesy et al., 1973).

EFFECTS OF COX-1 INHIBITORS ON THE GI TRACT

COX-1 deficiency or inhibition is compatible with normal small intestinal integrity (Sigthorsson et al., 2002). COX-1 knockout mice do not spontaneously develop GI lesions, demonstrating that the absence of COX-1 alone is not sufficient to induce GI pathology (Langenbach et al., 1995). COX-1-deficient (COX-1^{-/-}) mice are normal except for a decrease in intestinal PGE₂ levels (Sigthorsson et al., 2002). COX-1 inhibition alone does not cause GI injury. A selective COX-1 inhibitor (SC-560) did not cause intestinal damage in rats (Tanaka et al., 2002a). In an *in vitro* study of small intestine motility, SC-560 was devoid of significant effects on horse ileal motility (Menozzi et al., 2009). Another *in vitro* study utilized a pig ileal intestine ischemia model and found that exposure to SC-560 recovered injured tissue to control levels as assessed by transepithelial electrical resistance (Blikslager et al., 2002). The effects of SC-560, rofecoxib, and indomethacin on the healing of colon lesions induced by dextran sulfate sodium (DSS) in the rat were investigated. The investigators found that daily administration of indomethacin and rofecoxib significantly delayed the healing of colitis, with deleterious influences on histological restitution as well as mucosal inflammation, whereas SC-560 had

no effect (Tsubouchi et al., 2006). Okayama et al. (2001) found that SC-560 significantly worsened the severity of colonic damage in DSS-induced colitis in rats. Another study in a DSS-induced colitis mouse model found that rofecoxib ameliorated severe colitis and reduced the degree of inflammation by reducing neutrophil infiltration and IL-1 β levels (Martin et al., 2005). In healthy rats, neither the s-NSAID rofecoxib nor the COX-1 inhibitor SC-560 when given alone at 20 mg/kg induced gastric mucosal injury. However, when rats received concurrent treatment with both SC-560 and rofecoxib, severe gastric lesions developed (Gretzer et al., 2001). Recent data suggest that COX-1 inhibition via SC-560, but not COX-2-derived PGE₂ synthesis, is involved in augmentation of NSAID-induced gastric acid secretion in isolated rabbit stomach parietal cells by enhancing expression and activation of the proton pump (Nandi et al., 2009).

Studies in animal models suggest that inhibition of COX-1 and COX-2 is required for induction of gastric ulcerogenic action of ns-NSAIDs (Wallace et al., 2000; Tanaka et al., 2001, 2002a,b; Takeuchi et al., 2004). It is thought that NSAID-induced ulcerogenesis, at least in rats, is dependent on the amount of gastric acid secretion derived from increased proton pump expression and requires inhibition of both COX-1 and COX-2 (Zinkievich et al., 2010). For example, in an experimental mouse model, small intestinal ulcers were observed when celecoxib and SC-560 were administered concurrently, but no GI damage was observed when either compound was administered independently (Sigthorsson et al., 2002). The importance of COX-1 and COX-2 simultaneous inhibition to cause GI effects is further supported by findings by Wallace et al. and Tanaka et al. Wallace et al. (2001) reported that COX-1 inhibition in rats reduced gastric mucosal blood flow but did not increase leukocyte adherence to the mesenteric vessel wall. On the other hand, COX-2 inhibition increased leukocyte adherence but did not reduce gastric mucosal blood flow (Tanaka et al., 2001). Thus, in the normal gastric mucosa, at least in rats, increased leukocyte adherence and vasoconstriction act in concert to facilitate gastric mucosal damage and lesions develop only when mucosal microcirculation and leukocyte function are impaired simultaneously. Furthermore, no spontaneous GI lesions occurred in COX-1-knockout mice, although gastric PE₂ levels were <1% of those in wild-type animals (Langenbach et al., 1995). Similarly, no GI pathology was found in COX-2-deficient mice (Morham et al., 1995).

EFFECTS OF COX-2 S-NSAIDS ON THE GI TRACT

Several COX-2 s-NSAIDs are approved for use in human and veterinary medicine (Table 1-4). Numerous nonclinical studies have demonstrated and supported the reduced GI events of COX-2 s-NSAIDs. In rats, rofecoxib did not cause damage to the stomach or small intestine (Yokota et al., 2005). When administered either orally or subcutaneously in rats, rofecoxib did not produce pathological changes in the GI mucosa, which showed normal histology (Laudanno et al., 2001). Neither rofecoxib nor celecoxib (Celebrex) caused gastric damage in normal rats after oral administration; however, both drugs caused hemorrhagic gastric lesions in arthritic rats (Kato et al., 2002). However, another study investigated the effects of celecoxib

TABLE 1-4 Major COX-2 Selective NSAIDs

Generic name	Trade name
Rofecoxib	Vioxx
Celecoxib	Celebrex
Valdecoxib	Bextra
Lumiracoxib	Prexige
Etoricoxib	Arcoxia
Deracoxib	Deramaxx
Parecoxib	Dynastat
Firocoxib	Previcox
Robenacoxib	Onsior
Meloxicam	Mobic, Metacam
Mavacoxib	Trocoxil

and rofecoxib in an experimentally induced colitis rat model. Colitis was induced by intrarectal instillation of acetic acid, which caused hemorrhagic diarrhea and weight loss. Oral administration of celecoxib at 5 mg/kg or rofecoxib at 2.5 mg/kg given twice daily reduced the degree of hemorrhagic diarrhea and the weight loss and significantly reduced the degree of colonic injury (El-Medany et al., 2005).

Clinical studies have shown that unlike ns-NSAIDs (e.g., etodolac, naproxen, ibuprofen), rofecoxib (Vioxx) did not inhibit PG synthesis or cause GI mucosal injury, even at supratherapeutic doses (Laine et al., 1995, 1999; Hawkey et al., 2000; Wight et al., 2001). There was no difference in ulceration rates of rofecoxib-treated patients as compared with a placebo and a fourfold lower depression of PG synthesis than in ibuprofen-treated patients (Laine et al., 1999; Hawkey et al., 2000). The Vioxx Gastrointestinal Outcome Research Trial (VIGOR) was a large (conducted in 301 centers in 22 countries) 13-month placebo-controlled double-blind study that compared twice the recommended dose of rofecoxib (50 mg daily) with the most common dose of naproxen (1000 mg daily) in 8076 RA patients (Bombardier et al., 2000). The primary endpoint was symptomatic ulcers, including clinical upper GI events of perforation, obstruction, and bleeding. The secondary endpoint was complicated upper GI events (perforation, obstruction, and major bleeding, resulting in a drop of 2 g or more in hemoglobin, transfusion, or hypotension). The RA patient population of VIGOR was selected because RA patients use NSAIDs chronically and have a substantially higher risk of NSAID-related GI events than do patients with OA. Rofecoxib significantly decreased the incidence of all GI endpoints studied in VIGOR. The VIGOR study showed a 54% reduction in clinical ulcers and a 57% reduction in complicated upper GI events with rofecoxib as compared with naproxen (Bombardier et al., 2000). The rate of discontinuation for any GI events (including clinical endpoints) was significantly lower in the rofecoxib group than in the naproxen group (Bombardier et al., 2000). A trial of the assessment of differences between Vioxx and naproxen to ascertain gastrointestinal tolerability and effectiveness (ADVANTAGE) was a 12-week

double-blind randomized prospective trial in 5597 patients with OA in the United States and Sweden who were randomized to receive rofecoxib (25 mg daily) or naproxen (500 mg twice daily). Patients using low-dose aspirin (<81 mg/day) were included in the trial. The primary endpoint of ADVANTAGE was GI tolerability as defined by the incidence of discontinuations due to GI adverse events. The secondary endpoint was use of concomitant medication to treat GI symptoms. Most patients (71%) were women, and the mean age of study participants was 63 years. Twelve percent of patients used low-dose aspirin during the trial, and baseline characteristics of the treatment groups were similar. At the study end, a significantly lower rate of adverse GI event-related discontinuations had occurred with rofecoxib. Significantly fewer patients receiving rofecoxib required concomitant GI medications than patients receiving naproxen. Concomitant use of low-dose aspirin did not significantly affect relative rates of discontinuation due to adverse events, serious adverse events, or drug-related adverse events (Lisse et al., 2003).

Both nonclinical and clinical data show that COX-2 s-NSAIDs have a superior GI safety and improved GI tolerability profile to that of ns-NSAIDs. In dogs, no evidence of GI toxicity has been observed with celecoxib at supertherapeutic doses (Khan et al., 1997). In rats, celecoxib did not induce any damage to healthy stomachs or GI mucosa (Altinkaynak et al., 2003; Li et al., 2003), did not alter the gastric mucosal barrier (Coppelli et al., 2004), did not cause intestinal ulcers, and reduced the severity of experimental colitis (Cuzzocrea et al., 2001), but exacerbated inflammation-associated colonic injury in experimental colitis and damage induced in the stomach in a separate study (Khan et al., 1997; Zhang et al., 2004). In an experimental study in a rabbit model, the effects of valdecoxib on anastomotic healing 1 week following large bowel resection were investigated. Valdecoxib did not influence anastomotic healing or new vessel formation in the anastomotic region following large bowel resection (Neuss et al., 2009).

Similar to the nonclinical data, data from several clinical studies suggest that COX-2 s-NSAIDs have a superior GI safety profile to that of ns-NSAIDs. For example, CS-706, an s-NSAID, and naproxen were administered for 7 days to healthy men and women who did not have evidence of underlying GI lesions, and posttreatment upper GI endoscopy was conducted to assess and compare the development of GI petechiae, erosions, and ulcers. The extent of upper GI mucosal injury with CS-706 was statistically and significantly less than that for naproxen (Moberly et al., 2007). Another study compared the effects of valdecoxib (Bextra) and naproxen, administered for 6.5 days, on the upper GI mucosa of healthy older subjects (aged 65 to 75 years) as assessed by GI endoscopy. Valdecoxib was associated with a significantly lower rate of gastroduodenal, gastric, and duodenal ulcers than that of naproxen (Goldstein et al., 2006). In a 26-week clinical trial, the incidence of GI ulcers in patients receiving the COX-2 s-NSAID valdecoxib was significantly lower than in those receiving diclofenac. Additionally, valdecoxib was also associated with significantly improved GI tolerability than that with diclofenac (Pavelka et al., 2003). The incidence of upper GI bleeding and dyspeptic GI adverse experiences in patients with osteoarthritis was significantly lower with rofecoxib than with ns-NSAIDs (e.g., diclofenac, ibuprofen, nabumetone) (Langman

et al., 1999). The Therapeutic Arthritis Research and Gastrointestinal Event Trial (TARGET) study compared the GI safety of lumiracoxib (Prexige) with ibuprofen and naproxen. Lumiracoxib in this TARGET study showed a three- to fourfold reduction in ulcer complications (Schnitzer et al., 2004). A large body of data has been published comparing the GI safety of COX-2 s-NSAIDs, celecoxib, and varied ns-NSAIDs. The Celecoxib Long-Term Arthritis Safety Study (CLASS) was a double-blind randomized controlled trial carried out in 7968 patients from 386 centers in the United States and Canada that compared a celecoxib dose of 400 mg twice daily (which is two- and fourfold the maximum dosage for RA and OA, respectively) with two ns-NSAIDs (diclofenac at 75 mg twice daily or ibuprofen at 800 mg three times daily) (Silverstein et al., 2000). The primary endpoint in CLASS was the incidence of ulcer complications (ulcer perforation, gastric outlet obstruction, or upper GI bleeding). The secondary endpoint was complicated and symptomatic ulcer events. Celecoxib in this CLASS study was associated with a lower combined incidence of symptomatic ulcers and ulcer complications than was ibuprofen or diclofenac (Silverstein et al., 2000). When compared with naproxen, celecoxib-treated patients also had lower rates of gastric, duodenal, and gastroduodenal ulcers (Goldstein et al., 2001). The Successive Celecoxib Efficacy and Safety Study (SUCCESS) was a 12-week double-blind randomized trial in 13,274 patients from 39 countries. The SUCCESS trial compared the incidence of upper GI hospitalizations in patients with OA taking celecoxib (200 or 400 mg daily), diclofenac (100 mg daily), or naproxen (1000 mg daily) (Singh et al., 2006). The rate of hospitalization was significantly lower in the celecoxib group. In addition, there were fewer ulcer complications in the celecoxib group than in the diclofenac or naproxen group, both in patients taking concomitant aspirin and in those not taking aspirin (Singh et al., 2006). In a separate study, video capsule endoscopy in healthy volunteers showed that celecoxib induced significantly less small bowel erosion than naproxen combined with omeprazole (Goldstein et al., 2007). In the Multinational Etoricoxib and Diclofenac Arthritis Long-Term (MEDAL) trial, the effects on GI outcome of etoricoxib (Arcoxia) and diclofenac were assessed. There were significantly fewer upper GI clinical events with etoricoxib than with diclofenac (Laine et al., 2007). Another clinical study demonstrated that several COX-2 s-NSAIDs (i.e., celecoxib, rofecoxib, valdecoxib, etoricoxib, lumiracoxib) offer greater upper GI safety and are better tolerated compared with ns-NSAIDs (Rostom et al., 2007). Upper GI mucosal effects were investigated for parecoxib (Dynastat) in a two-center double-blind randomized placebo-controlled study. Healthy subjects aged 65 to 75 years who were shown at baseline endoscopy to have no gastric or duodenal lesions received either 40 mg of parecoxib sodium IV twice daily for 7 days or 15 mg of ketorolac IV once daily for 5 days. No gastric or duodenal ulcers occurred in any subjects receiving parecoxib sodium. On the other hand, 23% of the ketorolac subjects had at least one ulcer, 16% had gastric ulcers, and 6% had duodenal ulcers (Stoltz et al., 2002). In another multicenter randomized double-blind placebo-controlled design, 123 adults with endoscopically confirmed normal upper GI mucosa received parecoxib sodium 40 mg twice daily for 7 days or ketorolac 30 mg four times daily for 5 days. No subjects treated with parecoxib sodium or placebo developed GI ulcers. Additionally, parecoxib sodium was

comparable to placebo with respect to the combined incidence of erosions or ulcers. Thus, parecoxib sodium has a GI safety profile superior to that of ketorolac (Harris et al., 2004). The Meloxicam Large-Scale International Study Safety Assessment (MELISSA) trial was a large-scale double-blind randomized international trial conducted over 28 days in 9323 patients with symptomatic OA. Patients received either meloxicam 7.5 mg or diclofenac 100 mg, and significantly fewer adverse events were reported by patients receiving meloxicam than by those receiving diclofenac. Of the most common GI adverse events, there was significantly less dyspepsia, nausea and vomiting, abdominal pain, and diarrhea with meloxicam than with diclofenac. Thus, meloxicam has a significantly improved GI tolerability profile than that of diclofenac (Hawkey et al., 1998). Similarly, in another study called SELECT (the Safety and Efficacy Large-Scale Evaluation of COX-Inhibiting Therapies), 4320 patients with exacerbation of OA were treated with the recommended dose of meloxicam (7.5 mg) or piroxicam (20 mg) once daily for 28 days. There was a significantly lower incidence of GI adverse events in the meloxicam than in the piroxicam group (Dequeker et al., 1998).

Deracoxib (Deramaxx), a COX-2 s-NSAID approved for use in dogs, is indicated for the control of postoperative pain and inflammation associated with orthopedic surgery and osteoarthritis. Once absorbed, deracoxib protein binding is >90% and the half-life is 3 h. In a toxicology safety study, micronized deracoxib in gelatin capsules was administered once daily to healthy young dogs at doses of 10, 25, 50, and 100 mg/kg of body weight for up to 14 consecutive days. At the high doses of 25, 50, and 100 mg/kg, reduced body weight, vomiting, and melena occurred. Necropsy revealed gross GI lesions in dogs from all dose groups. The frequency and severity of the lesions increased with escalating doses. At 10 mg/kg, moderate diffuse congestion of gut-associated lymphoid tissues (GALT) and erosions or ulcers in the jejunum occurred. At the highest dose tested, 100 mg/kg, all dogs exhibited gastric ulcers and erosions or ulcerations of the small intestines (according to a package insert). In other 21-day and six-month toxicology studies in healthy dogs, deracoxib at lower doses of 2, 4, 6, 8, and 10 mg/kg per day did not cause abnormal GI findings as assessed by clinical observations or gross or histopathological examinations at any dose level tested (Roberts et al., 2009). Postapproval experience revealed GI events (i.e., vomiting, anorexia, diarrhea, melena, inappetence, hematemesis, hematochezia, weight loss, nausea, ulceration, perforation). However, it is not clear from this postapproval experience if deracoxib was used at the recommended doses or other NSAIDs or steroids were used. Deracoxib should only be used at approved dosages. In a retrospective study in dogs treated with deracoxib, it was found that 55% of dogs have received deracoxib at a dosage higher than that approved by the U.S. Food and Drug Administration for the particular indication being treated. In addition, it was found that 59% of dogs have received at least one other NSAID or a corticosteroid in close temporal association (within 24 h) with deracoxib administration (Lascelles et al., 2005a). Therefore, GI perforation has been observed in dogs that received deracoxib at a higher than approved dosage or had received at least one other ns-NSAID in close temporal association with deracoxib administration (Lascelles et al., 2005a). A randomized placebo-controlled trial compared gastroscopic findings in dogs given

aspirin (25 mg/kg) or deracoxib (1.5 mg/kg) for 28 days. The study found no significant differences in total scores between placebo and deracoxib-treated dogs on days 6, 14, and 28 and concluded that administration of deracoxib to healthy dogs resulted in significantly lower gastric lesion scores and fewer days of vomiting than with administration of aspirin (Sennello and Leib, 2006).

Another COX-2 s-NSAID, firocoxib (Previcox), has been proven clinically to control OA pain and inflammation in dogs (Pollmeier et al., 2006; Ryan et al., 2006). No adverse GI, hematological, or serum biochemical adverse effects were seen after oral daily administration of firocoxib for 29 days in healthy dogs (Stea-gall et al., 2007). In a large study with more than 1000 dogs with OA, a small withdrawal rate of 2.9% due to firocoxib GI-associated effects was observed, and no serious drug-related adverse events were reported (Ryan et al., 2006). The overall clinical efficacy of firocoxib to treat OA in horses was comparable to the ns-NSAID phenylbutazone (Doucet et al., 2008). In a study in healthy dogs, the gastric and duodenal effects of COX-2 s-NSAIDs after oral administration were investigated. Each dog received deracoxib (2 mg/kg), firocoxib (5 mg/kg), or meloxicam (0.2 mg/kg) for 3 days with a 4-week interval between successive treatments. No significant differences were found among these COX-2 s-NSAIDs regarding endoscopic GI mucosal scores, histologic scores, or COX-1 or COX-2 protein expression (Wooten et al., 2009). The effects of firocoxib on ischemic-injured jejunum mucosal recovery in horses were compared to those of flunixin meglumine. Transepithelial resistance of ischemic-injured jejunum from horses treated with flunixin meglumine was significantly lower than in firocoxib-treated horses (Cook et al., 2009). In a study in dogs, the effects of firocoxib on healing of induced gastric body and pyloric lesions were examined. Dogs were treated with firocoxib [5 mg/kg orally (PO) every 24 h] or placebo for 7 days. Healing was evaluated on days 2, 4, and 7 of treatment by endoscopic lesion scoring. Eicosanoid concentrations in plasma and at the lesion margins were determined on days 2, 4, and 7. The firocoxib group had larger pyloric lesions than the placebo, but mucosal PG production did not differ significantly from that with placebo (Goodman et al., 2009). In a blinded randomized crossover study design, cats were treated with firocoxib (1 mg/kg PO per day) and meloxicam (0.05 mg/kg PO per day) for 8 days. Blood samples and gastric and duodenal mucosal biopsy specimens were collected on days 0 (baseline; immediately before treatment), 3, and 8 of each treatment period. Firocoxib and meloxicam administration resulted in a lower plasma PGE₂ concentration than at baseline on days 3 and 8 of administration. Neither firocoxib nor meloxicam administration altered pyloric or duodenal PGE₁ synthesis (Goodman et al., 2010).

A recent COX-2 s-NSAID is robenacoxib (Onsior), which is prescribed to relieve pain and inflammation in cats and dogs. It contains four fluorine atoms and a carboxylic acid group and is chemically related to diclofenac and lumiracoxib. However, in contrast to most COX-2 s-NSAIDs, robenacoxib lacks a sulfur-containing group and is therefore considered to be chemically distinct from both the sulfone-containing rofecoxib and firocoxib class and the sulfonamide-containing celecoxib and deracoxib class (King et al., 2009). Significantly less gastric ulceration and intestinal permeability were noted in rats treated with robenacoxib

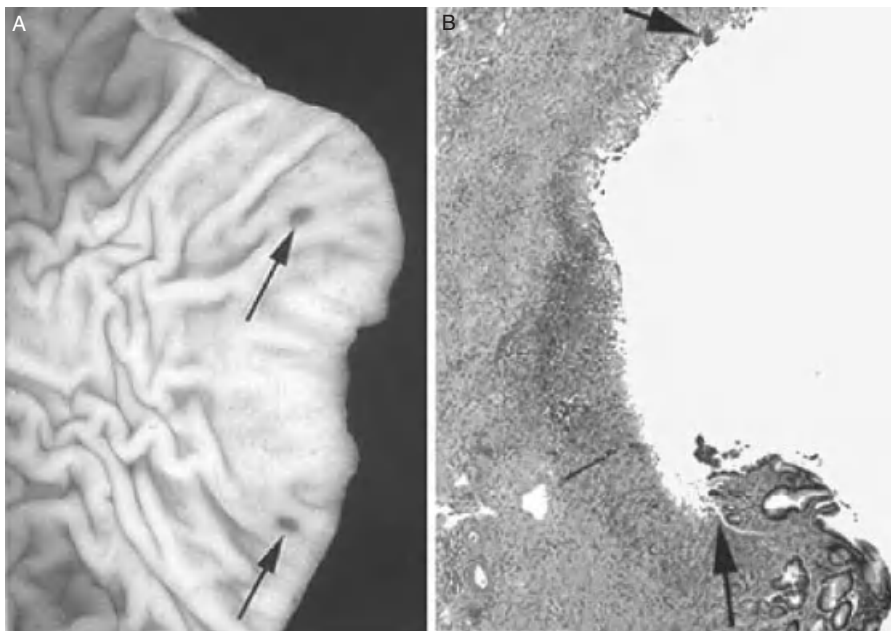


FIGURE 1-4 Meloxicam-induced gross (A) and microscopic (B) ulceration (between arrows) involving the mucosa in the pyloric region of the stomach of a dog. (Reprinted from Z. A. Radi and N. K. Khan, Effects of cyclooxygenase inhibition on the gastrointestinal tract, *Experimental and Toxicologic Pathology*, 58, pp. 163–173. Copyright © 2006, with permission from Elsevier.)

than in those treated with diclofenac (King et al., 2009). Another recent COX-2 s-NSAID is mavacoxib (Trococil), which is intended for the treatment of pain and inflammation associated with degenerative joint disease in dogs. No published GI safety data are currently available on this drug.

Other drugs previously compared to ns-NSAIDs for GI-related toxicity effects include meloxicam, L-745337, nimesulide, NS-398, and SC-58125. Meloxicam (Metacam, Mobic) is approved for use in dogs and cats and produced mild to moderate gastroduodenal lesions in dogs (Fig. 1-4) (Forsyth et al., 1998; Radi and Khan, 2006b; Radi, 2009); L-745,337 [5-methanesulfonamide-6-(2,4-difluorothiophenyl)-1-indanone] caused intestinal perforation in rats (Schmassmann et al., 1998); nimesulide did not cause any GI inflammation or ulcers in rats at excessive doses (Sigthorsson et al., 1998; Kataoka et al., 2000), prevented indomethacin-induced gastric ulcers in rats (Karmeli et al., 2000), and significantly decreased the extent of colitis induced by acetic acid in rats (Karmeli et al., 2000).

NS-398 produced little to no gastric ulceration in rats (Futaki et al., 1993; Masferrer et al., 1994) but had no beneficial effect on experimental colitis, whereas indomethacin did (Masferrer et al., 1994; Lesch et al., 1999). Similar to NS-398, SC-58125 yielded no GIT-related toxicity or beneficial effect in experimental colitis

in rats (Seibert et al., 1994; Lesch et al., 1999). The COX-2 s-NSAID NS-398 delayed healing after acid-induced gastric injury in rats (Sun et al., 2000).

PATHOPHYSIOLOGY AND MECHANISMS OF NSAID-ASSOCIATED GI TOXICITY

The GI tract is the site of entry into the body of orally administered drugs. Due to its high metabolic and mitotic rates, the GI system is susceptible to xenobiotics toxicity. Clinical signs of NSAID-associated GI system toxicoses (i.e., vomiting and diarrhea) are generally manifestations of the body's attempt to eliminate or reduce exposure to toxicants. The medullary emetic (vomiting) center can be stimulated by stomach irritation and distension. Bright red or dark-colored vomitus (hematemesis) indicates retention of blood in the stomach due to gastric ulceration. GI bleeding can be either in the upper GI tract (occurring in the stomach or duodenum) or in the lower GI tract (occurring in jejunum, ileum, colon, or rectum). The signs of GI bleeding include hematemesis, melena, hematochezia, or occult bleeding. Hematemesis indicates bloody vomitus that is either fresh, bright red blood, or dark, digested blood. Melena is black, tarry, foul-smelling stool caused by digestion of blood in the GI system. Hematochezia indicates fresh, bright red blood passed from the rectum. Occult bleeding is seen when trace amounts of blood are detected in normal-appearing stools. An ulcer is a local defect or excavation of the GI mucosal surface that is produced by sloughing of necrotic tissues and extends into the submucosa or deeper (Figs. 1-2 to 1-4) (Radi and Khan, 2006b). One of the consequences of GI mucosa inflammatory necrosis is ulceration. Erosion is a local defect of the GI tract that is confined to the mucosa and does not penetrate the submucosa and muscularis mucosa. The prevalence of endoscopically detectable gastroduodenal erosions associated with NSAID use in humans ranges from 14 to 60%, whereas the incidence of ulcers is 14 to 31% (La Corte et al., 1999). It is estimated that the annual number of hospitalizations in the United States from NSAID-associated GI complications is at least 103,000. Also, the estimated cost of such hospitalization is \$15,000 to \$20,000 per hospitalization, and the annual direct costs of such complications exceed \$2 billion (Wolfe et al., 1999). Although NSAIDs are known to produce GI lesions in various animal species, the intraanatomical incidence of ns-NSAID-induced GI lesions in veterinary medicine is unknown, but the gross and histopathological changes in dogs treated experimentally with loxoprofen sodium were erosions and ulcerations that were limited to the pyloric gastric mucosa, jejunum, and ileum mucosa (Korytko et al., 2003). GI-associated toxicity seen with ns-NSAIDs may be attributed to direct nonspecific irritation or to various biochemical and pharmacological mechanisms linked to local COX inhibition (Hawkey and Skelly, 2002; Radi and Khan, 2006b; Radi, 2009) (Fig. 1-1). The dual-insult hypothesis by Schoen and Vender (1989) suggests that NSAIDs exert a direct toxic effect on the GI mucosa and indirect effects through active hepatic metabolites and decreases in mucosal PGs. Hepatic metabolites are excreted into the bile and subsequently into the duodenum, where they cause mucosal damage to the stomach by duodenogastric reflux and mucosal

damage to the small intestine by antegrade passage through the GI tract. Detailed pathophysiological and potential mechanisms of NSAID-associated GI toxicity are discussed below.

Role of Cyclooxygenase Potency

Cyclooxygenase inhibitory potency is an important factor in NSAID GI toxicity. An indicator of the COX-1 versus COX-2 activity at therapeutic doses is the COX-1:COX-2 IC₅₀ ratio in human blood. The COX-1:COX-2 IC₅₀ ratio in human blood (the concentration of drug that inhibits 50% of the COX-1 activity in blood to that which inhibits COX-2 in the blood) is a good indicator of enzyme specificity; numbers greater than 1 are more COX-2 specific, and those below 1 are more COX-1 specific. There is wide variation between reports in the exact values, but the differences in COX selectivity of drugs tested have fairly good correlation between studies. Cryer and Feldman (1998) reported that the COX-1:COX-2 IC₅₀ ratio of aspirin was 0.32, whereas ibuprofen was 0.6, naproxen was 1.14, and NS-398 was 24. Another report by Chan et al. (1999) indicated that the COX-1:COX-2 IC₅₀ ratio in human blood for rofecoxib was 36, celecoxib was 6.6, and diclofenac was 0.4. As discussed previously, a lower incidence of adverse GI NSAID effects occurs more often with COX-2 s-NSAID. For example, substantial inhibition of platelet COX-1 will translate into an increased incidence of serious upper GI bleeding and complications (Patrino et al., 2001). Furthermore, the results of TARGET and VIGOR showed that ns-NSAIDs (naproxen and ibuprofen) cause more GI adverse events than do COX-2 s-NSAIDs (lumiracoxib and rofecoxib), which spare COX-1 activity at therapeutic dosing (Bombardier et al., 2000; Schnitzer et al., 2004).

Species Differences in NSAID-Associated Susceptibility to GI Injury

Although ns-NSAID-associated GI toxicity is prevalent throughout species, there are significant interspecies GI toxicity differences (Table 1-2) (Mahmud et al., 1996; Radi and Khan, 2006b). The degree and susceptibility of GI-associated toxicity can vary depending on the drug administered and the species tested (Radi and Khan, 2006b; Radi, 2009). For example, fenbufen has resulted in significantly fewer gastric lesions (hemorrhage and ulceration) in humans than have other ns-NSAIDs, such as naproxen and indomethacin (Lanza et al., 1983). Naproxen is well tolerated in mice, rabbits, nonhuman primates, and pigs, less well tolerated by rats, and poorly tolerated by dogs (Hallesy et al., 1973). The susceptibility of cats, dogs, and horses to the adverse effects of ns-NSAIDs is greater than that of humans (Mahmud et al., 1996). Dogs are considered a sensitive laboratory animal species for predicting the toxicity profile of NSAIDs. The no observed effect level (NOEL) dosages for GI toxicity in dogs are at or below clinical therapeutic dose levels for NSAIDs and are severalfold higher for COX-2 s-NSAIDs (Korytko et al., 2003). GI toxicity occurred at subtherapeutic ns-NSAID lloprofen exposures (Korytko et al., 2003). There are significant breed differences in susceptibility

to GI ulceration subsequent to ibuprofen exposure, with lower risk for the labrador breed and higher risk for the German shepherd breed (Poortinga and Hungerford, 1998). However, dogs tolerate ns-NSAIDs better than cats do. Since cats lack the glucuronyl transferase enzyme, they are delicately sensitive to the adverse effects of drugs that are glucuronidated before elimination (i.e., acetaminophen) (Court and Greenblatt, 1997). In addition, cats are at least twice as sensitive to ibuprofen as dogs are (Villar et al., 1998).

In addition, it is important not to extrapolate from studies performed in one species to another since various NSAID pharmacokinetics (PK) (a drug's absorption, distribution, metabolism, and elimination) are different across species (Lees et al., 2004). Some of the general PK properties of NSAIDs are (1) good bioavailability in monogastric species after oral dosing because of a medium to high level of lipid solubility, (2) dissolution in stomachs impaired by acidic pH, (3) possible delayed absorption by binding to digesta (e.g., horses), (4) a high degree of plasma protein binding of all drugs (except salicylate) in all species and small volume of distribution, (5) a low volume of distribution (some exceptions), and (6) marked species differences in clearance and terminal half-life (Lees et al., 2004). Such PK properties have implications in GI toxicity. For example, meloxicam has nearly 100% bioavailability after subcutaneous injection in cats, with an elimination half-life after a single dose estimated to be approximately 15 h. Therefore, the recommended dose of meloxicam (according to a package insert) in cats is 0.3 mg/kg, to be given subcutaneously only once, due to the narrow safety margin in cats. Repeated use of meloxicam in cats has been associated with diarrhea, vomiting, lethargy, and decreased appetite. Histopathological examination revealed gastrointestinal lesions ranging from GI mucosal inflammatory cell infiltration to erosions. In dogs, aspirin GI-associated side effects are dose- and preparation-related. A dose of 25 mg/kg (but not 10 mg/kg) of plain aspirin caused mucosal erosions in dogs, while no GI damage occurred in animals receiving buffered and enteric-coated preparations at similar doses of 25 mg/kg (Lipowitz et al., 1986).

GI Anatomical Differences

GI anatomical and physiological differences should be taken into consideration when NSAIDs are administered and potential GI toxicity is anticipated. For example, unlike humans, rats cannot vomit and are considered a nonvomiting species. This is due to a fold in the stomach that lies where the esophagus enters (Fox et al., 2002). Rats lack a gallbladder, and bile enters the duodenum continuously as it is made. Dogs, on the other hand, are very susceptible to vomition. Gut blood flow varies across species: 1.5, 7.5, 111, 216, 125, and 1100 mL/min in the mouse, rat, rabbit, dog, monkey, and human, respectively (Davies and Morris, 1993). Gut volume also varies across species: 1.5, 11.3, 120, 480, 230, and 1650 mL in the mouse, rat, rabbit, dog, monkey, and human, respectively (Davies and Morris, 1993). Humans, rhesus monkeys, and dogs are monogastric, and their stomachs are entirely secretory, whereas the stomachs of rodents, pigs, and horses have a glandular secretory portion and nonglandular bacterial digestion portion. Compared to humans, the GI length is shorter and

the gastric emptying time is longer in dogs. Particle size can affect the rate of gastric emptying. The rate of gastric emptying in minipigs of nondigestible tablets (11 mm diameter) and granules (1 mm diameter) is slower than that in humans and dogs (Aoyagi et al., 1992). The rate of gastric emptying of both dosages in the dog tended to be faster than or similar to that in humans (Aoyagi et al., 1992). Food delayed gastric emptying in dogs, especially for tablets (Aoyagi et al., 1992). Such anatomical differences can affect the rate and extent of absorption of some NSAIDs. For example, in humans, enteric-coated aspirin was designed to reduce stomach irritation by delaying absorption until the drug reached the small intestine. In a study where dogs were administered enteric-coated aspirin, oral absorption was incomplete, gastric retention of tablets occurred, and partially digested tablets were found in the feces of some dogs (Nap et al., 1990). Ruminants have a forestomach (comprised of rumen, reticulum, and omasum) that is followed by a true stomach (abomasum). The rumen is highly permeable to volatile fatty acids released from carbohydrate metabolism and is also capable of active sodium and chloride absorption. Therefore, the large size of the rumen affects the response to oral toxicants, and initial exposure to toxicants may result in dilution and slowing of the absorption rate. Because the horse is a monogastric animal, the aspirin is absorbed rapidly following oral administration but is also removed rapidly, due to its short $t_{1/2}$. One might assume that the recommended 100-mg/kg dose of aspirin to a cow might be quite toxic; however, in this case the rumen acts as an “anatomical sustained-release device,” slowly releasing the aspirin into the intestine for subsequent absorption. This slow release helps avoid potential aspirin-induced GI toxicity but allows for the maintenance of therapeutic drug concentrations (Langston and Clarke, 2002).

Enterohepatic Recirculation and NSAID Toxicity

The movement of a drug absorbed into the blood from the small intestine lumen, then carried into the liver by the hepatic portal vein, biotransformed in the liver, excreted into the bile, then through the bile duct into the lumen of duodenum, and reabsorbed into the blood via intestinal vessels is referred to as enterohepatic recirculation. Enterohepatic recirculation allows recycling of metabolized and nonmetabolized compounds and plays a role in NSAID-associated GI toxicity. Administration of NSAIDs that are not subject to enterohepatic recirculation did not produce intestinal damage in rats (Reuter et al., 1997). Additionally, ligation of the common bile duct prevented the damage normally observed after NSAID administration (Wax et al., 1970). Toxicological consequences of enterohepatic recirculation include increased drug half-life in blood, prolonged exposure, and inhibition of conjugate exports. For example, ibuprofen is particularly ulcerogenic in dogs because it undergoes enterohepatic recirculation. Indomethacin and piroxicam undergo substantial enterohepatic recirculation. Indomethacin enterohepatic recirculation is most extensive in dogs and rats and least extensive in rabbits and humans. In the dog, indomethacin remains in the enterohepatic circulation, even though it is reabsorbed from the gut, until its elimination in the feces. Biliary excretion of indomethacin and its conjugate is extensive and rapid in dogs, but slow in rats (Yesair et al., 1970). In

humans and nonhuman primates, most NSAIDs undergo less enterohepatic recirculation than in the dog and rat (Beck et al., 1990). Dogs are less tolerant than rats or humans to ns-NSAIDs and more at risk for ns-NSAID-induced gastropathy (Elliott et al., 1988; Forsyth et al., 1998). Many NSAIDs, except aspirin and salicylic acid, undergo enterohepatic recirculation in rats (Beck et al., 1990). Nabumetone is formulated as a nonacidic prodrug that does not undergo enterohepatic recirculation to improve its GI safety profile.

Role of Xenobiotic Glucuronidation

Glucuronidation, catalyzed by the UDP-glucuronosyltransferase (UGT) enzyme, is a major elimination and biotransformation pathway of endogenous and exogenous xenobiotic compounds. NSAIDs are eliminated primarily through conjugation with polar sugar moieties to form glucuronides. The UGTs catalyze the conjugation of compounds that possess a nucleophilic acceptor group with glucuronic acid, a relatively bulky, hydrophilic moiety, whose carboxylic acid functional group is ionized at physiological pH, thus forming metabolites with significantly different chemical and biochemical properties that in most cases have significantly decreased affinity for receptors or enzymes responsible for the biological activity of the parent compound (Siraki et al., 2005). A major biotransformation pathway for carboxylated NSAID is glucuronidation, with the resulting production of reactive acyl glucuronides (Siraki et al., 2005). Therefore, glucuronidation appears to play a role in NSAID GI-associated toxicity. Cats have remarkably low levels of UGT; therefore, they have a low capacity for hepatic glucuronidation and are more sensitive than other species to NSAID-associated GI toxicities (Court and Greenblatt, 1997; Steagall et al., 2009). Adduction, or covalent binding, of a toxicant to target macromolecules is considered a molecular mechanism of cellular injury of toxicants that damage tissues. For example, adducts detected by immunohistochemistry in the small intestine of diclofenac-treated rats represent covalent bonding of some diclofenac entity with intestinal macromolecules (Atchison et al., 2000). In addition, adduct formation after reactive metabolite generation by NSAIDs is one possible explanation for the mechanism of gut-induced toxicity. Rats given diclofenac orally at doses ranging from 10 to 100 mg/kg led to dose-dependent formation of adducts and ulcers only in the small intestine and only in animals with intact enterohepatic recirculation. Adducts formed within enterocytes by 1 h translocated to the brush border, preceded intestinal ulceration, and were intense at sites of ulceration (Atchison et al., 2000).

A major prerequisite for the enterohepatic recirculation of an NSAID is its conjugation by in the liver, which allows for hepatobiliary excretion of these highly polar metabolites. As discussed previously, in some NSAIDs (i.e., aspirin, diclofenac, ibuprofen, and indomethacin) intestinal toxicity is dependent on biliary excretion and enterohepatic circulation (Beck et al., 1990). Many carboxylic acid NSAIDs form ester glucuronides that are readily transported across the hepatic canalicular membrane by multidrug carrier systems. For example, diclofenac glucuronide is transported into bile by the canalicular conjugate export pump, Mrp2, in the rat (Seitz et al., 1998). Hepatocanalicular conjugate export pump-deficient

(TR⁻) rats were used to selectively block diclofenac enterohepatic circulation without interrupting bile flow. TR⁻ rats were refractory to diclofenac given either intraperitoneally or perorally. However, transfer of bile containing diclofenac glucuronide significantly increased the extent of ulcer formation in both normal and TR⁻ rats. Moreover, induction of glucuronosyltransferase aggravated intestinal ulceration (Seitz and Boelsterli, 1998).

Aging and Stress and NSAID GI Effects

Age appears to be a contributing factor in NSAID-induced GI toxicity. The exact mechanism of this is not fully understood. It is thought that the aging gastric mucosa has impaired mucosal defense mechanisms, due to decreased mucus and bicarbonate secretion, reduced gastric emptying rate, reduced GI motility, reduced GI blood flow, increased expression on villi of enterocytes and the function of the P-glycoprotein multidrug efflux pump, and reduced GI PG production. Neonates have a poorly developed intestinal mucosa barrier that can permit absorption of various xenobiotics. Some studies in humans have demonstrated a decline in gastric and duodenal mucosal PG content with aging, associated with an increase in gastric acid secretion (Cryer et al., 1992; Goto et al., 1992). Similarly, studies in animals have yielded similar results (Uchida et al., 1990; Lee and Feldman, 1994). Uchida et al. (1990) have demonstrated a marked decrease in gastric mucosal PGI₂ level between 20 and 40 weeks of age and between 60 and 86 weeks of age in normal and ulcer-bearing rats. In another study, gastric mucosal PGs synthesis decreases with age in rats, and aged animals were more susceptible to aspirin-induced acute gastric mucosal injury (Lee and Feldman, 1994).

In a study in humans, Feldman and Cryer (1998) demonstrated that in healthy subjects with normal gastric histology, advancing age was associated with a significant decline in gastric bicarbonate secretion (HCO₃⁻), Na⁺, and nonparietal fluid secretion, resulting in an increase in gastric acidity, while no age-related changes in acid and parietal fluid secretion were noted. Furthermore, animal studies have shown that aging was associated with significantly lower gastric luminal pH and bicarbonate output in the rat stomach and that aging also blunted PG-mediated increases in gastric HCO₃⁻ secretion (Lee, 1996). Moreover, Kim et al. (1990) have shown in anaesthetized rats that although aging does not affect basal duodenal bicarbonate secretion, the duodenal bicarbonate response to a fixed load of luminal acid declines progressively with age. Finally, some NSAID clearance is altered with aging. Clearance of phenylbutazone is twice as fast in 3-year-old horses as in 8- to 10-year-old horses (Tobin et al., 1986).

A syndrome in humans called stress-related mucosal disease (SRMD) is common in critically ill patients and can result in significant morbidity. Histologically, there does not appear to be a significant inflammatory component to the gastric mucosa. The pathophysiology of this condition is multifactorial, but local mucosal ischemia and gastric acid play a critical role in disease pathogenesis. It is thought that gastric mucosal damage results from an imbalance between factors promoting mucosal injury and host defenses. A major mucosal defense factor is impaired

mucosal blood flow. Aggregative factors include acid, pepsin, intramucosal acidosis, reperfusion injury, and free-radical formation (Duerksen, 2003). There does not seem to be a selective impairment of PG production in patients with SRMD. Therefore, there is no evidence that NSAIDs increase the susceptibility of critically ill patients to stress-related GI damage (Duerksen, 2003).

Disruption of GI Physiological Mucosal Defense Mechanisms

The GI system is involved primarily in breaking down food, ultimately absorbed into the body. This digestive process involves several phases: ingestion of food; secretion of mucus, water, and enzymes; fragmentation; chemical and mechanical digestion of food particles; absorption of digested food; and elimination of waste products by defecation. Fragmentation and initial digestion take place in the stomach. The stomach has gastric glands that release or secrete mucus, hydrochloric acid (HCl), gastrin, somatostatin, acetylcholine, histamine, and pepsinogen. The small intestine is a major GI site of digestion and absorption of nutrients and electrolytes. The small intestine is divided into the duodenum, jejunum, and ileum. The process of digestion is initiated in the stomach by the actions of HCl and pepsin, which break down food particles. The mucosa of the stomach and proximal duodenum are constantly exposed to gastric acid that can damage living cells. Acid secretion is stimulated by acetylcholine neurotransmitter, gastrin hormone, and histamine. PGs can inhibit acid secretion. The gastroduodenal lumen also contains bile salts and enzymes such as pepsins, lipases, proteases, and peptidases (Johnson et al., 2006). Proton pump inhibitors (PPIs) significantly decrease NSAID-induced gastric and duodenal ulcers (Lazzaroni and Porro, 2009). PPIs are a group of drugs whose main action is pronounced and long-lasting reduction of gastric acid production.

The GI mucosa has several physiological defense mechanisms that form a mucus coating called a mucosal barrier to protect itself from the damaging effects of such degradative enzymes and acidic pH. Major physical and chemical gastric mucosa defense mechanisms include a hydrophobic mucus layer, regulated intercellular tight junctions, specialized plasma membrane ion permeability, epidermal growth factors, HCO_3^- secretion, high rate of mucosal blood flow, mucosal cell hydrophobicity, and rapid epithelial turnover (Johnson et al., 2006). In addition, the gastric and duodenal mucosa are rich in PGs, which play a protective role in the GI tract via adequate perfusion of the gastroduodenal mucosa, epithelial cell secretion of bicarbonate, secretion of mucus, and maintenance of a neutral mucosa pH (Elliott et al., 1996; Scheiman, 1996).

The mucus hydrophobic layer traps secreted bicarbonate to maintain a neutral gastric mucosal pH and forms a stable water-insoluble glycoprotein gel that acts as a lubricant to prevent mechanical damage. The mucus–bicarbonate layer protects the gastric mucosa from diffusion of free hydrogen ions from the gastric lumen back into the mucosal cells (i.e., back-diffusion) (Johnson et al., 2006). If the integrity of the GI barrier is disturbed, the rate of back-diffusion of gastric acid and pepsin increases, leading to inflammation and hemorrhage. Inflammatory cells such as neutrophils and mast cells become activated and release inflammatory

mediators such as histamine, leukotriens, free radicals, and proteolytic enzymes. These mediators lead subsequently to vasodilation, vasoconstriction, increased vascular permeability, and edema. Such events lead to GI mucosal ischemia, reduced mucus secretion, and reduced PG production (McConnico et al., 2008).

Inhibition of PG synthesis and abrogation of protective mechanisms lead to GI injury (Hawkey and Skelly, 2002). Misoprostol is a synthetic PGE₁ analog used to overcome NSAID-induced PG deficiency in the gastric mucosa. In the six-month randomized Misoprostol Ulcer Complication Outcomes Safety Assessment (MUCOSA) trial, the effects of concurrent administration of misoprostol on the occurrence of serious upper GI complications in patients with RA who were receiving NSAID were investigated (Agrawal and Aziz, 1998). The results of the MUCOSA study showed that misoprostol resulted in a statistically significant reduction in the incidence of serious NSAID-induced upper GI complications compared with placebo in patients with RA (Agrawal and Aziz, 1998). NSAIDs can also decrease mucosal resistance in the diseased state (Rainsford, 1982) or cause direct chemical damage to the GI mucosa (Johnston and Budsberg, 1997). When the GI mucosal integrity is compromised, a cascade of pathological events follows, leading to further mucosal barrier layer damage. COX inhibition is suggested to increase the susceptibility of the gastric mucosa to injury by inhibiting secretion of the cytoprotective mucus and bicarbonate and altering the physicochemical nature of mucus (Kauffman, 1989). Indomethacin and SC-560, but not rofecoxib, attenuated mucosal acidification in the rat stomach (Takeuchi et al., 2006). This study suggests that EP₁ receptors are essential for the increase in the secretion of HCO₃⁻ in response to mucosal acidification in the rat stomach. In EP₃ receptor–knockout mice, the HCO₃⁻ stimulatory action of PGE₂ was observed in the stomach, whereas such action was absent in the EP₁ receptor–knockout mice (Takeuchi et al., 1999). Therefore, it appears that PGE₂ receptor subtypes (EP₁ in the stomach and EP₃ in the duodenum) and COX-1 are key regulators of HCO₃⁻ secretion in response to gastroduodenal mucosal acidification.

GI Disequilibrium

All segments of the GI from duodenum to distal colon have mechanisms for both absorbing and secreting water and electrolytes. GI secretions play a significant role in digestion and maintenance of pH levels and acid–base balance. Disequilibrium in GI motility and secretion by NSAIDs can lead to diarrhea, dehydration, and/or systemic acidosis or alkalosis. Respiratory alkalosis may occur from stimulation of the respiratory center by phenylbutazone. Major mechanisms of diarrhea are osmosis, active secretion, exudation, and/or altered motility. The Na⁺ gradient is the driving force for amino acid, oligopeptide, and sugar absorption. There are differences in Na⁺ entry mechanisms, sites of HCO₃⁻ secretion, and sites of active K⁺ transport. HCO₃⁻ is absorbed in the jejunum (via Na⁺/H⁺ exchange) and secreted in the duodenum, ileum, and colon. Na⁺ crosses the small intestinal and colonic brush borders via Na⁺/H⁺ exchange and in the small intestine also by the Na⁺ organic solute cotransport mechanism. In the distal colon, luminal Na⁺ is also absorbed via an aldosterone-sensitive Na⁺ channel. The intestines neither dilute

nor concentrate their contents, the osmolarity of which, except in the duodenum and proximal jejunum shortly after eating, is the same as the plasma osmolarity. Osmotic diarrhea occurs when these organic solutes are absorbed, salt is absorbed with them, and water follows osmotically (i.e., transport from enterocyte to lateral intercellular space creates a local osmotic gradient that initiates water flow) (Field, 2003).

In osmotic diarrhea, agents released from inflammatory cells (PGs and leukotrienes, platelet-activating factor, histamine, serotonin) can stimulate active secretion. GI mucosal-induced inflammation interferes with GI homeostatic control. PGE₂ activates mast cells, causing histamine release, which stimulates smooth muscle activity and induces the secretion of mucus and electrolytes. Electrolytes create osmotic force for the influx of water into the lumen. Therefore, the combination of excessive fluids and increased GI motility causes diarrhea. The pathogenic importance of intestinal hypermotility in the intestinal ulcerogenic response to indomethacin has been demonstrated in rats (Takeuchi et al., 2002). Additionally, indomethacin decreased gastric mucosal PGE₂ content and produced gross pathological mucosal damage with gastric hypermotility and expression of COX-2 mRNA (Takeuchi et al., 2004). In the same study by Takeuchi et al. (2004), although SC-560 did not produce damage, it caused a decrease in the PGE₂ content and an increase in gastric motility as well as the up-regulation of COX-2 expression. Duodenal HCO₃⁻ secretion and luminal release of PGE₂ in rats were increased in response to mucosal acidification. This response was significantly inhibited by indomethacin but not by NS-398 or nimesulide (Hirata et al., 1997).

In addition to transporting ions, nutrients, and water, the intestinal epithelium, comprised of both enterocytes and their tight junctions (zona occludens), functions as a barrier that restricts the flow of luminal contents into the blood and lymphatics, and vice versa. In the small intestine, tight junctions are, on average, of the low-resistance type, meaning that most of the passive permeability of the epithelium to small monovalent ions and water resides in these junctional complexes (tight junctions in villi have higher resistance than do those in crypts). Colonic intercellular junctions are tighter, their resistance increasing steadily from proximal to distal portions (Field, 2003).

Although these junctions, which comprise a number of discrete proteins, are extracellular, their permeability properties are regulated by intracellular structures, especially actin filaments. Therefore, when the intestinal epithelium's barrier function is compromised by NSAID-associated erosions and ulcerations, loss of epithelial cells, and/or disruption of tight junctions, hydrostatic pressure in blood vessels and lymphatics will cause water and electrolytes, mucus, and protein to accumulate lumenally, leading to exudative diarrhea.

Effects on Physiological GI Mucosal Cell Renewal Mechanisms After Mucosal Injury

The integrity of the intestinal mucosal surface barrier is generally reestablished rapidly, even after extensive damage, due to its enormous regenerative capability.

The rapid-healing mechanism of the surface mucosal epithelium is accomplished by epithelial cell migration from proliferative zones into wound, also termed epithelial restitution, epithelial cell proliferation, and differentiation. This healing mechanism is regulated by a highly complex network of factors, such as regulatory peptides within the intestinal tract mucosa, conventionally designated as growth factors and cytokines. These factors play an essential role in regulating differential epithelial cell functions to preserve normal homeostasis and integrity of the intestinal mucosa (Dignass, 2001; Sturm and Dignass, 2008). Mucosal villous contraction and the restitution mechanism represent primary repair mechanisms in the GI tract which allow resealing of the epithelial barrier within minutes or hours via reformation of tight junctions between cells (Dignass, 2001; Sturm and Dignass, 2008). Villous contraction is initiated by myofibroblasts that reside immediately beneath the epithelial basement membrane. Subsequent events include crawling of healthy epithelium adjacent to the wound, referred to as restitution. Restitution is a well-coordinated event that is dependent on epithelial cell migration but independent of cell proliferation and differentiation. The structural integrity of the mucosa is maintained by continuous cell renewal from mucosal progenitor cells. This continuous renewal is a well-coordinated process that is controlled by proliferation of progenitor cells, which enables replacement of damaged or aged surface epithelial cells. Actin filaments, focal adhesions, and focal adhesion kinase (FAK) play crucial roles in the cell motility essential for restitution (Szabó et al., 2002).

Indomethacin significantly delayed epithelial restitution in rats and reduced FAK phosphorylation and recruitment to adhesion points, as well as actin stress fiber formation in migrating surface epithelial cells (Szabó et al., 2002). NSAIDs have been found to affect intestinal restitution through decreased potassium channel [K(v)1] surface expression and trafficking (Freeman et al., 2007). In an *in vitro* study, intestinal epithelial cell migration in response to wounding was reduced by indomethacin, phenylbutazone, and NS-398 but not by SC-560 (Freeman et al., 2007). NSAID inhibition of intestinal cell migration was not associated with depletion of intracellular polyamines (Freeman et al., 2007). However, another study, using pig small intestinal ileal mucosa, showed that endogenous PGs, released when mucosal injury occurs, mediate local repair of small intestinal epithelium after damage by the deconjugated bile salt deoxycholate. Whereas ongoing epithelial restitution and villous contraction were prominent features of repairing mucosa, acute recovery of barrier function was uniquely dependent on PG-mediated resealing of tight junctions and lateral intercellular space. The authors conclude that failure to repair increases in paracellular pathway permeability may underlie barrier failure resulting from NSAID use in patients with underlying enteropathy (Gookin et al., 2003).

A number of other factors, such as extracellular matrix, blood clotting factors, phospholipids, short-chain fatty acids, adenine nucleotides, trace elements, and calpain, have been demonstrated to modulate intestinal epithelial repair mechanisms (Dignass, 2001; Sturm and Dignass, 2008). Calpains, cysteine proteases, are involved in numerous cellular processes, such as cell migration and invasion. Altered expression of calpain proteins contributes to NSAID effects on intestinal

epithelial restitution. A multistep functional microarray genomic study was conducted using intestinal epithelial cells to identify novel signaling pathways that contribute to NSAID inhibition of GI epithelial cell migration (Raveendran et al., 2008). Raveendran et al. demonstrated that indomethacin and NS-398 decreased the expression of calpains 1, 2, and 8 proteins, whereas SC-560 had no effect on the expression of calpain proteins. Functional data were also consistent with decreased expression of calpain protein in cells treated with either NS-398 or indomethacin.

In gastric glands, a single stem cell in every gastric gland undergoes division to produce committed progenitor cells, which further differentiate into an adult epithelial cell type (Modlin et al., 2003). The stem/progenitor cell niche is made up of proliferating and differentiating epithelial cells and surrounding mesenchymal cells (Leedham et al., 2006). Intestinal subepithelial myofibroblasts (ISEMFs) are important coordinating cells that possess significant influence on their environment by virtue of their receptor profile and the signals they produce. Characteristically, ISEMFs form a protective fenestrated sheath around the stem cell compartment, creating the stem cell niche—the optimal microenvironment for stem cells to give rise to differentiated progeny (Leedham et al., 2006). The ISEMFs generate growth factors and thus promote mesenchymal-to-epithelial crosstalk and signaling to maintain the niche progenitor cell survival. Cell proliferation of progenitor cells is controlled by growth factors. The major growth factor receptor in rats during gastric ulcer healing, expressed in gastric progenitor cells, is the epidermal growth factor receptor (EGF-R) (Tarnawski et al., 1992), and the major mitogenic growth factors that activate this receptor are transforming growth factor alpha (TGF α) and insulin-like growth factor 1 (IGF-1) (Nguyen et al., 2007). EGF peptide itself is absent in normal gastric mucosa. However, it is present in the gastric lumen and can stimulate progenitor cell proliferation in case of injury. In human gastric epithelial monolayers, EGF treatment significantly stimulated cell migration and actin stress fiber formation, and increased FAK localization to focal adhesions, and phosphorylation of FAK and tensin (Szabó et al., 2002). In gastric ulcers in rats, IGF-1 promoted actin polymerization, cell proliferation, reepithelialization, and induced COX-2 in a phosphatidylinositol 3-kinase-dependent manner (Nguyen et al., 2007).

Both ns- and COX-2 s-NSAIDs may delay the healing of damaged GI mucosa. NSAIDs may delay healing after injury to the GI tract by affecting GI epithelium proliferation in response to mediators such as growth factors and nitric oxide (NO). The effects of celecoxib on normal and damaged (acid or ethanol challenged) gastric mucosa of rats were compared to those of ns-NSAIDs (Berenguer et al., 2004). In the absence of acid or ethanol challenge, only ns-NSAIDs produced appreciable gastric lesions. However, following acid or ethanol challenge, both COX-2 s- and ns-NSAIDs impaired healing of gastric mucosal damage. In rats, NS-398, a COX-2 s-NSAID, delayed gastric healing after acid-induced injury (Sun et al., 2000). Increased COX-2 expression was noted after growth stimulation by addition of serum which contains growth factors to cultured rat gastric mucosal cells *in vitro* and after acid-induced gastric injury to rats *in vivo* (Sawaoka et al., 1997; Horie-Sakata et al., 1998; Erickson et al., 1999; Sun et al., 2000). These

serum growth factors were TGF α or the hepatocyte growth factor (HGF) (Horie-Sakata et al., 1998; Sawaoka et al., 1999). Celecoxib did not alter the gastric mucosal barrier or induce mucosal lesions in healthy or NO-deficient rat gastric mucosa (Copelli et al., 2004). Celecoxib appeared to worsen the flare of the colon in a rat model of inflammatory bowel disease (Singh et al., 2004). In an isolated rabbit gastric epithelial cells model, aspirin significantly retarded wound healing, but simultaneous addition of growth factors such as IGF-I and EGF significantly accelerated wound repair (Yoshizawa et al., 2000). PGE₂ and gastrin transactivate EGF-R and trigger the mitogen-activated protein kinase pathway, thereby stimulating cell proliferation and exerting a trophic action on mucosa, resulting in gastric and intestinal hypertrophy (Pai et al., 2002). Therefore, NSAIDs are contraindicated in patients with damaged GI mucosa (peptic ulceration or GI bleeding).

Effects on Leukocyte Adhesion Molecules and Trafficking

Infiltration of leukocytes into the mucosa in response to initial tissue injury has been implicated in NSAID GI injury (Reuter et al., 1997). Leukocyte–endothelial cell interactions are mediated by various cell adhesion molecules. These interactions are important for leukocyte extravasation and trafficking in many pathological conditions in several body systems, including the GI tract. There are various stages of leukocyte trafficking into sites of inflammation. An initial slowing of leukocytes on the vascular endothelium is mediated by selectins. This event is followed by (1) activation of β_2 integrins after leukocyte exposure to cytokines and proinflammatory mediators, (2) adherence of leukocyte β_2 integrins to vascular endothelial ligands [e.g., intercellular adhesion molecule-1 (ICAM-1)], (3) extravasation of leukocytes into tissues through tight junctions of endothelial cells mediated by the platelet and endothelial cell adhesion molecule 1 (PECAM-1), and (4) perivascular migration through the extracellular matrix via β_1 integrins. Inhibiting excessive leukocyte egress and subsequent free-radical-mediated damage caused by leukocyte components may attenuate or eliminate tissue damage (Radi et al., 2001). Both piroxicam and meloxicam interfered, in an *in vitro* experiment using flow cytometry, with neutrophil degranulation and cytokine-mediated activation changes in adhesion molecules (García-Vicu na et al., 1997). Due to their anti-inflammatory properties, NSAIDs have been used to modify leukocyte infiltration via their effects on different stages of leukocyte trafficking in various animal models (Radi et al., 2001). For example, celecoxib and indomethacin inhibited leukocyte migration induced by lipopolysaccharide injected into the cremaster muscle in a rat model. However, celecoxib was associated with reduced leukocyte rolling and adhesion, whereas indomethacin only inhibited cell adhesion (Menezes et al., 2008). A role for leukocyte trafficking, adhesion, and activation in NSAID GI-mediated toxicity has been proposed. In a study in rats, neutrophil adhesion to gastric mesenteric venules was increased by indomethacin and celecoxib but not by SC-560, whereas gastric mucosal blood flow was decreased by indomethacin and SC-560 but not by celecoxib (Wallace et al., 2000). These data suggest that the NSAID-induced decrease in gastric mucosal blood flow is COX-1-mediated, whereas NSAID-induced neutrophil vascular endothelial adhesion is COX-2-mediated. In another study in rats,

neutrophil- and oxygen radical–dependent microvascular injuries were found to have a role in gastric mucosal injury induced by ns-NSAIDs. Also, reactive oxygen species (ROS) produced by activated neutrophils after indomethacin treatment in rats caused gastric mucosal injury via ROS-mediated oxidation of such macromolecules as lipids, proteins, and DNA (Naito and Yoshikawa, 2006).

Effects of GI Physiological Local pH, Gut Absorption, and Fasting

Absorption is a process whereby xenobiotics gain entrance to the body via the circulatory or lymphatic system. There are five possible processes of intestinal absorption of xenobiotics: (1) active transport, (2) passive diffusion, (3) pinocytosis, (4) filtration through “pores,” and (5) lymphatic absorption. Most xenobiotics are transported across the GI mucosa by passive diffusion (Chhabra, 1979). GI physiology can have a significant impact on absorption. A number of factors, such as diet, GI motility, interference with GI flora, changes in the rate of gastric emptying, age of the animal, physical properties of a compound, and the dissolution rate of xenobiotics can influence the rate of GI absorption (Chhabra, 1979). Lipid-soluble compounds are more readily absorbed than water-soluble compounds. Additionally, xenobiotic absorption is highly dependent on local GI pH values. However, there are considerable species differences in pH along each segment of the GI tract (Table 1-5) (Smith, 1965; Dressman et al., 1990; Davies and Morris, 1993; McConnell et al., 2008).

The pH in the GI tract is a crucial factor, affecting the stability and solubility of drugs and their absorption through the mucosa (McConnell et al., 2008). The gastric acid secretion rate in the dog at the basal state is low compared to that in humans and rhesus monkeys. In an *in vitro* experiment, Legen and Kristl (2003) demonstrated that ketoprofen transport across the rat jejunum has pH- and energy-dependent transport mechanisms. Indomethacin-induced gastric mucosal damage in rats is markedly dependent on luminal pH (Elliott et al., 1996). Acidic compounds can potentially cause gastric toxicity. Although ibuprofen is more potent than aspirin as a cyclooxygenase inhibitor, it has less gastric toxicity in animals and humans. This is because ibuprofen is 10 times less soluble under the acidic pH conditions

TABLE 1-5 Comparative pH Values of Various Anatomical Regions of the Gastrointestinal Tract

Species	Stomach	Small intestine	Cecum	Colon
Human	1.7–6.7	5.4–7.5	6	7.5
Monkey	2.8	5.6–6	5	5.1
Dog	3.4	6.2–7.5	6.4	6.5
Rat	3.2–3.9	5–6	5.9–6.6	5.5–6.2
Mouse	3–4	4.8–5.2	4.4–4.6	4.4–5
Rabbit	1.9	6–8	6.6	7.2

in the stomach and thus is unlikely to be absorbed there (Beck et al., 1990). Unsuitable pH may cause the precipitation of acidic or basic drugs from solution or the degradation of labile compounds. The lowest pH is seen in the stomach in laboratory animals and humans. However, the fasting status affects gastric pH values. In dogs and cats, gastric acid secretion is intermittent and gastric pH during fasting can rise as high as 3 to 6.5. In rodents, gastric pH appeared higher in the fasted state (McConnell et al., 2008). These observations are unlike that seen in humans, where the gastric pH is lower in the fasting state than in the fed state (fasted pH 1.7 increases to 6.7 after meal ingestion in humans) (Dressman et al., 1990). The fasting status affects NSAID GI-associated toxicity. For example, the gastric toxicity of indomethacin, diclofenac, ibuprofen, and aspirin at various doses is relatively low after oral administration to rats having access to food (Beck et al., 1990). On the other hand, fasted rats were more vulnerable to similar toxicity at all doses of these NSAIDs (Beck et al., 1990). The presence of food retards fenoprofen stomach absorption and lowers peak concentration in plasma, which is usually achieved within 2 h. In horses, food can impair the oral absorption of some NSAIDs, such as phenylbutazone. Phenylbutazone absorption from the GI tract in horses is influenced by the dose administered and the relationship of dosing to feeding. Access to hay can delay the time of peak plasma concentration to 18 h or longer (Tobin et al., 1986). The fed state of rodents, similar to the situation in humans, had no effect on intestinal pH (McConnell et al., 2008). The low intestinal pH level in rodents could have implications for the *in vivo* testing of oral drugs in rats and mice. For example, drugs that require a basic pH to dissolve may precipitate at the lower pH values seen in rodents. This suggests that rodent models may not be the most appropriate to use to study pH-sensitive dosage forms targeted to the human lower intestine and colon (McConnell et al., 2008).

A pH gradient has been reported at the gastric mucosal surface in several species (human, dog, rat, mouse, rabbit) (Johnson et al., 2006). This pH gradient is relatively alkaline directly at tissue surfaces and becomes more acidic at distances farther away from the surface. This alkaline layer is caused by active bicarbonate secretion and is considered a major defense mechanism. Duodenal hemorrhagic lesions were induced when pH was decreased (acid hypersecretion) (Hirata et al., 1997). In addition, such lesions were induced by histamine in rats (Hirata et al., 1997). In fact, histamine H₂-receptor antagonists have been used to reduce NSAID-induced gastric ulcers (Lazzaroni and Porro, 2009).

NSAID Topical Effect-Mediated Injury

Variation in the physicochemical properties and pharmacological profiles among the individual NSAIDs translates into interagent differences regarding the propensity to cause adverse GI effects (Bannwarth, 2008). It has been suggested that NSAID-associated GI hemorrhage and erosion are related to a topical effect of the drugs in addition to COX inhibition (Tibble et al., 2000). Enteric-coated or IV-injected drugs result in considerably less acute GI injury. In rats, the intestinal tolerability of celecoxib is thought to be related to the absence of a topical

damaging effect and COX-2 selective inhibition (Tibble et al., 2000). Topical GI mucosal injury usually occurs after ingestion of the weakly acidic and lipid-soluble NSAIDs. These weak acids are not ionized in the acidic gastric environment and their lipid solubility allows them to diffuse freely across the plasma membrane into surface epithelial cells. At cellular pH, they dissociate into the ionized form, releasing hydrogen ions that are trapped within the cell (intracellular trapping hypothesis), leading to an increase in back-diffusion of gastric acids and disruption of cellular function (Wolfe et al., 1999). Topical acidic properties can cause GI mucosal damage. For example, although sulindac is administered as a non-toxic prodrug, its active metabolite, sulindac sulfide, is excreted into bile. Upon entry into the duodenum, sulindac sulfide causes duodenal topical mucosal injury by virtue of its acidic properties (Wolfe et al., 1999). After aspirin ingestion, gastric mucosal permeability is increased, as reflected by a decrease in the transmucosal potential difference (Baskin et al., 1976). This is caused by a direct topical effect.

Changes in GI Motility, Microcirculation, and Enterobacteria

The inner layer of the GI tract, which is in intimate contact with the contents of the lumen, is comprised of an epithelial cell layer called the mucosa. Subjacent to the mucosa is the submucosa, which is a loose connective tissue layer that contains blood vessels, lymphatics, and autonomic nerve fibers (Meissner plexus). Beneath the submucosa are circular and longitudinal muscle layers comprised of smooth muscle fibers. Contraction of these muscles is associated with mixing and propulsive movements of the intestinal contents (GI peristalsis and motility). The intestinal motility is regulated by the enteric nervous system. GI inflammation (e.g., inflammatory bowel disease) generally affects its motility. The exact pathophysiology of this dysmotility is poorly understood. However, changes in myenteric neurons and smooth muscle have been proposed (Fornai et al., 2005, 2006). Emerging data suggest that cyclooxygenases may play a role in the control of GI neuromuscular functions and motility (De Backer et al., 2003; Fornai et al., 2005; 2006). Fornai et al. reported that (1) in human colon, cyclooxygenases are involved in enteric circuitries exerting tonic inhibitory control on smooth muscle responses to endogenous acetylcholine; (2) both cyclooxygenase isoforms contribute to these regulatory actions; and (3) cholinergic neurons are modulated primarily by COX-1 activity, while COX-2 acts mainly at the muscular level to down-regulate muscarinic responses (Fornai et al., 2005). Gastric hypermotility occurred in indomethacin-treated rats (Takeuchi et al., 2004). Intestinal hypermotility has been implicated in NSAID-induced ulceration of the small intestine (Takeuchi et al., 2002). In an experimental study in rats, proximal duodenum motility was determined in the absence and presence of different NSAIDs. Treatment with rofecoxib at 5 mg/kg or parecoxib at 0.5 mg/kg induced duodenal motility, whereas SC-560 showed no effect (Pihl and Nylander, 2006). Another study demonstrated that COX-2 activation is a critical step in diminishing bowel propulsive motility in a trinitrobenzene sulfonic acid (TNBS)-induced colitis guinea pig model (Linden et al., 2004). In

this TNBS-induced colitis model, COX-2 inhibition with an s-NSAID, DFU, but not a COX-1 inhibitor, SC-560, restored to normal levels the electrical properties of myenteric neurons and the rate of propulsive motor activity (Linden et al., 2004). Thus, it is suggested that s-NSAIDs may be a possible therapeutic agent to improve bowel dysmotility.

GI mucosal and submucosal blood flow and microcirculation are important components of the gastroduodenal function and defense barrier. For example, in the stomach, the presence of luminal acid increases the delivery of vascular bicarbonate into the overlying mucus layer by mucosal microcirculation, thereby neutralizing H^+ ion invading from the lumen (Johnson et al., 2006). Indomethacin at an ulcerogenic dose of 25 mg/kg in rats enhances gastric motility and also induces microcirculatory disturbances at mucosal folds, which are caused by abnormal compression of the gastric mucosal wall and lead to increased microvascular permeability and cellular damage (Takeuchi et al., 1990). Wallace et al. (2000) reported that SC-560, but not celecoxib, produced a decrease in gastric mucosal blood flow in rats.

Enterobacterial invasion has also been implicated in NSAID-mediated GI pathophysiology. For example, the number of enterobacteria under both aerobic and anaerobic conditions is markedly increased in the intestinal mucosa following indomethacin treatment. Similarly, SC-560, with or without the coadministration of rofecoxib, increased the bacterial count in the mucosa, although rofecoxib alone did not (Takeuchi et al., 2010). The bacterial invasion in the intestinal mucosa following indomethacin treatment was blocked by prior administration of an ampicillin antibiotic, the numbers of bacteria being reduced even below control levels seen in the normal mucosa (Takeuchi et al., 2010). Enterobacteria and cytokines both play roles in the pathophysiology of NSAID-induced enteropathy. In addition, up-regulation of iNOS mRNA expression in the intestinal mucosa was observed in animals given SC-560 but not in animals given rofecoxib. Collectively, these data suggest that some NSAIDs cause GI hypermotility, followed by bacterial translocation, and GI microvascular disturbances, leading to the activation of neutrophils and expression of iNOS, and by doing so damage the intestine (Takeuchi et al., 2010).

Decreased Phosphatidylcholine Levels

A recent hypothesis related to the phosphatidylcholine (PC) role in the NSAID-associated toxicity mechanism has been proposed. Phosphatidylcholine is the major surfactant phospholipid that confers surface hydrophobic characteristics on the gastric mucosa. An improved safety profile of ibuprofen chemically associated with PC has been noted in elderly osteoarthritic patients (Lanza et al., 2008). It is possible that with age, surface phospholipid levels decrease below a critical threshold and that this reduction contributes to age-related NSAID intolerance (Lanza et al., 2008). In addition, age-associated decreases in surface hydrophobicity, PG levels, and impaired healing have been suggested to contribute to the deterioration of the barrier property of the gastric mucosa (Lanza et al., 2008). Hacklesberger et al.

(1998) observed a decrease in surface hydrophobicity in the antrum of the stomach, which is also one of the primary sites of NSAID-induced ulcers.

Impaired Drug Metabolism

Impaired drug metabolism with subsequent adverse drug effects can occur and is related to interindividual variability in drug metabolism due to polymorphisms in genes coded for drug-metabolizing enzymes such as cytochrome P450 (CYPs). Such impairment in drug metabolism would lead to increases in NSAID plasma concentrations and hence would increase the risk of developing adverse GI effects (Agúndez et al., 2009). Four NSAIDs—celecoxib, ibuprofen, lornoxicam, and piroxicam—are metabolized extensively by CYP2C9 and CYP2C8 enzymes, these enzymes being responsible for more than 90% of the primary metabolism of these drugs (Agúndez et al., 2009). Therefore, genetics has been suggested to predispose GI bleeding after NSAID use (Martinez et al., 2004). For example, inherited impairment in CYP2C9, an enzyme responsible for the metabolism of several NSAIDs, increases the risk for severe adverse drug reactions (i.e., GI bleeding) after NSAID use (Martinez et al., 2004; Pilotto et al., 2007). This suggests that CYP2C9 genotyping may identify subgroups of persons who are potentially at risk for NSAID-associated GI bleeding (Pilotto et al., 2007).

However, further investigation as to whether such GI bleeding is related to parent drugs or to metabolites is warranted. The impaired drug mechanism hypothesis would be relevant in long-term therapy because the drug would accumulate after multiple-dose exposure, but in many cases, patients with acute GI bleeding receive the NSAID only once, and the effect of an impaired metabolism in single-dose pharmacokinetics (PK) is less relevant, as can be expected in multiple-dose PK (Agúndez et al., 2009). An alternative mechanism for adverse GI drug effects that should be explored is whether impaired function of the main enzymes could drive the metabolism of the NSAIDs to alternative metabolic pathways and whether alternative metabolites may participate in the adverse effects (Agúndez et al., 2009).

Role of Toll-like Receptor (TLR)-4/MyD88 and Enteric Bacteria

Toll-like receptors (TLRs) comprise a family of conserved molecular structures (pathogen-associated molecular patterns) that function as sensors of microbial infection and play a central role in mucosal innate immune regulation (Rakoff-Nahoum et al., 2004). TLR activation leads to the production of cytokines and antimicrobial molecules important in the initial innate immune response. However, in addition to their function in host defense, recent findings indicate that activation of TLRs by commensal microflora is critical for protection against GI injury and associated mortality. Therefore, TLRs appear to control intestinal epithelial homeostasis and protection from injury (Rakoff-Nahoum et al., 2004). TLR-4 recognizes lipopolysaccharide (LPS), which is present in the cell wall of gram-negative bacteria. The interaction of LPS with TLR-4 and its coreceptor, MD-2, triggers signaling cascades mediated via the accessory protein MyD88-dependent pathways that lead

to translocation of the transcription factor nuclear factor κ B (NF κ B) and the production of proinflammatory cytokines (Medzhitov et al., 1998). TLR-4 signaling is important in the recruitment of inflammatory cells and the production of inflammatory cytokines in the intestine. In a mouse model of inflammatory bowel disease, TLR-4 was found to mediate PGE₂ production by regulation of COX-2 (Fukata et al., 2005, 2006). TLR-4 deficiency (TLR-4^{-/-}) in mice results in fewer inflammatory infiltrates in the lamina propria (Fukata et al., 2005). Furthermore, a study in mice assessed the role of TLR-4 activation and signaling through MyD88 in intestinal ischemia/reperfusion (I/R)-induced damage at 2 h postischemia (Moses et al., 2009). The investigators found that a lack of TLR-4 or MyD88 attenuated intestinal damage to approximately 50% of that seen in wild-type mice. The attenuated gut injury was accompanied by decreased proinflammatory mediators, including chemokines, cytokines, and PGE₂ production. The decreased PGE₂ appeared to be mediated by COX-2 activation (Moses et al., 2009). These studies support the hypothesis that TLR-4 expression affects the extent of intestinal damage by altering COX-2-mediated PGE₂ production. However, PGE₂ alone was not sufficient to restore damage in the TLR-4-altered mice, implicating additional mechanisms of TLR-4-mediated damage. Thus, these data indicate that TLR-4 stimulation of COX-2 activation of PGE₂ production is necessary but not sufficient for intestinal I/R-induced damage and inflammation. TLR-4^{-/-} mice also had defects in mucosal repair in response to dextran sodium sulfate (DSS)-induced colitis with decreased epithelial proliferation and increased rectal bleeding (Fukata et al., 2006). Collectively, these studies suggest that TLR-4 signaling may serve a dual role in the GI tract as a mediator of both inflammation and mucosal repair (Ungaro et al., 2009).

Intestinal epithelial cells showed up-regulated COX-2 expression in a TLR-4- and MyD88-dependent fashion in the DSS colitis mouse model (Fukata et al., 2006). TLR-4 has been implicated in ns-NSAID-induced (indomethacin) small intestine damage because TLR-4^{-/-} and MyD88^{-/-} mice showed resistance to ns-NSAID-induced small intestinal damage (Watanabe et al., 2008). The physiological importance of PGs in intestinal epithelial cells and its relationship to bacterial invasion have been demonstrated. In vitro infection of human intestinal epithelial cells with invasive bacteria has been shown to induce the expression of PGHS₂ and the production of PGE₂ and PGF_{2 α} (Eckmann et al., 1997). Furthermore, increased PGHS-2 expression was observed in intestinal epithelial cells in vivo after infection with invasive bacteria using a human intestinal xenograft model in SCID mice (Eckmann et al., 1997). The bacterial LPS/TLR-4 signaling pathway is also a key mechanism in NSAID-induced enteropathy. Elevation in enteric bacterial numbers and epithelial permeability of the small intestine was associated with enterohepatically recirculated ns-NSAIDs (Reuter et al., 1997). Another study investigated the effects of the *Lactobacillus casei* strain Shirota (LcS) on indomethacin-induced small intestine injury in rats. One-week treatment with viable LcS prevented indomethacin-induced intestinal injury. The investigators conclude that LcS exhibited a prophylactic effect on indomethacin-induced enteropathy by suppressing the LPS/TLR-4 signaling pathway (Watanabe et al.,

2009). Bacterial invasion in the intestinal mucosa following indomethacin treatment in rats was blocked by prior administration of the ampicillin antibiotic, the numbers of bacteria being reduced even below control levels seen in the normal mucosa (Takeuchi et al., 2010).

Role of Uncoupling of Mitochondrial Oxidative Phosphorylation

Several studies examined the role of the uncoupling of mitochondrial oxidative phosphorylation, leading to increased intestinal permeability and calcium release into the cytosol, in NSAID-mediated GI effects (Mahmud et al., 1996; Mathews, 1996; Somasundaram et al., 2000). NSAIDs increase mitochondrial respiration *in vivo* and *in vitro* without producing ATP. The higher pH inside the mitochondrial matrix deprotonates the NSAID, so protons are transported into the matrix. NSAIDs that directly uncouple or inhibit mitochondrial oxidative phosphorylation and ATP turnover include indomethacin, aspirin, diclofenac, meloxicam, and SC-236, an s-NSAID (Petrescu et al., 1997; Tibble et al., 2000; Krause et al., 2003). For example, indomethacin, but not celecoxib, uncoupled mitochondrial oxidative phosphorylation both *in vitro* and *in vivo*, caused a significant increase in small intestinal permeability, caused mucosal inflammation and a 90% decline in intestinal PGE levels, and was associated with multiple small intestinal ulcers in rats (Tibble et al., 2000). Sulindac sulfide, but not sulindac sulfone or sulindac itself, caused mitochondrial uncoupling in an isolated rat liver mitochondria (Leite et al., 2006). However, while the uncoupling of enterocyte mitochondrial oxidative phosphorylation leads to increased intestinal permeability and low-grade inflammation, concurrent decreases in mucosal prostanoids appear to be important in the development of ulcers (Somasundaram et al., 2000).

Role of Peroxisome Proliferator-Activated Receptor γ

Peroxisome proliferator-activated receptor γ (PPAR γ) is a ligand-activated nuclear receptor whose activation has been linked to several pathways, including regulation of intestinal inflammation (Issemann and Green, 1990). COX-2 is elaborated during I/R injury (Sato et al., 2005). Issemann and Green examined the importance of PPAR γ in inflammation and GI I/R-induced injury using a PPAR γ -knockout mouse model. PPAR γ -knockout mice showed exacerbated GI I/R-induced injury compared to wild-type mice. Histopathological examination of the small intestine revealed loss of villi (erosions and ulcers), hemorrhage, and inflammatory cell infiltrates. Furthermore, PPAR γ activation reduced the severity of GI I/R injury and blocked up-regulation of NF κ B, which is involved in the control of transcription of various inflammatory genes, such as TNF α (Issemann and Green, 1990). In a rodent model of I/R, NS-398, a COX-2 s-NSAID, reversed small intestine inflammation and injury and induced expression and nuclear translocation of PPAR γ (Sato et al., 2005). In addition, several ns-NSAIDs (e.g., naproxen, ibuprofen, indomethacin, fenpropfen) activate PPAR γ (Jaradat et al., 2001). In a porcine I/R model, injured ileum treated with NS-398, an s-NSAID, recovered to control levels within 3 h

(Blikslager et al., 2002). Therefore, PPAR γ appears to play a role in NSAID-mediated GI pathophysiological cellular mechanisms, and NSAID administration appears to have a protective effect in I/R GI conditions.

Role of Mitogen-Activated Protein Kinases

The mitogen-activated protein kinases (MAPKs) transduce a variety of extracellular signals to the transcription machinery and include three distinct mammalian types—extracellular signal-regulated kinases (ERKs), c-Jun NH₂-terminal kinases (JNKs), and p38 MAPKs (p38)—the latter having four isoforms of its own (α , β , γ , δ) (Radi and Khan, 2006a; Radi et al., 2009). p38 MAPKs have been shown to be crucial for COX-2 expression and PPAR γ (Scherle et al., 2000; Radi et al., 2009). In fact, the p38 MAPK pathway can activate the intestinal epithelial cells *cox-2* gene promoter directly (Grishin et al., 2006). It has been found that MAPKs regulate COX-2 expression and mucosal recovery in an in vitro porcine I/R ileum model (Shifflett et al., 2004). This suggests that the MAPK pathway can have a positive regulatory effect on COX expression in I/R GI conditions, which suggests that NSAID administration would be protective under such conditions.

NSAID GI Injury-Associated Risk Factors

Epidemiological studies suggest that there are several risk factors for the development of NSAID-associated GI events in humans. These include advancing age, a high dose of NSAID, use of more than two NSAIDs, concurrent paracetamol, concurrent anticoagulants, concurrent aspirin, and prior history of peptic ulcer disease, high alcohol consumption, cigarette smoking, and *H. pylori* infection (Rainsford, 2009).

CONCLUSIONS

The comparative pathophysiologic aspects of the GI tract and interspecies COX-1 and COX-2 expression levels and the pathophysiological role of cyclooxygenases (COX-1 and COX-2) and the effects of their inhibition in the GI system are discussed in this chapter. There are significant interspecies differences in both the level of COX-1 expression and the ratio of COX-1 and COX-2 expression and susceptibility to toxicity with COX inhibition in the GI tract. Nonselective NSAIDs are used to treat a variety of inflammatory disease conditions. The ns-NSAIDs have been associated with GI toxicity in many species. Examples of GI-related toxicities are bleeding, ulceration, erosions, and perforations, distributed across the pyloric region, gastric mucosa, jejunum, ileum, duodenum, and cecum. COX-2 s-NSAIDs have a superior and improved GI tolerability profile to that of ns-NSAIDs. The analgesic and anti-inflammatory benefits of NSAIDs are linked to COX-2 inhibition, while many of the GI toxicities and side effects have variably been linked to COX-1 and/or COX-2 inhibition and, in some cases, directly to the secondary pharmacologic properties of the select drugs. Several mechanisms involved in

the pathogenesis of these NSAID-associated toxicities include differences in COX enzyme potency, interspecies anatomical differences, changes in GI motility, aging, fasting status, disruption of GI physiologic mucosal defense mechanisms, effects on the physiologic GI mucosal cell renewal mechanisms, alterations in GI physiologic pH secretion regulation, inhibition of PG synthesis, impaired drug metabolism, effects of the enterohepatic recirculation, decreased phosphatidylcholine levels, the role of TLR-4/MyD88, PPARs, MAPKs, and glucuronidation, neutrophil adherence, and direct chemical damage in the GI tract. COX-2 s-NSAIDs have permitted comparable therapeutic benefit to conventional ns-NSAIDs without these attendant COX-1-mediated toxicities (Radi and Khan, 2006b).

REFERENCES

- Adams SS, Bough RG, Cliffe EE, Lessel B, et al. Absorption, distribution and toxicity of ibuprofen. *Toxicol Appl Pharmacol* 1969;15:310–330.
- Agrawal NM, Aziz K. Prevention of gastrointestinal complications associated with nonsteroidal antiinflammatory drugs. *J Rheumatol Suppl* 1998;51:17–20.
- Agúndez JA, García-Martín E, Martínez C. Genetically based impairment in CYP2C8- and CYP2C9-dependent NSAID metabolism as a risk factor for gastrointestinal bleeding: Is a combination of pharmacogenomics and metabolomics required to improve personalized medicine? *Expert Opin Drug Metab Toxicol* 2009;5:607–620.
- Aguwa CN. Incidence of gastric ulcers by indomethacin and piroxicam in rats. *Arch Toxicol* 1985;56:212–213.
- Aitken MM, Sanford J. Plasma levels following administration of sodium meclofenamate by various routes. *Res Vet Sci* 1975;19:241–244.
- al-Ghamdi MS, Dissanayake AS, Cader ZA, Jain S. Tenoxicam-induced gastropathy in the rat: a comparison with piroxicam and diclofenac sodium, and the inhibitory effects of ranitidine and sucralfate. *J Int Med Res* 1991;19:242–248.
- Allison SO, Halliday LC, French JA, Novikov DD, et al. Assessment of buprenorphine, carprofen, and their combination for postoperative analgesia in olive baboons (*Papio anubis*). *J Am Assoc Lab Anim Sci* 2007;46:24–231.
- Altinkaynak K, Suleyman H, Akcay F. Effect of nimesulide, rofecoxib and celecoxib on gastric tissue glutathione level in rats with indomethacin-induced gastric ulcerations. *Pol J Pharmacol* 2003;55:645–648.
- Anthony A, Dhillon AP, Sim R, Nygard G, et al. Ulceration, fibrosis and diaphragm-like lesions in the caecum of rats treated with indomethacin. *Aliment Pharmacol Ther* 1994;8:417–424.
- Aoyagi N, Ogata H, Kaniwa N, Uchiyama M, et al. Gastric emptying of tablets and granules in humans, dogs, pigs, and stomach-emptying-controlled rabbits. *J Pharm Sci* 1992;81:1170–1174.
- Arai I, Hamasaka Y, Futaki N, Takahashi S, et al. Effect of NS-398, a new nonsteroidal anti-inflammatory agent, on gastric ulceration and acid secretion in rats. *Res Commun Chem Pathol Pharmacol* 1993;81:259–270.
- Atchison CR, West AB, Balakumaran A, Hargus SJ, et al. Drug enterocyte adducts: possible causal factor for diclofenac enteropathy in rats. *Gastroenterology* 2000;119:1537–1547.
- Atzpodiën E, Mehdi N, Clarke D, Radhofer-Welte S. Subacute and chronic oral toxicity of lornoxicam in cynomolgus monkeys. *Food Chem Toxicol* 1997;35:465–474.
- Bannwarth B. Safety of the nonselective NSAID nabumetone: focus on gastrointestinal tolerability. *Drug Saf* 2008;31:485–503.
- Baskin WN, Ivey KJ, Krause WJ, Jeffrey GE, et al. Aspirin-induced ultrastructural changes in human gastric mucosa: correlation with potential difference. *Ann Intern Med* 1976;85:299–303.
- Beck WS, Schneider HT, Dietzel K, Nuernberg B, et al. Gastrointestinal ulcerations induced by anti-inflammatory drugs in rats: physicochemical and biochemical factors involved. *Arch Toxicol* 1990;64:210–217.

- Berenguer B, Alarcón de la Lastra C, Motilva V, La Casa C, et al. Effects of celecoxib on acid-challenged gastric mucosa of rats: comparison with metamizol and piroxicam. *Dig Dis Sci* 2004;49:937–947.
- Bhandari P, Bateman AC, Mehta RL, Patel P. Mucosal expression of cyclooxygenase isoforms 1 and 2 is increased with worsening damage to the gastric mucosa. *Histopathology* 2005;46:280–286.
- Bjorkman DJ. Nonsteroidal anti-inflammatory drug-induced gastrointestinal injury. *Am J Med* 1996;101:25S–32S.
- Blikslager AT, Zimmel DN, Young KM, Campbell NB, et al. Recovery of ischaemic injured porcine ileum: evidence for a contributory role of COX-1 and COX-2. *Gut* 2002;50:615–623.
- Bombardier C, Laine L, Reicin A, Shapiro D, et al. Comparison of upper gastrointestinal toxicity of rofecoxib and naproxen in patients with rheumatoid arthritis. VIGOR Study Group. *N Engl J Med* 2000;343:1520–1528.
- Bowen B, Yuan Y, James C, Rashid F, et al. Time course and pattern of blood loss with ibuprofen treatment in healthy subjects. *Clin Gastroenterol Hepatol* 2005;3:1075–1082.
- Brodie DA, Cook PG, Bauer BJ, Dagle GE. Indomethacin-induced intestinal lesions in the rat. *Toxicol Appl Pharmacol* 1970;17:615–624.
- Budsberg SC, Johnston SA, Schwarz PD, DeCamp CE, et al. Efficacy of etodolac for the treatment of osteoarthritis of the hip joints in dogs. *J Am Vet Med Assoc* 1999;214:206–210.
- Burdan F, Szumilo J, Gajjar B, Dudka J, et al. Immunorexpression of constitutive and inducible cyclo-oxygenase isoforms in the rat foetal and maternal digestive tract. *Folia Morphol (Warsz)* 2008;67:24–31.
- Campbell NB, Blikslager AT. The role of cyclooxygenase inhibitors in repair of ischaemic-injured jejunal mucosa in the horse. *Equine Vet J* 2000;32:59–64.
- Carrick JB, Papich MG, Middleton DM, Naylor JM, et al. Clinical and pathological effects of flunixin meglumine administration to neonatal foals. *Can J Vet Res* 1989;53:195–201.
- Cathers TE, Isaza R, Oehme F. Acute ibuprofen toxicosis in a ferret. *J Am Vet Med Assoc* 2000;216:1426–1428.
- Chan CC, Boyce S, Brideau C, Charleson S, et al. Rofecoxib [Vioxx, MK-0966; 4-(4'-methylsulfonylphenyl)-3-phenyl-2-(5H)-furanone]: a potent and orally active cyclooxygenase-2 inhibitor—pharmacological and biochemical profiles. *J Pharmacol Exp Ther* 1999;290:551–560.
- Chhabra RS. Intestinal absorption and metabolism of xenobiotics. *Environ Health Perspect* 1979;33:61–69.
- Collins LG, Tyler DE. Experimentally induced phenylbutazone toxicosis in ponies: description of the syndrome and its prevention with synthetic prostaglandin E2. *Am J Vet Res* 1985;46:1605–1615.
- Combe B, Swergold G, McLay J, McCarthy T, et al. Cardiovascular safety and gastrointestinal tolerability of etoricoxib vs. diclofenac in a randomized controlled clinical trial (the MEDAL study). *Rheumatology (Oxford)* 2009;48:425–432.
- Conforti A, Donini M, Brocco G, Del Soldato P, et al. Acute anti-inflammatory activity and gastrointestinal tolerability of diclofenac and nitrofenac. *Agents Actions* 1993;40:176–180.
- Conlon PD. Nonsteroidal drugs used in the treatment of inflammation. *Vet Clin North Am Small Anim Pract* 1988;18:1115–1131.
- Cook VL, Meyer CT, Campbell NB, Blikslager AT. Effect of firocoxib or flunixin meglumine on recovery of ischemic-injured equine jejunum. *Am J Vet Res* 2009;70:992–1000.
- Coppelli G, Guaita E, Spaggiari S, Coruzzi G, et al. Gastric effects of the selective cyclooxygenase-2 inhibitor, celecoxib, in the rat. *Dig Liver Dis* 2004;36:265–370.
- Cosenza SF. Drug-induced gastroduodenal ulceration in dogs. *Modern Vet Pract* 1984;65:923–925.
- Court MH, Greenblatt DJ. Molecular basis for deficient acetaminophen glucuronidation in cats: an interspecies comparison of enzyme kinetics in liver microsomes. *Biochem Pharmacol* 1997;53:1041–1047.
- Cryer B. Gastrointestinal safety of low-dose aspirin. *Am J Manag Care* 2002;8:S701–S708.
- Cryer B, Feldman M. Cyclooxygenase-1 and cyclooxygenase-2 selectivity of widely used nonsteroidal anti-inflammatory drugs. *Am J Med* 1998;104:413–421.
- Cryer B, Redfern JS, Goldschmiedt M, Lee E, et al. Effect of aging on gastric and duodenal mucosal prostaglandin concentrations in humans. *Gastroenterology* 1992;102:1118–1123.

- Cuzzocrea S, Mazzon E, Serraino I, Dugo L, et al. Celecoxib, a selective cyclooxygenase-2 inhibitor reduces the severity of experimental colitis induced by dinitrobenzene sulfonic acid in rats. *Eur J Pharmacol* 2001;431:91–102.
- Daeher MH. Transmural pyloric perforation associated with naproxen administration in a dog. *J Am Vet Med Assoc* 1986;189:694–695.
- Daffonchio L, Novellini R, Bertuglia S. Protective effect of ketoprofen lysine salt on interleukin-1beta and bradykinin induced inflammatory changes in hamster cheek pouch microcirculation. *Inflamm Res* 2002;51:223–228.
- Dannenberg AJ, Altorki NK, Boyle JO, Dang C, et al. Cyclo-oxygenase 2: a pharmacological target for the prevention of cancer. *Lancet Oncol* 2001;2:544–551.
- Davies B, Morris T. Physiological parameters in laboratory animals and humans. *Pharm Res* 1993;10:1093–1095.
- De Backer O, Leclere PG, Lefebvre RA. Pharmacological characterization of pre- and postsynaptic prostanoid receptors in pig gastric fundus. *Neuropharmacology* 2003;45:684–690.
- Deng X, Tolstanova G, Khomenko T, Chen L, et al. Mesalamine restores angiogenic balance in experimental ulcerative colitis by reducing expression of endostatin and angiostatin: novel molecular mechanism for therapeutic action of mesalamine. *J Pharmacol Exp Ther* 2009;331:1071–1078.
- Dequeker J, Hawkey C, Kahan A, Steinbrück K, et al. Improvement in gastrointestinal tolerability of the selective cyclooxygenase (COX)-2 inhibitor, meloxicam, compared with piroxicam: results of the safety and efficacy large-scale evaluation of COX-inhibiting therapies (SELECT) trial in osteoarthritis. *Br J Rheumatol* 1998;37:946–951.
- Dignass AU. Mechanisms and modulation of intestinal epithelial repair. *Inflamm Bowel Dis* 2001;7:68–77.
- DiPasquale G, Welaj P. Letter: Ulcerogenic potential of indomethacin in arthritic and non-arthritic rats. *J Pharm Pharmacol* 1973;25:831–832.
- Doan T, Massarotti E. Rheumatoid arthritis: an overview of new and emerging therapies. *J Clin Pharmacol* 2005;45:751–762.
- Doucet MY, Bertone AL, Hendrickson D, Hughes F, et al. Comparison of efficacy and safety of paste formulations of firocoxib and phenylbutazone in horses with naturally occurring osteoarthritis. *J Am Vet Med Assoc* 2008;232:91–97.
- Dressman JB, Berardi RR, Dermentzoglou LC, Russell TL, et al. Upper gastrointestinal (GI) pH in young, healthy men and women. *Pharm Res* 1990;7:756–761.
- Duerksen DR. Stress-related mucosal disease in critically ill patients. *Best Pract Res Clin Gastroenterol* 2003;17:327–244.
- Dugan DE, Hooke KF, Noll RM, Kwan C. Enterohepatic circulation of indomethacin and its role in intestinal irritation. *Biochem Pharmacol* 1975;24:1749–1754.
- Eckmann L, Stenson WF, Savidge TC, Lowe DC, et al. Role of intestinal epithelial cells in the host secretory response to infection by invasive bacteria: Bacterial entry induces epithelial prostaglandin H synthase-2 expression and prostaglandin E2 and F2alpha production. *J Clin Invest* 1997;100:296–309.
- Eling TE, Thompson DC, Foureman GL, Curtis JF, et al. Prostaglandin H synthase and xenobiotic oxidation. *Annu Rev Pharmacol Toxicol* 1990;30:1–45.
- Elliott GA, Purmalis A, Vandermeer DA, Denlinger RH. The propionic acids: gastrointestinal toxicity in various species. *Toxicol Pathol* 1988;16:245–250.
- Elliott SL, Ferris RJ, Giraud AS, Cook GA, et al. Indomethacin damage to rat gastric mucosa is markedly dependent on luminal pH. *Clin Exp Pharmacol Physiol* 1996;23:432–434.
- El-Medany A, Mahgoub A, Mustafa A, Arafa M, et al. The effects of selective cyclooxygenase-2 inhibitors, celecoxib and rofecoxib, on experimental colitis induced by acetic acid in rats. *Eur J Pharmacol* 2005;507:291–299.
- Erickson BA, Longo WE, Panesar N, Mazuski JE, et al. The effect of selective cyclooxygenase inhibitors on intestinal epithelial cell mitogenesis. *J Surg Res* 1999;81:101–107.
- Ewing GO. Indomethacin-associated gastrointestinal hemorrhage in a dog. *J Am Vet Med Assoc* 1972;161:1665–1668.
- Eyre P, Boulard C, Deline T. Local and systemic reactions in cattle to *Hypoderma lineatum* larval toxin: protection by phenylbutazone. *Am J Vet Res* 1981;42:25–28.

- Fang WF, Broughton A, Jacobson ED. Indomethacin-induced intestinal inflammation. *Am J Dig Dis* 1977;22:749–760.
- Feldman M, Cryer B. Effects of age on gastric alkaline and nonparietal fluid secretion in humans. *Gerontology* 1998;44:222–227.
- Field M. Intestinal ion transport and the pathophysiology of diarrhea. *J Clin Invest* 2003;111:931–943.
- Fornai M, Blandizzi C, Colucci R, Antonioli L, et al. Role of cyclooxygenases 1 and 2 in the modulation of neuromuscular functions in the distal colon of humans and mice. *Gut* 2005;54:608–616.
- Fornai M, Blandizzi C, Antonioli L, Colucci R, et al. Differential role of cyclooxygenase 1 and 2 isoforms in the modulation of colonic neuromuscular function in experimental inflammation. *J Pharmacol Exp Ther* 2006;317:938–945.
- Forsyth SF, Guilford WG, Haslett SJ, Godfrey J. Endoscopy of the gastroduodenal mucosa after carprofen, meloxicam and ketoprofen administration in dogs. *J Small Anim Pract* 1998;39:421–424.
- Fox J, Anderson LC, Loew FM, Quimby FW. *Laboratory Animal Medicine*, 2nd ed. San Diego, CA: Academic Press, 2002.
- Fox SM, Johnston SA. Use of carprofen for the treatment of pain and inflammation in dogs. *J Am Vet Med Assoc* 1997;210:1493–1498.
- Freeman LC, Narvaez DF, McCoy A, von Stein FB, et al. Depolarization and decreased surface expression of K channels contribute to NSAID-inhibition of intestinal restitution. *Biochem Pharmacol* 2007;74:74–85.
- Fukata M, Michelsen KS, Eri R, Thomas LS, et al. Toll-like receptor-4 is required for intestinal response to epithelial injury and limiting bacterial translocation in a murine model of acute colitis. *Am J Physiol Gastrointest Liver Physiol* 2005;288:G1055–G1065.
- Fukata M, Chen A, Klepper A, Krishnareddy S, et al. Cox-2 is regulated by Toll-like receptor-4 (TLR4) signaling: role in proliferation and apoptosis in the intestine. *Gastroenterology* 2006;131:862–877.
- Futaki N, Yoshikawa K, Hamasaka Y, Arai I, et al. NS-398, a novel non-steroidal anti-inflammatory drug with potent analgesic and antipyretic effects, which causes minimal stomach lesions. *Gen Pharmacol* 1993;24:105–110.
- García-Vicuña R, Díaz-González F, González-Alvaro I, del Pozo MA, et al. Prevention of cytokine-induced changes in leukocyte adhesion receptors by nonsteroidal antiinflammatory drugs from the oxicam family. *Arthritis Rheum* 1997;40:143–153.
- Girawan D, Abdurachman SA, Djumhana A, Roslia J, et al. Comparison of endoscopic gastric mucosa features after administration of piroxicam to meloxicam and their correlation with dyspepsia symptoms in elderly patient with knee osteoarthritis. *Acta Med Indones* 2004;36:202–206.
- Godshalk CP, Roush JK, Fingland RB, Sikkema D, et al. Gastric perforation associated with administration of ibuprofen in a dog. *J Am Vet Med Assoc* 1992;201:1734–1736.
- Goldstein JL, Correa P, Zhao WW, Burr AM, et al. Reduced incidence of gastroduodenal ulcers with celecoxib, a novel cyclooxygenase-2 inhibitor, compared to naproxen in patients with arthritis. *Am J Gastroenterol* 2001;96:1019–1027.
- Goldstein JL, Aisenberg J, Lanza F, Schwartz H, et al. A multicenter, randomized, double-blind, active-comparator, placebo-controlled, parallel-group comparison of the incidence of endoscopic gastric and duodenal ulcer rates with valdecoxib or naproxen in healthy subjects aged 65 to 75 years. *Clin Ther* 2006;28:340–351.
- Goldstein JL, Eisen GM, Lewis B, Gralnek IM, et al. Small bowel mucosal injury is reduced in healthy subjects treated with celecoxib compared with ibuprofen plus omeprazole, as assessed by video capsule endoscopy. *Aliment Pharmacol Ther* 2007;25:1211–1222.
- Goodman L, Torres B, Punke J, Reynolds L, et al. Effects of firocoxib and tepoxalin on healing in a canine gastric mucosal injury model: effects of firocoxib and tepoxalin on healing in a canine gastric mucosal injury model. *J Vet Intern Med* 2009;23:56–62.
- Goodman LA, Torres BT, Reynolds LR, Budsberg SC. Effects of firocoxib, meloxicam, and tepoxalin administration on eicosanoid production in target tissues of healthy cats. *Am J Vet Res* 2010;71:1067–1073.
- Gookin JL, Galanko JA, Blikslager AT, Argenzio RA. PG-mediated closure of paracellular pathway and not restitution is the primary determinant of barrier recovery in acutely injured porcine ileum. *Am J Physiol Gastrointest Liver Physiol* 2003;285:G967–G979.

- Goto H, Sugiyama S, Ohara A, Hoshino H, et al. Age-associated decreases in prostaglandin contents in human gastric mucosa. *Biochem Biophys Res Commun* 1992;186:1443–1448.
- Gretzer B, Maricic N, Respondek M, Schuligoi R, et al. Effects of specific inhibition of cyclooxygenase-1 and cyclo-oxygenase-2 in the rat stomach with normal mucosa and after acid challenge. *Br J Pharmacol* 2001;132:1565–1573.
- Grishin AV, Wang J, Potoka DA, Hackam DJ, et al. Lipopolysaccharide induces cyclooxygenase-2 in intestinal epithelium via a noncanonical p38 MAPK pathway. *J Immunol* 2006;176:580–588.
- Gullikson GW, Anglin CP, Kessler LK, Smeach S, et al. Misoprostol attenuates aspirin-induced changes in potential difference and associated damage in canine gastric mucosa. *Clin Invest Med* 1987;10:145–151.
- Hackelsberger A, Platzer U, Nilius M, Schultze V, et al. Age and *Helicobacter pylori* decrease gastric mucosal surface hydrophobicity independently. *Gut* 1998;43:465–469.
- Hallesy DW, Shott LD, Hill R. Comparative toxicology of naproxen. *Scand J Rheumatol* 1973;Suppl 2: 220–228.
- Harris SI, Stoltz RR, LeComte D, Hubbard RC. Parecoxib sodium demonstrates gastrointestinal safety comparable to placebo in healthy subjects. *J Clin Gastroenterol* 2004;38:575–580.
- Hawkey C, Kahan A, Steinbrück K, Alegre C, et al. Gastrointestinal tolerability of meloxicam compared to diclofenac in osteoarthritis patients. International MELISSA Study Group: Meloxicam Large-Scale International Study Safety Assessment. *Br J Rheumatol* 1998;37:937–945.
- Hawkey C, Laine L, Simon T, Beaulieu A, et al. Comparison of the effect of rofecoxib (a cyclooxygenase 2 inhibitor), ibuprofen, and placebo on the gastroduodenal mucosa of patients with osteoarthritis: a randomized, double-blind, placebo controlled trial. The Rofecoxib Osteoarthritis Endoscopy Multi-national Study Group. *Arthritis Rheum* 2000;43:370–377.
- Hawkey CJ, Skelly MM. Gastrointestinal safety of selective COX-2 inhibitors. *Curr Pharm Des* 2002;8:1077–1089.
- Haworth R, Oakley K, McCormack N, Pilling A. Differential expression of COX-1 and COX-2 in the gastrointestinal tract of the rat. *Toxicol Pathol.* 2005;33:239–245.
- Hirata T, Ukawa H, Kitamura M, Takeuchi K. Effects of selective cyclooxygenase-2 inhibitors on alkaline secretory and mucosal ulcerogenic responses in rat duodenum. *Life Sci* 1997;61:1603–1611.
- Horie-Sakata K, Shimada T, Hiraishi H, Terano A. Role of cyclooxygenase 2 in hepatocyte growth factor-mediated gastric epithelial restitution. *J Clin Gastroenterol* 1998;27 Suppl 1:S40–S46.
- Hull MA, Booth JK, Tisbury A, Scott N, et al. Cyclooxygenase 2 is up-regulated and localized to macrophages in the intestine of Min mice. *Br J Cancer* 1999;79:1399–1405.
- Issemann I, Green S. Activation of a member of the steroid hormone receptor superfamily by peroxisome proliferators. *Nature* 1990;347:645–650.
- Jackson LM, Wu KC, Mahida YR, Jenkins D, et al. Cyclooxygenase (COX) 1 and 2 in normal, inflamed, and ulcerated human gastric mucosa. *Gut* 2000;47:762–770.
- Jaradat MS, Wongsud B, Phornchirasilp S, Rangwala SM, et al. Activation of peroxisome proliferator-activated receptor isoforms and inhibition of prostaglandin H(2) synthases by ibuprofen, naproxen, and indomethacin. *Biochem Pharmacol* 2001;62:1587–1595.
- Johnson LR, Barret KE, Gishan FK, Merchant JL, Said HM, Wood JD (eds). *Physiology of the Gastrointestinal Tract*, 4th ed. New York: Elsevier, 2006, pp. 1259–1291.
- Johnston SA, Budsberg SC. Nonsteroidal anti-inflammatory drugs and corticosteroids for the management of canine osteoarthritis. *Vet Clin North Am Small Anim Pract* 1997;27:841–862.
- Johnston SA, Leib MS, Forrester SD, Marini M. The effect of misoprostol on aspirin-induced gastroduodenal lesions in dogs. *J Vet Intern Med* 1995;9:32–38.
- Julou L, Guyonnet JC, Ducrot R, Fournel J, et al. Ketoprofen (19.583R.P.) [2-(3-benzoylphenyl)propionic acid]. Main pharmacological properties: line of toxicological and pharmacokinetic data. *Scand J Rheumatol* 1976;1976:33–44.
- Kallings P, Johnston C, Dreveno S. Effects of flunixin on movement and performance of standardbred trotters on the track. *Equine Vet J* 1999;Suppl 30: 270–273.
- Karcher LF, Dill SG, Anderson WI, King JM. Right dorsal colitis. *J Vet Intern Med* 1990;4:247–253.
- Kargman S, Charleson S, Cartwright M, Frank J, et al. Characterization of prostaglandin G/H synthase 1 and 2 in rat, dog, monkey, and human gastrointestinal tracts. *Gastroenterology* 1996;111:445–454.

- Karmeli F, Cohen P, Rachmilewitz D. Cyclo-oxygenase-2 inhibitors ameliorate the severity of experimental colitis in rats. *Eur J Gastroenterol Hepatol* 2000;12:223–231.
- Kataoka H, Horie Y, Koyama R, Nakatsugi S, et al. Interaction between NSAIDs and steroid in rat stomach: safety of nimesulide as a preferential COX-2 inhibitor in the stomach. *Dig Dis Sci* 2000;45:1366–1375.
- Kato S, Ogawa Y, Kanatsu K, Okayama M, et al. Ulcerogenic influence of selective cyclooxygenase-2 inhibitors in the rat stomach with adjuvant-induced arthritis. *J Pharmacol Exp Ther* 2002;303:503–509.
- Kato S, Ito Y, Nishio H, Aoi Y, et al. Increased susceptibility of small intestine to NSAID-provoked ulceration in rats with adjuvant-induced arthritis: involvement of enhanced expression of TLR4. *Life Sci* 2007;81:1309–1316.
- Katz LB, Genna T, Fuller BL, Tolman EL, et al. Altered susceptibility of arthritic rats to the gastric lesion-inducing effects of aspirin or ethanol and the antileSION effect of rioprostil. *Agents Actions* 1987;22:134–143.
- Kauffman G. Aspirin-induced gastric mucosal injury: lessons learned from animal models. *Gastroenterology* 1989;96:606–614.
- Kearney D, Byrne A, Crean P, Cox D, et al. Optimal suppression of thromboxane A(2) formation by aspirin during percutaneous transluminal coronary angioplasty: no additional effect of a selective cyclooxygenase-2 inhibitor. *J Am Coll Cardiol* 2004;43:526–531.
- Kent TH, Cardelli RM, Stamler FW. Small intestinal ulcers and intestinal flora in rats given indomethacin. *Am J Pathol* 1969;54:237–249.
- Khan KN, Paulson S, Seibert K, Maziasz T. Gastrointestinal and renal safety of a specific COX-2 inhibitor versus NSAIDs in dogs. *Vet Pathol* 1997;34:509.
- Khan KN, Masferrer JL, Woerner BM, Soslow R, et al. Enhanced cyclooxygenase-2 expression in sporadic and familial adenomatous polyposis of the human colon. *Scand J Gastroenterol* 2001;36:865–869.
- Kim SW, Parekh D, Townsend CM Jr, Thompson JC. Effects of aging on duodenal bicarbonate secretion. *Ann Surg* 1990;212:332–337.
- King JN, Dawson J, Esser RE, Fujimoto R, et al. Preclinical pharmacology of robenacoxib: a novel selective inhibitor of cyclooxygenase-2. *J Vet Pharmacol Ther* 2009;32:1–17.
- Kishimoto Y, Wada K, Nakamoto K, Kawasaki H, et al. Levels of cyclooxygenase-1 and -2 mRNA expression at various stages of acute gastric injury induced by ischemia-reperfusion in rats. *Arch Biochem Biophys* 1998;352:153–157.
- Knapp DW, Richardson RC, Bottoms GD, Teclaw R, et al. Phase I trial of piroxicam in 62 dogs bearing naturally occurring tumors. *Cancer Chemother Pharmacol* 1992;29:214–218.
- Knapp DW, Richardson RC, Chan TC, Bottoms GD, et al. Piroxicam therapy in 34 dogs with transitional cell carcinoma of the urinary bladder. *J Vet Intern Med* 1994;8:273–278.
- Koki A, Khan NK, Woerner BM, Dannenberg AJ, et al. Cyclooxygenase-2 in human pathological disease. *Adv Exp Med Biol* 2002a;507:177–184.
- Koki AT, Khan NK, Woerner BM, Seibert K, et al. Characterization of cyclooxygenase-2 (COX-2) during tumorigenesis in human epithelial cancers: evidence for potential clinical utility of COX-2 inhibitors in epithelial cancers. *Prostaglandins Leukot Essent Fatty Acids* 2002b;66:13–18.
- Kopcha M, Ahl AS. Experimental uses of flunixin meglumine and phenylbutazone in food-producing animals. *J Am Vet Med Assoc* 1989;19:445–449.
- Korytko PJ, Senese PB, Sellers RS, Cai W, et al. Gastrointestinal and renal toxicity associated with loxoprofen sodium in dogs. *Preclinica* 2003;1:107–113.
- Krause MM, Brand MD, Krauss S, Meisel C, et al. Nonsteroidal antiinflammatory drugs and a selective cyclooxygenase 2 inhibitor uncouple mitochondria in intact cells. *Arthritis Rheum* 2003;48:1438–1444.
- La Corte R, Caselli M, Castellino G, Bajocchi G, et al. Prophylaxis and treatment of NSAID-induced gastroduodenal disorders. *Drug Saf* 1999;20:527–543.
- Laine L, Sloane R, Ferretti M, Cominelli F. A randomized double blind comparison of placebo, etodolac, and naproxen on gastrointestinal injury and prostaglandin production. *Gastrointest Endosc* 1995;42:428–433.

- Laine L, Harper S, Simon T, Bath R, et al. A randomized trial comparing the effect of rofecoxib, a cyclooxygenase 2-specific inhibitor, with that of ibuprofen on the gastroduodenal mucosa of patients with osteoarthritis. Rofecoxib Osteoarthritis Endoscopy Study Group. *Gastroenterology* 1999;117:776–783.
- Laine L, Curtis SP, Cryer B, Kaur A, et al. Assessment of upper gastrointestinal safety of etoricoxib and diclofenac in patients with osteoarthritis and rheumatoid arthritis in the Multinational Etoricoxib and Diclofenac Arthritis Long-Term (MEDAL) programme: a randomised comparison. *Lancet* 2007;369:465–473.
- Lamon TK, Browder EJ, Sohrabji F, Ihrig M. Adverse effects of incorporating ketoprofen into established rodent studies. *J Am Assoc Lab Anim Sci* 2008;47:20–24.
- Lanas A, Panes J, Pique JM. Clinical implications of COX-1 and/or COX-2 inhibition for the distal gastrointestinal tract. *Curr Pharm Des* 2003;9:2253–2266.
- Langenbach R, Morham SG, Tian HF, Loftin CD, et al. Prostaglandin synthase 1 gene disruption in mice reduces arachidonic acid-induced inflammation and indomethacin-induced gastric ulceration. *Cell* 1995;83:483–492.
- Langman MJ, Jensen DM, Watson DJ, Harper SE, et al. Adverse upper gastrointestinal effects of rofecoxib compared with NSAIDs. *J Am Med Assoc* 1999;282:1929–1933.
- Langston C, Clarke CR. The role of the clinical pharmacologist in animal health. *AAPS PharmSci* 2002;4:E36.
- Lanza FL, Nelson RS, Greenberg BP. Effects of fenbufen, indomethacin, naproxen, and placebo on gastric mucosa of normal volunteers: a comparative endoscopic and photographic evaluation. *Am J Med* 1983;75:75–79.
- Lanza FL, Marathi UK, Anand BS, Lichtenberger LM. Clinical trial: comparison of ibuprofen-phosphatidylcholine and ibuprofen on the gastrointestinal safety and analgesic efficacy in osteoarthritic patients. *Aliment Pharmacol Ther* 2008;28:431–442.
- Lascelles BD, Blikslager AT, Fox SM, Reece D. Gastrointestinal tract perforation in dogs treated with a selective cyclooxygenase-2 inhibitor: 29 cases (2002–2003). *J Am Vet Med Assoc* 2005a;227:1112–1117.
- Lascelles BD, McFarland JM, Swann H. Guidelines for safe and effective use of NSAIDs in dogs. *Vet Ther* 2005b;6:237–251.
- Laudanno OM, Cesolari JA, Esnarriaga J, Rista L, et al. Gastrointestinal damage induced by celecoxib and rofecoxib in rats. *Dig Dis Sci* 2001;46:779–784.
- Lazzaroni M, Porro GB. Management of NSAID-induced gastrointestinal toxicity: focus on proton pump inhibitors. *Drugs* 2009;69:51–69.
- Lee M, Feldman M. Age-related reductions in gastric mucosal prostaglandin levels increase susceptibility to aspirin-induced injury in rats. *Gastroenterology* 1994;107:1746–1750.
- Lee, M. Age-related changes in gastric mucosal bicarbonate secretion in rats. *Age* 1996;19:55–58.
- Leedham SJ, Brittan M, Preston SL, McDonald SA, et al. The stomach periglandular fibroblast sheath: all present and correct. *Gut* 2006;55:295–296.
- Lees P, Higgins AJ. Clinical pharmacology and therapeutic uses of non-steroidal anti-inflammatory drugs in the horse. *Equine Vet J* 1985;17:83–96.
- Lees P, Landoni MF, Giraudel J, Toutain PL. Pharmacodynamics and pharmacokinetics of non-steroidal anti-inflammatory drugs in species of veterinary interest. *J Vet Pharmacol Ther* 2004;27:479–490.
- Legen I, Kristl A. pH and energy dependent transport of ketoprofen across rat jejunum in vitro. *Eur J Pharm Biopharm* 2003;56:87–94.
- Leite S, Martins NM, Dorta DJ, Curti C, et al. Mitochondrial uncoupling by the sulindac metabolite, sulindac sulfide. *Basic Clin Pharmacol Toxicol* 2006;99:294–299.
- Le Loet X. Safety of ketoprofen in the elderly: a prospective study on 20,000 patients. *Scand J Rheumatol Suppl* 1989;83:21–27.
- Lesch CA, Kraus ER, Sanchez B, Gilbertsen R, et al. Lack of beneficial effect of COX-2 inhibitors in an experimental model of colitis. *Methods Find Exp Clin Pharmacol* 1999;21:99–104.
- Li JT, Li ZS, Zhan XB, Cui ZM, et al. Experimental study of the safety of the selective COX-2 inhibitor, celecoxib, for gastric mucosa. *Chin J Dig Dis* 2003;4:53–56.

- Linden DR, Sharkey KA, Ho W, Mawe GM. Cyclooxygenase-2 contributes to dysmotility and enhanced excitability of myenteric AH neurones in the inflamed guinea pig distal colon. *J Physiol* 2004;557:191–205.
- Lipowitz AJ, Boulay JP, Klausner JS. Serum salicylate concentrations and endoscopic evaluation of the gastric mucosa in dogs after oral administration of aspirin-containing products. *Am J Vet Res* 1986;47:1586–1589.
- Lipscomb GR, Wallis N, Armstrong G, Rees WD. Gastrointestinal tolerability of meloxicam and piroxicam: a double-blind placebo-controlled study. *Br J Clin Pharmacol* 1998;46:133–137.
- Lisse JR, Perlman M, Johansson G, Shoemaker JR, et al. Gastrointestinal tolerability and effectiveness of rofecoxib versus naproxen in the treatment of osteoarthritis: a randomized, controlled trial. *Ann Intern Med* 2003;139:539–546.
- Lohmander LS, McKeith D, Svensson O, Malmenäs M, et al. A randomised, placebo controlled, comparative trial of the gastrointestinal safety and efficacy of AZD3582 versus naproxen in osteoarthritis. *Ann Rheum Dis* 2005;64:449–456.
- Luna SP, Basílio AC, Steagall PV, Machado LP, et al. Evaluation of adverse effects of long-term oral administration of carprofen, etodolac, flunixin meglumine, ketoprofen, and meloxicam in dogs. *Am J Vet Res* 2007;68:258–264.
- MacAllister CG. Effects of toxic doses of phenylbutazone in ponies. *Am J Vet Res* 1983;44:2277–2279.
- MacAllister CG, Morgan SJ, Borne AT, Pollet RA. Comparison of adverse effects of phenylbutazone, flunixin meglumine, and ketoprofen in horses. *J Am Vet Med Assoc* 1993;202:71–77.
- Mackay RJ, French TW, Nguyen HT, Mayhew IG. Effects of large doses of phenylbutazone administration to horses. *Am J Vet Res* 1983;44:774–780.
- Magdalou J, Chajes V, Lafaurie C, Siest G. Glucuronidation of 2-arylpropionic acids pirofen, flurbiprofen, and ibuprofen by liver microsomes. *Drug Metab Dispos* 1990;18:692–697.
- Mahmud T, Rafi SS, Scott DL, Wrigglesworth JM, et al. Nonsteroidal antiinflammatory drugs and uncoupling of mitochondrial oxidative phosphorylation. *Arthritis Rheum* 1996;39:1998–2003.
- Martín AR, Villegas I, Alarcón de la Lastra C. The COX-2 inhibitor, rofecoxib, ameliorates dextran sulphate sodium induced colitis in mice. *Inflamm Res* 2005;54:145–151.
- Martínez C, Blanco G, Ladero JM, García-Martín E, et al. Genetic predisposition to acute gastrointestinal bleeding after NSAIDs use. *Br J Pharmacol* 2004;141:205–208.
- Masferrer JL, Zweifel BS, Manning PT, Hauser SD, et al. Selective inhibition of inducible cyclooxygenase 2 in vivo is antiinflammatory and nonulcerogenic. *Proc Natl Acad Sci USA* 1994;91:3228–3232.
- Mason JC. NSAIDs and the oesophagus. *Eur J Gastroenterol Hepatol* 1999;11:369–373.
- Mathews KA. Nonsteroidal anti-inflammatory analgesics in pain management in dogs and cats. *Can Vet J* 1996;37:539–545.
- Maziasz TJ, Khan KNM, Talley J, Gierse J, et al. The development of drugs that target cyclooxygenase-2. In: Harris RE (ed), *Cyclooxygenase 2 Blockade in Cancer Prevention and Therapy*. Clifton, UK: Humana Press, 2003, pp. 259–277.
- McCafferty DM, Granger DN, Wallace JL. Indomethacin induced gastric injury and leukocyte adherence in arthritic versus healthy rats. *Gastroenterology* 1995;109:1173–1180.
- McConnell EL, Basit AW, Murdan S. Measurements of rat and mouse gastrointestinal pH, fluid and lymphoid tissue, and implications for in-vivo experiments. *J Pharm Pharmacol* 2008;60:63–70.
- McConnico RS, Morgan TW, Williams CC, Hubert JD, et al. Pathophysiologic effects of phenylbutazone on the right dorsal colon in horses. *Am J Vet Res* 2008;69:1496–1505.
- Medzhitov R, Preston-Hurlburt P, Kopp E, Stadlen A, et al. MyD88 is an adaptor protein in the hToll/IL-1 receptor family signaling pathways. *Mol Cell* 1998;2:253–258.
- Melorange R, Gentry C, O'Connell C, Blower PR, et al. Anti-inflammatory and gastrointestinal effects of nabumetone or its active metabolite, 6MNA (6-methoxy-2-naphthylacetic acid): comparison with indomethacin. *Agents Actions* 1992;Spec No:C82–C83.
- Menezes GB, Rezende RM, Pereira-Silva PE, Klein A, et al. Differential involvement of cyclooxygenase isoforms in neutrophil migration in vivo and in vitro. *Eur J Pharmacol* 2008;598:118–122.
- Menozzi A, Pozzoli C, Poli E, Dacasto M, et al. Effects of nonselective and selective cyclooxygenase inhibitors on small intestinal motility in the horse. *Res Vet Sci* 2009;86:129–135.
- Mersereau WA, Hinchey EJ. Synergism between acid and gastric contractile activity in the genesis of ulceration and hemorrhage in the phenylbutazone-treated rat. *Surgery* 1981;90:516–522.

- Meschter CL, Gilbert M, Krook L, Maylin G, et al. The effects of phenylbutazone on the intestinal mucosa of the horse: a morphological, ultrastructural and biochemical study. *Equine Vet J* 1990a;22:255–263.
- Meschter CL, Gilbert M, Krook L, Maylin G, et al. The effects of phenylbutazone on the morphology and prostaglandin concentrations of the pyloric mucosa of the equine stomach. *Vet Pathol* 1990b;27:244–253.
- Moberly JB, Harris SI, Riff DS, Dale JC, et al. A randomized, double-blind, one-week study comparing effects of a novel COX-2 inhibitor and naproxen on the gastric mucosa. *Dig Dis Sci* 2007;52:442–450.
- Modlin IM, Kidd M, Lye KD, Wright NA. Gastric stem cells: an update. *Keio J Med* 2003;52:134–137.
- Möllenhoff A, Nolte I, Kramer S. Anti-nociceptive efficacy of carprofen, levomethadone and buprenorphine for pain relief in cats following major orthopaedic surgery. *J Vet Med A Physiol Pathol Clin Med* 2005;52:186–198.
- Moore JN, Garner HE, Shapland JE, Hatfield DG. Prevention of endotoxin-induced arterial hypoxaemia and lactic acidosis with flunixin meglumine in the conscious pony. *Equine Vet J* 1981;13:95–98.
- Morham SG, Langenbach R, Loftin CD, Tiano HF, et al. Prostaglandin synthase 2 gene disruption causes severe renal pathology in the mouse. *Cell* 1995;83:473–482.
- Moses T, Wagner L, Fleming SD. TLR4-mediated COX-2 expression increases intestinal ischemia/reperfusion-induced damage. *J Leukoc Biol* 2009;86:971–980.
- Murtaugh RJ, Matz ME, Labato MA, Boudrieau RJ. Use of synthetic prostaglandin E1 (misoprostol) for prevention of aspirin-induced gastroduodenal ulceration in arthritic dogs. *J Am Vet Med Assoc* 1993;202:251–256.
- Naito Y, Yoshikawa T. Oxidative stress involvement and gene expression in indomethacin-induced gastropathy. *Redox Rep* 2006;11:243–253.
- Nandi J, Das PK, Zinkievich JM, Baltodano JD, et al. Cyclo-oxygenase-1 inhibition increases acid secretion by modulating H⁺, K⁺-ATPase expression and activation in rabbit parietal cells. *Clin Exp Pharmacol Physiol* 2009;36:127–134.
- Nap RC, Breen DJ, Lam TJ, De Bruyne JJ. Gastric retention of enteric-coated aspirin tablets in beagle dogs. *J Vet Pharmacol Ther* 1990;13:148–153.
- Narita T, Sato R, Tomizawa N, Tani K, et al. Safety of reduced-dosage ketoprofen for long-term oral administration in healthy dogs. *Am J Vet Res* 2006;67:1115–1120.
- Neuss H, Raue W, Müller V, Schwenk W, et al. Effects of cyclooxygenase inhibition on anastomotic healing following large bowel resection in a rabbit model: a randomized, blinded, placebo-controlled trial. *Int J Colorectal Dis* 2009;24:551–557.
- Nguyen T, Chai J, Li A, Akahoshi T, et al. Novel roles of local insulin-like growth factor-1 activation in gastric ulcer healing: promotes actin polymerization, cell proliferation, re-epithelialization, and induces cyclooxygenase-2 in a phosphatidylinositol 3-kinase-dependent manner. *Am J Pathol* 2007;170:1219–1228.
- NygAard G, Anthony A, Khan K, Bounds SV, et al. Intestinal site-dependent susceptibility to chronic indomethacin in the rat: a morphological and biochemical study. *Aliment Pharmacol Ther* 1995;9:403–410.
- Oberto G, Conz A, Giachetti C, Galli CL. Evaluation of the toxicity of indomethacin in a 4-week study, by oral route, in the marmoset (*Callithrix jacchus*). *Fundam Appl Toxicol* 1990;15:800–813.
- Ofman JJ, Maclean CH, Straus WL, Morton SC, et al. Meta-analysis of dyspepsia and nonsteroidal antiinflammatory drugs. *Arthritis Rheum* 2003;49:508–518.
- Okayama M, Hayashi S, Aoi Y, Nishio H, et al. Aggravation by selective COX-1 and COX-2 inhibitors of dextran sulfate sodium (DSS)-induced colon lesions in rats. *Dig Dis Sci* 2007;52:2095–2103.
- Pai R, Soreghan B, Szabó IL, Pavelka M, et al. Prostaglandin E2 transactivates EGF receptor: a novel mechanism for promoting colon cancer growth and gastrointestinal hypertrophy. *Nat Med* 2002;8:289–293.
- Patoia L, Santucci L, Furno P, Dionisi MS, et al. A 4-week, double-blind, parallel-group study to compare the gastrointestinal effects of meloxicam 7.5mg, meloxicam 15mg, piroxicam 20mg and placebo by means of faecal blood loss, endoscopy and symptom evaluation in healthy volunteers. *Br J Rheumatol* 1996;35 Suppl 1: 61–67.

- Patrono C, Patrignani P, García Rodríguez LA. Cyclooxygenase-selective inhibition of prostanoid formation: transducing biochemical selectivity into clinical read-outs. *J Clin Invest* 2001;108:7–13.
- Pavelka K, Recker DP, Verburg KM. Valdecoxib is as effective as diclofenac in the management of rheumatoid arthritis with a lower incidence of gastroduodenal ulcers: results of a 26-week trial. *Rheumatology (Oxford)* 2003;42:1207–1215.
- Petrescu I, Tarba C. Uncoupling effects of diclofenac and aspirin in the perfused liver and isolated hepatic mitochondria of rat. *Biochim Biophys Acta* 1997;1318:385–394.
- Pihl L, Nylander O. Products of cyclooxygenase-2 depress duodenal function in rats subjected to abdominal surgery. *Acta Physiol (Oxford)* 2006;186:279–290.
- Pilotto A, Seripa D, Franceschi M, Scarcelli C, et al. Genetic susceptibility to nonsteroidal anti-inflammatory drug-related gastroduodenal bleeding: role of cytochrome P450 2C9 polymorphisms. *Gastroenterology* 2007;133:465–471.
- Pollmeier M, Toulemonde C, Fleishman C, Hanson PD. Clinical evaluation of firocoxib and carprofen for the treatment of dogs with osteoarthritis. *Vet Rec* 2006;159:547–451.
- Poortinga EW, Hungerford LL. A case–control study of acute ibuprofen toxicity in dogs. *Prev Vet Med* 1998;35:115–124.
- Radi ZA. Pathophysiology of cyclooxygenase inhibition in animal models. *Toxicol Pathol* 2009;37:34–46.
- Radi ZA, Khan NK. Comparative expression and distribution of c-fos, estrogen receptor alpha (eralpha), and p38 alpha in the uterus of rats, monkeys, and humans. *Toxicol Pathol* 2006a;34:327–335.
- Radi ZA, Khan NK. Effects of cyclooxygenase inhibition on the gastrointestinal tract. *Exp Toxicol Pathol* 2006b;58:163–173.
- Radi ZA, Kehrlí ME Jr, Ackermann MR. Cell adhesion molecules, leukocyte trafficking, and strategies to reduce leukocyte infiltration. *J Vet Intern Med* 2001;15:516–529.
- Radi ZA, Marusak RA, Morris DL. Species comparison of the role of p38 MAP kinase in the female reproductive system. *J Toxicol Pathol* 2009;22:109–124.
- Radi ZA, Heuvelman DM, Masferrer JL, Benson EL. Pharmacologic evaluation of sulfasalazine, FTY720, and anti-IL-12/23p40 in a TNBS-induced Crohn's disease model. *Dig Dis Sci* 2011;56:2283–2291.
- Raekallio MR, Hielm-Björkman AK, Kejonen J, Salonen HM, et al. Evaluation of adverse effects of long-term orally administered carprofen in dogs. *J Am Vet Med Assoc* 2006;228:876–880.
- Rainsford KD. The comparative gastric ulcerogenic activities of non-steroid anti-inflammatory drugs. *Agents Actions* 1977;7:573–577.
- Rainsford KD. An analysis of the gastro-intestinal side-effects of non-steroidal anti-inflammatory drugs, with particular reference to comparative studies in man and laboratory species. *Rheumatol Int* 1982;2:1–10.
- Rainsford KD. Ibuprofen: pharmacology, efficacy and safety. *Inflammopharmacology* 2009;17:275–342.
- Rainsford KD, Stetsko PI, Sirko SP, Debski S. Gastrointestinal mucosal injury following repeated daily oral administration of conventional formulations of indometacin and other non-steroidal anti-inflammatory drugs to pigs: a model for human gastrointestinal disease. *J Pharm Pharmacol* 2003;55:661–668.
- Rakoff-Nahoum S, Paglino J, Eslami-Varzaneh F, Edberg S, et al. Recognition of commensal microflora by Toll-like receptors is required for intestinal homeostasis. *Cell* 2004;118:229–241.
- Rampal P, Moore N, Van Ganse E, Le Parc JM, et al. Gastrointestinal tolerability of ibuprofen compared with paracetamol and aspirin at over-the-counter doses. *J Int Med Res* 2002;30:301–308.
- Raveendran NN, Silver K, Freeman LC, Narvaez D, et al. Drug-induced alterations to gene and protein expression in intestinal epithelial cell 6 cells suggest a role for calpains in the gastrointestinal toxicity of nonsteroidal anti-inflammatory agents. *J Pharmacol Exp Ther* 2008;325:389–399.
- Reed S. Nonsteroidal anti-inflammatory drug-induced duodenal ulceration and perforation in a mature rottweiler. *Can Vet J* 2002;43:971–972.
- Reimer ME, Johnston SA, Leib MS, Duncan RB, et al. The gastroduodenal effects of buffered aspirin, carprofen, and etodolac in healthy dogs. *J Vet Intern Med* 1999;13:472–477.
- Reuter BK, Davies NM, Wallace JL. Nonsteroidal anti-inflammatory drug enteropathy in rats: role of permeability, bacteria, and enterohepatic circulation. *Gastroenterology* 1997;112:109–117.

- Ricketts AP, Lundy KM, Seibel SB. Evaluation of selective inhibition of canine cyclooxygenase 1 and 2 by carprofen and other nonsteroidal anti-inflammatory drugs. *Am J Vet Res* 1998;59:1441–1446.
- Roberts ES, Van Lare KA, Marable BR, Salminen WF. Safety and tolerability of 3-week and 6-month dosing of Deramaxx (deracoxib) chewable tablets in dogs. *J Vet Pharmacol Ther* 2009;32:329–337.
- Roberts PJ, Morgan K, Miller R, Hunter JO, et al. Neuronal COX-2 expression in human myenteric plexus in active inflammatory bowel disease. *Gut* 2001;48:468–472.
- Robinson MG. New oral salicylates in the therapy of chronic idiopathic inflammatory bowel disease. *Gastroenterol Clin North Am* 1989;18:43–50.
- Rostom A, Muir K, DuBe C, Jolicoeur E, et al. Gastrointestinal safety of cyclooxygenase-2 inhibitors: a Cochrane Collaboration systematic review. *Clin Gastroenterol Hepatol* 2007;5:818–828.
- Roudebush P, Morse GE. Naproxen toxicosis in a dog. *J Am Vet Med Assoc* 1981;179:805–806.
- Rubio F, Seawall S, Pocelinko R, DeBarbieri B, et al. Metabolism of carprofen, a nonsteroid anti-inflammatory agent, in rats, dogs, and humans. *J Pharm Sci* 1980;69:1245–1253.
- Runkel R, Chaplin M, Boost G, Segre E, et al. Absorption, distribution, metabolism, and excretion of naproxen in various laboratory animals and human subjects. *J Pharm Sci* 1972;61:703–708.
- Ryan WG, Moldave K, Carithers D. Clinical effectiveness and safety of a new NSAID, firocoxib: a 1,000 dog study. *Vet Ther* 2006;7:119–126.
- Sato N, Kozar RA, Zou L, Weatherall JM, et al. Peroxisome proliferator-activated receptor gamma mediates protection against cyclooxygenase-2-induced gut dysfunction in a rodent model of mesenteric ischemia/reperfusion. *Shock* 2005;24:462–469.
- Sawant S, Snyman C, Bhoola K. Comparison of tissue kallikrein and kinin receptor expression in gastric ulcers and neoplasms. *Int Immunopharmacol* 2001;1:2063–2080.
- Sawaoka H, Tsuji S, Tsuji M, Gunawan ES, et al. Expression of the cyclooxygenase-2 gene in gastric epithelium. *J Clin Gastroenterol* 1997; S105–S110.
- Sawaoka H, Tsuji S, Tsuji M, Gunawan ES, et al. Involvement of cyclooxygenase-2 in proliferation and morphogenesis induced by transforming growth factor alpha in gastric epithelial cells. *Prostaglandins Leukot Essent Fatty Acids* 1999;61:315–322.
- Schattenkirchner M. Long-term safety of ketoprofen in an elderly population of arthritic patients. *Scand J Rheumatol Suppl* 1991;91:27–36.
- Scheiman JM. NSAIDs, gastrointestinal injury, and cytoprotection. *Gastroenterol Clin North Am* 1996;25:279–298.
- Scheiman JM. Gastrointestinal safety of cyclooxygenase-2 inhibitors. *Curr Pharm Des* 2003;9:2197–2206.
- Scheiman JM, Greenson JK, Lee J, Cryer B. Effect of cyclooxygenase-2 inhibition on human *Helicobacter pylori* gastritis: mechanisms underlying gastrointestinal safety and implications for cancer chemoprevention. *Aliment Pharmacol Ther* 2003;17:1535–1543.
- Scherkl R, Frey HH. Pharmacokinetics of ibuprofen in the dog. *J Vet Pharmacol Ther* 1987;10:261–265.
- Scherle PA, Ma W, Lim H, Dey SK, et al. Regulation of cyclooxygenase-2 induction in the mouse uterus during decidualization: an event of early pregnancy. *J Biol Chem* 2000;275:37086–37092.
- Schmassmann A, Peskar BM, Stettler C, Netzer P, et al. Effects of inhibition of prostaglandin endoperoxide synthase-2 in chronic gastro-intestinal ulcer models in rats. *Br J Pharmacol* 1998;123:795–804.
- Schnitzer TJ, Burmester GR, Mysler E, Hochberg MC, et al. Comparison of lumiracoxib with naproxen and ibuprofen in the Therapeutic Arthritis Research and Gastrointestinal Event Trial (TARGET), reduction in ulcer complications: randomised controlled trial. *Lancet* 2004;364:665–674.
- Schoen RT, Vender RJ. Mechanisms of nonsteroidal anti-inflammatory drug-induced gastric damage. *Am J Med* 1989;86:449–458.
- Schoenfeld P, Kimmey MB, Scheiman J, Bjorkman D, et al. Review article: nonsteroidal anti-inflammatory drug-associated gastrointestinal complications—guidelines for prevention and treatment. *Aliment Pharmacol Ther* 1999;13:1273–1285.
- Schrivver DA, White CB, Sandor A, Rosenthal ME. A profile of the rat gastrointestinal toxicity of drugs used to treat inflammatory diseases. *Toxicol Appl Pharmacol* 1975;32:73–83.
- Schwarz NT, Kalf J, Türler A, Engel BM, et al. Prostanoid production via COX-2 as a causative mechanism of rodent postoperative ileus. *Gastroenterology* 2001;121:1354–1371.
- Seibert K, Zhang Y, Leahy K, Hauser S, et al. Pharmacological and biochemical demonstration of the role of cyclooxygenase 2 in inflammation and pain. *Proc Natl Acad Sci USA* 1994;91:12013–12017.

- Seibert K, Zhang Y, Leahy K, Hauser S, et al. Distribution of COX-1 and COX-2 in normal and inflamed tissues. *Adv Exp Med Biol* 1997;400A:167–170.
- Seitz S, Boelsterli UA. Diclofenac acyl glucuronide, a major biliary metabolite, is directly involved in small intestinal injury in rats. *Gastroenterology* 1998;115:1476–1482.
- Seitz S, Kretz-Rommel A, Oude Elferink RP J, Boelsterli UA. Selective protein adduct formation of diclofenac glucuronide is critically dependent on the rat canalicular conjugate export pump (Mrp2). *Chem Res Toxicol* 1998;11:513–519.
- Sennello KA, Leib MS. Effects of deracoxib or buffered aspirin on the gastric mucosa of healthy dogs. *J Vet Intern Med* 2006;20:1291–1296.
- Shifflett DE, Jones SL, Moeser AJ, Blikslager AT. Mitogen-activated protein kinases regulate COX-2 and mucosal recovery in ischemic-injured porcine ileum. *Am J Physiol Gastrointest Liver Physiol* 2004;286:G906–G913.
- Shriver DA, Dove PA, White CB, Sandor A, et al. A profile of the gastrointestinal toxicity of aspirin, indomethacin, oxaprozin, phenylbutazone, and fentiazac in arthritic and Lewis normal rats. *Toxicol Appl Pharmacol* 1977;42:75–83.
- Sigthorsson G, Jacob M, Wrigglesworth J, Somasundaram S, et al. Comparison of indomethacin and nimesulide, a selective cyclooxygenase-2 inhibitor, on key pathophysiologic steps in the pathogenesis of nonsteroidal anti-inflammatory drug enteropathy in the rat. *Scand J Gastroenterol* 1998;33:728–735.
- Sigthorsson G, Simpson RJ, Walley M, Anthony A, et al. COX-1 and 2, intestinal integrity, and pathogenesis of nonsteroidal anti-inflammatory drug enteropathy in mice. *Gastroenterology* 2002;122:1913–1923.
- Silverstein FE, Faich G, Goldstein JL, Simon LS, et al. Gastrointestinal toxicity with celecoxib vs nonsteroidal anti-inflammatory drugs for osteoarthritis and rheumatoid arthritis: the CLASS study—a randomized controlled trial. Celecoxib Long-Term Arthritis Safety Study. *J Am Med Assoc* 2000;284:1247–1255.
- Singer II, Kawka DW, Schloemann S, Tessner T, et al. Cyclooxygenase 2 is induced in colonic epithelial cells in inflammatory bowel disease. *Gastroenterology* 1998;115:297–306.
- Singh G, Fort JG, Goldstein JL, Levy RA, et al. Celecoxib versus naproxen and diclofenac in osteoarthritis patients: SUCCESS-I Study. *Am J Med* 2006;119:255–266.
- Singh VP, Patil CS, Jain NK, Kulkarni SK. Aggravation of inflammatory bowel disease by cyclooxygenase-2 inhibitors in rats. *Pharmacology* 2004;72:77–84.
- Siraki AG, Chevaldina T, O'Brien PJ. Application of quantitative structure–toxicity relationships for acute NSAID cytotoxicity in rat hepatocytes. *Chem Biol Interact* 2005;151:177–191.
- Smith HW. Observations on the flora of the alimentary tract of animals and factors affecting its composition. *J Pathol Bacteriol* 1965;89:95–122.
- Somasundaram S, Sigthorsson G, Simpson RJ, Watts J, et al. Uncoupling of intestinal mitochondrial oxidative phosphorylation and inhibition of cyclooxygenase are required for the development of NSAID-enteropathy in the rat. *Aliment Pharmacol Ther* 2000;14:639–650.
- Soslow RA, Dannenberg AJ, Rush D, Woerner BM, et al. COX-2 is expressed in human pulmonary, colonic, and mammary tumors. *Cancer* 2000;89:2637–2645.
- Spangler RS. Gastrointestinal damage demonstrated with nabumetone or etodolac in preclinical studies. *Am J Med* 1993;95:35S–39S.
- Stanton ME, Bright RM. Gastroduodenal ulceration in dogs: retrospective study of 43 cases and literature review. *J Vet Intern Med* 1989;3:238–244.
- Steagall PV, Mantovani FB, Ferreira TH, Salcedo ES, et al. Evaluation of the adverse effects of oral firocoxib in healthy dogs. *J Vet Pharmacol Ther* 2008;30:218–223.
- Steagall PV, Moutinho FQ, Mantovani FB, Passarelli D, et al. Evaluation of the adverse effects of subcutaneous carprofen over six days in healthy cats. *Res Vet Sci* 2009;86:115–120.
- Stoltz RR, Harris SI, Kuss ME, LeComte D, et al. Upper GI mucosal effects of parecoxib sodium in healthy elderly subjects. *Am J Gastroenterol* 2002;97:65–71.
- Sturm A, Dignass AU. Epithelial restitution and wound healing in inflammatory bowel disease. *World J Gastroenterol* 2008;14:348–353.
- Sun WH, Tsuji S, Tsuji M, Gunawan ES, et al. Cyclo-oxygenase-2 inhibitors suppress epithelial cell kinetics and delay gastric wound healing in rats. *J Gastroenterol Hepatol* 2000;15:752–761.

- Szabó IL, Pai R, Jones MK, Ehring GR, et al. Indomethacin delays gastric restitution: association with the inhibition of focal adhesion kinase and tensin phosphorylation and reduced actin stress fibers. *Exp Biol Med (Maywood)* 2002;227:412–424.
- Takeuchi K, Okada M, Ebara S, Osano H. Increased microvascular permeability and lesion formation during gastric hypermotility caused by indomethacin and 2- deoxy-D-glucose in the rat. *J Clin Gastroenterol* 1990;12 Suppl 1:S76–S84.
- Takeuchi K, Ukawa H, Furukawa O, Kawauchi S, et al. Prostaglandin E receptor subtypes involved in stimulation of gastroduodenal bicarbonate secretion in rats and mice. *J Physiol Pharmacol* 1999;50:155–167.
- Takeuchi K, Miyazawa T, Tanaka A, Kato S, et al. Pathogenic importance of intestinal hypermotility in NSAID-induced small intestinal damage in rats. *Digestion* 2002;66:340–341.
- Takeuchi K, Tanaka A, Hayashi Y, Kubo Y. Functional mechanism underlying COX-2 expression following administration of indomethacin in rat stomachs: importance of gastric hypermotility. *Dig Dis Sci* 2004;49:180–187.
- Takeuchi K, Aihara E, Sasaki Y, Normura Y, et al. Involvement of cyclooxygenase-1, prostaglandin E2 and EP1 receptors in acid-induced HCO₃-secretion in stomach. *J Physiol Pharmacol* 2006;57:661–676.
- Takeuchi K, Tanaka A, Kato S, Amagase K, et al. Roles of COX inhibition in pathogenesis of NSAID-induced small intestinal damage. *Clin Chim Acta* 2010;411:459–466.
- Tanaka A, Araki H, Komoike Y, Hase S, et al. Inhibition of both COX-1 and COX-2 is required for development of gastric damage in response to nonsteroidal anti-inflammatory drugs. *J Physiol Paris* 2001;95:21–27.
- Tanaka A, Araki H, Hase S, Komoike Y, et al. Up-regulation of COX-2 by inhibition of COX-1 in the rat: a key to NSAID-induced gastric injury. *Aliment Pharmacol Ther* 2002a;16:90–101.
- Tanaka A, Hase S, Miyazawa T, Ohno R, et al. Role of cyclooxygenase (COX)-1 and COX-2 inhibition in nonsteroidal anti-inflammatory drug-induced intestinal damage in rats: relation to various pathogenic events. *J Pharmacol Exp Ther* 2002b;303:1248–1254.
- Tarnawski A, Stachura J, Durbin T, Sarfeh IJ, et al. Increased expression of epidermal growth factor receptor during gastric ulcer healing in rats. *Gastroenterology* 1992;102:695–698.
- Tatsuguchi A, Sakamoto C, Wada K, Akamatsu T, et al. Localisation of cyclooxygenase 1 and cyclooxygenase 2 in *Helicobacter pylori*-related gastritis and gastric ulcer tissues in humans. *Gut* 2000;46:782–789.
- Tibble JA, Sigthorsson G, Foster R, Bjarnason I. Comparison of the intestinal toxicity of celecoxib, a selective COX-2 inhibitor, and indomethacin in the experimental rat. *Scand J Gastroenterol* 2000;35:802–807.
- Tobin T, Chay S, Kamerling S, Woods WE, et al. Phenylbutazone in the horse: a review. *J Vet Pharmacol Ther* 1986;9:1–25.
- Tomlinson JE, Wilder BO, Young KM, Blikslager AT. Effects of flunixin meglumine or etodolac treatment on mucosal recovery of equine jejunum after ischemia. *Am J Vet Res* 2004;65:761–769.
- Traub JL, Gallina AM, Grant BD, Reed SM, et al. Phenylbutazone toxicosis in the foal. *Am J Vet Res* 1983;44:1410–1418.
- Traub-Dargatz JL, Bertone JJ, Gould DH, Wrigley RH, et al. Chronic flunixin meglumine therapy in foals. *Am J Vet Res* 1988;49:7–12.
- Tsubouchi R, Hayashi S, Aoi Y, Nishio H, et al. Healing impairment effect of cyclooxygenase inhibitors on dextran sulfate sodium-induced colitis in rats. *Digestion* 2006;74:91–100.
- Uchida M, Kawano O, Misaki N, Saitoh K, et al. Healing of acetic acid-induced gastric ulcer and gastric mucosal PGI₂ level in rats. *Dig Dis Sci* 1990;35:80–85.
- Ungaro R, Fukata M, Hsu D, Hernandez Y, et al. A novel Toll-like receptor 4 antagonist antibody ameliorates inflammation but impairs mucosal healing in murine colitis. *Am J Physiol Gastrointest Liver Physiol* 2009;296:G1167–G1179.
- Van Miert AS, Van Der Wal-Komproe LE, Van Duin CT. Effects of antipyretic agents on fever and ruminal stasis induced by endotoxins in conscious goats. *Arch Int Pharmacodyn Ther* 1977;225:39–50.
- Villar D, Buck WB, Gonzalez JM. Ibuprofen, aspirin and acetaminophen toxicosis and treatment in dogs and cats. *Vet Hum Toxicol* 1998;40:156–162.

- Villegas I, Alarcón de la Lastra C, Martín MJ, Motilva V, et al. Gastric damage induced by subchronic administration of preferential cyclooxygenase-1 and cyclooxygenase-2 inhibitors in rats. *Pharmacology* 2002;66:68–75.
- Vonderhaar MA, Salisbury SK. Gastroduodenal ulceration associated with flunixin meglumine administration in three dogs. *J Am Vet Med Assoc* 1993;203:92–95.
- Wallace JL, Keenan CM, Granger DN. Gastric ulceration induced by nonsteroidal anti-inflammatory drugs is a neutrophil-dependent process. *Am J Physiol* 1990;259:G462–G467.
- Wallace JL, McKnight W, Reuter BK, Vergnolle N. NSAID-induced gastric damage in rats: requirement for inhibition of both cyclooxygenase 1 and 2. *Gastroenterology* 2000;119:706–714.
- Watanabe T, Higuchi K, Kobata A, Nishio H, et al. Non-steroidal anti-inflammatory drug-induced small intestinal damage is Toll-like receptor 4 dependent. *Gut* 2008;57:181–187.
- Watanabe T, Nishio H, Tanigawa T, Yamagami H, et al. Probiotic *Lactobacillus casei* strain Shirota prevents indomethacin-induced small intestinal injury: involvement of lactic acid. *Am J Physiol Gastrointest Liver Physiol* 2009;297:G506–G513.
- Watson AD, Wilson JT, Turner DM, Culvenor JA. Phenylbutazone induced blood dyscrasias suspected in three dogs. *Vet Rec* 1980;107:239–241.
- Wax J, Clinger WA, Varner P, Bass P, et al. Relationship of the enterohepatic cycle to ulcerogenesis in the rat small bowel with flufenamic acid. *Gastroenterology* 1970;58:772–780.
- Wight NJ, Gottesdiener K, Garlick NM, Atherton CT, et al. Rofecoxib, a COX-2 inhibitor, does not inhibit human gastric mucosal prostaglandin production. *Gastroenterology* 2001;120:867–873.
- Wolfe MM, Lichtenstein DR, Singh G. Gastrointestinal toxicity of nonsteroidal antiinflammatory drugs. *N Engl J Med* 1999;340:1888–1899.
- Wooten JG, Blikslager AT, Marks SL, Law JM, et al. Effect of nonsteroidal anti-inflammatory drugs with varied cyclooxygenase-2 selectivity on cyclooxygenase protein and prostanoid concentrations in pyloric and duodenal mucosa of dogs. *Am J Vet Res* 2009;70:1243–1249.
- Yesair DW, Callahan M, Remington L, Kensler CJ. Role of the entero-hepatic cycle of indomethacin on its metabolism, distribution in tissues and its excretion by rats, dogs and monkeys. *Biochem Pharmacol* 1970;19:1579–1590.
- Yokota A, Taniguchi M, Takahira Y, Tanaka A, et al. Rofecoxib produces intestinal but not gastric damage in the presence of a low dose of indomethacin in rats. *J Pharmacol Exp Ther* 2005;314:302–309.
- Yoshizawa T, Watanabe S, Hirose M, Yamamoto J, et al. Effects of growth factors on aspirin-induced inhibition of wound repair in a rabbit gastric epithelial cell model. *Aliment Pharmacol Ther* 2000;Suppl 1: 176–182.
- Zhang L, Lu YM, Dong XY. Effects and mechanism of the selective COX-2 inhibitor, celecoxib, on rat colitis induced by trinitrobenzene sulfonic acid. *Chin J Dig Dis* 2004;5:110–114.
- Zinkievich JM, George S, Jha S, Nandi J, et al. Gastric acid is the key modulator in the pathogenesis of NSAID-induced ulceration in rats. *Clin Exp Pharmacol Physiol* 2010;37:654–661.

BONE–TENDON–LIGAMENT SYSTEM

INTRODUCTION

The skeletal system plays an essential role in providing mechanical support for body stature and locomotion, protecting vital body organs, and maintaining mineral homeostasis. A healthy skeleton must be maintained by constant bone modeling to carry out these crucial functions throughout life (Feng and McDonald, 2011). Musculoskeletal pain treatment is essential for improving healing of traumatic injuries and surgical procedures, and for improving patients' quality of life (O'Conner and Lysz, 2008). Cyclooxygenases (COX-1 and COX-2) are rate-limiting enzymes that catalyze the conversion of arachidonic acid to prostaglandins (PGs). COX-2 is induced at sites of inflammation, injury, and pain (Fig. 2-1) (Radi and Khan, 2005; Radi, 2009). Thus, COX inhibitors such as conventional nonselective NSAIDs (ns-NSAIDs) and COX-2 selective NSAIDs (COX-2 s-NSAIDs) are used to treat musculoskeletal pain, including postsurgical orthopedic analgesia. It has been hypothesized that NSAIDs can modulate bone, ligament, or tendon healing by modulating PG production (O'Conner and Lysz, 2008). The majority of evidence to support such hypotheses has been derived from nonclinical studies in various animal models, as no well-controlled large-scale clinical or epidemiological studies have been conducted (Radi and Khan, 2005).

In this chapter we examine nonclinical and clinical literature data on PG metabolism in the skeleton and NSAID pathophysiological impact on bone, ligament, and tendon healing.

COMPARATIVE PHYSIOLOGICAL AND ANATOMICAL ASPECTS OF THE SKELETON

The skeletal system consists of the bones of the skull, thorax, and vertebral column, which form the axial skeleton, and the bones of the upper and lower extremities, which form the appendicular skeleton. The long appendicular bones and the vertebral bodies are divided anatomically into four regions: (1) epiphysis, (2) metaphyseal growth plates (physis), (3) metaphysis, and (4) diaphysis. The skeleton is

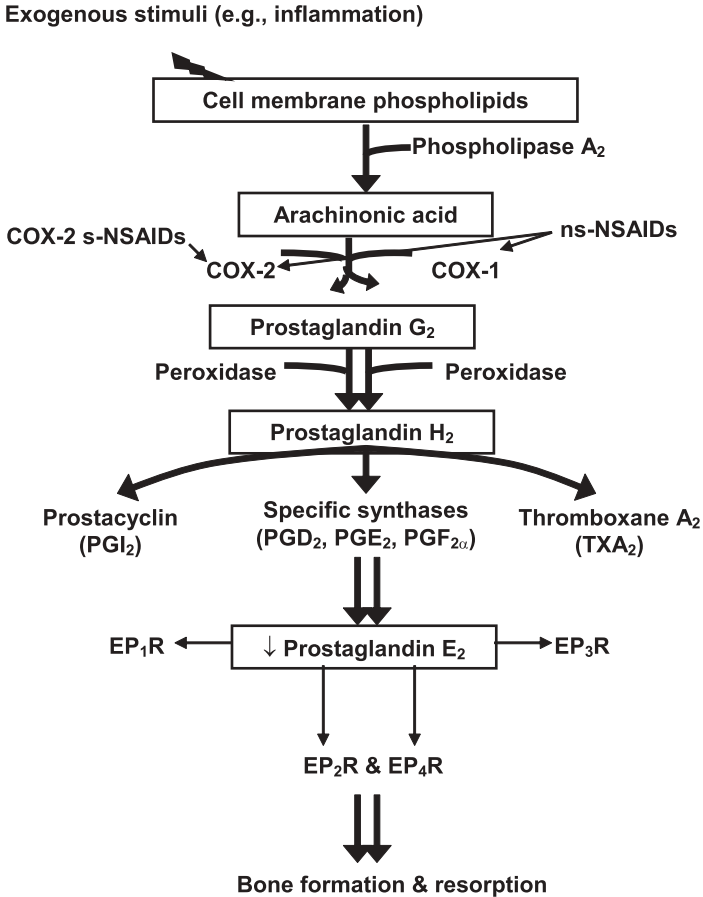


FIGURE 2-1 Role of prostaglandins (PGs) in bone metabolism in health and disease and effects of ns-NSAIDs and COX-2 s-NSAIDs. Following an exogenous stimulus (e.g., inflammation), cell membrane phospholipid is liberated to arachidonic acid (AA) by phospholipase A₂. Both COX-1 and COX-2 catalyze the conversion of AA into various PGs. PGE₂ is the most abundant PG produced by osteoblastic cells. PGE₂ interacts with four receptor types (EP₁R, EP₃R, EP₂R, and EP₄R), of which EP₂R and EP₄R stimulate bone formation and resorption. COX-1 is expressed constitutively by osteocytes and osteoblasts, while COX-2 expression is up-regulated during the initial stages of bone repair or under inflammatory or neoplastic conditions. Nonselective NSAIDs (e.g., carprofen, etodolac, flunixin meglumine, ketoprofen, indomethacin, meloxicam, phenylbutazone) inhibit COX-1 and COX-2, whereas COX-2 s-NSAIDs (e.g., celecoxib, lumiracoxib, parecoxib) spare COX-1 and inhibit only COX-2. (Reprinted with kind permission from Springer Science & Business Media: Z. A. Radi and N. K. Khan, *Inflammation Research*, 54(9), pp. 358–366. Copyright © 2005.)

composed of a dense cortical shell with a bone marrow space that contains trabecular bone and bone marrow elements. In addition, the skeleton is a metabolically active and dynamic organ that stores minerals (i.e., calcium, phosphorus, and carbonate), is a binding site for toxic ions such as lead, and undergoes continuous remodeling throughout life (Raisz, 1999a). There are two types of bones: cancellous and compact. Both are formed in layers and thus are called lamellar bone. Cancellous (spongy) bone is found in the interior of bones and is composed of trabeculae. Compact (cortical) bone has a densely packed calcified matrix. Bone is organized into osteons or haversian systems in the compact bone. Physical forces on the skeleton can lead to deformations and pathological conditions. This was recognized in the nineteenth century as Wolff's law, which is also called the "law of bone transformation" (Hert, 1990). Wolff's law, conceived in 1892 by Julius Wolff, a German anatomist, states that healthy bone will adapt to an applied force and loading stress. If loading on a particular bone increases, the bone will remodel itself over time to overcome such stress. The internal architecture of bone trabeculae undergoes adaptive changes, followed by secondary changes to the external cortical portion of the bone (Freiberg, 1902). This theory is known today as bone modeling and remodeling. Bone remodeling is the restructuring process of existing bone, which is in constant resorption and formation. Bone remodeling is vital for the structural and metabolic integrity of the skeleton. In aged rats, remodeling takes place in vertebral and tibial cancellous bone (Erben, 1996). Growth of the epiphysis contributes to the overall bone length. Growth of long bones depends on a functional metaphyseal growth plate (physis). The metaphyseal growth plate consists of hyaline cartilage and can be divided into three anatomical zones: resting or reserve, proliferative, and hypertrophic. The resting zone serves as a source of cells for the proliferating zone.

There are species differences in skeleton growth dynamics. In a nonhuman primate model (cynomolgus macaques), the status of full-thickness chondral defect repair was evaluated at different time points after microfracture (Gill et al., 2005). The chondral defects were created on the femoral condyles and trochlea of animals and evaluated by gross and histological examination at 6 and 12 weeks. At 6 weeks, there was limited chondral repair and ongoing resorption of subchondral bone. By 12 weeks, the defects were filled completely and showed more mature cartilage and bone repair. Thus, significant improvements in the extent and quality of cartilage repair were observed at the 6- to 12-week time points after microfracture in nonhuman primates (Gill et al., 2005).

The growth plate is thickest when there is rapid growth and becomes thin when growth slows. In larger mammals, growth plates close (become entirely replaced by bone) at skeletal maturity and longitudinal growth diminishes. In humans and rabbits, the growth plate is resorbed completely following puberty, resulting in fusion of the epiphysis to the metaphysis. This process of physal closure is primarily under the control of estrogen in both males and females (Weise et al., 2001). Rats and mice, however, maintain a growth plate until old age. Bone growth rate in rats increases between 1 and 5 weeks, then declines until skeletal maturity, which is achieved at approximately 11 to 13 weeks (Kember, 1973; Hunziker and Schenk, 1989). During the period of rapid growth (up to 5 weeks),

the height of the growth plate is greatest, whereas during the period when growth slows (8 to 16 weeks), the height of the growth plate decreases progressively (Roach et al., 2003). Some bones in the rat skeleton retain lifelong growth and do not fuse their epiphyses (Dawson, 1925). Many long bone epiphyseal growth plates in male rats remain open until 30 months of age (Dawson, 1925). In contrast, bone elongation at other skeleton sites, such as the proximal tibia and distal tibia, ceases at 15 and 3 months of age, respectively, in female rats (Dawson, 1925; Ke et al., 1993; Erben, 1996).

In humans, the mechanical properties of cortical bone specimens from human femora and tibiae were determined in terms of tension, torsion, and compression for a population ranging in age from 21 to 86 years (Burstein et al., 1976). No significant differences were found in the mechanical properties of males and females. Tibial bone had higher values of ultimate strength, stiffness, and ultimate strain than those for femoral bone. Consistent decreases with age of all mechanical properties except plastic modulus were found in the femoral but not in the tibial bone. No consistent significant differences in tension properties were found in specimens from normal, osteoporotic, and corticosteroid-treated persons. In addition, tensile testing to failure was carried out on 235 tensile cortical specimens (five per bone) that had been machined from 47 femora from human calvera (McCalden et al., 1993). The donors ranged in age from 20 to 102 years at the time of death. After mechanical testing, the porosity, mineralization, and microstructure were examined. Linear regression analysis showed that mechanical properties deteriorated markedly with age. Ultimate stress, strain, and energy absorption decreased by 5, 9, and 12% per decade, respectively. The porosity of bone increased significantly with age, whereas the mineral content was not affected. Microstructural analysis demonstrated that the amount of haversian bone increased with age. This demonstrates the importance of age-related changes in porosity to the decline in mechanical properties. Changes in porosity accounted for 76% of the reduction in strength (McCalden et al., 1993). Mineral content did not play a major role. Thus, the quantitative changes in aging bone tissue, rather than the qualitative changes, influence the mechanical competence of bone.

Another study analyzed iliac bone histomorphometric data from 58 healthy male and female subjects aged 1.5 to 23 years (Parfitt et al., 2000). There was a significant increase with age in core width, with corresponding increases in both cortical width and cancellous width. In cancellous bone there were increases in bone volume and trabecular thickness but not in trabecular number, wall thickness, interstitial thickness, and inferred erosion depth. Mineral apposition rates declined on the periosteal envelope and on all subdivisions of the endosteal envelope. The active osteoblast life span increased substantially. The bone formation rate was almost eight times higher on the outer than on the inner periosteum, and more than four times higher on the inner than on the outer endocortical surface. On the cancellous surface, the bone formation rate and activation frequency declined (Parfitt et al., 2000).

Age can also influence skeleton growth, and aging has been shown to diminish bone blood flow in rats and humans (Prisby et al., 2007). For example, blood flow was measured in conscious young adult (4 to 6 months old) and aged (24

to 26 months old) male Fischer 344 rats using radiolabeled microspheres. Blood flow of femurs in aged rats was 21% and 28% lower in the proximal and distal metaphyses, respectively, and 45% lower in the diaphyseal marrow (Prisby et al., 2007). Growth plates of femurs and tibiae in old Wistar rats 62 to 80 weeks old were compared to those from young rats 2 to 16 weeks old. Four categories of growth plate morphology were present in the old rats that were not present in younger rats: (1) formation of a bone band parallel to the metaphyseal edge of the growth plate; (2) extensive areas of acellularity, which were resistant to resorption and/or remodeling; (3) extensive remodeling and bone formation within cellular regions of the growth plate; and (4) direct bone formation by former growth plate chondrocytes (Roach et al., 2003). In a femoral fracture healing mouse model, healing was evaluated in mice either 7 to 9 or 52 to 56 weeks old. Aging in these mice was associated with a decreased rate of chondrogenesis, bone formation, callus vascularization, delayed remodeling, and altered expression of genes involved in bone repair and remodeling (Naik et al., 2009).

There are gender differences in skeleton dynamics. The dynamics of femoral midshaft collagen turnover was examined in adult humans. Males have a lower turnover rate than females when older but have a higher turnover rate when younger (Hedges et al., 2007). Male and female human femur cortical bone specimens were studied to determine if there are gender- and age-related differences. The degree of tissue mineralization decreased significantly with age in females but did not change in males. Total bone mineralization was higher in females than in males until 50 years of age but was lower in elderly females than in elderly males. Mineralization of osteons varied significantly with gender and age. Thus, in females, mineralization started at a higher level than in males but was lower in the sixth decade, falling below the level in males. Mineralization was far more stable throughout life in males (Bergot et al., 2009). A mutation in low-density lipoprotein receptor–related protein 5 (LRP5) has been shown to increase bone mass and density in humans and animals. Interestingly, within LRP5 mutant mice, there were significant gender-related differences in some of the trabecular bone structural parameters at various bone sites (distal femur, femoral neck, and vertebral body). However, unlike trabecular structural parameters, the gender-specific differences were not found in the trabecular strength of LRP5 transgenic mice (Dubrow et al., 2007). Gender can have an impact on NSAID elimination. For example, the elimination time for celecoxib in female rats is much longer than that in male rats (14 versus 4 h) (Paulson et al., 2000). This pharmacokinetic difference would affect drug concentration in the blood and should be taken into consideration when designing fracture-healing experimental studies in rodents.

Additionally, there are anatomical differences in the skeleton that can affect the rate of bone healing, such as vascular histology (e.g., the femur and mandible are more highly vascularized than the fibula), biomechanics (e.g., quadrupeds versus bipeds), wounding and healing histology and responses, and bone histomorphology (Auer et al., 2007). The base structure of the cortex in dogs and humans is composed of secondary osteons, whereas the sheep cortex is comprised predominantly of lamellar bone. However, during bone healing and remodeling, secondary osteons are activated in all of these species (Auer et al., 2007). Both animals and human

individuals have very different base levels of bone mass. Thus, genotype may influence specific structural and material properties (Judex et al., 2002). For example, material properties may differ by as much as 200% in different laboratory mice strains relative to structural morphology (Auer et al., 2007). There is significant genetic variation in the femur cross-sectional area, density, and mechanical properties between inbred mouse strains (Wergedal et al., 2005). Different anatomical sites may also influence the pattern of repair. This is multifactorial, partly because of the unique mechanobiology of different skeletal bones and partly as a consequence of biological differences (Auer et al., 2007). For example, the metacarpal and metatarsal bones of small ruminants are fused bones with minimal soft tissue coverage. Tendons and ligaments are found on the dorsal and palmar/plantar aspects of this bone. The tibia has a bone anatomy that provides a subcutaneous surface craniomedially and muscle cover laterocaudally. By contrast, the femur is predominantly covered by muscle on all aspects (Auer et al., 2007).

Healing within specific bones may also differ at bone anatomical sites with predominantly cortical healing at diaphyseal sites, and cancellous healing at metaphyseal sites (Auer et al., 2007). The extent of cancellous bone also differs between species and is generally limited in relation to the extent seen in humans. Bony defects of a size that will not heal during the lifetime of the animal may be termed critical size defects. Experiments on critical-size bone defects demonstrated species-dependent healing (Schmitz and Hollinger, 1986). A 4-mm circular craniomandibular bone defect in mice and 8-mm defect in rats are often both nonhealing without therapeutic intervention at 12 to 24 weeks. However, an 8-mm-diameter defect in a larger animal model (e.g., rabbit, dog, and sheep) will heal spontaneously since the surrounding soft tissue and remaining perimeter bone interfacial area are better able to supply signals and regenerative milieu to this relatively smaller defect volume. Critical-size calvarial defects increase to 17- to 35-mm diameters in larger animals (guinea pigs, rabbits, dogs, and sheep). Seemingly, the linear dimensions of a critical defect in bone do not translate simply across models, nor to humans, nor across different bone defect sites (e.g., cranial to long bone) (Auer et al., 2007). Additionally, the anatomical site of a critical defect has an effect on its size and, therefore, on possible nutrient transport limitations to healing. An 8-mm-diameter circular defect in rat parietal bones will heal spontaneously, whereas an 8-mm-diameter circular defect in the human parietal bone will not. These wound-site transport scaling effects also have a profound impact on the delivery of exogenous therapeutic and biotechnology components (living cells, growth factors, drugs) to fracture or defect sites (Auer et al., 2007).

The likelihood of surrounding soft tissue prolapse into the bone wound site as a function of increasing size can pose a problem during bone healing. The amount of repair and the time required to accomplish repair of 4-cm segmental fibular transplant in adult male dogs were determined at 2 to 48 weeks after transplantation by torsional stress testing, microradiography, and tetracycline labeling. The transplanted cortical bone was greatly weakened at 6 weeks to six months but was nearly normal at one year. The strength of the transplant appeared to be related to the amount of porosity of the matrix rather than to the quality or completeness of the biological repair. The repair was ordered rather than random. The

initial resorption caused increased porosity, which was slowly offset by apposition of new bone, a process that was dependent on general skeletal metabolic activity (Enneking et al., 1975). This effect extends beyond mammalian species in larger bone wounds relative to wound size. Relatively larger bone volumes will regenerate in rodents and amphibians (e.g., newt) compared to higher mammalian species (Auer et al., 2007). Animal physical activity levels should also be considered and quantified where possible, as it also modulates the bone repair process (Connolly et al., 2003). It was demonstrated that a femoral fracture mouse model that moved more had larger external calluses containing more cartilage and demonstrated lower torsional stiffness at the same time point (Connolly et al., 2003).

ROLE OF PROSTAGLANDINS IN SKELETON METABOLISM

The skeleton structural elements include bone cells (osteoclasts and osteoblasts), bone matrix [collagen fibers, bone morphogenic proteins (BMPs), and glycoproteins], and minerals. Osteoblasts express the receptor activator of nuclear factor κ B ligand (RANKL), which interacts with RANK expressed on osteoclasts to stimulate the formation of osteoclasts. Osteoprotegerin (OPG) is a secreted protein that is produced and released by activated osteoblastic cells. In 1965, Marshall Urist pioneered the concept of the presence of a substance naturally present in bone that is responsible for its regeneration and repair, called BMP, which is also known as osteogenic protein (OP) (Urist, 1965). BMPs are members of the transforming growth factor beta (TGF β) gene superfamily of growth and differentiation factors. Members of the BMP family were originally cloned and characterized by their ability to induce ectopic bone formation. The action of BMPs is mediated through receptor kinases and transcription factors called Smads (Vaibhav et al., 2007). BMPs are pleiotropic regulators mediating various sequential cellular responses: chemotaxis of cells, mitosis and proliferation of progenitor cells, differentiation into chondroblasts, cartilage calcification, vascular invasion, bone formation, remodeling and bone marrow differentiation. Sixteen different proteins (BMP-1 through BMP-16) have been identified. Of these various cloned BMPs, the bone inductive ability of BMP-7 and BMP-2 has been well characterized. Numerous studies have been conducted on large critically sized diaphyseal segmental defects in rats, rabbits, dogs, sheep, and nonhuman primates to evaluate the osteoinductive properties of BMPs. In these nonclinical studies it was observed that implantation of the BMPs with carrier matrices in bone defects led to biomechanically and biologically sound bone formation (Vaibhav et al., 2007). Furthermore, both BMP-7 and BMP-2 have been shown to have clinical utility in the healing of nonunion fractures (Govender et al., 2002; Dimitriou et al., 2005). The interaction between NSAIDs and the bone anabolic BMP-7 pathway was assessed in a study in C57BL/6 mice where BMP-7 expression and healing of fractures of the right femora were evaluated (Spiro et al., 2010). Each mouse was implanted with a 21-day-release pellet containing 2.5 mg diclofenac/pellet (5 mg diclofenac/kg body weight per day; the constant blood level of diclofenac is 0.238 μ g/mL). Contact x-rays were performed on all mice 5, 10,

15, and 20 days after BMP-7 implantation. At day 20 after implantation, all mice were euthanized, and radiographic, micro computed tomographic, histologic, and histomorphometric analyses were performed on ectopic bone nodules. Immunohistochemical analyses of fracture callus sections on days 10, 15, and 20 after surgery showed high expression of COX-2 and BMP-7 in osteoblasts, chondrocytes, and fibrous tissue of the fracture callus in both groups. This coexpression of COX-2 and BMP-7 indicated a possible role of both proteins during the fracture-healing process. Analyses of the fractured femora at day 20 following surgery revealed impairment of fracture healing due to diclofenac treatment. The callus bone volume per tissue volume was decreased significantly in diclofenac-treated mice compared to controls (Spiro et al., 2010).

It has been demonstrated, using human mesenchymal stem cells, that PGE₂ increases BMP-2 expression via binding to the EP₄ receptor (Arikawa et al., 2004). BMP-2 is used clinically to stimulate bone formation and accelerate repair. In an *in vitro* study, the effects of BMP-2 and PGE₂ on the expression of RANKL and OPG mRNA in bone marrow cultures from mice were assessed on days 4 to 6, prior to the peak of osteoclast formation (Blackwell et al., 2009). BMP-2 alone showed no effect on RANKL mRNA. Although BMP-2 decreased OPG mRNA 32 to 54% compared with the control, the RANKL/OPG ratio was not increased significantly. Treatment with PGE₂ both increased RANKL mRNA and decreased OPG mRNA compared with the control, resulting in an increased RANKL/OPG ratio. BMP-2 in combination with PGE₂ resulted in small, nonsignificant increases in RANKL and decreases in OPG compared with PGE₂ alone. However, the RANKL/OPG ratio was increased by BMP-2 and PGE₂ compared with PGE₂ alone by $64 \pm 29\%$ on day 6 in the experiment (Blackwell et al., 2009). Therefore, BMP-2 can increase osteoclast formation in response to PGE₂ by increasing the RANKL/OPG ratio in osteoblasts. This is supported by a study in a mouse collagen-induced arthritis model in which celecoxib was given orally at doses of 16 and 75 mg/kg. Celecoxib suppressed arthritis-related increase in bone resorption at low and high doses and prevented trabecular bone mass reduction at high doses. In addition, reduction in osteoclast surface number and suppression of osteoclast development in bone marrow through inhibition of the RANKL/OPG ratio, and IL-6 mRNA expression in inflammatory synovial tissue was noted (Taketa et al., 2008).

The bone remodeling cycle is divided into four phases: activation, resorption, reversal, and formation (Raisz, 1999a). Osteoblasts and osteoclasts, the most important contributors to the bone remodeling cycle, produce PGs, which are shown to modulate their function in normal bone metabolism and in bone healing (Okada et al., 2000, 2003; Raisz et al., 2001; Li X. et al., 2002; Gajraj et al., 2003). For example, in an *in vitro* model using rat femora, changes in PG synthesis and concentration were correlated with changes in the quantity of trabecular regeneration and acceleration of bone healing (Sun et al., 1999). Osteoblasts and osteoclasts cooperate to maintain bone homeostasis. Osteoblasts are mature “bone-building” metabolically active cells that differentiate from mesenchymal stem cells and are responsible for new bone formation and osteoid (unmineralized organic bone matrix that subsequently undergoes mineralization) secretion. Osteoclasts are multinucleated cells that arise from hematopoietic monocyte/macrophage precursors

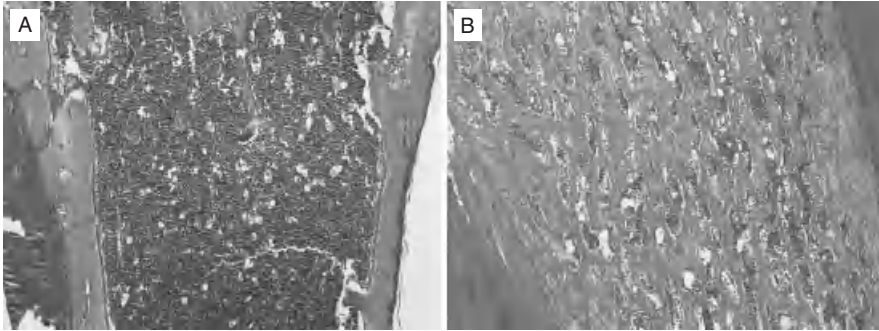


FIGURE 2-2 (A) Histopathology of a bone section from a control mouse. Hematoxylin and eosin (H&E) stain, original magnification $\times 10$. (B) Histopathology of a bone section from an *op/op* (osteopetrosis) mouse. Note that the bone marrow cavity is effaced by interweaving thick bony trabeculae consistent with osteopetrosis, H&E, original magnification $\times 20$.

and are the major resorptive cells of bone. Osteoclasts release hydrolytic enzymes that dissolve the bone matrix. Thus, osteoclasts are “bone-chewing” cells that function in the resorption of bone, removing the mineral and the organic matrix.

Macrophage colony-stimulating factor (M-CSF) induces monocyte/macrophage differentiation to osteoclasts and is critical to osteoclast replication and bone resorption (Radi et al., 2009, 2011). Thus, mice lacking M-CSF develop osteopetrosis, increased bone mass, in which affected bones are dense and lack a medullary cavity (Fig. 2-2) (Radi et al., 2009). Osteopetrosis also occurs in humans, dogs, horses, sheep, and cattle. The basis for osteopetrosis is the failure of osteoclasts to resorb bone and shape trabeculae. RANKL has been shown to be a marker and a mediator of bone loss in collagen-induced arthritis (CIA) models in rats (Stolina et al., 2005). RANKL-knockout mice develop severe osteopetrosis, a defect in tooth eruption, and completely lack osteoclasts as a result of an inability of osteoblasts to support osteoclastogenesis (Kong et al., 1999). RANKL was found to be expressed in activated T-cells, lymph nodes, the spleen, the thymus, intestinal lymphoid patches, and immature thymocytes (Anderson et al., 1997; Wong et al., 1997). Interestingly, RANKL-deficient mice lack all lymph nodes but have normal splenic structure and Peyer’s patches (Kong et al., 1999). OPG inhibits osteoblast–osteoclast interaction, and OPG treatment reverses bone loss. OPG-deficient mice display severe osteoporosis and a decrease in total bone density characterized by severe trabecular and cortical bone porosity, marked thinning of the parietal bones of the skull, and a high incidence of fractures (Bucay et al., 1998). In a CIA model in rats, OPG effectively prevented joint destruction, even though it had no impact on the inflammatory aspects of the disease. In addition, OPG depleted osteoclast numbers by over 75% and diminished bone erosion scores by over 60% (Romas et al., 2002).

Bone cells can produce several growth factors that affect bone formation or resorption, such as insulin growth factor 1 (IGF-1), fibroblast growth factor 2 (FGF-2), platelet-derived growth factor (PDGF), vascular endothelial growth factor (VEGF), and TGF β (Raisz, 1999a). The expression of VEGF in periodontal

disease and after COX-2 inhibition, using meloxicam, was investigated in Wistar rats (Oliveira et al., 2008). VEGF expression was significantly higher at diseased sites than at healthy sites. A reduction in alveolar bone resorption was observed after meloxicam treatment with a positive correlation between COX-2 and VEGF mRNA in gingival tissues and periodontal disease. Meloxicam significantly reduced the increased mRNA VEGF expression in diseased tissues after 14 days of treatment. Therefore, VEGF plays an important role in the progression of periodontal disease, and COX-2 inhibitor therapy can modify the progression of experimentally induced periodontitis in rats by reducing VEGF expression and alveolar bone loss (Oliveira et al., 2008).

PGs play an important role in the pathophysiologic processes of bone metabolism. PGE₂ is the most abundant PG produced by osteoblastic cells, and plays many roles in bone metabolism. PGE₂ has been shown to add bone-to-bone envelopes and to induce woven bone formation (Jee and Ma, 1997). In addition, systemic administration of PGE₂ stimulated bone formation and increased bone mass in infants and animals (Ringel et al., 1982; Marks and Miller, 1988; Yang et al., 1993; Saponitzky et al., 1998). PGE₂ infusion in rabbits increased blood flow to the bone, bone marrow, and muscle of the lower limbs, except in the osteotomy area (Keller et al., 1991). The release of PGE₂ and PGF from the tibiae of rabbits and the surrounding muscle *in vitro* after fracture and pinning, or pinning alone, has been compared to the release from unoperated tissues. The fractured tibiae released significantly more PGE₂ and PGF than did the control tibiae 3 to 14 days after the operation (Dekel et al., 1981). Furthermore, PGE₂ caused a dose-dependent stimulation of callus formation in rabbits (Keller et al., 1993). In dogs, the administration of PGE₂ increased the extent of mineralization on the bone surface of healing ribs, osteoid formation in all three envelopes, and the resorption surface in the cortical endosteal envelope, indicating accelerated remodeling (Shih and Norrdin, 1986; Norrdin and Shis, 1988). In rats, continuous systemic PGE₂ administration elevated metaphyseal cancellous bone mass to 3.5-fold that of the control (Ke et al., 1992). In dogs, subcutaneous administration of PGE₂ resulted in cancellous and cortical bone formation and increased skeletal turnover (High et al., 1987; Li et al., 1990).

In an *in vitro* study using OCCM-30 cells (a mouse cementoblast cell line), PGE₂ promoted cementoblast-mediated cementoclastogenesis by regulating the expression of RANKL and OPG via the EP₄ pathway (Oka et al., 2007). The effects of COX-2 expression regulation on calvarial osteoblastic proliferation and apoptosis was investigated *in vitro* using primary osteoblasts (POBs) that were cultured from calvariae of COX-2 wild-type (WT) and knockout (KO) mice. PGE₂ production and ALP activity were increased in WT cultures compared to KO cultures. In contrast, cell numbers were decreased in WT compared to KO cells by day 4 of culturing. Proliferation, measured on days 3 to 7 of culture, was twofold greater in KO than in WT POBs. There was no significant effect of COX-2 genotype on apoptosis under basal culture conditions on day 5 of culturing. Cell growth was decreased in KO POBs by the addition of the PGE₂ agonist and increased in WT POBs by the addition of NS398, a COX-2 s-NSAID. In contrast, differentiation and cell growth in marrow stromal cell (MSC) cultures were increased in MSCs from WT mice

compared to MSCs from KO mice, and exogenous PGE₂ increased cell growth in KO MSC cultures. Thus, PGs secondary to COX-2 expression decrease osteoblastic proliferation, at least in cultured calvarial mouse cells, but increase growth of osteoblastic precursors in MSC cultures (Xu et al., 2007). Physiologically, PGs may mediate the response to mechanical forces (Raisz et al., 1999b). In humans, impact loading was associated with an increased production of PG (Thorsen et al., 1996). Other possible roles for PGs in bone metabolism include stimulation of cAMP production and induction of COX-2, as demonstrated in mice osteoblasts (Sakuma et al., 2004). In pathological conditions, large amounts of PGE₂ have also been observed in chronic osteomyelitis and in osteoid osteoma, probably due to increased osteoblastic and osteoclastic activity (Plotquin et al., 1991; Mungo et al., 2002).

PGE₂ interacts with four receptor subtypes (EP₁R, EP₃R, EP₂R, and EP₄R), of which the latter two are shown to stimulate bone formation and bone resorption, as demonstrated in rat bone tissue and osteoblastic cells (Feyen et al., 1984; Kawaguchi et al., 1995; Lin et al., 1995; Jee and Ma, 1997; Wadleigh and Herschman, 1999; Suzawa et al., 2000; Weinreb et al., 2001). The skeletal phenotype of aged EP₄R-KO mice was studied and compared to the fracture healing in aged KO male mice versus WT mice (Li et al., 2005). There was no significant difference in body weight and femoral length between knockout KO and WT mice at 15 to 16 months of age. Radiographic bone analysis revealed lower bone mass in both axial and long bones of KO mice relative to WT mice. Microcomputed tomography images of the distal femurs showed thinner cortices, fewer trabeculae, and a deteriorated trabecular network in KO mice. Total bone content, trabecular content, and cortical content in the distal femur were lower in KO mice than in WT controls. Histomorphometric measurements showed that the trabecular bone volume and bone formation rate were significantly decreased, whereas osteoclast numbers on the trabecular, eroded, and endocortical surface were significantly increased in KO mice (Li et al., 2005). In addition, fracture healing was examined in KO and WT mice subjected to a transverse femoral fracture. Callus formation, the unorganized meshwork of woven bone that forms after a fracture, was significantly delayed in the fractured femurs of KO mice compared with those of WT mice. KO mice had significant decreases in total callus area, cartilaginous callus area, and bony callus area 2 weeks after a fracture. By 4 weeks, complete bony bridging was seen in WT mice but not in KO mice (Li et al., 2005). Some studies suggest that bone marrow stromal cells (BMSCs) play a major role in the anabolic effect of PGE₂ (Shamir et al., 2004). In a study in rats, a selective EP₄ antagonist, L-161,982, was used to investigate the effects on rat BMSCs *in vitro* and *in vivo*. *In vitro*, PGE₂ (100 nM) increased nodule formation and alkaline phosphatase (ALP) activity, a marker of bone formation, 1.5- to 2-fold in cultures of rat BMSCs. These effects were abolished by the EP₄ antagonist. Furthermore, PGE₂ increased the number of surviving adherent BMSCs by approximately 225%, and the EP₄ antagonist prevented this effect as well. The antagonist had no effect on basal levels of nodule formation and adherent cell number. *In vivo*, daily systemic administration of PGE₂ at 6 mg/kg for 2 weeks increased cancellous bone area (by approximately 50%) and increased nodule formation (measured as mineralized

area) in *ex vivo* stromal cultures by approximately 50%. Preadministration of the EP₄ antagonist at 10 mg/kg abrogated the increase in bone mass as well as the increase in nodule formation. The investigators conclude that PGE₂ stimulates osteoblastic commitment of BMSCs via activation of the EP₄ receptor (Shamir et al., 2004).

The sternum bone-healing effects after ONO-4819, an EP₄ agonist, was administered in a 300- μ g dose to diabetic Wistar rats was investigated. Sternum bone healing and incidence of sternal wound complications were evaluated 4 weeks after the operation. Sternum bone wound complications developed in five rats in the control group but in only one rat in the EP₄ group. Histological examination revealed an almost completely healed sternum filled with regenerated bone tissue only in the EP₄ group. Both bone mineral content and bone mineral density, as assessed with dual-energy x-ray absorptiometry, were higher in the EP₄ group than in the control group (Marui et al., 2006). Thus, EP₄ agonist accelerated sternal bone healing and decreased the incidences of sternal wound complications in diabetic rats. Another study investigated femur bone biomechanical properties of EP₄-KO transgenic female mice. EP₄-KO mice exhibited less structural (ultimate/yield load) and apparent material (ultimate/yield stress) strength in the femoral shaft and vertebral body than that in WT mice. Vertebral body stiffness and femoral neck ultimate load (structural strength) were marginally lower in the EP₄-KO than in the WT mice. In addition, the EP₄-KO mice had a smaller distal femur and vertebral bone volume/total volume trabecular thickness than that in the WT mice (Akhter et al., 2006).

Cultured calvarial cells from EP₄-KO mice had no increase in bone resorption when exposed to PGE₂ (Miyaura et al., 2000). Bone formation was induced in WT mice by infusion of an EP₄-selective agonist and not agonists specific for other EP subtypes (Yoshida et al., 2002). In a fracture-healing mouse model, COX-2-deficient (COX^{-/-}) mice showed delayed initiation and impaired endochondral bone repair, accompanied by a severe angiogenesis deficiency. Administration of an EP₄ agonist markedly improved the impaired healing, as evidenced by restoration of bony callus formation on day 14, a nearly complete reversal of bone formation, and an approximately 70% improvement in angiogenesis in the callus (Xie et al., 2009). In a study in 12-week-old rats, the effects of the administration of an EP₄ agonist, ONO-4819, on the healing of drill-hole injury in the femoral diaphysis bone was investigated. The rats were injected subcutaneously with the EP₄-agonist compound at 10 or 30 μ g/kg twice a day for 5, 7, 14, 21, and 28 days after the femoral bone injury was created (Tanaka et al., 2004). The regenerated cortical bone volume and content increased dose-dependently on days 14 and 21 following ONO-3819 treatment. In addition, the injured bone from the animals treated with a high dose of 30 μ g/kg of ONO-3819 had higher values of osteoclast surface and expression levels of osteocalcin and tartrate-resistant acid phosphatase (TRAP) mRNAs, an iron-containing protein that is highly expressed by osteoclasts, on day 14 day after treatment, and increased expression levels of EP₄, BMP-2, and RANKL mRNAs on day 7 day (Tanaka et al., 2004). In another study in rabbits, bioactive titanium plates were inserted into the tibia bone and examined histologically and biomechanically at 4,

8, and 16 weeks. An EP₄ agonist, ONO-AE-724, was administered systemically every 2 weeks after surgery. A low-dose group (10 µg/kg) and a high-dose group (100 µg/kg) were compared. The bonding strength of bioactive titanium in the EP₄-agonist groups was significantly higher than that in the control group at both 4 and 8 weeks, and enhanced bone remodeling and direct bonding around the bioactive titanium plates were observed only in the EP₄-agonist groups at 4 weeks. EP₄ agonist enhanced bone formation around the bioactive titanium plate and achieved early direct bone bonding (Onishi et al., 2008). An EP₂R agonist, CP-533,536, was delivered at doses of 0.3, 1 or 3 mg/kg into the bone marrow of the proximal tibial metaphysis of 6-week-old male rats by a single injection on day 1. The local anabolic bone effects were analyzed using peripheral quantitative computed tomography, bone histomorphometry, and biomechanical testing on day 7. The CP-533,536 dose-dependently stimulated local lamellar bone formation on trabecular, endocortical, and periosteal surfaces, and thus increased bone mineral content and bone strength at the injected site (Li et al., 2003).

The direct effects of selective EP₄ and EP₂ receptor (R) agonists with PGE₂ on the differentiation of cultured murine calvarial osteoblastic cells were investigated. Both the EP₄R agonist and PGE₂ increased alkaline phosphatase activity and osteocalcin mRNA levels in the osteoblastic cell cultures. The EP₂R agonist had a smaller effect. The investigators concluded that the anabolic effect of PGE₂ in calvarial osteoblastic cell cultures is largely mediated by activation of the EP₄R agonist, while activation of the EP₂R is less effective (Alander et al., 2006). In another study, the effects of the EP₂R agonist and PGE₂ on both calvarial primary osteoblasts (POBs) and marrow stromal cells (MSC) cultured from mice with deletion of one (Het) or both (KO) alleles of the EP₂R agonist were compared to their WT littermates. The 1-month-old mice used to provide cells in these studies did not show any significant differences in their femurs by static histomorphometry. EP₂R agonist enhanced osteoblastic differentiation as measured by ALP mRNA expression, and activity as well as osteocalcin, noncollagenous protein in bone extracellular matrix synthesized by osteoblastic cells, mRNA expression, and mineralization in the WT cell cultures from both marrow and calvariae. These effects were somewhat diminished in cultures from Het mice and abrogated in cultures from KO mice. PGE₂ effects were greater than those of the EP₂R agonist, particularly in POB cultures and were only moderately diminished in Het and KO cell cultures. Thus, activation of the EP₂R agonist is able to enhance differentiation of osteoblasts, and PGE₂ has an additional anabolic effect, probably mediated by the EP₄R (Choudhary et al., 2008a).

Prostaglandin E synthase (PGES) functions as the terminal enzyme in the biosynthesis of PGE₂ (Radi and Ostroski, 2007). The microsomal PGES-1 (mPGES-1) is known to play a critical role in the production of PGE₂ and is involved in various bone pathophysiological events (Yamakawa et al., 2008). Radiologic and histologic analyses were conducted on skeletons of mPGES-1-deficient mice and compared to WT mice. The mPGES-1-deficient mice had unaffected skeletal phenotypes or osteoarthritis under normal physiological conditions. In contrast, fracture healing was impaired by mPGES-1 deficiency, with half of the mice remaining in a bone fracture nonunion state after 21 days. Normal fracture

healing was restored by the reintroduction of mPGES-1. Further analyses revealed impaired chondrocytes proliferation in cartilage in mice with PGES-1 deficiency, at an early stage of fracture healing (Yamakawa et al., 2008).

Collectively, there is abundant evidence to support a significant role of PGs in bone metabolism in health and disease, which can be modulated by exogenous administration of PGs. PGE₂ and its receptors, EP₂R and EP₄R, appear to be the main contributors to bone metabolism and pathophysiological mechanisms.

THE PROCESS OF BONE HEALING AND POTENTIAL ROLE OF PROSTAGLANDINS

Bone healing is a dynamic process that involves various stages in which PGs and many other factors play an important role in completing the repair process (Radi and Khan, 2005). PGs can stimulate bone formation by increasing replication and differentiation of osteoblasts (Raisz, 1999b). Several studies in infants and experimental animals receiving systemic administration of PGE₂ have demonstrated the role of PGs in bone formation (Ringel et al., 1982; Marks and Miller, 1988; Yang et al., 1993; Jee and Ma, 1997; Suponitzky and Weinreb, 1998). Therefore, before examining the effects of ns-NSAIDs and COX-2 s-NSAIDs on the skeleton, a clear understanding of the pathophysiological process of bone healing and PG contributions to this process is a critical starting point. The bone-healing process can be subdivided into three phases: inflammatory response, bone resorption, and bone production (Fig. 2-3) (Radi and Khan, 2005).

Inflammatory Response

When the local blood supply is disrupted following bone fracture, several immediate events take place at the fracture line: hemorrhage and hematoma formation, hypoxia-mediated osteocyte necrosis, and clotting with fibrin mesh formation (Probst and Spiegel, 1997; Radi and Khan, 2005). Hematoma formation develops within the fracture site as a result of red blood cell extravasation (bleeding) and occurs acutely during the first few hours and days. The main function of this fracture hematoma is to prevent further hemorrhage via activation of platelets and the coagulation pathway and favors bone repair. The fracture hematoma microenvironment is rich in PGs, kinins, and noncollagenous proteins. Loss of stability decreased local oxygen, soft tissue injury, and ruptured vessels, and necrosis at the fracture site leads to an inflammatory response. The fracture site is sealed off by the fibrin mesh, which serves as a framework for inflammatory cell (macrophages, neutrophils, lymphocytes, and mast cells) infiltration and its by-products, such as cytokines (IL-1, IL-6, IL-18, TNF) and growth factors [platelet-derived growth factor (PDG), transforming growth factor 1 (TGFβ₁), fibroblast growth factor (FGF)] (Fig. 2-3A and B) (Einhorn, 1998; Radi and Khan, 2005). Platelets—disk-shaped anucleate cell fragments that are shed from megakaryocytes in the bone marrow into the bloodstream—are the first to arrive at the sites of bone fracture and they serve to control hemostasis (Probst and Spiegel, 1997). When vascular endothelium

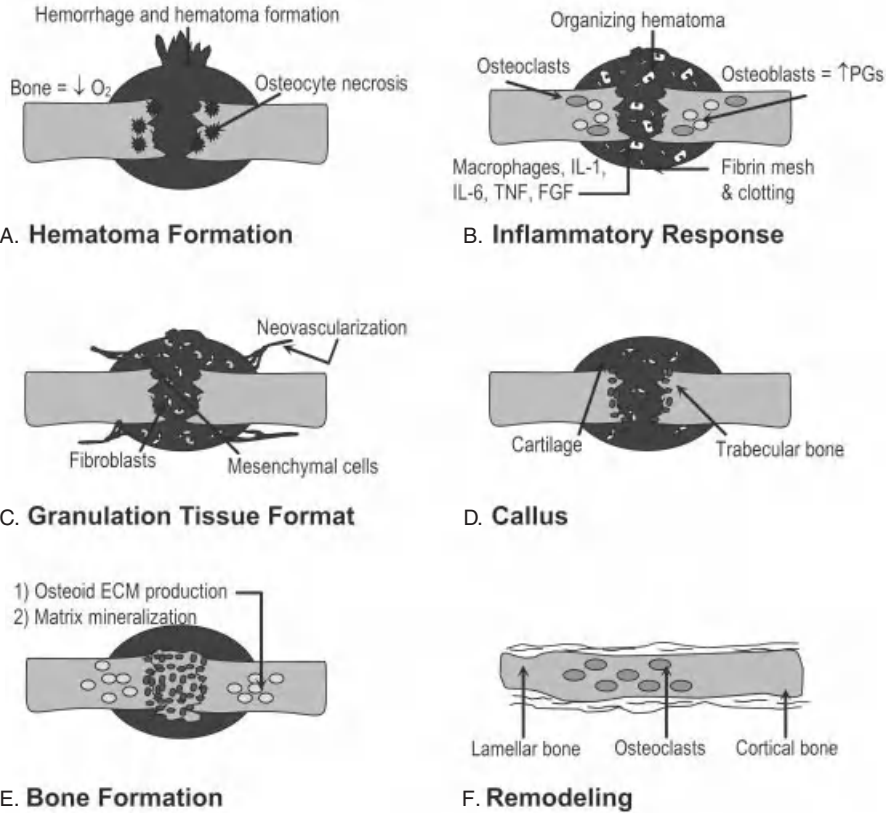


FIGURE 2-3 Sequence of events that occur during the process of bone healing. Immediately after bone fracture, there is hemorrhage with subsequent hematoma formation and osteocyte necrosis due to hypoxia (A). This is followed by an inflammatory response in which various inflammatory cells (e.g., macrophages), prostaglandins, cytokines (e.g., IL-6, TNF), and growth factors (e.g., FGF, PDGF) are released with fibrin mesh formation (B). Later, granulation tissue formation with fibroblast and mesenchymal cell migration and new capillary formation occurs (C). Bone resorption is then followed by cartilage and callus bone formation (D and E). In this process, osteoid extracellular matrix and matrix mineralization occur. Finally, bone formation and remodeling occurs (F). (Reprinted with kind permission from Springer Science & Business Media: Z. A. Radi and N. K. Khan, *Inflammation Research*, 54(9), pp. 358–366. Copyright © 2005.)

integrity is compromised and collagen in the subendothelium is exposed, platelets adhere to the exposed endothelium, a process leading to platelet activation and aggregation and release of such factors as PDGF, TGFβ, adenosine diphosphate (ADP), fibrinogen, and thromboxane A₂ (Probst and Spiegel, 1997). These factors contribute to the formation of a mature clot and stabilization of the primary hemostatic plug. In addition, this platelet aggregation process leads to increases in serum complement factors such as C5a, which possesses chemotactic activity for leukocytes leading to leukocyte infiltration into the fractured site. This process of

leukocyte trafficking is mediated by various adhesion molecules on leukocytes and vascular endothelial cells (Radi et al., 2001).

The first blood leukocytes to infiltrate the fractured site are neutrophils followed by monocytes, which differentiate into macrophages, and lymphocytes (Probst and Spiegel, 1997). Macrophages release various proteolytic enzymes, extracellular matrix proteins, and growth factors such as PDGF, IGF, and FGF. FGF leads to mesenchymal cell proliferation and stimulates fibroblasts and osteoblasts. FGFR-3 is a negative regulator of bone growth (Deng et al., 1996). Genetic disruption of the murine FGFR-3 results in prolongation of endochondral bone growth with expansion of the proliferating and hypertrophic zones of the growth plate (Colvin et al., 1996). The pathogenesis of achondroplasia, the most common form of human dwarfism, is due to a mutation in the FGFR-3 gene. Furthermore, PD176067, a reversible, selective ATP-competitive inhibitor of FGF receptor tyrosine kinase, was administered to mature (11 month old) female rats by gavage for 14 days at doses of 2.5, 5, and 10 mg/kg per day. Physeal dysplasia (distal femur, proximal tibia, and sternum) occurred in all drug-treated animals and was characterized by a dose-related increased thickness of the zones of chondrocyte proliferation and hypertrophy, and marked thickening of the zone of ossification. Cartilage hyperplasia was characterized by proliferation of chondrocytes along margins of the synchondrosis and subperiosteum of sternbrae (Brown et al., 2005). The inflammatory process, which peaks by 48 h and disappears by approximately 10 days, also helps immobilize the fractured bone by eliciting pain.

Proinflammatory stimuli and cytokines and growth factors release influence PG production, especially PGE₂ (Zhang et al., 2002; Gajraj, 2003; Gerstenfeld and Einhorn, 2004). PGs are produced abundantly by osteoblasts and are increased in fracture callus during the first 2 weeks following injury (Dekel et al., 1981; Gajraj, 2003; Gerstenfeld et al., 2003a). It was demonstrated that COX-2 mRNA levels showed peak expression during the first 2 weeks of fracture healing and then returned to basal levels by 3 weeks (Gerstenfeld et al., 2003b). The gene expression and role of COX-2 and inducible nitric oxide synthase (iNOS) in growth plate injury responses were analyzed. In addition, the effects of blocking COX-2 and iNOS activities with celecoxib and aminoguanidine, respectively, were assessed 2 days prior to and until 7 days after injury in a rat tibial growth plate injury model (Arasapam et al., 2006). Up-regulation of COX-2 expression was noted on days 1 and 4 and iNOS on day 1. Histological analysis of growth plate injury sites revealed significant reductions in inflammatory cell infiltrates (particularly neutrophils) on day 1 in treated groups compared to controls. While bony tissue proportions at injury sites were unaffected by either treatment, mesenchymal tissue proportions were larger, and bone remodeling appeared delayed, with a smaller bone marrow proportion on day 14 in both treatment groups. These findings suggest that COX-2 and iNOS mediate the injury-induced inflammatory response (Arasapam et al., 2006).

Furthermore, increased expression of cartilage-related (collagen-2, collagen-10, Sox-9) and bone-related molecules (osteocalcin, cbf α -1) suggested the involvement of both endochondral and direct bone formation mechanisms during bone repair (Arasapam et al., 2006). After the initial hematoma formation,

granulation tissue forms, which is characterized by neovascularization, mesenchymal cell migration, and ingrowth of fibroblasts and expression of several BMPs (Fig. 2-3C) (Radi and Khan, 2005). Hematoma and granulation tissue begin to develop into cartilaginous matrix, and chondrocyte proliferation and differentiation start to form fibrocartilage callus. In a mouse fracture-healing model, L-Sox5, Sox6, and Sox9, cartilage-related genes, were found to be involved in the activation and maintenance of chondrogenesis during fracture healing. In addition, enhanced chondrogenesis by BMP-2 was found to be mediated via an L-Sox5/Sox6/Sox9-dependent pathway (Usitalo et al., 2001).

Bone Resorption

The next phase is a proliferative and reparative phase that involves new capillary formation, a process called angiogenesis, and bony callus formation. Callus refers to an unorganized meshwork of woven bone that forms after a fracture. Several of the growth factors released by inflammatory cells contribute to the angiogenesis process. Bone is subject to continuous breakdown (resorption) by osteoclasts and rebuilding (formation) by osteoblasts in order to fulfill its functions (Radi and Khan, 2005). Osteoblasts secrete the organic matrix of bone, which is composed of approximately 90% of collagen I (Probst and Spiegel, 1997). Bone matrix contains growth factors such as IGF, PDGF, and TGF β in high concentrations. These growth factors are likely to exert anabolic effects on growth and/or maintenance of bone and cartilage tissue (Probst and Spiegel, 1997). During bone healing, osteoclasts release proteases that dissolve bone mineral matrix and collagen, remove damaged bone, and release matrix-bound growth factors. PGs increase the number and activity of osteoclasts and subsequent bone resorption (Raisz, 1999b). PGE₂ is the most potent agonist that stimulates bone resorption and formation (Yang et al., 1993). In addition, other PGs, such as PGI₂ and TXA₂ analogs, are shown to increase the number of multinuclear osteoclasts, osteoclastic bone resorption, and rate of orthodontic tooth movement, as noted in the rat, suggesting a role for these PGs in connective tissue remodeling (Gurton et al., 2004).

Parathyroid hormone (PTH) is a potent stimulator of osteoclastic bone resorption. Osteoblasts signal to osteoclast precursors and prepare the bone surface for osteoclast attachment and initiation of the resorption process. Production of PGs in bone and subsequent action on bone cells was enhanced indirectly by the induction of COX-2 (Tai et al., 1997; Raisz, 1999b). Osteoclasts do not have receptors for PTH, but osteoblasts do. Treatment of marrow stromal cell and calvarial osteoblast cultures with PTH stimulated osteoblast differentiation when COX-2 activity was inhibited by NS-398, a COX-2 s-NSAID (Choudhary et al., 2008b). Thus, it has been suggested that COX-2 and associated PG synthesis, when stimulated by PTH, play a critical role in advancing bone resorption, while cytokines such as IL-13 and IL-4 inhibit resorption, emphasizing the role of local environment in the production of COX-2 and PGs (Onoe et al., 1996; Okada et al., 2000; Radi and Khan, 2005). In fact, the correlation between the lack of COX-2 and PTH have been investigated in COX-2-KO and WT mice. In these 10-month-old male KO mice, serum calcium and PTH, but not phosphorus, levels were increased compared with

those in WT mice. 1,25-Dihydroxyvitamin D₃ levels were markedly elevated in KO mice. Skeletal analysis showed small nonsignificant decreases in cortical bone density and either an increase (distal femur, by microcomputed tomography) or no difference (distal femur, by static histomorphometry) in trabecular bone density in KO mice. There was a trend toward an increased percentage of osteoblastic and osteoclastic surfaces, and the rates of trabecular bone formation and mineral apposition were increased in KO mice relative to WT mice. However, rates of trabecular bone formation and mineral apposition were increased in 10-month-old WT females compared with males and did not increase further in female KO mice. The authors conclude that COX-2-KO mice with intact renal function have primary hyperparathyroidism, and the effects of increased PTH and 1,25-dihydroxyvitamin D₃ are to increase bone turnover, which may be compensated for by the absence of COX-2 (Xu et al., 2005). COX-2-KO mice in inbred strains can have renal dysfunction with secondary hyperparathyroidism (HPTH), making direct effects of COX-2 KO on bone difficult to assess. The effects of COX-2 KO on bone responses after 3 weeks of intermittent PTH were investigated in healthy male COX-2-KO mice. Intermittent PTH increased femoral bone mineral density and cortical bone area more in KO mice than in WT mice and increased trabecular bone volume in the distal femur in both WT and KO mice. PTH also increased serum markers of bone formation and resorption more in KO than in WT mice but increased the ratio of osteoblastic surface to osteoclastic surface only in the KO mice. In addition, PTH increased femoral mineral apposition rates and bone formation rates in KO mice more than in WT mice (Xu et al., 2010). Therefore, COX-2 deficiency leads to increased anabolic responses to PTH. Using murine MC3T3-E1 and MC-4 cells that are stably transfected with murine COX-2, a role for the calcium–calcineurin–nuclear factor of activated T-cell (NFAT) signaling pathway in the PTH induction of COX-2 has been proposed (Huang et al., 2010).

Other essential factors involved in bone resorption include the osteoclast differentiation factor, a member of the TNF ligand family that is identical to RANKL, and the previously mentioned EP₂R and EP₄R (Tsukii et al., 1998; Raisz, 1999b; Okada et al., 2003). Specifically, EP₄R is essential for osteoclast formation, as demonstrated by stimulated bone formation and prevention of bone loss upon activation (Ono et al., 2003; Yoshida et al., 2002). In addition, EP₂- and EP₄-KO mice have impaired osteoclastogenesis and bone resorption, respectively (Li et al., 2000; Miyaura et al., 2000; Sakuma et al., 2000). In a femoral fracture-healing mouse model, the effects of EP₄ agonist administration on bone healing were evaluated in either young (7 to 9 week old) or aged (52 to 56 week old) mice (Naik et al., 2009). Local administration of an EP₄ agonist to the fracture repair site in aged mice enhanced the rate of chondrogenesis and bone formation to levels observed in young mice (Naik et al., 2009). The effects of global or targeted deletion of the EP₄R on the response of osteoblasts to PG *in vitro* and on bone histomorphometry in aged mice were studied. The study compared WT, global heterozygote (G-HET), targeted heterozygote (T-HET), and KO mice. KO mice had one targeted and one global deletion of the EP₄R. In cultures of calvarial osteoblasts, PGE₂ increased ALP activity in cells from WT mice, and this effect was decreased significantly in cells from either G-HET or T-HET mice and decreased further in cells from

KO mice. A selective agonist for the EP₄R increased ALP activity and osteocalcin mRNA levels in cells from WT mice but not those from KO mice. A COX-2 s-NSAID, NS-398, decreased osteoblast differentiation in WT but not in KO cells. At 15 to 18 months of age there were no differences in serum creatinine, calcium, PTH, body weight, or bone mineral density among the various genotypes. Histomorphometry showed no consistent changes in bone volume or bone formation (Gao et al., 2009).

Bone Formation

Bone remodeling occurs via osteoclastic resorption of the new woven bone with subsequent osteoblastic replacement of matrix with lamellar bone (Cruess and Dumont, 1975). The steps involved in bone formation in adults include mesenchymal stem cell recruitment, proliferation, and differentiation with endochondral and intramembranous bone ossification (Bruder et al., 1994; Einhorn, 1998; Radi and Khan, 2005). Mesenchymal cells play a critical role in endochondral bone ossification. Mesenchymal cells first differentiate into chondrocytes, which subsequently undergo terminal differentiation and apoptosis, leading to calcification of the matrix. This calcified matrix lays the ground for primary bone formation by serving as a template, whereby osteoblasts deposit bone directly onto calcified cartilage (de Crombrugge et al., 2001). In intramembranous bone ossification, the mesenchymal cells differentiate directly into osteoblasts (de Crombrugge et al., 2001). Signaling pathway gene signatures that take place during intramembranous bone regeneration were examined in a unilateral femoral ablation model using 6-month-old Sprague–Dawley male rats (Kuroda et al., 2005). During inflammation (days 1 to 5), several genes, including COX-1 and COX-2, were down-regulated. Other proinflammatory cytokines, TNF α and IL-1 β , exhibited increasing levels around day 5. During repair (days 3 to 10), growth factors, receptors, and inhibitor genes for TGF β ; FGF; BMP-2, BMP-4, and BMP-7; VEGF; and IGF-I were up-regulated. The fracture-site microenvironment is acidic and hypoxic. The pH of the fracture hematoma was shown to be acidic immediately after the trauma, becoming alkaline with ongoing fracture repair (Brighton and Krebs, 1972). Interestingly, osteoblast expression of VEGF is modulated by such an extracellular microenvironment. For example, whereas there is an increased osteoblast expression of VEGF in hypoxia (Steinbrech et al., 2001), acidic pH decreased VEGF production significantly under hypoxic conditions (Spector et al., 2000). In addition, markers of osteoblast function such as alkaline phosphatase (ALP), collagen type I, osteonectin, osteopontin, and osteocalcin exhibited peak expression at day 5 or 7. The remodeling phase (days 10 to 14) was characterized by peaks for cytokines associated with osteoclastic activity, including RANKL, cathepsin K, TNF α , IL-6, and COX-2 (Kuroda et al., 2005).

The structure of the adult skeleton is determined, in large part, by its genome (Judex et al., 2002). The differential response of trabecular bone to an anabolic (low-level mechanical vibration) and a catabolic (disuse) mechanical stimulus was evaluated in three strains of adult mice. In low-bone-mineral-density C57BL/6J mice, the low-level mechanical signal caused significantly larger bone formation

rates (BFRs) in the proximal tibia, but the removal of functional weight bearing did not significantly alter the BFRs. In mid-bone-mineral-density BALB/cByJ mice, mechanical stimulation also increased BFRs, whereas disuse significantly decreased BFRs. In contrast, neither anabolic nor catabolic mechanical signals influenced any index of bone formation in high-bone-mineral-density C3H/HeJ mice (Judex et al., 2002). It is suggested that PGs release from cells at times of mechanical loading, which is a primary cellular mechanism of bone formation (Li J. et al., 2002). For example, infants with congenital heart disease who are given infusions of PGE₁ to maintain patency of the ductus arteriosus exhibit striking new periosteal bone formation (Faye-Petersen et al., 1996). Cultures of primary bone cells from the iliac crest of postmenopausal women have increased PGE₂ and PGI₂ production after fluid shear mechanical stress (Joldersma et al., 2000). As mentioned previously, fracture healing is also affected (Thorsen et al., 1996).

The role that COX-2 may play in the initiation of periosteal cortical bone healing was investigated in a mouse femoral grafting model (Xie et al., 2008). In this model, fresh femur cortical bone grafts from COX-2-KO mice were transplanted into both KO and WT mice. Similarly, grafts from WT mice were transplanted into both WT and KO mice. Histologic analyses showed that WT-to-WT transplantation resulted in normal endochondral bone healing, as evidenced by marked induction of neovascularization and periosteal bone formation on the donor graft. In contrast, transplantation of a KO graft into a KO host led to a marked, 96%, reduction in bone formation and near-elimination of donor cell-initiated periosteal bone formation. Transplantation of a WT graft into a KO host resulted in an 87% reduction of bone formation; however, when a KO graft was transplanted into a WT host, KO donor periosteal cell-initiated endochondral bone formation was restored. Histomorphometric analyses demonstrated a 10-fold increase in bone formation and three-fold increase in cartilage formation compared to KO-to-KO transplantation, suggesting that COX-2-deficient donor cells were capable of differentiating and forming bone when placed in a WT host. Thus, the authors suggested that COX-2 is critical for initiation of periosteal cortical bone healing and that elimination of COX-2 at the early stage of bone healing could lead to detrimental effects on periosteal progenitor cell-initiated cortical bone repair (Xie et al., 2008).

In summary, the process of bone formation (osteogenesis) involves three main steps: extracellular organic matrix (osteoid) production, mineralization of the matrix to form bone, and bone remodeling by resorption and reformation (Fig. 2-3D to F) (Gajraj, 2003; Radi and Khan, 2005). Bone matrix synthesis and the secretion of a collagen-rich ground substance by osteoblasts are essential for later mineralization and are thus involved in osteogenesis (Gajraj, 2003).

COX-1 AND COX-2 EXPRESSION IN BONE, TENDON, AND LIGAMENT DURING REPAIR AND IN PATHOLOGICAL CONDITIONS

The expression of COX-1 and COX-2 in normal bone, during repair, and in pathological conditions is summarized in Table 2-1 (Radi and Khan, 2005). Studies have

TABLE 2-1 Summary of COX-1 and COX-2 Expression in Normal Bone cells, During Repair, and Under Pathological Conditions

COX-1	COX-2
Osteocytes	Canine osteosarcoma
Osteoblasts	Fracture healing
Osteoclasts	Periodontal inflammation (osteoblasts and cementoblasts)
Canine osteosarcoma	Canine pulmonary osteosarcoma
Canine pulmonary osteosarcoma	Activated human articular chondrocytes Pediatric human osteosarcoma

Source: Reprinted with kind permission from Springer Science & Business Media: Z. A. Radi, and N. K. Khan, *Inflammation Research* 54(9), pp. 358–366. Copyright © 2005.

shown that COX-1 is expressed constitutively by osteocytes and osteoblasts that surround alveolar bone (Mungo et al., 2002; Miyauchi et al., 2004). COX-1 was expressed constitutively in the callus and quantities remained unchanged during the healing process in a rat model of fractured femur. COX-1 and COX-2 expression were evaluated in various articular structures from 21-day-old male rat fetuses. COX-1, but not COX-2, was expressed in the anterior and posterior cruciate ligament of the knee joint and the labrum of the hip and shoulder. Both COX-1 and COX-2 were detected in the articular cartilage and joint capsule and the intraarticular disk of the temporomandibular joint and meniscus of the knee joint (Burdan et al., 2009). Oxygen plays a physiological role during bone repair and fracture sites and is generally hypoxic (Heppenstall et al., 1975). The role of hypoxia on PG release and COX expression was investigated in hypoxic osteoblasts in vitro (Lee et al., 2010). PGE₂ levels alone were significantly elevated under hypoxic conditions. COX-1 and COX-2 expression, using Western blot analysis, did not change. Treatment of cells with resveratrol, a COX-1 inhibitor, significantly reduced PGE₂ levels in media from hypoxic osteoblasts at 12 h. Furthermore, NS-398, a COX-2 s-NSAID, had no effect on PGE₂ levels from hypoxic osteoblasts at 6 h; however, treatment for 12 or 24 h significantly reduced the levels of PGE₂ released from cells. Therefore, COX may play a role in hypoxia-induced PGE₂ production (Lee et al., 2010).

COX-1 and COX-2 expression that takes place during intramembranous bone regeneration was examined in a unilateral femoral ablation model using 6-month-old Sprague–Dawley male rats (Kuroda et al., 2005). During inflammation (days 1 to 5), COX-1 and COX-2 were down-regulated (Kuroda et al., 2005). A recent study investigated COX gene expression of the healing and remodeling process initiated by fatigue loading in the rat ulna. Stress fracture healing involved direct remodeling that progressed along the fracture line as well as woven bone proliferation at the site of the fracture. At 4 days there was a significant increase in COX-1 mRNA expression (Kidd et al., 2010). At 4 h after fracture, there was a prominent peak increase in COX-2 mRNA expression (Kidd et al., 2010). The effects of metabolic acidosis on COX-1 and COX-2 expression were assessed in vitro using primary

cells isolated from neonatal CD-1 mouse calvariae that were cultured in a neutral or physiologically acidic medium. The mRNA levels for COX-1 and COX-2 were measured by quantitative real-time polymerase chain reaction (RT-PCR), and the protein levels were measured by immunoblot analysis (Krieger et al., 2007). The investigators found that incubation of calvarial bone cells in an acidic medium significantly increased COX-2 mRNA and protein levels without a change in COX-1 expression levels. In addition, increased COX-2 protein levels in response to acidity were also observed in cultured calvariae bone cells (Krieger et al., 2007). Therefore, it is suggested, at least *in vitro*, that COX-2 expression is critical for acid-induced cell-mediated bone resorption.

COX-1, but not COX-2, was expressed in osteoblasts and osteoclasts of dog normal skeleton (Mohammed et al., 2004). COX-1 and COX-2 expression was evaluated in a naturally occurring canine model of secondary osteoarthritis (OA). Hip joint capsules (HJCs) with synovial tissue and femoral head (FH) subchondral bones were collected from normal dogs and dogs undergoing total hip replacement for coxofemoral joint OA (Lascelles et al., 2009). There was no significant difference in COX-1 expression. However, significantly more COX-1 and COX-2 were present in OA FH tissue than in normal FH tissue (Lascelles et al., 2009). Additionally, significantly more COX-2 protein was present in the OA HJCs than in normal joints (Lascelles et al., 2009). Thus, COX-2 is an appropriate target for pain management in OA. In neoplastic skeleton tumors in dogs, COX-1 was present in 8 of 13 osteosarcoma, and COX-2 was present in 3 of the 13 tumors (Mohammed et al., 2004). This suggests a role for COX-2 in skeleton neoplasms. Furthermore, COX-2 expression has been documented in other skeleton neoplastic conditions (e.g., bone sarcomas, osteoid osteomas) (Dickens et al., 2002; Mullins et al., 2004). The expression levels of COX-2 were evaluated in patients with extremity osteosarcoma. COX-2 was expressed in most of the cases. No correlation was found between COX-2 expression intensity and variables such as gender, age, anatomical site, necrosis after chemotherapy, and surgical stage. However, strong COX-2 expression was associated with low metastasis-free survival. An age older than 20 years and strong COX-2 expression independently predicted increased risk of metastasis. These data suggest that COX-2 overexpression in the primary tumor correlates with the occurrence of distant metastasis in patients with osteosarcoma (Urakawa et al., 2009). High COX-2 expression was observed in human chondrosarcomas (Schrage et al., 2010). Human osteoblastomas and osteosarcomas show high COX-2 expression (Hosono et al., 2007). Increased COX-2 expression by osteoblasts and cementoblasts has also been observed in deep periodontal tissue after application of lipopolysaccharide and in activated human articular chondrocytes (Geng et al., 1995; Miyauchi et al., 2004).

In an *in vitro* study using rat bone cell lines, ultrasound stimulation (US) increased COX-2 expression and PGE₂ formation, as detected by Western blotting analysis, PCR, and enzyme-linked immunosorbent assay (ELISA) (Tang et al., 2006). The signaling pathway involved in this US-induced COX-2 expression in rat osteoblasts is through up-regulation of cell membrane integrins and activation of FAK, phosphatidylinositol 3-kinase (PI3K), Akt, ERK, and NFκB. Long-term US stimulation enhanced the differentiation of osteoblasts and bone nodule formation

because of the increase in COX-2 expression (Tang et al., 2006). Another study examined the effects of US on human chondrocytes and found that US stimulation transiently increased the surface expression of $\alpha 2, \alpha 5, \beta 1$, or $\beta 3$ but not $\alpha 3$ or $\alpha 4$ integrins in human chondrocytes (Hsu et al., 2007). US stimulation increased PGE₂ formation as well as the protein and mRNA levels of COX-2. Antibodies against either anti-integrin $\beta 1$ and $\beta 3$ or anti-integrin $\beta 1$ and $\beta 3$ integrin, using small interference RNA, attenuated the US-induced COX-2 expression. Integrin-linked kinase (ILK) inhibitor (KP-392), Akt inhibitor, NF- κ B inhibitor (PDTC), or I κ B protease inhibitor (TPCK) also inhibited the potentiating action of US. Ultrasound stimulation promotes kinase activity of ILK and the phosphorylation of Akt. In addition, US stimulation also induces IKK α/β phosphorylation, I κ B α phosphorylation, I κ B α degradation, p65 phosphorylation at Ser276, p65 and p50 translocation from the cytosol to the nucleus, and κ B-luciferase activity. The binding of p65 to the NF κ B element, as well as the recruitment of p300 and the enhancement of p50 acetylation on the COX-2 promoter, were enhanced by US (Hsu et al., 2007). Therefore, US stimulation increases COX-2 expression, at least in human chondrocytes in vitro, via the integrin/ILK/Akt/NF- κ B, and p300 signaling pathway. COX expression after exposure of human primary bone cells to mechanical stress was investigated in vitro. Cells were obtained from the iliac crest of elderly (56 to 80 year-old) women. Increased COX-2, but not COX-1, mRNA expression was observed in this study (Joldersma et al., 2000).

In a femoral fracture-healing mouse model, COX-2 expression was evaluated in either young (7- to 9-week-old) or old (52- to 56-week-old) mice (Naik et al., 2009). COX-2 expression in young mice peaked at 5 days, coinciding with the transition of mesenchymal progenitors to cartilage and the onset of expression of early cartilage markers. COX-2 was expressed primarily in early cartilage precursors. COX-2 expression was reduced by 75% and 65% in fractures from aged mice compared with young mice on days 5 and 7, respectively (Naik et al., 2009). At the site of bone fracture, COX-2 mRNA was elevated, with peak levels expressed during the first 14 days of healing followed by return to basal level at 21 days and complete normalization by 42 days (Gerstenfeld et al., 2003a). These results are consistent with other data and suggest that COX-2 is important in early or activated stages of healing, but probably exhibits little effect on the long-term healing process (Gerstenfeld et al., 2003a).

COX-1 and COX-2 mRNA expression was evaluated in the human patellar tendon in rest and after exercise. Patellar tendon biopsy samples were taken from six people (three men and three women) before and 4 h after a bout of resistance exercise (RE) (three sets of 10 repetitions at approximately 70% of one-repetition maximum) and from a separate group of six (three men and three women) before and 24 h after RE. Samples were analyzed by RT-PCR. COX-1's were the most abundant COX mRNAs before exercise and remained unchanged after exercise. COX-2 was also expressed in tendon tissue at rest and was unchanged after exercise (Trappe et al., 2008). Application to human periodontal ligament cells of a compressive force of 2 g/cm² for 3 to 48 h significantly stimulated COX-2 expression in both time- and age-dependent manners. These increases in COX-2 expression were dramatically larger in periodontal ligament cells obtained from human donors

over the age of 35, thus implicating aging as a factor that stimulates COX-2 expression and PGE₂ after compressive force application to such cells (Mayahara et al., 2007). Another *in vitro* study investigated the effects of applying mechanical force on human periodontal ligament cells COX-2 expression. Cyclic tension force application to human periodontal ligament cells resulted in PGE₂ release to the culture medium in a time-dependent manner. Although hardly detectable in controls, COX-2 mRNA expression increased dramatically on days 3 and 5 in response to tension force. In contrast, COX-1 mRNA levels detected in controls were not affected by tension force. As assessed by immunohistochemistry, COX-2 protein was increased significantly by tension force around the unstained cell nucleus in a time-dependent manner. When NS-398, a COX-2 s-NSAID, was added to the medium, PGE₂ synthesis increased by tension force was completely inhibited (Shimizu et al., 1998). In a rat supraspinatus tendon overuse injury model, mRNA expression levels of COX-2 were initially increased at 3 days, decreased by 1 week, peaked at 8 weeks, and decreased by 16 weeks of overuse (Perry et al., 2005).

In a study in rabbits, the expression of genes associated with tendon degeneration after static loads was studied. Flexor tendons were obtained from New Zealand white rabbits and secured in a tissue-loading system. A static load of 0, 2, 4, or 6 MPa was applied to tendons for 20 h, and COX-2 mRNA expression was measured by reverse transcription–polymerase chain reaction (RT-PCR). COX-2 expression was increased only at the high stress load of 6 MPa (Asundi and Rempel, 2008). COX-2 expression was evaluated in the rotator cuff tear in rabbits. A rotator cuff tear was surgically created and the expression of PGE₂ and COX-2 was analyzed. In the supernatant of the tissue culture of the torn tendon, PGE₂, the mediator of pain and the product of COX-2, was detected. The production of PGE₂ increased significantly 7 days after injury, and then decreased by day 21. RT-PCR analysis confirmed the mRNA expression of COX-2 in the torn tendon. In addition, immunohistochemical study demonstrated that cells in the tendon stump were immunopositive for COX-2. Furthermore, in the joint affected, articular chondrocytes in the remote area from the tear had strong COX-2 expression (Koshima et al., 2007). Using a rabbit model of flexor tendon injury, COX-2 mRNA levels were assessed by RT-PCR at 3, 6, 12, and 24 days after injury. Increased levels of COX-2 mRNA were detected in both tendon and tendon sheath following injury in a time-dependent manner. COX-2 was increased predominantly in the tendon (Berglund et al., 2007).

The effects of cast immobilization on COX-2 expression were studied after rat Achilles tendon rupture. RT-PCR was performed at 8 and 17 days postrupture to assess COX-1 and COX-2 in the healing region. At 8 days postinjury, tendon mRNA levels were comparable in both groups. However, by day 17, COX-1 mRNA levels in the mobilized group increased significantly. Corresponding mRNA levels in the immobilized group decreased during the same period. There were no significant differences in the expression of COX-2 among the various groups, indicating that injury-associated expression of these molecules is not overtly influenced by loading (Bring et al., 2009).

In summary and consistent with other organ systems, COX-1 expression is generally observed in normal bone, tendon, and ligament. COX-2 expression

is increased during the initial stages of the bone repair process or inflammatory conditions or skeleton neoplasms.

EFFECTS OF ns-NSAIDs ON BONE HEALING

Nonselective NSAIDs are widely used in patients with bone and joint pathology and acute musculoskeletal injury (Brooks and Day, 1991; Vaile and Davis, 1998). The use of NSAIDs can have therapeutic benefits in osteoporosis and bone loss prevention in older women (Bauer et al., 1996). For example, in an *in vitro* study with or without basic fibroblast growth factor (b-FGF) stimulation, NSAIDs (indomethacin and etodolac) have been shown to reduce osteoclast formation and bone resorption (Bell et al., 1994; Hurley et al., 1998; Kawaguchi et al., 2000; Raisz et al., 2001). Furthermore, several studies have demonstrated that NSAIDs can be used for the prevention of heterotopic ossification following joint replacement and as a prophylactic against heterotopic bone formation in humans (Wahlstrom et al., 1991; Kjaersgaard-Andersen et al., 1993; Moed et al., 1994; Burssens et al., 1995; Persson et al., 1998; Vielpeau et al., 1999; Wurnig et al., 1999; Burd et al., 2003; Grohs et al., 2007; Saudan et al., 2007) and in nonclinical animal models (Moed et al., 1994; Radi and Khan, 2005; Rapuano et al., 2008).

Variable results were noted when NSAIDs evaluated in nonclinical models of bone healing following fracture, osteotomy, or other surgical orthopedic procedures. For example, impaired bone healing was observed in rats and rabbits after treatment with aspirin, diclofenac, ibuprofen, indomethacin, and tenoxicam (Bo et al., 1976; Sudmann and Bang, 1979; Sudmann et al., 1979; Allen et al., 1980; Tornkvist et al., 1980; Lindholm and Tornkvist, 1981; Sato et al., 1986; Keller et al., 1987; Engesaeter et al., 1992; Hogevoid et al., 1992; Obeid et al., 1992; Altman et al., 1995; Glassman et al., 1998; Bichara et al., 1999; Beck et al., 2003; Giordano et al., 2003; Jaffre et al., 2003; Riew et al., 2003; Brown et al., 2004). In those nonclinical models the bone effects included inhibition of haversian (cortical bone) remodeling, alterations in spinal fusions, poor mineralization of bone matrix, decreased osteoid formation and callus bone formation, decreased bone mineral content, reduced mechanical strength of replacement tissue, decreased amounts of cortical bone, and inhibition of new bone formation (Bo et al., 1976; Lindholm et al., 1981; Keller et al., 1987; Lane et al., 1990; Obeid et al., 1992; Dimar et al., 1996; Glassman et al., 1998; Ho et al., 1998; Ankarath et al., 2003; Seidenberg and An, 2004). One of the earliest experiments of ns-NSAID effects on bone healing took place in the 1980s. Allen et al. (1980) examined the effects of indomethacin and aspirin in 45-day-old male CD rats by subjecting them under anesthesia to fractures of the right ulna and radius. Indomethacin was given at a 2- or 4-mg/kg per day dose and aspirin at a 100-, 200-, or 300-mg/kg per day dose for 21 days. After 21 days, the rats were euthanized and histological sections of the fracture sites were examined in a blinded fashion to evaluate the effects on healing. The results showed a drug- and dose-related retardation of fracture healing which was statistically significant at all dose levels of indomethacin and at the highest level of aspirin (100, 200, and 300 mg/kg per day), as compared to controls. In another

study in Wistar rats, the short-term (up to 3 days) effects of indomethacin therapy at a 2-mg/kg per day dose on the healing of intramedullary pinned osteotomies of the femur were investigated. The indomethacin-treated rats showed statistically significant decreases in bone strength, absorbed energy, and bending rigidity when tested mechanically in cantilever bending (Hogevold et al., 1992). Similarly, Altman et al. (1995) studied the effects of ibuprofen at a 30-mg/kg per day dose and indomethacin at a 1-mg/kg per day dose administered orally for up to 12 weeks to rats with femur fractures. Both ibuprofen and indomethacin retarded fracture healing, with significant differences in mechanical healing found between the control and experimental groups after 10 weeks of drug administration. Both drugs also induced qualitative histological changes manifested by delayed maturation of callus, which was noticeable earlier than the difference found by mechanical testing of bone (Altman et al., 1995). In older rats (six to nine months), high doses of indomethacin were associated with histological evidence of increased fibrogenesis and decreased osteogenesis and remodeling of bone fractures (Elves et al., 1982). Indomethacin treatment was associated with increased collagen synthesis in fracture callus in rats as assessed *in vitro* via [³H]proline incorporation (Ro et al., 1978).

The effects of ibuprofen on the healing and remodeling of bone and cartilage in the temporomandibular joint of rabbits were investigated in a 4-week study. Three groups of rabbits were operated on to create a groove and a hole in the articular surface of both the right and left mandibular condyles. Following surgery, one group was used as a control and did not receive any medication, a second group was given a daily dose of 17 mg/kg of ibuprofen, and the third group was given a daily dose of 34 mg/kg of ibuprofen. A highly significant difference in the healing of bone and cartilage as assessed clinically and histologically was observed between the control group and the ibuprofen-treated group (Obeid et al., 1992). The skeletal abnormalities were assessed after ibuprofen oral administration at doses of 180, 60, 20, and 7.5 mg/kg per day to pregnant rats from days 1 to 20 of pregnancy and from day 1 of pregnancy to parturition (Adams et al., 1969). Although different types of skeletal abnormalities were found, these generally fell within the accepted range of normal variation and were similar to those of untreated control rats (Adams et al., 1969). In another study, the prenatal skeletal developmental effect of several ns-NSAIDs (tolmetin, ibuprofen, piroxicam) and a COX-2 s-NSAID, DUF, were investigated after intragastrical administration to pregnant Wistar rats from days 7 to 21 of gestation. The initial dose was set at 8.5 mg/kg per dose for tolmetin and ibuprofen and at 0.3 and 0.2 mg/kg per dose for piroxicam and DFU, respectively. The middle dose was increased 10 times. The highest dose, except for ibuprofen, was increased 100 times. The highest dose for ibuprofen was set at 200 mg/kg. Tolmetin and ibuprofen were administered three times a day. Piroxicam and DFU were dosed once daily. The epiphysis (epiphyseal chondrocytes of long bones and menisci), as well as cells in periosteum, articular capsule, and ligaments of the 21-day-old fetuses, had normal physiological expression of COX-1 and COX-2, as well as cathepsin K; collagen types I, II, and X; osteopontin; osteocalcin; and TNF α . Increased developmental skeletal variation was noted in groups exposed to the highest dose of these ns-NSAIDs. Bone variations, including decrease of bone mineralization, limited to various parts of the axial skeleton and metacarpal

bodies, were noted. Occasionally, increases in primary ossification centers were seen in fetuses obtained from two litters exposed to the lowest dose of tolmetin and DFU. Unlike nonselective NSAIDs, DFU caused a significant decrease of fetal length only. Unlike the increased number of skeletal variations observed in fetuses exposed to the highest doses of ns-NSAIDs, both COX-2 s- and ns-NSAIDs did not disturb joint formation and morphology of femoral epiphyses when administered even at high maternal toxic doses. No histological differences in joint formation were noted in the NSAID-treated group compared with controls (Burdan et al., 2005).

The postnatal developmental effects of piroxicam were assessed in rabbits and rats after oral administration at 2, 5, and 10 mg/kg per day. No adverse-effect postnatal developments were observed (Perraud et al., 1984). Etodolac was tested in a 12-week-old Wistar rat fracture model by altering the period of administration from early to late. After closed fractures had been created in the middle of femoral shafts, a 20-mg/kg per day dose of etodolac was administered intraperitoneally in three ways: Group I received it for 3 weeks, group II for just the first week after operation, and group III for just the third (final) week. Bone maturation was estimated by a radiographic scoring system and mechanically by a three-point bending test. In both the radiographic and mechanical studies, groups I and II showed lower scores, indicating that even a short period of administration of etodolac in the early phase of fracture healing creates a risk of delayed healing (Endo et al., 2005). The effects of several NSAIDs—diclofenac sodium, piroxicam, parecoxib, lornoxicam, meloxicam, ketoprofen, and ketorolac—on bone marrow mesenchymal stem cell (MSC) proliferation and osteogenic and chondrogenic differentiation were investigated *in vitro* using trabecular bone MSC from healthy volunteers (Pountos et al., 2010). It was found that none of the NSAIDs tested at a broad range of concentrations significantly affected MSC proliferation or osteogenic differentiation. However, NSAIDs affected chondrogenic potential with a reduction in soluble glycosaminoglycan content by 45% and 55% with diclofenac and ketorolac, respectively. Thus, these data suggest that NSAIDs may inhibit bone formation via blockage of MSC chondrogenic differentiation, which is an important intermediate phase in normal endochondral bone formation (Pountos et al., 2010).

Phenylbutazone (PBZ), an ns-NSAID, is often used in horses for the management of pain associated with conditions such as osteoarthritis. Recommendations typically include administration of PBZ at a 4.4-mg/kg dose. The effects of PBZ on bone activity and bone formation were investigated in 1- to 2-year-old healthy horses. Biopsy was conducted to obtain unicortical bone specimens from one tibia on day 0 and from the contralateral tibia on day 14. Fluorochromic markers were administered intravenously (IV) 2 days prior to and on days 0, 10, 15, and 25 after the biopsy was performed. PBZ was administered orally once at 4.4 mg/kg of body weight dose. Osteonal density and activity, the mineral apposition rate (MAR), and the percentage of mineralized tissue filling of the biopsy-induced defects in cortical bone were assessed. The MAR was decreased significantly in horses treated with PBZ. Although a regional acceleratory phenomenon was observed in cortical bone in PBZ-treated and control groups, such a phenomenon was decreased significantly in horses treated with PBZ. Osteonal activity was similar at all time

points in all horses. In control horses, the percentage of mineralized tissue filling of the cortical defects was significantly greater in defects present for 30 days than in defects present for 14 days. Differences in the percentages of mineralized tissue were not detected in horses treated with PBZ. Thus, PBZ decreased the MAR in cortical bone and appeared to decrease the healing rate of cortical defects in horses (Rohde et al., 2000). In another experimental study in horses, PBZ was administered orally twice daily at a dose of 4.4 mg/kg for 3 days and subsequently at a dose of 2.2 mg/kg for 7 days to adult female horses without clinical or radiographic evidence of joint disease. Biomarkers of cartilage aggrecan synthesis (chondroitin sulfate 846) and type II collagen synthesis (procollagen type II C-propeptide) and degradation (collagen type II cleavage) were assayed. Biomarkers of bone synthesis (osteocalcin) and resorption (C-terminal telopeptide of type I collagen) were also measured. No significant differences were found between control and treatment groups or temporally for the biomarkers chondroitin sulfate 846, procollagen type II C-propeptide, collagen type II cleavage, and C-terminal telopeptide of type I collagen in serum or synovial fluid. However, a significant increase in osteocalcin concentration occurred in synovial fluid during treatment in the treated group. No treatment effect was detected for serum osteocalcin concentration. Therefore, continuous PBZ administration at recommended doses altered some biomarkers in healthy equine joints after short periods of administration (Fradette et al., 2007).

The exact mechanism of potential effects on bone healing is under debate. Studies have suggested that osteoblastic proliferation is involved, but not via inhibition of PG synthesis (Ho et al., 1998,1999). Others have demonstrated that PGE₂ is markedly reduced, as in the LPS-challenged synovial explants equine model, treated with phenylbutazone, flunixin meglumine, ketoprofen, carprofen, and meloxicam (Moses et al., 2001). Edwall et al. (1992) demonstrated in male Sprague–Dawley rats that IGF-I was increased at 8 days after tibial fracture and that this level was depressed after indomethacin administration at a dose of 3 mg/kg per day given via the intramuscular route, thus implicating IGF-I both in fracture healing and in ns-NSAID inhibitory response.

In contrast, other studies suggest that NSAIDs have no significant effect on bone repair or that their effects can be attributed only partially to the inhibition of PG synthesis (Sudmann et al., 1979, 1982; Mbugua et al., 1989; Huo et al., 1991; Reikeraas and Engebratsen, 1998; Akman et al., 2002; Seidenberg and An, 2004). For example, no effects on collagen synthesis, an important marker of bone healing, were observed *in vitro* in rat fracture callus (Ro et al., 1978). In a separate study, quantitative histomorphometric indices of bone formation and resorption, as well as cartilage histology, were not significantly different between rats treated with indomethacin and nontreated rats (Boiskin et al., 1988). In a rabbit distal tibia fracture model, the effects of two ns-NSAIDs, piroxicam and flunixin, on post-fracture limb swelling, joint stiffness, and torsional bone strength were examined. After 3 weeks of treatment, limb swelling in rabbits treated with low-dose piroxicam was reduced by 39%, and high-dose piroxicam reduced limb swelling by 86%. Flunixin reduced swelling by 53%. Neither piroxicam nor flunixin affected fracture healing as measured by ankle stiffness or tibia torsional strength (More et al., 1989). β -Tricalcium phosphate (β -TCP) is a biomaterial used in oral and

maxillofacial surgery because it can induce a rapid proliferation of woven bone (Nyangoga et al., 2010). In a study in New Zealand rabbits, ketoprofen, a ns-NSAID, was given for 8 and 28 days to evaluate its effects on the healing of β -TCP bone graft. β -TCP induced metaplastic bone trabeculae as early as 8 days postsurgery. Ketoprofen did not affect the amount of bone formed or the number of macrophages labeled. No significant alterations in fracture biomechanics, as measured by torsion testing and fracture stage, were observed in mature (Nyangoga et al., 2010) Sprague–Dawley rats after daily oral administration of ibuprofen at a 30-mg/kg dose, starting 3 days following fracture, over a 12-week interval. Fracture histology and serum osteocalcin levels were no different in the ibuprofen-treated animals from those in controls. Furthermore, the histomorphometric parameters of bone remodeling, including bone volume and the bone formation rate in the intact tail vertebrae of these animals with unilateral femur fractures, were no different between ibuprofen-treated and control rats (Huo et al., 1991).

In Wistar rats, the left tibia were osteotomized, stabilized with a Kirschner wire, and rats were randomized into four groups (Krischak et al., 2007). Group 1 received a placebo, group 2 received a central analgesic, tramadol, at 20 mg/kg per day throughout the study; and groups 3 and 4 were treated with sodium diclofenac at 5 mg/kg per day. Group 3 received diclofenac for 7 days, followed by placebo until euthanasia (short term), and group 4 animals received diclofenac for the full period (long term). Animals were euthanized 21 days after osteotomy. All osteotomies, as assessed by histopathological examination, healed successfully and independent of the drug treatment. Delayed callus maturation, as assessed by histomorphometry, was observed in the long-term diclofenac-treated mice, with significantly higher amounts of cartilage and less bone, particularly in the outermost region of periosteal callus. Short-term diclofenac application did not significantly alter callus differentiation (Krischak et al., 2007). In a randomized placebo-controlled crossover study in mongrel dogs, indomethacin and phenylbutazone did not affect bone healing (Mbugua et al., 1989). The effect of an ns-NSAID, etodolac, on a beagle dog model of osteoarthritis in the right temporomandibular joint (TMJ) was investigated using radiology and histopathological examination 8 weeks postsurgical operation. From 2 to 6 weeks after surgery, the dogs were given 15 mg/kg of etodolac daily. The etodolac-treated dogs had fewer morphological differences between the unoperated control (left) and the operated (right) TMJ, and steoarthritic changes in the TMJ were significantly less severe in the treated group than in the untreated controls (Miyamoto et al., 2007). A middiaphyseal transverse osteotomy (stabilized with an intramedullary pin) of the right tibia was performed in each dog. The effects of carprofen administration on healing of a tibial osteotomy were investigated in dogs. Dogs received carprofen (2.2 mg/kg PO every 12 h) for 120 days. At 120 days after surgery, stiffness, elastic modulus, and flexural rigidity values in the carprofen group were significantly lower than corresponding values in the control group. Furthermore, histological evaluation revealed that the cartilage area within the callus in the carprofen group was significantly greater than that in the control group (Ochi et al., 2011). Thus, 120-day administration of carprofen appeared to inhibit bone healing in dogs that underwent tibial osteotomy. In a study of Dutch milk goats, the effects of NSAID treatment on bone graft ingrowth were

evaluated. Allograft bone was obtained from the sternum of 3 donor goats; the other 27 goats were divided into three groups. The first group did not receive any NSAID, the second group received ketoprofen subcutaneously in a 2.2-mg/kg dose once daily, and the third group received meloxicam subcutaneously in a 0.5-mg/kg dose once daily. The treatment period was 6 weeks for all goats. No difference in bone in-growth in titanium bone chambers was noted, whether the goats were treated with ketoprofen or meloxicam or with medication at all. Furthermore, there was comparable in-growth of bone irrespective of whether an autograft, rinsed allograft, or irradiated rinsed allograft was used (van der Heide et al., 2008).

Clinical studies that assessed the effects of ns-NSAIDs on bone healing are few. Giannoudis et al. (2000) looked retrospectively at 377 patients treated with intramedullary nailing for femoral shaft fractures. Femur diaphysis fracture nonunion had occurred in 32 of these patients. Of those remaining, the investigators selected 67 patients of similar gender and age whose fractures had united. They then examined several differences among those patients, including postoperative ns-NSAID use, between the two groups. Significant association between nonunion and the use of ns-NSAIDs after injury and delayed healing was noted in patients who took NSAIDs and whose fractures had united. Another study looked at the association between NSAID use and the incidence of humeral shaft fracture nonunion. Of the 9995 humeral shaft fractures, 105 patients developed nonunions (1.1%), and 1032 (10.3%) were exposed to NSAIDs in the 90 days after fracture. NSAID exposure within the first 90 days was associated significantly with nonunion. Exposure to ns-NSAIDs in the period 61 to 90 days after a humeral shaft fracture was associated with nonunion (Bhattacharyya et al., 2005). However, these associations are not necessarily causal. Similarly, Butcher and Marsh (1996) retrospectively examined 94 patients who had sustained tibial fractures. The authors found that patients who received ns-NSAIDs as part of their treatment had an average length of time to union 7.6 weeks longer: from 16.7 weeks to 24.3 weeks. The Canadian Multicentre Osteoporosis Study is a longitudinal randomly selected population-based community cohort study that looked at the effects of the COX-2 s-NSAIDs, celecoxib and rofecoxib on bone mineral density (BMD). Data were from men ($n = 2004$) and postmenopausal women age 65 and older ($n = 2776$) who underwent a BMD measurement and structured interview in the fifth year of the study. To assess dose effects, rofecoxib and celecoxib doses were standardized such that starting daily doses for osteoarthritis (12.5 mg for rofecoxib and 200 mg for celecoxib) were considered equivalent. For patients taking higher doses of these medications, their dose was considered as a multiple of these starting doses. For purposes of analysis, each subject was categorized into nonuser, low-dose daily user (25 mg equivalent dose), and high-dose daily user (50 mg equivalent dose) and the relationship between dose and BMD was assessed. Persons were considered daily users of rofecoxib or celecoxib if they reported taking the medication every day. In men, daily use of COX-2 s-NSAIDs was associated with a 2.4 to 5.3% lower hip and spine BMD compared with that of nonusers. However, in postmenopausal women not using estrogen replacement therapy, daily COX-2 s-NSAID use was associated with a 0.9 to 5.7% higher BMD at most sites. COX-2 s-NSAIDs did not have an effect in women on estrogen replacement therapy (Richards et al., 2006).

This may indicate a gender difference in the effects of NSAIDs on BMD between men and women older than 65 years.

A retrospective study looked at whether patients (112 patients) with an acetabular fracture who received the ns-NSAID indomethacin for prophylaxis against heterotopic ossification (HO) were at risk of bone fractures, delayed healing, or nonunion (Burd et al., 2003). Those patients at risk for HO were randomized to receive either radiation or indomethacin; the remaining patients served as controls. The results demonstrated a higher incidence of nonunion of long bone fractures in the indomethacin group (11 of 38 patients, or 26%) versus in the nonindomethacin (radiation and control) group (5 of 74 patients, or 7%) (Burd et al., 2003). In a randomized double-blind study involving 42 postmenopausal women 52 to 79 years old with a displaced Colles' fracture, the effects of the ns-NSAID piroxicam given at 20 mg/day PO for 8 weeks on posttraumatic osteopenia reduction and recovery were investigated. The patients were treated with a below-elbow plaster slab for 4 weeks after the reduction. The bone mineral content of the forearm bones was measured with a single-photon absorptiometer 8 weeks after the fracture. Piroxicam actually reduced the osteopenia caused by external fixation (Adolphson et al., 1991, 1993). No significant differences were found in the bone mineral decrease in the radius (mean of 7%) and the ulna (mean of 5%) among the patients treated with piroxicam versus 10% in the radius and 7% in the ulna in the placebo group. Furthermore, piroxicam did not decrease the rate of fracture healing. The patients who received piroxicam had significantly less pain during plaster treatment, but there was no difference in the rate of functional recovery between the groups (Adolphson et al., 1991; 1993). The effect of 1 week of treatment with naproxen on the formation of HO after cemented total hip arthroplasty was studied in a prospective trial. Twenty-seven patients received 500 mg naproxen twice daily for 7 days postoperatively and were compared with a control group of 23 patients from a previous study who had not received any type of NSAID. Three months after the operation, HO had developed in 52% patients in the control group and in 11% patients in the naproxen-treated group. One year after the operation, 17% patients in the naproxen-treated group and 52% in the control group had HO. Severe ossification developed in three patients in the control group and in none of the naproxen-treated group. Thus, naproxen given for 1 week can decrease the incidence of HO after total hip arthroplasty (Gebuhr et al., 1995). A retrospective cohort study was conducted in a general medical practice setting in the UK (using data from the General Practice Research Database). Regular NSAID users (who received three or more NSAID prescriptions) aged 18 years or older were compared with matched control patients and incidental NSAID users. The study comprised 214,577 regular NSAID users, 286,850 incidental NSAID users, and 214,577 control patients. The relative rate of nonvertebral fractures during regular NSAID treatment compared with control was 1.47 and that of hip fracture 1.08. No differences in nonvertebral fractures were found between the regular and incidental NSAID users. The rate of nonvertebral fractures among users of diclofenac and naproxen was similar to that of ibuprofen. Thus, the results of this study are not supportive of clinically significant effects of NSAIDs on bone metabolism (van Staa et al., 2000). In a case study, a patient with an ankle joint fracture-dislocation was treated preoperatively with indomethacin.

Indomethacin was found to have an inhibitory effect on bone formation (Sudmann and Hagen, 1976). The effect of 2-week flurbiprofen treatment fracture healing was investigated in patients with distal radial fracture, and no effects were noted (Davis and Ackroyd, 1988). In a retrospective observational study, ketorolac had no effect on spinal fusion when used at a dose of 30 mg IV every 6 h for 48 h in humans after spinal fusion surgery (Pradhan et al., 2008).

In summary, NSAIDs are effective anti-inflammatory drugs that have been used for the treatment of various orthopedic conditions and are not associated with adverse effects on normal bones or joints. However, the effects of these drugs on bone healing have variable findings among animal models and humans.

EFFECTS OF COX-2 s-NSAIDs ON BONE HEALING

COX-2 s-NSAIDs spare the COX-1 pathway (Fig. 2-1) (Radi and Khan, 2005). Several studies using these drugs have shown minimal effects on bone metabolism. For example, in an *in vitro* study using bone culture, treatment of neonatal mouse calvarial with celecoxib, a COX-2 s-NSAID, inhibited IL-1 β -stimulated bone resorption completely, but not PTH-induced bone resorption (Igarashi et al., 2002). Bone formation that occurred after mechanical loading and osteoclast formation following stimulation with b-FGF was inhibited after NS-398 treatment (Forwood, 1996; Hurley et al., 1998; Kawaguchi et al., 2000). In another study, the effects of parecoxib and NS-398 on osteoclast and osteoblast differentiation and activity were tested *in vitro*. Cells were harvested from the tibiae and femora of 8- to 12-week-old mice. The COX-2 s-NSAIDs parecoxib and NS398 both significantly inhibited osteoclast differentiation by 93%, 94%, and 74% of the control for 100 μ M indomethacin, 100 μ M parecoxib, and 3 μ M NS398, respectively. In addition, COX-2 inhibition reduced the resorption activity of mature osteoclasts. COX inhibition also significantly inhibited osteoblast differentiation from human mesenchymal stem cells. Simultaneously, the number of adipocytes was increased significantly. The molecular mechanism of induced adipocyte differentiation is unclear and needs further investigation (Kellinsalmi et al., 2007). A series of four inhibitors with differing selectivities for COX-1 and COX-2 each inhibited b-FGF-induced calcium release from cultured mouse calvariae with an order of potency indicating COX-2 to be the primary actor (Kawaguchi et al., 2000). However, under *in vivo* conditions, NS-398 did not affect new periosteal bone formation on the tibiae of rats (Forwood 1996; Li J. et al., 2002). Prostaglandin E₂ production was significantly reduced in marrow cultures from mice lacking PGHS-2 (PGHS-2^{-/-}). Furthermore, the decreases in PGE₂ production and osteoclastogenesis that were noted after NS-398 treatment of bone marrow cell cultures were reversible upon addition of PGE₂ to cultures (Okada et al., 2000). In female Sprague–Dawley rats, the effects of celecoxib on closed femoral fracture healing and PGs production was studied. Celecoxib treatment at a dose of 4 mg per/kg/day reduced fracture callus PGE₂ and PGF_{2 α} levels by more than 60% (Simon and O’Conner, 2007).

Experimental data generated in COX-2-KO mice are unreplicable in humans or other animal models, and is, therefore, questionable (Radi and Khan, 2005). Effects on bone fracture healing that were observed in COX-2-KO models included impaired fracture healing and decreased bone density, reduced bone resorption and osteoclast formation, and lack of inflammatory response (Okada et al., 2000; Simon et al., 2002). This inhibition of fracture healing was correlated with the reduced capacity of COX-2-KO mice to produce differentiated bone cells. Therefore, the relation between COX-2 gene ablation in mice and the clinical effects of pharmacological inhibition of COX-2 on bone healing remains undefined (Zhang et al., 2002). The effects noted in COX-2-KO mice included alterations of intramembranous and endochondral bone formation, suggesting a possible role of COX-2 on osteoblasts and osteoclast formation, and osteoclastogenesis, as indicated by *in vitro* bone marrow cell cultures (Li et al., 2000; Zhang et al., 2002; Ono et al., 2003). Bone morphology in multiple trabecular and cortical regions within the distal and diaphyseal femur of 4-month-old WT and KO (COX-2^{-/-}) male and female mice was investigated using microcomputed tomography. COX-2^{-/-} female mice had normal bone geometry and trabecular microarchitecture at four months of age, whereas the male KO mice displayed reduced bone volume fractions within the distal femoral metaphysis. Furthermore, male COX-2^{-/-} mice had a significant reduction in cortical bone mineral density within the central cortical diaphysis and distal epiphysis and metaphysis. Biomechanical testing via four-point bending showed that male COX-2^{-/-} mice had a significant increase in postyield deformation, indicating a ductile bone phenotype in male COX-2^{-/-} mice (Robertson et al., 2006). However, bones of COX-2-KO mice exhibited no gross or histological bone abnormalities in a separate study (Okada et al., 2000). The effect of COX-2 on bone response after placement of titanium implants in the middle of the femurs of 9-week-old male WT (COX-2^{+/+}) and COX-2^{-/-} mice was investigated (Chikazu et al., 2007). Mice were evaluated at 1, 2, 4, 7, and 56 days after implantation. COX-2 and osteocalcin expression was induced in bone surrounding implants in COX-2^{+/+} mice but not in COX-2^{-/-} mice. In cortical bone, the implant surface was in direct contact with newly formed bone lamellae in COX-2^{+/+} mice, and new bone formation was minimal in COX-2^{-/-} mice (Chikazu et al., 2007). Thus, the authors suggested that COX-2 may interfere with osseointegration of dental implants.

Similar to studies with ns-NSAIDs, results on the effects of COX-2 on bone fracture healing with COX-2 s-NSAIDs have been variable (Tables 2-2 and 2-3) (Radi and Khan, 2005). Studies in rats and rabbits have suggested that celecoxib and rofecoxib impaired bone healing, as evidenced by delayed fracture healing, reduced intramembranous and endochondral bone formation, decreased osteoblastogenesis and osteoclastogenesis, persistence of mesenchyme and cartilage in the callus, reduction or absence of cartilage in the fracture callus, and reduced bony in-growth (Elder et al., 2001; Zhang et al., 2001, 2002; Goodman et al., 2002; Simon et al., 2002; Radi and Khan, 2005; Radi, 2009). However, celecoxib did not significantly inhibit the rate of spinal fusion in rats, rabbits, or humans, whereas indomethacin showed biomechanical and radiographic evidence of delayed healing at 4 weeks postsurgery (Long et al., 2002; Brown et al., 2004). PGs regulate bone

TABLE 2-2 Variable Nonclinical Findings on Bone Healing After Celecoxib Treatment

Animal model	Celecoxib daily dose (mg/kg)	Bone model	Post-fracture dosing duration	Post-fracture healing assessment duration	Findings vs. controls	Reference
Rat Male	3	Femur fracture	4, 8, 12 weeks	4, 8, 12 weeks	Celecoxib did not delay healing	Brown et al., 2004
Female	3, 6	Femur fracture	10 days	8 weeks	Significant ↓ in fracture healing	Bergenstock et al., 2005
Mouse (male)	10, 50	Tibia fracture	4, 8, 12 weeks	4, 8, 12 weeks	No significant differences in biomechanical, biochemical, or histological parameters	Mullis et al., 2006
Dog (female)	100, 200	Knee osteoarthritis (OA)	15 weeks after knee surgery	15 weeks after knee OA surgery	No detrimental effects on proteoglycan turnover and content of osteoarthritic cartilage	Mastbergen et al., 2006
Mouse	25	Bone allograft healing	2, 5 weeks after bone allograft	2, 5 weeks after bone allograft	↓ new bone in-growth	O'Keefe et al., 2006
Rat Female	2, 4, 8	Femur fracture	5, 15 days	8 weeks	Significant ↓ in fracture callus and ↑ nonunions at all doses	Simon and O'Conner, 2007
Male	5 to 30	Femur fracture	2, 4, 8, 12 weeks	2, 4, 8, 12 weeks	↓ biomechanical strength	Herbenick et al., 2008

TABLE 2-3 Variable Nonclinical Findings on Wound Healing After Celecoxib Treatment

Animal model	Celebrex daily dose (mg/kg)	Wound model	Post-injury dosing duration	Post-Injury healing assessment duration	Findings vs. controls	Reference
Mouse	7.5, twice a day	<i>ob/ob</i> diabetic	8 days	8 days	No significant effects	Kämpfer et al., 2005
Rat Male	10	Rotator cuff repair	2, 4, 8 weeks	2, 4, 8 weeks	Significant ↓ in tendon-to-bone healing	Cohen et al., 2006
Female	10	Patellar tendon transection	14 days	14 days	↓ failure load and healing strength	Ferry et al., 2007
Male	1500 ppm	Fasciocutaneous flap survival, revascularization and healing	12 hrs	12 h	No effects on healing	Wax et al., 2007
Mouse	20	Hemophilia B	2, 4, 6, 8, 10, 12, 15 days	2, 4, 6, 8, 10, 12, 15 days	No delay in cutaneous wound healing	Hoffman et al., 2009

formation and resorption via their direct actions on both osteoblasts and osteoclasts, and the effects of various mediators of bone cell functions are enhanced via the induction of COX-2 in these cells. PGE₂ is the most abundant PG produced by osteoblasts, which plays a critical role in bone-to-bone formation, woven bone formation, and bone resorption, primarily through the PGE₂ and PGE₄ (EP₂ and EP₄) receptor subtypes (Radi and Khan, 2005; Radi et al., 2009). The mechanism of COX effects have not been established definitively, but may be related to marked reductions in PGE₂ and osteoblastic proliferation with or without PG inhibition (Radi and Khan, 2005; Radi, 2009). Nonclinical studies have suggested that celecoxib may have an effect on bone and wound healing, as evidenced by delayed bone fracture and wound healing (Tables 2-2 and 2-3). Brown et al. (2004) examined the effects of the daily administration (beginning 1 day after fracture) of celecoxib (3 mg/kg per day) for up to 12 weeks on femur fracture healing in adult male Wistar rats. The data from this study indicated that celecoxib did not delay healing at either 4, 8, or 12 weeks following fracture. However, histological analysis of bone fractures revealed the presence of more fibrous tissue (fibrous healing) and less woven bone formation (endochondral and immature bone formation) at 4 and 8 weeks in the celecoxib-treated rats, but mechanical strength and radiographic signs of healing were similar to those in the control rats. Bergenstock et al. (2005) measured fracture healing at 8 weeks in female Sprague–Dawley rats treated once daily for 10 days after fracture with celecoxib at 3 and 6 mg/kg per day. Celecoxib treatment caused a significant decrease in fracture healing (Bergenstock et al., 2005). Mullis et al. (2006) did a bone biomechanical, biochemical, and histological assessment at 4, 8, and 12 weeks after fracture creation in the tibiae of male C57BL/6N mice given dosages of 10 and 50 mg/kg per day of celecoxib for up to 12 weeks. No differences in biomechanical, biochemical, or histological parameters were noted in the celecoxib-treated mice. The effects of low-intensity pulsed ultrasound (LIPUS) and celecoxib on ulna stress fractures were investigated in rats. Animals were treated for 5 days per week with celecoxib at 5 mg/kg. One to three hours following drug administration, all animals were treated with unilateral active-LIPUS, and the contralateral inactive-LIPUS and ulnas were evaluated histologically at 2, 4, and 8 weeks following induction of stress fractures. Neither LIPUS nor celecoxib influenced bone resorption, but each had significant and opposite effects on the intracortical bone formation rate. There was no interaction between LIPUS and celecoxib, indicating that the beneficial LIPUS effect was not mediated by the cyclooxygenase-2 pathway. LIPUS accelerated stress fracture healing, whereas celecoxib delayed repair. When used in combination, the beneficial LIPUS effect was not impaired by celecoxib (Li et al., 2007).

In a study by Simon and O’Connon (2007), the authors examined the effects of celecoxib on femur fracture following daily administration (before and after fracture) of celecoxib at 2, 4, and 8 mg/kg per day in rats for at least 8 weeks. Beginning 4 h after fracture and continuing for 5 or 15 days, the results showed that all doses of celecoxib reduced the mechanical properties of the fracture callus and caused a significant increase in the proportion of nonunion fractures. Conversely, when celecoxib treatment was given prior to fracture or 14 days (delayed) after fracture, no significant decline in the fracture-healing process was noted. In another

study, structural femoral bone allograft healing was delayed in C57BL/6 mice given celecoxib at doses of 25 mg/kg per day for 2 or 5 weeks (O’Keefe et al., 2006). Delayed ulna stress fracture repair was noted in male rats following treatment 5 days per week with 5 mg/kg of celecoxib for up to 8 weeks (Li et al., 2007). Herbenick et al. (2008) found that daily supplementation to male Sprague–Dawley rats of celecoxib, at a mean dose of 3.2 mg/day, for up to 12 weeks decreased femur biomechanical strength but did not affect callus formation, and the effect on the strength of fracture callus was most pronounced in the early inflammatory phase (Herbenick et al., 2008). Celecoxib at 4 mg/kg administered daily for up to 2 weeks following femur fracture in female Sprague–Dawley rats resulted in the reduction of the callus cell proliferation rate at day 4 but not at day 2, 7, or 10 (Cottrel and O’Conner, 2009). However, celecoxib 10 mg/kg did not significantly inhibit the rate of spinal fusion in rabbits (Long et al., 2002). In addition, there were no detrimental effects of celecoxib on proteoglycan turnover and the content of osteoarthritic cartilage in a female beagle dog osteoarthritis model when celecoxib was administered at 100 or 200 mg/kg per day for at least 15 weeks after knee surgery (Mastbergen et al., 2006).

The effects of celecoxib on fracture healing were compared to acetaminophen. Mid-diaphyseal femur fractures were produced in female Sprague–Dawley rats, and the rats were given once-daily oral dosing of 60 or 300 mg/kg of acetaminophen or 3 or 6 mg/kg of celecoxib for 10 days after fracture. Fracture healing was measured after 8 weeks by radiographic examination, mechanical testing, and histology. Radiographic scoring revealed that acute celecoxib treatment impaired fracture healing significantly, whereas acetaminophen treatment had no effect. Mechanical testing supported the radiographic observations. No negative effects of celecoxib or acetaminophen treatment on the structural properties (peak torque and torsional rigidity) of the healing were detected. Celecoxib treatment, but not acetaminophen treatment, significantly reduced the material properties (maximum shear stress and shear modulus) of the healing femurs. Postmechanical testing examination of the healing femurs found that 73% of the vehicle- or acetaminophen-treated femurs had healed as unions, 27% failed as incomplete unions, and none failed as nonunions. In contrast, only 21% of the fractured femurs from the celecoxib-treated rats had healed as unions, 53% failed as incomplete unions, and 26% failed as nonunions. The proportion of nonunions among the celecoxib-treated rats was significantly higher than that of the control and acetaminophen-treated rats. Histological examination indicated that celecoxib treatment altered normal fracture callus morphology in which cartilage rather than new bone abutted the fracture site (Bergensstock et al., 2005). The effects of twice-daily oral administration of celecoxib; loxoprofen, an ns-NSAID; and SC-58560, a COX-1 s-NSAID, were compared using an adjuvant-induced arthritis (AIA) rat model. Drugs were given for 10 days beginning 15 days after adjuvant injection. Celecoxib was administered at 3 mg/kg per day, eloxoprofen at 3 mg/kg per day, and SC-58560 at 10 mg/kg per day. The therapeutic effects on three-dimensional architectural bone changes under arthritic conditions (e.g., the bone volume/total tissue volume ratio and the amount of trabecular bone pattern factor) were determined using microcomputed tomography (micro-CT). In addition, dual-energy x-ray absorptiometry two-dimensional bone analysis

was performed to compare with micro-CT analysis. The AIA rats had substantial inflammatory bone destruction and erosion, which allows for significant changes in the three-dimensional architectural index. This inflammatory bone destruction was potently suppressed by celecoxib, only moderately suppressed by eloxoprofen, and not at all suppressed by SC-58560 (Noguchi et al., 2008). The clinical and joint destruction (radiographic and histopathological) effects of twice-daily oral administration of 0.01 to 3 mg/kg celecoxib and 0.013 to 3 mg/kg eloxoprofen were evaluated in the AIA model. The drugs were given by twice-daily oral administration for 10 days beginning 15 days after adjuvant injection. Celecoxib significantly inhibited paw swelling, hyperalgesic response, and joint destruction (both radiographic and histopathological findings) in these arthritic rats. These bone efficacy effects of celecoxib were superior to those of eloxoprofen (Noguchi et al., 2005). In a mouse collagen-induced arthritis model, celecoxib, deracoxib, 5-lipoxygenase (5-LO), or leukotriene A₄ (LTA₄) hydrolase inhibitor, administered by oral gavage twice daily in a 0.1-mL volume, when administered alone decreased severity but had little effect on disease incidence, defined as any sign of redness and swelling in the paws. However, the combination of COX-2 s-NSAIDs with 5-LO inhibitors produced significant decreases in both incidence and severity, and normal-appearing COX-2/LT inhibitor paws in all experiments were examined histologically and found to have no signs of infiltration or cartilage joint destruction (Anderson et al., 2009). Therefore, results from these nonclinical studies suggest that celecoxib may have an effect on bone healing, especially at earlier stages, but appears to bear no significant impact on the ultimate long-term outcome.

The effects of administration of rofecoxib at 12.5 mg once-daily dosing on fibula osteotomy healing in male New Zealand white rabbits was compared to administration of ibuprofen at 150 mg once a day for 28 days after surgery. Bone healing was assessed by histomorphometry at 3 and 6 weeks after osteotomy, and at 6 and 12 weeks by torsional mechanical testing (O'Connor et al., 2009). Fracture callus morphology was abnormal in the rofecoxib-treated rabbits, and torsional mechanical testing showed that fracture healing was impaired. Ibuprofen treatment caused persistence of cartilage within the fracture callus and reduced peak torque at 6 weeks after osteotomy. In the fracture allowed to progress to possible healing, nonunion was seen in some of the fibulae from the rofecoxib- and ibuprofen-treated animals (O'Connor et al., 2009). In another study in adult male New Zealand rabbits, the short-term (for 5 days) effects of several NSAIDs (indometacin, meloxicam, or rofecoxib) on healing after middiaphyseal osteotomy of the right ulna were investigated. Radiological, biomechanical, and histomorphometric evaluation were performed at 6 weeks (Karachalios et al., 2007). The incidence of radiologically incomplete union in the rofecoxib-treated rabbits was similar to that in the control group. Statistically, all the biomechanical parameters were significantly lower in the indometacin and meloxicam groups than in the control group. Only the fracture load values were found to be statistically significantly lower in the rofecoxib group. Histomorphometric parameters were adversely affected in all groups, with the specimens of the rofecoxib group showing the least negative effect. The effects of rofecoxib dosed at 3 mg/kg once a day on femoral fractures in male rats was investigated and revealed impaired

fracture healing based on histopathological and radiologic observations (Simon et al., 2002). Thus, short-term administration of low therapeutic doses of a rofecoxib had a minor negative effect on bone healing (Karachalios et al., 2007). NS-398 had no effect on periosteal bone formation in the rat tibia (Forwood, 1996; Li J. et al., 2002). In a study in mice, animals underwent surgery to induce an open transverse middiaphyseal femoral fracture, which was then fixed using a custom-made external fixator, and rofecoxib was administered orally at 5 mg/kg per day. Effects on fracture healing were investigated using radiographic assessment, histological analysis, biomechanical testing, and laser Doppler flowmetry to assess blood flow across the fracture gap. Poor healing was observed by radiography only on day 32. Histological analysis demonstrated that the control animals healed more quickly (at days 24 and 32) and had more callus and less fibrous tissue (at days 8 and 32) than those of the rofecoxib-treated animals. Biomechanical testing revealed that the control animals were stronger at day 32. The rofecoxib-treated mice exhibited a lower median flow from day 4 onward that was significant at days 4, 16, and 24 (Murnaghan and Marsh, 2006). Thus, rofecoxib reduced blood flow across the fracture gap and correlated with reduced fracture-healing outcomes in mice. In a study in male Wistar rats, a closed, nondisplaced femoral fracture was induced, and rofecoxib at 8 mg/kg or ibuprofen at 30 mg/kg was provided in food for 4 weeks. Both rofecoxib and ibuprofen diminished fracture-healing parameters during the early stages of fracture repair. Compared with ibuprofen, rofecoxib was significantly more likely to produce nonunions. Gross nonunions were noted in 64.7% of rofecoxib-treated rats, 17.6% of ibuprofen-treated rats, and 0% in placebo controls. Mean callus width was 8.9 mm for rofecoxib, 8.9 mm for ibuprofen, and 8 mm for placebo controls. Mean healing maturity was 1.6 in the rofecoxib-treated group, 1.7 in the ibuprofen-treated group, and 2.7 in the placebo controls. Mean fracture angulation was 30.8° for rofecoxib, 14.3° for ibuprofen, and 13.4° for placebo. Mean histologic healing was 5.75 for rofecoxib, 6.35 for ibuprofen, and 8.25 for placebo (Leonelli et al., 2006).

The effects of an orally administered ns-NSAID, ketorolac, and a COX-2 s-NSAID, valdecoxib, on fracture healing in rats for either 7 or 21 days were assessed with biomechanical, histological, and biochemical analyses (Gerstenfeld et al., 2007). No significant effects on the rate of fracture nonunion were noted at either 21 or 35 days. The 21-day treatment produced significantly more nonunions in valdecoxib-treated rats than in either ketorolac-treated or control animals, but these differences disappeared by 35 days. The reversibility of the effects after drug withdrawal was assessed in fracture calluses. The assessment showed that ketorolac treatment led to two- to threefold lower levels of PGE₂ than those with valdecoxib. Histological analysis showed delayed remodeling of calcified cartilage and reduced bone formation in association with valdecoxib treatment (Gerstenfeld et al., 2007).

The long-term effect of intraperitoneal administration of parecoxib sodium daily at a 1.06-mg/kg dose for 7 days on middiaphyseal bone healing in rats, when applied in a pattern similar to clinical treatment patterns, that is, in a high dose and for a short period after bone fracture, was evaluated (Akritopoulos et al., 2009). Bone union and callus formation fracture healing were evaluated by x-rays at 28 and 42 days after surgery. No statistically significant differences were noted in the

parecoxib-treated rats (Akritopoulos et al., 2009). In another study in female Wistar rats, parecoxib was also administered intraperitoneally at 0.05 mg per 100 g body weight for 7 days after a closed tibial fracture. At 2, 3, and 6 weeks after surgery, bone mineral density (BMD) at the fracture site was measured using dual-energy x-ray absorptiometry (DEXA). The BMD at the fracture site was calculated as the average of the results after 2, 3, and 6 weeks. Mean BMD was lower in the parecoxib group than in the control group. However, there were no statistically significant differences in mechanical properties of the healing fractures after 6 weeks (Dimmen et al., 2008). Furthermore, parecoxib at 0.05 mg per 100 g body weight and indomethacin at 0.0625 mg per 100 g body weight were administered to female Wistar rats for 7 days after being subjected to a closed tibial fracture stabilized with an intramedullary nail. Two and three weeks after surgery, the bone density at the fracture site was measured using DEXA. Parecoxib decreased BMD at the fracture site 3 weeks after fracture and indomethacin after 2 weeks. Both parecoxib and indomethacin reduced the ultimate bending moment and the bending stiffness of the healing fractures after 3 weeks (Dimmen et al., 2009). Gregory and Forwood (2007) studied woven bone in female Wistar rats. Periosteal woven bone callus was initiated in the right tibia following a single bout of four-point bending applied as a haversine wave for 300 cycles at a frequency of 2 Hz and a magnitude of 65 N. The rats were injected daily with a COX-2 s-NSAID, 5,5-dimethyl-3-(3-fluorophenyl)-4-(4-methylsulfonyl)phenyl-2(5*H*)-furanone (DFU) at 2 mg/kg starting 7 days postloading, and the tibiae were examined 2, 3, 4, and 5 weeks postloading. No significant difference in peak woven bone area was observed in the DFU-treated rats. Treatment with DFU resulted in a temporal defect in woven bone formation, where the achievement of peak woven bone area was delayed by 1 week. However, woven bone remodeling was observed in DFU-treated rats at 21 days postloading, demonstrating that remodeling of the periosteal callus is not prevented in the presence of a COX-2 s-NSAID in the rat. The effect of meloxicam on bone healing of calvarial defects was assessed in male Wistar rats. A linear incision was made through the skin of the scalp, a full-thickness flap was reflected, and a 4-mm round defect was made with a trephine drill. The animals were injected daily via the subcutaneous route with 3 mg/kg of meloxicam for 15 or 45 days. The bone filling was measured histometrically. Intergroup comparisons demonstrated that the meloxicam groups had a significant reduction in bone healing compared to their respective controls (Gurgel et al., 2005). In a rat AIA model, etoricoxib was given orally at a 0.6-mg/kg dose, twice daily, starting on day 0 and until euthanasia on day 21, and the effects on bone were evaluated and radiographs were taken from adjuvant injected and noninjected hind paws on days 0 and 21. Etoricoxib treatment resulted in a clear reduction in adjuvant-induced radiographic changes of bone and joint structures compared with the vehicle group (Riendeau et al., 2001).

In summary, nonclinical data regarding the effects of NSAIDs on bone healing have been variable and results do suggest that nonselective NSAIDs and COX-2 selective NSAIDs may have some effect on bone fracture healing. Such an effect is apparent at the earlier stages of the healing process but bears no significant impact on the overall long-term healing of the fracture (Ho et al., 1998;

Gerstenfeld et al., 2003b; Brown et al., 2004; Radi and Khan, 2005; Radi 2009; Nyangoga et al., 2010).

EFFECTS OF ns-NSAIDs ON LIGAMENT AND TENDON HEALING

In comparison to bone fracture healing, little information is available to evaluate the effects of NSAIDs on ligament and tendon healing. With the exception of some *in vitro* data, long-term NSAID use has not been associated with adverse effects on normal tendon or ligament healing. Nonclinical models have shown variable results on the healing of these structures, both beneficial and deleterious (Radi and Khan, 2005). In an *in vitro* study, diclofenac and aceclofenac had no significant effect on tendon cell proliferation or glycosaminoglycan synthesis; however, indomethacin and naproxen inhibited cell proliferation within patella tendons and inhibited glycosaminoglycan synthesis in both the digital flexor and patella tendons of rabbits (Riley et al., 2001). Treatment of nonhuman primates with oral ibuprofen significantly reduced the force required for tendon gliding following flexor tendon injury and reduced the breaking strength of completely divided and repaired extensor tendons (Kulick et al., 1986). Flurbiprofen treatment following Achilles tendon transection in rats resulted in better organization of the extracellular collagenous matrix, but decreased the cross-sectional area and failure load (Yuan et al., 2003). Indomethacin, by contrast, improved tendon healing after tendon transection in rats, as demonstrated by the reduced cross-sectional area, without change in failure load (Forslund et al., 2003). Furthermore, indomethacin significantly increased tensile strength at 16 weeks after tenotomy of plantaris longus tendons in rabbits, but did not change the total collagen content (Forslund et al., 2003). Piroxicam treatment on days 1 to 6 after injury to medial contralateral ligaments of rats also resulted in a 42% increase in the strength of ligaments at day 14 postinjury (Dahners et al., 1988). In contrast, continuous treatment with indomethacin had no significant effect on mechanical performance or histologic appearance at 2 or 6 weeks after tenotomy of rabbit Achilles tendons, and treatment for 14 days with ibuprofen had no effect on mechanical strength at 14 or 28 days after injury to medial contralateral ligaments of rabbits (Carlstedt et al., 1986; Moorman et al., 1999). Additionally, neither indomethacin- nor ibuprofen-treated rabbits regained their torsional strength after 5 or 8 weeks of treatment (Thomas et al., 1991). Diclofenac had no effect on tendon healing (Tornkvist et al., 1984). From these observations, it can be concluded that treatment with NSAIDs in experimental animal models has shown variable intra- and interspecies effects (Radi and Khan, 2005). The effects of several NSAIDs (ibuprofen, acetaminophen, naproxen, piroxicam, celecoxib, valdecoxib) on patellar tendon healing were investigated in Sprague–Dawley rats that underwent transection of the patellar tendon at the inferior pole of the patella (Ferry et al., 2007). At 14 days the repair site tissue was analyzed biochemically. The control group demonstrated greater maximum load than did the celecoxib, valdecoxib, and piroxicam groups. The acetaminophen and ibuprofen groups were also significantly stronger than the celecoxib group, but not statistically different from the control

group. The investigators concluded that with the exception of ibuprofen, these NSAIDs had a detrimental effect on healing strength at the bone–tendon junction, as demonstrated by decreased failure loads and increased failures of the cerclage suture. Acetaminophen had no effect on healing strength. The biomechanical properties closely paralleled the total collagen content at the injury site, suggesting that these agents may alter healing strength by decreasing collagen content (Ferry et al., 2007).

EFFECTS OF COX-2 s-NSAIDs ON LIGAMENT AND TENDON HEALING

Similar to ns-NSAIDs, COX-2 s-NSAIDs have not been widely evaluated in non-clinical models of ligament and tendon healing (Table 2-3) (Radi and Khan, 2005). In a rat model of Achilles tendon transection, parecoxib showed an adverse effect on early tendon repair (postinjury days 1 to 5), but improved tendon remodeling when given during later stages of repair (days 6 to 14) (Virchenko et al., 2004). When given throughout the healing phase, both indomethacin and celecoxib improved the outcome after Achilles tendon transection in rats (Yuan et al., 2003). In another study, celecoxib administration for 6 days after surgical transection of the right medial collateral ligament in rats was associated with a 32% lower load to failure on day 14 compared to untreated/transected ligaments (Elder et al., 2001). In the same model, SC-560, a relatively selective COX-1 inhibitor, had no effect on the strength of injured ligaments (Bogatov et al., 2003). Because an ns-NSAID was not evaluated concurrently in the celecoxib study, direct comparison of COX-2 selective versus nonselective COX inhibition was not possible (Radi and Khan, 2005). Ekman (2002) discussed several additional shortcomings associated with this investigation in a “Letter to the Editor” and suggests alternatively that celecoxib use is actually beneficial in ankle injury in humans.

Nonclinical studies on the effects of celecoxib on wound healing are highly variable and contradictory. Significant inhibition of tendon-to-bone healing was noted after celecoxib treatment in a Sprague–Dawley rat model of acute rotator cuff repair (Cohen et al., 2006). Ferry et al. (2007) examined the effects of daily administration of celecoxib, 10 mg/kg, for 14 days on patellar tendon healing in female Sprague–Dawley rats and found that celecoxib decreased healing at the bone–tendon junction. In contrast, using a diabetic *ob/ob* mouse model, Kämpfer et al. (2005) demonstrated that celecoxib, 7.5 mg/kg, given twice daily for at least 8 days beginning at day 5 following wounding, did not impair wound healing. In an in vitro cell proliferation study, celecoxib administration was shown to result in a dose-dependent inhibition of rat Achilles tendon cell proliferation and migration; however, no effects on types I and II collagen expression were observed (Tsai et al., 2007). Celecoxib, as a supplement to food at a dose of 1500 ppm, showed no deleterious effects on fasciocutaneous flap survival, revascularization, and healing for up to 12 h postdose in a Sprague–Dawley male rat model (Wax et al., 2007). Celecoxib therapy may inhibit adhesion formation during tendon healing, with subsequent improvement in functional recovery. Another study found that celecoxib,

at a higher dose, 20 mg/kg, for up to 15 days does not delay cutaneous wound healing in a hemophilia B mouse model (Hoffman et al., 2009). In a study in adult rats, bilateral transection of the knee medial collateral ligaments was performed and animals were treated 5 days per week with celecoxib at 5 mg/kg. One to three hours after drug administration, all animals were treated with unilateral active low-intensity pulsed ultrasound (US) and contralateral inactive low-intensity pulsed US. Equal numbers of animals were tested mechanically at 2, 4, and 12 weeks after injury. US and celecoxib treatment did not influence ligament mechanical properties at any time point. After 2 weeks, ligaments treated with active low-intensity pulsed US were 34.2% stronger, 27% stiffer, and could absorb 54.4% more energy before failure than could ligaments treated with inactive low-intensity pulsed US, whereas ligaments from the celecoxib-treated group could absorb 33.3% less energy than could ligaments from the control group. There were no US or celecoxib effects after 4 and 12 weeks of intervention. Thus, low-intensity pulsed US accelerated, but did not improve, ligament healing, whereas celecoxib delayed, but did not impair, healing (Warden et al., 2006). Collectively, the effects of celecoxib on wound healing in nonclinical studies appear highly variable.

CONCLUSIONS

In this chapter we described the nonclinical and clinical roles of PGs in bone metabolism and healing, data to illustrate these roles, expression of COX-1/COX-2 in normal and diseased states of bone, and an overall assessment of the effects of nonselective NSAIDs versus COX-2 s-NSAIDs on healing. PGs are known modulators of tissue metabolism, including bone, ligament, and tendons, via the action of osteoclasts and osteoblasts. PGE₂ is the most abundant PG produced by osteoblasts, and has been demonstrated to play a critical role in bone-to-bone formation, woven bone formation, and bone resorption, primarily through the EP₂ and EP₄ PG receptor subtypes. PGs are additionally demonstrated to release in response to mechanical force and stimulate cAMP. These roles of PGs in metabolism translate to bone healing. In the inflammatory stage of healing, PGs, particularly PGE₂, are produced abundantly by osteoblasts and accumulate in the fracture callus, creating a rich microenvironment of PG activity. PGE₂, PGI₂, and TXA₂ then stimulate bone resorption via increase and activity of osteoclasts, followed by bone remodeling and/formation (Radi and Khan, 2005). The production of PGs in bone has been enhanced indirectly by COX-2 induction. COX-1 is constitutively present in normal skeleton and COX-2 is up-regulated during initial stages of bone repair, inflammation, or in neoplastic skeleton conditions.

Nonclinical models revealed that NSAIDs and COX-2 s-NSAIDs could impair bone, tendon, and ligament healing with variable results. The exact mechanism of COX effects is not well defined but may be related to significant reductions in PGE₂ and osteoblastic proliferation with or without PG inhibition. Results from animal models do suggest that ns-NSAIDs and COX-2 s-NSAIDs may have a minimal effect on bone, tendon, and ligament healing, especially at earlier stages, but bear no significant impact on the ultimate long-term outcome

(Radi and Khan, 2005). Despite the abundant nonclinical evidence that PGs produce effects on bone metabolism, little relevant clinical evidence is available to adequately assess the significance of PG inhibition by nonselective or COX-2 selective inhibitors. Although inhibition of COX-2 may play a role in these effects, there is no clear convincing evidence that COX-2 s-NSAIDs are any more deleterious than conventional ns-NSAIDs.

Overall, the relevance of the available nonclinical data to humans is unknown due to (1) no replicable data of associated orthopedic problems with ns-NSAIDs or COX-2 s-NSAIDs in humans from randomized large, controlled clinical reports; (2) inconsistent results from nonclinical studies that ns-NSAIDs or COX-2 s-NSAIDs affect the long-term outcome of bone, tendon, or ligament healing; (3) intra- and interspecies dose and sensitivity differences; (4) undefined compensating systemic and local factors that may also regulate bone repair; (5) the unknown effects of underlying conditions (age, rate of bone turnover, or disease affliction) that may influence bone healing; (6) differences in dosing duration and levels between experimental animal models and clinical applications; and (7) the lack of large controlled clinical trials needed to better assess the orthopedic effects of these drugs (Radi and Khan, 2005; Radi, 2009).

REFERENCES

- Adams SS, Bough RG, Cliffe EE, Lessel B, et al. Absorption, distribution and toxicity of ibuprofen. *Toxicol Appl Pharmacol* 1969;15:310–330.
- Adolphson P, Jonsson U, Dalen N. Piroxicam-induced reduction in osteopenia after external fixation of rabbit tibia. *Acta Orthop Scand* 1991;62:363–366.
- Adolphson P, Abbaszadegan H, Jonsson U, Dalen N, et al. No effects of piroxicam on osteopenia and recovery after Colles' fracture: a randomized, double-blind, placebo-controlled, prospective trial. *Arch Orthop Trauma Surg* 1993;112:127–130.
- Akhter MP, Cullen DM, Pan LC. Bone biomechanical properties in EP4 knockout mice. *Calcif Tissue Int* 2006;78:357–362.
- Akman S, Gogus A, Sener N, Bilgic B, et al. Effect of diclofenac sodium on union of tibial fractures in rats. *Adv Ther* 2002;19:119–125.
- Akritopoulos P, Papaioannidou P, Hatzokos I, Haritanti A, et al. Parecoxib has non-significant long-term effects on bone healing in rats when administered for a short period after fracture. *Arch Orthop Trauma Surg* 2009;129:1427–1432.
- Alander CB, Raisz LG. Effects of selective prostaglandins E2 receptor agonists on cultured calvarial murine osteoblastic cells. *Prostaglandins Other Lipid Mediat* 2006;81:178–183.
- Allen HL, Wase A, Bear WT. Indomethacin and aspirin: effect of nonsteroidal anti-inflammatory agents on the rate of fracture repair in the rat. *Acta Orthop Scand* 1980;51:595–600.
- Altman RD, Latta LL, Keer R, Renfree K, et al. Effect of nonsteroidal antiinflammatory drugs on fracture healing: a laboratory study in rats. *J Orthop Trauma* 1995;9:392–400.
- Anderson DM, Maraskovsky E, Billingsley WL, et al. A homologue of the TNF receptor and its ligand enhance T-cell growth and dendritic-cell function. *Nature* 1997;390:175–179.
- Anderson GD, Keys KL, De Ciechi PA, Masferrer JL. Combination therapies that inhibit cyclooxygenase-2 and leukotriene synthesis prevent disease in murine collagen induced arthritis. *Inflamm Res* 2009;58:109–117.
- Ankarath S, Raman R, Giannoudis PV. Non-steroidal anti-inflammatory drugs in orthopaedic practice: an update. *Curr Orthop* 2003;17:144–149.
- Arasapam G, Scherer M, Cool JC, Foster BK, et al. Roles of COX-2 and iNOS in the bony repair of the injured growth plate cartilage. *J Cell Biochem* 2006;99:450–461.

- Arikawa T, Omura K, Morita I. Regulation of bone morphogenetic protein-2 expression by endogenous prostaglandin E2 in human mesenchymal stem cells. *J Cell Physiol* 2004;200:400–406.
- Asundi KR, Rempel DM. MMP-1, IL-1beta, and COX-2 mRNA expression is modulated by static load in rabbit flexor tendons. *Ann Biomed Eng* 2008;36:237–243.
- Auer JA, Goodship A, Arnoczky S, Pearce S, et al. Refining animal models in fracture research: seeking consensus in optimising both animal welfare and scientific validity for appropriate biomedical use. *BMC Musculoskelet Disord* 2007;8:72.
- Bauer DC, Orwoll ES, Fox KM, Vogt TM, et al. Aspirin and NSAID use in older women: effect on bone mineral density and fracture risk. Study of Osteoporotic Fractures Research Group. *J Bone Miner Res* 1996;11:29–35.
- Beck A, Krischak G, Sorg T, Augat P, et al. Influence of diclofenac (group of nonsteroidal anti-inflammatory drugs) on fracture healing. *Arch Orthop Trauma Surg* 2003;123:327–332.
- Bell NH, Hollis BW, Shary JR, Eyre DR, et al. Diclofenac sodium inhibits bone resorption in postmenopausal women. *Am J Med* 1994;96:349–353.
- Bergenstock M, Min W, Simon AM, Sabatino C, et al. A comparison between the effects of acetaminophen and celecoxib on bone fracture healing in rats. *J Orthop Trauma* 2005;19:717–723.
- Berglund M, Hart DA, Wiig M. The inflammatory response and hyaluronan synthases in the rabbit flexor tendon and tendon sheath following injury. *J Hand Surg Eur Vol* 2007;32:581–587.
- Bergot C, Wu Y, Jolivet E, Zhou LQ, et al. The degree and distribution of cortical bone mineralization in the human femoral shaft change with age and sex in a microradiographic study. *Bone* 2009;45:435–442.
- Bhattacharyya T, Levin R, Vrahas MS, Solomon DH. Nonsteroidal antiinflammatory drugs and nonunion of humeral shaft fractures. *Arthritis Rheum* 2005;53:364–367.
- Bichara J, Greenwell H, Drisko C, Wittwer JW, et al. The effect of postsurgical naproxen and a bioabsorbable membrane on osseous healing in intrabony defects. *J Periodontol* 1999;70:869–877.
- Blackwell KA, Hortschansky P, Sanovic S, et al. Bone morphogenetic protein 2 enhances PGE(2)-stimulated osteoclast formation in murine bone marrow cultures. *Prostaglandins Other Lipid Mediat* 2009;90:76–80.
- Bo J, Sudmann E, Marton PF. Effect of indomethacin on fracture healing in rats. *Acta Orthop Scand* 1976;47:588–599.
- Bogatov VB, Weinhold P, Dahners LE. The influence of a cyclooxygenase-1 inhibitor on injured and uninjured ligaments in the rat. *Am J Sports Med* 2003;31:574–576.
- Boiskin I, Epstein S, Ismail F, Fallon MD, Levy W. Long term administration of prostaglandin inhibitors in vivo fail to influence cartilage and bone mineral metabolism in the rat. *Bone Miner* 1988;4:27–36.
- Brighton CT, Krebs AG. Oxygen tension of healing fractures in the rabbit. *J Bone Joint Surg Am* 1972;54:323–332.
- Bring D, Reno C, Renstrom P, Salo P, Hart D, Ackermann P. Prolonged immobilization compromises up-regulation of repair genes after tendon rupture in a rat model. *Scand J Med Sci Sports* 2009;20:411–417.
- Brooks PM, Day RO. Nonsteroidal antiinflammatory drugs: differences and similarities. *N Engl J Med* 1991;324:1716–1725.
- Brown AP, Courtney CL, King LM, Groom SC, Graziano MJ. Cartilage dysplasia and tissue mineralization in the rat following administration of a FGF receptor tyrosine kinase inhibitor. *Toxicol Pathol* 2005;33:449–455.
- Brown KM, Saunders MM, Kirsch T, Donahue HJ, Reid JS. Effect of COX-2-specific inhibition on fracture-healing in the rat femur. *J Bone Joint Surg Am* 2004;86-A:116–123.
- Bruder SP, Fink DJ, Caplan AI. Mesenchymal stem cells in bone development, bone repair, and skeletal regeneration therapy. *J Cell Biochem* 1994;56:283–294.
- Bucay N, Sarosi I, Dunstan CR. Osteoprotegerin-deficient mice develop early onset osteoporosis and arterial calcification. *Genes Dev* 1998;12:1260–1268.
- Burd TA, Hughes MS, Anglen JO. Heterotopic ossification prophylaxis with indomethacin increases the risk of long-bone nonunion. *J Bone Joint Surg Br* 2003;85:700–705.
- Burdan F, Szumilo J, Marzec B, Klepacz R, et al. Skeletal developmental effects of selective and non-selective cyclooxygenase-2 inhibitors administered through organogenesis and fetogenesis in Wistar CRL:(WI)WUBR rats. *Toxicology* 2005;216:204–223.

- Burdan F, Szumilo J, Dworzański W, Szumilo M, et al. Immunoexpression of constitutive and inducible cyclooxygenase isoforms in distinguishing and accessory structures of synovial joints in rat fetuses. *Folia Morphol (Warsz)* 2009;68:59–64.
- Burssens A, Thiery J, Kohl P, Molderez A, et al. Prevention of heterotopic ossification with tenoxicam following total hip arthroplasty: a double-blind, placebo-controlled dose-finding study. *Acta Orthop Belg* 1995;61:205–211.
- Burstein AH, Reilly DT, Martens M. Aging of bone tissue: mechanical properties. *J Bone Joint Surg Am* 1976;58:82–86.
- Butcher CK, Marsh DR. Non steroidal anti-inflammatory drugs delay tibial fracture union. *Injury* 1996;27:375.
- Carlstedt CA, Madsen K, Wredmark T. The influence of indomethacin on tendon healing: a biomechanical and biochemical study. *Arch Orthop Trauma Surg* 1986;105:332–336.
- Chikazu D, Tomizuka K, Ogasawara T, Saijo H, et al. Cyclooxygenase-2 activity is essential for the osseointegration of dental implants. *Int J Oral Maxillofac Surg* 2007;36:441–446.
- Choudhary S, Alander C, Zhan P, Gao Q, et al. Effect of deletion of the prostaglandin EP2 receptor on the anabolic response to prostaglandin E2 and a selective EP2 receptor agonist. *Prostaglandins Other Lipid Mediat* 2008a;86:35–40.
- Choudhary S, Huang H, Raisz L, Pilbeam C. Anabolic effects of PTH in cyclooxygenase-2 knockout osteoblasts in vitro. *Biochem Biophys Res Commun* 2008b;372:536–541.
- Cohen DB, Kawamura S, Ehteshami JR, Rodeo SA. Indomethacin and celecoxib impair rotator cuff tendon-to-bone healing. *Am J Sports Med* 2006;34:362–369.
- Colvin JS, Bohne BA, Harding GW, et al. Skeletal overgrowth and deafness in mice lacking fibroblast growth factor receptor-3. *Nat Genet* 1996;12:390–397.
- Connolly CK, Li G, Bunn JR, Mushipe M, Dickson GR, Marsh DR. A reliable externally fixated murine femoral fracture model that accounts for variation in movement between animals. *J Orthop Res* 2003;21:843–849.
- Cottrell JA, O'Connor JP. Pharmacological inhibition of 5-lipoxygenase accelerates and enhances fracture-healing. *J Bone Joint Surg Am* 2009;91:2653–2665.
- Cruess RL, Dumont J. Fracture healing. *Can J Surg* 1975;18:403–413.
- Dahners LE, Gilbert JA, Lester GE, Taft TN, et al. The effect of a nonsteroidal antiinflammatory drug on the healing of ligaments. *Am J Sports Med* 1988;16:641–646.
- Davis TR, Ackroyd CE. Non-steroidal anti-inflammatory agents in the management of Colles' fractures. *Br J Clin Pract* 1988;42:184–189.
- Dawson AB. The age order of epiphyseal union in the long bones of the albino rat. *Anat Rec* 1925;31:1–17.
- de Crombrugge B, Lefebvre V, Nakashima K. Regulatory mechanisms in the pathways of cartilage and bone formation. *Curr Opin Cell Biol* 2001;13:721–727.
- Dekel S, Lenthall G, Francis MJ. Release of prostaglandins from bone and muscle after tibial fracture: an experimental study in rabbits. *J Bone Joint Surg Br* 1981;63-B:185–189.
- Deng C, Wynshaw-Boris A, Zhou F, et al. Fibroblast growth factor receptor 3 is a negative regulator of bone growth. *Cell* 1996;84:911–921.
- Dickens DS, Kozielski R, Khan J, Forus A, et al. Cyclooxygenase-2 expression in pediatric sarcomas. *Pediatr Dev Pathol* 2002;5:356–364.
- Dimar JR 2nd, Ante WA, Zhang YP, Glassman SD. The effects of nonsteroidal anti-inflammatory drugs on posterior spinal fusions in the rat. *Spine* 1996;21:1870–1876.
- Dimitriou R, Dahabreh Z, Katsoulis E, Matthews SJ, et al. Application of recombinant BMP-7 on persistent upper and lower limb non-unions. *Injury* 2005;36 Suppl 4:S51–S59.
- Dimmen S, Nordsletten L, Engebretsen L, Steen H, Madsen JE. Negative effect of parecoxib on bone mineral during fracture healing in rats. *Acta Orthop* 2008;79:438–444.
- Dimmen S, Nordsletten L, Madsen JE. Parecoxib and indomethacin delay early fracture healing: a study in rats. *Clin Orthop Relat Res* 2009;467:1992–1999.
- Dubrow SA, Hruby PM, Akhter MP. Gender specific LRP5 influences on trabecular bone structure and strength. *J Musculoskelet Neuronal Interact* 2007;7:166–173.
- Edwall D, Prissel PT, Levinovitz A, Jennische E, et al. Expression of insulin-like growth factor I messenger ribonucleic acid in regenerating bone after fracture: influence of indomethacin. *J Bone Miner Res* 1992;7:207–213.

- Einhorn TA. The cell and molecular biology of fracture healing. *Clin Orthop Relat Res* 1998;S7–S21.
- Ekman EF. A cyclooxygenase-2 inhibitor impairs ligament healing in the rat. *Am J Sports Med* 2002;30:457.
- Elder CL, Dahners LE, Weinhold PS. A cyclooxygenase-2 inhibitor impairs ligament healing in the rat. *Am J Sports Med* 2001;29:801–805.
- Elves MW, Bayley I, Roylance PJ. The effect of indomethacin upon experimental fractures in the rat. *Acta Orthop Scand* 1982;53:35–41.
- Endo K, Sairyo K, Komatsubara S, Sasa T, et al. Cyclooxygenase-2 inhibitor delays fracture healing in rats. *Acta Orthop* 2005;76:470–474.
- Engesaeter LB, Sudmann B, Sudmann E. Fracture healing in rats inhibited by locally administered indomethacin. *Acta Orthop Scand* 1992;63:330–333.
- Enneking WF, Burchardt H, Puhl JJ, Piotrowski G. Physical and biological aspects of repair in dog cortical-bone transplants. *J Bone Joint Surg Am* 1975;57:237–252.
- Erben RG. Trabecular and endocortical bone surfaces in the rat: modeling or remodeling? *Anat Rec* 1996;246:39–46.
- Faye-Petersen OM, Johnson WH Jr, Carlo WA, Hedlund GL, et al. Prostaglandin E1–induced hyperostosis: clinicopathologic correlations and possible pathogenetic mechanisms. *Pediatr Pathol Lab Med* 1996;16:489–507.
- Feng X, McDonald JM. Disorders of bone remodeling. *Annu Rev Pathol* 2011;6:121–145.
- Ferry ST, Dahners LE, Afshari HM, Weinhold PS. The effects of common anti-inflammatory drugs on the healing rat patellar tendon. *Am J Sports Med* 2007;35:1326–1333.
- Feyen JH, van der Wilt G, Moonen P, Di Bon A, et al. Stimulation of arachidonic acid metabolism in primary cultures of osteoblast-like cells by hormones and drugs. *Prostaglandins* 1984;28:769–781.
- Forslund C, Bylander B, Aspenberg P. Indomethacin and celecoxib improve tendon healing in rats. *Acta Orthop Scand* 2003;74:465–469.
- Forwood MR. Inducible cyclo-oxygenase (COX-2) mediates the induction of bone formation by mechanical loading in vivo. *J Bone Miner Res* 1996;11:1688–1693.
- Fradette ME, Céleste C, Richard H, Beauchamp G, et al. Effects of continuous oral administration of phenylbutazone on biomarkers of cartilage and bone metabolism in horses. *Am J Vet Res* 2007;68:128–133.
- Freiberg AH. Wolff's law and the functional pathogenesis of deformity. *J Bone Joint Surg Am* 1902;15:200–220.
- Gajraj NM. The effect of cyclooxygenase-2 inhibitors on bone healing. *Reg Anesth Pain Med* 2003;28:456–465.
- Gao Q, Zhan P, Alander CB, Kream BE, et al. Effects of global or targeted deletion of the EP4 receptor on the response of osteoblasts to prostaglandin in vitro and on bone histomorphometry in aged mice. *Bone* 2009;45:98–103.
- Gebuhr P, Wilbek H, Soelberg M. Naproxen for 8 days can prevent heterotopic ossification after hip arthroplasty. *Clin Orthop Relat Res* 1995;314:166–169.
- Geng Y, Blanco FJ, Cornelissen M, Lotz M. Regulation of cyclooxygenase-2 expression in normal human articular chondrocytes. *J Immunol* 1995;155:796–801.
- Gerstenfeld LC, Einhorn TA. COX inhibitors and their effects on bone healing. *Expert Opin Drug Saf* 2004;3:131–136.
- Gerstenfeld LC, Cullinane DM, Barnes GL, Graves DT, et al. Fracture healing as a post-natal developmental process: molecular, spatial, and temporal aspects of its regulation. *J Cell Biochem* 2003a;88:873–884.
- Gerstenfeld LC, Thiede M, Seibert K, Mielke C, et al. Differential inhibition of fracture healing by non-selective and cyclooxygenase-2 selective non-steroidal anti-inflammatory drugs. *J Orthop Res* 2003b;21:670–675.
- Gerstenfeld LC, Al-Ghawas M, Alkhiary YM, Cullinane DM, et al. Selective and nonselective cyclooxygenase-2 inhibitors and experimental fracture-healing: reversibility of effects after short-term treatment. *J Bone Joint Surg Am* 2007;89:114–125.
- Giannoudis PV, MacDonald DA, Matthews SJ, Smith RM, et al. Nonunion of the femoral diaphysis: the influence of reaming and non-steroidal anti-inflammatory drugs. *J Bone Joint Surg Br* 2000;82:655–658.

- Gill TJ, McCulloch PC, Glasson SS, Blanchet T, et al. Chondral defect repair after the microfracture procedure: a nonhuman primate model. *Am J Sports Med* 2005;33:680–685.
- Giordano V, Giordano M, Knackfuss IG, Apfel MI, Gomes RD. Effect of tenoxicam on fracture healing in rat tibiae. *Injury* 2003;34:85–94.
- Glassman SD, Rose SM, Dimar JR, Puno RM, Campbell MJ, Johnson Jr. The effect of postoperative nonsteroidal anti-inflammatory drug administration on spinal fusion. *Spine* 1998;23:834–838.
- Goodman S, Ma T, Trindade M, Ikenoue T, et al. COX-2 selective NSAID decreases bone ingrowth in vivo. *J Orthop Res* 2002;20:1164–1169.
- Govender S, Csimma C, Genant HK, Valentin-Opran A, et al. Recombinant human bone morphogenetic protein-2 for treatment of open tibial fractures: a prospective, controlled, randomized study of four hundred and fifty patients. *J Bone Joint Surg Am* 2002;84-A:2123–2134.
- Gregory LS, Forwood MR. Cyclooxygenase-2 inhibition delays the attainment of peak woven bone formation following four-point bending in the rat. *Calcif Tissue Int* 2007;80:176–183.
- Grohs JG, Schmidt M, Waniwenhaus A. Selective COX-2 inhibitor versus indomethacin for the prevention of heterotopic ossification after hip replacement: a double-blind randomized trial of 100 patients with 1-year follow-up. *Acta Orthop* 2007;78:95–98.
- Gurgel BC, Ribeiro FV, Silva MA, Nociti FH Jr, et al. Selective COX-2 inhibitor reduces bone healing in bone defects. *Braz Oral Res* 2005;19:312–316.
- Gurton AU, Akin E, Sagdic D, Olmez H. Effects of PGI₂ and TxA₂ analogs and inhibitors in orthodontic tooth movement. *Angle Orthod* 2004;74:526–532.
- Hedges RE, Clement JG, Thomas CD, O'Connell TC. Collagen turnover in the adult femoral mid-shaft: modeled from anthropogenic radiocarbon tracer measurements. *Am J Phys Anthropol* 2007;133:808–816.
- Heppenstall RB, Grislis G, Hunt TK. Tissue gas tensions and oxygen consumption in healing bone defects: tissue gas tensions and oxygen consumption in healing bone defects. *Clin Orthop Relat Res* 1975;106:357–365.
- Herbenick MA, Sprott D, Stills H, Lawless M. Effects of a cyclooxygenase 2 inhibitor on fracture healing in a rat model. *Am J Orthop (Belle Mead NJ)* 2008;37:E133–E137.
- Hert J. Wolff's law of transformation after 100 years. *Acta Chir Orthop Traumatol Cech* 1990;57:465–476.
- High WB. Effects of orally administered prostaglandin E-2 on cortical bone turnover in adult dogs: a histomorphometric study. *Bone* 1987;8:363–373.
- Ho ML, Chang JK, Wang GJ. Effects of ketorolac on bone repair: a radiographic study in modeled demineralized bone matrix grafted rabbits. *Pharmacology* 1998;57:148–159.
- Ho ML, Chang JK, Chuang LY, Hsu HK, et al. Effects of nonsteroidal anti-inflammatory drugs and prostaglandins on osteoblastic functions. *Biochem Pharmacol* 1999;58:983–990.
- Hoffman M, Pradhan S, Monroe DM. Celecoxib does not delay cutaneous wound healing in haemophilia B mice. *Haemophilia* 2009;15:615–616.
- Hogevold HE, Groggaard B, Reikeras O. Effects of short-term treatment with corticosteroids and indomethacin on bone healing: a mechanical study of osteotomies in rats. *Acta Orthop Scand* 1992;63:607–611.
- Hosono A, Yamaguchi U, Makimoto A, Endo M, et al. Utility of immunohistochemical analysis for cyclo-oxygenase 2 in the differential diagnosis of osteoblastoma and osteosarcoma. *J Clin Pathol* 2007;60:410–414.
- Hsu HC, Fong YC, Chang CS, Hsu CJ, et al. Ultrasound induces cyclooxygenase-2 expression through integrin, integrin-linked kinase, Akt, NF-kappaB and p300 pathway in human chondrocytes. *Cell Signal* 2007;19:2317–2328.
- Huang H, Chikazu D, Voznesensky OS, Herschman HR, et al. Parathyroid hormone induction of cyclooxygenase-2 in murine osteoblasts: role of the calcium–calcineurin–NFAT pathway. *J Bone Miner Res* 2010;25:819–829.
- Hunziker EB, Schenk RK. Physiological mechanisms adopted by chondrocytes in regulating longitudinal bone growth in rats. *J Physiol* 1989;414:55–71.
- Huo MH, Troiano NW, Pelker RR, Gundberg CM, et al. The influence of ibuprofen on fracture repair: biomechanical, biochemical, histologic, and histomorphometric parameters in rats. *J Orthop Res* 1991;9:383–390.

- Hurley MM, Lee SK, Raisz LG, Bernecker P, et al. Basic fibroblast growth factor induces osteoclast formation in murine bone marrow cultures. *Bone* 1998;22:309–316.
- Igarashi K, Woo JT, Stern PH. Effects of a selective cyclooxygenase-2 inhibitor, celecoxib, on bone resorption and osteoclastogenesis in vitro. *Biochem Pharmacol* 2002;63:523–532.
- Jaffre B, Watrin A, Loeuille D, Gillet P, et al. Effects of antiinflammatory drugs on arthritic cartilage: a high-frequency quantitative ultrasound study in rats. *Arthritis Rheum* 2003;48:1594–601.
- Jee WS, Ma YF. The in vivo anabolic actions of prostaglandins in bone. *Bone* 1997;21:297–304.
- Joldersma M, Burger EH, Semeins CM, Klein-Nulend J. Mechanical stress induces COX-2 mRNA expression in bone cells from elderly women. *J Biomech* 2000;33:53–61.
- Judex S, Donahue LR, Rubin C. Genetic predisposition to low bone mass is paralleled by an enhanced sensitivity to signals anabolic to the skeleton. *FASEB J* 2002;16:1280–1282.
- Kämpfer H, Schmidt R, Geisslinger G, Pfeilschifter J, et al. Wound inflammation in diabetic ob/ob mice: functional coupling of prostaglandin biosynthesis to cyclooxygenase-1 activity in diabetes-impaired wound healing. *Diabetes* 2005;54:1543–1551.
- Karachalios T, Boursinos L, Pountsides L, Khaldi L, et al. The effects of the short-term administration of low therapeutic doses of anti-COX-2 agents on the healing of fractures: an experimental study in rabbits. *J Bone Joint Surg Br* 2007;89:1253–1260.
- Kawaguchi H, Pilbeam CC, Harrison JR, Raisz LG. The role of prostaglandins in the regulation of bone metabolism. *Clin Orthop Relat Res* 1995;313:36–46.
- Kawaguchi H, Chikazu D, Nakamura K, Kumegawa M, et al. Direct and indirect actions of fibroblast growth factor 2 on osteoclastic bone resorption in cultures. *J Bone Miner Res* 2000;15:466–473.
- Ke HZ, Jee WS, Mori S, Li XJ, Kimmel DB. Effects of long-term daily administration of prostaglandin-E2 on maintaining elevated proximal tibial metaphyseal cancellous bone mass in male rats. *Calcif Tissue Int* 1992;50:245–252.
- Ke HZ, Jee WS, Ito H, Setterberg RB, et al. Greater bone formation induction occurred in aged than young cancellous bone sites. *Bone* 1993;14:481–485.
- Keller J, Bunger C, Andreassen TT, Bak B, et al. Bone repair inhibited by indomethacin: effects on bone metabolism and strength of rabbit osteotomies. *Acta Orthop Scand* 1987;58:379–383.
- Keller J, Hansen ES, He SZ, Kjaersgaard-Andersen P, et al. Early hemodynamic response to tibial osteotomy in rabbits: influence of indomethacin and prostaglandin E2. *J Orthop Res* 1991;9:539–544.
- Keller J, Klamer A, Bak B, Suder P. Effect of local prostaglandin E2 on fracture callus in rabbits. *Acta Orthop Scand* 1993;64:59–63.
- Kellinsalmi M, Parikka V, Risteli J, Hentunen T, et al. Inhibition of cyclooxygenase-2 down-regulates osteoclast and osteoblast differentiation and favours adipocyte formation in vitro. *Eur J Pharmacol* 2007;572:102–110.
- Kember NF. Aspects of the maturation process in growth cartilage in the rat tibia. *Clin Orthop* 1973;95:288–294.
- Kidd LJ, Stephens AS, Kuliwaba JS, Fazzalari NL, et al. Temporal pattern of gene expression and histology of stress fracture healing. *Bone* 2010;46:369–378.
- Kjaersgaard-Andersen P, Nafei A, Teichert G, Kristensen O, et al. Indomethacin for prevention of heterotopic ossification: a randomized controlled study in 41 hip arthroplasties. *Acta Orthop Scand* 1993;64:639–642.
- Kong YY, Yoshida H, Sarosi I, Tan HL, et al. OPGL is a key regulator of osteoclastogenesis, lymphocyte development and lymph-node organogenesis. *Nature* 1999;397:315–323.
- Koshima H, Kondo S, Mishima S, Choi HR, et al. Expression of interleukin-1beta, cyclooxygenase-2, and prostaglandin E2 in a rotator cuff tear in rabbits. *J Orthop Res* 2007;25:92–97.
- Krieger NS, Frick KK, LaPlante Strutz K, et al. Regulation of COX-2 mediates acid-induced bone calcium efflux in vitro. *J Bone Miner Res* 2007;22:907–917.
- Krischak GD, Augat P, Sorg T, Blakytyn R, et al. Effects of diclofenac on periosteal callus maturation in osteotomy healing in an animal model. *Arch Orthop Trauma Surg* 2007;127:3–9.
- Kulick MI, Smith S, Hadler K. Oral ibuprofen: evaluation of its effect on peritendinous adhesions and the breaking strength of a tenorrhaphy. *J Hand Surg [Am]* 1986;11:110–120.
- Kuroda S, Viridi AS, Dai Y, Shott S, et al. Patterns and localization of gene expression during intramembranous bone regeneration in the rat femoral marrow ablation model. *Calcif Tissue Int* 2005;77:212–225.

- Lane N, Coble T, Kimmel DB. Effect of naproxen on cancellous bone in ovariectomized rats. *J Bone Miner Res* 1990;5:1029–1035.
- Lascelles BD, King S, Roe S, Marcellin-Little DJ, Jones S. Expression and activity of COX-1 and 2 and 5-LOX in joint tissues from dogs with naturally occurring coxofemoral joint osteoarthritis. *J Orthop Res* 2009;27:1204–1208.
- Lee CM, Genetos DC, Wong A, Yellowley CE. Prostaglandin expression profile in hypoxic osteoblastic cells. *J Bone Miner Metab* 2010;28:8–16.
- Leonelli SM, Goldberg BA, Safanda J, Bagwe MR, et al. Effects of a cyclooxygenase-2 inhibitor (rofecoxib) on bone healing. *Am J Orthop (Belle Mead NJ)* 2006;35:79–84.
- Li J, Burr DB, Turner CH. Suppression of prostaglandin synthesis with NS-398 has different effects on endocortical and periosteal bone formation induced by mechanical loading. *Calcif Tissue Int* 2002;70:320–329.
- Li J, Waugh LJ, Hui SL, Burr DB, et al. Low-intensity pulsed ultrasound and nonsteroidal anti-inflammatory drugs have opposing effects during stress fracture repair. *J Orthop Res* 2007;25:1559–1567.
- Li M, Ke HZ, Qi H, Healy DR, et al. A novel, non-prostanoid EP2 receptor-selective prostaglandin E2 agonist stimulates local bone formation and enhances fracture healing. *J Bone Miner Res* 2003;18:2033–2042.
- Li M, Healy DR, Li Y, Simmons HA, et al. Osteopenia and impaired fracture healing in aged EP4 receptor knockout mice. *Bone* 2005;37:46–54.
- Li X, Okada Y, Pilbeam CC, Lorenzo JA, et al. Knockout of the murine prostaglandin EP2 receptor impairs osteoclastogenesis in vitro. *Endocrinology* 2000;141:2054–2061.
- Li X, Pilbeam CC, Pan L, Breyer RM, Raisz LG. Effects of prostaglandin E2 on gene expression in primary osteoblastic cells from prostaglandin receptor knockout mice. *Bone* 2002;30:567–573.
- Li XJ, Jee WS, Li YL, Patterson-Buckendahl P. Transient effects of subcutaneously administered prostaglandin E2 on cancellous and cortical bone in young adult dogs. *Bone* 1990;11:353–364.
- Lin CH, Jee WS, Ma YF, Setterberg RB. Early effects of prostaglandin E2 on bone formation and resorption in different bone sites of rats. *Bone* 1995;17:255S–259S.
- Lindholm TS, Tornkvist H. Inhibitory effect on bone formation and calcification exerted by the anti-inflammatory drug ibuprofen: an experimental study on adult rat with fracture. *Scand J Rheumatol* 1981;10:38–42.
- Long J, Lewis S, Kuklo T, Zhu Y, et al. The effect of cyclooxygenase-2 inhibitors on spinal fusion. *J Bone Joint Surg Am* 2002;84-A:1763–1768.
- Marks SC Jr, Miller S. Local infusion of prostaglandin E1 stimulates mandibular bone formation in vivo. *J Oral Pathol* 1988;17:500–505.
- Marui A, Hirose K, Maruyama T, Arai Y, et al. Prostaglandin E2 EP4 receptor-selective agonist facilitates sternal healing after harvesting bilateral internal thoracic arteries in diabetic rats. *J Thorac Cardiovasc Surg* 2006;131:587–593.
- Mastbergen SC, Marijnissen AC, Vianen ME, Zoer B, et al. Inhibition of COX-2 by celecoxib in the canine groove model of osteoarthritis. *Rheumatology (Oxford)* 2006;45:405–413.
- Mayahara K, Kobayashi Y, Takimoto K, Suzuki N, et al. Aging stimulates cyclooxygenase-2 expression and prostaglandin E2 production in human periodontal ligament cells after the application of compressive force. *J Periodont Res* 2007;42:8–14.
- Mbugua SW, Skoglund LA, Lokken P. Effects of phenylbutazone and indomethacin on the post-operative course following experimental orthopaedic surgery in dogs. *Acta Vet Scand* 1989;30:27–35.
- McCalden RW, McGeough JA, Barker MB, Court-Brown CM. Age-related changes in the tensile properties of cortical bone. The relative importance of changes in porosity, mineralization, and microstructure. *J Bone Joint Surg Am* 1993;75:1193–1205.
- Miyamoto H, Onuma H, Shigematsu H, Suzuki S, et al. The effect of etodolac on experimental temporomandibular joint osteoarthritis in dogs. *J Craniomaxillofac Surg* 2007;35:358–363.
- Miyauchi M, Hiraoka M, Oka H, Sato S, et al. Immuno-localization of COX-1 and COX-2 in the rat molar periodontal tissue after topical application of lipopolysaccharide. *Arch Oral Biol* 2004;49:739–746.
- Miyaura C, Inada M, Suzawa T, Sugimoto Y, et al. Impaired bone resorption to prostaglandin E2 in prostaglandin E receptor EP4-knockout mice. *J Biol Chem* 2000;275:19819–19823.

- Moed BR, Resnick RB, Fakhouri AJ, Nallamothu B, et al. Effect of two nonsteroidal antiinflammatory drugs on heterotopic bone formation in a rabbit model. *J Arthroplasty* 1994;9:81–87.
- Mohammed SI, Khan KN, Sellers RS, Hayek MG, et al. Expression of cyclooxygenase-1 and 2 in naturally-occurring canine cancer. *Prostaglandins Leukot Essent Fatty Acids* 2004;70:479–483.
- Moorman CT 3rd, Kukreti U, Fenton DC, Belkoff SM. The early effect of ibuprofen on the mechanical properties of healing medial collateral ligament. *Am J Sports Med* 1999;27:738–741.
- More RC, Kody MH, Kabo JM, Dorey FJ, et al. The effects of two nonsteroidal anti-inflammatory drugs on limb swelling, joint stiffness, and bone torsional strength following fracture in a rabbit model. *Clin Orthop* 1989;247:306–312.
- Moses VS, Hardy J, Bertone AL, Weisbrode SE. Effects of anti-inflammatory drugs on lipopolysaccharide-challenged and -unchallenged equine synovial explants. *Am J Vet Res* 2001;62:54–60.
- Mullins MN, Lana SE, Dernell WS, Ogilvie GK, et al. Cyclooxygenase-2 expression in canine appendicular osteosarcomas. *J Vet Intern Med* 2004;18:859–865.
- Mullis BH, Copland ST, Weinhold PS, Miclau T, et al. Effect of COX-2 inhibitors and non-steroidal anti-inflammatory drugs on a mouse fracture model. *Injury* 2006;37:827–837.
- Mungo DV, Zhang X, O’Keefe RJ, Rosier RN, et al. COX-1 and COX-2 expression in osteoid osteomas. *J Orthop Res* 2002;20:159–162.
- Murnaghan M, Li G, Marsh DR. Nonsteroidal anti-inflammatory drug-induced fracture nonunion: An inhibition of angiogenesis? *J Bone Joint Surg Am* 2006;88 Suppl 3: 140–147.
- Naik AA, Xie C, Zuscik MJ, Kingsley P, et al. Reduced COX-2 expression in aged mice is associated with impaired fracture healing. *J Bone Miner Res* 2009;24:251–264.
- Noguchi M, Kimoto A, Kobayashi S, Yoshino T, et al. Effect of celecoxib, a cyclooxygenase-2 inhibitor, on the pathophysiology of adjuvant arthritis in rat. *Eur J Pharmacol* 2005;513:229–235.
- Noguchi M, Kimoto A, Sasamata M, Miyata K. Micro-CT imaging analysis for the effect of celecoxib, a cyclooxygenase-2 inhibitor, on inflammatory bone destruction in adjuvant arthritis rats. *J Bone Miner Metab* 2008;26:461–468.
- Norrdin RW, Shih MS. Systemic effects of prostaglandin E2 on vertebral trabecular remodeling in beagles used in a healing study. *Calcif Tissue Int* 1988;42:363–368.
- Nyangoga H, Aguado E, Goyenvalle E, Baslé MF, et al. A non-steroidal anti-inflammatory drug (ketoprofen) does not delay beta-TCP bone graft healing. *Acta Biomater* 2010;6:3310–3317.
- Obeid G, Zhang X, Wang X. Effect of ibuprofen on the healing and remodeling of bone and articular cartilage in the rabbit temporomandibular joint. *J Oral Maxillofac Surg* 1992;50:843–849.
- Ochi H, Hara Y, Asou Y, Harada Y, et al. Effects of long-term administration of carprofen on healing of a tibial osteotomy in dogs. *Am J Vet Res* 2011;72:634–641.
- O’Connor JP, Lysz T. Celecoxib, NSAIDs and the skeleton. *Drugs Today (Barc)* 2008;44:693–709.
- O’Connor JP, Capo JT, Tan V, Cottrell JA, et al. A comparison of the effects of ibuprofen and rofecoxib on rabbit fibula osteotomy healing. *Acta Orthop* 2009;80:597–605.
- Oka H, Miyauchi M, Sakamoto K, et al. PGE2 activates cementoclastogenesis by cementoblasts via EP4. *J Dent Res* 2007;86:974–979.
- Okada Y, Lorenzo JA, Freeman AM, Tomita M, et al. Prostaglandin G/H synthase-2 is required for maximal formation of osteoclast-like cells in culture. *J Clin Invest* 2000;105:823–832.
- Okada Y, Pilbeam C, Raisz L, Tanaka Y. Role of cyclooxygenase-2 in bone resorption. *J Uoeh* 2003;25:185–195.
- O’Keefe RJ, Tiyapananaputi P, Xie C, Li TF, et al. COX-2 has a critical role during incorporation of structural bone allografts. *Ann NY Acad Sci* 2006;1068:532–542.
- Oliveira TM, Sakai VT, Machado MA, Dionísio TJ, et al. COX-2 inhibition decreases VEGF expression and alveolar bone loss during the progression of experimental periodontitis in rats. *J Periodontol* 2008;79:1062–1069.
- Onishi E, Fujibayashi S, Takemoto M, Neo M, et al. Enhancement of bone-bonding ability of bioactive titanium by prostaglandin E2 receptor selective agonist. *Biomaterials* 2008;29:877–883.
- Ono K, Akatsu T, Kugai N, Pilbeam CC, et al. The effect of deletion of cyclooxygenase-2, prostaglandin receptor EP2, or EP4 in bone marrow cells on osteoclasts induced by mouse mammary cancer cell lines. *Bone* 2003;33:798–804.
- Onoe Y, Miyaura C, Kaminakayashiki T, Nagai Y, et al. IL-13 and IL-4 inhibit bone resorption by suppressing cyclooxygenase-2-dependent prostaglandin synthesis in osteoblasts. *J Immunol* 1996;156: 758–764.

- Parfitt AM, Travers R, Rauch F, Glorieux FH. Structural and cellular changes during bone growth in healthy children. *Bone* 2000;27:487–494.
- Paulson SK, Zhang JY, Breau AP, Hribar JD, et al. Pharmacokinetics, tissue distribution, metabolism, and excretion of celecoxib in rats. *Drug Metab Dispos* 2000;28:514–521.
- Perraud J, Stadler J, Kessedjian MJ, Monro AM. Reproductive studies with the anti-inflammatory agent, piroxicam: modification of classical protocols. *Toxicology* 1984;30:59–63.
- Perry SM, McIlhenny SE, Hoffman MC, Soslowsky LJ. Inflammatory and angiogenic mRNA levels are altered in a supraspinatus tendon overuse animal model. *J Shoulder Elbow Surg* 2005;14:79S–83S.
- Persson PE, Sodemann B, Nilsson OS. Preventive effects of ibuprofen on periarticular heterotopic ossification after total hip arthroplasty: a randomized double-blind prospective study of treatment time. *Acta Orthop Scand* 1998;69:111–115.
- Plotquin D, Dekel S, Katz S, Danon A. Prostaglandin release by normal and osteomyelitic human bones. *Prostaglandins Leukot Essent Fatty Acids* 1991;43:13–15.
- Pountos I, Giannoudis PV, Jones E, English A, et al. NSAIDs inhibit in vitro MSC chondrogenesis but not osteogenesis. *J Cell Mol Med* 2010;15:525–534.
- Pradhan BB, Tatsumi RL, Gallina J, Kuhns CA, et al. Ketorolac and spinal fusion: Does the perioperative use of ketorolac really inhibit spinal fusion? *Spine (Phila Pa 1976)* 2008;33:2079–2082.
- Prisby RD, Ramsey MW, Behnke BJ, Dominguez JM 2nd, et al. Aging reduces skeletal blood flow, endothelium-dependent vasodilation, and NO bioavailability in rats. *J Bone Miner Res* 2007;22:1280–1288.
- Probst A, Spiegel HU. Cellular mechanisms of bone repair. *J Invest Surg* 1997;10:77–86.
- Radi ZA. Pathophysiology of cyclooxygenase inhibition in animal models. *Toxicol Pathol* 2009;37:34–46.
- Radi ZA, Koza-Taylor PH, Bil RR, Obert LA, et al. Increased serum enzyme levels associated with kupffer cell reduction with no signs of hepatic or skeletal muscle injury. *Am J Pathol* 2011;179:240–247.
- Radi ZA, Khan NK. Effects of cyclooxygenase inhibition on bone, tendon, and ligament healing. *Inflamm Res* 2005;54(9):358–366.
- Radi ZA, Ostroski R. Pulmonary and cardiorenal cyclooxygenase-1 (COX-1), -2 (COX-2), and microsomal prostaglandin E synthase-1 (mPGES-1) and -2 (mPGES-2) expression in a hypertension model. *Mediators Inflamm* 2007;2007:85091.
- Radi ZA, Kehrl ME Jr, Ackermann MR. Cell adhesion molecules, leukocyte trafficking, and strategies to reduce leukocyte infiltration. *J Vet Intern Med* 2001;15:516–529.
- Radi ZA, Guzman RE, Bell RR. Increased connective tissue extracellular matrix in the op/op model of osteopetrosis. *Pathobiology* 2009;76:199–203.
- Raisz LG. Physiology and pathophysiology of bone remodeling. *Clin Chem* 1999a;45:1353–1358.
- Raisz LG. Prostaglandins and bone: physiology and pathophysiology. *Osteoarthritis Cartilage* 1999b;7:419–421.
- Raisz LG. Potential impact of selective cyclooxygenase-2 inhibitors on bone metabolism in health and disease. *Am J Med* 2001;110 Suppl 3A:43S–45S.
- Rapuano BE, Boursiquot R, Tomin E, MacDonald DE, et al. The effects of COX-1 and COX-2 inhibitors on prostaglandin synthesis and the formation of heterotopic bone in a rat model. *Arch Orthop Trauma Surg* 2008;128:333–344.
- Reikeraas O, Engebretsen L. Effects of ketorolac tromethamine and indomethacin on primary and secondary bone healing: an experimental study in rats. *Arch Orthop Trauma Surg* 1998;118:50–52.
- Richards JB, Joseph L, Schwartzman K, Kreiger N, et al. The effect of cyclooxygenase-2 inhibitors on bone mineral density: results from the Canadian Multicentre Osteoporosis Study. *Osteoporos Int* 2006;17:1410–1419.
- Riendeau D, Percival MD, Brideau C, Charleson S, et al. Etoricoxib (MK-0663): preclinical profile and comparison with other agents that selectively inhibit cyclooxygenase-2. *J Pharmacol Exp Ther* 2001;296:558–566.
- Riew KD, Long J, Rhee J, Lewis S, et al. Time-dependent inhibitory effects of indomethacin on spinal fusion. *J Bone Joint Surg Am* 2003;85-A:632–634.
- Riley GP, Cox M, Harrall RL, Clements S, et al. Inhibition of tendon cell proliferation and matrix glycosaminoglycan synthesis by non-steroidal anti-inflammatory drugs in vitro. *J Hand Surg [Br]* 2001;26:224–228.

- Ringel RE, Brenner JI, Haney PJ, Burns JE, et al. Prostaglandin-induced periostitis: a complication of long-term PGE1 infusion in an infant with congenital heart disease. *Radiology* 1982;142:657–658.
- Ro J, Langeland N, Sander J. Effect of indomethacin on collagen metabolism of rat fracture callus in vitro. *Acta Orthop Scand* 1978;49:323–328.
- Roach HI, Mehta G, Oreffo RO, Clarke NM, et al. Temporal analysis of rat growth plates: cessation of growth with age despite presence of a physis. *J Histochem Cytochem* 2003;51:373–383.
- Robertson G, Xie C, Chen D, Awad H, et al. Alteration of femoral bone morphology and density in COX-2^{-/-} mice. *Bone* 2006;39:767–772.
- Rohde C, Anderson DE, Bertone AL, Weisbrode SE. Effects of phenylbutazone on bone activity and formation in horses. *Am J Vet Res* 2000;61:537–543.
- Romas E, Sims NA, Hards DK, et al. Osteoprotegerin reduces osteoclast numbers and prevents bone erosion in collagen-induced arthritis. *Am J Pathol* 2002;161:1419–1427.
- Sakuma Y, Tanaka K, Suda M, Yasoda A, et al. Crucial involvement of the EP4 subtype of prostaglandin E receptor in osteoclast formation by proinflammatory cytokines and lipopolysaccharide. *J Bone Miner Res* 2000;15:218–227.
- Sakuma Y, Li Z, Pilbeam CC, Alander CB, et al. Stimulation of cAMP production and cyclooxygenase-2 by prostaglandin E(2) and selective prostaglandin receptor agonists in murine osteoblastic cells. *Bone* 2004;34:827–834.
- Sato S, Kim T, Arai T, Maruyama S, et al. Comparison between the effects of dexamethasone and indomethacin on bone wound healing. *Jpn J Pharmacol* 1986;42:71–78.
- Saudan M, Saudan P, Perneger T, Riand N, et al. Celecoxib versus ibuprofen in the prevention of heterotopic ossification following total hip replacement: a prospective randomised trial. *J Bone Joint Surg Br* 2007;89:155–159.
- Schmitz JP, Hollinger JO. The critical size defect as an experimental model for craniomandibulofacial nonunions. *Clin Orthop Relat Res* 1986;205:299–308.
- Schrage YM, Machado I, Meijer D, Briaire-de Bruijn I, et al. COX-2 expression in chondrosarcoma: A role for celecoxib treatment? *Eur J Cancer* 2010;46:616–624.
- Seidenberg AB, An YH. Is there an inhibitory effect of COX-2 inhibitors on bone healing? *Pharmacol Res* 2004;50:151–156.
- Shamir D, Keila S, Weinreb M. A selective EP4 receptor antagonist abrogates the stimulation of osteoblast recruitment from bone marrow stromal cells by prostaglandin E2 in vivo and in vitro. *Bone* 2004;34:157–162.
- Shih MS, Norrdin RW. Effect of prostaglandin E2 on rib fracture healing in beagles: histomorphometric study on periosteum adjacent to the fracture site. *Am J Vet Res* 1986;47:1561–1564.
- Shimizu N, Ozawa Y, Yamaguchi M, Goseki T, et al. Induction of COX-2 expression by mechanical tension force in human periodontal ligament cells. *J Periodontol* 1998;69:670–677.
- Simon AM, Manigrasso MB, O'Connor JP. Cyclo-oxygenase 2 function is essential for bone fracture healing. *J Bone Miner Res* 2002;17:963–976.
- Simon AM, O'Connor JP. Dose and time-dependent effects of cyclooxygenase-2 inhibition on fracture-healing. *J Bone Joint Surg Am* 2007;89:500–511.
- Spector JA, Mehrara BJ, Greenwald JA, Saadeh PB, et al. Osteoblast expression of vascular endothelial growth factor is modulated by the extracellular microenvironment. *Am J Physiol Cell Physiol* 2001;280:C72–C80.
- Spiro AS, Beil FT, Baranowsky A, Barvencik F, et al. BMP-7-induced ectopic bone formation and fracture healing is impaired by systemic NSAID application in C57BL/6-mice. *J Orthop Res* 2010;28:785–791.
- Steinbrech DS, Mehrara BJ, Saadeh PB, Greenwald JA, et al. VEGF expression in an osteoblast-like cell line is regulated by a hypoxia response mechanism. *Am J Physiol Cell Physiol* 2000;278:C853–C860.
- Stolina M, Adamo S, Ominsky M, et al. RANKL is a marker and mediator of local and systemic bone loss in two rat models of inflammatory arthritis. *J Bone Miner Res* 2005;20:1756–1765.
- Sudmann E, Bang G. Indomethacin-induced inhibition of haversian remodelling in rabbits. *Acta Orthop Scand* 1979;50:621–627.
- Sudmann E, Hagen T. Indomethacin-induced delayed fracture healing. *Arch Orthop Unfallchir* 1976;85:151–154.

- Sudmann E, Dregelid E, Bessesen A, Morland J. Inhibition of fracture healing by indomethacin in rats. *Eur J Clin Invest* 1979;9:333–339.
- Sudmann E, Tveita T, Hald J Jr. Lack of effect of indomethacin on ordered growth of the femur in rats. *Acta Orthop Scand* 1982;53:43–49.
- Sun JS, Tsuang YH, Lin FH, Liu HC, et al. Bone defect healing enhanced by ultrasound stimulation: an in vitro tissue culture model. *J Biomed Mater Res* 1999;46:253–261.
- Suponitzky I, Weinreb M. Differential effects of systemic prostaglandin E2 on bone mass in rat long bones and calvariae. *J Endocrinol* 1998;156:51–57.
- Suzawa T, Miyaura C, Inada M, Maruyama T, et al. The role of prostaglandin E receptor subtypes (EP1, EP2, EP3, and EP4) in bone resorption: an analysis using specific agonists for the respective EPs. *Endocrinology* 2000;141:1554–1559.
- Tai H, Miyaura C, Pilbeam CC, Tamura T, et al. Transcriptional induction of cyclooxygenase-2 in osteoblasts is involved in interleukin-6-induced osteoclast formation. *Endocrinology* 1997;138:2372–2379.
- Taketa T, Sakai A, Tanaka S, Nakai K, et al. Selective cyclooxygenase-2 inhibitor prevents reduction of trabecular bone mass in collagen-induced arthritic mice in association with suppression of RANKL/OPG ratio and IL-6 mRNA expression in synovial tissues but not in bone marrow cells. *J Bone Miner Metab* 2008;26:143–151.
- Tanaka M, Sakai A, Uchida S, Tanaka S, et al. Prostaglandin E2 receptor (EP4) selective agonist (ONO-4819.CD) accelerates bone repair of femoral cortex after drill-hole injury associated with local upregulation of bone turnover in mature rats. *Bone* 2004;34:940–948.
- Tang CH, Yang RS, Huang TH, Lu DY, et al. Ultrasound stimulates cyclooxygenase-2 expression and increases bone formation through integrin, focal adhesion kinase, phosphatidylinositol 3-kinase, and Akt pathway in osteoblasts. *Mol Pharmacol* 2006;69:2047–2057.
- Thomas J, Taylor D, Crowell R, Assor D. The effect of indomethacin on Achilles tendon healing in rabbits. *Clin Orthop Relat Res* 1991;308–311.
- Thorsen K, Kristoffersson AO, Lerner UH, Lorentzon RP. In situ microdialysis in bone tissue: stimulation of prostaglandin E2 release by weight-bearing mechanical loading. *J Clin Invest* 1996;98:2446–2449.
- Tornkvist H, Lindholm TS. Effect of ibuprofen on mass and composition of fracture callus and bone: an experimental study on adult rat. *Scand J Rheumatol* 1980;9:167–171.
- Tornkvist H, Lindholm TS, Netz P, Stromberg L, et al. Effect of ibuprofen and indomethacin on bone metabolism reflected in bone strength. *Clin Orthop Relat Res* 1984; 255–259.
- Trappe TA, Carroll CC, Jemiolo B, Trappe SW, et al. Cyclooxygenase mRNA expression in human patellar tendon at rest and after exercise. *Am J Physiol Regul Integr Comp Physiol* 2008;294:R192–R199.
- Tsai WC, Hsu CC, Chou SW, Chung CY, et al. Effects of celecoxib on migration, proliferation and collagen expression of tendon cells. *Connect Tissue Res* 2007;48:46–51.
- Tsukii K, Shima N, Mochizuki S, Yamaguchi K, et al. Osteoclast differentiation factor mediates an essential signal for bone resorption induced by 1 alpha,25-dihydroxyvitamin D3, prostaglandin E2, or parathyroid hormone in the microenvironment of bone. *Biochem Biophys Res Commun* 1998;246:337–341.
- Urakawa H, Nishida Y, Naruse T, Nakashima H, et al. Cyclooxygenase-2 overexpression predicts poor survival in patients with high-grade extremity osteosarcoma: a pilot study. *Clin Orthop Relat Res* 2009;467:2932–2938.
- Urist M. Bone formation by osteoinduction. *Science* 1965;150:893–899.
- Usitalo H, Hiltunen A, Ahonen M, Gao TJ, et al. Accelerated up-regulation of L-Sox5, Sox6, and Sox9 by BMP-2 gene transfer during murine fracture healing. *J Bone Miner Res* 2001;16:1837–1845.
- Vaibhav B, Nilesh P, Vikram S, Anshul C. Bone morphogenic protein and its application in trauma cases: a current concept update. *Injury* 2007;38:1227–1235.
- Vaile JH, Davis P. Topical NSAIDs for musculoskeletal conditions: a review of the literature. *Drugs* 1998;56:783–799.
- van der Heide HJ, Hannink G, Buma P, Schreurs BW. No effect of ketoprofen and meloxicam on bone graft ingrowth: a bone chamber study in goats. *Acta Orthop* 2008;79:548–554.
- van Staa TP, Leufkens HG, Cooper C. Use of nonsteroidal anti-inflammatory drugs and risk of fractures. *Bone* 2000;27:563–568.

- Vielpeau C, Joubert JM, Hulet C. Naproxen in the prevention of heterotopic ossification after total hip replacement. *Clin Orthop Relat Res* 1999; 279–288.
- Virchenko O, Skoglund B, Aspenberg P. Parecoxib impairs early tendon repair but improves later remodeling. *Am J Sports Med* 2004;32:1743–1747.
- Wadleigh DJ, Herschman HR. Transcriptional regulation of the cyclooxygenase-2 gene by diverse ligands in murine osteoblasts. *Biochem Biophys Res Commun* 1999;264:865–870.
- Wahlstrom O, Risto O, Djerf K, Hammerby S. Heterotopic bone formation prevented by diclofenac: prospective study of 100 hip arthroplasties. *Acta Orthop Scand* 1991;62:419–421.
- Warden SJ, Avin KG, Beck EM, DeWolf ME, et al. Low-intensity pulsed ultrasound accelerates and a nonsteroidal anti-inflammatory drug delays knee ligament healing. *Am J Sports Med* 2006;34:1094–1102.
- Wax MK, Reh DD, Levack MM. Effect of celecoxib on fasciocutaneous flap survival and revascularization. *Arch Facial Plast Surg* 2007;9:120–124.
- Weinreb M, Machwate M, Shir N, Abramovitz M, et al. Expression of the prostaglandin E(2) [PGE(2)] receptor subtype EP(4) and its regulation by PGE(2) in osteoblastic cell lines and adult rat bone tissue. *Bone* 2001;28:275–281.
- Weise M, De-Levi S, Barnes KM, et al. Effects of estrogen on growth plate senescence and epiphyseal fusion. *Proc Natl Acad Sci USA* 2001;98:6871–6876.
- Wergedal JE, Sheng MH, Ackert-Bicknell CL, Beamer WG, et al. Genetic variation in femur extrinsic strength in 29 different inbred strains of mice is dependent on variations in femur cross-sectional geometry and bone density. *Bone* 2005;36:111–122.
- Wong BR, Rho J, Arron J, Robinson E, et al. TRANCE is a novel ligand of the tumor necrosis factor receptor family that activates c-Jun N-terminal kinase in T cells. *J Biol Chem* 1997;272:25190–194.
- Wurnig C, Schwameis E, Bitzan P, Kainberger F. Six-year results of a cementless stem with prophylaxis against heterotopic bone. *Clin Orthop Relat Res* 1999;361:150–158.
- Xie C, Ming X, Wang Q, Schwarz EM, et al. COX-2 from the injury milieu is critical for the initiation of periosteal progenitor cell mediated bone healing. *Bone* 2008;43:1075–1083.
- Xie C, Liang B, Xue M, Lin AS, et al. Rescue of impaired fracture healing in COX-2^{-/-} mice via activation of prostaglandin E2 receptor subtype 4. *Am J Pathol* 2009;175:772–785.
- Xu M, Choudhary S, Goltzman D, Ledgard F, et al. Do cyclooxygenase-2 knockout mice have primary hyperparathyroidism? *Endocrinology* 2005;146:1843–1853.
- Xu M, Choudhary S, Voznesensky O, Gao Q, et al. Basal bone phenotype and increased anabolic responses to intermittent parathyroid hormone in healthy male COX-2 knockout mice. *Bone* 2010;47:341–352.
- Xu Z, Choudhary S, Okada Y, Voznesensky O, et al. Cyclooxygenase-2 gene disruption promotes proliferation of murine calvarial osteoblasts in vitro. *Bone* 2007;41:68–76.
- Yamakawa K, Kamekura S, Kawamura N, Saegusa M, et al. Association of microsomal prostaglandin E synthase 1 deficiency with impaired fracture healing, but not with bone loss or osteoarthritis, in mouse models of skeletal disorders. *Arthritis Rheum* 2008;58:172–183.
- Yang RS, Liu TK, Lin-Shiau SY. Increased bone growth by local prostaglandin E2 in rats. *Calcif Tissue Int* 1993;52:57–61.
- Yoshida K, Oida H, Kobayashi T, Maruyama T, et al. Stimulation of bone formation and prevention of bone loss by prostaglandin E EP4 receptor activation. *Proc Natl Acad Sci USA* 2002;99:4580–4585.
- Yuan J, Murrell GA, Wei AQ, Appleyard RC, et al. Addition of nitric oxide via nitroflurbiprofen enhances the material properties of early healing of young rat Achilles tendons. *Inflamm Res* 2003;52:230–237.
- Zhang X, Morham SG, Langenbach R, Young DA, et al. Evidence for a direct role of cyclo-oxygenase 2 in implant wear debris-induced osteolysis. *J Bone Miner Res* 2001;16:660–670.
- Zhang X, Schwarz EM, Young DA, Puzas JE, et al. Cyclooxygenase-2 regulates mesenchymal cell differentiation into the osteoblast lineage and is critically involved in bone repair. *J Clin Invest* 2002;109:1405–1415.

RENAL SYSTEM

INTRODUCTION

In the kidney, prostaglandins (PGs) are important mediators of hemodynamic regulation, salt and water homeostasis, and renin (REN) release (Harris and Breyer, 2001). The main PGs in the kidney are PGE₂ and prostacyclin (PGI₂), which is synthesized from arachidonic acid (AA) by enzymatic reactions, particularly cyclooxygenases and prostaglandin E synthases (PGESs) (Whorton et al., 1978; Radi and Ostroski, 2007). Cyclooxygenase (COX)-derived PGs have two membrane-anchored isoenzymes, COX-1 and COX-2. COX-1 is expressed constitutively and found in most normal body tissues, while COX-2 is expressed in normal tissues at a low level and is strongly induced by proinflammatory mediators (Radi and Ostroski, 2007; Radi, 2009). The membrane-associated PGES-1 (mPGES-1) is inducible and linked functionally to COX-2, while mPGES-2 is constitutive and coupled to both COX isoforms (Radi and Ostroski, 2007). These PG-derived COXs and PGEs play a role in the kidney, and their inhibition can contribute to alterations in renal homeostasis. For example, because COX-1 is expressed in the collecting ducts of the nephron, an active area in the regulation of sodium excretion in both laboratory animals and humans (Currie and Needleman, 1984), it is not surprising that blood pressure increases in COX-1-deficient mice compared with wild-type controls (Kawada et al., 2005).

Nonselective nonsteroidal anti-inflammatory drugs (ns-NSAIDs), which inhibit both COX-1 and COX-2, may aggravate REN-independent sodium-sensitive hypertension, possibly in part by inhibition of the COX-1 responsible for sodium excretion (Okumura et al., 2002). Thus, the reduction in renal blood flow and sodium and water retention contributes to the adverse effects of NSAIDs on the kidney, especially in humans or animals suffering from conditions with altered renal function, such as salt depletion, lupus nephritis, liver cirrhosis, or nephritic syndrome. The incidence of NSAID-associated renal side effects ranges from 1 to 5% (DeMaria and Weir, 2003). However, it is important to consider the interspecies renal physiological and anatomical differences that may exist and differences in the involvement of COX in the generation of renal PGs under normal and altered kidney function. The comparative aspects of the renal system

are reviewed in this chapter, with a discussion of the pathophysiological effects of COX inhibition on electrolyte handling and the renal system.

COMPARATIVE PHYSIOLOGICAL, DEVELOPMENTAL, AND ANATOMICAL ASPECTS OF THE RENAL SYSTEM

Understanding the comparative physiological, developmental, and anatomical aspects of renal function in diverse species is important for an understanding of the pathological and toxicological consequences of COX inhibition in the kidney. The kidneys are paired organs located in the posterior part of the abdomen. The mammalian kidney develops through three overlapping, successive stages: the pronephrons, the mesonephrons, and the metanephrons (the adult permanent kidney) (Dressler, 2006). The metanephric kidney undergoes three basic phases of growth. The first phase is called nephrogenesis, the development of new nephrons. Nephrogenesis varies across species and is completed during the perinatal period in most mammalian species. In humans, nephrogenesis starts during week 5 of gestation and is complete at 36 weeks of fetal gestation (MacDonald and Emery, 1959). The period between gestation weeks 18 to 32 is a critical point in renal development in humans because nephrogenetic development reaches its peak (Gasser et al., 1993). Nephrogenesis continues after birth for 2 weeks in the dog (Kleinman and Reuter, 1973), 4 to 6 weeks in the rat (Solomon, 1977), and 3 weeks in the pig (Friis, 1980). The puppy kidney is immature in both structure and function at birth (Evan et al., 1979). Changes in glomerular and tubular growth in the dog are complete by approximately 2 months of age. In monkeys, nephrogenesis is complete at birth (Lumbers, 1995), and in mice, sheep, and guinea pig, nephrogenesis completes before birth (Fouser and Avner, 1993; Lumbers, 1995).

Cyclooxygenase-2 may be involved in nephrogenesis in humans, and its inhibition using NSAID inhibitors during the third trimester may be responsible for fetal renal syndromes (Khan et al., 2001b). In utero exposure to early prolonged high-dose indomethacin or ibuprofen resulted in kidney structural abnormalities in the developing human fetus and renal failure in neonates (Kaplan et al., 1994). Kidney postnatal development was evaluated in COX-2 null mice. Mice homozygous for a targeted deletion of COX-2 ($-/-$) were compared with wild-type littermates ($+/+$). Beginning at postnatal day 10 (PN10), kidney growth was suppressed in COX-2 ($-/-$) mice. By PN10, kidneys from COX-2 ($-/-$) mice had thin nephrogenic cortices and small, crowded subcapsular glomeruli. The kidney pathological changes increased with age with progressive outer cortical dysplasia, cystic subcapsular glomeruli, loss of proximal tubules, and tubular atrophy and cyst formation. Therefore, deficiency of COX-2, at least in null mice, resulted in progressive and specific renal architectural disruption and functional deterioration beginning in the final phases of nephrogenesis (Norwood et al., 2000). Chronic suppression of PG synthesis by indomethacin, an ns-NSAID, in the pregnant rhesus monkey during late gestation resulted in fetal renal dysgenesis (Novy, 1978). In a recent study

using the flatworm *Schmidtea mediterranea*, interference with the expression of epidermal growth factor receptor (EGFR5) during the regeneration process showed that protonephridia could no longer undergo branching morphogenesis. Thus, EGFR5 appears to be a crucial regulator of branching morphogenesis and maintenance (Rink et al., 2011). Such a model could be relevant for studying kidney physiology, nephrogenesis, and regeneration and the effects of NSAIDs in mammalian species.

The kidney is bean-shaped in most mammals, whereas it is heart-shaped in the horse and lobulated in the ox (Braun, 1991; Hoffmann et al., 2000). Regarding blood flow, in humans and most mammals, each kidney is supplied by a single renal artery, but it is not uncommon for one or more accessory renal arteries to be present (el-Galley and Keane, 2000). Two distinct anatomical regions can be identified on the cut surface of the kidney: an outer region called the cortex and an inner region called the medulla (Fig. 3-1). In the mammalian kidney, renal blood flow is regulated via the afferent arterioles. In avian species, however; the primary nutrient blood source to the renal cortex is the renal portal system via the afferent renal portal vein. The primary blood supply to the avian glomeruli and distal convoluted tubules is the central artery, located between the intralobular (central) vein and the cortex (Meteyer et al., 2005). Normal renal function is predicated on adequate perfusion (pressure and volume). Although the kidneys are only about 0.5% of body weight, they typically receive 20 to 25% of the cardiac output. Only about 10% of oxygen consumption occurs in the kidneys. There is heterogeneity in intrarenal flow distribution in the kidney. Approximately 85% of renal flow can be associated with cortex, 14% with outer medulla, and 1% with inner medulla (Khan et al., 2011). The very low oxygen tension in the renal medulla makes it vulnerable to NSAID-mediated hypoxic injury, which can be prevented by PGs (Brezis and Rosen, 1995).

The comparative anatomical aspects of the mammalian renal pelvis and medulla have been investigated (Pfeiffer, 1968). Simple renal medulla is present in most mammals (rabbits, guinea pigs, cats, dogs, pigs, humans). Complex renal medulla is present in animals with a high urine-concentrating ability (rat, mouse, desert sand rat). The medulla in the kidney of nonhuman primates (rhesus macaques, cynomolgus macaques) is relatively small compared to the medulla in the kidney of human. In humans, beavers, and pigs, the renal medulla is divided into striated conical masses (pyramids), and thus the kidney from these species is termed multipapillate. Cats, horses, dogs, rats, nonhuman primates, and many other laboratory animals have a single renal pyramid, and the kidney in these species is called unipapillate. The renal pelvis is lined by transitional epithelium and represents the expanded portion of the upper urinary tract. In mammals possessing a unipapillate kidney, the papilla is surrounded directly by the renal pelvis (Pfeiffer, 1968). In some species, such as horses, many mucous glands are present in the renal pelvis (Mutoh et al., 1992).

The primary functions of kidneys can be divided into four major categories: (1) control of the body's fluid and electrolytes, (2) elaboration of hormones, (3) excretion of the waste products of metabolism, and (4) selected metabolic activities. Nitrogenous waste products consisting of urea, creatinine, and ammonia

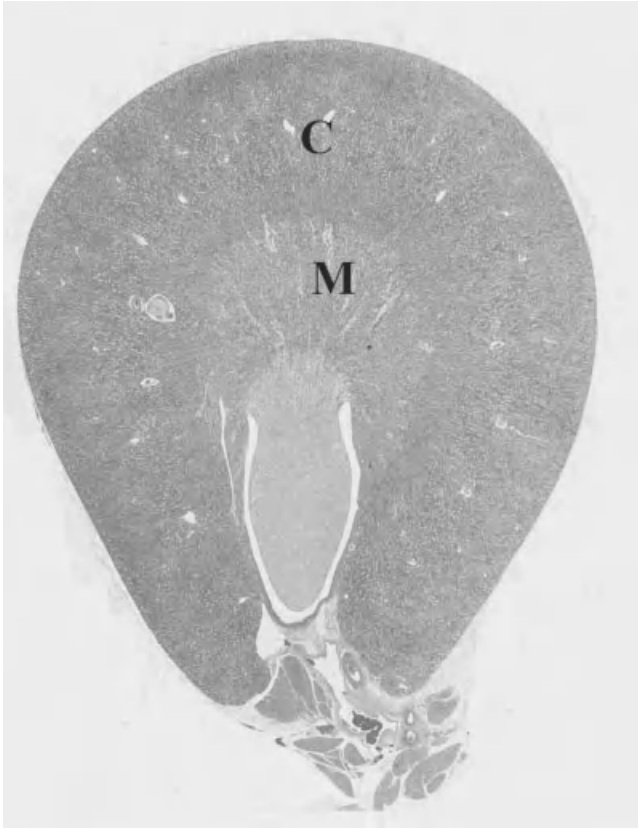


FIGURE 3-1 Two distinct anatomical regions can be identified on the cut surface of the kidney: an outer region called the cortex (C) and an inner region called the medulla (M).

ion are excreted in the urine; thus, any significant alterations in renal function are manifested in retention of these waste products in the body (Khan et al., 2011). The kidney excretes nitrogenous waste products and is central to body water and solute homeostasis. In avian species, during embryonic development of the bird within the shelled egg, nitrogenous waste products accumulate and cannot be voided. Insoluble uric acid is the main by-product rather than urea (Lierz, 2003). About 65% of uric acid is chemically bound to proteins. Thus, hyperuricemia is an indication of kidney injury in birds. In pigs and rabbits, secretion of urate commonly occurs by the proximal tubules (Chonko, 1980; Roch-Ramel et al., 1980). In humans, tubular reabsorption of filtered urate predominates, but tubular secretion also occurs (Roch-Ramel, 1979).

The nephron is the basic structural and functional unit of the kidney that performs such primary functions. The main nephron components consist of the renal or malpighian corpuscle (glomerulus and Bowman's capsule), the proximal tubule, the thin limbs, the distal tubule, and the connecting segment or connecting tubule (Khan et al., 2011). There are species differences in kidney nephron numbers. For

example, each human kidney contains about 1,000,000 nephrons, adult rat kidney approximately 30,000 nephrons, dog kidney approximately 500,000 nephrons, cat kidney approximately 200,000 nephrons, and pig kidney approximately 1,250,000 nephrons. Furthermore, the interspecies and strain differences in the number of nephrons can have an impact on the development of renal pathologies. The F344 rat strain is shown to be more vulnerable to development of progressive kidney damage, due to the relatively low nephron number (Szabó et al., 2008). Spontaneously hypertensive rats (SHR) have 10 to 25% fewer nephrons than do their normotensive counterparts (Skov et al., 1994). There is evidence that fetal growth restriction is associated with impaired nephrogenesis and reduced numbers of mature nephrons (Hinchliffe et al., 1992; Bassan et al., 2000). In addition, because of the fewer nephrons, the younger animals have much less capacity to concentrate urine than do the adults. In mice with a null mutation of the gene for COX-2, there is a severe reduction in the number of functional nephrons developed in the fetal kidney (Dinchuk et al., 1995). In Sprague–Dawley rats, reduction in COX-2 activity during the nephrogenic period leads to a modest but significant reduction in nephron number. However, the consequent age-dependent deterioration of the renal structure and renal function is significantly enhanced only in male rats (Sáez et al., 2009). The comparative lengths of various nephron segments are detailed in Table 3-1.

Two main populations of nephrons are those possessing a short loop of Henle and those with a long loop of Henle (juxtamedullary). In birds, cortical (reptilian type) nephrons are most common (up to 90%) and are located in the lobule cortex. Their glomeruli are smaller and they do not possess the loop of Henle. Medullary (mammalian type) nephrons have long loops of Henle, reaching far into the medulla (Lierz, 2003). This is important because the countercurrent hypothesis for urine concentration states that the maximal urine concentration that can be achieved is related directly to the length of loops of Henle (Gottschalk and Mylle, 1958). Within the mammalian kidney, urea concentration (creating hypertonicity) within the medulla is the key factor enabling concentration of urine. As urea is not an important product of metabolism in birds and loops of Henle are absent in 90% of avian nephrons, the capacity of the kidney in birds to concentrate urine is less than in mammals. Water is conserved by resorption within the coprodeum and rectum (Lierz, 2003).

TABLE 3-1 Comparative Lengths of Various Nephron Segments

Species	Range of nephron segment length (mm)			References
	Proximal tubule	Distal tubule	Loop of Henle	
Human	7.2–23.1	1.6–4.2	0–5.6	Pai, 1935
Nonhuman primate (rhesus monkey)	3.6–9.6	1.4–6.6	0.9–1.9	Bennet et al., 1968
Dog	9–24	3–3.9	5.2–15	Watson, 1966; Bennet et al., 1968
Rat	9–13.5	2.5–2.7	5–7.3	Walker and Oliver, 1941

The glomeruli, capillary networks lined by a thin layer of endothelial cells, have a central region of mesangial cells (glomerular mesangium) with surrounding mesangial matrix material, visceral epithelial cells (podocytes) and an associated basement membrane, parietal epithelial cells of Bowman's capsule and glomerular basement membrane, and Bowman's space or urinary space (narrow cavity between the two visceral and parietal epithelial layers) (Khan et al., 2011). The four main functions of the glomeruli are (1) plasma ultrafiltration and removal of plasma solutes (e.g., glucose, urea, electrolytes) and water; (2) regulation of blood pressure through various molecules, such as angiotensin and aldosterone; (3) regulation of tubular metabolism via regulating peritubular blood flow; and (4) removal of macromolecules (e.g., soluble immune complexes) from the circulation (Robertson, 1998). Thus, the glomerular filtration rate (GFR) is the basic determinant in urine formation and a key measurement of kidney function. GFR continues to increase after birth and reaches adult levels at 1 to 2 years of age in humans (Gomez et al., 1999). In rats, GFR increases sharply during the first weeks of postnatal life (Horster, 1977). Discrimination in GFR for larger molecules occurs based on molecular size, configuration, and charge. For example, small molecules (approximately 5000 Dal) pass through the glomerular barrier, and molecules such as albumin (approximately 68,000 Dal) do not pass the barrier. Any pathophysiological process that interferes with the structural integrity and function of the glomerulus can result in abnormal loss of protein in the urine, predominantly albumin. Therefore, a hallmark of drugs that damage glomerular epithelial cells in mammals is the induction of proteinuria. However, in contrast to most other mammals, proteinuria is normal in mice, with the highest levels in sexually mature male mice (Wicks, 1941). Mice excrete only a drop or two of urine at a time, and it is highly concentrated (Fox et al., 2002). The filtering system per gram of tissue is twice that of the rat. They can concentrate urine to 4300 mOsm/L compared to 1160 mOsm/L for humans. Large amounts of protein, including creatinine, in the urine are normal, which is different from the situation in other mammals (Fox et al., 2002). To some extent, the high total solids content of urine and high specific gravity reflect this passage of protein into the urine (Parfentjev and Perlzweig, 1933). In addition, there are gender and strain differences in the mouse kidney, and sexual maturity in male mice leads to sexual dimorphism in the kidney, as evidenced by larger renal cortices, larger renal corpuscles, and cuboidal epithelium lining the parietal layer of Bowman's capsule (Ahmadizadeh et al., 1984). The parietal epithelium layer is mainly squamous in DBA female mice (Ahmadizadeh et al., 1984). Furthermore, sexual dimorphism in renal and plasma potassium content was demonstrated in adult male CD1 mice. These mice have a higher plasma potassium concentration than that of females or 40-day-old male mice (Cremades et al., 2003). Such anatomical differences can play a role in susceptibility to toxic renal insults. The glomeruli of neonatal pigs are permeable to colostral protein for a few days (Bergelin and Karlsson, 1974). Administration of indomethacin, an ns-NSAID, to women in threatened preterm labor results in abnormalities in glomerular and tubular morphology in the fetal kidney and a loss of fetal and neonatal urine production (Kaplan et al., 1994; van der Heijden et al., 1994).

Visceral epithelium is continuous with the parietal epithelium at the vascular pole, where the afferent and efferent arterioles enter and exit the glomerulus, and the parietal layer of Bowman's capsule continues into the epithelium of the proximal tubule at the urinary pole. The average diameter of the glomerulus is approximately 120, 130, and 200 μm in the rat, beagle dog, and human kidney, respectively (Khan et al., 1991). Glomerular growth during human childhood has been evaluated. It was found that the estimated mean maximum glomerular diameter, which is 112 μm for newborns, increased approximately 3.6 μm per year, reaching 167 μm at age 15. Glomerular size correlated better with age than with height, weight, or body mass index, and glomeruli in the inner cortex were significantly larger than those in the middle and outer cortex. Glomerular size was significantly greater in female children than in male children over the age range examined (Moore et al., 1993). As mentioned above, the glomerulus is responsible for the production of an ultrafiltrate of plasma. Filtration barrier between the blood and the urinary space is composed of fenestrated endothelium, peripheral glomerular basement membrane, and slit pores between the foot processes of the visceral epithelial cells. Vascular endothelial growth factor (VEGF) is produced by the visceral epithelial cells, and VEGF receptors are expressed on the surface of glomerular endothelial cells. VEGF is an important regulator of endothelial cell function and permeability, induces the mobilization of caveolae and formation of fenestrae, and is important for endothelial cell survival and repair in glomerular diseases that result in endothelial cell damage (Veron et al., 2010). The effects of an s-NSAID, celecoxib, on fetal renal growth in rabbits were evaluated. Celecoxib was given orally at a dose level of 30 mg/kg per day from 13 to 20 days of gestation (group 1) or from day 13 to day 28 of gestation (group 2). The fetuses were delivered by cesarean section at 29 days of gestation. This maternal administration of celecoxib at therapeutic doses did not affect maternal fetal renal growth in either group. However, VEGF levels were elevated in group 2 (Hartleroad et al., 2005).

Visceral epithelial cells (podocytes) are the largest cells in the glomerulus. They have long cytoplasmic processes (trabeculae) that extend from the main cell body and divide into individual foot processes called pedicels that come into direct contact with the lamina rara externa of the glomerular basement membrane (GBM). The GBM is a size-dependent barrier, and particles with radius greater than 3.5 nm do not pass through such a barrier. Podocytes are capable of endocytosis, and the heterogeneous content of their lysosomes reflects the uptake of proteins and other components from the ultrafiltrate. In addition, large numbers of microtubules, microfilaments, and intermediate filaments are present in the cytoplasm of podocytes. Filtration slit or slit pore is bridged by a thin membrane called the filtration slit membrane or slit diaphragm. Nephritin and CD2-associated protein (CD2AP) are required for normal filtration to occur. Nephritin is a transmembrane protein that belongs to the immunoglobulin family of adhesion molecules and located in the slit diaphragm. CD2AP is an adapter molecule that binds to nephritin and is believed to connect nephritin to the cytoskeleton (Pavenstädt et al., 2003). It has been demonstrated that preexisting expression of podocyte COX-2 in a mouse strain (B6/D2) that otherwise is resistant to adriamycin injury sensitized the podocytes to injury,

indicated by foot process effacement and albuminuria (Cheng et al., 2007). These responses were associated with a further increase in endogenous podocyte COX-2 expression and a decrease in nephrin expression. Long-term treatment with the s-NSAID SC58236 attenuated the albuminuria and foot process effacement and restored nephrin expression. In addition, in BALB/c mice endogenous podocyte COX-2 expression also increased in association with adriamycin-induced podocyte injury (Cheng et al., 2007). Thus, overexpression of COX-2 predisposes to podocyte injury. Podocin is connected to both nephrin and CD2AP. Podocin is an integral membrane protein that is expressed in the foot process membrane at the site of insertion of the slit diaphragm (Takeda, 2003; Fukasawa et al., 2009).

Podocyte injury is a major cause of progressive glomerular damage. Prostaglandin synthesis has been demonstrated in rat glomerular epithelial cells (Kreisberg et al., 1982). Increased podocyte COX-2 expression has been reported in rat models of subtotal renal ablation (Wang et al., 1998; Kong et al., 2003) and diabetic nephropathy (Komers et al., 2001). Various membrane components have been identified on the surface of podocytes. Podocalyxin is a principal sialoprotein on the urinary surface of the podocytes. Plasma membrane of the foot processes has a negatively charged surface coat rich in sialic acid (Takeda, 2003). Podoplanin is a 43-kDa membrane protein identified in the plasma membrane, which has a role in the maintenance of podocyte shape. Anionic sites on the podocytes as well as the presence of an intact slit diaphragm are important in establishing the permi-selective properties of the filtration barrier. Recent data suggest that podocyte injury can be repaired via parietal epithelial cells of Bowman's capsule, which may represent a potential source for podocyte regeneration. An abnormal proliferative response of renal progenitors to podocyte injury can generate hyperplastic glomerular lesions, which are observed in several glomerular disorders (Smeets et al., 2009; Romagnani, 2011).

The glomerular mesangium represents the central region of the glomerulus and is comprised of mesangial cells (intercapillary arrays) and their surrounding matrix material and separated from the capillary lumen by the endothelium. In mammals, the glomerular capillaries form a complex network of anastomosing channels; while in birds single unbranched glomerular capillary coils are present around the periphery of the renal corpuscle (Casotti and Braun, 1995). Mesangial cells represent a specialized pericyte and possess many of the functional properties of smooth muscle cells (Mené, 1996). The contractile mesangial cell processes bridge the gap in the glomerular basement membrane encircling the capillary, prevent capillary wall distention secondary to elevation of intracapillary pressure, and play a role in the regulation of glomerular filtration. Contraction decreases glomerular filtration by reducing blood flow through capillary loops. Cell contraction is stimulated by a variety of vasoactive agents such as angiotensin II (Ang II), leukotrienes, and platelet-activating factor (Mené, 1996). Mesangial cells possess membrane receptors for peptidic and nonpeptidic hormones, have signaling pathways involving intracellular cAMP and cGMP accumulation, and synthesize proteins such as extracellular matrix protein (ECM) and serine proteases. Mesangial cells exhibit phagocytic properties and participate in the clearance or disposal

of macromolecules from the mesangium (Mené, 1996). The mesangial matrix possesses fixed, negatively charged sites that influence the filtration of macromolecules. Thus, mesangial cells play a central role in the physiology and pathophysiology of the glomerulus.

There are significant species differences in the glomerulus mesangium. In the glomerulus of humans, only contractile resident mesangial cells (and not resident macrophages) have been identified (Sraer et al., 1993). Macrophages are detected only in pathological conditions in human kidney glomeruli, which suggests that they are not resident but rather, infiltrating cells. Mesangial receptors, most notably Ang II receptors, are present on mesangial cell membranes and are linked to PGE₂ synthesis and to cell contraction. In humans, spontaneous prostanoid synthesis is low and is increased by the induction of cyclooxygenase by sodium butyrate in the medium. The amount of PGE₂ synthesized by human mesangial cells is quantitatively low compared with that in rats (Sraer et al., 1993). In rats, the role of the renin–angiotensin system in the glomerulus is clearly demonstrated, including the presence of Ang II receptors on isolated glomeruli and mesangial cells. Mesangial cells play a role in the regulation of single-nephron GFR. In humans, Ang II also exerts control on GFR, but a direct contractile effect of Ang II on mesangial cells is more difficult to demonstrate (Sraer et al., 1993). Cyclooxygenase-2 may participate in a number of pathological processes in immune-mediated renal glomerular diseases. In human mesangial cells *in vitro*, progressive accumulation of collagen I in the extracellular medium induced a significant increase in COX-2 expression. Focal adhesion kinase (FAK), the phosphatidylinositol 3-kinase (PI3K)/AKT pathway, and cAMP response element (CRE) activation were demonstrated with such increased COX-2 expression. Thus, collagen type I increases COX-2 expression via the FAK/PI3K/AKT/cAMP response element binding protein signaling pathway (Alique et al., 2011). Engulfment and cell motility 1 (ELMO1), a bipartite guanine nucleotide exchange factor (GEF) for the small GTPase Rac 1, was identified as a susceptibility gene for glomerular disease. In human mesangial cells *in vitro*, ELMO1 interacted with COX-2 and ELMO1 was identified as a posttranslational regulator of COX-2 activity, and COX-2 activity increased fibronectin (an ECM) promoter activity (Yang and Sorokin, 2011).

Glomerular basement membrane (GBM) is 100 to 300 nm thick and is composed of a central dense layer, the lamina densa, and two thinner, more electron-lucent layers, the lamina rara externa and the lamina rara interna (Takami et al., 1991). Special stains such as methenamine silver and periodic acid–Schiff (PAS) can be used to visualize the GBM by light microscopy. Collagen IV is the major constituent of the GBM. Glomerular basement membrane is produced by the podocytes. Anionic sites exist in all three layers of the GBM, which consist of glycosaminoglycans rich in heparan sulfate (Timpl, 1986). Glomerular basement membrane plays a role in establishing the permeability to plasma proteins. Glomerular capillary wall possesses both size- and charge-selective properties and therefore restricts the passage of molecules the size of albumin or larger. Prostaglandins may play a role in GBM immunologic diseases. For example, in an experimental rat model of membranous nephropathy, a thromboxane A₂ (TXA₂) synthase inhibitor that was given after proteinuria is fully developed decreased the deposition of both

rabbit immunoglobulin G and rat immunoglobulin G on GBM in these nephritic rats (Nagao et al., 1996). Thus, thromboxanes may exacerbate glomerular pathology.

The glomerular juxtaglomerular apparatus is located at the vascular pole of the glomerulus. It contains two distinct cell types: juxtaglomerular granular cells of the afferent arteriole that contain renin and Ang II and agranular extraglomerular mesangial cells (laci cells or pseudomeissnerian cells of Goormaghtigh), located between the afferent and efferent arterioles. In addition, there is a specialized tubule component called macula densa (MD), which is a specialized region of the thick ascending limb adjacent to the hilus of the glomerulus (Khan et al., 2011). The MD senses change in the distal tubule in the luminal concentrations of sodium and chloride via absorption of sodium and chloride across the luminal membrane by the $\text{Na}^+ - \text{K}^+ - \text{Cl}^-$ cotransporter. Signals generated by acute changes in sodium chloride concentration are transferred via the MD cells to the glomerular arterioles to control the glomerular filtration rate and to the renin-secreting cells in the afferent arteriole. The immunohistochemical expression of COX-2 has been evaluated in human fetal kidneys ranging between 15 and 23 weeks of gestational age. Strong expression of COX-2 was localized primarily in the MD and the thick ascending limb of the loop of Henle, and in rare glomerular podocytes and vascular endothelial cells. There was a progressive decrease in COX-2 immunoreactivity from the most immature nephrons adjacent to the metanephric regions to the well-developed nephrons in the middle to inner cortex (Khan et al., 2001b). Data in rats suggest that COX-2, which is expressed in the MD, regulates tubuloglomerular feedback, at least partly, via two mechanisms: (1) generation of TXA_2 or related agonists of thromboxane/PGH₂ receptor and (2) reduction of neuronal nitric oxide synthase-dependent nitric oxide (Araujo and Welch, 2009). COX-2 colocalizes with neuronal nitric oxide synthase (nNOS) in the MD. Up-regulation of COX-2 expression has been demonstrated in porcine kidney MD with chronic NOS inhibition (Kommareddy et al., 2011). The MD-derived COX-2 products could counteract renal vasoconstriction in NOS inhibition-induced hypertension and maintain renin synthesis/secretion (Kommareddy et al., 2011).

The renin-angiotensin-aldosterone system (RAAS) plays an important role in the control of cardiovascular and renal homeostasis by regulating vascular tone, blood pressure (BP), and fluid volume. Ang II is a physiologically active component of the RAAS, produced via an enzymatic cascade that begins with angiotensinogen (AGT) cleaving REN to form Ang I, which is then cleaved by the angiotensin-converting enzyme (ACE) to form Ang II. Ang II causes vasoconstriction directly by activating Ang II type 1 (AT1) receptors on vascular smooth muscle and affects fluid volume via AT1 receptor activation in the proximal tubule, resulting in renal sodium and water reabsorption. Ang II regulates fluid balance by stimulating aldosterone secretion from the adrenal glands (Radi and Ostroski, 2007). PGs are modulators of physiological functions and contribute to REN release, regulation of renal microvascular hemodynamics, salt balance, and BP control via mechanisms involving the regulation of vascular tone and renal excretory function (Radi and Ostroski, 2007). A baseline absence of REN in juxtaglomerular cells was observed in the Toll-like receptor 4-knockout mouse. This was specific to juxtaglomerular cells, as REN was easily detected in other arteriolar segments (El-Achkar et al.,

2007). Dopamine, a neurotransmitter, serves important physiological functions in the mammalian kidney and is a major regulator of proximal tubule salt reabsorption and is a modulator of REN release. There is crosstalk between intrarenal dopaminergic and COX-2 systems. In an experimental study in male Sprague–Dawley rats, acute treatment with a D1-like agonist, fenoldopam, inhibited REN release. Two mechanisms have been proposed for such intrarenal dopaminergic and COX-2 system crosstalk: (1) indirect inhibition via decreasing proximal salt reabsorption and modulating MD COX-2 expression and activity, and (2) direct stimulation of REN via activation of D1-like receptors (Zhang et al., 2009). In birds, oriental white-backed vultures, a proposed mechanism by which the ns-NSAID diclofenac induced renal failure is through the inhibition of the modulating effect of PG on Ang II-mediated adrenergic stimulation. It is proposed that renal portal valves open in response to adrenergic stimulation, redirecting portal blood to the caudal vena cava and bypassing the kidney. If diclofenac removes a modulating effect of PGs on the renal portal valves, indiscriminant activation of these valves would redirect the primary nutrient blood supply away from the renal cortex. Therefore, this leads to ischemic necrosis of the cortical proximal convoluted tubules in these birds (Meteyer et al., 2005).

The length of various nephron segments (proximal tubule, loop of Henle, distal tubule) varies across species. Proximal convoluted tubules (PCTs) begin at the urinary pole of the glomerulus. PCTs have three morphologically distinct segments (S1, S2, S3) in the rat, rabbit, mouse, and rhesus monkey (Khan et al., 2011). There are species and strains differences in PCT. For example, Sprague–Dawley rats have somewhat fewer, but longer, PCTs than those of Wistar rats (Solomon, 1977). PCTs have brush borders that form the apical or luminal surface of the tubules with microvilli. Basolateral plasma membrane contains receptors for various peptide hormones, such as insulin, growth hormone, and parathyroid hormone (Corvilain et al., 1962). Megalin is a 600-kDa glycoprotein belonging to the low-density-lipoprotein receptor gene family and represents the antigen for the rat Heymann nephritis model of membranous glomerulonephritis. Megalin is located in the brush border, coated pits, and endocytic vesicles. It mediates the reabsorption of numerous proteins and polypeptides and serves as a receptor for numerous ligands (e.g., β_2 -microglobulin, lysozyme, cytochrome *c*, epidermal growth factor, albumin, insulin, prolactin, vitamin B₁₂, vitamin D) (Christensen and Verroust, 2002).

The major function of PCTs is reabsorption of Na^+ , HCO_3^- , Cl^- , K^+ , Ca^{2+} , PO_4^{3-} , calcium, water, and organic solutes (glucose and amino acids). Approximately half of the ultrafiltrate is reabsorbed. Fluid reabsorption mechanism is coupled with an active transport of Na^+ . The rate of fluid absorption from the proximal tubule to the peritubular capillaries is influenced by the hydraulic and oncotic pressures across the tubule and capillary wall, the main anions transported being HCO_3^- and Cl^- with HCO_3^- . Approximately 70% of potassium is reabsorbed in the PCTs (Khan et al., 2011). Unlike most mammals, where calcium and magnesium are excreted mainly in the bile, urine is the major route of calcium and magnesium excretion in rabbits (Cheeke and Amberg, 1973). Peritubular interstitial cells produce erythropoietin, a glycoprotein hormone that regulates survival, proliferation, and maturation of erythroid progenitor cells into mature red blood cells,

whose deficiency leads to anemia (Jelkmann, 1992). This hormone is produced in peritubular interstitial cells in several experimental animals, including rats, mice, sheep, and nonhuman primates (Fisher et al., 1996). PGE₂ can affect erythropoietin activity under hypoxic conditions (Gross et al., 1976). Renal secretion of organic electrolytes of diverse chemical structures plays a critical role in limiting the body's exposure to toxic compounds of exogenous and endogenous origin. The active renal secretion of drugs occurs via a transport process in the proximal tubules, which consists of uptake from systemic circulation via the basolateral membrane and subsequent efflux into urine through the luminal membrane by efflux transporters or passive permeability (Dresser et al., 2001). Uptake of substances in the systemic circulation may subsequently lead to efflux of such substances across the brush-border membrane of proximal tubule cells by various efflux transporters, such as the multidrug resistance P-glycoprotein (P-gp) or the breast cancer resistance protein (BCRP) (Deeley et al., 2006). Other transporters, such as the multidrug and toxin extrusion proteins 1 and 2 (MATE1, MATE2-K), have been identified in the brush-border membrane of proximal tubular cells in humans and mice (Omote et al., 2006) and play an important role in the renal secretion of xenobiotics with highly diverse chemical structures (Ohta et al., 2009).

Renal secretion of organic cations (OCs) (including bases) and organic anions (OAs) (including acids) has physiological, pharmacological, and toxicological implications. Transporters that are involved in the uptake of OC and OA across the basolateral membrane into the cells of PTCs have been identified in human kidney (Hosoyamada et al., 1999). In general, substrates for pathways involved in renal OC transport include a diverse array of primary, secondary, tertiary, or quaternary amines that have a net positive charge on the amine nitrogen at physiological pH. Renal organic ion transporters [e.g., organic anion transporter (OAT1) and organic cation transporters (OCT1 and OCT2)] play an important role in the excretion of numerous commonly used drugs, including NSAIDs. For example, ns-NSAIDs such as ketoprofen and naproxen are effective in altering the pharmacokinetic behavior of acyclovir, a guanosine analog antiviral drug, by inhibiting the OAT-mediated tubular secretion of acyclovir in rats (Gwak et al., 2005). Some studies revealed that a prototypic substrate and/or inhibitor of the renal OAT1 system consists of a hydrophobic core to which at least one negatively charged group, often a carboxyl, is attached (Ullrich, 1997). PGs are secreted into the urine by OAT system in renal proximal tubules (Nagai et al., 2006). The role of human OAT1 (hOAT1) renal transporters in adefovir-mediated transport and cytotoxicity and its relationship to NSAIDs was investigated using several NSAIDs of varied structures in both the hydrophobic core and the carboxylic acid moiety (Mulato et al., 2000). In general, the inhibitory potency did not seem to be influenced significantly by the type of carboxylic acid. Diflunisal, the most potent inhibitor of adefovir transport, which contains a carboxyl moiety attached directly to the hydrophobic aromatic ring, was only slightly more potent than some of ns-NSAIDs containing a propionic acid side chain (i.e., ketoprofen, flurbiprofen, naproxen) or acetic acid side chain (i.e., indomethacin, diclofenac). However, etodolac, which is also a derivative of acetic acid, was a poor hOAT1 inhibitor. Etodolac was the only ns-NSAID with an alkyl substituent in the immediate

vicinity of the carboxylic acid side chain, which presumably decreased the planarity of the molecule and may reduce its interaction with the substrate-binding site of hOAT1. Two ns-NSAIDs lacking the carboxyl moiety (phenacetin and piroxicam) clearly showed less inhibitory effect. With respect to the hydrophobic part of the molecule, two aromatic rings linked by a short spacer appear to be characteristic for ns-NSAIDs with the highest inhibitory potency (i.e., diflunisal, ketoprofen, and flurbiprofen) (Mulato et al., 2000).

In general, there was a correlation between the inhibitory potency of NSAIDs in the adenosine transport assay and their cytoprotective effect. Ketoprofen, flurbiprofen, and naproxen were potent inhibitors of adenosine transport and exhibited cytoprotection superior to that of probenecid, a uricosuric drug that increases uric acid excretion in the urine. For diclofenac and ibuprofen, both the inhibitory activities and the cytoprotective effects were comparable to those of probenecid. Diclofenac, the most potent hOAT1 inhibitor among the NSAIDs tested, still showed a distinct cytoprotective effect, despite being tested at a significantly lower concentration, due to its intrinsic cytotoxicity. Furthermore, piroxicam, one of the least potent inhibitors, showed only a minor reduction in the hOAT1-specific cytotoxicity of adenosine. In contrast, indomethacin did exhibit almost no cytoprotection in hOAT1-expressing cells despite its efficient inhibition of hOAT1 transport activity (Mulato et al., 2000). Another study, using the rat homolog of hOAT1, found that acetylsalicylate, salicylate, and indomethacin were taken up by OAT1, and the uptake rate of these NSAIDs was enhanced by the outwardly directed dicarboxylate gradient (Apiwattanakul et al., 1999). Rat OAT1 shares 88% amino acid residues with hOAT1 and showed a higher degree of homology with hOAT1 (Cihlar et al., 1999).

The distal nephron is composed of distal convoluted tubules (DCTs), thick ascending limb (TAL), and collecting ducts (Khan et al., 2011). Sodium and water reabsorption and potassium addition take place in the distal nephron. Sodium is transported passively in the TAL but actively elsewhere in the distal nephron and is responsive to aldosterone. In contrast, chloride is transported actively in the TAL (Khan et al., 2011). The effect of aldosterone on the distal nephron is an increase in sodium reabsorption in exchange for potassium. Normal water intake occurs in response to thirst, which is stimulated by hypertonicity. Hypertonicity leads to the release of vasopressin, also called antidiuretic hormone (ADH). Vasopressin binds to receptors in the distal nephron and collecting duct cells and activates adenyl cyclase and increases intracellular cyclic AMP. Prostaglandins inhibit the response to vasopressin, and COX inhibitors can increase the action of ADH. In rats, bradykinin regulates ion transport in the TAL via a COX-2-mediated mechanism (Rodriguez et al., 2004). In a Sprague–Dawley rats sepsis model, Toll-like receptor 4 (TLR-4) was found to be necessary for COX-2 expression only in cortical and medullary thick ascending loops (cTAL and mTAL) which express and secrete Tamm–Horsfall protein (El-Achkar et al., 2007). Thus, dependence of sepsis-induced renal COX-2 expression on TLR-4 is tubule specific in the distal nephron. The collecting ducts are composed of two cell types: principal cells and intercalated cells. Principal cells resorb sodium and water and secrete potassium,

and intercalated cells secrete either hydrogen or bicarbonate and reabsorb potassium. In an experiment in mouse collecting duct principal cells it was found that (1) a short-term increase of extracellular osmolarity decreases aquaporin-2 (AQP2) expression through inhibition of AQP2 gene transcription; (2) a long-term increase of extracellular tonicity, but not osmolarity, enhances AQP2 expression via stimulation of AQP2 gene transcription, and (3) long-term hypertonicity and cAMP-protein kinase increases AQP2 expression through synergistic but independent mechanisms (Hasler et al., 2005). In addition, the collecting ducts contain heat shock protein-70 (HSP-70), which is an osmotic stress protein (Khan et al., 2011). In rats, COX-2 inhibition reduced medullary HSP-70 expression and induced papillary apoptosis in dehydration (Neuhofer et al., 2004).

ROLE OF PROSTAGLANDINS IN THE RENAL SYSTEM

PGs are lipid mediators derived from the enzymatic metabolism of arachidonic acid initiated by COX. PGs commonly have a carboxylic acid group with pK_a values of approximately 5 and exist as charged molecules at physiological pH (Nagai et al., 2006). Prostanoid synthases include PGE synthase (PGES), prostacyclin synthase (PGIS), PGD synthase (PGDS), PGF synthase (PGFS), and thromboxane (TX) synthase, responsible for PGE₂, PGI₂, PGD₂, PGF_{2 α} , and TXA₂ biosynthesis, respectively (Radi, 2009). Renal COX-1 and COX-2 activity produces five primary prostanoids: PGE₂, PGF_{2 α} , PGI₂, TXA₂, and PGD₂. These prostanoids act locally via specific transmembrane G-protein-coupled receptors designated EP (for E-prostanoid receptor), FP, DP, IP, and TP, respectively (Breyer and Breyer, 2001). The kidney is capable of synthesizing all types of PGs, especially PGE₂ and PGI₂, which influence urinary sodium excretion directly through inhibition of the tubular transport function and indirectly through the regulation of RAAS system activity. A summary of various PGs and their effects on the kidney is provided in Table 3-2.

PGE₂ synthesis is predominant along the renal tubules, the main sites of synthesis being the medullary collecting tubule and, to a lesser extent, the cortical collecting tubule (CCT) and the thin limb of Henle's loop (Bonvalet et al., 1987). The NaK-ATPase maintains transmembrane electrochemical gradients in mammalian cells through the extracellular transport K⁺ in exchange for intracellular Na⁺, and inhibition of such Na⁺ transport in CCT leads to natriuresis. PGE₂ regulates renal tubular transport processes and can be involved in natriuresis and diuresis or the regulation of renin release. PGE₂ reduced sodium reabsorption in the juxtamedullary nephrons (Stokes and Kokko, 1977) and inhibited sodium absorption in the rabbit CCT (Warden and Stokes, 1993). Indomethacin given to patients with malignant hypertension in a 25-mg dose three times daily caused sodium retention (Frolich et al., 1976). However, some studies have suggested, using EP₁-deficient mice, that PGE₂ modulates urine concentration by acting at the EP₁ receptors, not in the CCT, within the hypothalamus to promote arginine-vasopressin synthesis in response to acute water deprivation (Kennedy et al., 2007). Thus, it is thought that PGE₂ affects at least three signaling mechanisms in the CCT via (1) increased cAMP generation, (2) inhibition of vasopressin-stimulated cAMP accumulation,

TABLE 3-2 Summary of Various Prostaglandins and their Effects in the Kidney

PG	Renal synthesis location	Renal effects
PGE ₂	Medullary collecting tubule, cortical collecting tubule, thin limb of Henle's	Diuresis, vasodilatation; stimulates renin release, maintains renal blood flow and GFR, increases erythropoietin
PGI ₂	Vasculature, macula densa, cortical thick ascending limb	Vasodilation and renal blood flow, renin release, diuresis, natriuresis, maintains GFR
PGE ₁	Vasculature, cortical tubules	Vasodilation maintains renal blood flow and GFR; decreases macrophage infiltration
PGD ₂	Glomeruli	Increases renin release and renal blood flow; antifibrotic
PGF _{2α}	Glomeruli, medulla	Vasodilation, natriuresis, diuresis
TXA ₂ /TXB ₂	Glomeruli, smooth muscle cells in renal arterioles, transitional cell epithelium of renal pelvis, distal convoluted tubules, collecting tubules, connecting tubules	Vasoconstriction, renal hemodynamics, and GFR, renovascular actions of angiotensin II, glomerular thrombosis
PGA ₂	Cortical and medullary tubules	Increases renal blood flow and erythropoietin release

and (3) increased intracellular calcium (Hébert et al., 1991). Some in vitro studies have shown that EP₂ and EP₁ mediate the regulatory effects of PGE₁ and PGE₂ on the transcription of the Na⁺, K⁺-ATPase in Madin–Darby canine kidney (MDCK) cells (Matlhagela et al., 2006). Using primary proximal tubule cell culture system, chronic incubation with PGE₁ and PGE₂ resulted in an increase in the levels of mRNA for Na,K-ATPase as well as the total level of cellular Na,K-ATPase (Herman et al., 2010). In another in vitro study of renal cortex incubated with PGE₂, it was demonstrated that PGE₂ inhibited both phosphate and volume absorption in mouse proximal convoluted tubules perfused in vitro and reduced brush-border membrane vesicle NaPi-2a protein abundance in the renal cortex (Syal et al., 2006).

Overproduction of PGE₂ has been shown to be associated with increased GFR in diabetic nephropathy (DeRubertis and Craven, 1993). Oral administration of an antagonist selective for the PGE receptor EP₁ subtype, ONO-8713, at a dose of 1000 ppm in regular chow prevented the progression of nephropathy in streptozotocin-induced diabetic rats. ONO-8713 reduced renal and glomerular hypertrophy, decreased mesangial expansion, inhibited transcriptional activation of transforming growth factor beta (TGFβ) and fibronectin, and completely suppressed proteinuria (Makino et al., 2002). Urinary excretion of PGE₂ is significantly elevated in type 1 (insulin-dependent) diabetic women with nephropathy compared with normoalbuminuric type 1 diabetic women and nondiabetic women, and indomethacin treatment, 150 mg/day, induced a significant reduction in urinary

PGE₂ excretion (Hommel et al., 1987). These data indicate that the PGE₂–EP₁ system plays a crucial role in the development of diabetic renal injury. Antidiuretic hormone (ADH) increases renal PGE₂ synthesis (Walker et al., 1978). In hypophysectomized dogs, indomethacin increased urine osmolality in response to ADH (Anderson et al., 1975).

It is known that PGE₂ can cause either vasodilatation, via activating EP₂/EP₄ receptors, or vasoconstriction, via activating EP₁/EP₃ receptors. Thus, a role for the PGE₂/EP₁ signaling pathway in the development of renal injury in hypertension has been proposed and investigated. Oral administration of an EP₁-selective antagonist prevented the progression of renal damage in stroke-prone spontaneously hypertensive rats (SHRSP), a model of human malignant hypertension (Suganami et al., 2003). EP₁-deficient mice have a urine concentration defect due to decreased vasopressin release, resulting in hypotension (Kennedy et al., 2007). In the *db/db* mouse (with homozygote mutation in leptin receptor) model of type 2 diabetes, systolic blood pressure was significantly elevated compared with control heterozygote male mice. Exogenous application of PGE₂ or a selective agonist of the EP₁ receptor elicited arteriolar constrictions that were significantly enhanced in *db/db* mice compared with controls. Moreover, oral administration of an EP₁ receptor antagonist, AH6809, at 10 mg/kg per day for 4 days significantly reduced the systolic blood pressure in *db/db* but not in control mice. The investigators concluded that activation of EP₁ receptors increases arteriolar tone, which could contribute to the development of hypertension in the *db/db* mice (Rutkai et al., 2009). PGE₂ can maintain GFR by dilating the afferent arterioles (Edwards, 1985; Schlondorff, 1993). In addition, medullary PGE₂ promotes renal sodium excretion via the EP₂ receptor. For example, C57BL/6J mice placed on a high-NaCl diet exhibited increased medullary COX-2 and mPGES1 expression (Chen et al., 2008). In addition, COX-2 expression dramatically increased in the MD and cortical thick ascending limb in both humans and rodents with salt and volume depletion (Harris et al., 1994; Komhoff et al., 2000). Some human syndromes, such as Bartter-like syndrome, are associated with significant renal salt and water loss. In this syndrome, there is also marked by increased urinary PGE₂ excretion (Komhoff et al., 2000). The MD cells synthesize and release PGE₂ during reduced luminal salt content, and this response is important in the control of renin release and renal vascular resistance during salt deprivation (Peti-Peterdi et al., 2003). In vitro studies of glomerular podocytes have shown that PGE₂ regulates distinct cellular functions via the EP₁ and EP₄ receptors, thereby increasing Ca²⁺ and cAMP, respectively (Bek et al., 1999). PGE₂ evoked cAMP production and renin secretion by juxtaglomerular cells from salt-deprived rats was significantly higher than with cells obtained from salt-loaded animals (Jensen et al., 1999). Thus, renocortical PGE₂ stimulates renin secretion and maintains renal blood flow during low-salt states, whereas medullary PGE₂ promotes salt excretion in response to a high salt intake (Jensen et al., 1999).

PGE₁ is a potent vasodilator of all arterioles. The protective role of PGE₁ in the kidney has been demonstrated in several studies. PGE₁ suppressed macrophage-infiltration and ameliorated injury in an experimental model of macrophage-dependent glomerulonephritis (Cattell et al., 1990). In a rat model of

acute macrophage-dependent glomerular injury, administration of 15(*s*)-15-methyl PGE₁ (M-PGE₁) ameliorated proteinuria by day 4, decreased glomerular hypercellularity, and reduced the numbers of infiltrating macrophages (Cattell et al., 1990). PGE₁ in pharmacological quantities retarded the development of an autoimmune, lupus-like disorder in an MRL mouse model. The effects included (1) prevention of peripheral T-lymphoid hyperplasia, (2) preservation of T-cell mitogenic responses, (3) inhibition of immune complex-mediated glomerulonephritis, and (4) reduction in the amounts of circulating immune complexes (Kelley et al., 1981). In a study of male Wistar rats, oral administration of 200 µg/kg of a PGE₁ analog, misoprostol, for 5 days was protective against toxic and ischemic renal injury induced by cisplatin (Ozer et al., 2011). In a female Sprague–Dawley rat model of acute renal microvascular injury, PGE₁ decreased the capillary loss, relieved hypoxia, and protected renal function (Sun et al., 2011). In another study in a Sprague–Dawley rat model of acute aristolochic acid nephropathy, PGE₁ significantly ameliorated the renal microvascular injury, decreased hypoxia, and protected renal function (Sun et al., 2011). In dogs, PGE₁ infusion increased renal blood flow and significantly attenuated the postischemic fall in GFR and renal concentrating ability as well as the postischemic increase of plasma creatinine and blood urea nitrogen (Johnston et al., 1967; Torsello et al., 1989). In humans it has been suggested that PGE₁ may prevent renal dysfunction after cardiopulmonary bypass (Abe et al., 1993).

TXA₂ receptors (TPs) have been found in various regions of the kidney. Thromboxane synthase has been detected in the glomeruli of rat kidneys (Vitzthum et al., 2002). In the rat kidney, TX receptor mRNA, using *in situ* hybridization, was localized in glomeruli, smooth muscle cells in renal arterioles, and transitional cell epithelium of renal pelvis (Abe et al., 1995). Similarly, immunostainable TX receptor was observed in the rat kidney in the glomeruli, arterial walls, luminal membranes of thick ascending limbs of Henle's loop, the luminal and basolateral membranes of either distal convoluted tubules or connecting tubules, and the basolateral membranes of collecting tubules (Takahashi et al., 1996). Another study investigated the localization of thromboxane A₂/prostaglandin H₂ (TXA₂/PGH₂) receptor protein in the rat kidney. In the mouse kidney, TXA₂ receptor mRNA was expressed most abundantly in the glomerulus, followed by the distal convoluted tubule, proximal tubule, thick ascending limb of Henle, and outer medullary collecting duct (Asano et al., 1996). The investigators found that the receptor localized both in glomeruli and in tubules. In the glomeruli, the receptor was most prominent along the lumen of glomerular capillary loops. Parietal epithelial cells of the Bowman's capsule, podocytes, and mesangial cells also had receptor expression. In the tubules, the receptor was localized most prominently at the base of the brush border of proximal tubules and at the luminal surface of thick ascending limbs and distal convoluted tubules (Bresnahan et al., 1996).

TXA₂ is a potent vasoconstrictor. In fact, injection of synthetic TXA₂ in a dose of 20 ng/kg directly into the renal artery of anesthetized pigs resulted in a dose-related decrease in renal blood flow (Cirino et al., 1990). In addition, TXA₂ regulates mesangial cell contraction through elevation of intracellular cAMP (Mené and Dunn, 1988). Improved renal function was noted in a randomized clinical

crossover study in which eight patients with lupus nephritis were given a TXA₂ synthetase inhibitor, DP-1904, orally at a dose of 400 mg/day twice daily for 4 days (Yoshida et al., 1996). In a study in male Sprague–Dawley rats, the effects on renal function of acute bile duct ligation were studied for 2 days. The consequences of administration of a TX receptor antagonist, BAYu3405, given at a total dose of 10 mg/kg per day via intraperitoneal injections, were then examined. It was shown that TX receptor antagonist can partially prevent renal dysfunction in experimental cholestasis (Holt et al., 1999). A role for TXA₂ in glomerular thrombosis has been suggested. For example, in a rat model of type 2 diabetes, Otsuka Long–Evans Tokushima Fatty strain, the progress of nephropathy as evidenced by an increase in proteinuria paralleled an increase in the urinary excretion of 2,3-dinor-TXB₂. An inhibitor of TXA₂ synthase, OKY-046, at 100 mg/kg in these rats suppressed the proteinuria and the formation of glomerular thrombi (Okumura et al., 2003). Thromboxane receptors play a role in the renovascular actions of angiotensin II (Ang II). For example, the selective TP receptor antagonist terutroban attenuated renal damage in a double-transgenic (harboring human renin and angiotensinogen genes) rat model of hypertension (Sebeková et al., 2008). TXA₂ plays a role in the regulation of renal hemodynamics. For example, TP-KO mice had normal basal mean arterial blood pressure (MAP) and GFR but reduced renal blood flow and increased filtration fraction (FF) and renal vascular resistance (RVR) and markers of reactive oxygen species (ROS) (Kawada et al., 2004). Ang II infusion into TP-KO mice reduced Ang I and increased aldosterone, but caused a blunted increase in MAP and failed to increase FF and ROS (Kawada et al., 2004). Thus, it is suggested that TP receptors regulate renal hemodynamics during Ang II slow pressor response. An additional role for TXA₂ in renal pathophysiology has been suggested. In TP-receptor-KO mice, the glomerular heat-aggregated bovine serum albumin content was lower than that of WT mice. Furthermore, a stable analog of TXA₂, U-46619, increased in a dose-dependent manner the uptake of heat-aggregated bovine serum albumin by mesangial cells in WT mice but not in TP-KO mice (Nagao et al., 2001). These findings suggest that TXA₂ retarded the clearance of aggregated protein in nephritic glomeruli (Nagao et al., 2001). Another study found that a thromboxane receptor antagonist, S18886, attenuated renal oxidant stress and proteinuria in a diabetic apolipoprotein E-deficient mouse model (Xu et al., 2006).

PGI plays a role in vasodilatation and is localized in vasculature in the rat kidney (Vitzthum et al., 2002). Some studies showed that PGIS is expressed in the MD and cortical thick ascending limb in 5/6-nephrectomized rats (Tomida et al., 2001). In the MD, PGI₂ mediated renin release (Ito et al., 1989). Some studies showed that PGIS deletion is associated with ischemic kidney damage and have demonstrated a role for PGI₂ in maintaining RBF (Yokoyama et al., 2002). These PGI₂-deficient mice developed progressive morphological abnormalities in the kidneys, characterized by renal atrophy, surface irregularity, fibrosis, cyst, arterial sclerosis, and hypertrophy of vessel walls. Thickening of the thoracic aortic media and adventitia was also observed (Yokoyama et al., 2002). Interestingly, the IP receptor deficiency in mice does not result in the same kidney damage as that seen in PGIS deficiency (Murata et al., 1997), suggesting that other signaling mechanisms (e.g., renin pathway) may contribute to PGI₂'s effect on RBF. The systemic

blood pressure and plasma renin effects after intravenous injection of PGI₂ were investigated. A dose-dependent antihypertensive effect in conscious rats with spontaneous and chronic renal hypertension was observed. In addition, PGI₂ induced an increase of plasma renin activity in anesthetized rats (Schölkens, 1978). The effects of increased renal PGI₂, using kidney-specific PGI₂ transgenic (Tg) mice, on endotoxin-induced acute kidney injury (AKI) were investigated (Wang et al., 2007). Increased sensitivity to endotoxin was noted in the PGI₂ Tg mice compared with the wild-type mice. The authors concluded that an excess of renal PGI₂ in mice may obscure beneficial effects against endotoxemia-related AKI by activating the PGI₂-cyclic AMP-renin pathway (Wang et al., 2007). PGI₂ can lead to natriuresis (Villa et al., 1997).

PGD₂ is produced localized in renal glomeruli (Hassid et al., 1979). The exact role of PGD₂ in the kidney is poorly understood. Dose-response renal effects of PGD₂ (0.125, 0.25, 0.5, and 0.75 µg/kg per minute) infused intravenously in dogs were studied. PGD₂ administration resulted in a significant dose-dependent increase in renal artery flow, urine output, creatinine clearance, plasma renin activity, sodium excretion, potassium excretion, and pulmonary artery pressure. A significant decrease occurred in renal resistance and arterial PO₂. There were no appreciable changes in mean arterial pressure, heart rate, hematocrit, platelet count, arterial pH, and PCO₂ (Rao et al., 1987). These results suggest that PGD₂ given under these experimental conditions and doses can improve renal blood flow and function, at least in dogs. In an *in vitro* study using rat kidney cells, it was shown that PGD₂ in the renal papilla plays a role in the maintenance of phosphatidylcholine biosynthesis (Fernandez-Tome et al., 2004). An antifibrotic role for PGD₂ has been suggested (Zhang et al., 2006). Lipocalin-type prostaglandin D synthase/β-trace (L-PGDS) is an enzyme-synthesizing prostaglandin D₂(PGD₂) and a secretory protein of the lipocalin superfamily. It is synthesized in choroid plexus or leptomeninges in the brain and secreted steadily through cerebrospinal fluid into circulating blood. L-PGDS has a small molecular mass of 26,000 Da. Thus, L-PGDS can easily pass through glomerular capillary walls of the kidney, and its urinary levels may reflect a change in the permeability of glomerular capillary walls and can be used as a biomarker to predict renal injury in type 2 diabetic patients (Uehara et al., 2009). In fact, the urinary and serum concentrations of L-PGDS increased in patients with type 2 diabetes and hypertension (Ragolia et al., 2005; Ogawa et al., 2006). Atherosclerosis and diabetic nephropathy are two common pathologies associated with type 2 diabetes. Thus, the L-PGDS role in the kidney has been investigated using L-PGDS-KO mice. L-PGDS-KO mice became glucose-intolerant and insulin-resistant at an accelerated rate compared with the C57BL/6 control strain of mice. In addition, these mice developed kidney structural changes indicative of diabetic nephropathy, such as glomerular hypertrophy, fibrosis, and basement membrane thickening, and these changes were further exacerbated on the diabetogenic diet. Furthermore, RT-PCR showed that L-PGDS mRNA is expressed in kidney cortex and outer medulla in mice (Ragolio et al., 2005). Thus, urinary levels of L-PGDS have also been proposed to be a relevant biomarker for renal injury (Ragolio et al., 2005; Ogawa et al., 2006). PGA₂ is localized in the renal cortical and medullary tubules (Perez and McGuckin, 1972). PGA₂ can increase

renal blood flow, lead to vasodilation, and increase erythropoietin release (Gross et al., 1976; Banks and Jacobson, 1985). $\text{PGF}_{2\alpha}$ is localized in the renal medulla (Lee et al., 1967; Gross et al., 1976). $\text{PGF}_{2\alpha}$ contributes to diuresis and natriuresis (Zook and Strandhoy, 1981) and causes vasodilation (Lebel and Grose, 1991). The local synthesis and accumulation of prostanoids in the kidney can play a role in urinary tract obstruction. Increased kidney concentrations of PGE_2 , $\text{PGF}_{2\alpha}$, and TXB_2 have been demonstrated to be predominantly in the renal inner medulla, with the highest concentration 12 h after the occlusion and then largely normalized at 24 h (Nørregaard et al., 2010).

PG receptors have been localized in various microanatomic regions of the kidney. E-type prostanoid receptors (EPs) are the receptors that mediate the actions of PGE_2 and are members of the superfamily of G-protein-coupled receptors. There are four PGE_2 receptors, designated EP_1 , EP_2 , EP_3 , and EP_4 (Morath et al., 1999). These receptors can play a role in regulation of Na^+ handling, vasodilatation, vasoconstriction, and/or blood pressure. It is well accepted that PGE_2 stimulation of the EP_1 receptor is linked to smooth muscle contraction and increased intracellular Ca^{2+} . Thus, PGE_2 stimulation of EP_1 receptors produces contractile responses. Expression of the EP_1 receptor subtype protein in renal tissue was detected in human kidney mainly in connecting segments, cortical and medullary collecting ducts, and in the media of arteries and afferent and efferent arterioles (Morath et al., 1999). In rabbit kidney cell cultures, EP_1 receptor mRNA expression predominates in the cortical collecting duct (Guan et al., 1998). It is suggested, at least in rabbit kidneys, that EP_1 receptor activation mediates PGE_2 -dependent inhibition of Na^+ absorption in the collecting duct, thereby contributing to its natriuretic effects (Guan et al., 1998). EP_1 -deficient mice exhibit lower systolic blood pressure and increased plasma renin levels (Stock et al., 2001). In addition, oral administration of an EP_1 receptor antagonist, SC-51322, reduced blood pressure in spontaneously hypertensive rats (Guan et al., 2007). Furthermore, some studies have shown that the EP_1 receptor facilitates Ang II-mediated vasoconstriction (Guan et al., 2007). Selective genetic disruption of the EP_1 receptor in mice blunted the acute pressor response to Ang II and reduced chronic Ang II-driven hypertension (Guan et al., 2007). In primary cultures of inner medullary collecting duct (IMCD) cells, EP_1 receptor activation prevented the aldosterone-induced epithelial sodium channel (αENaC), the rate-limiting step for Na^+ reabsorption, and up-regulation (González et al., 2009). Furthermore, infusion of Ang II to rats caused an increase in plasma aldosterone and induced a significant increase in αENaC mRNA and protein in kidney cortex and medulla. This effect of Ang II infusion on αENaC expression was blocked by coadministration of spironolactone, a mineralocorticoid receptor (MR) antagonist, indicating an MR-dependent effect (González et al., 2009). This work suggested that activation of EP_1 receptor during RAAS activation can modify the aldosterone-mediated αENaC expression in the renal medulla (González et al., 2009). However, renal concentrating and diluting ability in the EP_1 receptor-KO mice appears comparable to that of WT mice, although the KO mice may have altered vasopressin release (Kennedy et al., 2007). Arginine-vasopressin (AVP) or ADH has been established as an intrarenal vasoconstrictor, capable of decreasing perfusion, mostly of the inner medulla, with less impact in the outer medulla.

AVP facilitates water reabsorption in renal collecting duct principal cells by activation of vasopressin V2 receptors and the subsequent translocation of water channels (aquaporin-2, AQP2) from intracellular vesicles into the plasma membrane (Tamma et al., 2003). The EP₁ receptor is abundantly expressed in the principal cells of the collecting duct, where it is thought to offset the buffering influence of EP₃ receptors on the antidiuretic actions of AVP (Tamma et al., 2003). Prostaglandin E₂ antagonizes AVP-induced water reabsorption. Using primary rat inner medullary collecting duct (IMCD) cells, Tamma et al. (2003) showed that stimulation of prostaglandin EP₃ receptors induced ρ activation and actin polymerization in resting IMCD cells but did not modify the intracellular localization of AQP2. However, AVP-, dibutyryl cAMP-, and forskolin-induced AQP2 translocation was strongly inhibited. This inhibitory effect was independent of increases in cAMP and cytosolic Ca²⁺. In addition, stimulation of EP₃ receptors inhibited the AVP-induced ρ inactivation and the AVP-induced F-actin depolymerization. Thus, the signaling pathway underlying the diuretic effects of PGE₂ includes cAMP- and Ca²⁺-independent ρ activation and F-actin formation.

The EP₃ receptor mRNA, using *in situ* hybridization, was detected in medullary thick ascending limb and cortical and medullary collecting ducts with intense labeling, while no labeling of glomeruli, proximal tubules, or cortical thick ascending limbs was observed in rabbit kidney (Breyer et al., 1993). EP₃ counteracts AVP action by reducing cAMP production (Hébert et al., 1993). Activation of EP₃ leads to acute inhibition of sodium–potassium–chloride transporter 2 (NKCC2) and aquaporin 2 (AQP2) because the apical trafficking of these proteins is dependent on cAMP (Nielsen et al., 1995; Ortiz, 2006). In a study of EP₃-receptor expression in the developing rabbit kidney. The investigators found that the highest levels of EP₃ mRNA were observed at 2 weeks of age. EP₃ mRNA was observed in the medullary thick ascending limb, cortical collecting duct, and inner medullary collecting duct of adult and immature kidneys (Bonilla-Felix and Jiang, 1996). In the mouse kidney, EP₃ receptor mRNA was located in the tubules in the outer medulla and in the distal tubules in the cortex (Sugimoto et al., 1994). EP₃-deficient mice concentrated and diluted their urine normally in response to a series of physiological stimuli (Fleming et al., 1998). A study in male mice found that EP₃ receptors mediate renal vasoconstriction and are capable of buffering PGE₂-mediated renal vasodilation (Audoly et al., 2001). In human kidneys, RNA for the GI-coupled EP₃ receptor was expressed primarily in the cortical and outer medullary collecting duct as well as in the medullary thick ascending limb; however, it was absent from the inner medullary collecting duct (Breyer et al., 1996). Another study found that EP₃ receptor subtype protein, using immunohistochemistry, is strongly expressed in glomeruli, Tamm–Horsfall negative late distal convoluted tubules, connecting segments, and cortical and medullary collecting ducts, as well as in the media and the endothelial cells of arteries and arterioles of human kidney (Morath et al., 1999).

The EP₂ receptor subtype protein was detectable only in the media of arteries and arterioles of human kidney (Morath et al., 1999). Although only low levels of EP₂ receptor mRNA are detected in the kidney and its precise intrarenal

localization is uncertain, mice with targeted disruption of the EP₂ receptor exhibit salt-sensitive hypertension, suggesting that this receptor may also play an important role in salt excretion. In contrast, EP₄ receptor mRNA is expressed predominantly in the glomerulus, where it may contribute to the regulation of glomerular hemodynamics and renin release. The IP receptor mRNA is highly expressed near the glomerulus, in the afferent arteriole, where it may also dilate renal arterioles and stimulate renin release. Conversely, TP receptors in the glomerulus may counteract the effects of these dilator prostanoids and increase glomerular resistance. At present there is little evidence for DP receptor expression in the kidney (Breyer and Breyer, 2001; Imig, 2006). In a mouse model of LPS-induced renal glomerular inflammation, it was demonstrated that EP₂ and EP₄ receptors modulate expression of the chemokine CCL2 (MCP-1) (Zahner et al., 2009). Some studies show that EP₄ and EP₂ receptor agonists improve renal function and/or increase survival in the mercury chloride rat model of acute renal failure, supporting a protective role of EP_{2/4} in the maintenance of renal function (Vukicevic et al., 2006).

Three PGE synthases have been identified: microsomal PGE synthase-1 (mPGES-1), microsomal PGE synthase-2 (mPGES-2), and cytosolic PGE synthase (cPGES). Expression of mPGES-1 is induced by cytokines and inflammatory stimuli. In contrast, the expression of cPGES and mPGES-2 is not inducible (Radi and Ostroski, 2007). In general, mPGES-1 is located in the perinuclear compartment of the cell preferentially and couples to COX-2, whereas cPGES couples predominantly with constitutive COX-1. Also, mPGES-2 couples with both COX isoforms. The expression of mPGES was investigated in the rat and mouse kidney. It was shown that there is a parallel expression with COX-2 in the cortical thick ascending limb and macula densa, and coexpression with COX-1 in glomerular mesangial cells, distal convoluted tubule, connecting tubule, and nonintercalated collecting duct cells, where COX-2 was absent (Campean et al., 2003). Cortical fibroblasts were positive for COX-1 and PGES in mice, and medullary interstitial cells expressed all three enzymes (Campean et al., 2003). Another study have shown that mPGES-1 is highly expressed in rabbit distal convoluted tubule, medullary collecting ducts, and cortical collecting ducts, predominantly colocalizing with COX-1 and, to a lesser extent, is coexpressed with COX-2 in macula densa and medullary interstitial cells (Schneider et al., 2004). High expression of mPGES-1 is present in the collecting duct (Vitzthum et al., 2002; Campean et al., 2003; Schneider et al., 2004). Also, mPGES-1 has been detected in the thick ascending limb and MD (Campean et al., 2003). Low levels of mPGES-1 can be detected in the cortical and medullary interstitial cells (Campean et al., 2003; Schneider et al., 2004; Vitzthum et al., 2002). It is thought that mPGES-1 is coupled functionally to COX-2, due to colocalization of mPGES1 and COX-2 in the cortical thick ascending limb and medullary interstitial cells (Murakami et al., 2002). Low levels of mPGES2 and cPGES are also detected in the kidney (Yang et al., 2006; Zhang et al., 2003).

COX-1 AND COX-2 EXPRESSION IN THE KIDNEY

The early immunohistochemical localization of COX in rat, rabbit, guinea pig, sheep, and cow in the renal cortex began in 1978 (Smith and Bell, 1978). COX-1 is the most abundant isoform of COX in the kidney and is localized in the renal vasculature, collecting ducts, and papillary interstitial cells across various species (Smith and Bell, 1978; Khan et al., 1998; Sellers et al., 2004; Radi and Ostroski, 2007; Radi, 2009). Table 3-3 summarizes the comparative renal expression of COX-1 (Radi and Ostroski 2007; Radi, 2009). No differences in COX-1 renal regional localization were found among various species (Khan et al., 1998). Evidence in various species (cow, dog, guinea pig, human, monkey, mouse, rabbit, rat, and sheep) demonstrated that high levels of COX-1 expression occurred in the collecting ducts (Smith et al., 1978; Khan et al., 1998; Campean et al., 2003). In kidney cells isolated from Sprague–Dawley rats, COX-1 mRNA was found to be widely distributed and expressed at substantial levels along the entire collecting duct, in MTAL segments, in glomeruli freed of adherent MD, and in cultured renal interstitial cells, mesangial, and collecting duct-derived cell lines. Low or high dietary salt did not affect COX-1 expression (Yang et al., 1998). COX-1 expression has been investigated in various pathological conditions. Nephrogenic diabetes insipidus (NDI) is a renal disorder characterized by an inability to concentrate urine despite normal or elevated plasma concentrations of the antidiuretic hormone (ADH) arginine vasopressin (Morello and Bichet, 2001). Nephrogenic diabetes insipidus is caused either by mutation in the vasopressin type 2 receptor (*AVPR2*) or aquaporin-2 (*AQP2*) gene, hypercalcemia, or lithium treatment (Singer et al., 1972; Morello and Bichet, 2001; Faerch et al., 2009). In NDI there is a peripheral resistance to ADH and polyuria (excessive or abnormally large production and/or passage of urine), with hyposthenuria (excretion of urine of low specific gravity) and polydipsia (excessive thirst) being the cardinal clinical manifestations of the disease. NSAIDs have been used to treat patients with NDI (Usberti et al., 1980; Pattaragarn and Alon, 2003). Therefore, COX expression has been investigated in animal models of NDI. In

TABLE 3-3 Comparative Expression of COX-1 in the Kidney^a

Renal microanatomical location	Species				
	Human	Monkey	Dog	Rat	Mouse
Vasculature	+	+	+/-	+	++
Collecting duct	+	+	+	+	+++
Interstitial cells	++	++	+++	+++	++

Source: The final, definitive version of this table was published in Z. A. Radi, *Toxicologic Pathology*, 37(1), 2009, pp. 34–46. Copyright © Sage Publications. All rights reserved.

^a + minimal; ++ mild; +++ moderate; ++++ marked.

an NDI model, Wistar rats were treated with lithium for 4 weeks to induce the disease. There was a marked decrease in the expression of COX-1 in the inner medulla of the kidney, and COX-1 expression was marginally reduced in the inner stripe of outer medulla in this NDI model (Kotnik et al., 2005). COX-1 expression was studied in a two-kidney/one-clip (2K1C) Goldblatt hypertensive rat model. In this 2K1C hypertension model, the defect is highly dependent on the enhanced activity of the RAAS. Decreased renal perfusion pressure in the compromised kidney maximally activates RAAS and its inability to balance the rise in blood pressure, which is partly the result of elevated Ang II levels (Theilig et al., 2006). Immunoreactive COX-1 in the 2K1C model was localized to the extraglomerular mesangium and distal convoluted tubules (DCTs), connecting tubule, and cortical collecting duct, with the exception of the intercalated cells (Theilig et al., 2006). In a hypertension transgenic mouse model that expresses the human renin and angiotensinogen genes, the highest degree of renal COX-1 expression occurred in the DCTs, cortical collecting ducts, and medullary collecting ducts, while mild-to-moderate COX-1 expression occurred in other microanatomic renal locations. PCT lacked COX-1 expression (Radi and Ostroski, 2007).

In kidney sections from CD1 mice, COX-1 expression before and after NSAID treatment was investigated (Meskell and Ettarh, 2011). Immunohistochemical analysis before NSAID treatment and in control kidneys revealed COX-1 expression in the renal cortex and medulla, with significantly more expression evident within the cortex. Immunoreactivity in the superficial cortex was more pronounced than in the rest of the cortex or the medulla. COX-1 protein was expressed in the glomeruli and parietal cells of the glomerular capsule, epithelial cells of the proximal and distal convoluted tubules, and the collecting ducts. Cytoplasmic COX-1 protein within the distal tubule was present in the juxtaglomerular region, adjacent to the glomerulus. Interstitial cells in the renal cortex did not show reactivity for COX-1. Within the medulla, pronounced expression of COX-1 was apparent within the endothelial cells of the renal vasculature, but the epithelial cells of the medullary collecting ducts and the interstitial cells in the medulla showed poor reactivity for COX-1 (Meskell and Ettarh, 2011). In kidneys treated with the ns-NSAID indomethacin, COX-1 immunostaining was present in the cortical and medullary areas. COX-1 immunoreactive protein was apparent in the outer parietal layer of the Bowman's capsule and in some cells of the glomerulus. COX-1 expression was observed within cells of the proximal and distal convoluted tubules and the cortical collecting ducts. COX-1 expression was present within the endothelial cells of the renal blood vessels, and the medullary collecting duct expression was minimal (Meskell and Ettarh, 2011). There was no staining for COX-1 immunoreactive protein in the cortical or the medullary interstitium (Meskell and Ettarh, 2011). Thus, at therapeutic doses of 10 mg/kg, indomethacin did not alter renal COX-1 expression, at least by immunohistochemistry, relative to immunoreactivity in untreated control kidney. In the same study in mice, the ns-NSAID nimesulide was used and renal COX-1 expression was examined (Meskell and Ettarh, 2011). Significant expression of COX-1 protein was present in the superficial cortical region adjacent to the renal capsule and evidence of some COX-1 immunoreactivity in the outer parietal epithelial cell layer of Bowman's capsule. Very minimal COX-1

immunoreactivity was evident in the proximal convoluted tubule. There was COX-1 protein expression within cells of the cortical distal convoluted tubules, with significant localization within the cortical collecting ducts. Focal immunostaining was seen in endothelial cells of blood vessels and collecting duct cells in the renal medulla (Meskell and Ettarh, 2011). Therefore, the investigators concluded that a therapeutic dose of 15 mg/kg of nimesulide reduced renal COX-1 expression within the first 24 h of treatment.

The ontogeny of renal COX expression has been investigated. In a study in developing rats, COX mRNA expression changes was examined in renal medulla and in cortex at various ages (Ogawa et al., 2001). COX-1 mRNA expression did not change with age in either the cortex or medulla. COX-2 mRNA expression was highest in 1-week-old rats and lowest in 4- and 8-week-old rats. Lipopolysaccharide (LPS) treatment did not alter COX-1 mRNA expression in infantile or adult rats. In adults, LPS at 1, 5, and 10 mg/kg induced COX-2 mRNA expression in renal medulla; the higher doses, 5 and 10 mg/kg, induced COX-2 expression in cortex. In infantile rats, COX-2 mRNA, which was already high in the unmanipulated state, was increased further by only 1 mg/kg LPS in both renal cortex and medulla (Ogawa et al., 2001). Another study examined the age-related changes in COX mRNA expression induced by hypoxia in the renal cortex and medulla of developing rats (Ogawa et al., 2002). Expression of COX-1 mRNA did not change in response to hypoxia in the cortex or medulla in either infantile or adult rats. In infantile rats, COX-2 mRNA expression was not induced by 1 or 4 h of hypoxia. In adults, 1- and 4-h exposures to hypoxia induced COX-2 mRNA in the renal cortex, and 1 h of exposure induced COX-2 mRNA in the medulla (Ogawa et al., 2002). Thus, age-related changes in COX-2 mRNA expression in the developing rats were observed after acute exposure to hypoxia.

Since COX-1 is expressed in the collecting ducts of the nephron, an active area in the regulation of sodium excretion in both laboratory animals and humans (Currie and Needleman, 1984), it is not surprising that BP increases in COX-1-deficient mice compared with WT controls (Kawada et al., 2005). Thus, ns-NSAIDs may aggravate renin-independent sodium-sensitive hypertension, possibly in part by inhibition of the COX-1 responsible for sodium excretion (Okumura et al., 2002). In rats infused with the COX-2 s-NSAID NS-398 or meloxicam, direct renal interstitial volume expansion significantly increased renal interstitial hydrostatic pressure and fractional excretion of sodium (Gross et al., 1999).

In humans, COX-1 expression was examined in kidney tissues obtained from patients aged 17 to 97 years old. These patients' deaths were unrelated to renal or cardiovascular pathologies (mostly car accidents). Strong immunoreactivity was detected in the collecting duct epithelium, and less intense staining was seen in the descending thin loops of Henle and interstitial cells in the papilla. Many of the arcuate arteries also expressed COX-1, which appeared to be confined to the tunica media (Nantel et al., 1999). In another study of adult normal human kidney, COX-1 expression was noted in the collecting duct cells, interstitial cells, endothelial cells, and smooth muscle cells of pre- and postglomerular vessels. In fetal human kidney, COX-1 was expressed primarily in podocytes and collecting duct

cells. Expression levels of COX-1 in both cell types increased markedly from sub-capsular to juxtamedullary cortex (Komhoff et al., 1997). Another study examined COX-1 expression in normal human kidney tissues using immunohistochemistry, Western blotting, and RT-PCR. Autopsy samples from healthy trauma victims and samples from biopsy surgical specimens were included in the study. COX-1 was found in blood vessels, interstitial cells, smooth muscle cells, platelets, and mesothelial cells (Zidar et al., 2009).

COX-2 is generally an inducible enzyme under settings of inflammation. In the kidney, COX-2 is expressed constitutively in macula densa and thick ascending limb in cortex and inner medulla (Ferreri et al., 1999; Campean et al., 2003) and can be found in interstitial cells (Yang et al., 1999). Enhanced COX-2 expression has been demonstrated in several renal pathologies, such as glomerulonephritis (Schneider et al., 1999), passive Heymann nephritis (Heise et al., 1998), and lupus nephritis (Tomasoni et al., 1998). COX-2-deficient mice exhibited severe disruption of renal development and function, suggesting an important role for COX-2 in renal development (Dinchuk et al., 1995; Morham et al., 1995). COX-2 is expressed in variable locations in the kidney across species (Khan et al., 1998, 2001b). COX-2 expression was studied in human fetal kidneys ranging between 15 and 23 weeks of gestational age. Strong expression of COX-2 was localized primarily in the MD and the thick ascending limb of the loop of Henle, and in rare glomerular podocytes and vascular endothelial cells. There was a progressive decrease in COX-2 immunoreactivity from the most immature nephrons adjacent to the metanephric regions to the well-developed nephrons in the middle to inner cortex. In contrast to the adult human kidney, this temporal and spatial expression of COX-2 in the fetal kidney suggests that COX-2 enzyme may be involved in nephrogenesis, and its inhibition by NSAIDs during the third trimester may be responsible for fetal renal syndromes (Khan et al., 2001b). The temporal expression of COX-2 throughout embryonic and fetal development was investigated in the rat by immunohistochemistry and *in situ* hybridization. COX-2 expression was not detectable in any tissues from developing embryos during gestation days 7 to 13, but was observed in the fetal growth period (gestation days 15 to 20) in several organs, including the kidney (Stanfield et al., 2003). Interspecies differences may exist for the involvement of COX-2 in the generation of renal PGs in states of normal and altered kidney function (Khan and Alden, 2002). For example, normal rodent and canine kidneys have prominent constitutive COX-2 expression in the MD and thick ascending limb of loop of Henle; whereas COX-2 is absent at these sites in the normal nonhuman primate and human kidney (Sellers et al., 2004). COX-2 levels also differ according to maturation, with high levels expressed in the macula densa and thick ascending limbs of fetal kidneys and minimal expression upon renal maturation (Khan et al., 2001b; Khan and Alden, 2002). In rat kidney cells, COX-2 mRNA was restricted to the MD, cortical thick ascending limb, and at significantly lower levels, in the inner medullary collecting duct (Yang et al., 1998). Divergent regulation of COX-2 in cortex and medulla by dietary salt has been suggested (Yang et al., 1998). In the inner medulla of rats treated with a high-salt diet, COX-2 mRNA increased 4.5-fold and protein levels increased 9.5-fold. In contrast, cortical COX-2 mRNA levels decreased 2.9-fold in rats on a high-salt diet and increased 3.3-fold in rats

on a low-salt diet. A low-salt diet increased COX-2 mRNA 7.7-fold in MD and 3.3-fold in CTAL (Yang et al., 1998).

The role for MD COX-2 in the regulation of renin in renovascular hypertension has been proposed (Hartner et al., 1998). For example, the expression of COX-2 and renin was investigated in the kidneys of rats with two-kidney/one-clip renovascular hypertension. COX-2 mRNA levels were increased in clipped kidneys but remained unchanged or slightly decreased in nonclipped kidneys. COX-2 protein was expressed mainly in the MD and occasionally in distal tubular cells not associated with the MD (Hartner et al., 1998). COX-2 mRNA and protein expression, but not COX-1, is markedly decreased in the cortex and increased in the inner medulla in response to unilateral ureteral obstruction (Chou et al., 2003) and bilateral ureteral obstruction (Cheng et al., 2004). COX-2 expression was examined in kidney tissues obtained from patients aged 17 to 97 years old. These patients' deaths were unrelated to renal or cardiovascular pathologies (mostly car accidents). In the cortex, COX-2 immunoreactivity was identified in the MD, in the glomerular afferent arteriole, in podocytes in a subset of glomeruli, and in a limited number of thick loops of Henle. In the medulla, COX-2 immunoreactivity was limited to interstitial cells and the tunica media of arcuate arteries. The presence of COX-2 in the MD was more evident in kidney specimens obtained from older subjects. COX-2 immunoreactivity was detected in the MD of all kidneys from subjects aged 48 years or greater. Only two of five kidneys (40%) from subjects less than 40 years of age showed COX-2 MD immunoreactivity. COX-2-positive immunostaining was also detected within podocytes of the some glomeruli in six of 10 kidneys (60%) (Nantel et al., 1999).

There is a regulatory association between COX-2 and renin (Schnermann, 2001). It has been suggested that COX-2 mediates increased renin content induced by a low-sodium diet in mice. A low-sodium diet in mice increased renal renin content, but this increase was blocked by treatment with the COX-2 *s*-NSAID NS-398. In addition, treatment with NS-398 reduced renin mRNA in response to a low-sodium diet (Harding et al., 1997). Demonstration that indomethacin and SC-58236, a COX-2 *s*-NSAID, can decrease BP and suppress plasma renin activity in rats lends further support to this association (Jackson et al., 1981; Wang et al., 1999). In a streptozotocin-induced diabetes mouse model, increased podocyte expression of COX-2 increased susceptibility to development of diabetic nephropathy, and the podocyte injury was due in part to increased expression and activity of the pro-renin receptor. These mice exhibited significant renal changes characterized by albuminuria, foot process effacement, and GBM thickening (Cheng et al., 2011). In addition, the role that Ang II can play in modulating the regulation of renin release has been proposed. Administration of the angiotensin-converting (ACE) inhibitor captopril to rats fed a normal or sodium-deficient diet resulted in an increase in COX-2 mRNA and renal cortical COX-2 immunoreactivity, with the most pronounced expression in the macula densa (Cheng et al., 1999). Administration of an Ang I receptor antagonist, losartan, also significantly increased cortical COX-2 mRNA expression and COX-2 immunoreactivity in rats on control diet and further increased COX-2 expression in salt-deficient animals (Cheng et al., 1999). To investigate the role of an Ang I receptor in the regulation of cTALH/MD

COX-2 expression, mutant mice homozygous for both *Agtr1a* and *Agtr1b* null mutations (*Agtr1a*^{-/-}, *Agtr1b*^{-/-}) were used. These mice had large increases in immunoreactive COX-2 expression in the cTALH/MD (Cheng et al., 1999). Rats were treated with captopril for 1 week with or without the COX-2 s-NSAID SC58236. Plasma renin activity increased significantly in the captopril group, and this increase was inhibited significantly by simultaneous treatment with SC-58236. Thus, these studies indicated that Ang II inhibitors augment up-regulation of renal cortical COX-2 in states of volume depletion, suggesting that negative feedback by the renin–angiotensin system modulates renal cortical COX-2 expression and that COX-2 is a mediator of increased renin production in response to inhibition of Ang II production (Cheng et al., 1999). Conversely, COX-2-KO mice had reduced renin content and activity (Yang et al., 2000).

Endogenous glucocorticoids play a complex physiological role in modulating renal electrolyte balance and blood flow. These endogenous glucocorticoids act via glucocorticoid receptors and indirectly enhance sodium reabsorption in epithelial cells isolated from proximal tubules (Gong et al., 2008). One of the glucocorticoid metabolizing enzymes is 11 β -hydroxysteroid dehydrogenase (11 β -HSD1). The normal human kidney expresses functional 11 β -HSD1 protein in proximal tubules and in medullary interstitial cells. Interestingly, in the normal human kidney, 11 β -HSD1 colocalizes with COX-2 in proximal tubule cells (Gong et al., 2008).

EFFECTS OF ns-NSAIDs ON THE KIDNEY

Over-the-counter and prescription NSAIDs are widely used by the adult population in the United States (Paulose-Ram et al., 2003). The incidence of NSAID-associated renal side effects was investigated. In one study that used a computerized medical records system, the incidence of ibuprofen-associated renal impairment and risk factors for its development was 18% in 1908 patients treated with ibuprofen (Murray et al., 1990). In a recent survey of a total of 12,065 adult (aged 20 years or older), the use (nearly every day for 30 days or longer) of any NSAID (ibuprofen, naproxen, sulindac, piroxicam, indomethacin, tolmetin, or diclofenac) was reported by 2.5%, 2.5%, and 5% of the U.S. population with no, mild, and moderate-to-severe chronic kidney disease (CKD), respectively (Plantinga et al., 2011). NSAIDs have been associated with greater risk for development of acute kidney injury in the general population (Huerta et al., 2005) and with increased risk for rapid CKD progression in a community-based elderly population (Gooch et al., 2007). The most common renal side effects of ns-NSAIDs are functional and include interference with fluid and electrolyte homeostasis. Other less frequent side effects include acute renal failure, interstitial nephritis, nephritic syndrome, atrophy of subcapsular cortex in dogs, and renal papillary necrosis (Whelton, 1999; Rossert, 2001; Khan and Alden, 2002). Elderly persons are more predisposed to NSAID-associated renal adverse effects for several reasons: (1) age-associated changes in renal function; (2) the prevalence of comorbid conditions (congestive heart failure, hypertension, hepatic cirrhosis, renal insufficiency), and (3) the pervasive use of concomitant drugs that affect kidney function (diuretics, antihypertensives) (Ailabouni and Eknoyan, 1996).

NSAIDs contribute to changes in blood pressure and edema, resulting from renal flow and fluid retention imbalance. NSAIDs may aggravate renin-independent sodium-sensitive hypertension, possibly in part by inhibition of the COX-1 responsible for sodium excretion (Okumura et al., 2002). In addition, NSAIDs may elevate blood pressure and antagonize the blood pressure-lowering effect of antihypertensive medication to an extent that may potentially increase hypertension-related morbidity (Johnson et al., 1994). Inhibition of cortical and medullary PGs production by NSAIDs can lead to electrolyte abnormalities and fluid retention, such as sodium, potassium, and water retention. However, clinically detectable edema occurs in less than 5% of patients and is easily managed in patients and readily reversible upon discontinuation of the use of NSAID (Whelton and Hamilton, 1991). Furosemide is a loop diuretic used in the treatment of congestive heart failure and edema. Renal function and excretion of water and salt were evaluated in furosemide-treated patients with well-controlled congestive heart failure. In addition, four doses of naproxen (500 mg) were given every 12 h in a double-blind crossover design. Naproxen significantly decreased the urinary excretion of water (19%), sodium (26%), and chloride (26%), and decreased osmolal clearance (18%). Plasma renin activity, aldosterone, or free water clearance did not change significantly with treatment (Eriksson et al., 1987). The effects of ibuprofen and indomethacin on renal function and electrolytes in the presence and absence of furosemide in healthy volunteers who are on a restricted sodium diet were evaluated (Passmore et al., 1990). Neither indomethacin (50 mg) nor ibuprofen (400 and 800 mg) affected renal blood flow, GFR, or electrolyte excretion before furosemide. However, renal blood flow and GFR were increased significantly in the first 20 min after furosemide, and these changes were attenuated significantly by indomethacin compared with placebo and ibuprofen 400 mg (Passmore et al., 1990). In a placebo-controlled double-blind crossover design study, the effects of 7-day oral administration of naproxen in a 500-mg dose in the morning and a 250-mg dose in the evening in patients with polyarthritis and stable impaired renal function were investigated (Eriksson et al., 1990). Naproxen reduced GFR and renal plasma flow by 18% and 13%, respectively. Plasma renin activity decreased by 38% during naproxen treatments. No significant change in plasma aldosterone was observed during treatment, but urinary aldosterone declined significantly by 34% and albuminuria decreased by 41%. No discernible effects on base excess, on excretion of water, sodium, or potassium, or on osmolal clearance were noted. However, serum potassium increased slightly but significantly during naproxen treatment (Eriksson et al., 1990). The effect of a single 500-mg dose of naproxen on renal function in healthy volunteers was studied. No effects on GFR were noted. Over the first 4 to 8 h of the study, fractional excretion of sodium was reduced by approximately 50% (Dixey et al., 1987). Thus, naproxen should be used with caution in patients with fluid retention, hypertension, or heart failure. Another study examined renal function in healthy volunteers who received ibuprofen, naproxen, or sulindac in a randomized double-blind fashion. Renal function and plasma renin activity were not affected (Brater et al., 1985). On the average, 0.6% of a dose of ketoprofen or naproxen was found in the urine of normal male volunteers assayed immediately after its collection (Upton et al., 1980). Between approximately 60

and 85% of the dose of these drugs can be excreted in the urine as conjugates, which rapidly hydrolyze at body temperature, at room temperature, and even during frozen storage, thereby regenerating the parent drug. Thus, only a small fraction of naproxen is excreted unchanged in vivo (Upton et al., 1980). Only a small fraction of the filtered naproxen amount was excreted into the urine (Cox et al., 1990). This means that naproxen must be reabsorbed extensively. Reabsorption is probably a passive process, dependent on the urinary flow and pH (Cox et al., 1990). As a result of active uptake of naproxen across the basolateral membrane and facilitated diffusion across the brush-border membrane, naproxen can accumulate in the tubular cells (Cox et al., 1990). In isolated perfused rat kidneys naproxen accumulates considerably. Increasing the naproxen-perfused concentration results in a decrease in the K/P ratio which may be related to the saturation of active secretion of naproxen (Cox et al., 1990).

The effects of NSAIDs on urinary sodium and potassium excretion were studied in the rat. Diclofenac (30 mg/kg) and flurbiprofen (125 mg/kg) were administered orally once daily for 4 days. Urine was collected 0 to 8 h after each dose, and urinary sodium and potassium excretion and urine flow rate were compared with placebo. Both diclofenac, and flurbiprofen significantly reduced the excretion rate of sodium and potassium (Harirforoosh and Jamali, 2005). The effects of the ns-NSAID sodium meclofenamate at a 5-mg/kg dose given intravenously in pentobarbital-anesthetized and sodium-replete dogs were investigated. Sodium meclofenamate significantly reduced the urinary excretion of sodium by 47% but did not affect mean arterial blood pressure, renal blood flow, GFR, or urine volume (Blasingham and Nasjletti, 1980). In nonclinical toxicology studies, the acute 2-week oral toxicity profile of naproxen was determined in Swiss Webster albino mice, Sprague–Dawley rats, Golden Syrian hamsters, and beagle dogs with multiples of the maximum human therapeutic dose of 107, 47, 357, and 87, respectively. Subacute (1- and 3-month) repeated oral dosing studies were also conducted in mice, rats, rabbits, dogs, monkeys, and pigs with multiples of the maximum human therapeutic dose up to 1.3-fold. These acute and subacute studies showed that repeated oral dosing of naproxen did not cause significant histopathological changes in the kidney and was well tolerated by mice, rabbits, monkeys, and pigs, less well by rats, and poorly by dogs. Based on these results, rats, monkeys, and pigs were animals of choice for the chronic studies. Rats dosed for up to 2.6 times the maximum human therapeutic dose per day for 6 and 22 months showed no significant kidney histopathological changes but had increased urinary volume, decreased body weight gain, and a shorter survival time than did control rats or rats given 0.2 or 0.9 times the maximum human dose per day. No meaningful renal changes were seen for monkeys given oral doses up to 10.4 times the maximum human per day for six months or for pigs given doses up to 3.9 times the maximum human per day for one year (Hallesy et al., 1973).

NSAID-induced hyperkalemia most often occurs from impaired renal potassium excretion (Perazella, 2000). Potassium homeostasis is impaired by NSAIDs through the inhibition of renal PG (PGE₂ and PGI₂) synthesis (Garella and Matarese, 1984). These PGs stimulate renal synthesis of renin and influence the subsequent synthesis of aldosterone (Garella and Matarese, 1984). This

leads to a hyporeninemic hypoaldosteronism state, which is probably the major mechanism by which NSAIDs cause hyperkalemia (Tan et al., 1979). Up to 46% of patients treated with indomethacin develop hyperkalemia (Zimran, 1985).

Nonselective NSAIDs can reduce GFR and renal blood flow (Clive and Stoff, 1984; Dunn et al., 1988) and may aggravate renin-independent sodium-sensitive hypertension, possibly in part by inhibition of the COX-1 responsible for sodium excretion (Okumura et al., 2002). However, studies in which the effect of naproxen was examined using healthy volunteers showed no reduction in GFR (Brater et al., 1985; Dixey et al., 1987). The physiological status (i.e., exercise, salt restriction, and dehydration) can affect the outcome of NSAID use. For example, the renal effects of the maximal recommended dose of ibuprofen at 1.2 g/day versus a placebo in humans subjected to progressive renal stresses (e.g., treadmill exercise, heat, dehydration, fasting) were tested. These combined stressors caused dramatic decreases in effective renal plasma flow, GFR, and sodium excretion. Baseline GFR decreased in all groups including placebo, with a significantly greater decrease in GFR in the ibuprofen-treated group. Ibuprofen treatment showed small but statistically significant effects on GFR during exercise in a sodium- and volume-depleted state (Farquhar et al., 1999). In another randomized double-blind three-way crossover study with placebo, the effects of 2 weeks of treatment with ibuprofen and etodolac on renal hemodynamics (GFR, RPF) and filtration fraction (FF), tubular function and plasma concentrations of the hormones, and renin (PRC) and arginine vasopressin (AVP) in healthy subjects were examined (Svendsen et al., 2000). In addition, the effects on the urinary excretion of albumin and α -GST as markers of renal injury were also studied. No differences were found between the three treatments (i.e., placebo, ibuprofen, and etodolac) in the effects on GFR, RPF, FF, free water clearance, urinary output, or fractional excretion of potassium and sodium. However, in contrast to etodolac, ibuprofen caused a significant decrease in both lithium clearance and the fractional excretion of lithium, suggesting an increase in the reabsorption in the proximal tubules. PRC was reduced significantly by ibuprofen but not by etodolac. None of the drugs changed AVP. Fourteen days of treatment with ibuprofen caused a significant decrease in the urinary excretion of α -GST, while no changes were seen after etodolac. None of the drugs changed the urinary excretion of albumin (Svendsen et al., 2000). Thus, a 14-day administration of etodolac or ibuprofen in therapeutic doses did not affect renal hemodynamics, the net excretion of electrolytes, or the urinary excretion of albumin in healthy subjects.

However, in contrast to etodolac, ibuprofen caused a reduction in PRC, suggesting that COX-1 may be involved in basal renin release in humans. In addition, ibuprofen decreased lithium excretion, suggesting that COX-1 is involved in the reabsorption of sodium and/or water in the proximal tubules. The reduction in the urinary excretion of α -GST by ibuprofen may be caused by an inhibition of the detoxification enzyme by ibuprofen. Overall, the study indicated that only small differences in the effects of the two drugs on renal function in healthy subjects exist during a treatment period of 2 weeks (Svendsen et al., 2000). In another clinical study, normal volunteers received placebo, ibuprofen, naproxen, or sulindac in a randomized double-blind fashion. After control periods assessing the effect of

the NSAIDs alone, a 40-mg dose of furosemide was administered. Renal function, plasma renin activity, and urinary PGs were not affected during control collections, while all three ns-NSAIDs decreased TXB₂. After furosemide, all ns-NSAIDs decreased fractional excretions of Na⁺ and Cl⁻, renin, and TXB₂. Sulindac and ibuprofen decreased urinary PGE₂, whereas naproxen did not (Brater et al., 1985). The effects of 600 mg of ibuprofen given three times daily on renal water and sodium excretion was measured during fasting in a randomized placebo-controlled double-blind crossover study of 17 healthy humans. The subjects received a standardized diet on day 1, fasted at day 2, and received an IV infusion of 3% NaCl on day 3. Ibuprofen decreased fractional excretion of sodium and increased the urinary beta fraction of the epithelial sodium channel during a 24-h fasting period, during the first 2 h after 24 h of fasting, and during the following period with hypertonic saline infusion. In addition, ibuprofen decreased urinary excretions of aquaporin 2 and PGE₂ at all parts of the study. Ibuprofen did not change the response in AVP, urinary cAMP, urinary output, and free water clearance during any of these periods (Lauridsen et al., 2011). Thus, urinary sodium excretion decreases considerably in healthy men during fasting, so a state with an increased PGs synthesis and a possible role for epithelial sodium channels is suggested. Ibuprofen elimination is through hepatic biotransformation to inactive metabolites excreted by kidney filtration and secretion. About 70% of ibuprofen is excreted in the urine as metabolites or unchanged drug.

An acute ibuprofen overdose in dogs, cats, and ferrets is associated with renal signs of toxicosis (Villar et al., 1998). At doses greater than 175 mg/kg in dogs, there was an increased risk of acute renal failure (polyuria, polydipsia, oliguria, and uremia). The effects of anesthesia on renal function were examined in beagle dogs. Acetaminophen was given at 15 mg/kg and ibuprofen at 10 mg/kg intravenously. Both drugs decreased RBF and GFR by approximately 20 to 30% in normal anesthetized sodium-repleted dogs. Although acetaminophen produced similar changes in RBF and GFR in the low-sodium dogs, ibuprofen caused a significantly greater renal vasoconstriction (Colletti et al., 1999). In general, the healthy newborn, in particular the premature infant, have a low GFR, and drugs that may affect GFR and electrolyte handling (i.e., NSAIDs) should be given with caution to young individuals. In an experiment with New Zealand white rabbits, increasing doses of ibuprofen (0.02, 0.2, 2.0 mg/kg body weight) were given to newborn rabbits. This resulted in a significant, dose-dependent decrease in RBF and GFR. This was accompanied by a reduction in urinary volume and urinary sodium excretion, whereas mean arterial pressure remained unchanged. There was a very steep rise in renal vascular resistance (Chamaa et al., 2000). Thus, when NSAIDs are given to neonates, renal function has to be followed very carefully. The effects of clinically comparable doses of ibuprofen and indomethacin on renal vascular perfusion were investigated in newborn piglets (Speziale et al., 1999). The newborn piglets were injected with two ns-NSAIDs, ibuprofen (20 mg/kg) and indomethacin (0.3 mg/kg). Ibuprofen increased renal cortical and medullary resistance by 44 and 52% while indomethacin raised renal cortical and medullary resistance by 66 and 71% at 60 min postinjection, respectively. Indomethacin and, to a lesser extent, ibuprofen increased renal vascular resistance (Speziale et al., 1999). No significant

changes in pulmonary vascular pressures of strenuously exercising thoroughbreds have been observed after phenylbutazone administration in horses (Manohar et al., 1996). In addition, NSAIDs may elevate blood pressure and antagonize the blood pressure–lowering effect of antihypertensive medication to an extent that may potentially increase hypertension-related morbidity (Johnson et al., 1994).

Analgesic nephropathy is characterized by chronic interstitial nephritis and renal papillary necrosis or calcifications. The hallmark of analgesic nephropathy is renal papillary necrosis (RPN) (Fig. 3-2). The only permanent renal complication of NSAIDs is RPN, which is very rare (Whelton and Hamilton, 1991). Studies in rats show that NSAIDs readily cause RPN; however, studies have shown that laboratory animals (i.e., rats, dogs, rabbits) are unusually susceptible to RPN, which is related to their unique renal anatomy and physiology compared to other species (Wiseman and Reinert, 1975; Khan et al., 1998). Thus, laboratory animals are not necessarily a good model for predicting RPN in humans. The effects of two papillotoxic agents, including an ns-NSAID, indomethacin, and a chemical agent, 2-bromoethanamine hydrobromide (2-BEA), on COX-1 and COX-2 in the renal papilla in female Wistar rats during the development of RPN were investigated. Indomethacin was given at 75 mg/kg as a single dose or as a daily dose of 10 mg/kg for 5 days. 2-BEA

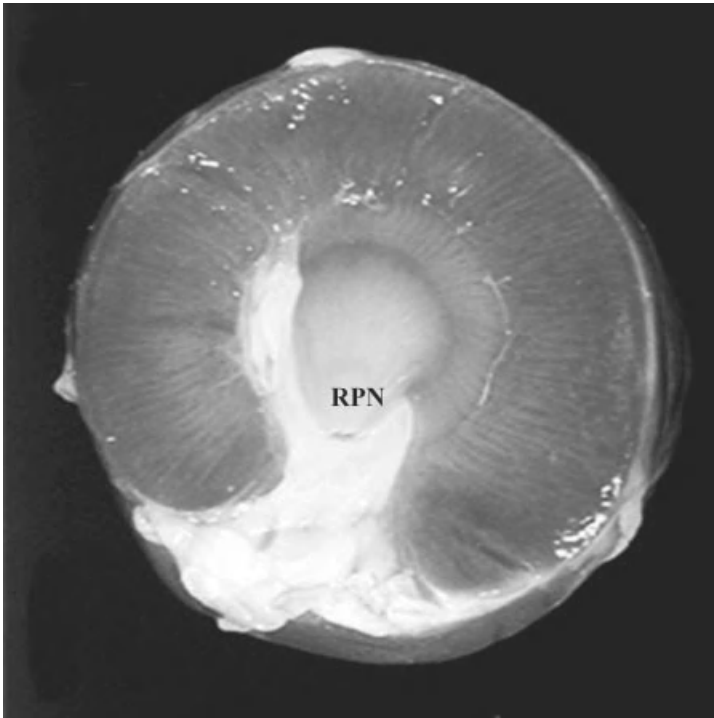


FIGURE 3-2 Analgesic nephropathy (renal papillary necrosis). Courtesy of Dr. N. Khan. [The final, definitive version of this figure was published in Z. A. Radi, *Toxicologic Pathology*, 37(1), 2009, pp. 34–46. Copyright © Sage Publications. All rights reserved.]

was given in a daily dose of 100 mg/kg for 4 days to induce lesions of RPN. The single 75-mg/kg dose of indomethacin did not cause light microscopic changes of RPN. However, RPN was observed in rats administered indomethacin 10 mg/kg per day for 1 week or 2-BEA for 5 days. The immunohistochemical analyses of kidneys showed that both COX-1 and COX-2 were present in the renal papilla of control rats. In animals treated with indomethacin (75 mg/kg), a slight to moderate decrease in both COX isoforms was observed in essentially normal renal papillary cells within 2 h, followed by an increase in COX-2 immunoreactivity in the renal papilla, macula densa, and thick ascending limbs (at both 10 and 75 mg/kg). No changes in the expression of COX isoforms in the intact papilla occurred as a result of 2-BEA; however, cells undergoing degeneration and necrosis lost immunoreactivity to both COX isoforms (Khan et al., 1998). The earliest lesions of RPN are characterized by loss of interstitial glycosaminoglycans and focal interstitial cell degeneration near the tip of the papilla, which represents precursor lesions of RPN (Bennett et al., 1996). Papillary interstitial cells are the first cell type to undergo morphological changes in NSAID-related RPN. These cells have limited proliferating capacity; therefore, repeated injury is irreversible and may result in a local loss of vasodilatory PGs and development of secondary ischemia (Khan et al., 1998). In cases with full expression of injury, degeneration and necrosis extended to the vascular endothelium and the epithelial cells of the loops of Henle, and the collecting ducts also involved a larger portion of the papilla (Khan et al., 1998). It has been speculated that the papillae of rats and dogs are susceptible to chemical injury owing to sluggish blood flow, which predisposes to ischemia and accumulation of toxic substances (Khan and Alden, 2002). Two mechanisms of RPN have been proposed (Duggin, 1980). The first mechanism involves metabolic or functional features of the renal papilla, which makes it susceptible to ischemia resulting from decreased RBF. The second mechanism is the selective concentration of the drug within the renal papilla (Duggin, 1980).

NSAIDs are commonly used in the neonatal period to treat or prevent patent ductus arteriosus (PDA) in preterm infants. The renal effect of ibuprofen treatment for patent ductus arteriosus (PDA) in very preterm infants during the first month of life was examined. Infants aged 27 to 31 weeks of gestation were assigned to two different groups according to ibuprofen exposure during care of their PDA status assessed by echocardiography. Renal function was evaluated at baseline and weekly for one month. GFR decreased significantly in the ibuprofen group after treatment withdrawal. Adjusted analysis proved this decreased GFR to be sustained during the first month of life. Tubular function was also impaired during the first month in ibuprofen-treated infants (Vieux et al., 2010). The renal effects of ibuprofen and indomethacin on suckling and weanling Sprague–Dawley rat were investigated. Newborn rats received intraperitoneal injections of either ibuprofen (10 mg/kg) on the first day of postnatal life (P1) followed by 5 mg/kg on P2 and P3 or indomethacin (0.2 mg/kg) on P1, followed by 0.1 mg/kg indomethacin on P2 and P3. No kidney histological differences were noted among the groups. However, in suckling rats, indomethacin suppressed PGE₂ and COX-2 expression and increased PGF_{2 α} , whereas ibuprofen increased COX-2 and Ang II. Although both ns-NSAIDs suppressed 6-ketoPGF_{1 α} and TXB₂ levels in suckling rats, the effect was sustained

in weanling rats with indomethacin (Hasan et al., 2008). Therefore, renal function of infants receiving ns-NSAIDs should be monitored carefully and drugs that are eliminated by glomerular filtration handled cautiously during this period (Vieux et al., 2010).

In the human, glomerulogenesis is complete at 36 weeks of gestation. The metanephron develops at 5 weeks of gestation, with vesicular glomeruli development occurring at 18 weeks of gestation. Glomerular tubular development occurs from 24 weeks of gestation and is complete at 36 weeks (Abrahamson, 1991; Horster et al., 1999; Naruse et al., 2000). The mesangial cells in almost all glomeruli at the late M stage acquire the adult phenotype before birth. In the rat, glomerulogenesis continues after birth until 14 days of life (Lasaitiene et al., 2003). At birth, the neonatal rat kidney is similar to that of a 24-week-gestation human fetus. Some ns-NSAIDs, such as indomethacin, are often effective in delaying delivery for 24 to 48 h. Indomethacin suppresses preterm labor by interfering with PG-induced myometrial contractions. However, investigators have shown that indomethacin treatment given to pregnant women as a short course (the last 2 days of pregnancy) can lead to a significant functional impairment of the kidneys in their offspring, manifested as suppression of both GFR and urine production (van der Heijden et al., 1988). Some studies have shown that maternal indomethacin exposure immediately before delivery was shown not to be associated with increased neonatal complications for infants delivered between 24 and 32 weeks of gestation (Vermillion and Newman, 1999). The effects of several ns-NSAIDs on glomerulogenesis were investigated in Sprague–Dawley pregnant dams. Rat pups were given indomethacin, intraperitoneally at a dose of 0.2 mg/kg, ibuprofen at 10 mg/kg, or indomethacin at 0.1 mg/kg and gentamicin at 2.5 mg/kg for the first 5 days of their postnatal life and were euthanized at 14 days of age at completion of glomerulogenesis. The rat pups were given the drugs for the first 5 days of their postnatal life, which covers a more extensive period of glomerulogenesis (24 to 30 weeks of gestation). There was no difference between treatment groups in total number of glomeruli per kidney. Significantly fewer glomeruli per gram of kidney were noted in those rat pups that had received indomethacin or ibuprofen. The body and kidney weights of those rat pups given the higher doses of indomethacin and ibuprofen were significantly greater (13 to 25%) than those of control pups and those given the lower dose of indomethacin. The results should be interpreted with caution, due to the timing of the drug regimens and the time the rats were euthanized at 14 days of life. The reduction in the number of glomeruli per gram of kidney may indicate augmented growth of nephron tubules and/or collecting ducts and/or be a consequence of edema secondary to drug exposure (Kent et al., 2009). Another study investigated the type of renal changes found on light (LM) and electron microscopy (EM) following administration of indomethacin, ibuprofen, and gentamicin in a neonatal rat model. Rat pups were exposed to indomethacin or ibuprofen and/or gentamicin antenatally for 5 days before birth or postnatally for 5 days from day 1 of life, and pups were euthanized at 14 days of age. LM examination in all indomethacin- and ibuprofen-treated pups both antenatally and postnatally showed vacuolization of the proximal tubular epithelium, interstitial edema, and intratubular protein deposition but no significant glomerular changes. EM examination showed

pleomorphic mitochondria and loss of microvilli in the renal tubules. The glomeruli showed extensive foot process effacement and irregularities of the glomerular basement membrane. EM changes were most marked in pups treated antenatally with ibuprofen, and indomethacin with gentamicin postnatally. Indomethacin, ibuprofen, and gentamicin cause significant change in glomerular and tubular structure in this neonatal rat model (Kent et al., 2007).

EFFECTS OF COX-2 s-NSAIDs ON THE KIDNEY

Complete COX-2 gene disruption results in severe nephropathy (Morham et al., 1995). Gross pathological examination of kidneys from 8-week-old male COX-2 homozygous mutant mice revealed that the kidneys were small and pale and had a granular appearance of the capsular surface. Kidneys from wild-type (WT) animals were normal in appearance. Light microscopic examination of kidneys from WT male and female mice revealed no histologic abnormalities. In contrast, the kidneys of all adult homozygous mice had mild to marked renal lesions. Mild renal lesions of the nephropathy were characterized by multifocal areas of abnormal subcapsular parenchyma comprised of small immature glomeruli and tubules, consistent with nephron hypoplasia. In some cases, the cortex appeared thin, and the numbers of glomeruli were reduced in comparison with WT kidneys. Glomeruli that are not within the hypoplastic region of the kidney were frequently found to be enlarged. Other histopathological findings included cortical areas of tubular atrophy and regeneration, protein and cellular casts within tubular lumens, tubular dilation, interstitial inflammation and fibrosis, and papillary mineralization. In general, these histopathological changes were more severe in male than in female homozygous mutants, and lesion severity increased with advancing age. The 8-week-old homozygous mutant mice kidneys had few small scattered foci of tubular atrophy and interstitial fibrosis that were not present in the 6-week-old homozygous mutant mice. The single homozygous mutant male that survived to necropsy at 16 weeks of age had severe focal interstitial fibrosis and tubular atrophy, associated with focal segmental and global glomerular sclerosis. Renal arteries and arterioles were unremarkable. To ascertain the general time frame in which the renal pathology developed, a litter of 3-day-old pups was euthanized and their kidneys were examined. The renal histopathology of the COX-2-deficient mice did not differ from that of the wild type, and the 3-day-old homozygous mice had a normal subcapsular zone of immature nephrogenic tissue and normal numbers of glomeruli in the kidney cortex. This is in contrast with the 6-week and older homozygous mice, which had abnormal nephron hypoplasia in the subcapsular region and abnormally low numbers of glomeruli in the kidney cortex. Thus, COX-2 null mice show postnatal developmental abnormalities in their kidneys that then deteriorate progressively with increasing age (Morham et al., 1995). The renal effects of COX-2 knockdown were investigated in mice. In these mice, COX-2 expression was suppressed to an extent similar to that achieved with COX-2 s-NSAIDs, but was not eliminated. In LPS-challenged macrophages and cytokine-stimulated endothelial cells obtained from these COX-2 knockdown mice, COX-2 expression was reduced 70 to 90%.

These mice developed a mild renal phenotype compared with COX-2 mice possessing an active site mutation with minimal signs of renal dysfunction as measured by inulin clearance and blood urea nitrogen (Seta et al., 2009). These mice have no notable alterations in systemic blood pressure compared to control mice (Seta et al., 2009).

Postnatal (PN) development and progression of renal dysplasia was investigated in COX-2 null mice (Norwood et al., 2000). No differences in renal morphology were detected between COX-2^{-/-} mice and their controls on the day of birth, postnatal day 3 (PN3), and PN7. By PN10, early cystic changes were identifiable in some kidneys from COX-2^{-/-} mice, and the lesion was affecting several different tubule sections and glomeruli, and crowded, small, subcapsular glomeruli were noted. A distinctive lack of the normal proximal tubular mantle was also noted in COX-2^{-/-} animals. Not all PN10 COX-2^{-/-} kidneys exhibited identifiable abnormalities, suggesting that the rate of pathological progression may vary slightly among animals. However, by PN14, kidneys from all COX-2^{-/-} mice could be differentiated from their WT littermates. Kidneys from PN14 and PN28 COX-2^{-/-} mice had progressive outer cortical dysplasia with cystic subcapsular glomeruli, loss of proximal tubular mass and brush-border definition, and tubular atrophy and cyst formation. Hypertrophy of juxtamedullary glomeruli and tubules was observed by PN28. The severity of pathological changes continued to increase with age. Adult (PN42) homozygous null kidneys had profound diffuse tubular dilation and cyst formation, outer cortical glomerular hypoplasia and periglomerular fibrosis, focally variable glomerular sclerosis, inner cortical nephron hypertrophy, and diffuse interstitial fibrosis. No significant inflammatory infiltrate or vascular pathology was seen. Some degree of variability in the severity of adult pathology was noted among littermates, with some animals showing more severe cystic degeneration than others (Norwood et al., 2000).

PGs also play a role in renal pathophysiology by modulating the release of renin. The macula densa in the kidney is involved in regulating afferent arteriolar tone and renin release by sensing alterations in luminal chloride (Persson et al., 1991). Low plasma renin levels have been demonstrated in COX-2-deficient mice (Kim et al., 2007). It has been demonstrated that COX-2 s-NSAIDs can significantly decrease plasma renin levels and blood pressure in rats (Wang et al., 1999; Cheng et al., 2001). COX-derived prostanoids act in an autocrine or paracrine fashion, exert complex and diverse functions, and serve as physiological buffers within the kidney (Hao and Breyer, 2008). COX-derived prostanoids can modulate RBF and GFR. Modulation of renal physiology is driven by COX-2 catalysis from AA of PGE₂ and PGI₂; both are important PGs for the maintenance of RBF. PGI₂ is the main factor involved in endothelial dysfunction in hypertensive rats, whereas other prostanoids are more critically involved in endothelial dysfunction under normotensive conditions (Blanco-Rivero et al., 2005). Some studies have suggested that nitric oxide, in addition to PGI₂, plays a significant role in the restoration of endothelial function in hypertensive patients treated with ACE-Is (Yamanari et al., 2004). Thus, COX-2 metabolites have been implicated to play a role in regulation of renal sodium excretion, renin release, and maintenance of RBF. A high-salt diet markedly increases renal medullary COX-2 expression

(Yang et al., 1998). The importance of renal medullary COX-2 in promoting natriuresis and maintaining blood pressure during high dietary sodium intake has been demonstrated in rats after intramedullary infusion with NS-398, a COX-2 s-NSAID (Zewde and Mattson, 2004). In nonclinical safety studies with celecoxib, transient sodium retention was reported in rats up through 6 weeks of treatment (Khan et al., 2002). Rats given celecoxib for 3 weeks caused a 30-mm Hg increase in systolic blood pressure, whereas the same dose given hypertensive rats increased systolic blood pressure by 33 mmHg (Muscara et al., 2000a). In another study, however, celecoxib did not alter blood pressure in hypertensive rats, and it has been suggested that the natriuretic response to increased blood pressure may be preserved during inhibition of COX-2 (Richter et al., 2004). In rats infused with NS-398 or meloxicam, responses to increased renal interstitial hydrostatic pressure, induced by direct renal interstitial volume expansion and fractional excretion of sodium, were preserved (Gross et al., 1999). Variations between rat strains in the effects of COX-2 inhibitors on blood pressure have been reported. A study comparing the effects of diclofenac, celecoxib, and rofecoxib in Dahl salt-sensitive rats found that after 8 weeks of treatment, celecoxib slightly (4%), but significantly, reduced systemic blood pressure compared to controls and diclofenac and rofecoxib minimally, but significantly increased systemic blood pressure (1%) (Hermann et al., 2005). In another study, COX-2 inhibition in Sprague–Dawley rats had no effect on systemic blood pressure (Vanecková et al., 2005). Beneficial effects of COX-2 inhibition on the renal system have been reported. In male Wistar and stroke-prone spontaneously hypertensive (SHRSP) rats, the postischemic increase in fractional sodium excretion was blunted after celecoxib treatment (Knight and Johns, 2008). A study in male Sprague–Dawley rats found that celecoxib might reduce proteinuria in nephritic syndrome without impairing renal function (Lee et al., 2009). Streptozotocin-diabetic rats treated with a COX-2 s-NSAID, SC-58236, showed a marked reduction in albuminuria, a reduction in kidney weight-to-body weight ratio, and TGF β excretion and a marked decrease in the urinary excretion of TNF α (Quilley et al., 2011).

Nimesulide, a COX-2 s-NSAID, infusion (infused as a continuous bolus dose) in anesthetized mongrel dogs with normal sodium intake had no effects on mean arterial pressure (MAP) or renal hemodynamics, but did reduce urinary sodium excretion and urine flow rate. However, during low sodium intake, nimesulide infusion increased arterial pressure and decreased RBF and urine flow rate. Urinary PGE₂ excretion was decreased, but plasma renin activity did not change (Rodriguez et al., 2000). In dogs given nimesulide, a moderate elevation in blood pressure was observed after intravenous infusion of glucose (Brands et al., 2001). Nimesulide given as a single intravenous bolus dose of 3 mg/kg nimesulide elicited a decrease in MAP in both induced and noninduced Cyp1a1–Ren2 transgenic hypertensive rats. However, the decrease in MAP was greater in hypertensive rats than in normotensive rats. Nimesulide also decreased GFR and RPF in hypertensive rats but did not alter GFR or RPF in normotensive rats (Opay et al. 2006). NS-398 given intraperitoneally in a 5-mg/kg per day dose significantly ameliorated an increase in systolic blood pressure and proteinuria and decreased portal hypertension in Sprague–Dawley rats (Tsugawa et al., 1999; Tomida et al., 2003).

In a rat model of hypertension, it has been suggested that COX-2 plays a significant role in the development of two-kidney/one-clip and one-kidney/one-clip renovascular hypertension (Okumura et al., 2002). PGs seem to contribute to portal hypertension, and both COX-1 and COX-2 blockades reduced the portal pressure and visceral blood flow volume of the portal vein and gastric mucosa in rats (Tsugawa et al., 1999). Studies in COX-1 null mice under conditions of reduced sodium intake have revealed a mild but significant reduction in blood pressure over control mice (Athirakul et al., 2001). The COX-2 s-NSAID SC-58236 had no effect on blood pressure in a 5/6 nephroctomized rat hypertension model, but reduced blood pressure and plasma renin activity in a renovascular rat hypertension model (Wang et al., 1999,2000). Another COX-2 s-NSAID, MF-tricyclic, did not decrease RBF and had no effect on blood pressure in normal and volume-depleted dogs (Black et al., 1998).

In salt-depleted subjects, celecoxib was given for 7 days in 200- and 400-mg twice-daily doses. Celecoxib caused sodium and potassium retention and had no effect on systemic blood pressure (Rossat et al., 1999). Short-term and transient decreases in RBF and GFR were found at the highest dose of 400 mg on day 1 (Rossat et al., 1999). In another study, no individual age category of normotensive subjects had blood pressure or renal function effects significantly altered by short-term treatment with standard doses of celecoxib (200 mg twice a day) (Dilger et al., 2002). In a study in healthy elderly volunteers placed on a fixed sodium intake, rofecoxib at 50 mg once daily for 14 days did not affect GRR and caused a transient retention of sodium, reduced sodium excretion by 20% during the first 3 days of drug administration, and then returned to normal (Catella-Lawson et al., 1999). The effects of rofecoxib on renal function were investigated in the elderly, who received a low-sodium diet. In the first study, single doses of rofecoxib of 250 mg were administered to 15 patients. In the second study, multiple doses of rofecoxib at 12.5 or 25 mg/day were administered to 60 patients. The single and multiple doses of rofecoxib decreased GFR and serum and urinary sodium and potassium values (Swan et al., 2000). The safety and tolerability profile of orally administered meloxicam 15 mg given once daily over a 28-day treatment period was investigated in renally impaired patients with rheumatic disease. No adverse events related to the urinary system or increases in serum urea or potassium were recorded (Bevis et al., 1996). It is implied that COX-2 inhibition would disrupt the antihypertensive effects of ACE-I. However, high doses of celecoxib (400 mg twice a day) showed no significant effect on the activity of the ACE-I lisinopril (White et al., 2002). In another study, celecoxib had no significant change in blood pressure during a 24-h ambulatory blood pressure outcome, but increased systolic blood pressure at peak in the presence of ACE-I, a trandolapril (Izhar et al., 2004).

POTENTIAL MECHANISMS OF NSAID EFFECTS ON THE RENAL SYSTEM

Both COX-2 s-NSAIDs and ns-NSAIDs could contribute to changes in RBF and fluid retention imbalance. Several potential mechanisms of the effects

of ns-NSAIDs on renal pathophysiology have been proposed (Radi, 2009). These mechanisms include (1) inhibition of COX, which reduces systemic and renal PG synthesis (Meade et al., 1993; Wen, 1997); (2) inhibition of PGs by NSAIDs counteracting the hypotensive effects of ACE-I, which blocks ACE and successively increases bradykinin levels, allowing increased renal release of vasodilatory and natriuretic PGs (Blumberg et al., 1977; Linz et al., 1995); (3) alterations in systemic vascular resistance and cardiac output (de Leeuw, 1996); and (4) alterations in the renin–angiotensin–aldosterone system (Lopez-Ovejero et al., 1978; Sahloul et al., 1990; Houston, 1991; Wen, 1997). It is interesting that aldosterone can promote endothelial dysfunction independent of blood pressure through COX-2-derived PGI₂ vasoconstriction in both normotensive and hypertensive conditions in rats (Blanco-Rivero et al., 2005).

Structurally different COX-2 inhibitors vary in their potency as inhibitors of the COX-2 enzyme (Clark et al., 2004). Selectivity and potency of COX-2 s-NSAIDs may differ between tissues and types of cells from the same tissue. Rofecoxib appears more selective and potent than celecoxib (Clark et al., 2004). In addition, differences in metabolism could contribute to effects on blood pressure regulation. Rofecoxib is a sulfone that is not well distributed in tissues and is metabolized principally by cytosolic reduction. Therefore, the NSAID chemotype (i.e., chemically distinct) is an important consideration. Cystosol reductase metabolizes a number of vasoactive hormones in addition to COX. It has been suggested that COX-2 may competitively inhibit the metabolism of these hormones, particularly aldosterone, significant in fluid and sodium retention, both important in blood pressure regulation (Liew and Krum, 2002). Thus, inhibition of carbonic anhydrase leads to diuretic action that partially offsets blood pressure elevations in the kidney. In addition, rofecoxib can readily decompose to reactive metabolites that may account for peroxy radical formation (Reddy and Corey, 2005). Celecoxib is a sulfonamide that is well distributed in tissues and is metabolized by the cytochrome P450 system (Tacconelli et al., 2004). Additional studies designed exclusively to evaluate the influence of structural differences, selectivity, and potency are needed to delineate the potential contribution of NSAIDs to these effects.

CONCLUSIONS

It is important to consider the renal anatomical, developmental, and physiological interspecies differences when considering the pathophysiological effects of COX inhibition on the kidney. In the kidney, COX-1 is expressed constitutively and in the most abundant isoform in various microanatomical locations, while COX-2 is usually expressed constitutively in the macula densa across various species and up-regulated during various pathological renal conditions. Studies show that COX-2 s-NSAIDs can, like ns-NSAIDs, affect renal function adversely in some experimental models. However, in some models, COX-2 s-NSAIDs have had no effect or have had beneficial effects such as decreased plasma renin activity or decreased renal injury. Several mechanisms are proposed for the effects on NSAIDs

on the renal system. Further studies are needed to better understand the potential for chemotype-mediated renal effects.

REFERENCES

- Abe K, Fujino Y, Sakakibara T. The effect of prostaglandin E1 during cardiopulmonary bypass on renal function after cardiac surgery. *Eur J Clin Pharmacol* 1993;45:217–220.
- Abe T, Takeuchi K, Takahashi N, Tsutsumi E, et al. Rat kidney thromboxane receptor: molecular cloning, signal transduction and intrarenal expression localization. *J Clin Invest* 1995;96:657–664.
- Abrahamson DR. Glomerulogenesis in the developing kidney. *Semin Nephrol* 1991;11:375–389.
- Ahmadizadeh M, Echt R, Kuo CH, Hook JB. Sex and strain differences in mouse kidney: Bowman's capsule morphology and susceptibility to chloroform. *Toxicol Lett* 1984;20:161–171.
- Ailabouni W, Eknayan G. Nonsteroidal anti-inflammatory drugs and acute renal failure in the elderly. A risk-benefit assessment. *Drugs Aging* 1996;9:341–351.
- Alique M, Calleros L, Luengo A, Griera M, et al. Changes in extracellular matrix composition regulate cyclooxygenase-2 expression in human mesangial cells. *Am J Physiol Cell Physiol* 2011;300:C907–C918.
- Anderson RJ, Berl T, McDonald KM, Schrier RW. Evidence for an in vivo antagonism between vasopressin and prostaglandin in the mammalian kidney. *J Clin Invest* 1975;56:420–426.
- Apiwattanakul N, Sekine T, Chairoungdua A, Kanai Y, et al. Transport properties of nonsteroidal anti-inflammatory drugs by organic anion transporter 1 expressed in *Xenopus laevis* oocytes. *Mol Pharmacol* 1999;55:847–854.
- Araujo M, Welch WJ. Cyclooxygenase 2 inhibition suppresses tubuloglomerular feedback: roles of thromboxane receptors and nitric oxide. *Am J Physiol Renal Physiol* 2009;296:F790–F794.
- Asano K, Taniguchi S, Nakao A, Maruyama T, et al. Distribution of thromboxane A2 receptor mRNA along the mouse nephron segments. *Biochem Biophys Res Commun* 1996;226:613–617.
- Athirakul K, Kim HS, Audoly LP, Smithies O, et al. Deficiency of COX-1 causes natriuresis and enhanced sensitivity to ACE inhibition. *Kidney Int* 2001;60:2324–2329.
- Audoly LP, Ruan X, Wagner VA, Goulet JL, et al. Role of EP(2) and EP(3) PGE(2) receptors in control of murine renal hemodynamics. *Am J Physiol Heart Circ Physiol* 2001;280:H327–H333.
- Banks RO, Jacobson ED. Renal vasodilation with ureteral occlusion and prostaglandins: attenuation by histamine H1 antagonists. *Am J Physiol* 1985;249:F851–F857.
- Bassan H, Trejo L, Kariv N, et al. Experimental intrauterine growth retardation alters renal development. *Pediatr Nephrol* 2000;15:192–195.
- Bek M, Nusing RM, Kowark P, Henger A, et al. Characterization of prostanoid receptors in podocytes. *J Am Soc Nephrol* 1999;10:2084–2093.
- Bennett CM, Brenner BM, Berliner RW. Micropuncture study of nephron function in the rhesus monkey. *J Clin Invest* 1968;47:203–216.
- Bennett WM, Henrich WL, Stoff JS. The renal effects of nonsteroidal anti-inflammatory drugs: summary and recommendations. *Am J Kidney Dis* 1996;28:S56–S62.
- Bergelin I, Karlsson B. Colostrum, serum and kidney proteins in the urine of the developing neonatal pig. *Int J Biochem* 1974;5:885–894.
- Bevis PJ, Bird HA, Lapham G. An open study to assess the safety and tolerability of meloxicam 15mg in subjects with rheumatic disease and mild renal impairment. *Br J Rheumatol* 1996;35:56–60.
- Black SC, Brideau C, Cirino M, Bellef M, et al. Differential effect of a selective cyclooxygenase-2 inhibitor versus indomethacin on renal blood flow in conscious volume depleted dogs. *J Cardiovasc Pharmacol* 1998;32:686–694.
- Blanco-Rivero J, Cachofeiro V, Lahera V, Aras-Lopez R, et al. Participation of prostacyclin in endothelial dysfunction induced by aldosterone in normotensive and hypertensive rats. *Hypertension* 2005;46:107–112.
- Blasingham MC, Nasjletti A. Differential renal effects of cyclooxygenase inhibition in sodium-replete and sodium-deprived dog. *Am J Physiol* 1980;239:F360–F365.

- Blumberg AL, Denny SE, Marshall GR, Needleman P. Blood vessel–hormone interactions: angiotensin, bradykinin, and prostaglandins. *Am J Physiol* 1977;232:H305–H310.
- Bonilla-Felix M, Jiang W. Expression and localization of prostaglandin EP3 receptor mRNA in the immature rabbit kidney. *Am J Physiol* 1996;271(1Pt 2):F30–F36.
- Bonvalet JP, Pradelles P, Farman N. Segmental synthesis and actions of prostaglandins along the nephron. *Am J Physiol* 1987;253:F377–F387.
- Brands MW, Hailman AE, Fitzgerald SM. Long-term glucose infusion increases arterial pressure in dogs with cyclooxygenase-2 inhibition. *Hypertension* 2001;37:733–738.
- Brater DC, Anderson S, Baird B, Campbell WB. Effects of ibuprofen, naproxen, and sulindac on prostaglandins in men. *Kidney Int* 1985;27:66–73.
- Braun U. Ultrasonographic examination of the right kidney in cows. *Am J Vet Res* 1991;52:1933–1929.
- Bresnahan BA, Le Breton GC, Lianos EA. Localization of authentic thromboxane A₂/prostaglandin H₂ receptor in the rat kidney. *Kidney Int* 1996;49:1207–1213.
- Breyer MD, Breyer RM. G protein-coupled prostanoid receptors and the kidney. *Annu Rev Physiol* 2001;63:579–605.
- Breyer MD, Jacobson HR, Davis LS, Breyer RM. In situ hybridization and localization of mRNA for the rabbit prostaglandin EP3 receptor. *Kidney Int* 1993;44:1372–1378.
- Breyer MD, Davis L, Jacobson HR, Breyer RM. Differential localization of prostaglandin E receptor subtypes in human kidney. *Am J Physiol* 1996;270:F912–F918.
- Brezis M, Rosen S. Hypoxia of the renal medulla: its implications for disease. *N Engl J Med* 1995;332:647–655.
- Campean V, Theilig F, Paliege A, Breyer M, et al. Key enzymes for renal prostaglandin synthesis: sitespecific expression in rodent kidney (rat, mouse). *Am J Physiol Renal Physiol* 2003;285:F19–F32.
- Casotti G, Braun EJ. Structure of the glomerular capillaries of the domestic chicken and desert quail. *J Morphol* 1995;224:57–63.
- Catella-Lawson F, McAdam B, Morrison BW, Kapoor S, et al. Effects of specific inhibition of cyclooxygenase-2 on sodium balance, hemodynamics, and vasoactive eicosanoids. *J Pharmacol Exp Ther* 1999;289:735–741.
- Cattell V, Smith J, Cook HT. Prostaglandin E1 suppresses macrophage infiltration and ameliorates injury in an experimental model of macrophage-dependent glomerulonephritis. *Clin Exp Immunol* 1990;79:260–265.
- Chamaa NS, Mosig D, Drukker A, Guignard JP. The renal hemodynamic effects of ibuprofen in the newborn rabbit. *Pediatr Res* 2000;48:600–605.
- Cheeke PR, Amberg JW. Comparative calcium excretion by rats and rabbits. *J Anim Sci* 1973;37:450–454.
- Chen J, Zhao M, He W, Milne GL, et al. Increased dietary NaCl induces renal medullary PGE₂ production and natriuresis via the EP2 receptor. *Am J Physiol Renal Physiol* 2008;295:F818–F825.
- Cheng H, Wang S, Jo YI, Hao CM, et al. Overexpression of cyclooxygenase-2 predisposes to podocyte injury. *J Am Soc Nephrol* 2007;18:551–559.
- Cheng H, Fan X, Moeckel GW, Harris RC. Podocyte COX-2 exacerbates diabetic nephropathy by increasing podocyte (pro)renin receptor expression. *J Am Soc Nephrol* 2011;22:1240–1251.
- Cheng HF, Wang JL, Zhang MZ, Miyazaki Y, et al. Angiotensin II attenuates renal cortical cyclooxygenase-2 expression. *J Clin Invest* 1999;103:953–961.
- Cheng HF, Wang JL, Zhang MZ, Wang SW, et al. Genetic deletion of COX-2 prevents increased renin expression in response to ACE inhibition. *Am J Physiol Renal Physiol* 2001;280:F449–F456.
- Cheng X, Zhang H, Lee HL, Park JM. Cyclooxygenase-2 inhibitor preserves medullary aquaporin-2 expression and prevents polyuria after ureteral obstruction. *J Urol* 2004;172:2387–2390.
- Chonko AM. Urate secretion in isolated rabbit renal tubules. *Am J Physiol* 1980;239:F545–F551.
- Chou SY, Cai H, Pai D, Mansour M, et al. Regional expression of cyclooxygenase isoforms in the rat kidney in complete unilateral ureteral obstruction. *J Urol* 2003;170:1403–1408.
- Christensen EI, Verroust PJ. Megalin and cubilin, role in proximal tubule function and during development. *Pediatr Nephrol* 2002;17:993–999.
- Cihlar T, Lin DC, Pritchard JB, Fuller MD, et al. The antiviral nucleotide analogs cidofovir and adefovir are novel substrates for human and rat renal organic anion transporter 1. *Mol Pharmacol* 1999;56:570–580.

- Cirino M, Morton H, MacDonald C, Hadden J, et al. Thromboxane A2 and prostaglandin endoperoxide analogue effects on porcine renal blood flow. *Am J Physiol* 1990;258:F109–F114.
- Clark DW, Layton D, Shakir SA. Do some inhibitors of COX-2 increase the risk of thromboembolic events? Linking pharmacology with pharmacoepidemiology. *Drug Saf* 2004;27:427–456.
- Clive DM, Stoff JS. Renal syndromes associated with nonsteroidal antiinflammatory drugs. *N Engl J Med* 1984;310:563–572.
- Colletti AE, Vogl HW, Rahe T, Zambraski EJ. Effects of acetaminophen and ibuprofen on renal function in anesthetized normal and sodium-depleted dogs. *J Appl Physiol* 1999;86:592–597.
- Corvilain J, Abramo M, Bergans A. Some effects of human growth hormone on renal hemodynamics and on tubular phosphate transport in man. *J Clin Invest* 1962;41:1230–1235.
- Cox PG, Moons WM, Russel FG, van Ginneken CA. Renal disposition and effects of naproxen and its *l*-enantiomer in the isolated perfused rat kidney. *J Pharmacol Exp Ther* 1990;255:491–496.
- Cremades A, Vicente-Ortega V, Peñafiel R. Influence of murine renal sexual dimorphism on amiloride-induced hyperkalemia. *Nephron Physiol* 2003;95:57–66.
- Currie MG, Needleman P. Renal arachidonic acid metabolism. *Annu Rev Physiol* 1984;46:327–341.
- Deeley RG, Westlake C, Cole SP. Transmembrane transport of endo- and xenobiotics by mammalian ATP-binding cassette multidrug resistance proteins. *Physiol Rev* 2006;86:849–899.
- de Leeuw PW. Nonsteroidal anti-inflammatory drugs and hypertension. The risks in perspective. *Drugs* 1996;51:179–187.
- DeMaria AN, Weir MR. Coxibs—beyond the GI tract: renal and cardiovascular issues. *J Pain Symptom Manag* 2003;25:S41–S49.
- DeRupertis FR, Craven PA. Eicosanoids in the pathogenesis of the functional and structural alterations of the kidney in diabetes. *Am J Kidney Dis* 1993;22:727–735.
- Dilger K, Herrlinger C, Peters J, Seyberth HW, et al. Effects of celecoxib and diclofenac on blood pressure, renal function, and vasoactive prostanoids in young and elderly subjects. *J Clin Pharmacol* 2002;42:985–994.
- Dinchuk JE, Car BD, Focht RJ, Johnston JJ, et al. Renal abnormalities and an altered inflammatory response in mice lacking cyclooxygenase II. *Nature* 1995;378:406–409.
- Dixey JJ, Noormohamed FH, Lant AF, Brewerton DA. The effects of naproxen and sulindac on renal function and their interaction with hydrochlorothiazide and piretanide in man. *Br J Clin Pharmacol* 1987;23:55–63.
- Dresser MJ, Leabman MK, Giacomini KM. Transporters involved in the elimination of drugs in the kidney: organic anion transporters and organic cation transporters. *J Pharm Sci* 2001;90:397–421.
- Dressler GR. The cellular basis of kidney development. *Annu Rev Cell Dev Biol* 2006;22:509–529.
- Duggin GG. Mechanisms in the development of analgesic nephropathy. *Kidney Int* 1980;18:553–561.
- Dunn MJ, Simonson M, Davidson EW, Scharschmidt LA, et al. Nonsteroidal anti-inflammatory drugs and renal function. *J Clin Pharmacol* 1988;28:524–529.
- Edwards RM. Effects of prostaglandins on vasoconstrictor action in isolated renal arterioles. *Am J Physiol Renal Physiol* 1985;248:F779–F784.
- El-Achkar TM, Plotkin Z, Marcic B, Dagher PC. Sepsis induces an increase in thick ascending limb COX-2 that is TLR4 dependent. *Am J Physiol Renal Physiol* 2007;293:F1187–F1196.
- el-Galley RE, Keane TE. Embryology, anatomy, and surgical applications of the kidney and ureter. *Surg Clin North Am* 2000;80:381–401.
- Eriksson LO, Beermann B, Kallner M. Renal function and tubular transport effects of sulindac and naproxen in chronic heart failure. *Clin Pharmacol Ther* 1987;42:646–654.
- Eriksson LO, Sturfelt G, Thysell H, Wollheim FA. Effects of sulindac and naproxen on prostaglandin excretion in patients with impaired renal function and rheumatoid arthritis. *Am J Med* 1990;89:313–321.
- Evan AP Jr, Stoeckel JA, Loemker V, et al. Development of the intrarenal vascular system of the puppy kidney. *Anat Rec* 1979;194:187–199.
- Faerch M, Christensen JH, Rittig S, Johansson JO, et al. Diverse vasopressin V2 receptor functionality underlying partial congenital nephrogenic diabetes insipidus. *Am J Physiol Renal Physiol* 2009;297:F1518–F1525.
- Farquhar WB, Morgan AL, Zambraski EJ, Kenney WL. Effects of acetaminophen and ibuprofen on renal function in the stressed kidney. *J Appl Physiol* 1999;86:598–604.

- Fernandez-Tome M, Kraemer L, Federman SC, Favale N, et al. COX-2-mediated PGD2 synthesis regulates phosphatidylcholine biosynthesis in rat renal papillary tissue. *Biochem Pharmacol* 2004;15:245–254.
- Ferreri NR, An SJ, McGiff JC. Cyclooxygenase-2 expression and function in the medullary thick ascending limb. *Am J Physiol* 1999;277:F360–F368.
- Fisher JW, Koury S, Ducey T, Mendel S. Erythropoietin production by interstitial cells of hypoxic monkey kidneys. *Br J Haematol* 1996;95:27–32.
- Fleming EF, Athirakul K, Oliverio MI, Key M, et al. 1998. Urinary concentrating function in mice lacking EP3 receptors for prostaglandin E2. *Am J Physiol Renal Physiol* 1998;275:F955–F961.
- Fouser L, Avner ED. Normal and abnormal nephrogenesis. *Am J Kidney Dis* 1993;21:64–70.
- Fox J, Anderson LC, Loew FM, Quimby FW. *Laboratory Animal Medicine*, 2nd ed. San Diego, CA: Academic Press, 2002.
- Friis C. Postnatal development of the pig kidney: ultrastructure of the glomerulus and the proximal tubule. *J Anat* 1980;130:513–526.
- Frolich JC, Hollifield JW, Dormois JC, Frolich BL, et al. Suppression of plasma renin activity by indomethacin in man. *Cir Res* 1976;39:447–452.
- Fukasawa H, Bornheimer S, Kudlicka K, Farquhar MG. Slit diaphragms contain tight junction proteins. *J Am Soc Nephrol* 2009;20:1491–1503.
- Garella S, Matarese RA. Renal effects of prostaglandins and clinical adverse effects of nonsteroidal anti-inflammatory agents. *Medicine* 1984;63:165–181.
- Gasser B, Mauss Y, Ghnassia JP, et al. A quantitative study of normal nephrogenesis in the human fetus: its implication in the natural history of kidney changes due to low obstructive uropathies. *Fetal Diagn Ther* 1993;8:371–384.
- Gomez RA, Sequeira Lopez ML, Fernandez L, et al. The maturing kidney: development and susceptibility. *Renal Fail* 1999;21:283–291.
- Gong R, Morris DJ, Brem AS. Human renal 11beta-hydroxysteroid dehydrogenase 1 functions and co-localizes with COX-2. *Life Sci* 2008;82:631–637.
- González AA, Céspedes C, Villanueva S, Michea L, et al. E Prostanoid-1 receptor regulates renal medullary alphaENaC in rats infused with angiotensin II. *Biochem Biophys Res Commun* 2009;389:372–377.
- Gooch K, Culleton BF, Manns BJ, Zhang J, et al. NSAID use and progression of chronic kidney disease. *Am J Med* 2007;120:280, e1–e7.
- Gottschalk CW, Mylle M. Evidence that the mammalian nephron functions as a countercurrent multiplier system. *Science* 1958;128:594.
- Gross DM, Brookins J, Fink GD, Fisher JW. Effects of prostaglandins A2, E2 and F2 alpha on erythropoietin production. *J Pharmacol Exp Ther* 1976;198:489–496.
- Gross JM, Dwyer JE, Knox FG. Natriuretic response to increased pressure is preserved with COX-2 inhibitors. *Hypertension* 1999;34:1163–1167.
- Guan Y, Zhang Y, Breyer RM, Fowler B, et al. Prostaglandin E2 inhibits renal collecting duct Na⁺ absorption by activating the EP1 receptor. *J Clin Invest* 1998;102:194–201.
- Guan Y, Zhang Y, Wu J, Qi Z, et al. Antihypertensive effects of selective prostaglandin E2 receptor subtype 1 targeting. *J Clin Invest* 2007;117:2496–2505.
- Gwak HS, Oh JH, Han HK. Effects of non-steroidal anti-inflammatory drugs on the pharmacokinetics and elimination of acyclovir in rats. *J Pharm Pharmacol* 2005;57:393–398.
- Hallesy DW, Shott LD, Hill R. Comparative toxicology of naproxen. *Scand J Rheumatol Suppl* 1973;2:20–28.
- Hao CM, Breyer MD. Physiological regulation of prostaglandins in the kidney. *Annu Rev Physiol* 2008;70:357–377.
- Harding P, Sigmon DH, Alfie ME, Huang PL, et al. Cyclooxygenase-2 mediates increased renal renin content induced by low-sodium diet. *Hypertension* 1997;29:297–302.
- Harirforoosh S, Jamali F. Effect of nonsteroidal anti-inflammatory drugs with varying extent of COX-2–COX-1 selectivity on urinary sodium and potassium excretion in the rat. *Can J Physiol Pharmacol* 2005;83:85–90.

- Harris RC, Breyer MD. Physiological regulation of cyclooxygenase-2 in the kidney. *Am J Physiol Renal Physiol* 2001;281:F1–F11.
- Harris RC, McKanna JA, Akai Y, Jacobson HR, Dubois RN, Breyer MD. Cyclooxygenase-2 is associated with the macula densa of rat kidney and increases with salt restriction. *J Clin Invest* 1994;94:2504–2510.
- Hartleroad JY, Beharry KD, Hausman N, et al. Effect of maternal administration of selective cyclooxygenase (COX)-2 inhibitors on renal size, growth factors, proteinases, and COX-2 secretion in the fetal rabbit. *Biol Neonate* 2005;87:246–253.
- Hartner A, Goppelt-Struebe M, Hilgers KF. Coordinate expression of cyclooxygenase-2 and renin in the rat kidney in renovascular hypertension. *Hypertension* 1998;31:201–205.
- Hasan J, Beharry KD, Gharraee Z, Stavitsky Y, et al. Early postnatal ibuprofen and indomethacin effects in suckling and weanling rat kidneys. *Prostaglandins Other Lipid Mediat* 2008;85:81–88.
- Hasler U, Vinciguerra M, Vandewalle A, Martin PY, et al. Dual effects of hypertonicity on aquaporin-2 expression in cultured renal collecting duct principal cells. *J Am Soc Nephrol* 2005;16:1571–1582.
- Hassid A, Konieczkowski M, Dunn MJ. Prostaglandin synthesis in isolated rat kidney glomeruli. *Proc Natl Acad Sci USA* 1979;76:1155–1159.
- Hébert RL, Jacobson HR, Breyer MD. Prostaglandin E2 inhibits sodium transport in rabbit cortical collecting duct by increasing intracellular calcium. *J Clin Invest* 1991;87:1992–1998.
- Hébert RL, Jacobson HR, Fredin D, Breyer MD. Evidence that separate PGE2 receptors modulate water and sodium transport in rabbit cortical collecting duct. *Am J Physiol* 1993;265:F643–F650.
- Heise G, Grabensee B, Schrör K, Heering P. Different actions of the cyclooxygenase 2 selective inhibitor flosulide in rats with passive Heymann nephritis. *Nephron* 1998;80:220–226.
- Herman MB, Rajkhowa T, Cutuli F, Springate JE, et al. Regulation of renal proximal tubule Na,K-ATPase by prostaglandins. *Am J Physiol Renal Physiol* 2010 Feb 3.
- Hermann M, Shaw S, Kiss E, Camici G, et al. Selective COX-2 inhibitors and renal injury in salt-sensitive hypertension. *Hypertension* 2005;45:193–197.
- Hinchliffe SA, Lynch MR, Sargent PH, et al. The effect of intrauterine growth retardation on the development of renal nephrons. *Br J Obstet Gynaecol* 1992;99:296–301.
- Hoffmann KL, Wood AK, McCarthy PH. Ultrasonography of the equine neonatal kidney. *Equine Vet J* 2000;32:109–113.
- Holt S, Marley R, Fernando B, Harry D, et al. Acute cholestasis-induced renal failure: effects of antioxidants and ligands for the thromboxane A2 receptor. *Kidney Int* 1999;55:271–277.
- Hommel E, Mathiesen E, Larsen SA, Edsberg B, et al. Effects of indomethacin on kidney function in type 1 (insulin-dependent) diabetic patients with nephropathy. *Diabetologia* 1987;30:78–81.
- Horster M. Nephron function and perinatal homeostasis. *Ann Rech Vet* 1977;8:468–482.
- Horster MF, Braun GS, Huber SM. Embryonic renal epithelia: induction, nephrogenesis, and cell differentiation. *Physiol Rev* 1999;79:1157–1191.
- Hosoyamada M, Sekine T, Kanai Y, Endou H. Molecular cloning and functional expression of a multispecific organic anion transporter from human kidney. *Am J Physiol* 1999;276:F122–F128.
- Houston MC. Nonsteroidal anti-inflammatory drugs and antihypertensives. *Am J Med* 1991;90:42S–47S.
- Huerta C, Castellsague J, Varas-Lorenzo C, García Rodríguez LA. Nonsteroidal anti-inflammatory drugs and risk of ARF in the general population. *Am J Kidney Dis* 2005;45:531–539.
- Imig JD. Eicosanoids and renal vascular function in diseases. *Clin Sci* 2006;111:21–34.
- Ito S, Carretero OA, Abe K, Beierwaltes WH, et al. Effect of prostanoids on renin release from rabbit isolated afferent arterioles with and without attached macula densa. *Kidney Int* 1989;35:1138–1144.
- Izhar M, Alausa T, Folker A, Hung E, et al. Effects of COX inhibition on blood pressure and kidney function in ACE inhibitor-treated blacks and hispanics. *Hypertension* 2004;43:573–577.
- Jackson EK, Oates JA, Branch RA. Indomethacin decreases arterial blood pressure and plasma renin activity in rats with aortic ligation. *Circ Res* 1981;49:180–185.
- Jelkmann W. Erythropoietin: structure, control of production, and function. *Physiol Rev* 1992;72:449–489.
- Jensen BL, Mann B, Skott O, Kurtz A. Differential regulation of renal prostaglandin receptor mRNAs by dietary salt intake in the rat. *Kidney Int* 1999;56:528–537.

- Johnson AG, Nguyen TV, Day RO. Do nonsteroidal anti-inflammatory drugs affect blood pressure? A meta-analysis. *Ann Intern Med* 1994;121:289–300.
- Johnston HH, Herzog JP, Lauler DP. Effect of prostaglandin E1 on renal hemodynamics, sodium and water excretion. *Am J Physiol* 1967;213:939–946.
- Kaplan BS, Restaino I, Raval DS, Gottlieb RP, Bernstein J. Renal failure in the neonate associated with in utero exposure to non-steroidal anti-inflammatory agents. *Pediatr Nephrol* 1994;8:700–704.
- Kawada N, Dennehy K, Solis G, et al. TP receptors regulate renal hemodynamics during angiotensin II slow pressor response. *Am J Physiol Renal Physiol* 2004;287:F753–F759.
- Kawada N, Solis G, Ivey N, et al. Cyclooxygenase-1-deficient mice have high sleep-to-wake blood pressure ratios and renal vasoconstriction. *Hypertension* 2005;45:1131–1138.
- Kelley VE, Winkelstein A, Izui S, Dixon FJ. Prostaglandin E1 inhibits T-cell proliferation and renal disease in MRL/l mice. *Clin Immunol Immunopathol* 1981;21:190–203.
- Kennedy CR, Xiong H, Rahal S, Vanderluit J, et al. Urine concentrating defect in prostaglandin EP1-deficient mice. *Am J Physiol Renal Physiol* 2007;292:F868–F875.
- Kent AL, Maxwell LE, Koina ME, Falk MC, et al. Renal glomeruli and tubular injury following indomethacin, ibuprofen, and gentamicin exposure in a neonatal rat model. *Pediatr Res* 2007;62:307–312.
- Kent AL, Douglas-Denton R, Shadbolt B, Dahlstrom JE, et al. Indomethacin, ibuprofen and gentamicin administered during late stages of glomerulogenesis do not reduce glomerular number at 14 days of age in the neonatal rat. *Pediatr Nephrol* 2009;24:1143–1149.
- Khan KN, Venturini CM, Bunch RT, et al. Interspecies differences in renal localization of cyclooxygenase isoforms: implications in nonsteroidal antiinflammatory drug-related nephrotoxicity. *Toxicol Pathol* 1998;26:612–620.
- Khan KN, Stanfield KM, Trajkovic D, Knapp DW. Expression of cyclooxygenase-2 in canine renal cell carcinoma. *Vet Pathol* 2001a;38:116–119.
- Khan KN, Stanfield KM, Dannenberg A, Seshan SV, et al. Cyclooxygenase-2 expression in the developing human kidney. *Pediatr Dev Pathol* 2001b;4:461–466.
- Khan N, Hard G, Radi Z. Chapter 11: New horizons in toxicity prediction: a comprehensive overview of the current status and application of predictive toxicology. In: *In Vivo Approaches: Renal Toxicity*. San Diego, CA: Academic Press, 2011.
- Khan NK, Alden CL, Chapter 29: Kidney. In: Haschek WM, Rousseaux CG (eds), *Handbook of Toxicologic Pathology*, 2nd ed. San Diego, CA: Academic Press, 2002.
- Kim SM, Chen L, Mizel D, Huang YG, et al. Low plasma renin and reduced renin secretory responses to acute stimuli in conscious COX-2-deficient mice. *Am J Physiol Renal Physiol* 2007;292:F415–F422.
- Kleinman LI, Reuter JH. Maturation of glomerular blood flow distribution in the new-born dog. *J Physiol* 1973;228:91–103.
- Knight S, Johns EJ. Renal functional responses to ischaemia-reperfusion injury in normotensive and hypertensive rats following non-selective and selective cyclooxygenase inhibition with nitric oxide donation. *Clin Exp Pharmacol Physiol* 2008;35:11–16.
- Komers R, Lindsley JN, Oyama TT, et al. Immunohistochemical and functional correlations of renal cyclooxygenase-2 in experimental diabetes. *J Clin Invest* 2001;107:889–898.
- Komhoff M, Grone HJ, Klein T, Seyberth HW, et al. Localization of cyclooxygenase-1 and -2 in adult and fetal human kidney: implication for renal function. *Am J Physiol* 1997;272:460–468.
- Komhoff M, Jeck ND, Seyberth HW, et al. Cyclooxygenase-2 expression is associated with the renal macula densa of patients with Bartter-like syndrome. *Kidney Int* 2000;58:2420–2424.
- Kommareddy M, McAllister RM, Ganjam VK, Turk JR, et al. Upregulation of cyclooxygenase-2 expression in porcine macula densa with chronic nitric oxide synthase inhibition. *Vet Pathol* 2011; 1125–1133.
- Kong WX, Ma J, Gu Y, Yang HC, Zuo YQ, Lin SY. Renal protective effects of specific cyclooxygenase-2 inhibitor in rats with subtotal renal ablation. *Zhonghua Nei Ke Za Zhi* 2003;42:186–190.
- Kotnik P, Nielsen J, Kwon TH, Krzysnik C, et al. Altered expression of COX-1, COX-2, and mPGES in rats with nephrogenic and central diabetes insipidus. *Am J Physiol Renal Physiol* 2005;288:F1053–F1068.
- Kreisberg JI, Karnovsky MJ, Levine L. Prostaglandin production by homogeneous cultures of rat glomerular epithelial and mesangial cells. *Kidney Int* 1982;22:355–359.

- Lasaitiene D, Chen Y, Guron G, Marcussen N, et al. Perturbed medullary tubulogenesis in neonatal rat exposed to renin-angiotensin system inhibition. *Nephrol Dial Transplant* 2003;18:2534–2541.
- Lauridsen TG, Vase H, Starklint J, Graffe CC, et al. Increased renal sodium absorption by inhibition of prostaglandin synthesis during fasting in healthy man: a possible role of the epithelial sodium channels. *BMC Nephrol* 2010;11:28.
- Lebel M, Grose JH. Renal eicosanoids and renal hemodynamics in early borderline hypertension. *Clin Invest Med* 1991;14:525–534.
- Lee DW, Kwak IS, Lee SB, Song SH, et al. Effects of celecoxib and nordihydroguaiaretic acid on puromycin aminonucleoside-induced nephrosis in the rat. *J Korean Med Sci* 2009;24 Suppl:S183–S188.
- Lee JB, Crowshaw K, Takman BH, Attrep KA. The identification of prostaglandins E(2), F(2alpha) and A(2) from rabbit kidney medulla. *Biochem J* 1967;105:1251–1260.
- Lierz M. Avian renal disease: pathogenesis, diagnosis, and therapy. *Vet Clin North Am Exot Anim Pract* 2003;6:29–55.
- Liew D, Krum H. The role of aldosterone receptor blockade in the management of cardiovascular disease. *Curr Opin Invest Drugs* 2002;3:1468–1473.
- Linz W, Wiemer G, Gohlke P, Unger T, et al. Contribution of kinins to the cardiovascular actions of angiotensin-converting enzyme inhibitors. *Pharmacol Rev* 1995;47:25–24.
- Lopez-Ovejero JA, Weber MA, Drayer JJ, Sealey JE, et al. Effects of indomethacin alone and during diuretic or beta-adrenergic blockade therapy on blood pressure and the renin system in essential hypertension. *Clin Sci Mol Med* 1978;55:203S–205S.
- Lumbers ER. Functions of the renin-angiotensin system during development. *Clin Exp Pharmacol Physiol* 1995;22:499–505.
- MacDonald MS, Emery JL. The late intrauterine and postnatal development of human renal glomeruli. *J Anat* 1959;93:331–340.
- Makino H, Tanaka I, Mukoyama M, et al. Prevention of diabetic nephropathy in rats by prostaglandin E receptor EP1-selective antagonist. *J Am Soc Nephrol* 2002;13:1757–1765.
- Manohar M, Goetz TE, Griffin R, Sullivan E. Pulmonary vascular pressures of strenuously exercising thoroughbreds after administration of phenylbutazone. *Am J Vet Res* 1996;57:1354–1358.
- Matlhagela K, Taub M. Involvement of EP1 and EP2 receptors in the regulation of the Na,K-ATPase by prostaglandins in MDCK cells. *Prostaglandins Other Lipid Mediat* 2006;79:101–113.
- Meade EA, Smith WL, DeWitt DL. Differential inhibition of prostaglandin endoperoxide synthase (cyclooxygenase) isozymes by aspirin and other non-steroidal anti-inflammatory drugs. *J Biol Chem* 1993;268:6610–6614.
- Mené P. Physiology and pathophysiology of the mesangial cell. *Nefrologia* 1996;XVIsupl 3.
- Mené P, Dunn MJ. Eicosanoids and control of mesangial cell contraction. *Circ Res* 1988;62:916–925.
- Meskill M, Eitarh R. Immunohistochemical localisation of renal cyclooxygenase-1 expression in non-steroidal anti-inflammatory drug-treated mice. *Exp Toxicol Pathol* 2011;63:39–42.
- Meteyer CU, Rideout BA, Gilbert M, Shivaprasad HL, et al. Pathology and proposed pathophysiology of diclofenac poisoning in free-living and experimentally exposed oriental white-backed vultures (*Gyps bengalensis*). *J Wildl Dis* 2005;41:707–716.
- Moore L, Williams R, Staples A. Glomerular dimensions in children under 16 years of age. *J Pathol* 1993;171:145–150.
- Morath R, Klein T, Seyberth HW, Nüsing RM. Immunolocalization of the four prostaglandin E2 receptor proteins EP1, EP2, EP3, and EP4 in human kidney. *J Am Soc Nephrol* 1999;10:1851–1860.
- Morello JP, Bichet DG. Nephrogenic diabetes insipidus. *Annu Rev Physiol* 2001;63:607–630.
- Morham SG, Langenbach R, Loftin CD, et al. Prostaglandin synthase 2 gene disruption causes severe renal pathology in the mouse. *Cell* 1995;83:473–482.
- Mulato AS, Ho ES, Cihlar T. Nonsteroidal anti-inflammatory drugs efficiently reduce the transport and cytotoxicity of adefovir mediated by the human renal organic anion transporter 1. *J Pharmacol Exp Ther* 2000;295:10–15.
- Murakami M, Nakatani Y, Tanioka T, Kudo I. Prostaglandin E synthase. *Prostaglandins Other Lipid Mediat* 2002;68–69:383–399.
- Murata T, Ushikubi F, Matsuoka T, et al. Altered pain perception and inflammatory response in mice lacking prostacyclin receptor. *Nature* 1997;388:678–682.

- Murray MD, Brater DC, Tierney WM, Hui SL, et al. Ibuprofen-associated renal impairment in a large general internal medicine practice. *Am J Med Sci* 1990;299:222–229.
- Muscara MN, Vergnolle N, Lovren F, Triggle CR, et al. Selective cyclo-oxygenase-2 inhibition with celecoxib elevates blood pressure and promotes leukocyte adherence. *Br J Pharmacol* 2000a;129:1423–1430.
- Muscara MN, McKnight W, Lovren F, Triggle CR, et al. Antihypertensive properties of a nitric oxide-releasing naproxen derivative in two-kidney, one-clip rats. *Am J Physiol* 2000b;279:H528–H535.
- Mutoh K, Watanabe S, Wakuri H. Histochemical study on the gland of pelvis renalis in the horse. *Kitasato Arch Exp Med* 1992;65:117–122.
- Nagai J, Taogoshi T, Tokunaga A, Nishikawa H, et al. Characterization of prostaglandin E1 transport in rat renal brush-border membrane. *Drug Metab Pharmacokinet* 2006;21:186–193.
- Nagao T, Nagamatsu T, Suzuki Y. Effect of DP-1904, a thromboxane A2 synthase inhibitor, on passive Heymann nephritis in rats. *Eur J Pharmacol* 1996;316:73–80.
- Nagao T, Koseki J, Suzuki Y, Nagamatsu T. Thromboxane A₂ causes retarded clearance of aggregated protein in glomeruli of nephritic mice. *Eur J Pharmacol* 2001;413:271–279.
- Nantel F, Meadows E, Denis D, Connolly B, et al. Immunolocalization of cyclooxygenase-2 in the macula densa of human elderly. *FEBS Lett* 1999;457:475–477.
- Naruse K, Fujieda M, Miyazaki E, Hayashi Y, et al. An immunohistochemical study of developing glomeruli in human fetal kidneys. *Kidney Int* 2000;57:1836–1846.
- Neuhofer W, Holzapfel K, Fraek ML, Ouyang N, et al. Chronic COX-2 inhibition reduces medullary HSP70 expression and induces papillary apoptosis in dehydrated rats. *Kidney Int* 2004;65:431–441.
- Nielsen S, Chou CL, Marples D, Christensen EI, et al. Vasopressin increases water permeability of kidney collecting duct by inducing translocation of aquaporin-CD water channels to plasma membrane. *Proc Natl Acad Sci USA* 1995;90:11663–11667.
- Nøregaard R, Jensen BL, Topcu SO, Wang G, et al. Urinary tract obstruction induces transient accumulation of COX-2-derived prostanoids in kidney tissue. *Am J Physiol Regul Integr Comp Physiol* 2010;298:R1017–R1025.
- Norwood VF, Morham SG, Smithies O. Postnatal development and progression of renal dysplasia in cyclooxygenase-2 null mice. *Kidney Int* 2000;58:2291–2300.
- Novy MJ. Effects of indomethacin on labor, fetal oxygenation, and fetal development in rhesus monkeys. *Adv Prostaglandin Thromboxane Res* 1978;4:285–300.
- Ogawa M, Hirawa N, Tsuchida T, et al. Urinary excretions of lipocalin-type prostaglandin D2 synthase predict the development of proteinuria and renal injury in OLETF rats. *Nephrol Dial Transplant* 2006;21:924–934.
- Ogawa T, Tomomasa T, Hikima A, Kobayashi Y, et al. Developmental changes in cyclooxygenase mRNA expression in the kidney of rats. *Pediatr Nephrol* 2001;16:618–622.
- Ogawa T, Tomomasa T, Morikawa A. Developmental changes in cyclo-oxygenase mRNA induction by hypoxia in rat kidney. *Pediatr Int* 2002;44:675–679.
- Ohta KY, Imamura Y, Okudaira N, Atsumi R, Inoue K, Yuasa H. Functional characterization of multidrug and toxin extrusion protein 1 as a facilitative transporter for fluoroquinolones. *J Pharmacol Exp Ther* 2009;328:628–634.
- Okumura T, Hayashi I, Ikezawa T, et al. Cyclooxygenase-2 inhibitors attenuate increased blood pressure in renovascular hypertensive models, but not in deoxycorticosterone-salt hypertension. *Hypertension Res* 2002;25:927–938.
- Okumura M, Imanishi M, Okamura M, et al. Role for thromboxane A2 from glomerular thrombi in nephropathy with type 2 diabetic rats. *Life Sci* 2003;72:2695–2705.
- Omote H, Hiasa M, Matsumoto T, Otsuka M, Moriyama Y. The MATE proteins as fundamental transporters of metabolic and xenobiotic organic cations. *Trends Pharmacol Sci* 2006;27:587–593.
- Opay AL, Mouton CR, Mullins JJ, Mitchell KD. Cyclooxygenase-2 inhibition normalizes arterial blood pressure in CYP1A1-REN2 transgenic rats with inducible ANG II-dependent malignant hypertension. *Am J Physiol Renal Physiol* 2006;29:F612–F618.
- Ortiz PA. cAMP increases surface expression of NKCC2 in rat thick ascending limbs: role of VAMP. *Am J Physiol* 2006;290:F608–F616.

- Ozer MK, Asci H, Oncu M, Calapoglu M, et al. Effects of misoprostol on cisplatin-induced renal damage in rats. *Food Chem Toxicol* 2011;49:1556–1559.
- Pai HC. Dissection of nephrons from the human kidney. *J Anat* 1935;69(Pt 3): 344–349.
- Parfentjev IA, Perlzweig WA. The composition of the urine of white mice. *J Biol Chem* 1933;100: 551–555.
- Passmore AP, Copeland S, Johnston GD. The effects of ibuprofen and indomethacin on renal function in the presence and absence of frusemide in healthy volunteers on a restricted sodium diet. *Br J Clin Pharmacol* 1990;29:311–319.
- Pattaragarn A, Alon US. Treatment of congenital nephrogenic diabetes insipidus by hydrochlorothiazide and cyclooxygenase-2 inhibitor. *Pediatr Nephrol* 2003;18:1073–1076.
- Paulose-Ram R, Hirsch R, Dillon C, Losonczy K, et al. Prescription and non-prescription analgesic use among the US adult population: results from the third National Health and Nutrition Examination Survey (NHANES III). *Pharmacoepidemiol Drug Saf* 2003;12:315–326.
- Pavenstädt H, Kriz W, Kretzler M. Cell biology of the glomerular podocyte. *Physiol Rev* 2003;83:253–307.
- Perazella MA. Drug-induced hyperkalemia: old culprits and new offenders. *Am J Med* 2000;109: 307–314.
- Perez G, McGuckin J. Cellular localiation of prostaglandin A2 in the rat kidney. *Prostaglandins* 1972;2:393–398.
- Persson AE, Salomonsson M, Westerlund P, Greger R, et al. Macula densa cell function. *Kidney Int Suppl* 1991;32:S39–S44.
- Peti-Peterdi J, Komlosi P, Fuson AL, et al. 2003. Luminal NaCl delivery regulates basolateral PGE2 release from macula densa cells. *J Clin Invest* 2003;112:76–82.
- Pfeiffer EW. Comparative anatomical observations of the mammalian renal pelvis and medulla. *J Anat* 1968;102:321–331.
- Plantinga L, Grubbs V, Sarkar U, Hsu CY, et al. Nonsteroidal anti-inflammatory drug use among persons with chronic kidney disease in the United States. *Ann Fam Med* 2011;9:423–430.
- Quilley J, Santos M, Pedraza P. Renal protective effect of chronic inhibition of COX-2 with SC-58236 in streptozotocin-diabetic rats. *Am J Physiol Heart Circ Physiol* 2011;300:H2316–H2322.
- Radi ZA. Pathophysiology of cyclooxygenase inhibition in animal models. *Toxicol Pathol* 2009;37:34–46.
- Radi ZA, Ostroski R. Pulmonary and cardiorenal cyclooxygenase-1 (COX-1), -2 (COX-2), and microsomal prostaglandin E synthase-1 (mPGES-1) and -2 (mPGES-2) expression in a hypertension model. *Mediators Inflamm* 2007;2007:85091.
- Ragolia L, Palaia T, Hall CE, et al. Accelerated glucose intolerance, nephropathy, and atherosclerosis in prostaglandin D2 synthase knock-out mice. *J Biol Chem* 2005;280:29946–29955.
- Rao PS, Cavanagh D, Dietz JR, Marsden KA, et al. Dose-dependent effects of prostaglandin D2 on hemodynamics, renal function and blood gas analyses. *Am J Obstet Gynecol* 1987;156:843–851.
- Reddy LR, Corey EJ. Facile air oxidation of the conjugate base of rofecoxib (Vioxx), a possible contributor to human toxicity. *Tetrahedron Lett* 2005;46:927–929.
- Richter CM, Godes M, Wagner C, Maser-Gluth C, et al. Chronic cyclooxygenase-2 inhibition does not alter blood pressure and kidney function in renovascular hypertensive rats. *J Hypertens* 2004;22:191–198.
- Rink JC, Vu HT, Sánchez Alvarado A. The maintenance and regeneration of the planarian excretory system are regulated by EGFR signaling. *Development* 2011;138:3769–3780.
- Robertson JL. Chemically induced glomerular injury: a review of basic mechanisms and specific xenobiotics. *Toxicol Pathol* 1998;26:64–72.
- Roch-Ramel F. Renal excretion of uric acid in mammals. *Clin Nephrol* 1979;12:1–6.
- Roch-Ramel F, White F, Vowles L, Simmonds HA, et al. Micropuncture study of tubular transport of urate and PAH in the pig kidney. *Am J Physiol* 1980;239:F107–F112.
- Rodríguez F, Llinas MT, Gonzalez JD, Rivera J, et al. Renal changes induced by a cyclooxygenase-2 inhibitor during normal and low sodium intake. *Hypertension* 2000;36:276–281.
- Rodríguez JA, Vio CP, Pedraza PL, McGiff JC, et al. Bradykinin regulates cyclooxygenase-2 in rat renal thick ascending limb cells. *Hypertension* 2004;44:230–235.
- Romagnani P. Parietal epithelial cells: their role in health and disease. *Contrib Nephrol* 2011;169:23–36.

- Rossat J, Maillard M, Nussberger J, Brunner HR, et al. Renal effects of selective cyclooxygenase-2 inhibition in normotensive salt-depleted subjects. *Clin Pharmacol Ther* 1999;66:76–84.
- Rossett J. Drug-induced acute interstitial nephritis. *Kidney Int* 2001;60:804–187.
- Rutkai I, Feher A, Erdei N, Henrion D, et al. Activation of prostaglandin E2 EP1 receptor increases arteriolar tone and blood pressure in mice with type 2 diabetes. *Cardiovasc Res* 2009;83:148–154.
- Sáez F, Reverte V, Salazar F, et al. Hypertension and sex differences in the age-related renal changes when cyclooxygenase-2 activity is reduced during nephrogenesis. *Hypertension* 2009;53:331–337.
- Sahloul MZ, al-Kiek R, Ivanovich P, Mujais SK. Nonsteroidal anti-inflammatory drugs and antihypertensives. Cooperative malfeasance. *Nephron* 1990;56:345–352.
- Schlondorff D. Renal complications of nonsteroidal anti-inflammatory drugs. *Kidney Int* 1993;44:643–653.
- Schneider A, Harendza S, Zahner G, Jocks T, et al. Cyclooxygenase metabolites mediate glomerular monocyte chemoattractant protein-1 formation and monocyte recruitment in experimental glomerulonephritis. *Kidney Int* 1999;55:430–441.
- Schneider A, Zhang Y, Zhang M, et al. Membrane-associated PGE synthase-1 (mPGES-1) is coexpressed with both COX-1 and COX-2 in the kidney. *Kidney Int* 2004;65:1205–1213.
- Schnermann J. Cyclooxygenase-2 and macula densa control of renin secretion. *Nephrol Dial Transplant* 2001;17:35–1738.
- Schölkens BA. Antihypertensive effect of prostacyclin (PGI₂) in experimental hypertension and its influence on plasma renin activity in rats. *Prostaglandins Med* 1978;1:359–372.
- Sebeková K, Ramuscak A, Boor P, Heidland A, et al. The selective TP receptor antagonist, S18886 (terutroban), attenuates renal damage in the double transgenic rat model of hypertension. *Am J Nephrol* 2008;28:47–53.
- Sellers RS, Senese PB, Khan KN. Interspecies differences in the nephrotoxic response to cyclooxygenase inhibition. *Drug Chem Toxicol* 2004;27:111–122.
- Seta F, Chung AD, Turner PV, Mewburn JD, et al. Renal and cardiovascular characterization of COX-2 knockdown mice. *Am J Physiol Regul Integr Comp Physiol* 2009;296:R1751–R1760.
- Singer I, Rotenberg D, Puschet JB. Lithium-induced nephrogenic diabetes insipidus: in vivo and in vitro studies. *J Clin Invest* 1972;51:1081–1091.
- Skov K, Nyengaard JR, Korsgaard N, et al. Number and size of renal glomeruli in spontaneously hypertensive rats. *J Hypertens* 1994;12:1373–1376.
- Smeets B, Angelotti ML, Rizzo P, et al. Renal progenitor cells contribute to hyperplastic lesions of podocytopathies and crescentic glomerulonephritis. *J Am Soc Nephrol* 2009;20:2593–2603.
- Smith WL, Bell TG. Immunohistochemical localization of the prostaglandin-forming cyclooxygenase in renal cortex. *Am J Physiol Renal Physiol* 1978;235:F451–F457.
- Solomon S. Developmental changes in nephron number, proximal tubular length and superficial nephron glomerular filtration rate of rats. *J Physiol* 1977;272:573–589.
- Speziale MV, Allen RG, Henderson CR, Barrington KJ, et al. Effects of ibuprofen and indomethacin on the regional circulation in newborn piglets. *Biol Neonate* 1999;76:242–252.
- Sraer JD, Adida C, Peraldi MN, Rondeau E, et al. Species-specific properties of the glomerular mesangium. *J Am Soc Nephrol* 1993;3:1342–1350.
- Stanfield KM, Bell RR, Lisowski AR, English ML, et al. Expression of cyclooxygenase-2 in embryonic and fetal tissues during organogenesis and late pregnancy. *Birth Defects Res A Clin Mol Teratol* 2003;67:54–58.
- Stock JL, Shinjo K, Burkhardt J, Roach M, et al. The prostaglandin E2 EP1 receptor mediates pain perception and regulates blood pressure. *J Clin Invest* 2001;107:325–331.
- Stokes JB, Kokko JP. Inhibition of sodium transport by prostaglandin E2 across the isolated, perfused rabbit collecting tubule. *J Clin Invest* 1977;59:1099–1104.
- Suganami T, Mori K, Tanaka I, et al. Role of prostaglandin E receptor EP1 subtype in the development of renal injury in genetically hypertensive rats. *Hypertension* 2003;42:1183–1190.
- Sugimoto Y, Namba T, Shigemoto R, Negishi M, et al. Distinct cellular localization of mRNAs for three subtypes of prostaglandin E receptor in kidney. *Am J Physiol* 1994;266(Renal Fluid Electrolyte Physiol 35):F823–F828.
- Sun D, Liu CX, Ma YY, Zhang L. Protective effect of prostaglandin E1 on renal microvascular injury in rats of acute aristolochic acid nephropathy. *Renal Fail* 2011;33:225–232.

- Svensden KB, Bech JN, Sørensen TB, Pedersen EB. A comparison of the effects of etodolac and ibuprofen on renal haemodynamics, tubular function, renin, vasopressin and urinary excretion of albumin and alpha-glutathione-S-transferase in healthy subjects: a placebo-controlled cross-over study. *Eur J Clin Pharmacol* 2000;56:383–388.
- Swan SK, Rudy DW, Lasseter KC, Ryan CF, et al. Effect of cyclooxygenase-2 inhibition on renal function in elderly persons receiving a low-salt diet: a randomized, controlled trial. *Ann Intern Med* 2000;133:1–9.
- Syal A, Schiavi S, Chakravarty S, Dwarakanath V, et al. Fibroblast growth factor-23 increases mouse PGE2 production in vivo and in vitro. *Am J Physiol Renal Physiol* 2006;290:F450–F455.
- Szabó AJ, Muller V, Chen GF, et al. Nephron number determines susceptibility to renal mass reduction-induced CKD in Lewis and Fisher 344 rats: implications for development of experimentally induced chronic allograft nephropathy. *Nephrol Dial Transplant* 2008;23:2492–2495.
- Tacconelli S, Capone ML, Patrignani P. Clinical pharmacology of novel selective COX-2 inhibitors. *Curr Pharm Des* 2004;10:589–601.
- Takahashi N, Takeuchi K, Abe T, et al. Immunolocalization of rat thromboxane receptor in the kidney. *Endocrinology* 1996;137:5170–5173.
- Takami H, Naramoto A, Shigematsu H, Ohno S. Ultrastructure of glomerular basement membrane by quick-freeze and deep-etch methods. *Kidney Int* 1991;3, 9: 659–664.
- Takeda T. Podocyte cytoskeleton is connected to the integral membrane protein podocalyxin through Na⁺/H⁺-exchanger regulatory factor 2 and ezrin. *Clin Exp Nephrol* 2003;7:260–269.
- Tamma G, Wiesner B, Furkert J, Hahm D, et al. The prostaglandin E2 analog sulprostone antagonizes vasopressin-induced antidiuresis through activation of Rho. *J Cell Sci* 2003;116:3285–3294.
- Tan SY, Shapiro R, Franco R, Stockard H, et al. Indomethacin-induced prostaglandin inhibition with hyperkalemia. *Ann Intern Med* 1979;90:783–785.
- Theilig F, Debiec H, Nafz B, Ronco P, et al. Renal cortical regulation of COX-1 and functionally related products in early renovascular hypertension (rat). *Am J Physiol Renal Physiol* 2006;291:F987–F994.
- Timpl, R. Recent advances in the biochemistry of glomerular basement membrane. *Kidney Int* 1986;30:293–298.
- Tomasoni S, Noris M, Zappella S, Gotti E, et al. Upregulation of renal and systemic cyclooxygenase-2 in patients with active lupus nephritis. *J Am Soc Nephrol* 1998;9:1202–1212.
- Tomida T, Numaguchi Y, Matsui H, et al. Altered expression of prostacyclin synthase in a subset of the thick ascending limb cells and mesangial cells in 5/6- nephrectomized rats. *Hypertens Res Clin Exp* 2001;24:411–419.
- Tomida T, Numaguchi Y, Nishimoto Y, Tsuzuki M, et al. Inhibition of COX-2 prevents hypertension and proteinuria associated with a decrease of 8-iso-PGF2alpha formation in L-NAME-treated rats. *J Hypertens* 2003;21:601–609.
- Torsello G, Schrör K, Szabó Z, Kutkuhn B, et al. Effects of prostaglandin E1 (PGE1) on experimental renal ischaemia. *Eur J Vasc Surg* 1989;3:5–13.
- Tsugawa K, Hashizume M, Migou S, Kishihara F, et al. A selective cyclo-oxygenase-2 inhibitor, NS-398, may improve portal hypertension without inducing gastric mucosal injury. *J Gastroenterol Hepatol* 1999;14:642–651.
- Uehara Y, Makino H, Seiki K, Urade Y L-PGDS Clinical Research Group of Kidney. Urinary excretions of lipocalin-type prostaglandin D synthase predict renal injury in type-2 diabetes: a cross-sectional and prospective multicentre study. *Nephrol Dial Transplant* 2009;24:475–482.
- Ullrich KJ. Renal transporters for organic anions and organic cations. Structural requirements for substrates. *J Membr Biol* 1997;158:95–107.
- Upton RA, Buskin JN, Williams RL, Holford NH, et al. Negligible excretion of unchanged ketoprofen, naproxen, and probenecid in urine. *J Pharm Sci* 1980;69:1254–1257.
- Uberti M, Dechaux M, Guillot M, Seligmann R, et al. Renal prostaglandin E₂ in nephrogenic diabetes insipidus: effects of inhibition of prostaglandin synthesis by indomethacin. *J Pediatr* 1980;97:476–478.
- van der Heijden AJ, Provoost AP, Nauta J, Grose W, et al. Renal functional impairment in preterm neonates related to intrauterine indomethacin exposure. *Pediatr Res* 1988;24:644–648.
- van der Heijden BJ, Carlus C, Narcy F, et al. Persistent anuria, neonatal death, and renal microcystic lesions after prenatal exposure to indomethacin. *Am J Obstet Gynecol* 1994;171:617–623.

- Vanecková I, Skaroupková P, Dvorák P, Certíková Chábová V, et al. Effects of sodium restriction and cyclooxygenase-2 inhibition on the course of hypertension, proteinuria and cardiac hypertrophy in Ren-2 transgenic rats. *Physiol Res* 2005;54:17–24.
- Vermillion ST, Newman RB. Recent indomethacin tocolysis is not associated with neonatal complications in preterm infants. *Am J Obstet Gynecol* 1999;181:1083–1086.
- Veron D, Reidy KJ, Bertuccio C, Teichman J, et al. Overexpression of VEGF-A in podocytes of adult mice causes glomerular disease. *Kidney Int* 2010;77:989–999.
- Vieux R, Desandes R, Boubred F, Semama D, et al. Ibuprofen in very preterm infants impairs renal function for the first month of life. *Pediatr Nephrol* 2010;25:267–274.
- Villa E, Garcia-Robles R, Haas J, Romero JC. Comparative effect of PGE2 and PGI2 on renal function. *Hypertension* 1997;30:664–666.
- Villar D, Buck WB, Gonzalez JM. Ibuprofen, aspirin and acetaminophen toxicosis and treatment in dogs and cats. *Vet Hum Toxicol* 1998;40:156–162.
- Vitzthum H, Abt I, Einhellig S, Kurtz A. Gene expression of prostanoid forming enzymes along the rat nephron. *Kidney Int* 2002;62:1570–1581.
- Vukicevic S, Simic P, Borovecki F, et al. Role of EP2 and EP4 receptor-selective agonists of prostaglandin E₂ in acute and chronic kidney failure. *Kidney Int* 2006;70:1099–1106.
- Walker AM, Oliver J. Methods for the collection of fluid from single glomeruli and tubules of the mammalian kidney. *Am J Physiol* 1941;134:562–579.
- Walker LA, Whorton AR, Smigel M, France R, et al. Antidiuretic hormone renal increases prostaglandin synthesis in vivo. *Am J Physiol* 1978;235:F180–F185.
- Wang JL, Cheng HF, Zhang MZ, McKanna JA, Harris RC. Selective increase of cyclooxygenase-2 expression in a model of renal ablation. *Am J Physiol* 1998;275:F613–F622.
- Wang JL, Cheng HF, Harris RC. Cyclooxygenase-2 inhibition decreases renin content and lowers blood pressure in a model of renovascular hypertension. *Hypertension* 1999;34:96–101.
- Wang JL, Cheng HF, Shappell S, Harris RC. A selective cyclooxygenase-2 inhibitor decreases proteinuria and retards progressive renal injury in rats. *Kidney Int* 2000;57:2334–2342.
- Wang W, Zolty E, Falk S, Summer S, et al. Prostacyclin in endotoxemia-induced acute kidney injury: cyclooxygenase inhibition and renal prostacyclin synthase transgenic mice. *Am J Physiol Renal Physiol* 2007;293:F1131–F1136.
- Warden DH, Stokes JB. EGF and PGE2 inhibit rabbit CCD Na⁺ transport by different mechanisms: PGE2 inhibits Na⁺ – K⁺ pump. *Am J Physiol* 1993;264:F670–F677.
- Watson JF. Potassium reabsorption in the proximal tubule of the dog nephron. *J Clin Invest* 1966;45:1341–1348.
- Wen SF. Nephrotoxicities of nonsteroidal anti-inflammatory drugs. *J Formos Med Assoc* 1997;96:157–171.
- Whelton A. Nephrotoxicity of nonsteroidal anti-inflammatory drugs: physiologic foundations and clinical implications. *Am J Med* 1999;106:13S–24S.
- Whelton A, Hamilton CW. Nonsteroidal anti-inflammatory drugs: effects on kidney function. *J Clin Pharmacol* 1991;31:588–598.
- White WB, Faich G, Whelton A, Maurath C, et al. Comparison of thromboembolic events in patients treated with celecoxib, a cyclooxygenase-2 specific inhibitor, versus ibuprofen or diclofenac. *Am J Cardiol* 2002;89:425–430.
- Whorton AR, Smigel M, Oates JA, Frölich JC. Regional differences in prostacyclin formation by the kidney: Prostacyclin is a major prostaglandin of renal cortex. *Biochim Biophys Acta* 1978;529:176–180.
- Wicks LE. Sex and proteinuria I mice. *Proc Soc Exp Biol Med* 1941;48:395–400.
- Wiseman EH, Reinert H. Anti-inflammatory drugs and renal papillary necrosis. *Agents Actions* 1975;5:322–325.
- Xu S, Jiang B, Maitland KA, et al. The thromboxane receptor antagonist S18886 attenuates renal oxidant stress and proteinuria in diabetic apolipoprotein E-deficient mice. *Diabetes* 2006;55:110–119.
- Yamanari H, Nakamura K, Kakishita M, Ohe T. Effects of cyclooxygenase inhibition on endothelial function in hypertensive patients treated with angiotensin-converting enzyme inhibitors. *Clin Cardiol* 2004;27:523–527.

- Yang C, Sorokin A. Upregulation of fibronectin expression by COX-2 is mediated by interaction with ELMO1: upregulation of fibronectin expression by COX-2 is mediated by interaction with ELMO1. *Cell Signal* 2011;23:99–104.
- Yang G, Chen L, Zhang Y, Zhang X, et al. Expression of mouse membrane-associated prostaglandin E₂ synthase-2 (mPGES-2) along the urogenital tract. *Biochim Biophys Acta* 2006;1761:1459–1468.
- Yang T, Singh I, Pham H, Sun D, et al. Regulation of cyclooxygenase expression in the kidney by dietary salt intake. *Am J Physiol Renal Physiol* 1998;274:F481–F489.
- Yang T, Sun D, Huang YG, Smart A, et al. Differential regulation of COX-2 expression in the kidney by lipopolysaccharide: role of CD14. *Am J Physiol* 1999;277:F10–F16.
- Yang T, Endo Y, Huang YG, et al. Renin expression in COX-2-knockout mice on normal or low-salt diets. *Am J Physiol Renal Physiol* 2000;279:F819–F825.
- Yokoyama C, Yabuki T, Shimonishi M, et al. Prostacyclin-deficient mice develop ischemic renal disorders, including nephrosclerosis and renal infarction. *Circulation* 2002;106:2397–2403.
- Yoshida T, Kameda H, Ichikawa Y, Tojo T, et al. Improvement of renal function with a selective thromboxane A₂ synthetase inhibitor, DP-1904, in lupus nephritis. *J Rheumatol* 1996;23:1719–1724.
- Zahner G, Schaper M, Panzer U, Kluger M, et al. Prostaglandin EP2 and EP4 receptors modulate expression of the chemokine CCL2 (MCP-1) in response to LPS-induced renal glomerular inflammation. *Biochem J* 2009;422:563–570.
- Zewde T, Mattson DL. Inhibition of cyclooxygenase-2 in the rat renal medulla leads to sodium-sensitive hypertension. *Hypertension* 2004;44:424–428.
- Zhang A, Dong Z, Yang T. Prostaglandin D₂ inhibits TGF- β 1-induced epithelial-to-mesenchymal transition in MDCK cells. *Am J Physiol Renal Physiol* 2006;291:F1332–F1342.
- Zhang MZ, Yao B, Fang X, Wang S, et al. Intrarenal dopaminergic system regulates renin expression. *Hypertension* 2009;53:564–570.
- Zhang Y, Schneider A, Rao R, Lu WJ, et al. 2003. Genomic structure and genitourinary expression of mouse cytosolic prostaglandin E₂ synthase gene. *Biochim Biophys Acta* 2003;1634:15–23.
- Zidar N, Odar K, Glavac D, Jerse M, et al. Cyclooxygenase in normal human tissues: Is COX-1 really a constitutive isoform, and COX-2 an inducible isoform? *J Cell Mol Med* 2009;13:3753–3763.
- Zimran A, Kramer M, Plaskin M, Hershko C. Incidence of hyperkalaemia induced by indomethacin in a hospital population. *BMJ* 1985;29:107–108.
- Zook TE, Strandhoy JW. Mechanisms of the natriuretic and diuretic effects of prostaglandin F₂ alpha. *J Pharmacol Exp Ther* 1981;217:674–680.

CARDIOVASCULAR SYSTEM**INTRODUCTION**

The conversion of arachidonic acid (AA) into prostaglandin H₂(PGH₂) is catalyzed by cyclooxygenase (COX). PGH₂ is subsequently converted by synthases to various prostanoids, such as PGE₂, PGI₂, PGF_{2α}, and thromboxane A₂(TXA₂) (Eling et al., 1990; Dannenberg et al., 2001). These prostanoids play a role (1) in cardiovascular homeostasis and vascular tone (Fitzgerald, 2004) and (2) in altering renal blood flow, glomerular filtration rate (GFR), and electrolytes (Radi, 2009). COX-1 isoenzyme is expressed constitutively in most normal tissues; COX-2 is highly induced by proinflammatory mediators in the setting of inflammation, injury, and pain (Fig. 4-1) (Parente and Perretti, 2003; Radi, 2009; Sellers et al., 2010). Inhibitors of COX activity include nonselective nonsteroidal anti-inflammatory drugs (ns-NSAIDs) such as naproxen, ibuprofen, diclofenac, and phenylbutazone and COX-2 selective NSAIDs (COX-2 s-NSAIDs) such as firocoxib (Previcox), robenacoxib (Onsior), and celecoxib (Celebrex) (Radi and Khan, 2006; Joubert, 2009; Radi, 2009; Sellers et al., 2010). In therapeutic doses, ns-NSAIDs inhibit both COX-1 and COX-2 (Fig. 4-1), whereas COX-2 s-NSAIDs inhibit predominantly COX-2 (Krotz et al., 2005; Sellers et al., 2010).

The potential for cardiovascular events associated with COX-2 selective and ns-NSAID inhibitors, particularly in people with underlying cardiovascular disease, has been addressed in the last few years (Krotz et al., 2005). Nonclinical studies failed to identify these risks in a variety of animal species and models. Although a variety of experimental models have assessed the effects of both selective and ns-NSAIDs, the outcome in these models has been variable (Sellers et al., 2010). In this chapter we discuss the expression of COX-1 and COX-2 in the cardiovascular system, the role of prostaglandins and COX in cardiovascular homeostasis and pathophysiology, and the effects on the cardiovascular system of COX-2 s-NSAIDs and ns-NSAIDs.

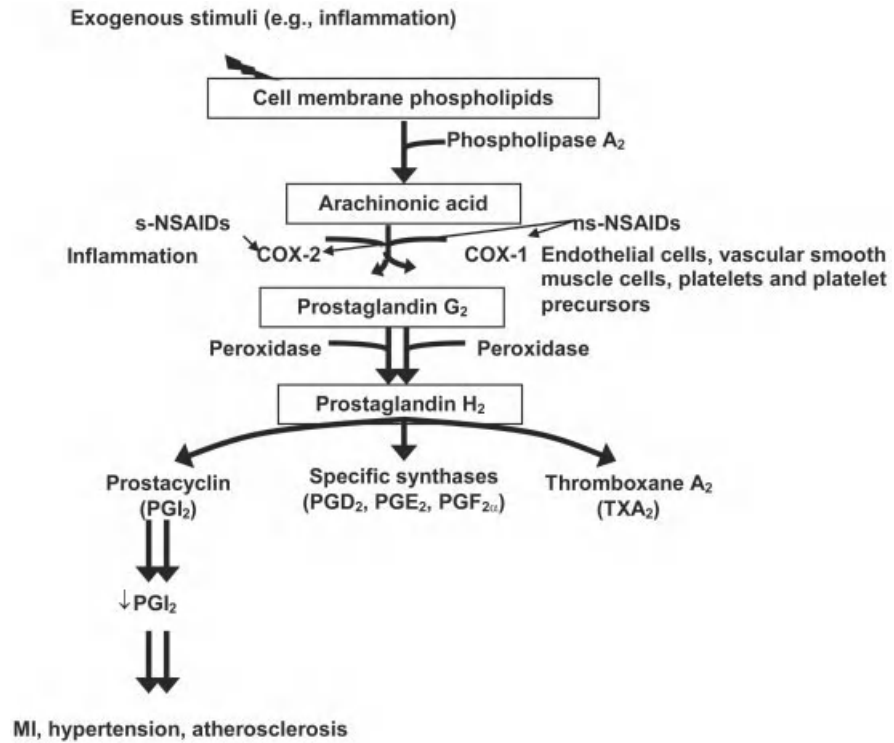


FIGURE 4-1 Prostaglandin synthesis: the role of prostaglandins (PGs) in the cardiovascular system in health and disease and the effects of nonselective and nonsteroidal anti-inflammatory drugs (ns-NSAIDs) and COX-2 s-NSAIDs. Following an exogenous stimulus (e.g., inflammation), cell membrane phospholipid is liberated to arachidonic acid (AA) by phospholipase A₂. Two cyclooxygenases, COX-1 and COX-2, catalyze the conversion of AA into various PGs. COX-1 is expressed in endothelial cells, platelets, platelet precursors, and vascular smooth muscle cell, whereas COX-2 expression is up-regulated during inflammatory or neoplastic conditions. Nonselective NSAIDs (e.g., carprofen, etodolac, flunixin meglumine, ketoprofen, indomethacin, meloxicam, phenylbutazone) inhibit COX-1 and COX-2; COX-2 s-NSAIDs (e.g., celecoxib, deracoxib, lumiracoxib, robenacoxib, rofecoxib) spare COX-1 and inhibit only COX-2. [The final, definitive version of this table was published in R. A. Sellers, Z. A. Radi, and N. K. Khan, *Veterinary Pathology*, 47(4), 2010, pp. 601–613. Copyright © Sage Publications. All rights reserved.]

COMPARATIVE PHYSIOLOGICAL AND ANATOMICAL ASPECTS OF THE CARDIOVASCULAR SYSTEM

The Heart

Understanding the comparative physiological and anatomical aspects of cardiovascular function in diverse species is important for an understanding of the pathological and toxicological consequences of COX inhibition in the cardiovascular

system. The heart is a hollow muscular pump that is located within the mediastinum. The main function of the heart is to send oxygenated arterial blood to the body and pump deoxygenated blood into the pulmonary circulation. As arteries enter tissues, they become smaller (arterioles), and from there they become capillaries to provide nutrients and oxygen and remove carbon dioxide. The shape of the normal heart varies from elongated (horse heart) to ovoid (dog heart) to trapezoidal (human) (Crick et al., 1998). The heart of a normal human female is smaller than that of a normal male. Anatomically, the heart is enclosed in a double-walled fibroserous inelastic sac called the pericardium or pericardial sac. The heart wall consists of three layers: epicardium, endocardium, and myocardium (Gavaghan, 1998). The outermost layer of the heart, the epicardium, also known as the visceral pericardium, consists of epithelial cells that form a serous membrane that covers the entire heart (the inner surface of the pericardial sac). The outer surface of the pericardial sac is called the parietal pericardium. Humans have a much thicker pericardium than that of animals (Holt, 1970). The innermost layer of the heart is known as the endocardium. It is a serous membrane that lines the inner surface of the heart, its valves, and the chordae tendineae, which are the cords that connect the free edges of the atrioventricular valves with the papillary muscles. The papillary muscles are muscle eminences on the walls of the ventricles. The endocardium is continuous with the intima (e.g., the inner lining of arteries). The thick middle layer of the heart is the muscular layer known as the myocardium. It is responsible for the major pumping action of the ventricles. The myocardial cells have an intrinsic ability to contract in the absence of stimuli (i.e., automaticity) and in a rhythmic manner (i.e., rhythmicity), and to transmit nerve impulses (i.e., conductivity).

Rhythmicity is the regular generation of an action potential (i.e., transmission of electrical impulses) by the conduction system of the heart. The heart has four chambers: the right and left atriums and the right and left ventricles. The four valves of the heart—the mitral, tricuspid, pulmonary, and aortic valves—are involved in the filling and pumping action of the heart (Zimmerman, 1966; Gavaghan, 1998). The mitral or bicuspid valve is located between the left atrium and the left ventricle. It has two leaves that slightly overlap each other when the valve is closed. The tricuspid (i.e., three cusp) valve lies between the right atrium and the right ventricle. It has three valves, which are thinner than those of the mitral valve. The leaves of both valves are attached to strong fibrous strands called the chordae tendineae. These cords arise from the trabeculae carneae muscle bundles in the inner ventricles. Two groups of papillary muscles arise from the trabeculae carneae in the left ventricle and three arise in the right ventricle. The aortic (separates the left ventricle from the ascending aorta) and pulmonary valves are called semilunar (i.e., half moon) valves because they have three cusps that are cuplike in nature. The atrioventricular (i.e., mitral and tricuspid) valves prevent backflow of blood from the ventricles into the atria during systole. The semilunar (i.e., aortic and pulmonary) valves prevent backflow from the aorta and pulmonary artery during diastole (Gavaghan, 1998). Cardiac valve injury can lead to valve regurgitation, where blood flows in a reverse direction (valve insufficiency), or stenosis, where blood outflow is obstructed (Cannistra, 2005).

The contraction and relaxation of cardiac muscle is mediated by the sliding of interdigitating thick filaments and thin filaments. Thick myofilaments are composed of a protein called myosin. Thin myofilaments are composed of three proteins: actin, troponin, and tropomyosin. The control of cardiac muscle function is Ca^{2+} -based and resides in the thin filament. This process involves cardiac troponin (cTn) complex in interaction with tropomyosin (Tm). Cardiac Tn is a complex composed of three subunits, each of which interacts with the other two. Tropomyosin is a long, flexible coil that is in equilibrium among three states of myosin–actin–troponin binding: blocked (Ca^{2+} not bound to troponin C, myosin not bound to actin), closed (Ca^{2+} bound to troponin C, myosin weakly bound to actin), and open (Ca^{2+} bound to troponin C, myosin strongly bound to actin). Subtle changes in the structure and protein contacts within cardiac troponin lead to significant changes throughout the complex which alter Tm dynamics and cardiac troponin–actin interactions (Manning et al., 2011).

Cardiovascular Blood Flow

Blood flow through the heart follows a specific route. The right side of the heart receives venous blood from the body (deoxygenated blood) and sends it to the lung, while the left side receives arterial blood from the lung (oxygenated blood) and sends it to the body. When the blood returns from the systemic circulation to the right atrium, it goes through the tricuspid valve to the right ventricle. From the right ventricle, blood is ejected through the pulmonary valve to the lungs to get oxygenated. The oxygenated blood returns from the lungs to the left atrium, and from there goes through the mitral valve to the left ventricle. Blood is pumped through the aortic valve to the aorta and the systemic circulation (Rudolph, 1985; Reece, 2007). The fetal circulation is significantly different from the adult circulation (Murphy, 2005). In the fetus, gas exchange and oxygenation occurs in the placenta, which receives deoxygenated blood from the fetal systemic organs and returns its oxygen-rich venous drainage to the fetal systemic arterial circulation. Deoxygenated blood gets to the placenta via the umbilical arteries and is returned to the fetus in the umbilical vein. In addition, in the fetal cardiovascular system, most of the highly oxygenated blood is delivered to the myocardium and brain. Because of the preferential streaming of oxygenated blood and the presence of intracardiac and extracardiac shunts, the fetal circulation has been defined as “shunt-dependent” circulation (Murphy, 2005).

Cardiac Conduction System and Blood Pressure

The cardiac conduction system generates and transmits impulses that stimulate myocardial contraction. The components of the cardiac conduction system are (1) the sinoatrial (SA) node, (2) the atrioventricular (AV) node and bundle, and (3) the right and left bundle branches (RBB and LBB) (Lev, 1964). The cardiac cycle is defined as the period from the beginning of one heartbeat to the

beginning of the next beat. It includes the systole (i.e., heart chamber contraction during emptying), the diastole (i.e., relaxation of heart chamber during filling), and a short pause called the diastasis cordis (when both atria and ventricles relax) (Gavaghan, 1998). Systolic blood pressure (SBP) is the pressure within the arterial system at the peak of the systole. The SBP is controlled by the stroke volume of the heart, the rate of systolic ejection, and the distensibility of the arterial tree (Koch-Weser, 1973). Diastolic blood pressure (DBP), when the heart is relaxed, is controlled by peripheral resistance. Elevated SBP is a recognized risk factor for cardiovascular complications among older patients, but when this elevation is due to a stiffened arterial tree, DBP is necessarily reduced (Smulyan and Safar, 1997). If arteries lose their elasticity due to pathological conditions (e.g., sclerosis), BP rises (i.e., hypertension) during both systole and diastole. The systolic/diastolic BP values vary across adult species: human (120/70 mmHg), rhesus monkey (130/100 mmHg), dog (120/70 mmHg), horse (130/95 mmHg), cow (140/80 mmHg), cat (140/90 mmHg), rat (110/70 mmHg), and mouse (111/80 mmHg) (Smith and Ansevin, 1957; Detweiler, 1993). In the fetus of humans, BP in the aorta is approximately 30 mmHg at 20 weeks of gestation and increases to approximately 45 mmHg at 40 weeks of gestation (Struijk et al., 2008). Intrauterine recording of the intraventricular pressure in human fetuses has been evaluated. There was an increase in ventricular systolic and end diastolic pressures with advancing gestation. Systemic systolic pressure increased from 15 to 20 mmHg at 16 weeks to 30 to 40 mmHg at 28 weeks. No differences between left and right ventricular pressures were noted, and atrial pressures were equal and remained constant (Johnson et al., 2000). There are species differences in the fetal circulation. The human fetus appears to circulate less blood through the placenta, to shunt less through the ductus venosus and foramen ovale, but to direct more blood through the lungs than does the fetal sheep (Kiserud and Acharya, 2004). In addition, the ductus arteriosus, a short temporary vessel in the fetus that connects the pulmonary trunk and the aorta and conducts most of the blood directly from the right ventricle to the aorta, bypassing the lungs, is important in maintaining adequate aortic circulation in the fetus. After birth, constriction of the ductus arteriosus takes place and PGE₂ plays a major role in ductal patency (Clyman et al., 1978). Furthermore, PGE₁ can play a significant role in the regulation of ductus arteriosus tone in the elevated oxygen environment of the newborn as well as in the low-oxygen environment of the fetus (Clyman et al., 1977).

Hypertension is defined as a sustained increase in systemic arterial BP. Cardiac output (CO), the volume of blood ejected per minute, is defined as being the product of stroke volume and heart rate. Stroke volume is determined by (1) preload (volume of blood that fills the ventricles during diastole and degree of stretch of myocardial fibers), (2) afterload (resistance or pressure the ventricles must overcome to eject blood out), and (3) contractility (force generated by the myocardium when it contracts) (Gavaghan, 1998). Cardiac hypertrophy is an adaptive response of the heart to an imposed load. Two distinct patterns of hypertrophy are discussed, pathological and physiological, which differ in their mechanical and

biochemical features (Scheuer and Buttrick, 1987). Several signaling molecules, such as endothelin, angiotensin II and cardiotrophin-1 have been proposed as the mediators promoting pressure overload-induced cardiac hypertrophy (Ito et al., 1994; Senbonmatsu et al., 2000; Takimoto et al., 2002; van de Schans et al., 2007). In the adult circulation, the stroke volume of the right ventricle should equal that of the left ventricle. In the fetus, because of the intracardiac and extracardiac shunting, the stroke volume of the fetal left ventricle is not equal to the stroke volume of the right ventricle. The right ventricle receives about 65% of the venous return and the left ventricle about 35% (Murphy, 2005). Mean arterial BP is determined by the product of CO and total peripheral resistance.

Several physiological factors contribute to arterial BP reflex control, including adrenergic receptors, force of contraction, antidiuretic hormone (ADH) activity, venous capacitance, filling pressure, intravascular volume, stroke volume, and heart rate (Bakris and Mensah, 2003). Thus, factors that may contribute to the pathophysiology of hypertension are increased sympathetic nervous system activity, overproduction of sodium-retaining hormones and vasoconstrictors, increased or inappropriate renin secretion with resulting increased production of Ang II and aldosterone, genetics, environmental factors, deficiencies of vasodilators, vascular reactivity, vascular remodeling, increased peripheral resistance, renal parenchymal and nervous stimulation, production of inflammatory mediators, and endothelial dysfunction (Bakris and Mensah, 2003; Vargas Alarcón, 2006). In cats, chronic kidney disease, adrenal diseases, and hyperthyroidism are the most frequent causes of systemic hypertension (Brown et al., 2007). A diagnosis of hypertension should be considered strongly in a cat with Doppler forelimb SBP ≥ 160 mmHg or oscillometric tail cuff SBP ≥ 140 to 160 mmHg (Stepien, 2011). In dogs, hyperadrenocorticism (i.e., Cushing's disease; an endocrine disorder characterized by chronic elevations in the circulating concentrations of adrenal cortisol hormone) and renal failure are the primary causes of hypertension (Lien et al., 2010). The chromaffin cells of the adrenal gland synthesize and secrete various catecholamines, including epinephrine and norepinephrine, which lead to a variety of physiological effects, including increased cardiac contraction and vasoconstriction. Pheochromocytoma, a tumor of the adrenal gland, can lead in several species to hypertension, which is related to the rapid and massive release of catecholamines from the tumor (Prejbisz et al., 2011). In addition, reversible dilated or hypertrophic cardiomyopathy is a well-established cardiac manifestation of pheochromocytoma in humans (Prejbisz et al., 2011). There are species differences in sensitivity to hypertension. For example, the rhesus monkey is more susceptible than the dog to the morbid effects (cardiac hypertrophy) of hypertension (Frank, 1963). Dogs exhibited marked differences in susceptibility or resistance to the development of chronic hypertension (Schroeder and Goldman, 1952). Approximately two-thirds of dogs return to normotension within a year after constriction of one renal artery (Schroeder and Goldman, 1952). Furthermore, in certain breeds of dogs (i.e., the terrier breeds), hypertension was easily induced experimentally (Schroeder and Goldman, 1952). In nonhuman primates, experimental renal hypertension developed consistently after unilateral renal artery constriction and was maintained for 19 to 35 months and became more marked after contralateral renal constriction or nephrectomy (Frank, 1963).

Heart Rate

Heart rate (HR) is the frequency of cardiac cycle and is measured by the number of beats per minute. Generally, small animals have a higher heart rate than that of larger animals (Reece, 2007). Heart rate values vary significantly among species: human (60 to 90 beats/min), rhesus monkey (180 to 210 beats/min), horse (32 to 44 beats/min), cow (60 to 70 beats/min), dog (70 to 120 beats/min), and cat (111 to 130 beats/min) (Reece, 2007). In the mouse, the heart rate ranges from 310 to 840 beats/min, and there is a wide variation in HR and BP among mouse strains (Fox et al., 2002). When the HR is too slow, it is termed bradycardia, and when HR is too fast, it is termed tachycardia. Heart rate is regulated by the autonomic nervous system. Sympathetic stimulation enhances myocardial performance and increases HR activities (i.e., rate and force of contraction, rate of impulse conduction, and amount of coronary blood flow), and parasympathetic (vagal) stimulation decreases all HR activities (McCorry, 2007; Reece, 2007). HR regulation can vary between neonates and adults. Pharmacological blockade of sympathetic (propranolol) and parasympathetic (atropine) efferent nerves can be used to assess effects on HR. The autonomic control of resting HR was assessed using atropine and propranolol in neonatal (2 to 3 week old) male rhesus monkeys. It was found that the autonomic control of resting HR is mediated by the autonomic nervous system and the sympathetic system, the latter having a dominant influence. This is in contrast to the adult rhesus, where the parasympathetic nervous system controls resting HR (Goldberg and Moberg, 1985). The sympathetic nervous system predominates during emergency “fight-or-flight,” with the primary neurotransmitter being norepinephrine (McCorry, 2007). Main receptors for norepinephrine are adrenergic (β_1 , α_1 , and α_2). Beta 1 receptors are the primary adrenergic receptor on the heart (a small percentage of the adrenergic receptors on the myocardium are β_2). Both subtypes of beta receptors on the heart are excitatory, and stimulation leads to an increase in cardiac output, lipolysis, or renin (Bakris and Mensah, 2003; McCorry, 2007). In sympathetic nervous stimulation, norepinephrine or catecholamine bind to β -adrenergic receptors on the cell membrane of cardiac cells, leading to increased cellular calcium influx and subsequently increased contractile strength of the heart (McCorry, 2007). The parasympathetic nervous system predominates during resting conditions, with the primary neurotransmitter being acetylcholine (McCorry, 2007). Main receptors for acetylcholine are cholinergic (nicotinic and muscarinic) (McCorry, 2007). In vagal stimulation, acetylcholine is released and binds to nicotinic receptors, causing rapid increase in the cellular permeability to sodium and calcium ions, which causes depolarization (McCorry, 2007). Parasympathetic control of the heart is attenuated in heart failure (HF). In experimentally induced HF in dogs, vagal transmission is reduced, acetylcholinesterase activity is decreased, and muscarinic receptor density and composition are altered (Dunlap et al., 2003).

The Frank–Starling law of the heart describes the length–tension relationship and relates resting muscle length, expressed as the volume of blood in the heart at the end of diastole, to tension generation (Shiels and White, 2008). Heart

failure is characterized by a lower length–tension curve. The Frank–Starling law of the heart applies to all classes of vertebrates and is found in both adult and embryonic myocardium (Asnes et al., 2006; Shiels and White, 2008). The cellular mechanisms underlying the Frank–Starling response include three cooperative mechanisms: (1) an increase in myofilament sensitivity for calcium, (2) decreased myofilament lattice spacing, and (3) increased thin filament (Shiels and White, 2008). In the Laplace law or surface tension law, the tension in the wall (T) is directly proportional to intraventricular pressure (P) and internal radius (R) ($T = P \times R$) and inversely to the wall thickness (Strain and Olson, 1975). Dilated cardiomyopathy is an example of Laplace’s law, in which the heart chambers become dilated and the radius of ventricle increases. As a consequence of this and to create the same pressure during blood ejection, cardiac muscle develops more wall tension. In hypertension, all parts of the Laplace law equation apply (i.e., intraventricular pressure changes, and with left ventricular hypertrophy, both internal radius and wall thickness are altered) (James et al., 2000). Laplace’s law has been used widely to explain the constancy of arterial wall thickness to the lumen radius needed to maintain constant stress in the wall of the pressurized cylinder in a wide range of circumstances. The relationship among carotid BP, arterial geometry, and wall stress was investigated to determine the impact of hypertension, smoking, and their interaction on these relationships (Liang et al., 2001). The investigators found that carotid artery wall remodeling follows Laplace’s law. However, this was insufficient to prevent an increase in circumferential stress in hypertensive patients. Smoking did not influence the lumen-to-wall ratio but has a significant effect on wall stiffness (Liang et al., 2001).

Renin–Angiotensin–Aldosterone in the Cardiovascular System

The renin–angiotensin–aldosterone system (RAAS) plays an important role in the control of the cardiovascular homeostatic physiological processes by regulating vascular tone, BP, and fluid volume. Angiotensin II (Ang II) is a physiologically active component of the RAAS, produced via an enzymatic cascade that begins with angiotensinogen (AGT) (synthesized mainly in the liver) cleaving renin, aspartyl protease enzyme, to form Ang I, which is then cleaved by the angiotensin-converting enzyme (ACE) to form Ang II. Ang II has two subtypes of receptors, AT₁ and AT₂, but the AT₁ receptor subtype drives most of the biological functions of Ang II. Ang II causes vasoconstriction, most pronounced in arteries and arterioles and less in veins, directly by activating Ang II type 1 (AT₁) receptors on vascular smooth muscle. Ang II also affects fluid volume via AT₁ receptor activation in the renal proximal tubule, resulting in renal sodium and water reabsorption. Ang II regulates fluid balance by stimulating aldosterone secretion from the adrenal glands (Meune et al., 2003; Mehta and Griendling, 2007; Radi and Ostroski, 2007). Ang II is also a growth promoter in cardiovascular tissues and has been implicated in cardiovascular system inflammation, endothelial dysfunction, atherosclerosis, hypertension, and congestive heart failure (Mehta and Griendling, 2007). In vascular smooth muscle cell contraction, AT₁ receptors can, via G-protein

signaling, mobilize calcium from the sarcoplasmic reticulum and promote the interaction of actin and myosin filaments to allow for contraction and migration of cells. Ang II has been shown to phosphorylate and activate phospholipase A₂, which leads to the production of arachidonic acid (AA) and its metabolites. In addition, Ang II can maintain a balance between vasoconstriction and vasodilation in various vascular beds (Mehta and Griendling, 2007). One of the major pathways activated by G-protein interaction with AT₁ receptors led to the activation of protein kinase C (PKC) and the ERK pathway, which are implicated in contraction as well as cellular growth (Mehta and Griendling, 2007). In addition, Ang II, via the AT₁, activates intracellular signaling pathways that promote atherothrombosis through inflammation, endothelial dysfunction, growth, altered fibrinolysis, and potentiation of low-density lipoprotein (LDL) oxidation (Jacoby and Rader, 2003). Thus, RAAS contributes directly to coronary ischemic events via atherosclerosis, altered postinfarct remodeling, and reduced fibrinolysis.

Inhibition of the RAAS has antiatherosclerotic activity, independent of BP, which has been demonstrated in animal models of atherosclerosis (Chobanian, 1990; Miyazaki et al., 1999; Jacoby and Rader, 2003). Chymase is stored intracellularly in the secretory granules of mast cells and is released upon mast cell activation. In the cardiovascular system in dogs, monkeys, hamsters, and humans, chymase is a local Ang II-generating enzyme (Kunori et al., 2005). Interestingly, chymase inhibition using TY-51469, a novel chymase inhibitor, at a dose 0.1 mg/kg per day, reduced the progression to heart failure in an autoimmune myocarditis Lewis rat model (Palaniyandi et al., 2007). PGs are modulators of physiological functions and contribute to renin release, regulation of hemodynamics, salt balance, and BP control via mechanisms involving the regulation of vascular tone (Meune et al., 2003; Mehta and Griendling, 2007; Radi and Ostroski, 2007).

Natriuretic Peptides in the Cardiovascular System

Natriuretic peptides (NPs) are hormones involved in the regulation of sodium excretion (natriuresis), diuresis, vasodilation, reflex tachycardia inhibition, water balance, blood volume, and decreased systemic vascular resistance and arterial blood pressure (Woodard and Rosado, 2008). NPs include atrial (ANP), brain NP (BNP), C-type NP (CNP), dendroaspis-type NP (DNP), and urodilatin. All the natriuretic peptides have been shown to induce vasorelaxant effects in the coronary circulation (Woodard and Rosado, 2008). The actions of these NPs are mediated by the specific binding to three cell surface receptors: type A natriuretic peptide receptor (NPR-A), type B natriuretic peptide receptor (NPR-B), and type C natriuretic peptide receptor (NPR-C) (Woodard and Rosado, 2008). In the heart of rhesus monkey, APRA mRNA, using *in situ* hybridization, is expressed most abundantly in endocardial endothelial cells of the right and left atrium and right ventricle, while APRC mRNA is expressed most prominently in endocardial endothelial cells of all four heart chambers but was also found throughout the myocardium only in the right atrium (Wilcox et al., 1991). In the rat heart, distribution of the APRA and APRB receptor transcripts was relatively homogeneous; in contrast, the C-type mRNA was concentrated principally in the atria, with no difference between

the left and right sides of the heart. In human heart, APRA and APRB receptors were found after amplification of the left (but not the right) ventricle, and APRC receptor expression was similar in both ventricles (Nunez et al., 1992). ANP is synthesized and secreted by normal adult mammalian atrial cardiocytes in response to wall stretch resulting from BP and volume loading and causes natriuresis, diuresis, and inhibition of smooth muscle contraction, and aldosterone and renin release (Ruskoaho et al., 1987). The expression of ANP is low in the ventricles in the physiological state (Woodard and Rosado, 2008). Increased ANP levels have been demonstrated in heart failure in humans (Burnett et al., 1986), in Wistar–Kyoto rats that spontaneously develop biventricular hypertrophy (Lee et al., 1988), in cats with congestive heart failure (Connolly et al., 2009), in dogs with mitral valve disease and congestive heart failure (Tarnow et al., 2009), and upon volume and pressure overload in mice (Mori et al., 2004). BNP is a cardiac hormone secreted predominantly from the ventricle, and its synthesis, secretion, and clearance differs from those of ANP (Mukoyama et al., 1991). BNP has emerged as a useful biomarker for the diagnosis and prognosis of adult patients and children with heart failure (Ekure et al., 2011). The cardiovascular effects of CNP are more likely to be mediated by local effects on blood vessel or by central actions on vasopressin and adrenocorticotropin release (Woodard and Rosado, 2008). DNP is an endogenous human natriuretic peptide that relaxes human arteries more than veins (Best et al., 2002). Urodilatin is synthesized in kidney tubular cells and is secreted into kidney tubules. It has been claimed that urodilatin has beneficial effects in patients with congestive heart failure and lowered preload, increased diuresis and natriuresis, decreased systemic vascular resistance, increased cardiac index, and lowered cardiac filling (Kentsch et al., 1992; Elsner et al., 1995; Mitrovic et al., 2006). The correlation between PGs and NPs in the cardiovascular system has been investigated. Using perfused beating rat atria, the effects of various PGs on the regulation of ANP and signaling molecules involved in PG-mediated ANP secretion were investigated. The study revealed that $\text{PGF}_{2\alpha}$ and PGD_2 , but not PGE_2 , PGJ_2 , PGI_2 , and TBA_2 , increase ANP secretion and positive inotropy through the FP receptor. $\text{PGF}_{2\alpha}$ was found to be the most potent stimulator and secretagogue of ANP secretion through a signaling pathway involving phospholipase C (PLC), inositol 3-phosphate (IP_3), PKC, and myosin light-chain kinase (MLCK). In two-kidney/one-clip hypertensive rat atria, $\text{PGF}_{2\alpha}$ -induced ANP secretion was attenuated, whereas COX-2 inhibitor nimesulide-induced ANP secretion was augmented. The expression of COX-2 was increased and FP receptor mRNA was decreased in hypertrophied atria. The authors conclude that the regulation of ANP secretion by COX-2 and $\text{PGF}_{2\alpha}$ is due to increased expression of COX-2 and decreased expression FP receptor, which may partly relate to the development of renal hypertension (Bai et al., 2009).

Cardiovascular Research and Animal Models

In cardiovascular function and disease research studies, each experimental animal model, each animal species, and each endpoint has its own advantages and disadvantages, and appreciating these will help the investigator select the most

appropriate animal model for the particular question under investigation (Hearse and Sutherland, 2000). In addition, nonclinical-to-clinical translation and relevance to the human condition is an important factor to consider in cardiovascular research (Hearse and Sutherland, 2000). A cautious approach is mandatory when experimental findings in animal models are extrapolated to human hypertension (Lerman et al., 2005). In hypertension cardiovascular research, the first animal model of hypertension was in dogs and was introduced in 1934 and was induced by unilateral constriction of the renal artery (2K1C model) (Goldblatt et al., 1934). Hypertension models fall into a variety of categories and include renovascular (e.g., two kidneys, one clip), renal injury (e.g., partial or total nephrectomy), vasoactive intervention (e.g., pressor prostaglandins), endocrine and dietary (e.g., Dahl salt-sensitive), neurogenic (e.g., baroreceptor denervation), and phenotype-driven (e.g., RAAS, Dahl salt-sensitive rat, SHR-stroke prone) (Lerman et al., 2005). In animal models, the most commonly used indirect method for monitoring BP is the cuff technique, in which BP is measured in a tail or limb by determining the cuff pressure at which changes in blood flow occur during occlusion or release of the cuff. It is important that investigators also use optimal methods for measuring BP. The investigator needs to keep in mind that many environmental factors can affect BP, including, but not limited to, ambient room temperature, light cycle, noise levels, duration of human contact, number of animals per caging unit, proximity to other animals undergoing experimental procedures, cage unit size and design, and access to supplemental items such as toys, treadmills, and hiding spaces within the cage unit (Kurtz et al., 2005). In addition, systemic anesthetics can also exert major effects on cardiovascular function and should be avoided whenever possible (Kurtz et al., 2005). In atherosclerosis and dyslipidemia cardiovascular research, animal models should share the pathophysiology of the disease with humans (Moghadasian et al., 2001). In addition, interspecies differences in cholesterol are important considerations. For example, many characteristics typical of human serum LDL are found in those of the pig, rhesus monkey, and baboon (Chapman and Goldstein, 1976). Unlike humans and several other animals, wild-type (WT) mice and rats do not possess plasma cholesteryl ester transfer protein (CETP), and approximately 70% of their plasma total cholesterol is found in high-density lipoprotein (HDL) particles and therefore are resistant to atherogenesis (Moghadasian et al., 2001). Hyperlipidemia alone is not sufficient to result in atherogenesis in rats. The poor response to dietary cholesterol supplementation is a limitation for using mice in experimental atherogenesis (Moghadasian et al., 2001). However, unlike their WT counterparts, transgenic rodent models (e.g., Apo E knockout mouse) provide investigators with an excellent opportunity to study the interactions of gene and environment in atherogenesis (Moghadasian et al., 2001). Rabbits share with humans several aspects of lipoprotein metabolism, such as similarities in composition of apolipoprotein B-containing lipoproteins (Chapman, 1980). Unlike humans, rabbits need a very high plasma cholesterol to induce atherosclerosis, are hepatic lipase-deficient, and do not have an analog of human Apo A-II (Chapman, 1980; Warren et al, 1991; Moghadasian et al., 2001). Pigeons (e.g., White Carneau strain) have relatively high levels of plasma cholesterol, most

of it in HDL particles (St. Clair, 1983; Jerome and Lewis, 1985). In dogs, spontaneous atherosclerosis is rare (Moghadasian et al., 2001). Hypothyroidism has been associated with atherosclerosis in dogs (Liu et al., 1986).

Generally, the heart of pig is anatomically similar to that of humans, a notable exception being the presence of a left azygous (hemiazygous) vein, which drains the intercostal system into the coronary sinus (Swindle et al., 1986). The pig cardiovascular system has many features that make pigs an attractive model of human cardiovascular disease. Features of the pig cardiovascular system include (1) very similar cardiac output to that of humans (Tranquilli et al., 1982), (2) a high heart rate (112.0 ± 3.5 beats/min) (Poletto et al., 2011), (3) blood pressure (mean arterial pressure of 112.8 ± 2.8 mmHg, SBP of 134.0 ± 3.3 mmHg, and DBP of 102.2 ± 2.6 mmHg) (Poletto et al., 2011), (4) a prominent left azygous vein entered on the left side of the heart drained via the coronary sinus instead of the precava (Crick et al., 1998), (5) a vaso vasorum in the aorta, (6) coronary artery anatomy and distribution of blood supply more similar to those of humans than those of other mammals (Weaver et al., 1986), (7) a coronary system similar to that of 90% of the human population in anatomy and function and no preexisting collateral vessels in the myocardium, (8) heart weight/body weight ratio in young pigs similar to that in normal adult human (5 g/kg) (Hughes, 1986), (9) similar chemical, immunological, physical, and physiological properties of the major apolipoprotein in human and pig HDL (Jackson et al., 1973), and (10) the physicochemical characteristics of LDL most closely resembling those of humans (Chapman and Goldstein, 1976).

Cardiovascular Atherosclerosis

In humans and nonhuman primates, atherosclerosis is one of the most important contributors to cardiovascular disease (Sellers et al., 2010). Atherosclerosis is a complex inflammatory disease of medium-sized and large vessels and is characterized by thickening and hardening of the arteries. Vascular thickening and hardening results from the accumulation of lipids, lipid-laden macrophages, matrix, mineral, and other inflammatory cells, as well as smooth muscle cell proliferation (Moubayed et al., 2007). Pathologically, atherosclerosis begins with endothelial cell dysfunction and inflammation, and thus it is considered to be predominantly an inflammatory disease. During the early initiation of atherosclerotic plaques, lipid accumulation, leukocyte recruitment, and expression of proinflammatory cytokines in the vascular wall with subsequent cytokine, cell signaling, and enzyme production promote plaque growth (Ross, 1993; Libby, 2002; Bonetti et al., 2003; Cipollone and Fazia, 2006). Animal models of atherosclerosis have shed light on the pathogenesis of this disease and the roles of COX-1 and COX-2 on both the development and progression of atherosclerotic plaques (Sellers et al., 2010). Mammalian species other than nonhuman primates do not develop atherosclerosis spontaneously under normal conditions, and atherosclerosis in nonhuman primates is generally associated with aging (Sellers et al., 2010). This species difference certainly presents limitations in the evaluation of cardiovascular risks associated with atherosclerosis in the typical nonclinical toxicology species and in the relatively young primates used in such nonclinical

toxicology studies (Sellers et al., 2010). Animal models of atherosclerosis include the PGI₂ receptor-deficient mouse (*Ptgir*^{-/-}), apolipoprotein E-deficient mouse (*ApoE*^{-/-}), the LDL receptor-deficient mouse (*Ldlr*^{-/-}), the ApoE*3-Leiden transgenic mouse [*Tg(APOE*3,APOC1)2Lmh*], as well as high-fat-diet-induced atherosclerosis in hamsters and Watanabe rabbits (Kowala et al., 1993; Kobayashi et al., 2004; Egan et al., 2005; Zadelaar et al., 2007; van der Hoorn et al., 2008).

COX-1 AND COX-2 EXPRESSION IN THE CARDIOVASCULAR SYSTEM

COX-1 is the predominant COX isoform that is expressed constitutively in the normal vascular endothelium and smooth muscles (Smith et al., 2000; Koki et al., 2002; Parente et al., 2003; Zidar et al., 2007, 2009; Streicher and Wang, 2008; Sellers et al., 2010; Radi and Ackermann, 2011). In endothelial cells prepared from rabbit or pig aortas, COX-1 activity supports prevention of platelet adhesion via the production of the antithrombotic PG prostacyclin (Moncada et al., 1976). Endothelial cells line the luminal surface of blood vessels and are exposed continuously to hemodynamic shear stress. The level of hemodynamic shear stress endothelial cells experience varies from region to region within the vasculature, and physiologic fluid shear stress has been proposed to have an atheroprotective effects. Atherosclerotic lesions develop invariably in regions with lowered shear stress or vortices, whereas the regions of increased shear stress are protected (Cheng et al., 2006). In areas of high laminar shear stress, endothelial cells are elongated, aligned, and protected from inflammation (Potter et al., 2011). COX isoform expression under static or shear stress was investigated using porcine aortic endothelial cells (PAECs) (Potter et al., 2011). PAECs cultured under static or shear stress conditions readily expressed detectable levels of COX-1, with low levels of COX-2 in all regions of the well. Shear stress did not affect the relative expression of COX-1 and COX-2 immunoreactivity in cells at either 24 h or 7 days. Endothelial cell medium contained low levels of the prostacyclin metabolite 6-keto-PGF_{1α} when cells were grown under static or sheared conditions for up to 7 days. Interestingly, levels of COX-1 or COX-2 did not vary significantly in aligned versus nonaligned endothelial cells (Potter et al., 2011). In another study, human umbilical vein endothelial cells (HUVECs) were exposed to uniform laminar shear stress for 6 h, and COX-1 and COX-2 expression was investigated. COX-2 protein was induced significantly, whereas COX-1 and the downstream synthases were not modulated significantly (Di Francesco et al., 2009). Thus, COX-1 is the predominant COX isoform in the healthy peripheral vasculature (Sellers et al., 2010).

COX-1 expression in the heart of adult humans and animals is in both endothelial cells and vascular smooth muscle (Stanfield et al., 2001; Koki et al., 2002; Radi and Ostroski, 2007; Zadelaar et al., 2007; Zidar et al., 2007; Sellers et al., 2010). In normal human heart, COX-1 is expressed in endothelial and smooth muscle cells of blood vessels and in endothelial cells of the endocardium. In myocardial infarction in humans, COX-1 is expressed in inflammatory cells as

well as in myofibroblasts and capillaries of granulation and fibrous tissue (Zidar et al., 2007). In Finnish domestic pig normal heart, COX-1 mRNA was detected in the left ventricular wall (Uotila et al., 2001).

In a renin–angiotensinogen transgenic mouse model of human hypertension, COX-1 expression was noted in vascular endothelial cells and vascular smooth muscle cells of the heart, while cardiac myocytes lacked COX-1 expression (Radi and Ostroski, 2007). In the aorta of spontaneously hypertensive rats, endothelium-dependent contractions were associated with multiple dysfunctions in both the endothelial and the smooth muscle cells. The endothelial dysfunction was due to the release of endothelium-derived contracting factors that counteracted the vasodilator effect of nitric oxide, with no or minor alteration of its production (Félétou et al., 2009). Endothelial cell dysfunction included abnormal calcium handling, increased COX-1 expression, enhanced production of reactive oxygen species, and increased prostacyclin synthase expression (Félétou et al., 2009). COX isoform gene expression was quantified by real-time PCR using isolated endothelial cells and smooth muscle cells (SMCs) from the aorta of Wistar–Kyoto and spontaneously hypertensive rats (Tang and Vanhoutte, 2008). Aging caused overexpression of COX-1, COX-2, endothelial nitric oxide synthase, thromboxane A (TXA) synthase, PGD synthase, mPGE synthase-2, and PGF synthase in endothelial cells and COX-1 and PGE₂ receptors in SMC. In hypertension, the expression of COX-1, PGI synthase, TXA synthase, and PGD synthase were augmented in endothelial cells and PGD₂, EP₃, and EP₄ receptors in SMC. The authors conclude that in aging and hypertension, at least in Wistar–Kyoto and the spontaneously hypertensive rat model, the endothelium has greater propensity to release COX-derived vasoconstrictive prostanoids (Tang and Vanhoutte, 2008). In dogs, COX-1 expression in the heart has been localized to the fibrous connective tissue of the tricuspid valve and chordae tendinae and in the microvasculature of the heart, aorta, and renal artery (Stanfield et al., 2001). In the normal aortic endothelium of male beagle dogs and humans, high levels of COX-1 and PGI synthase (PGIS) expression was observed in the endothelium. In addition, intense COX-1/PGIS double labeling, indicating PGIS and COX-1 colocalization was detected throughout the endothelium of both species. Quantification of the immunolabeling in the dog indicated that 55% of the aortic endothelium exhibited COX-1 expression compared to 8% for COX-2 (Kawka et al., 2007). In Sprague–Dawley rats, COX-1 has been identified in the endothelial cells of the heart but not in cardiomyocytes (Sellers et al., 2010). There are strain differences in cardiac COX expression. No COX-1 mRNA expression was noted in Fisher 344 and brown Norway strains of rats (Okamoto and Hino, 2000). In the fetal pig, the ductus arteriosus contains COX-1 almost exclusively (Guerguerian et al., 1998).

Cyclooxygenase activity is induced in human atherosclerosis (Belton et al., 2003). Prostaglandins (PGs) promote atherosclerosis by altering the inflammatory response and expression of matrix metalloproteinases (MMPs) as well as by acting as a mitogen for various cell types, including vascular smooth muscle cells (VSMCs) (Sellers et al., 2010). Up-regulation of MMP-2 and MMP-9 in plaques has been demonstrated to be mediated in part by COX-2- and COX-1-derived PGE₂ (Cipollone and Fazio, 2006), and probably contribute to plaque rupture (Sellers

et al., 2010). COX-1 mRNA expression was investigated in atherosclerotic aortic plaques and adjacent normal aorta samples obtained from postmortem human cases. COX-1 mRNA levels were only 1.1-fold higher in plaque tissue. There was no relationship between gender, age, or cause of death and COX-2 or COX-1 levels (McGeer et al., 2002). COX-1 expression was analyzed in biopsies from human atherosclerotic carotid arteries and from healthy mammary arteries and saphenous veins. COX-1 was found in the endothelium in healthy and in atherosclerotic vessels (Stemme et al., 2000). TXA₂ increases in atherosclerosis, and platelet COX-1 plays an important role in the early stages of lesion development in the ApoE^{-/-} knockout mouse model of atherosclerosis (Belton et al., 2003). Suppression of TXA₂ biosynthesis retards atherogenesis (Cyrus et al., 2007).

In contrast to COX-1, COX-2 is generally not expressed in the majority of normal endothelial or vascular smooth muscle cells; however, it is induced rapidly with vessel trauma or inflammation (Smith et al., 2000; Dannenberg et al., 2001; Koki et al., 2002; Zidar et al., 2007, 2009; Sellers et al., 2010). The 5' flanking region of the COX-2 gene contains transcription factor binding sites for nuclear factor κ B (NF κ B), nuclear factor for interleukin-6/CCAAT enhancer-binding protein (NF-IL6/C/EBP), and cyclic AMP response element (CRE) (Kirtikara et al., 2000; Smith et al., 2000; Streicher and Wang, 2008). This is consistent with a COX-2 role in inflammation. Cyclic stretch induces COX-2 gene expression in vascular endothelial cells via activation of NF κ B (Zhao et al., 2009). Blood vessels are constantly subjected to mechanical forces in the form of stretch, encompassing cyclic mechanical strain due to the pulsatile nature of blood flow and shear stress. Significant variations in mechanical forces, of a physiological or physiopathological nature, occur in vivo (Lehoux et al., 2006). Exposure of human umbilical vein endothelial cells to laminar shear stress in the physiological range up-regulated the expression of COX-2 (Inoue et al., 2002). Cardiac hypertrophy is an increase in the size of individual myofiber and, consequently, in the size of the heart. In response to pathophysiological stress, the adult heart undergoes hypertrophic enlargement. Although cardiac hypertrophy is initially a compensatory response, sustained hypertrophy is a leading predictor for the development of heart failure. At the cellular and molecular level, disease-related stimuli invoke endocrine, paracrine, and autocrine regulatory circuits, which directly influence cardiomyocyte hypertrophy, in part, through membrane-bound G-protein-coupled receptors and receptor tyrosine kinases. These membrane receptors activate intermediate signal transduction pathways within the cytoplasm, such as mitogen-activated protein kinases (MAPKs), protein kinase C (PKC), and calcineurin, which directly modify transcriptional regulatory factors, promoting alterations in cardiac gene expression (Bueno and Molkentin, 2002). Interestingly, stimulation of either PKC or Ras signaling enhances MAPK activity, which, in turn, activates transcription of COX-2 (Chun and Surh, 2004). In fact, PKC- ϵ was found to play a significant role in COX-2 expression in mice after ischemic preconditioning (Xuan et al., 2005). COX-2 expression in the normal heart is limited. In histologically normal coronary arteries of humans (Baker et al., 1999) and in nonatheromatous aorta of humans (Schönbeck et al., 1999), undetectable or little COX-2 protein immunostaining was observed.

COX-2 expression, using immunohistochemistry, was found to be restricted in aortic vascular endothelial cells in the normal beagle dog and Sprague–Dawley rat, and no expression has been identified in the human aorta (Kawka et al., 2007). In the cardiomyocytes of normal adult humans, COX-2 expression was either not present or it was present in occasional myocytes (Zidar et al., 2007). Extensive COX-1 and COX-2 immunohistochemical staining was observed in heart cardiomyocytes of humans, Wistar rats, and CD-1 mice (Testa et al., 2007). Such extensive staining may be explained by the use of a rabbit polyclonal COX-1 and COX-2 antibody in the immunohistochemical staining of heart sections. Rabbit polyclonal antibodies stain the myocardium extensively, regardless of antigen, and are thus felt to be unreliable for the immunohistochemical evaluation of rodent hearts (Sellers et al., 2010).

COX-2 is readily observed in pathological cardiac conditions and injured cardiac tissues both in humans and in animal models of myocardial disease. Myocardial infarction (MI) is caused by interruption of coronary blood flow to the myocardium, which if persistent would lead to myocyte necrosis and chronic heart failure. COX-2 expression was induced in cardiomyocytes in MI in humans (Zidar et al., 2007). COX-2 mRNA and protein expression was increased in the left ventricular wall after cardioplegic arrest in the heart of pigs (Uotila et al., 2001). In the heart of rabbits, brief episodes of myocardial ischemia with reperfusion resulted in a rapid increase in COX-2 mRNA levels followed by a robust induction of COX-2 protein 24 h later. The enhanced expression of COX-2 was associated with a marked increase in the myocardial content of PGE₂ and 6-keto-PGF_{1α} (Shinmura et al., 2000). Immunohistochemical evaluation of COX-1 and COX-2 expression in human hearts with postmyocardial infarction was investigated. COX-2 staining was observed through the entire peri-infarct region, and uniformly from the epicardial to the endocardial layer, being present in the vast majority of cardiomyocytes. In addition, COX-2 expression in cardiomyocytes occurs 10 days to two months after acute myocardial infarction and is associated with an increased rate of postinfarction myocardial apoptosis (Abbate et al., 2004). In human patients who have suffered from an MI, COX-2 protein expression was induced in cardiomyocytes as well as in interstitial inflammatory cells and in capillaries and myofibroblasts in granulation tissue (Zidar et al., 2007). In a Lewis rat model of chronic MI and heart failure, strong immunohistochemical COX-2 protein expression was observed mainly in the cardiomyocytes, macrophages, endocardium, and vascular endothelial cells in the infarcted myocardium and in the cardiomyocytes and endothelial cells of the noninfarcted myocardium (Saito et al., 2004). The strongest expression of COX-2 in all cells was seen 2 weeks after coronary artery ligation, and decreased slightly thereafter except in macrophages, where it was prominent throughout the study (Saito et al., 2004). Because COX-2 is an inducible enzyme in settings of inflammation, it is not surprising that COX-2 expression has been identified in the hearts of patients with septicemia and inflammation of heart myocardium, myocarditis (Cuenca et al., 2006; Streicher et al., 2008). In the region of atherosclerotic plaques, COX-2 expression is present in endothelial cells, VSMCs, and macrophages (Belton et al., 2003). COX-2 mRNA expression was investigated in atherosclerotic aortic plaques and adjacent normal aorta samples obtained from postmortem human cases.

COX-2 levels were 4.8-fold higher in plaque tissue than in normal artery (McGeer et al., 2002). COX-2 immunoreactivity was seen in macrophages and foam cells, intimal and medial smooth muscle cells, and endothelial cells of vasa vasorum in transplant atherosclerosis (Baker et al., 1999). As in humans, mouse and rabbit models of atherosclerosis have COX-2 expression in fatty streaks and atherosclerotic vessels (Belton et al., 2000; Hong et al., 2000; Stemme et al., 2000; Wong et al., 2001; Burleigh et al., 2005b). These data indicate that in animal models of atherosclerosis, the expression of COX isoforms is similar to that of humans (Sellers et al., 2010).

PATHOPHYSIOLOGICAL ROLE OF PROSTAGLANDINS IN THE CARDIOVASCULAR SYSTEM

The role of prostanoids in homeostasis and vascular tone has been well established. The effects of prostanoids are often opposing, which is important for maintaining a balance between vasoconstriction and vasodilation and anti- and prothrombotic effects (Sellers et al., 2010). Platelets are essential cells for hemostasis, in which they aggregate and cooperate with the coagulation system. The vasoconstriction and vasodilation and anti- and prothrombotic balance are mediated through PGI₂ and platelet-derived TXA₂, and to a lesser extent, PGE₂. The balance between PGI₂ and TXA₂ is a critical factor determining a thrombotic tendency. TXA₂ is a largely platelet-derived (to a lesser extent, monocytes) potent vasoconstrictor (Rossi et al., 1996). Because TXA₂ is platelet derived, it is primarily COX-1-dependent. Platelets express only COX-1 in both humans and nonclinical species; platelets have neither baseline nor induced expression of COX-2 (Kay-Mugford et al., 2000; Zidar et al., 2007). TXA₂ causes local vasoconstriction, platelet aggregation, and smooth muscle cell proliferation. TXA₂ actions are mediated by G-protein-coupled thromboxane–prostanoid (TP) receptors. Infusion of the TP receptor agonist U-46619 causes transient increases in blood pressure followed by cardiovascular collapse in wild-type (WT) mice, but U-46619 caused no hemodynamic effect in TP^{-/-} mice. These knockout (KO) TP^{-/-} mice have a mild bleeding disorder and altered vascular responses to TXA₂ and arachidonic acid (Thomas et al., 1998). During myocardial ischemia, TXA₂ is released in large quantities by activated platelets in the coronary circulation of patients with coronary artery disease (Hirsh et al., 1981). Injections of the TXA₂ mimetic U-46619 at 10 and 20 μg into the left atrium of anesthetized rabbits evoked decreases in HR and arterial BP by stimulation of cardiac vagal afferent nerves (Wacker et al., 2002). Receptors for prostanoids on platelets include the EP₃ receptor for which the natural agonist is PGE₂ produced in atherosclerotic plaques, and EP₃ has been implicated in atherothrombosis (Heptinstall et al., 2008). DG-041, a direct-acting EP₃ antagonist, potentiated the protective effects of PGE₂ on platelet aggregation by inhibiting the proaggregatory effect via EP₃ stimulation (Heptinstall et al., 2008). PGI₂, which is primarily COX-2 derived, is a vasodilator with antithrombotic effects and is expressed primarily by endothelial and vascular smooth muscle cells (Dannenberg et al., 2001; Koki et al., 2002; Zadelaar et al., 2007; Streicher et al., 2008).

The interplay between TXA₂ and PGI₂ in platelet–vascular wall interaction regulation has been studied in rodent models. PGI₂ is important for balancing the prothrombotic and vasoconstrictive effects of TXA₂ (Fitzgerald, 2004; Kearney et al., 2004). The exact source of baseline PGI₂ is uncertain, as there is little to no COX-2 expression in normal human endothelium (Koki et al., 2002). However, COX-2 induction in damaged or inflamed endothelial cells promotes production of prostacyclin, which tempers prothrombotic events at those sites. While PGE₂ can cause vasodilation and can modulate the effects of TXA₂ on platelet aggregation, it does not participate directly in homeostasis (Sellers et al., 2010). Mice lacking the receptor for PGI₂ (IP KO) develop salt-sensitive hypertension, cardiac hypertrophy, and severe cardiac fibrosis. Coincidental deletion of the TP receptor does not prevent the development of hypertension, but cardiac hypertrophy is ameliorated and fibrosis is prevented in IPTP double knockouts (Francois et al., 2005). Decreased susceptibility to renovascular hypertension has been reported in mice lacking the receptor for PGI₂ (Fujino et al., 2004). While a balance exists between TXA₂ and PGI₂ to control thrombosis, studies in PGI₂ receptor–deficient (*Ptgir*^{-/-}) and TXA₂-overexpressing mice (B6;129Sv-*Tbxa2*^{Y385F}) have demonstrated that shifting the balance between these factors does not result in increased platelet aggregation or thrombosis under normal physiological conditions (Murata et al., 1997; Cheng et al., 2002). It is likely, therefore, that other homeostatic mechanisms play a role on clotting under normal conditions (Sellers et al., 2010). Such molecules would include nitric oxide, carbon monoxide, and CD39, to name only a few, which play an important role not only in endothelial protection but also in pro- and antithrombotic events and vascular tone (Marcus et al., 2002).

With injury, however, the importance of a balance between PGI₂ and TXA₂ to modulate platelet aggregation becomes apparent. Vascular injury up-regulates COX-2 activity and therefore local PGI₂ production. If PGI₂ receptor–deficient mice are subjected to vascular injury, they are significantly more prone to thrombotic events than are WT controls (Murata et al., 1997; Cheng et al., 2002). Similar to PGI₂ receptor–deficient mice, mice overexpressing the TXA₂ receptor displayed increased neointimal hyperplasia, intimal cell proliferation, and platelet activation after mechanical artery injury (Cheng et al., 2002). These data indicate that the importance of a balance between PGI₂ and TXA₂ is essential, particularly with vascular trauma, although redundant controls via other molecules may predominate under normal physiological conditions (Sellers et al., 2010).

Genetically engineered and knockout mice have allowed a better understanding of the role of prostanoids and COX in the cardiovascular system (Sellers et al., 2010). Using mice null for COX-2 to evaluate cardiac function and histology has had limited value because COX-2 (*Ptgs2*) null mice often die at birth and rarely survive to 6 months of age (Dinchuk et al., 1995). These null mice develop myocardial fibrosis. However, because the mice have significantly underdeveloped kidneys and poor renal function, discerning whether this cardiac change is primary or secondary is challenging (Sellers et al., 2010). The use of site-specific and inducible gene modulating technology has promoted a better understanding of organ and time-specific changes in gene expression, particularly for genes whose mutation results in early death (Sellers et al., 2010). The role of COX-2 in the adult mouse

heart was investigated using a cardiomyocyte-specific inducible deletion of *Ptgs2*. Two weeks after the cardiomyocyte-specific deletion of COX-2 in postweanling animals, the mice had reduced systolic ventricular function, decreased heart rate, increased susceptibility to induced ventricular arrhythmias, and decreased exercise tolerance (Wang et al., 2009). When afterload was increased through aortic banding, the null mice had greater cardiomyocyte hypertrophy and fibrosis than those of their WT littermates (Wang et al., 2009). Interestingly, Connexin 43, an important gap junction protein, was reduced in the COX-2-deficient cardiomyocytes compared to littermates, and fibroblasts obtained from these hearts had greater expression of atrial natriuretic peptide (ANP), B-type natriuretic peptide (BNP), and MMP-9. A study by Seta et al. (2009) utilized a complete disruption of the murine gene encoding COX-2 (*Ptgs2*) knockdown approach in an effort to mimic the effect of COX-2 s-NSAID inhibition. The study revealed that mice with marked (but not complete) COX-2 inhibition had greater platelet aggregation along vessel walls after FeCl₃-induced vascular injury than that of their (WT) littermates. Ex vivo platelet activation studies demonstrated no significant difference in platelet activation by thrombin or TXA₂ production between the COX-2 knockdown and the WT littermates. Thus, the increased platelet aggregation was probably attributable to COX-2-related changes in the vascular wall physiology. In addition, these mice had no alterations in the mean arterial pressure, suggesting that under normal conditions, reductions in COX-2 do not notably alter blood pressure in mice (Seta et al., 2009).

PGE₂, derived from both COX-1 and COX-2, promotes vasodilatation and although not by itself thrombogenic promotes the thrombogenic potential of TXA₂ (Gross et al., 2007; Sellers et al., 2010). PGE₂ was released from both ischemic and nonischemic cardiac regions during myocardial ischemia in anesthetized mongrel dogs (Berger et al., 1976). The receptors for PGE₂, EP₁₋₄, are G-protein-coupled receptors. Each of these receptors has differing signaling cascades (Degousee et al., 2008). The highest expression level of EP₄ mRNA was found in cardiac ventricle in mice (Xiao et al., 2004). The histopathological features of myocardial reperfusion injury induced by temporary occlusion of the coronary artery were first described in 1960 in the dog. Cardiac pathological features included cell swelling, contracture of myofibrils, disruption of the sarcolemma, and the appearance of intramitochondrial calcium phosphate particles (Jennings et al., 1960). The cardiac ventricle in mice has the highest expression level of EP₄ mRNA (Xiao et al., 2004). The role of PGE₂ via its receptor subtype EP₄ in cardiac ischemia with reperfusion (I/R) injury has been examined in EP₄^{-/-}-KO mice. EP₄^{-/-} mice had larger infarct size than WT mice in an I/R model (Xiao et al., 2004). In addition, isolated and perfused EP₄^{-/-} hearts had greater functional and biochemical derangements than WT hearts in response to I/R (Xiao et al., 2004). However, a different cardiac effect was noted if EP₄ function was deleted only in cardiomyocytes. Cardiac remodeling and function were investigated in cardiac-specific EP₄ receptor-KO mice. No difference was noted in infarct size between KO mice and controls. The KO mice showed less myocyte cross-sectional area and interstitial collagen fraction than those of controls and reduced ejection fraction. Cardiomyocyte-EP₄

deletion decreased cardiac hypertrophy, fibrosis, and activation of STAT-3. However, cardiac function was unexpectedly worsened in these KO mice. Thus, cardiac myocyte EP₄ may have a cardioprotective role in cardiac hypertrophy via activation of STAT-3 (Qian et al., 2008). EP₄ knockdown in cardiac myocytes in aged male KO mice is, in part, shown to be associated with increased fibrosis, reduced ejection fraction, and dilated cardiomyopathy (Harding et al., 2010). EP₄ has been found to mediate regulation of inflammatory cytokines in macrophages and neutrophils in vitro by PGE₂ (Sakamoto et al., 2004). An EP₄ agonist, ONO-AE1-329, was administered to rats at one of three concentrations (1, 3, or 10 µg/kg via hourly bolus intravenous injection). Infusion of the EP₄ agonist at 3 and 10 µg/kg per hour attenuated lipopolysaccharide (LPS)-induced hypotension and hyporeactivity to norepinephrine. In addition, the EP₄ agonist significantly attenuated the LPS-induced increases in serum concentrations of TNF α and IL-6. Furthermore, EP₄ agonist attenuated increases in left ventricular and aortic expression of mRNAs encoding TNF α and inducible nitric oxide (Sakamoto et al., 2004). In another study, an EP₄-selective agonist, EP4RAG, was administered to rats at doses of 1 or 3 mg/kg, and the effects on cardiac function after myocardial I/R injury were investigated. EP4RAG significantly reduced myocardial infarction area and ischemia and improved left ventricular contraction and dilatation compared with that of the vehicle control. In addition, EP4RAG attenuated the recruitment of inflammatory cells, especially macrophages, and cardiac interstitial fibrosis (Hishikari et al., 2009).

Interestingly, high concentrations of PGE₂ will inhibit platelet aggregation by activating the PGI₂ receptor (IP) nonspecifically. However, low concentrations of PGE₂ potentiate the activation of partially activated platelets, increasing platelet aggregation. This potentiation is primarily through activation of the PGE₂ receptor EP₃ (Gross et al., 2007). Interestingly, prostaglandins may also play a role in myocardial hypertrophy. Overexpression of the PGE₂ receptor gene *Ptger3* in mice using the α -myosin heavy-chain promoter resulted in marked myocardial hypertrophy with increased expression of TGF β , ANP, cardiac ankyrin repeat protein, and connective tissue growth factor with increased interstitial fibrosis in TG mice compared to their WT littermates (Meyer-Kirchrath et al., 2009). These mice had marked increases in end diastolic and end systolic volumes at 5 to 6 weeks of age compared to their WT littermates. In addition, the left ventricular ejection fraction was markedly decreased in the TG mice, suggesting reductions in contractility. Hypertrophic effects of *Ptger3* overexpression in these mice was thought to be mediated by increased activation of the calcineurin signaling pathway. Thus, PGE₂ may be a factor in the development of myocardial hypertrophy. However, to identify whether the reduction of PGE₂ signaling could cause myocardial atrophy and dysfunction, deletion of *Ptger3* in the heart would be required. In another study, the effect of cardiospecific overexpression of EP₃ was studied. In the hearts of these mice, ischemic contracture was markedly delayed compared with WT hearts, and the ischemia-induced increase in left ventricular end-diastolic pressure was reduced by 55%. Creatine kinase and lactate dehydrogenase release were decreased significantly, by 85% and 73%, respectively, compared with WT hearts (Martin et al., 2005).

The importance of PGs in the development of atherosclerosis has been demonstrated using several animal models of atherosclerosis. Increases in PGI₂ are the result of both COX isoforms in the endothelium, although much of the PGI₂ increase in atherosclerosis has been attributed to COX-2 up-regulation at the site of the plaque (Belton et al., 2000). Studies by Kobayashi et al. (2004) using mice mutant for both *Apoe* and either the PGI receptor (*Ptgir*) or the TXA₂ receptor (*Tbxa2r*) has helped to elucidate the importance of prostacyclin and thromboxane in the development of atherosclerosis (Sellers et al., 2010). In *Apoe*^{-/-} *Ptgir*^{-/-} mice, atherogenesis was accelerated compared to *Apoe*^{-/-} mice. In contrast, in *Apoe*^{-/-} *Tbxa2r*^{-/-} mice atherogenesis was delayed compared to *Apoe*^{-/-} mice. The PGI₂ system is essential for endothelial progenitor cells (EPCs) to accomplish their function, and it plays a critical role in the regulation of vascular remodeling in mice (Kawabe et al., 2010). Injury-induced vascular proliferation and platelet activation were enhanced in mice that are genetically deficient in the PGI₂ receptor (IP) but were depressed in mice genetically deficient in the TXA₂ receptor (TP) or treated with a TP antagonist (Cheng et al., 2002). These data collectively indicate that PGI₂ is protective against the atherosclerosis, whereas TXA₂ is important in the initiation and progression of atherosclerosis (Kobayashi et al., 2004; Egan et al., 2005). This is due, in part, to modulation of platelet aggregation and leukocyte–endothelial cell interactions through alterations in the adhesion molecules ICAM-1 and PECAM-1. Studies in *Apoe*^{-/-} *Ptgs1*^{-/-} (COX-1) mice fed a 1% cholesterol diet for 8 weeks showed decreased atherosclerotic lesion development compared to control mice (McClelland et al., 2009). These data implicate COX-1 in the early pathogenesis of atherosclerosis. Interestingly, platelet adhesion to vessel walls was not notably different between double mutant and controls under normal conditions; however, reductions in platelet adhesion were evident after vascular ligation injury in the *Apoe*^{-/-} *Ptgs1*^{-/-} mice compared to controls. This suggests that COX-1 is also important in promoting platelet adhesion to damaged vessel walls and is probably mediated through TXA₂ production (Sellers et al., 2010). Studies in hamsters have also demonstrated that the fact that PGI₂ imparts atheroprotective properties and that PGI₂ analogs retarded atherogenesis in hamsters is consistent with results in genetically engineered mouse studies (Kowala et al., 1993).

Systemic inflammation induces various adaptive responses, including inflammatory tachycardia. The role of various prostanoids in inflammatory tachycardia was examined using mice lacking each prostanoid receptor (Takayama et al., 2005). The tachycardia induced in WT mice by injection of LPS was greatly attenuated in TP- or FP-deficient mice and was completely absent in mice lacking both TP and FP. A TP agonist and PGF_{2α} increased the beating rate of the isolated atrium of WT mice via TP and FP, respectively. In addition, the inflammatory cytokine-induced increase in the beating rate in vitro was significantly diminished in atria from mice lacking either TP or FP. The beta-blocker propranolol did not block the LPS-induced increase in heart rate in WT mice. Inflammatory tachycardia was caused by direct action on the heart of TXA₂ and PGF_{2α} formed under systemic inflammatory conditions (Takayama et al., 2005). A pattern of LPS-induced tachycardia was noted in mice with impaired febrile response and lacking EP₃ (Ushikubi

et al., 1998). This suggests that febrile response and inflammatory tachycardia are independent events. Interestingly, the effects of NSAIDs on inflammatory tachycardia were examined in humans in a randomized double-blind placebo-controlled trial of intravenous ibuprofen [10 mg/kg body weight (maximal dose, 800 mg) given every 6 h in eight doses] in 455 patients who had sepsis, defined as fever, tachycardia, tachypnea, and acute failure of at least one organ system. Ibuprofen treatment reduced levels of PGI₂ and TXA₂ and decreased fever, tachycardia, and oxygen consumption (Bernard et al., 1997).

EFFECTS OF NSAIDs ON THE CARDIOVASCULAR SYSTEM

The COX-1-inhibitory effects of NSAIDs have been associated with decreased platelet aggregation, and these effects have been studied extensively (Campbell et al., 2007). The effects of COX-2 inhibitors, however, have been mixed and often contradictory. In nonclinical studies, this may be due at least in part to variations in study design, genetic backgrounds, drug exposure, and the environment (Sellers et al., 2010). In addition, under normal physiological conditions, alterations in platelet aggregation would probably not be identified with COX-2 inhibition, as was demonstrated in studies of PGI₂ receptor-KO and TXA₂-overexpressing mice (Sellers et al., 2010). The *ex vivo* antiplatelet effects of COX-2 s- and ns-NSAIDs were investigated in healthy volunteers to determine whether NSAIDs antagonize the effect of aspirin (Gladding et al., 2008). All ns-NSAIDs tested (buprofen, indomethacin, naproxen, and tiaprofenic acid) blocked the antiplatelet effect of aspirin. The COX-2 s-NSAIDs sulindac and celecoxib did not demonstrate any significant antiplatelet effect or reduce the antiplatelet effect of aspirin. In another study, the effects of 200 mg twice daily celecoxib on the inhibition of platelet COX-1 activity by aspirin (100 mg daily) were investigated in human patients with osteoarthritis and stable ischemic heart disease. Celecoxib did not interfere with the inhibition of platelet COX-1 activity and function by aspirin despite a comparable suppression of COX-2 *ex vivo* in these patients (Renda et al., 2006). Thus, in studies in healthy humans and normal animal models it is not anticipated that COX-2 inhibition would cause significant reductions in PGI₂ or TXA₂ levels in vascular tissues (Sellers et al., 2010). It is also not anticipated that significant COX-2 inhibition would alter platelet aggregation *ex vivo*.

EFFECTS OF COX-1 AND COX-2 INHIBITION ON MYOCARDIAL ISCHEMIA, INFARCTION, AND THROMBOSIS

Animal models of myocardial infarction generally fall into four main categories: myocardial infarction (MI), ischemia with reperfusion (I/R), I/R with ischemic preconditioning, and I/R with postconditioning (Ferdinandy et al., 2007). Myocardial

infarction is caused by interruption of coronary blood flow to the myocardium. Reperfusion induces an exaggerated hydrolysis of cell membrane phospholipids, causing an unphysiological rise in unesterified arachidonic acid associated with enhanced phospholipase A₂ (PLA₂) activity. Phospholipases A₂ are ubiquitous enzymes that hydrolyze the *sn*-2-acyl bond of phospholipids present in cell membranes and lipoproteins and yield free fatty acids and lysophospholipids, precursors of various bioactive lipid mediators (Balsinde et al., 2002). Myocardial phospholipids serve as primary reservoirs of arachidonic acid (AA), which is liberated through the rate-determining hydrolytic action of cardiac phospholipases A₂. A predominant PLA₂ in myocardium is calcium-independent phospholipase A_{2β} (iPLA_{2β}), which through its calmodulin and ATP-binding domains is regulated by alterations in local cellular calcium concentrations and cardiac bioenergetic status, respectively (Jenkins et al., 2009). PLA₂ have been implicated in playing a critical role in the pathogenesis of myocardial ischemia (Jenkins et al., 2009). Group V secretory phospholipase A₂ (sPLA₂-V) is expressed strongly in the heart and has been found to play an important role in the pathogenesis of myocardial I/R injury in mice, at least partly in concert with the activation of cytosolic PLA₂ (Yano et al., 2011). Myocardial injury and echocardiographic LV dysfunction after I/R were reduced in sPLA₂-V^{-/-} mice, including a reduction in myocardial apoptosis (Yano et al., 2011). The accumulation of AA and the extent of reperfusion injury have been shown to be closely related. The release of the cytosolic enzyme lactate dehydrogenase (LDH) during reperfusion is a measure of loss of cellular integrity. Prolonged duration of ischemia leads to a substantial reduction in ATP (<25% of preischemic value) and accumulation of adenosine and inosine in the myocardium (De Windt et al., 2001).

Contradictory results have been noted in animal models that investigate the effects of COX inhibition in myocardial ischemia (Tables 4-1 to 4-3) (Sellers et al., 2010). The majority of animal models evaluating the cardiac effects of COX inhibition have utilized either MI (complete coronary artery ligation) or I/R (coronary artery ligation for several hours followed by reperfusion) with or without ischemic preconditioning. While reperfusion after ischemia is necessary for tissue survival, reperfusion also results in the release of reactive oxygen species, which may incite further cell death (Sellers et al., 2010). The duration of the ischemic event prior to reperfusion affects the degree of tissue injury (Ferdinandy et al., 2007). Summaries of the drugs, types of studies, and outcomes are given in Tables 4-1 to 4-3 (Sellers et al., 2010). In a study by Inseret et al. (2009), transgenic (TG) mice carrying human COX-2 specifically overexpressed in cardiomyocytes were subjected to transient coronary artery occlusion (without preconditioning) followed by reperfusion. Histopathological and echocardiographic analysis revealed no differences in the phenotype of COX-2 TG and WT mice. Improved contractility during the reperfusion phase and decreased hypercontracture, infarct area, and LDH release were noted compared to that in the WT mice. The magnitude of this effect was similar to that seen with ischemic preconditioning. In both WT and COX-2-overexpressing mice, levels of PGE₂, PGI₂, and PGF_{2α} were increased but not the level of TXA₂. However, only PGE₂ was significantly higher in TG mice than in WT mice, suggesting that this molecule is important in the prevention of cell death during I/R

TABLE 4-1 Examples of Myocardial Infarction (MI) and Ischemia with Reperfusion (I/R) in Various Animal Models with the COX-1 NSAID Acetylsalicylic Acid

Animal model	Model	Study duration	Findings vs. controls	Reference
Rat: Sprague–Dawley	MI	2 weeks	No difference in MI size Increased MI wall thickness No loss of ischemic preconditioning protection	Alhaddad et al., 1995
Dog	I/R	2 h	No difference in MI size	Alcindor et al., 2004
	MI	6 weeks	No difference in MI size	Brown et al., 1983
	MI	Acute	Decreased infarct size	Such et al., 1983
Rat	MI	3 months	No difference in MI size	Saito et al., 2000
Guinea pig	I/R	Isolated perfused heart	Greater dysfunction	Heindl and Becker, 2001
Rabbit	I/R	Isolated heart	Greater dysfunction	Rossoni et al., 2002
Pig Landrace	MI	3 h	No difference in MI size Increased premature ventricular contractions	Wainwright et al., 2002
Pig	I/R	3 h	No difference in MI size	Jaloway et al., 1998

Source: The final, definitive version of this table was published in R. A. Sellers, Z. A. Radi, and N. K. Khan, *Veterinary Pathology*, 47(4), 2010, pp. 601–613. Copyright © Sage Publications. All rights reserved.

events. These data provided direct evidence that constitutive COX-2 expression in cardiomyocytes has a cardioprotective effect that is independent of its influence on hemodynamic factors or on blood constituents (Inserte et al., 2009). PGE₂ receptor (*Ptger3*)–overexpressing mice subjected to ischemia with reperfusion also demonstrated significant protection against ischemia-associated creatine phosphokinase (CPK) release and left ventricular contracture (Meyer-Kirchrath et al., 2009). The authors hypothesized that this is related to the blunting of ischemia-induced endogenous catecholamines by attenuation of the cAMP-mediated calcium influx into cardiomyocytes. However, induced MI in microsomal prostaglandin E₂ synthase 1 (*Ptgs1*) null mice revealed similar effects on post-MI survival, infarct size, or CPK and cardiac troponin I levels compared to control animals, indicating that inflammation-induced PGE₂ may not contribute significantly to the outcome in MI

TABLE 4-2 Findings of Myocardial Infarction (MI) and Ischemia with Reperfusion (I/R) in Various Animal Models with Use of Nonselective Nonsteroidal Anti-inflammatory Drugs

ns-NSAID	Animal model	Model	Study duration	Findings controls	Reference
Azapropazone	Rat	MI	48 h	Decreased infarct size	Estrela et al., 1987
	Rabbit	I/R	60 min	Decreased infarct size	Mousa et al., 1990
Ibuprofen	Dog	I/R	5 h	Limitation of infarct size	Mousa et al., 1989
	Rat	Isoprenaline hydrochloride induced	1, 5, 12, 21 days	Increased infarct size	Lal and Sharma, 1992
	Cat	MI	24 h	Decreased infarct size	Flynn et al., 1984
Meclofenamate	Dog	MI	Acute	No change in infarct size	Such et al., 1983
	Dog	MI	6 weeks	Decreased infarct size; increased scar thinning	Brown et al., 1983
	Dog	MI	Acute	Decreased infarct size	Such et al., 1983
Meloxicam	Rabbit	I/R	Isolated heart	Greater dysfunction than control	Rossoni et al., 2002
	Rabbit	I/R	Isolated heart	No change in infarct size	Liu et al., 1992
	Guinea pig	I/R	Isolated perfused heart	No difference	Heindl and Becker, 2001

Naproxen	Dog	MI	3 days	No difference in infarct size	Bolli et al., 1981
	Rabbit	I/R	Isolated heart	No difference	Aitchison and Coker, 1999
Indomethacin	Rabbit	I/R	3 days	No difference in infarct size	Shizukuda et al., 1991
		I/R	Isolated rabbit heart	No difference in infarct size	Aitchison and Coker 1999
	Pig	I/R	2 h	No difference in infarct size Abolished weak ischemic preconditioning	Gres et al., 2002
		I/R	2 h	No difference in infarct size	Jalowy et al., 1998
		I/R	3 h	Increased infarct size	Hohlfeld et al., 1993
	Dog	MI	6 h	No difference in infarct size	Fiedler and Mardin, 1985
		MI	2 days	Increased infarct size	Jugdutt et al., 1979
		MI	7 days	Increased infarct size, decreased scar thinning	Hammerman et al., 1983
		MI	6 weeks	Increased scar thinning	Such et al., 1983
Sulfimpyrazon	Dog	MI	3 days	No difference in infarct size	Bolli et al., 1981
	Rat	MI	3 weeks	Decreased infarct size	Innes and Weisman, 1981

Source: The final, definitive version of this table was published in R. A. Sellers, Z. A. Radi, and N. K. Khan, *Veterinary Pathology*, 47(4), 2010, pp. 601–613. Copyright © Sage Publications. All rights reserved.

TABLE 4-3 Findings of Myocardial Infarction (MI) and Ischemia with Reperfusion (I/R) in Various Animal Models with COX-2 Selective NSAID Use

COX-2 s-NSAID	Animal model	Model	Study duration	Findings vs. controls	Reference
Celecoxib	Pig	MI	6 weeks	LV rupture	Timmers et al., 2007
	Dog	I/R	3 h	No difference in infarct size Abolished ischemic preconditioning	Alcindor et al., 2004
Parecoxib	Rabbit	I/R	Isolated heart	Greater dysfunction than control	Rossoni et al., 2002
	Mice: B6	MI	7 days	↓ apoptosis in peri-infarct region	Abbate et al., 2007
	Rat: Wistar	MI	7 days	Attenuation of LV dysfunction vs. control	Straino et al., 2007
				↓ apoptosis in peri-infarct region	
DFU	Rat: Lewis	MI	3 months	Improved LV function and ↓ infarct size	Saito et al., 2004
	Rat: Lewis	MI	3 days	↓ infarct size	Saito et al., 2003
DuP-697	Rabbit	I/R	Isolated heart	Greater dysfunction than control	Rossoni et al., 2002
	Mice: B6/J	MI	2 weeks	No difference in infarct size	LaPointe et al., 2004
NS-398	Mice: B6129F2/J	I/R	24 h	No difference in infarct size Abolished ischemic preconditioning	Guo et al., 2000
Merck tricyclic	Mice: CD-1	Adriamycin-induced heart failure	35 days	Attenuated progression of heart failure	Delgado et al., 2004
Rofecoxib	Mice	MI	2 weeks	No difference in infarct size Abolished ischemic preconditioning	LaPointe et al., 2004
SC-236	Dog	MI	30 min	No different from control	Camieto et al., 2009
	Rat: Sprague-Dawley	Doxirubicin	Acute	Aggravated acute cardiac injury	Dowd et al., 2001
SC-58125	Guinea pig	I/R	Isolated perfused heart	No effect on cardiac function	Heindl and Becker, 2001

Source: The final, definitive version of this table was published in R. A. Sellers, Z. A. Radi, N. K. Khan, *Veterinary Pathology*, 47(4), 2010, pp. 601–613. Copyright © Sage Publications. All rights reserved.

(Wu et al., 2009). Adiponectin (APN) is an adipocyte-specific cytokine that suppresses inflammatory responses and myocardial production of TNF α *in vitro* and *in vivo* (Shibata et al., 2005). The role of COX-2 signaling in the cardioprotective action of adiponectin *in vivo* was investigated. The COX-2 s-NSAID NS-398 was given daily via intraperitoneal injections to mice in a 5-mg/kg dose from 3 days before surgery until study termination. NS-398 did not affect infarct size in APN-KO mice, but abrogated the infarct-sparing actions of exogenous adiponectin by 53% in WT and 48% in APN-KO mice. These data indicated that COX-2-dependent signaling contributes to the protective action of adiponectin in myocardial I/R injury through the suppression of inflammatory cytokines and improved cell survival (Shibata et al., 2005).

The findings from COX inhibition in acute MI studies can be divided into short- and long-term findings, with most studies having a duration of less than 7 days (Sellers et al., 2010). Myocardial infarction and congestive heart failure (CHF) were induced in Lewis rats by ligating of the left coronary artery. Treatment of rats with the COX-2 s-NSAID 5,5-dimethyl-3-(3-fluorophenyl)-4-(4-methylsulfonyl-2(5H)-fluranone (DFU), at 5 mg/kg per day for 3 days and three months revealed that DFU-treated rats had a smaller infarct size, with significant improvement in left ventricular (LV) end-diastolic pressure and LV systolic pressure over that of vehicle-treated animals (Saito et al., 2003, 2004). Improved cardiac function and cardioprotective effects were noted in Wistar rats given the COX-2 s-NSAID parecoxib 0.75 mg/kg intraperitoneally for 5 days beginning 2 days postcoronary artery occlusion. These rats had smaller end-diastolic and end-systolic diameters and greater fractional shortening. Systolic thickness in the anterior infarct wall was also significantly greater in the parecoxib-treated animals, whereas the posterior wall was not significantly affected. Aneurysmal dilatation of the left ventricle was more frequent in saline-treated versus parecoxib-treated animals. In addition, parecoxib treatment was associated with lower apoptotic rates and preservation of arteriolar density in the peri-infarct area (Straino et al., 2007). The effects of COX-2 inhibition after prolonged heart failure were investigated in Wistar rats. These rats underwent coronary artery ligation to induce ischemic congestive heart failure. Rats were treated one year after the ligation with daily intraperitoneal parecoxib injections at a dose of 0.75 mg/kg per day for 7 days. An echocardiogram to measure end-diastolic diameter showed no changes, and there was an increase in myocardial function in the peri-infarct area (Abbate et al., 2007). In another study, parecoxib was given to mice at an intraperitoneal dose of 0.75 mg/kg per day for 7 days. Parecoxib reduced mortality, improved ventricular function, reduced LV cavity size, and reduced peri-infarct apoptosis in this mouse model of acute MI (Salloum et al., 2009).

Dogs, rats, and mice that undergo several cycles of ischemic preconditioning (4 to 5 min of ischemia followed by 4 to 5 min of reperfusion repeated four or five times) have reduced myocardial injury when this preconditioning is followed by prolonged ischemia with reperfusion (Fiedler et al., 1985; Guo et al., 2000; Alcindor et al., 2004; Sellers et al., 2010). The ischemic preconditioning effect is lost if celecoxib or NS-398 is administered prior to surgery, while the protective effect of preconditioning on the myocardium is not lost with pretreatment with

ASA (Guo et al., 2000; Alcindor et al., 2004). This demonstrates the importance of COX-2, not COX-1, in ischemic preconditioning associated myocardial protection. Studies of the effect of COX inhibition in I/R without preconditioning are also limited. Many of these studies focus on the early or immediate effects of COX inhibition in reperfusion rather than on the long-term consequences in remodeling (Sellers et al., 2010). A study in dogs treated with the COX-2 s-NSAID rofecoxib prior to 3 h of cardiac ischemia followed by 30 min of reperfusion showed no detectable differences in CPK-MB or troponin I, biomarkers of cardiac injury, compared to controls (Carnieto et al., 2009), suggesting that acute injury is not altered in I/R injury with COX-2 inhibition. A longer-term study in rats exposed to 8 h of cardiac ischemia followed by 2 weeks of reperfusion and ASA therapy revealed no differences in infarct size or septal or left ventricular wall thickness compared to vehicle-treated animals (Alhaddad et al., 1995).

Landrace pigs given 10 mg/kg aspirin (ASA) orally for 7 days before MI showed no difference in infarct size or heart function compared to vehicle-treated animals. However, those treated with a 60-mg/kg oral dose of a nitro derivative of ASA, NCX 4016, did have reduced infarct size following combined ischemia and reperfusion compared to ASA- or vehicle-treated pigs (Wainwright et al., 2002). In dogs, the effects of ASA on cardiac infarct were investigated after intravenous (IV) administration of aspirin at a dose of 3 mg/kg 10 min before occlusion of the left anterior descending coronary artery. Aspirin-treated dogs did not differ from control dogs in percent ventricle at risk, percent infarct weight/left ventricle, or percent infarct weight/weight of ventricle at risk (Bonow et al., 1981). In an acute model of transmural infarction in anesthetized open-chest dogs, the effects of various COX inhibitors on infarct size were evaluated. ASA, 30 mg/kg IV, and meclofenamic acid, 1 mg/kg IV, decreased infarct size without altering other parameters except for an increase in retrograde flow produced by ASA (Such et al., 1983). Indomethacin, 10 mg/kg IV, increased infarct size and ectopic rate and decreased retrograde flow while developing greater tachycardia and less hypotension than in controls (Such et al., 1983). In another study, mongrel dogs underwent 180 min of left anterior descending coronary artery occlusion followed by 30 min of reperfusion. Dogs were treated with rofecoxib at a single 50-mg/day dose that was given orally with their chow during the 48 h preceding the surgical procedure. Rofecoxib was not associated with early detrimental effects on the hemodynamic profile or the gross extent of infarction (Carnieto et al., 2009). Experimental studies to assess the effects of ibuprofen on MI and scar thinning were conducted. Four groups of dogs were studied: a control (untreated) group; ibuprofen 12.5 mg/kg IV 15 min and 6, 12, 18, and 24 h after occlusion (high dose); ibuprofen 12.5 mg/kg IV 15 min and 3 h after occlusion (low dose); and aspirin 30 mg/kg IV 15 min and 3 h after proximal left anterior descending coronary artery occlusion for 6 weeks. Assessment of infarct size was determined at 6 weeks post-MI and revealed no difference in infarct size from control animals in ASA-treated dogs and reduced infarct size in ibuprofen-treated dogs (Brown et al., 1983). Dogs treated with ibuprofen for up to 24 h or ASA for up to 3 h after MI had increased scar thinning 6 weeks after MI compared to vehicle-treated animals (Brown et al., 1983).

The effects of thrombus formation can be devastating and lead to myocardial infarction and stroke. The effects of NSAIDs on platelet aggregation and thrombosis have been investigated in human and animal models. The effects of celecoxib on COX-1-dependent platelet TXA₂ and on systemic biosynthesis of PGI₂ production were investigated in healthy volunteers. Celecoxib was given at doses of 100, 400, or 800 mg and ibuprofen in an 800-mg dose. Ibuprofen (but not celecoxib) significantly inhibited TXA₂-dependent aggregation. Neither NSAID altered platelet aggregation induced by a thromboxane mimetic, U46619. Ibuprofen reduced serum TXB₂ and urinary excretion of the major TX metabolite (McAdam et al., 1999). Thus, celecoxib up to 800 mg did not inhibit COX-1-dependent platelet aggregation and function but suppressed excretion of both the hydration product, 6-keto PGF_{1α}, and the major urinary metabolite of prostacyclin, 2,3 dinor-6-keto PGF_{1α} (PGI-M). Prostacyclin receptor-deficient mice show increased thrombosis (Murata et al., 1997). In an African green monkey thrombosis model, animals were exposed for 5 days to placebo, rofecoxib, celecoxib, naproxen, or aspirin and were evaluated following electrolytic injury to the carotid artery and jugular vein. Neither rofecoxib nor celecoxib had any effect on either arterial or venous thrombosis compared to placebo. Animals treated with naproxen, however, demonstrated significantly prolonged times to both arterial and venous thrombosis compared to placebo. The time to thrombosis in the aspirin group had a significantly prolonged time to arterial thrombosis and a numerically increased time to venous thrombosis. These data suggest that COX-2 s-NSAIDs have no effect on thrombosis, and ns-NSAIDs exhibit antithrombotic effects similar to those of aspirin (FDA, 2005).

Rofecoxib (Vioxx) and celecoxib (Celebrex) were the first COX-2 s-NSAID inhibitors to reach the market. Celecoxib and rofecoxib were approved in 1998 and 1999, respectively. Celecoxib exhibits anti-inflammatory, analgesic, and antipyretic activities in animal models and was approved in the United States in December 1998 and in Europe (Sweden) in December 2000 for the indications of symptomatic relief in the treatment of osteoarthritis (OA) and rheumatoid arthritis (RA) in humans. In subsequent years, the U.S. Food and Drug Administration (FDA) placed a boxed warning on all prescription NSAIDs. In humans, the cardiovascular (CV) events (MI, stroke, CV deaths, and peripheral events) of rofecoxib were analyzed in a randomized long-term Vioxx gastrointestinal outcomes research (VIGOR) clinical trial. In the VIGOR study, rofecoxib was used at a daily dose of 50 mg ($n = 4047$) and naproxen was used at a daily dose of 100 mg ($n = 4029$). Compared with naproxen, rofecoxib showed increased CV risk events (MI, unstable angina, ischemic stroke, and transient ischemic attacks) (FDA, 2001). In the Adenomatous Polyp Prevention on Vioxx (APPROVe) multicenter randomized placebo-controlled double-blind trial, a total of 2586 patients with a history of colorectal adenomas underwent randomizations in which 1287 received 25 mg of rofecoxib daily, and 1299 received placebo. Thrombotic, MI, and ischemic cerebrovascular events were increased in the rofecoxib groups (Bresalier et al., 2005). In a retrospective population-based cohort study of elderly adults (<65 years old), the influence of various COX-2 s- and ns-NSAIDs on the risk for a first myocardial infarction was assessed. An increased risk for acute MI in users of rofecoxib with no history of MI was noted (Lévesque et al., 2005).

The effects of long-term treatment (up to one year) with celecoxib and the ns-NSAIDs ibuprofen and diclofenac were investigated in the Celecoxib Long-Term Arthritis Safety Study (CLASS) (White et al., 2002). Celecoxib was given 400 mg twice daily ($n = 2320$), ibuprofen 800 mg three times daily, or diclofenac 75 mg twice daily ($n = 3987$). The incidences of serious CV thromboembolic events were similar, and not significantly different, between celecoxib and ns-NSAID (combined or individually). Therefore, rates of serious adverse cardiac events, regardless of causality, were not different between the treatment groups (White et al., 2002). In another study, CV events (MI, stroke, or heart failure) among 2035 patients with a history of colorectal neoplasia were analyzed. This Adenoma Prevention with Celecoxib (APC) study compared the efficacy and safety of 200 mg of celecoxib twice daily, 400 mg of celecoxib twice daily, and placebo in reducing the occurrence of adenomatous polyps in the colon and rectum one and three years after endoscopic polypectomy. CV events were noted in 7 of 679 patients in the placebo group compared with 16 of 685 patients who received 200 mg of celecoxib twice daily and with 23 of 671 patients who received 400 mg of celecoxib twice daily (Solomon et al., 2005). Thus, a CV risk was shown in patients with colorectal neoplasia receiving celecoxib after approximately one year of continuous treatment. However, differing results of CV event were noted in the Prevention of Colorectal Sporadic Adenomatous Polyps (PreSAP) clinical trial, in which celecoxib was given daily in a single 400-mg dose (Arber et al., 2006). Adjudicated serious CV events occurred in 2.5% of subjects in the celecoxib group and 1.9% of those in the placebo group (Arber et al., 2006). A metaanalysis of randomized clinical trials of the CV events risk in patients receiving celecoxib was conducted. Such analyses failed to demonstrate an increased CV risk with celecoxib relative to placebo and demonstrated a comparable rate of CV events with celecoxib treatment compared with ns-NSAIDs (White et al., 2007). There is an ongoing study to assess the long-term CV safety of the COX-2 s-NSAID celecoxib versus ns-NSAIDs. The Prospective Randomized Evaluation of Celecoxib Integrated Safety Versus Ibuprofen or Naproxen (PRECISION) trial is designed to evaluate the CV safety of celecoxib, ibuprofen, and naproxen. PRECISION is a randomized double-blind triple-dummy multinational multicenter study and will include approximately 20,000 patients with symptomatic osteoarthritis or rheumatoid arthritis at high risk for, or with, established cardiovascular disease. The primary endpoint of the study is the composite of cardiovascular death, nonfatal myocardial infarction, or nonfatal stroke (Becker et al., 2009).

Collectively, nonclinical studies suggest that COX-2 inhibition may reduce the inflammatory response and infarct size at the site of acute MI. COX-1 inhibition may have little impact on short- and long-term effects of MI. The reduction in local inflammation may be acutely valuable but may have long-term consequences in tissue breakdown and scar formation (Sellers et al., 2010). While the findings after long-term inhibition of COX-2 after infarction are variable, there is a trend in these studies indicating decreased collagen density and normal wall remodeling at the infarct site (Sellers et al., 2010). COX-2 is an important mediator in the protective effect of preconditioning in I/R studies. However, neither COX-1 nor COX-2 inhibition appears to affect the outcome in I/R studies

significantly in several animal species (Sellers et al., 2010). No evidence of COX-2 s-NSAIDs prothrombotic potential was observed in acute animal models of thrombosis.

EFFECTS OF COX-1 AND COX-2 INHIBITION ON CORONARY BLOOD FLOW AND BLOOD PRESSURE

The effects of COX inhibition on local blood flow in the coronary artery have been evaluated in dog models. These models have evaluated the ability of COX inhibitors to modulate AA- and acetylcholine (ACH)-induced coronary vasodilatation and blood flow. The effects of celecoxib and aspirin administration on left circumflex coronary artery blood flow and thrombosis were evaluated in a dog model (Hennan et al., 2001). Before the administration of celecoxib, the intracoronary administration of 30 and 100 μg of AA or 100 and 300 ng of ACH, an endothelium-dependent vasodilator, increased coronary blood flow. In the same animal, 60 min after intravenous administration of 3 mg/kg of celecoxib, the vasodilator responses to 30 and 100 μg of AA were decreased, whereas the responses to ACH remained unchanged. Time controls were used to evaluate coronary responses over the course of the experiment, and no significant changes in the vasodilator responses to AA or ACH were observed (Hennan et al., 2001). Intracoronary administration of AA (3 to 300 μg) caused a dose-related increase in arterial volume blood flow, characterized as a dose-dependent increase in peak flow, followed by a dose-related prolongation in the vasodilator response. Both the peak response to AA and the duration of the response were suppressed equally by SC-560, a COX-1 inhibitor, at 0.3 mg/kg IV, nimesulide (5 mg/kg IV), and naproxen (3 mg/kg IV). The changes in volume blood flow to graded 10- to 300-ng doses of ACH were not altered after the administration of SC-560, nimesulide, or naproxen (Hong et al., 2008). Thus, AA-induced coronary blood flow is attenuated by pretreatment with ASA, nimesulide, naproxen, and celecoxib (Hennan et al., 2001; Hong et al., 2008). In contrast, coronary vasodilation was induced by direct intracoronary injection of ACH and AA in control animals. This ACH-induced coronary vasodilatation (nitric oxide-dependent pathway) in dogs was unaffected by pretreatment with 10 mg/kg naproxen and 15 mg/kg SC-58236, an experimental COX-2 s-NSAID, and SC-58236 failed to attenuate significantly either AA- or ACH-induced vasodilatation (Gross and Moore, 2004). These data suggest that the effects of AA, at least in the dog, are primarily COX-1 dependent.

As described previously, COX-1 and COX-2 have effects on localized vascular bed pressure. Systemic BP is maintained primarily by the RAAS, and hypertension is often due to abnormal renal vascular control homeostasis (Radi, 2009). Genetically engineered mice with reductions (“knockdown”) in COX-2 expression to levels interpreted to be similar to that which would be induced by COX-2 s-NSAID administration had no alterations in mean arterial pressure, heart rate, or diastolic or systolic pressure in knockdown mice compared to WT littermates (Seta et al., 2009; Sellers et al., 2010). These two studies indicate that COX-2 is

essential for normal cardiac function, but reductions in COX-2 expression (compared to deletion of COX-2 expression) do not significantly affect myocardial function (Sellers et al., 2010). Mice that overexpress COX-2 in the heart demonstrate no differences in cardiac function, weight, or histopathology under normal conditions (Inserre et al., 2009). *Drosophila* serves as a model for human cardiac pharmacology (Wolf et al., 2006). Celecoxib effects on cardiac rhythm in *Drosophila* hearts and rat cardiomyocytes (the cardiomyocytes were obtained from rat fetuses at gestation stage 20 just 1 day before birth) were investigated. Heart rate in *Drosophila* was reduced significantly by exposure to 3 μM celecoxib. Celecoxib has been shown to predispose to arrhythmia in *Drosophila* hearts and in rat neonatal cardiomyocytes in vitro by modulating delayed rectifier K^+ channel function. However, this has been attributed to an off-target effect independent of COX pathways because *Drosophila* lacks cyclooxygenases (Frolov et al., 2008). Studies in COX-1 null mice revealed that BP in COX-1^{-/-} mice was near normal and that under conditions of reduced sodium intake these mice have a mild, but significant reduction in BP over control mice (Athirakul et al., 2001). The data in this study indicate that COX-1 is important in maintaining BP indirectly by maintaining sodium retention (Sellers et al., 2010). In addition, blood pressure has a circadian pattern, with reductions in BP during sleep (Kawada et al., 2005). COX-1 null mice have impaired reductions in BP during sleep (Kawada et al., 2005), indicating that COX-1 mediates a suppressed sympathetic nervous activity and enhanced nitric oxide and may be important in maintaining normal circadian rhythms in blood pressure. When COX-2 expression is suppressed to an extent similar to that achieved with COX-2 s-NSAIDs, COX-2-knockdown mice have no notable alterations in systemic BP compared to those in control mice (Seta et al., 2009). These data indicate that under normal physiological conditions, COX effects on systemic blood pressure are probably mediated primarily through its actions on renal sodium retention and excretion (Sellers et al., 2010).

The effect of COX inhibition on blood pressure in nonclinical species has been variable. Studies in normal animals indicate that ns-NSAIDs and/or COX-2 s-NSAIDs have little effect on systemic arterial BP (Manohar et al., 1996; Black et al., 1998; Birck et al., 2000; Brands et al., 2001). While blood pressure studies in dogs appear to be consistent, there is reported variation between rat strains in the effects of COX-2 inhibition on blood pressure (Sellers et al., 2010). A study compared the effects of diclofenac, celecoxib, and rofecoxib in Dahl salt-sensitive rats. Rats were fed 4% NaCl-enriched chow for 8 weeks, and from week 6 to week 8, NSAIDs were given in food: diclofenac (6 mg/kg per day), rofecoxib (2 mg/kg per day), celecoxib (25 mg/kg per day). By 5 and 8 weeks, BP increase in DS rats was more pronounced with rofecoxib and diclofenac treatment, but was attenuated in the celecoxib-treated rats. After 8 weeks of treatment, celecoxib slightly (approximately 4%), but significantly, reduced systemic BP compared to controls, and diclofenac and rofecoxib minimally but significantly increased systemic BP (approximately a 1% increase) (Hermann et al., 2005). In addition, celecoxib, but not rofecoxib or diclofenac, normalized proteinuria, decreased renal injury, and reduced cellular inflammation in this rat model of salt-sensitive hypertension (Hermann et al., 2005). In another study, COX-2 inhibition for 26 days using NS-398 at 1 mg/kg per day

in Hannover Sprague–Dawley rats had no effect on systemic BP and MAP, and the rats remained normotensive throughout the study (Vaneckova et al., 2005). In a 2K1C model of renovascular hypertension using Wistar–Kyoto (WKY) or Sprague–Dawley rats, COX-2 inhibition using 1 and 15 mg/kg celecoxib per day and 1 mg/kg NS-398 per day, has been shown to be effective in the kidney, and up to 6 weeks of treatment resulted in no significant effect on BP (Hartner et al., 2003; Richter et al., 2004). In contrast, COX-2 inhibition has been found to increase BP in normotensive and hypertensive Wistar rats (Muscara et al., 2000; Höcherl et al., 2002b). Daily oral treatment of rofecoxib at a dose of 10 or 30 mg/kg resulted in a significant increase in systolic BP in normotensive WKY rats after 1 week compared to vehicle-treated rats. Rofecoxib at a dose of 3 mg/kg increased BP after 2 weeks, whereas 1 mg/kg of rofecoxib increased systolic BP after 3 weeks of the beginning of the treatment compared to vehicle-treated rats. At the end of the treatment the mean systolic BP of rofecoxib-treated rats was 15, 17, 21, and 23 mmHg higher than that of vehicle-treated rats, respectively (Höcherl et al., 2002b). Hypertensive rats were treated orally with celecoxib at 10 mg/kg, a dose selected based on inflammatory PGE₂ synthesis and inhibition of COX-2 activity, and BP measurements were performed using the tail cuff method prior to initiating treatment and at 1-week intervals for a total of 3 weeks. Hypertension was induced through the addition of *N*-nitro-*L*-arginine methyl ester (L-NAME) to the drinking water. Two weeks after beginning treatment with L-NAME, the rats began to receive celecoxib for 3 weeks. Daily treatment with celecoxib resulted in a significant increase in BP over that in the vehicle-treated group at all three time points, the greatest increase being seen at the end of the fifth week of the study (mean increase of 33 ± 2 mmHg) (Muscara et al., 2000).

It may be that some COX-1 inhibition along with COX-2 may be important to prevent thrombotic events in at-risk populations (Krotz et al., 2005). Salt-sensitive (DS) rats were fed a high-sodium diet (4% NaCl) for 56 days. From days 35 to 56, diclofenac (6 mg/kg per day), rofecoxib (2 mg/kg per day), or celecoxib (25 mg/kg per day) was added to the chow. Blood pressure increased with the sodium diet in the DS groups, which was more pronounced after diclofenac and rofecoxib treatment but was slightly decreased by celecoxib. In addition, celecoxib improved endothelial dysfunction and reduced oxidative stress (Hermann et al., 2003). This may point to differential effects of COX-2 s-NSAIDs in salt-induced hypertension (Hermann et al., 2003). Cardiac dysfunction and BP were evaluated in male Sprague–Dawley rats undergoing IV infusion of lipopolysaccharides. Rats were divided into two groups: the control group and the treated group, which received rofecoxib at 20 mg/kg. A significant decrease in BP and myocardial dysfunction was observed in the control group, whereas no changes were observed in the rofecoxib-treated group (Höcherl et al., 2002a).

In normotensive human patients, blood pressure and renal function were not altered significantly by short-term treatment with standard doses of celecoxib 200 mg twice a day (Dilger et al., 2002). The contribution of COX-2 activity to endothelial dysfunction was investigated in human patients with hypertension. Brachial artery vasodilator function was evaluated using ultrasound in 29

hypertensive patients before and after treatment with celecoxib at 200 mg in a randomized double-blind study. Brachial artery flow-mediated dilation improved from a baseline 3 h after the first dose and after 1 week of treatment with celecoxib (Widlansky et al., 2003). Thus, COX-2 may contribute to endothelial dysfunction in hypertension, and treatment with a COX-2 s-NSAID could have a beneficial effect (Widlansky et al., 2003). The effects of celecoxib 400 mg daily for 2 weeks on endothelial function, measured by high-resolution ultrasound, in patients with severe coronary artery disease were studied in a double-blind placebo-controlled crossover design. In addition, plasma levels of oxidized LDL (ox-LDL) and high-sensitivity C-reactive protein (hs-CRP), both of which have been implicated in atherogenesis and represent sensitive markers of oxidative stress and low-grade chronic inflammation, respectively, were studied. Celecoxib significantly improved endothelial function, and both ox-LDL and hs-CRP were lower after celecoxib therapy (Chenevard et al., 2003). The effects on 24-h mean systolic BP of celecoxib (200 mg once daily), rofecoxib (25 mg once daily), and naproxen (500 mg twice daily) treatment for 12 weeks was investigated in patients with type 2 diabetes, hypertension, and osteoarthritis in a double-blind randomized trial. The mean 24-h systolic BP following 6 weeks of therapy was increased significantly by rofecoxib, but not by celecoxib or naproxen (Sowers et al., 2005).

The effects of COX inhibition on aged humans and animals may be of greater significance clinically (Sellers et al., 2010). Studies of the aortic endothelium from aged rats demonstrated increased *Ptsg1* (COX-1) and *Ptsg2* (COX-2) gene expression (Kim et al., 2001; Tang et al., 2008). In the rat, COX-2 mRNA and protein levels in the heart increased with aging, whereas those of COX-1 showed no change (Kim et al., 2001). In the aorta of Wistar-Kyoto rats, aging caused overexpression of COX-1 and COX-2 in endothelial cells and of COX-1 and PGE₂ and EP₄ receptors in smooth muscle cells. Hypertensive rats had increased expression of COX-1 in endothelial cells and PGD₂, EP₃, and EP₄ receptors in smooth muscle cells (Tang et al., 2008). Thus, aortic endothelial cells from hypertensive rats had increased COX-1 gene expression, and this increased COX-1 expression may explain why, in aging, endothelial cells tend to secrete more COX-derived vasoconstrictive prostanoids than in younger animals (Kim et al., 2001; Tang et al., 2008). Studies in aged animals are uncommon; thus, studies of the effects of COX inhibition in aged animals are limited (Sellers et al., 2010). Interestingly, one study found that in aged humans (mean age 66 ± 3 years) with coronary artery disease, COX-2 inhibition was associated with improved coronary artery endothelium-dependent vasodilation (Chenevard et al., 2003). Some studies have indicated that COX inhibition may attenuate the effects of some antihypertensive therapeutics. In a 6-week randomized parallel-group double-blind trial of COX-2 inhibitors in human patients taking antihypertensives, 200 mg/day celecoxib or 25 mg/day rofecoxib increased both systolic and diastolic BP, but to different severities depending on the drug (e.g., the effects on blood BP were greater in patients treated with rofecoxib than in those treated with celecoxib) (Whelton et al., 2001, 2002). Patients on ACE inhibitors treated with high doses of celecoxib had no statistically significant effects on BP (White et al., 2002).

EFFECTS OF COX-1 AND COX-2 INHIBITION ON ATHEROGENESIS

Studies in atherosclerotic mouse models have been divided into evaluation of initiation and evaluation of progression (Sellers et al., 2010). Studies in *Apoe*-null mice have demonstrated that COX-1 inhibition appears consistently to modify the initiation and/or progression of atherosclerosis (antiatherogenic) (Belton et al., 2003; Cyrus et al., 2006). Furthermore, the importance of TXA₂ and COX-1 in atherogenesis is evident in low-density lipoprotein receptor-deficient mice on a high-fat diet (*Ldlr* deletion mice) treated with TXA₂ receptor and COX-1 inhibitors. When treated with COX-1 inhibitor, these mice using SC-560 at 15 mg/kg per day and the TP antagonist BM-573 at 10 mg/L for up to 12 weeks have reductions in atherogenesis compared to untreated animals (Cyrus et al., 2007). In cholesterol-fed rabbits, 25 mg/day indomethacin, an ns-NSAID, given for 12 weeks significantly reduced platelet aggregation and urinary TXB₂, 6-keto-PGF_{1α}, and PGF_{2α} excretion, reduced the progression of atherosclerotic lesions, and improved endothelium-mediated vascular responses (Srisawat et al., 2003). COX-2 inhibition with 5 mg/kg rofecoxib once daily for 3 days promoted early atherosclerotic lesion formation in *Ldlr*-deficient mice, and COX-2 inhibition for 3 weeks with Merck Frosst (MF) tricyclic at 12 or 24 mg/kg per day increased both the early atherosclerotic lesion area and atherosclerotic plaque destabilization in *Apoe*-deficient mice (Rott et al., 2003; Burtleigh et al., 2005b). In *Apoe*-deficient mice, COX-2 inhibition using SC-236 at 15 mg/kg per day demonstrated that despite selective reduction in PGI₂ generation, there was no effect on lesion development or platelet interactions with the vessel wall (Belton et al., 2003). Other studies demonstrated that chronic (up to four months) administration of COX-2 s-NSAIDs (celecoxib and MF-tricyclic) did not influence or have an effect on the composition of advanced atherosclerotic lesions in the same *Apoe* mouse strain (Pratico et al., 2001; Olesen et al., 2002; Bea et al., 2003). Treatment of *Apoe*-deficient mice with 900 ppm of celecoxib for 16 weeks led to a significant, 81% reduction in atherosclerotic lesions in the proximal aortas (Jacob et al., 2008). In another *Apoe*-deficient mouse atherosclerosis model, celecoxib was provided at a dose of 75 mg/kg (according to the authors, this dose is equivalent to a daily dose of 400 mg for a 60-kg person) and/or atorvastatin at a dose of 20 mg/kg body weight (according to the authors, this dose is equivalent to a daily dose of 80 mg for a 60-kg person) for 12 weeks (Raval et al., 2010). Diet supplemented with a combination of atorvastatin and celecoxib led to a significant reduction in established plaque in the aortas of these mice. Thus, combining statins with COX-2 inhibitors provides a greater benefit in reducing the size of established plaque than either atorvastatin or celecoxib alone, which appears to be due, in part, to a reduction in inflammation and adhesion molecules (Raval et al., 2010). In a carotid artery balloon injury Sprague–Dawley rat model, 50 mg/kg celecoxib was administered daily by oral gavage for 3 days before the balloon injury and were continued for 2 weeks after injury. At 2 weeks after injury, the vehicle-treated group had abundant neointimal hyperplasia. The celecoxib-treated group showed significant suppression of neointimal hyperplasia. In contrast, the

aspirin-treated group (50 mg/kg) showed no significant reduction in neointimal hyperplasia. The levels of phosphorylated Akt and GSK-3 β , both molecules that regulate cellular processes such as apoptosis, proliferation, migration, and survival, were significantly suppressed in the celecoxib-treated group compared with the vehicle- and aspirin-treated groups (Yang et al., 2004). Ultimately, the data from animal models suggest that while COX-2 is highly expressed in atherosclerotic plaques, it probably plays a lesser role in lesion development and progression than does COX-1. In healthy human volunteers, sulindac and celecoxib had no effect on the antithrombotic effect of ASA (Wilner et al., 2002; Gladding et al., 2008).

CONCLUSIONS

COX-1 and COX-2 isoforms are essential in normal cardiovascular system physiology. Postmarketing withdrawal of some COX-2 s-NSAIDs (e.g., rofecoxib and lumiracoxib) due to concerns of CV complications has raised a question as to why no adverse CV findings were identified in nonclinical studies prior to clinical use. There are drug-specific differences that may have played a role in the CV mechanism and the magnitude of CV risk. Chemically, rofecoxib and celecoxib belonged to a diaryl-substituted class of compounds. However, celecoxib is a sulfonamide-substituted 1,5-diaryl pyrazole compound, whereas rofecoxib is a methylsulfonylphenyl compound. Extensive review of nonclinical toxicology studies, which included hemodynamic and detailed morphological assessments, revealed no treatment-related adverse findings in cardiovascular function or histopathology at a broad range of doses of celecoxib, valdecoxib, and rofecoxib after repeated dosing in multiple rodent and nonrodent species (Sellers et al., 2010). The two-year chronic toxicity studies indicated that standard nonclinical safety pharmacology and toxicology studies in multiple species at broad dose ranges and up to two years in duration did not predict the adverse CV safety events identified in long-term clinical studies (Sellers et al., 2010). NSAID effects on infarct size and MI in animal models have been variable. Animal models of cardiovascular diseases and genetically engineered mice have provided some indirect information in understanding potential functions of COX-mediated PGs in homeostasis and disease (Sellers et al., 2010). However, whereas disease models may be considered in assessing the overall safety profile of a new therapeutic candidate, species and strain variations in response may not be predictive of human risk (Sellers et al., 2010).

REFERENCES

- Abbate A, Santini D, Biondi-Zoccai GG, Scarpa S, et al. Cyclo-oxygenase-2 (COX-2) expression at the site of recent myocardial infarction: Friend or foe? *Heart* 2004;90:440–443.
- Abbate A, Salloum FN, Ockaili RA, Fowler AA 3rd, et al. Improvement of cardiac function with parecoxib, a cyclo-oxygenase-2 inhibitor, in a rat model of ischemic heart failure. *J Cardiovasc Pharmacol* 2007; 49:416–418.

- Aitchison KA, Coker SJ. Cyclooxygenase inhibition converts the effect of nitric oxide synthase inhibition from infarct size reduction to expansion in isolated rabbit hearts. *J Mol Cell Cardiol* 1999;31:1315–1324.
- Alcindor D, Krolikowski JG, Pagel PS, Warltier DC, et al. Cyclooxygenase-2 mediates ischemic, anesthetic, and pharmacologic preconditioning in vivo. *Anesthesiology* 2004;100:547–554.
- Alhaddad IA, Tkaczewski L, Siddiqui F, Mir R, Brown EJ Jr. Aspirin enhances the benefits of late reperfusion on infarct shape: a possible mechanism of the beneficial effects of aspirin on survival after acute myocardial infarction. *Circulation* 1995;91:2819–2823.
- Arber N, Eagle CJ, Spicak J, Rácz I, et al. Celecoxib for the prevention of colorectal adenomatous polyps. *N Engl J Med* 2006;355:885–895.
- Asnes CF, Marquez JP, Elson EL, Wakatsuki T. Reconstitution of the Frank–Starling mechanism in engineered heart tissues. *Biophys J* 2006;91:1800–1810.
- Athirakul K, Kim HS, Audoly LP, Smithies O, et al. Deficiency of COX-1 causes natriuresis and enhanced sensitivity to ACE inhibition. *Kidney Int* 2001;60:2324–2329.
- Bai G, Gao S, Shah A, Yuan K, et al. Regulation of ANP secretion from isolated atria by prostaglandins and cyclooxygenase-2. *Peptides* 2009;30:1720–1728.
- Baker CS, Hall RJ, Evans TJ, Pomerance A, et al. Cyclooxygenase-2 is widely expressed in atherosclerotic lesions affecting native and transplanted human coronary arteries and colocalizes with inducible nitric oxide synthase and nitrotyrosine particularly in macrophages. *Arterioscler Thromb Vasc Biol* 1999;19:646–655.
- Bakris GL, Mensah GA. Pathogenesis and clinical physiology of hypertension. *Curr Probl Cardiol* 2003;28:137–155.
- Balsinde J, Winstead MV, Dennis EA. Phospholipase A(2) regulation of arachidonic acid mobilization. *FEBS Lett* 2002;531:2–6.
- Bea F, Blessing E, Bennett BJ, Kuo CC, et al. Chronic inhibition of cyclooxygenase-2 does not alter plaque composition in a mouse model of advanced unstable atherosclerosis. *Cardiovasc Res* 2003;60:198–204.
- Becker MC, Wang TH, Wisniewski L, Wolski K, et al. Rationale, design, and governance of prospective randomized evaluation of celecoxib integrated safety versus ibuprofen or naproxen (PRECISION), a cardiovascular end point trial of nonsteroidal anti-inflammatory agents in patients with arthritis. *Am Heart J* 2009;157:606–612.
- Belton O, Byrne D, Kearney D, Leahy A, et al. Cyclooxygenase-1 and -2-dependent prostacyclin formation in patients with atherosclerosis. *Circulation* 2000;102:840–845.
- Belton OA, Duffy A, Toomey S, Fitzgerald DJ. Cyclooxygenase isoforms and platelet vessel wall interactions in the apolipoprotein E knockout mouse model of atherosclerosis. *Circulation* 2003;108:3017–3023.
- Berger HJ, Zaret BL, Speroff L, Cohen LS, et al. Regional cardiac prostaglandin release during myocardial ischemia in anesthetized dogs. *Circ Res* 1976;38:566–571.
- Bernard GR, Wheeler AP, Russell JA, Schein R, et al. The effects of ibuprofen on the physiology and survival of patients with sepsis. The Ibuprofen in Sepsis Study Group. *N Engl J Med* 1997;336:912–918.
- Best PJ, Burnett JC, Wilson SH, Holmes DR Jr, et al. Dendroaspis natriuretic peptide relaxes isolated human arteries and veins. *Cardiovasc Res* 2002;55:375–384.
- Birck R, Krzossok S, Knoll T, Braun C, et al. Preferential COX-2 inhibitor, meloxicam, compromises renal perfusion in euvoletic and hypovolemic rats. *Exp Nephrol* 2000;8:173–180.
- Black SC, Brideau C, Cirino M, Belley M, et al. Differential effect of a selective cyclooxygenase-2 inhibitor versus indomethacin on renal blood flow in conscious volume-depleted dogs. *J Cardiovasc Pharmacol* 1998;32:686–694.
- Bolli R, Goldstein RE, Davenport N, Epstein SE. Influence of sulfinpyrazone and naproxen on infarct size in the dog. *Am J Cardiol* 1981;47:841–847.
- Bonetti PO, Lerman LO, Lerman A. Endothelial dysfunction: a marker of atherosclerotic risk. *Arterioscler Thromb Vasc Biol* 2003;23:168–175.
- Bonow RO, Lipson LC, Sheehan FH, Capurro NL, et al. Lack of effect of aspirin on myocardial infarct size in the dog. *Am J Cardiol* 1981;47:258–264.

- Brands MW, Hailman AE, Fitzgerald SM. Long-term glucose infusion increases arterial pressure in dogs with cyclooxygenase-2 inhibition. *Hypertension* 2001;37:733–738.
- Bresalier RS, Sandler RS, Quan H, Bolognese JA, et al. Cardiovascular events associated with rofecoxib in a colorectal adenoma chemoprevention trial. *N Engl J Med* 2005;352:1092–1102.
- Brown EJ Jr, Kloner RA, Schoen FJ, Hammerman H, et al. Scar thinning due to ibuprofen administration after experimental myocardial infarction. *Am J Cardiol* 1983;51:877–883.
- Brown S, Atkins C, Bagley R, Carr A, et al. Guidelines for the identification, evaluation, and management of systemic hypertension in dogs and cats. *J Vet Intern Med* 2007;21:542–558.
- Bueno OF, Molkentin JD. Involvement of extracellular signal-regulated kinases 1/2 in cardiac hypertrophy and cell death. *Circ Res* 2002;91:776–781.
- Burleigh ME, Babaev VR, Patel MB, Crews BC, et al. Inhibition of cyclooxygenase with indomethacin phenethylamide reduces atherosclerosis in apoE-null mice. *Biochem Pharmacol* 2005a;70:334–342.
- Burleigh ME, Babaev VR, Yancey PG, Major AS, et al. Cyclooxygenase-2 promotes early atherosclerotic lesion formation in ApoE-deficient and C57BL/6 mice. *J Mol Cell Cardiol* 2005b;39:443–452.
- Burnett JC Jr, Kao PC, Hu DC, Hesser DW, et al. Atrial natriuretic peptide elevation in congestive heart failure in the human. *Science* 1986;231:1145–1147.
- Campbell CL, Smyth S, Montalescot G, Steinhubl Sr. Aspirin dose for the prevention of cardiovascular disease: a systematic review. *J Am Med Assoc* 2007;297:2018–2024.
- Cannistra AJ. Adult valvular heart disease: a practical approach. *Prim Care* 2005;32:1109–1114.
- Carnieto A Jr, Dourado PM, da Luz PL, Chagas AC. Selective cyclooxygenase-2 inhibition protects against myocardial damage in experimental acute ischemia. *Clinics (Sao Paulo)* 2009;64:245–252.
- Chapman MJ. Animal lipoproteins: chemistry, structure, and comparative aspects. *J Lipid Res* 1980;21:789–853.
- Chapman MJ, Goldstein S. Comparison of the serum low density lipoprotein and of its apoprotein in the pig, rhesus monkey and baboon with that in man. *Atherosclerosis* 1976;25:267–291.
- Chenevard R, Hurlimann D, Bechir M, Enseleit F, et al. Selective COX-2 inhibition improves endothelial function in coronary artery disease. *Circulation* 2003;107:405–409.
- Cheng C, Tempel D, van Haperen R, van der Baan A, et al. Atherosclerotic lesion size and vulnerability are determined by patterns of fluid shear stress. *Circulation* 2006;113:2744–2753.
- Cheng Y, Austin SC, Rocca B, Koller BH, et al. Role of prostacyclin in the cardiovascular response to thromboxane A₂. *Science* 2002;296:539–541.
- Chobanian AV. The effects of ACE inhibitors and other antihypertensive drugs on cardiovascular risk factors and atherogenesis. *Clin Cardiol* 1990;13:VII43–VII48.
- Chun KS, Surh YJ. Signal transduction pathways regulating cyclooxygenase-2 expression: potential molecular targets for chemoprevention. *Biochem Pharmacol* 2004;68:1089–10100.
- Cipollone F, Fazia ML. Cyclooxygenase-2 inhibition: vascular inflammation and cardiovascular risk. *Curr Atheroscler Rep* 2006;8:245–251.
- Clyman RI, Heymann MA, Rudolph AM. Ductus arteriosus responses to prostaglandin E₁ at high and low oxygen concentrations. *Prostaglandins* 1977;13:219–223.
- Clyman RI, Mauray F, Roman C, Rudolph AM. PGE₂ is a more potent dilator of the lamb ductus arteriosus than is either PGI₂ or 6-keto PGF_{1α}. *Prostaglandins* 1978;16:259–264.
- Connolly DJ, Soares Magalhaes RJ, Fuentes VL, Boswood A, et al. Assessment of the diagnostic accuracy of circulating natriuretic peptide concentrations to distinguish between cats with cardiac and non-cardiac causes of respiratory distress. *J Vet Cardiol* 2009;11:S41–S50.
- Crick SJ, Sheppard MN, Ho SY, Gebstein L, et al. Anatomy of the pig heart: comparisons with normal human cardiac structure. *J Anat* 1998;193:105–119.
- Cuenca J, Martin-Sanz P, Alvarez-Barrientos AM, Bosca L, et al. Infiltration of inflammatory cells plays an important role in matrix metalloproteinase expression and activation in the heart during sepsis. *Am J Pathol* 2006;169:1567–1576.
- Cyrus T, Yao Y, Tung LX, Pratico D. Stabilization of advanced atherosclerosis in low-density lipoprotein receptor-deficient mice by aspirin. *Atherosclerosis* 2006;184:8–14.
- Cyrus T, Yao Y, Ding T, Dogne JM, et al. Thromboxane receptor blockade improves the antiatherogenic effect of thromboxane A₂ suppression in LDLR KO mice. *Blood* 2007;109:3291–3296.
- Dannenber AJ, Altorki NK, Boyle JO, Dang C, et al. Cyclo-oxygenase 2: a pharmacological target for the prevention of cancer. *Lancet Oncol* 2001;2:544–551.

- Degouse N, Fazel S, Angoulvant D, Stefanski E, et al. Microsomal prostaglandin E2 synthase-1 deletion leads to adverse left ventricular remodeling after myocardial infarction. *Circulation* 2008;117:1701–1710.
- Delgado RM 3rd, Nawar MA, Zewail AM, Kar B, et al. Cyclooxygenase-2 inhibitor treatment improves left ventricular function and mortality in a murine model of doxorubicin-induced heart failure. *Circulation* 2004;109:1428–1433.
- Detweiler DK. Control mechanisms of the circulatory system. In: Swenson MJ, Reece WO (eds), *Duke's Physiology of Domestic Animals*, 11th ed. Ithaca, NY: Cornell University Press, 1993, p. 185.
- De Windt LJ, Willems J, Roemen TH, Coumans WA, et al. Ischemic-reperfused isolated working mouse hearts: membrane damage and type IIA phospholipase A2. *Am J Physiol Heart Circ Physiol* 2001;280:H2572–H2580.
- Di Francesco L, Totani L, Dovizio M, Piccoli A, et al. Induction of prostacyclin by steady laminar shear stress suppresses tumor necrosis factor- α biosynthesis via heme oxygenase-1 in human endothelial cells. *Circ Res* 2009;104:506–513.
- Dilger K, Herrlinger C, Peters J, Seyberth HW, et al. Effects of celecoxib and diclofenac on blood pressure, renal function, and vasoactive prostanoids in young and elderly subjects. *J Clin Pharmacol* 2002;42:985–994.
- Dinchuk JE, Car BD, Focht RJ, Johnston JJ, et al. Renal abnormalities and an altered inflammatory response in mice lacking cyclooxygenase II. *Nature* 1995;378:406–409.
- Dowd NP, Scully M, Adderley SR, Cunningham AJ, et al. Inhibition of cyclooxygenase-2 aggravates doxorubicin-mediated cardiac injury in vivo. *J Clin Invest* 2001;108:585–590.
- Dunlap ME, Bibevski S, Rosenberry TL, Ernsberger P. Mechanisms of altered vagal control in heart failure: influence of muscarinic receptors and acetylcholinesterase activity. *Am J Physiol Heart Circ Physiol* 2003;285:H1632–H1640.
- Egan KM, Wang M, Fries S, Lucitt MB, et al. Cyclooxygenases, thromboxane, and atherosclerosis: plaque destabilization by cyclooxygenase-2 inhibition combined with thromboxane receptor antagonism. *Circulation* 2005;111:334–342.
- Ekure EN, Okoromah CA, Ajuluchukwu JN, Mbakwem A, et al. Diagnostic usefulness of N-terminal pro-brain natriuretic peptide among children with heart failure in a tertiary hospital in Lagos, Nigeria. *West Afr J Med* 2011;30:29–34.
- Eling TE, Thompson DC, Foureman GL, Curtis JF, et al. Prostaglandin H synthase and xenobiotic oxidation. *Annu Rev Pharmacol Toxicol* 1990;30:1–45.
- Elsner D, Muders F, Müntze A, Kromer EP, et al. Efficacy of prolonged infusion of urodilatin [ANP-(95–126)] in patients with congestive heart failure. *Am Heart J* 1995;129:766–773.
- Estrela JM, Montoro JB, Vina JR, Vina J. Glutathione metabolism under the influence of hydroperoxides in the lactating mammary gland of the rat: effect of glucose and extracellular ATP. *Biosci Rep* 1987;7:23–31.
- FDA. Cardiovascular safety review of rofecoxib. http://www.fda.gov/ohrms/dockets/ac/01/briefing/3677b2_06_cardio.pdf. FDA Advisory Committee, Rockville, MD, 2001.
- FDA Advisory Committee Meeting. Merck Briefing Document. Feb 2005.
- Félétou M, Verbeuren TJ, Vanhoutte PM. Endothelium-dependent contractions in SHR: a tale of prostanoid TP and IP receptors. *Br J Pharmacol* 2009;156:563–574.
- Ferdinandy P, Schulz R, Baxter GF. Interaction of cardiovascular risk factors with myocardial ischemia/reperfusion injury, preconditioning, and postconditioning. *Pharmacol Rev* 2007;59:418–458.
- Fiedler VB, Mardin M. Effects of nafazotrom and indomethacin on experimental myocardial ischemia in the anesthetized dog. *J Cardiovasc Pharmacol* 1985;7:983–989.
- Fitzgerald GA. Prostaglandins: modulators of inflammation and cardiovascular risk. *J Clin Rheumatol* 2004;10:S12–S17.
- Flynn PJ, Becker WK, Vercellotti GM, Weisdorf DJ, et al. Ibuprofen inhibits granulocyte responses to inflammatory mediators. A proposed mechanism for reduction of experimental myocardial infarct size. *Inflammation* 1984;8:33–44.
- Fox J, Anderson LC, Loew FM, Quimby FW. *Laboratory Animal Medicine*, 2nd ed. San Diego, CA: Academic Press, 2002.

- Francois H, Athirakul K, Howell D, Dash R, et al. Prostacyclin protects against elevated blood pressure and cardiac fibrosis. *Cell Metab* 2005;2:201–207.
- Frank MH. Renin in experimental renal hypertension in monkeys. *Circ Res* 1963;12:241–255.
- Frolov RV, Berim IG, Singh S. Inhibition of delayed rectifier potassium channels and induction of arrhythmia: a novel effect of celecoxib and the mechanism underlying it. *J Biol Chem* 2008;283:1518–1524.
- Fujino T, Nakagawa N, Yuhki K, Hara A, et al. Decreased susceptibility to renovascular hypertension in mice lacking the prostaglandin I₂ receptor IP. *J Clin Invest* 2004;114:805–812.
- Gavaghan M. Cardiac anatomy and physiology: a review. *AORN J* 1998;67:802–822.
- Gladding PA, Webster MW, Farrell HB, Zeng IS, et al. The antiplatelet effect of six non-steroidal anti-inflammatory drugs and their pharmacodynamic interaction with aspirin in healthy volunteers. *Am J Cardiol* 2008;101:1060–1063.
- Goldberg JM, Moberg GP. Autonomic control of heart rate in the neonatal rhesus monkey. *J Med Primatol* 1985;14:19–27.
- Goldblatt H, Lynch J, Hanzal RF, Summerville WW. Studies on experimental hypertension: I. The production of persistent elevation of systolic blood pressure by means of renal ischemia. *J Exp Med* 1934;59:347–379.
- Gres P, Schulz R, Jansen J, Umschlag C, et al. Involvement of endogenous prostaglandins in ischemic preconditioning in pigs. *Cardiovasc Res* 2002;55:626–632.
- Gross GJ, Moore J. Effect of COX-1/COX-2 inhibition versus selective COX-2 inhibition on coronary vasodilator responses to arachidonic acid and acetylcholine. *Pharmacology* 2004;71:135–142.
- Gross S, Tilly P, Hentsch D, Vonesch JL, et al. Vascular wall–produced prostaglandin E₂ exacerbates arterial thrombosis and atherothrombosis through platelet EP₃ receptors. *J Exp Med* 2007;204:311–320.
- Guerguerian AM, Hardy P, Bhattacharya M, Olley P, et al. Expression of cyclooxygenases in ductus arteriosus of fetal and newborn pigs. *Am J Obstet Gynecol* 1998;179:1618–1626.
- Guo Y, Bao W, Wu WJ, Shinmura K, et al. Evidence for an essential role of cyclooxygenase-2 as a mediator of the late phase of ischemic preconditioning in mice. *Basic Res Cardiol* 2000;95:479–484.
- Hammerman H, Kloner RA, Schoen FJ, Brown EJ Jr, et al. Indomethacin-induced scar thinning after experimental myocardial infarction. *Circulation* 1983;67:1290–1295.
- Harding P, Yang XP, Yang J, Shesely E, et al. Gene expression profiling of dilated cardiomyopathy in older male EP₄ knockout mice. *Am J Physiol Heart Circ Physiol* 2010;298:H623–H632.
- Harterner A, Cordasic N, Goppelt-Strube M, Veelken R, et al. Role of macula densa cyclooxygenase-2 in renovascular hypertension. *Am J Physiol Renal Physiol* 2003;284:F498–F502.
- Hearse DJ, Sutherland FJ. Experimental models for the study of cardiovascular function and disease. *Pharmacol Res* 2000;41:597–603.
- Heindl B, Becker BF. Aspirin, but not the more selective cyclooxygenase (COX)-2 inhibitors meloxicam and SC 58125, aggravates postischemic cardiac dysfunction, independent of COX function. *Naunyn Schmiedeberg Arch Pharmacol* 2001;363:233–240.
- Hennan JK, Huang J, Barrett TD, Driscoll EM, et al. Effects of selective cyclooxygenase-2 inhibition on vascular responses and thrombosis in canine coronary arteries. *Circulation* 2001;104:820–825.
- Heptinstall S, Espinosa DI, Manolopoulos P, Glenn JR, et al. DG-041 inhibits the EP₃ prostanoid receptor: a new target for inhibition of platelet function in atherothrombotic disease. *Platelets* 2008;19:605–613.
- Hermann M, Camici G, Fratton A, Hurlimann D, et al. Differential effects of selective cyclooxygenase-2 inhibitors on endothelial function in salt-induced hypertension. *Circulation* 2003;108:2308–2311.
- Hermann M, Shaw S, Kiss E, Camici G, et al. Selective COX-2 inhibitors and renal injury in salt-sensitive hypertension. *Hypertension* 2005;45:193–197.
- Hirsh PD, Hillis LD, Campbell WB, Firth BG, et al. Release of prostaglandins and thromboxane into the coronary circulation in patients with ischemic heart disease. *N Engl J Med* 1981;304:685–691.
- Hishikari K, Suzuki J, Ogawa M, Isobe K, et al. Pharmacological activation of the prostaglandin E₂ receptor EP₄ improves cardiac function after myocardial ischemia/reperfusion injury. *Cardiovasc Res* 2009;81:123–132.
- Höcherl K, Dreher F, Kurtz A, Bucher M. Cyclooxygenase-2 inhibition attenuates lipopolysaccharide-induced cardiovascular failure. *Hypertension* 2002a;40:947–953.

- Höcherl K, Endemann D, Kammerl MC, Grobecker HF, et al. Cyclo-oxygenase-2 inhibition increases blood pressure in rats. *Br J Pharmacol* 2002b;136:1117–1126.
- Hohlfeld T, Strobach H, Schrör K. Stimulation of endogenous prostacyclin protects the reperfused pig myocardium from ischemic injury. *J Pharmacol Exp Ther* 1993;264:397–405.
- Holt JP. The normal pericardium. *Am J Cardiol* 1970;26:455–465.
- Hong BK, Kwon HM, Lee BK, Kim D, et al. Coexpression of cyclooxygenase-2 and matrix metalloproteinases in human aortic atherosclerotic lesions. *Yonsei Med J* 2000;41:82–88.
- Hong TT, Huang J, Barrett TD, Lucchesi BR. Effects of cyclooxygenase inhibition on canine coronary artery blood flow and thrombosis. *Am J Physiol Heart Circ Physiol* 2008;294:H145–H155.
- Hughes HC. Swine in cardiovascular research. *Lab Anim Sci* 1986;36:348–350.
- Innes IR, Weisman H. Reduction in the severity of myocardial infarction by sulfinpyrazone. *Am Heart J* 1981;102:153–157.
- Inoue H, Taba Y, Miwa Y, Yokota C, et al. Transcriptional and posttranscriptional regulation of cyclooxygenase-2 expression by fluid shear stress in vascular endothelial cells. *Arterioscler Thromb Vasc Biol* 2002;22:1415–1420.
- Inserte J, Molla B, Aguilar R, Traves PG, et al. Constitutive COX-2 activity in cardiomyocytes confers permanent cardioprotection constitutive COX-2 expression and cardioprotection. *J Mol Cell Cardiol* 2009;46:160–168.
- Ito H, Hiroe M, Hirata Y, Fujisaki H, et al. Endothelin ET_A receptor antagonist blocks cardiac hypertrophy provoked by hemodynamic overload. *Circulation* 1994;89:2198–2203.
- Jackson RL, Baker HN, Taunton OD, Smith LC, et al. A comparison of the major apolipoprotein from pig and human high density lipoproteins. *J Biol Chem* 1973;248:2639–2644.
- Jacob S, Laury-Kleintop L, Lanza-Jacoby S. The select cyclooxygenase-2 inhibitor celecoxib reduced the extent of atherosclerosis in apo E^{-/-} mice. *J Surg Res* 2008;146:135–142.
- Jacoby DS, Rader DJ. Renin-angiotensin system and atherothrombotic disease: from genes to treatment. *Arch Intern Med* 2003;163:1155–1164.
- Jalowy A, Schulz R, Dörge H, Behrends M, et al. Infarct size reduction by AT₁-receptor blockade through a signal cascade of AT₂-receptor activation, bradykinin and prostaglandins in pigs. *J Am Coll Cardiol* 1998;32:1787–1796.
- James MA, Saadeh AM, Jones JV. Wall stress and hypertension. *J Cardiovasc Risk* 2000;7:187–190.
- Jenkins CM, Cedars A, Gross RW. Eicosanoid signalling pathways in the heart. *Cardiovasc Res* 2009;82:240–249.
- Jennings RB, Sommers HM, Smyth GA, Flack HA, et al. Myocardial necrosis induced by temporary occlusion of a coronary artery in the dog. *Arch Pathol* 1960;70:68–78.
- Jerome WG, Lewis JC. Early atherogenesis in White Carneau pigeons: II. Ultrastructural and cytochemical observation. *Am J Pathol* 1985;119:210–222.
- Johnson P, Maxwell DJ, Tynan MJ, Allan LD. Intracardiac pressures in the human fetus. *Heart* 2000;84:59–63.
- Joubert KE. The effects of firocoxib (Previcox) in geriatric dogs over a period of 90 days. *J S Afr Vet Assoc* 2009;80:179–184.
- Jugdutt BI, Hutchins GM, Bulkley BH, Pitt B, et al. Effect of indomethacin on collateral blood flow and infarct size in the conscious dog. *Circulation* 1979;59:734–743.
- Kawabe J, Yuhki K, Okada M, Kanno T, et al. Prostaglandin I₂ promotes recruitment of endothelial progenitor cells and limits vascular remodeling. *Arterioscler Thromb Vasc Biol* 2010;30:464–470.
- Kawada N, Solis G, Ivey N, Connors S, et al. Cyclooxygenase-1-deficient mice have high sleep-to-wake blood pressure ratios and renal vasoconstriction. *Hypertension* 2005;45:1131–1138.
- Kawka DW, Ouellet M, Hetu PO, Singer II, et al. Double-label expression studies of prostacyclin synthase, thromboxane synthase and COX isoforms in normal aortic endothelium. *Biochim Biophys Acta* 2007;1771:45–54.
- Kay-Mugford PA, Benn SJ, LaMarre J, Conlon PD. Cyclooxygenase expression in canine platelets and Madin–Darby canine kidney cells. *Am J Vet Res* 2000;61:1512–1516.
- Kearney D, Byrne A, Crean P, Cox D, et al. Optimal suppression of thromboxane A(2) formation by aspirin during percutaneous transluminal coronary angioplasty: no additional effect of a selective cyclooxygenase-2 inhibitor. *J Am Coll Cardiol* 2004;43:526–531.

- Kentsch M, Ludwig D, Drummer C, Gerzer R, et al. Haemodynamic and renal effects of urodilatin bolus injections in patients with congestive heart failure. *Eur J Clin Invest* 1992;22:662–669.
- Kim JW, Baek BS, Kim YK, Herlihy JT, et al. Gene expression of cyclooxygenase in the aging heart. *J Gerontol A Biol Sci Med Sci* 2001;56:B350–B355.
- Kirtikara K, Raghov R, Laulederkind SJ, Goorha S, et al. Transcriptional regulation of cyclooxygenase-2 in the human microvascular endothelial cell line, HMEC-1: control by the combinatorial actions of AP2, NF-IL-6 and CRE elements. *Mol Cell Biochem* 2000;203:41–51.
- Kiserud T, Acharya G. The fetal circulation. *Prenat Diagn* 2004;24:1049–1059.
- Kobayashi T, Tahara Y, Matsumoto M, Iguchi M, et al. Roles of thromboxane A(2) and prostacyclin in the development of atherosclerosis in apoE-deficient mice. *J Clin Invest* 2004;114:784–794.
- Koch-Weser J. The therapeutic challenge of systolic hypertension. *N Engl J Med* 1973;289:481–483.
- Koki A, Khan NK, Woerner BM, Dannenberg AJ, et al. Cyclooxygenase-2 in human pathological disease. *Adv Exp Med Biol* 2002;507:177–184.
- Kowala MC, Mazzucco CE, Hartl KS, Seiler SM, et al. Prostacyclin agonists reduce early atherosclerosis in hyperlipidemic hamsters. Octimibate and BMY 42393 suppress monocyte chemotaxis, macrophage cholesteryl ester accumulation, scavenger receptor activity, and tumor necrosis factor production. *Arterioscler Thromb* 1993;13:435–444.
- Krotz F, Schiele TM, Klauss V, Sohn HY. Selective COX-2 inhibitors and risk of myocardial infarction. *J Vasc Res* 2005;42:312–324.
- Kunori Y, Muroga Y, Iidaka M, Mitsuhashi H, et al. Species differences in angiotensin II generation and degradation by mast cell chymases. *J Recept Signal Transduct Res* 2005;25:35–44.
- Kurtz TW, Griffin KA, Bidani AK, Davisson RL, et al. Recommendations for blood pressure measurement in humans and experimental animals: Part 2. Blood pressure measurement in experimental animals: a statement for professionals from the Subcommittee of Professional and Public Education of the American Heart Association Council on High Blood Pressure Research. *Arterioscler Thromb Vasc Biol* 2005;25:e22–e33.
- Lal A, Sharma ML. Failure to reduce experimental myocardial infarct size with ibuprofen pre-treatment in rats. *Indian J Physiol Pharmacol* 1992;36:133–134.
- LaPointe MC, Mendez M, Leung A, Tao Z, et al. Inhibition of cyclooxygenase-2 improves cardiac function after myocardial infarction in the mouse. *Am J Physiol Heart Circ Physiol* 2004;286:H1416–H1424.
- Lee RT, Bloch KD, Pfeffer JM, Pfeffer MA, et al. Atrial natriuretic factor gene expression in ventricles of rats with spontaneous biventricular hypertrophy. *J Clin Invest* 1988;81:431–434.
- Lehoux S, Castier Y, Tedgui A. Molecular mechanisms of the vascular responses to haemodynamic forces. *J Intern Med* 2006;259:381–392.
- Lerman LO, Chade AR, Sica V, Napoli C. Animal models of hypertension: an overview. *J Lab Clin Med* 2005;146:160–173.
- Lev M. The normal anatomy of the conduction system in man and its pathology in atrioventricular block. *Ann NY Acad Sci* 1964;111:817–829.
- Lévesque LE, Brophy JM, Zhang B. The risk for myocardial infarction with cyclooxygenase-2 inhibitors: a population study of elderly adults. *Ann Intern Med* 2005;142:481–489.
- Liang YL, Shiel LM, Teede H, Kotsopoulos D, et al. Effects of blood pressure, smoking, and their interaction on carotid artery structure and function. *Hypertension* 2001;37:6–11.
- Libby P. Inflammation in atherosclerosis. *Nature* 2002;420:868–784.
- Lien YH, Hsiang TY, Huang HP. Associations among systemic blood pressure, microalbuminuria and albuminuria in dogs affected with pituitary- and adrenal-dependent hyperadrenocorticism. *Acta Vet Scand* 2010;52:61.
- Liu GS, Stanley AW, Downey J. Cyclooxygenase products are not involved in the protection against myocardial infarction afforded by preconditioning in rabbit: cyclooxygenase pathway's involvement in preconditioning. *Am J Cardiovasc Pathol* 1992;4:157–164.
- Liu SK, Tilley LP, Tappe JP, Fox PR. Clinical and pathologic findings in dogs with atherosclerosis: 21 cases (1970–1983). *J Am Vet Med Assoc* 1986;189:227–232.
- Manning EP, Tardiff JC, Schwartz SD. A model of calcium activation of the cardiac thin filament. *Biochemistry* 2011;50:7405–7413.

- Manohar M, Goetz TE, Griffin R, Sullivan E. Pulmonary vascular pressures of strenuously exercising thoroughbreds after administration of phenylbutazone. *Am J Vet Res* 1996;57:1354–1358.
- Marcus AJ, Broekman MJ, Pinsky DJ. COX inhibitors and thromboregulation. *N Engl J Med* 2002;347:1025–1026.
- Martin M, Meyer-Kirchath J, Kaber G, Jacoby C, et al. Cardiospecific overexpression of the prostaglandin EP3 receptor attenuates ischemia-induced myocardial injury. *Circulation* 2005;112:400–406.
- McAdam BF, Catella-Lawson F, Mardini IA, Kapoor S, et al. Systemic biosynthesis of prostacyclin by cyclooxygenase (COX)-2: the human pharmacology of a selective inhibitor of COX-2. *Proc Natl Acad Sci USA* 1999;96:272–277.
- McClelland S, Gawaz M, Kennerknecht E, Konrad CS, et al. Contribution of cyclooxygenase-1 to thromboxane formation, platelet–vessel wall interactions and atherosclerosis in the ApoE null mouse. *Atherosclerosis* 2009;202:84–91.
- McCorry LK. Physiology of the autonomic nervous system. *Am J Pharm Educ* 2007;71:78.
- McGeer PL, McGeer EG, Yasojima K. Expression of COX-1 and COX-2 mRNAs in atherosclerotic plaques. *Exp Gerontol* 2002;37:925–929.
- Meune C, Mourad JJ, Bergmann JF, Spaulding C. Interaction between cyclooxygenase and the renin–angiotensin–aldosterone system: rationale and clinical relevance. *J Renin Angiotensin Aldosterone Syst* 2003;4:149–154.
- Mehta PK, Griendling KK. Angiotensin II cell signaling: physiological and pathological effects in the cardiovascular system. *Am J Physiol Cell Physiol* 2007;292:C82–C97.
- Meyer-Kirchath J, Martin M, Schooss C, Jacoby C, et al. Overexpression of prostaglandin EP3 receptors activates calcineurin and promotes hypertrophy in the murine heart. *Cardiovasc Res* 2009;81:310–318.
- Mitrovic V, Seferovic PM, Simeunovic D, Ristic AD, et al. Haemodynamic and clinical effects of ularitide in decompensated heart failure. *Eur Heart J* 2006;27:2823–3282.
- Miyazaki M, Sakonjo H, Takai S. Anti-atherosclerotic effects of an angiotensin converting enzyme inhibitor and an angiotensin II antagonist in cynomolgus monkeys fed a high-cholesterol diet. *Br J Pharmacol* 1999;128:523–529.
- Moghadasian MH, Frohlich JJ, McManus BM. Advances in experimental dyslipidemia and atherosclerosis. *Lab Invest* 2001;81:1173–1183.
- Moncada S, Gryglewski R, Bunting S, Vane Jr. An enzyme isolated from arteries transforms prostaglandin endoperoxides to an unstable substance that inhibits platelet aggregation. *Nature* 1976;263:663–665.
- Mori T, Chen YF, Feng JA, Hayashi T, et al. Volume overload results in exaggerated cardiac hypertrophy in the atrial natriuretic peptide knockout mouse. *Cardiovasc Res* 2004;61:771–779.
- Moubayed SP, Heinonen TM, Tardif JC. Anti-inflammatory drugs and atherosclerosis. *Curr Opin Lipidol* 2007;18:638–644.
- Mousa SA, Cooney JM, Thoolen MJ, Timmermans PB. Myocardial cytoprotective efficacy of azapropazone in a canine heart model of regional ischemia and reperfusion. *J Cardiovasc Pharmacol* 1989;14:542–548.
- Mousa SA, Brown R, Thoolen MJ, Smith RD. Evaluation of the effect of azapropazone on neutrophil migration in regional myocardial ischaemia/reperfusion injury in rabbits. *Br J Pharmacol* 1990;100:379–382.
- Mukoyama M, Nakao K, Hosoda K, Suga S, et al. Brain natriuretic peptide as a novel cardiac hormone in humans. Evidence for an exquisite dual natriuretic peptide system, atrial natriuretic peptide and brain natriuretic peptide. *J Clin Invest* 1991;87:1402–1412.
- Murata T, Ushikubi F, Matsuoka T, Hirata M, et al. Altered pain perception and inflammatory response in mice lacking prostacyclin receptor. *Nature* 1997;388:678–682.
- Murphy PJ. The fetal circulation. *Contin Educ Anaesth Crit Care Pain* 2005;5:107–112.
- Muscara MN, Vergnolle N, Lovren F, Triggle CR, et al. Selective cyclo-oxygenase-2 inhibition with celecoxib elevates blood pressure and promotes leukocyte adherence. *Br J Pharmacol* 2000;129:1423–1430.
- Nunez DJ, Dickson MC, Brown MJ. Natriuretic peptide receptor mRNAs in the rat and human heart. *J Clin Invest* 1992;90:1966–1971.

- Okamoto T, Hino O. Expression of cyclooxygenase-1 and -2 mRNA in rat tissues: tissue-specific difference in the expression of the basal level of mRNA. *Int J Mol Med* 2000;6:455–457.
- Olesen M, Kwong E, Meztli A, Kontny F, et al. No effect of cyclooxygenase inhibition on plaque size in atherosclerosis-prone mice. *Scand Cardiovasc J* 2002;36:362–367.
- Palaniyandi SS, Nagai Y, Watanabe K, Ma M, et al. Chymase inhibition reduces the progression to heart failure after autoimmune myocarditis in rats. *Exp Biol Med (Maywood)* 2007;232:1213–1221.
- Parente L, Perretti M. Advances in the pathophysiology of constitutive and inducible cyclooxygenases: two enzymes in the spotlight. *Biochem Pharmacol* 2003;65:153–159.
- Poletto R, Janczak AM, Marchant-Forde RM, Marchant-Forde JN, et al. Identification of low and high frequency ranges for heart rate variability and blood pressure variability analyses using pharmacological autonomic blockade with atropine and propranolol in swine. *Physiol Behav* 2011;103:188–196.
- Potter CM, Lundberg MH, Harrington LS, Warboys CM, et al. Role of shear stress in endothelial cell morphology and expression of cyclooxygenase isoforms. *Arterioscler Thromb Vasc Biol* 2011;31:384–391.
- Pratico D, Tillmann C, Zhang ZB, Li H, et al. Acceleration of atherogenesis by COX-1-dependent prostanoid formation in low density lipoprotein receptor knockout mice. *Proc Natl Acad Sci USA* 2001;98:3358–3363.
- Prejbisz A, Lenders JW, Eisenhofer G, Januszewicz A. Cardiovascular manifestations of pheochromocytoma. *J Hypertens* 2011;29(11): 2049–2060.
- Qian JY, Harding P, Liu Y, Shesely E, et al. Reduced cardiac remodeling and function in cardiac-specific EP4 receptor knockout mice with myocardial infarction. *Hypertension* 2008;51:560–566.
- Radi ZA. Pathophysiology of cyclooxygenase inhibition in animal models. *Toxicol Pathol* 2009;37:34–46.
- Radi ZA, Ackermann MR. Ontogeny of pulmonary cyclooxygenase-1 (COX-1) and -2 (COX-2). *Pathophysiology* 2011;18:215–219.
- Radi ZA, Khan NK. Effects of cyclooxygenase inhibition on the gastrointestinal tract. *Exp Toxicol Pathol* 2006;58:163–173.
- Radi ZA, Ostroski R. Pulmonary and cardiorenal cyclooxygenase-1 (COX-1), -2 (COX-2), and microsomal prostaglandin E synthase-1 (mPGES-1) and -2 (mPGES-2) expression in a hypertension model. *Mediators Inflamm* 2007;2007:85091.
- Raval M, Frank PG, Laury-Kleintop L, Yan G, et al. Celecoxib combined with atorvastatin prevents progression of atherosclerosis. *J Surg Res* 2010;163:e113–e122.
- Reece WO. *Functional Anatomy and Physiology of Domestic Animals*, 4th ed. Ames, IA: Iowa State University Academic Press, 2007.
- Renda G, Tacconelli S, Capone ML, Sacchetta D, et al. Celecoxib, ibuprofen, and the antiplatelet effect of aspirin in patients with osteoarthritis and ischemic heart disease. *Clin Pharmacol Ther* 2006;80:264–274.
- Richter CM, Godes M, Wagner C, Maser-Gluth C, et al. Chronic cyclooxygenase-2 inhibition does not alter blood pressure and kidney function in renovascular hypertensive rats. *J Hypertens* 2004;22:191–198.
- Ross R. Rous-Whipple Award Lecture. Atherosclerosis: a defense mechanism gone awry. *Am J Pathol* 1993;143:987–1002
- Rossi P, Kuukasjarvi P, Riutta A, Salenius JP, et al. Prostacyclin and thromboxane A2 synthesis are increased in acute lower limb ischaemia. *Prostaglandins Leukot Essent Fatty Acids* 1996;55:433–436.
- Rossoni G, Muscara MN, Cirino G, Wallace JL. Inhibition of cyclo-oxygenase-2 exacerbates ischaemia-induced acute myocardial dysfunction in the rabbit. *Br J Pharmacol* 2002;135:1540–1546.
- Rott D, Zhu J, Burnett MS, Zhou YF, et al. Effects of MF-tricyclic, a selective cyclooxygenase-2 inhibitor, on atherosclerosis progression and susceptibility to cytomegalovirus replication in apolipoprotein-E knockout mice. *J Am Coll Cardiol* 2003;41:1812–1819.
- Rudolph AM. Distribution and regulation of blood flow in the fetal and neonatal lamb. *Circ Res* 1985;57:811–821.
- Ruskoaho H, Lang RE, Toth M, Ganten D, et al. Release and regulation of atrial natriuretic peptide (ANP). *Eur Heart J* 1987;8:99–109.
- Saito T, Rodger IW, Hu F, Shennib H, et al. Inhibition of cyclooxygenase-2 improves cardiac function in myocardial infarction. *Biochem Biophys Res Commun* 2000;273:772–775.

- Saito T, Rodger IW, Shennib H, Hu F, et al. Cyclooxygenase-2 (COX-2) in acute myocardial infarction: cellular expression and use of selective COX-2 inhibitor. *Can J Physiol Pharmacol* 2003;81:114–119.
- Saito T, Rodger IW, Hu F, Robinson R, et al. Inhibition of COX pathway in experimental myocardial infarction. *J Mol Cell Cardiol* 2004;37:71–77.
- Sakamoto A, Matsumura J, Mii S, Gotoh Y, et al. A prostaglandin E2 receptor subtype EP4 agonist attenuates cardiovascular depression in endotoxin shock by inhibiting inflammatory cytokines and nitric oxide production. *Shock* 2004;22:76–81.
- Salloum FN, Hoke NN, Seropian IM, Varma A, et al. Parecoxib inhibits apoptosis in acute myocardial infarction due to permanent coronary ligation but not due to ischemia-reperfusion. *J Cardiovasc Pharmacol* 2009;53:495–498.
- Scheuer J, Buttrick P. The cardiac hypertrophic responses to pathologic and physiologic loads. *Circulation* 1987;75:163–168.
- Schönbeck U, Sukhova GK, Graber P, Coulter S, et al. Augmented expression of cyclooxygenase-2 in human atherosclerotic lesions. *Am J Pathol* 1999;155:1281–1291.
- Schroeder HA, Goldman ML. Arterial hypertension in dogs: I. Methods. *Circulation* 1952;5:730–741.
- Sellers RS, Radi ZA, Khan NK. Pathophysiology of cyclooxygenases in cardiovascular homeostasis. *Vet Pathol* 2010;47:601–613.
- Senbonmatsu T, Ichihara S, Price E, Gaffney FA, et al. Evidence for angiotensin II type 2 receptor-mediated cardiac myocyte enlargement during in vivo pressure overload. *J Clin Invest* 2000;106:R25–R29.
- Seta F, Chung AD, Turner PV, Mewburn JD, et al. Renal and cardiovascular characterization of COX-2 knockdown mice. *Am J Physiol Regul Integr Comp Physiol* 2009;296:R1751–R1760.
- Shibata R, Sato K, Pimentel DR, Takemura Y, et al. Adiponectin protects against myocardial ischemia-reperfusion injury through AMPK- and COX-2-dependent mechanisms. *Nat Med* 2005;11:1096–1103.
- Shiels HA, White E. The Frank–Starling mechanism in vertebrate cardiac myocytes. *J Exp Biol* 2008;211:2005–2013.
- Shinmura K, Tang XL, Wang Y, Xuan YT, et al. Cyclooxygenase-2 mediates the cardioprotective effects of the late phase of ischemic preconditioning in conscious rabbits. *Proc Natl Acad Sci USA* 2000;97:10197–10202.
- Shizukuda Y, Miura T, Ishimoto R, Itoya M, et al. Effect of prednisolone on myocardial infarct healing: characteristics and comparison with indomethacin. *Can J Cardiol* 1991;7:447–454.
- Smith CC, Ansevin A. Blood pressure of the normal rhesus monkey. *Proc Soc Exp Biol Med* 1957;96:428–432.
- Smith WL, DeWitt DL, Garavito RM. Cyclooxygenases: structural, cellular, and molecular biology. *Annu Rev Biochem* 2000;69:145–182.
- Smulyan H, Safar ME. Systolic blood pressure revisited. *J Am Coll Cardiol* 1997;29:1407–1413.
- Solomon SD, McMurray JJ, Pfeffer MA, Wittes J, et al. Cardiovascular risk associated with celecoxib in a clinical trial for colorectal adenoma prevention. *N Engl J Med* 2005;352:1071–1080.
- Sowers JR, White WB, Pitt B, Whelton A, et al. The Effects of cyclooxygenase-2 inhibitors and nonsteroidal anti-inflammatory therapy on 24-hour blood pressure in patients with hypertension, osteoarthritis, and type 2 diabetes mellitus. *Arch Intern Med* 2005;165:161–168.
- Srisawat S, Phivthong-Ngam L, Unchern S, Chantharaksri U, et al. Improvement of vascular function by chronic administration of a cyclo-oxygenase inhibitor in cholesterol-fed rabbits. *Clin Exp Pharmacol Physiol* 2003;30:405–412.
- Stanfield KM, Khan KN, Gralinski MR. Localization of cyclooxygenase isozymes in cardiovascular tissues of dogs treated with naproxen. *Vet Immunol Immunopathol* 2001;80:309–314.
- St. Clair RW. Metabolic changes in the arterial wall associated with atherosclerosis in the pigeon. *Fed Proc* 1983;42:2480–2485.
- Stemme V, Swedenborg J, Claesson H, Hansson GK. Expression of cyclooxygenase-2 in human atherosclerotic carotid arteries. *Eur J Vasc Endovasc Surg* 2000;2:146–152.
- Stepien RL. Feline systemic hypertension: diagnosis and management. *J Feline Med Surg* 2011;13:35–43.
- Strain RE, Olson WH. Selective damage of large diameter peripheral nerve fibers by compression: an application of Laplace's law. *Exp Neurol* 1975;47:68–80.

- Straino S, Salloum FN, Baldi A, Ockaili RA, et al. Protective effects of parecoxib, a cyclo-oxygenase-2 inhibitor, in postinfarction remodeling in the rat. *J Cardiovasc Pharmacol* 2007;50:571–577.
- Streicher JM, Wang Y. The role of COX-2 in heart pathology. *Cardiovasc Hematol Agents Med Chem* 2008;6:69–79.
- Struijk PC, Mathews VJ, Loupas T, Stewart PA, et al. Blood pressure estimation in the human fetal descending aorta. *Ultrasound Obstet Gynecol* 2008;32:673–681.
- Such L, Morcillo EJ, Fortana A, Alberola A, et al. Effects of anti-inflammatory drugs in a model of acute transmural infarction in the dog. *J Pharmacol* 1983;14:283–293.
- Swindle MM, Horneffer PJ, Gardner TJ, Gott VL, et al. Anatomic and anesthetic considerations in experimental cardiopulmonary surgery in swine. *Lab Anim Sci* 1986;36:357–361.
- Takayama K, Yuhki K, Ono K, Fujino T, et al. Thromboxane A2 and prostaglandin F2alpha mediate inflammatory tachycardia. *Nat Med* 2005;11:562–566.
- Takimoto Y, Aoyama T, Iwanaga Y, Izumi T, et al. Increased expression of cardiotrophin-1 during ventricular remodeling in hypertensive rats. *Am J Physiol* 2002;282:H896–H901.
- Tang EH, Vanhoutte PM. Gene expression changes of prostanoid synthases in endothelial cells and prostanoid receptors in vascular smooth muscle cells caused by aging and hypertension. *Physiol Genomics* 2008;32:409–418.
- Tarnow I, Olsen LH, Kvart K, Høglund K, et al. Predictive value of natriuretic peptides in dogs with mitral valve disease. *Vet J* 2009;180:195–201.
- Testa M, Rocca B, Spath L, Ranalletti FO, et al. Expression and activity of cyclooxygenase isoforms in skeletal muscles and myocardium of humans and rodents. *J Appl Physiol* 2007;103:1412–1418.
- Thomas DW, Mannon RB, Mannon PJ, Latour A, et al. Coagulation defects and altered hemodynamic responses in mice lacking receptors for thromboxane A2. *J Clin Invest* 1998;102:1994–2001.
- Timmers L, Sluijter JP, Verlaan CW, Steendijk P, et al. Cyclooxygenase-2 inhibition increases mortality, enhances left ventricular remodeling, and impairs systolic function after myocardial infarction in the pig. *Circulation* 2007;115:326–332.
- Tranquilli WJ, Parks CM, Thurmon JC, Benson GJ, et al. Organ blood flow and distribution of cardiac output in nonanesthetized swine. *Am J Vet Res* 1982;43:895–897.
- Uotila P, Saraste A, Vähäsilita T, Kentala E, et al. Stimulated expression of cyclooxygenase-2 in porcine heart after bypass circulation and cardioplegic arrest. *Eur J Cardiothorac Surg* 2001;20:992–995.
- Ushikubi F, Segi E, Sugimoto Y, Murata T, et al. Impaired febrile response in mice lacking the prostaglandin E receptor subtype EP3. *Nature* 1998;395:281–284.
- van der Hoorn JW, Jukema JW, Bekkers ME, Princen HM, et al. Negative effects of rofecoxib treatment on cardiac function after ischemia-reperfusion injury in APOE3Leiden mice are prevented by combined treatment with thromboxane prostanoid-receptor antagonist S18886 (terutroban). *Crit Care Med* 2008;36:2576–2582.
- van de Schans VA, van den Borne SW, Strzelecka AE, Janssen BJ, et al. Interruption of Wnt signaling attenuates the onset of pressure overload-induced cardiac hypertrophy. *Hypertension* 2007;49:473–480.
- Vaneckova I, Skaroupkova P, Dvorak P, Certiková Chábová V, et al. Effects of sodium restriction and cyclooxygenase-2 inhibition on the course of hypertension, proteinuria and cardiac hypertrophy in Ren-2 transgenic rats. *Physiol Res* 2005;54:17–24.
- Vargas Alarcón G. Physiopathogenesis of hypertension. *Arch Cardiol Mex* 2006;76 Suppl 2:S157–S160.
- Wacker MJ, Tehrani RN, Smoot RL, Orr JA. Thromboxane A(2) mimetic evokes a bradycardia mediated by stimulation of cardiac vagal afferent nerves. *Am J Physiol Heart Circ Physiol* 2002;282:H482–H490.
- Wainwright CL, Miller AM, Work LM, Del Soldato P. NCX4016 (NO-aspirin) reduces infarct size and suppresses arrhythmias following myocardial ischaemia/reperfusion in pigs. *Br J Pharmacol* 2002;135:1882–1888.
- Wang D, Patel VV, Ricciotti E, Zhou R, et al. Cardiomyocyte cyclooxygenase-2 influences cardiac rhythm and function. *Proc Natl Acad Sci USA* 2009;106:7548–7552.
- Warren RJ, Ebert DL, Mitchell A, Barter PJ. Rabbit hepatic lipase cDNA sequence: Low activity is associated with low messenger RNA levels. *J Lipid Res* 1991;32:1333–1339.

- Weaver ME, Pantely GA, Bristow JD, Ladley HD. A quantitative study of the anatomy and distribution of coronary arteries in swine in comparison with other animals and man. *Cardiovasc Res* 1986;20:907–917.
- Whelton A, Fort JG, Puma JA, Normandin D, et al. Cyclooxygenase-2-specific inhibitors and cardiorenal function: a randomized, controlled trial of celecoxib and rofecoxib in older hypertensive osteoarthritis patients. *Am J Ther* 2001;8:85–95.
- Whelton A, White WB, Bello AE, Puma JA, et al. Effects of celecoxib and rofecoxib on blood pressure and edema in patients $>$ or $=$ 65 years of age with systemic hypertension and osteoarthritis. *Am J Cardiol* 2002;90:959–963.
- White WB, Faich G, Whelton A, Maurath C, et al. Comparison of thromboembolic events in patients treated with celecoxib, a cyclooxygenase-2 specific inhibitor, versus ibuprofen or diclofenac. *Am J Cardiol* 2002;89:425–230.
- White WB, West CR, Borer JS, Gorelick PB, et al. Risk of cardiovascular events in patients receiving celecoxib: a meta-analysis of randomized clinical trials. *Am J Cardiol* 2007;99:91–98.
- Widlansky ME, Price DT, Gokce N, Eberhardt RT, et al. Short- and long-term COX-2 inhibition reverses endothelial dysfunction in patients with hypertension. *Hypertension* 2003;42:310–315.
- Wilcox JN, Augustine A, Goeddel DV, Lowe DG. Differential regional expression of three natriuretic peptide receptor genes within primate tissues. *Mol Cell Biol* 1991;11:3454–3462.
- Wilner KD, Rushing M, Walden C, Adler R, et al. Celecoxib does not affect the antiplatelet activity of aspirin in healthy volunteers. *J Clin Pharmacol* 2002;42:1027–1030.
- Wolf MJ, Amrein H, Izatt JA, Choma MA, et al. *Drosophila* as a model for the identification of genes causing adult human heart disease. *Proc Natl Acad Sci USA* 2006;103:1394–1399.
- Wong E, Huang JQ, Tagari P, Riendeau D. Effects of COX-2 inhibitors on aortic prostacyclin production in cholesterol-fed rabbits. *Atherosclerosis* 2001;157:393–402.
- Woodard GE, Rosado JA. Natriuretic peptides in vascular physiology and pathology. *Int Rev Cell Mol Biol* 2008;268:59–93.
- Wu D, Mennerich D, Arndt K, Sugiyama K, et al. The effects of microsomal prostaglandin E synthase-1 deletion in acute cardiac ischemia in mice. *Prostaglandins Leukot Essent Fatty Acids* 2009;81:31–33.
- Xiao CY, Yuhki K, Hara A, Fujino T, et al. Prostaglandin E2 protects the heart from ischemia–reperfusion injury via its receptor subtype EP4. *Circulation* 2004;109:2462–2468.
- Xuan YT, Guo Y, Zhu Y, Wang OL, et al. Role of the protein kinase C-epsilon-Raf-1-MEK-1/2-p44/42 MAPK signaling cascade in the activation of signal transducers and activators of transcription 1 and 3 and induction of cyclooxygenase-2 after ischemic preconditioning. *Circulation* 2005;112:1971–1978.
- Yang HM, Kim HS, Park KW, You HJ, et al. Celecoxib, a cyclooxygenase-2 inhibitor, reduces neointimal hyperplasia through inhibition of Akt signaling. *Circulation* 2004;110:301–308.
- Yano T, Fujioka D, Saito Y, Kobayashi T, et al. Group V secretory phospholipase A2 plays a pathogenic role in myocardial ischaemia–reperfusion injury. *Cardiovasc Res* 2011;90:335–343.
- Zadelaar S, Kleemann R, Verschuren L, de Vries–Van der Weij J, et al. Mouse models for atherosclerosis and pharmaceutical modifiers. *Arterioscler Thromb Vasc Biol* 2007;27:1706–1721.
- Zhao H, Hiroi T, Hansen BS, Rade JJ. Cyclic stretch induces cyclooxygenase-2 gene expression in vascular endothelial cells via activation of nuclear factor kappa-beta. *Biochem Biophys Res Commun* 2009;389:599–601.
- Zidar N, Dolenc-Strazar Z, Jeruc J, Jerse M, et al. Expression of cyclooxygenase-1 and cyclooxygenase-2 in the normal human heart and in myocardial infarction. *Cardiovasc Pathol* 2007;16:300–304.
- Zidar N, Odar K, Glavac D, Jerse M, et al. Cyclooxygenase in normal human tissues: Is COX-1 really a constitutive isoform, and COX-2 an inducible isoform? *J Cell Mol Med* 2009;13:3753–3763.
- Zimmerman J. The functional and surgical anatomy of the heart. *Ann R Coll Surg Engl* 1966;39:348–366.

OCULAR SYSTEM**INTRODUCTION**

Ocular tissues respond to physiological and pathophysiological stimuli via activation of phospholipases and subsequent release of biologically active metabolites such as prostaglandins (PGs) from membrane phospholipids (Bazan et al., 1997; Radi and Render, 2008). PGs have receptors localized in a variety of ocular tissues, and affect the physiology and pathophysiology of the eye (Hardy et al., 1994; Radi and Render, 2008). Cyclooxygenase isoenzymes (COX-1 and -2) catalyze the conversion of arachidonic acids (AAs) to PGs (Fig. 5-1) (Radi and Render, 2008). The COX-1 isoenzyme is expressed in a variety of ocular tissues, and this expression is variable among different animal species (Radi and Render, 2008). In inflamed tissues, eicosanoids are thought to play a significant role in angiogenesis (Yamada et al., 1999). COX-2 and vascular endothelial growth factor (VEGF) affect vascular permeability and angiogenesis and may be induced by hyperglycemia and tissue hypoxia (Bonazzi et al., 2000; Wilkinson-Berka, 2004). COX-2 inhibition has been associated with attenuating angiogenesis and down-regulating VEGF and bFGF (Masferrer et al., 1999). Among their many uses, NSAIDs are employed for various ophthalmic indications. In this chapter we discuss the expression of COX-1 and COX-2 in the ocular system, the role of prostaglandins and COX in ocular physiology and pathophysiology, and the effects of COX-2 s-NSAIDs and ns-NSAIDs in the treatment of ophthalmic conditions.

COMPARATIVE PHYSIOLOGICAL AND ANATOMICAL ASPECTS OF THE OCULAR SYSTEM

The ocular (visual) system is one of the most complex organs in the body. Understanding the comparative physiological and anatomical aspects of the ocular system is important for an understanding of the pathophysiological consequences of COX inhibition on this system. The eyes allow people and animals to see and interpret their surroundings by collecting light and focusing it onto the retina. The major layers of the eye are the (1) cornea, (2) anterior chamber, (3) lens, (4) vitreous, (5) retina, and (6) optic nerve. The cornea is a transparent, highly specialized tissue

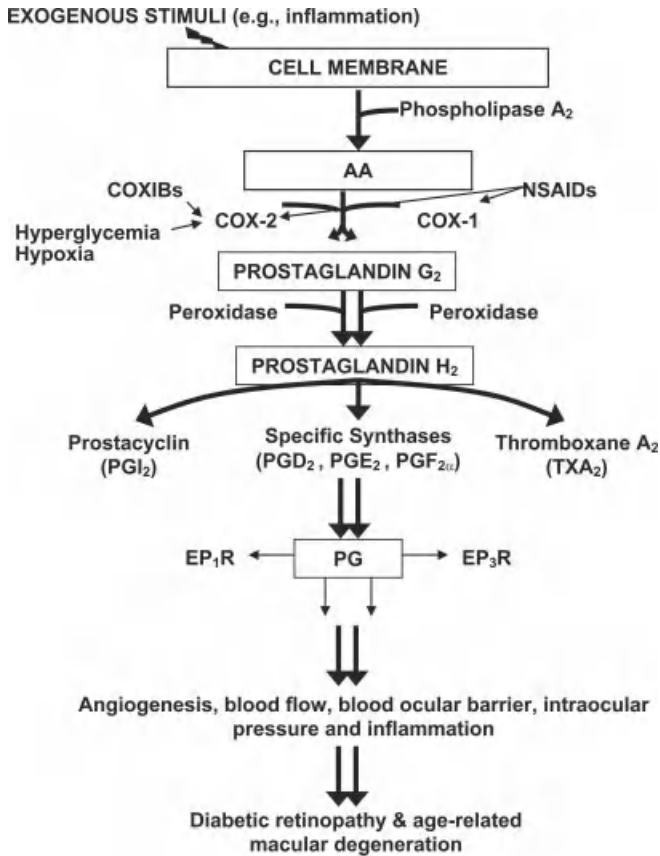


FIGURE 5-1 Role of prostaglandins (PGs) in the eye in health, disease, and the effects of COX-2 s-NSAIDs and ns-NSAIDs. Following an exogenous stimulus (e.g., inflammation), cell membrane phospholipid is liberated to arachidonic acid (AA) by phospholipase A₂. Both COX-1 and COX-2 catalyze the conversion of AA into various PGs. COX-1 is the predominant isoform in the normal eye that is expressed in a variety of ocular tissues, while COX-2 expression is up-regulated during pathological conditions (e.g., hyperglycemia and hypoxia). Nonselective NSAIDs (e.g., diclofenac, fluriprofen, ketorolac, indomethacin) inhibit COX-1 and COX-2, while COX-2 s-NSAIDs (e.g., Celecoxib, Rofecoxib) spare COX-1 and inhibit COX-2. Hyperglycemia and hypoxia can induce COX-2 and participate in vascular permeability. PGs can alter the blood–ocular barrier, affect intraocular pressure, produce miosis and conjunctival hyperemia and retinal and corneal angiogenesis, affect the integrity of the retinal blood–aqueous barrier, and mediate ocular allergic reactions and pain responses. [Reprinted with permission from Z. A. Radi and J. A. Render, *Ocular Pharmacology and Therapeutics*, 24(2), pp. 141–151. Copyright © 2008 Mary Ann Liebert, Inc. Publications. All rights reserved.]

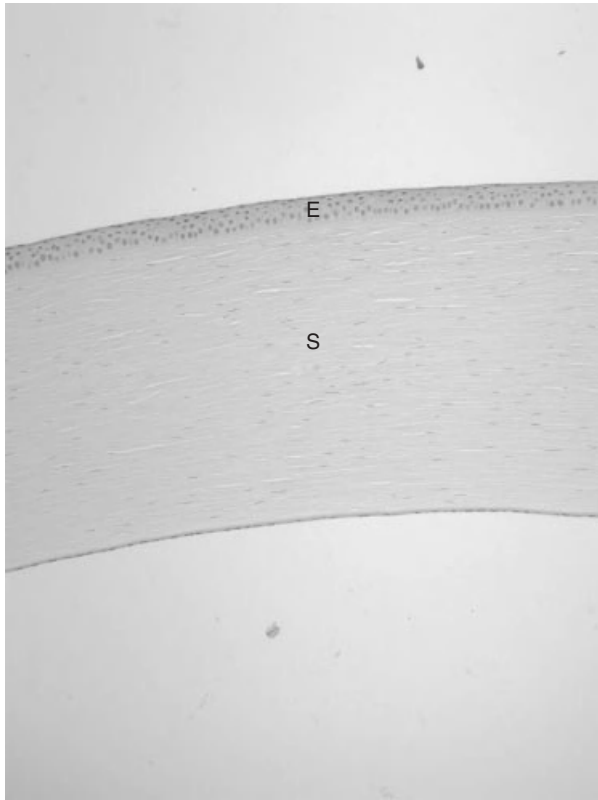


FIGURE 5-2 Normal nonhuman primate cornea anatomic structures. Note epithelium (E) and stroma (S). Hematoxylin and eosin stain, original magnification $\times 10$.

that must maintain transparency to visible light, regularly refract visible light and resist adverse external forces such as dehydration, microbial invasion, and trauma. Structurally, the cornea is an avascular (devoid of blood vessels) convex uniform nonpigmented, nonkeratinized tissue composed histologically of five layers from the outside to the inside: the epithelium, Bowman's layer, the stroma, Descemet's membrane, and the endothelium (Fig. 5-2). The cornea receives nutrition from tears, aqueous humor, and capillaries in the limbus. The corneal epithelium is the barrier of the cornea to the exterior and is a tight epithelium with a relatively low ionic conductance (Ehlers and Hjortdal, 2005). The anterior part of the stroma, known as Bowman's membrane, is acellular, and by light microscopy it appears homogeneous. Bowman's membrane is transparent, continuous, and homogeneous and is prominent in human and nearly all nonhuman primate (except the lemur) corneas (Merindano et al., 2002). Bowman's layer is absent in all carnivores (Merindano et al., 2002). The fibrils in Bowman's membrane are thinner (20 nm) than those of the stroma, and accordingly, show a higher type V/type I collagen ratio (Ehlers and Hjortdal, 2005). Corneal stroma comprises nearly 90% of corneal thickness, is very poorly cellular, and is composed predominantly of highly ordered extracellular

type I collagen fibrils with interspersed cells, the keratocytes. Keratocytes are the predominant cell type in the stroma and play a role in maintaining its organization. These stellar-shaped cells contact each other by long cytoplasmic extensions (morphologic and functional syncytium) and also interact with the corneal epithelium (Willoughby et al., 2010). Type I collagen fibrils are uniform in size and spacing, specialization that allows the transmission of visible light. The endothelium and Descemet's membrane regulate the hydration status of the stroma, and the epithelium and Bowman's layer provide protection against the environment (Holland and Mannis, 2002). A large decrease in central endothelial cell density occurs during maturation of the cornea in several species (Bahn et al., 1986). During the first months of life, central endothelial cell counts of developing corneas of cat, dog, and rabbit decrease rapidly. This rapid decrease in endothelial cell density correlates with growth of the cornea to adult size. Despite a wide variation in corneal size, central endothelial cell counts of adult cat, cow, deer, dog, pig, rabbit, and human corneas were similar (2500 cells/mm²). Hypertrophy of individual cells is primarily responsible for this adult cell density of 2500 cells/mm² for these species (Bahn et al., 1986).

Embryologically, the human cornea can be identified at an early stage of development (week 6) (Ehlers and Hjortdal, 2005). At birth the cornea is relatively large compared to the eyeball. The cornea is one of the most densely innervated tissues in the body. It is estimated that there are approximately 7000 nociceptors/mm² in the human cornea (Ehlers and Hjortdal, 2005). A tear film covers the surface of the epithelium. This thin layer of fluid maintains the optical quality of the cornea (Ehlers and Hjortdal, 2005). The cornea may also be divided into a central part and a peripheral or limbal zone (Ehlers and Hjortdal, 2005). The cornea is avascular and the branches of the anterior ciliary arteries stop at the limbus, where they form arcades that supply the peripheral cornea. Thus, the peripheral and central cornea is very distinct in terms of physiology and pathology (Willoughby et al., 2010). The epithelium and endothelium utilize most of the corneal oxygen and receive the most oxygen from the atmosphere. Oxygen diffuses through the tear film, and aerobic metabolism expels CO₂ into the atmosphere. Thus, the cornea is metabolically active and has three exchange routes for metabolites and accumulated breakdown products: the anterior epithelial surface, the posterior endothelial surface, and the peripheral limbus (Ehlers and Hjortdal, 2005). The cornea is the main route for drug transport to the anterior chamber (Willoughby et al., 2010). The abundant presence of hydrated collagen in the stroma may hamper the diffusion of highly lipophilic drugs (Willoughby et al., 2010). The endothelium is more permeable and allows the passage of hydrophilic drugs and macromolecules between the aqueous layer and the stroma due to the presence of "leaky tight junctions" called desmosomes or macula adherens. The passage of topical ocular drugs through the corneal route depends on their lipophilicity, molecular weight, charge, and degree of ionization. Small lipophilic drugs in particular can permeate easily through the cornea (Willoughby et al., 2010). There are species differences in corneal anatomy and physiology. The relative size of the cornea varies among animal species living under different conditions, being generally large in night-living (nocturnal) animals and small in those active

in daylight. Corneal thickness is different across species. Corneal thickness in various species is as follows: human (mean central corneal thickness is 0.548 ± 0.037 mm) (Rüfer et al., 2009), rhesus nonhuman primate (mean central corneal thickness is 0.468 ± 0.02 mm) (Ollivier et al., 2003), cynomolgus nonhuman primate (0.4 mm) (Ehlers and Hjortdal, 2005), horse (0.786 mm) (Plummer et al., 2003), dog (0.562 ± 0.06 mm) (Gilger et al., 1993), cat (0.578 ± 0.06 mm) (Gilger et al., 1993), Fisher 344 rat (0.15 ± 0.02 mm) (Tuft et al., 1986), ox (0.8 mm) (Ehlers and Hjortdal, 2005), rabbit (0.4 mm) (Ehlers and Hjortdal, 2005), and C57BL/6J mouse (0.083 mm) (Dimasi et al., 2011). Corneal thickness is of importance for the estimation of intraocular pressure (IOP) and in the diagnosis of corneal and systemic disorders. Pathological conditions can affect corneal thickness. Sustained ocular hypertension in humans causes an increase in corneal thickness (Ventura et al., 2001). Increased corneal thickness can adversely affect IOP measurements (Brusini et al., 2000). Corneal endothelium was evaluated in patients with diabetes mellitus types 1 and 2. There was a statistically significant decrease in endothelial cell density (ECD) in type 1 disease compared with healthy subjects. Corneas from diabetic patients were thicker than normal and the HbA1c level was correlated inversely with the ECD and the mean endothelial cell area. In addition, significant correlation was observed between the endothelial morphology and grade of diabetic retinopathy (Módis et al., 2010).

The cornea is highly innervated and heals rapidly without scarring. Corneal wound healing is a complex physiological process and plays a critical role in the maintenance of corneal structural integrity and clarity. Several growth factors and cytokines are released following an epithelial injury in the cornea and contribute to corneal healing pathophysiology. These factors play essential roles in epithelial–stromal interaction leading to successful corneal wound healing. Growth factors such as keratinocyte growth factor (KGF) and hepatocyte growth factor (HGF) are believed to be produced by keratocytes, while IL-1 and platelet-derived growth factor (PDGF) are secreted by the epithelium. Other growth factors, such as the epidermal growth factor (EGF) family, insulin-like growth factor (IGF), and transforming growth factor beta ($TGF\beta$), regulate both the epithelium and stroma, and the crosstalk among various growth factors determines the outcome of a corneal epithelial wound (Yu et al., 2010). EGFR is generated in response to cell injury to intracellular signaling pathways, particularly extracellular signal-regulated kinase (ERK) and phosphatidylinositol 3-kinase (PI_3K), and regulates corneal epithelial wound healing. In cultured porcine corneas, inhibition of ERK and PI_3K pathways impaired *ex vivo* epithelial wound healing (Xu et al., 2004). Other growth factors, such as insulin, IGF, and HGF, are known to transactivate EGFR (Yu et al., 2010). Cellular components such as ATP and lysophosphatidic acid (LPA) released from injured cells act as “alarmins” to initiate cell response by transactivating EGFR and to signal potential further damage to the cornea, such as infection. Thus, EGFR represents a pivotal point of cell signaling accessible to a variety of stimuli in response to pathophysiological challenge in the cornea (Yu et al., 2010). There are species differences in reactions to corneal injury and in the healing process. The horse had the longest healing time, whereas cow corneal healing is rapid. Corneal neovascularization occurs following corneal trauma or chemical injury. It has been

shown that vascular endothelial growth factor (VEGF) is an important mediator of angiogenesis in a rat model of corneal neovascularization (Edelman et al., 1999). Vascularization can enhance the corneal healing process and increase the likelihood of scarring.

The anterior chamber (AC) of the eye is the front part of the eye between the cornea and the iris. The AC is filled with aqueous humor, an optically clear, colorless, watery, and slightly alkaline fluid. The aqueous humor (AH) provides nutrition to the cornea and lens and removes waste products. Several immunosuppressive substances are present within the normal aqueous humor, such as TGF β , which inhibits antigen processing and presentation, and suppresses both T-lymphocyte activation and certain aspects of nonspecific inflammation (Streilein and Cousins, 1990). Recent data show that AH suppressed lineage commitment and acquisition of the Th1 and Th17 effector function of naive T cells, manifested as a reduction in lineage-specific transcription factors and cytokines. AH promoted its massive conversion to Foxp3⁺ regulatory T-cells (Tregs), which expressed CD25, glucocorticoid-induced tumor necrosis factor receptor family-related gene (GITR), cytotoxic T-lymphocyte antigen 4 (CTLA-4), and CD103 and were functionally suppressive. TGF β and retinoic acid were both needed and synergized for Treg conversion by AH, with TGF β -enhancing T-cell expression of retinoic acid receptor α (Zhou et al., 2011). Other immunosuppressive factors found in the low-molecular-weight fraction (< 5 kDa) of aqueous humor include neuropeptide α -melanocyte-stimulating hormone (MSH α), which suppresses immunogenic inflammation, neuropeptide vasoactive intestinal peptide (VIP), and somatostatin (Taylor et al., 1994; Taylor and Yee, 2003). There is a delicate balance between the production and drainage of the aqueous humor, which maintains the normal physiological range of intraocular pressure at 10 to 20 mmHg (Philipp et al., 1990). In certain pathological conditions, aqueous humor accumulates within the eye and IOP increases, which can lead to glaucoma (i.e., increased pressure inside the eye due to the decreased aqueous humor outflow) (Philipp et al., 1990). Nonhuman primates have been used as a model for ocular hypertension, which leads to optic neuropathy, which closely reflects the optic neurodegeneration associated with human glaucoma (Rasmussen and Kaufman, 2005). Glaucoma is one of the most frequent ophthalmic diseases in dogs and is characterized by high IOP (> 25 to 30 mmHg in dogs and > 31 mmHg in cats).

The lens is a biconvex transparent structure that lies posterior to the iris. It is avascular, lacks a nerve supply, and contains a high concentration of protein, carbonic anhydrase, and glutathione (Friedland and Maren, 1984; Giblin, 2000). The normal human lens contains about 65% water and 35% organic matter, the latter being mainly (greater than 90%) structural proteins (Lerman, 1983). Lens thickness across species is 4 mm (human), 2.98 mm (monkey), 7.85 mm (dog), 8.5 mm (cat), and 3.87 mm (rat) (Vakkur and Bishop, 1963; Massof and Chang, 1972; Lapuerta and Schein, 1995; Mutti et al., 1999). The lens is attached to the ciliary body by zonules. Contraction and relaxation cause changes in the lens configuration, increasing and decreasing its focusing power. This process called accommodation is necessary in focusing on both near and distant objects. The lens of a human eye is only twice as thick as that of the mouse (Zhou et al.,

2007). Glutathione functions as an essential antioxidant vital for maintenance of the lens's transparency (Giblin, 2000). The lens is surrounded by a lens capsule. The lens depends on the aqueous humor and vitreous for nutrition and elimination of waste products. Sodium–potassium–adenosine triphosphatase (Na,K-ATPase) regulates electrolyte concentrations in the lens (Tseng and Tang, 1999). Hexokinase enzyme contributes to glucose metabolism in the lens. In the mouse lens, high levels of hexokinase mRNAs were noted relative to aldose reductase mRNAs. This favors metabolism of glucose via the glycolytic pathway rather than the sorbitol pathway in the mouse; while the opposite is true for the rat lens (Wen and Bekhor, 1993). Cataract is a clouding of the lens. The word *cataract* is derived from the Greek word *cataractos*, which means “waterfall.” Cataracts are most commonly caused by chemical changes within the lens of the eye. Diabetic cataracts are caused by an elevation of polyols within the lens of the eye catalyzed by the enzyme aldose reductase (Head, 2001). Pathophysiological mechanisms of cataract formation include deficient glutathione levels, which lead to defective antioxidant defense system within the lens. Nutrients that can increase glutathione levels and activity include lipoic acid, vitamins E and C, and selenium. Cataract patients also tend to be deficient in vitamin A and the carotenes lutein and zeaxanthin (Head, 2001). Lens epithelia from patients with senile cataracts have a decreased amount of Na,K-ATPase α -subunit with increased cataract severity (Tseng and Tang, 1999). It has been demonstrated that the rat lens microsomal preparations possess the ability to convert exogenous arachidonic acid into PGE₂ and PGF_{2 α} (Keeting et al., 1985).

The vitreous humor is a hydrogel that fills the space between the lens and the retina. More than 95% of the content of the gelatinous vitreous body by weight is water (Kleinberg et al., 2011). The volume of the vitreous in adult mammals varies: 1 to 2 mL in rabbit, 3.2 mL in pig, 3 to 4 mL in monkey, and 4 to 5 mL in humans (Kleinberg et al., 2011). The vitreous of rabbit has a high concentration of total protein (2.2 mg/mL) (Manzanas et al., 1992). Cattle, lamb, pig, and dog contain much less protein in the vitreous than do nonhuman primates (Chen and Chen, 1981). Physiological levels (approximately 100 pg/mL) of PGs were found in vitreous from human eyes undergoing cataract extraction. Eyes with vitreous hemorrhage, retinal detachment, or cystoid macular edema had similarly low levels. Vitreous PGs were mildly elevated in trauma and endophthalmitis and markedly elevated in aphakic bullous keratopathy (Thomas et al., 1985). Transmission electron microscopy of the human vitreous revealed the presence of parallel collagen fibrils packed in bundles and no membraneous structures (Sebag and Balazs, 1989). Thus, the gelatinous nature of the vitreous body is related to hyaluronic acid–collagen complex, with aggregation of collagen fibrils into bundles (Sebag and Balazs, 1989; Kleinberg et al., 2011). The presence of both hyaluronic acid (HA) and collagen determine the viscoelastic properties of the vitreous (Kleinberg et al., 2011). The amount of vitreal HA varies across species. Rhesus monkeys and human vitreal HA concentrations are similar (approximately 200 μ g/mL) (Kleinberg et al., 2011). In other species, concentrations range from 20 to 60 μ g/mL in the dog, cat, rabbit, and pig (Weber et al., 1982; Kleinberg et al., 2011) to approximately 470 μ g/mL in cattle (Gherezghiher et al., 1987). At birth, the human vitreous

is entirely gelatinous. However, within the human life span, a linear increase in the volume of the liquid portion of the central vitreous is observed (Kleinberg et al., 2011). In rabbits, a central structure of the vitreous body is defined by a well-demarcated central channel called Cloquet's canal, a remnant of the hyaloid artery (Los et al., 1999). A typical well-defined Cloquet's canal is not normally observed in humans, although a similar arrangement of vitreous fibers is present (Kleinberg et al., 2011). Although the central vitreous is a completely gelatinous structure at birth in primates, a progressive liquefaction develops with aging (Kleinberg et al., 2011). Age-related liquefaction of the vitreous gel has been associated with lens opacification (Harocopos et al., 2004). Rabbits, cats, dogs, sheep, and cattle show relatively small changes with age in the vitreous body (Kleinberg et al., 2011). By contrast, in rhesus monkeys and humans, vitreous liquefies over time, with the portion of the liquefied tissue increasing with age (Denlinger et al., 1980; Los, 2008; Kleinberg et al., 2011). The rabbit is a frequently used animal model for studies on vitreous function and pathobiology (Los et al., 1999). However, the pig and nonhuman primate could be better animal models than the rabbit (Kleinberg et al., 2011). Drugs can be removed from the vitreous through diffusion into the anterior chamber or by the blood–retinal barrier (Willoughby et al., 2010).

The light continues through the vitreous humor back to a clear focus on the retina, behind the vitreous. The retina is the most complex ocular structure and is composed of 10 layers: retinal pigmented epithelium (RPE), inner and outer segments of rods and cones, outer limiting membrane, outer nuclear layer, inner nuclear layer, inner plexiform layer, ganglion cell layer, nerve fiber layer, and inner limiting membrane. The RPE is a monolayer of cuboidal epithelial cells intercalated between the photoreceptors and choriocapillaries (Willoughby et al., 2010). RPE cells rest on the Bruch's membrane, a trilaminar structure consisting of the basement membrane of RPE cells, an intervening elastocollagen layer, and an outer layer derived from the basal layer of the choriocapillaris. This layering is more evident in nonhuman primates than in mice (Zeiss, 2010). Numerous pigment (melanin and lipofuscin) granules are present in the apical cytoplasm of RPE cells. Functions of RPE include the maintenance of photoreceptor function (phagocytosis of photoreceptor waste), retinal adhesion, storage and metabolism of vitamin A, the production of growth factors, and blood–retinal barrier (BRB) function (Willoughby et al., 2010). The retina is exposed to high levels of light throughout the day, and RPE prevent potential noxious effects of such light exposure. Light filtration by RPE pigments functions as a preventive mechanism against photooxidation, and RPE cells can repair considerable damage to DNA, proteins, and lipids (Kevany and Palczewski, 2010). The RPE and the retinal capillary endothelium are the main barriers for systemically administered drugs (Willoughby et al., 2010). The BRB selectively controls the traverse of substances and pharmaceuticals after systemic and periocular administration to the retina (Willoughby et al., 2010). The BRB has a functional outer barrier that is formed by the RPE and an inner barrier formed by the endothelial cells of retinal vessels (Willoughby et al., 2010). Transcellular passive permeation is the main route for the inward/outward traverse of small molecules across the BRB, whereas the paracellular permeability of RPE is

quite low. An inverse correlation exists between the molecular weight and permeability (Willoughby et al., 2010). Choroid/PRE-specific PGD₂ synthase gene was found to be expressed in a much higher level in mouse than in human and guinea pig (Zhou et al., 2007).

The process of vision begins with collection of light by photoreceptor cells in the retina (Kevany and Palczewski, 2010). Photoreceptor cells are comprised of two types: rods, which govern vision in low-light settings, and cones, which collect photons in ambient light and discern color differences (Kevany and Palczewski, 2010). In most mammals, rods are the dominant population throughout the retina (Szél et al., 1996). In humans, rods are approximately 20 times more abundant than cones. The average human retina contains 4.6 million cones (4.08 to 5.29 million). Peak foveal cone density averages 199,000 cones/mm² and is highly variable between individuals (100,000 to 324,000 cones/mm²). The average human retina contains 92 million rods (77.9 to 107.3 million) (Curcio et al., 1990). In nonhuman primates (i.e., pigtail macaques), the retina contains an average of 3.1 million cones (2.8 to 3.3 million), with an average peak foveal cone density of 210,000 cones/mm² (190,000 to 260,000 cones/mm²) (Packer et al., 1989). There are three types of photopigments: red, green, and blue. Damage to the fovea and/or macular area causes reduced color and central vision. The photoreceptors are responsible for phototransduction, the conversion of light into an electrical signal (Willoughby et al., 2010). Rod cells are very sensitive to light but have a low photon saturation threshold, whereas cones have an extremely high saturation threshold but a relatively low sensitivity. Each rod and cone cell consists of four distinct components: a synaptic terminal, an outer segment (OS), an inner segment, and a cilium connecting the outer and inner segments (Kevany and Palczewski, 2010). Photoreceptor cells maintain a roughly constant length by continuously generating new outer segments from their base while simultaneously releasing mature outer segments engulfed by the RPE (Kevany and Palczewski, 2010). The density of rods and cones varies between different regions of the retina. In humans, about 50% of the cones are located in the central 30% of the visual field, corresponding roughly with the macula (Willoughby et al., 2010). There are species differences in retinal maturity. In humans, the retina is mature at birth. In dogs, the rod and cone inner and outer segments are first observed microscopically in the third week after birth. Further differentiation of the rod and cone segments and other retinal layers occurs from week 5 to week 8 (Gum et al., 1984). In cats, retinal maturation process is presumably finished between the fourth and fifth months of life (Vogel, 1978).

The macula lutea is an area in the retina between the temporal vascular arcades containing xanthophyll pigment. Histologically, the macula has several layers of ganglion cells, whereas in the surrounding peripheral retina the ganglion cell layer is only one cell thick. The excavation near the center of the macula is called the fovea (Willoughby et al., 2010). The macula mediates high-acuity central vision and is present in primates as well as in some birds and reptiles (Zeiss, 2010). The mouse lacks a macula and has a much lower proportion of cones in its retina (Zeiss, 2010). Age-related macular degeneration (AMD) is a degenerative progressive condition of the retinal pigment epithelium, its supporting basement membrane, and the overlying photoreceptors. AMD is regarded as the leading cause of blindness in

humans older than 65 years. AMD results from variable contributions of age, environment, and genetic predisposition (Zeiss, 2010). Normal aging is accompanied by thickening of the Bruch's membrane and minor accumulation within the macula of small discrete sub-RPE deposits known as hard drusen. The biochemical composition of drusen includes complement components such as complement C3 and C5b-9 terminal complexes, immunoglobulins, apolipoproteins B and E, fibrinogen, vitronectin, and amyloid β (Zeiss, 2010). AMD is characterized by fragmentation and calcification of Bruch's membrane, as well as accumulation of soft drusen (Zeiss, 2010). Rodents and nonhuman primates are the primary models in which choroidal neovascularization is induced and antiangiogenic therapies of AMD are tested (Zeiss, 2010). Although the mouse does not have a macula, it is the most commonly utilized animal model of AMD because (1) the histological anatomy of the primary site of AMD (RPE, Bruch's membrane, and choriocapillary layer) is well preserved across species, and (2) the mouse is genetically manipulable and is thus the most practical model in which to test the numerous genetic alterations associated with AMD (Zeiss, 2010). Macular degeneration occurs in rhesus and cynomolgus macaques. In both, retinal lesions are characterized by drusen accumulation in the central retina. However, the onset of fundus changes and inheritance patterns differ in these two primate species. Macular degeneration in the cynomolgus macaque appears to be a model for early-onset maculopathies rather than AMD. In contrast, adult-onset macular degeneration in rhesus macaques resembles human AMD (Zeiss, 2010). COX-2 immunohistochemical expression was evaluated in sections of choroidal neovascular membranes excised from 16 patients with AMD. Increased expression of COX-2 in human choroidal neovascular membranes was noted and may suggest a possible role for cyclooxygenases in age-related macular degeneration pathogenesis (Maloney et al., 2009).

The optic nerve carries electrical signals from the retina to the brain visual cortex region for processing. In the normal adult human optic nerve, there are an estimated 1.2 million axons per nerve (Balazsi et al., 1984). In normal cynomolgus monkeys, the mean total number of fibers in the optic nerve is 1.2 million. The mean diameter of axons is 0.8 μm (Sanchez et al., 1986). The optic nerve is visible on ophthalmic examination and corresponds to the physiologic blind spot. Other anatomical components of the eye are the conjunctiva, meibomian glands, the uveal tract, and the choroid. The conjunctiva is a vascular mucous membrane that lines the upper and lower eyelids. The portion covering the sclera is termed the bulbar conjunctiva, and that covering the inner lid is termed the palpebral conjunctiva. The conjunctiva provides mucous to lubricate the surface, which is secreted by the goblet cells. Membrane-associated mucins such as MUC1 and MUC4 decorate the membranes of human conjunctival epithelial cells (Berry et al., 2000). The conjunctiva contains lymphoid tissue, consisting of intraepithelial lymphocytes, subepithelial lymphoid follicles, and adjacent lymphatics and blood vessels. This conjunctiva-associated lymphoid tissue (CALT) plays a key role in protection of the ocular surface by initiating and regulating immune responses (Steven and Gebert, 2009). Meibomian glands are oil-secreting sebaceous glands composed of secretory acini that are connected via smaller ductules to the larger long straight central duct. The numerous secretory acini, which have an elongated or spherical shape

approximately 150 to 200 μm in diameter, are completely filled with secretory cells called meibocytes. The meibomian glands of the human have a dense meshwork of unmyelinated nerve fibers (nerve plexus) around the acini (Knop et al., 2011).

The uveal tract consists of the iris, ciliary body, and the choroid. The uveal tract forms the central vascular bed for the eye. The iris and ciliary body are referred to as the anterior uvea, and the choroid is referred to as the posterior uvea. The uveal tract contains rich networks of both resident macrophages and MHC class II dendritic cells, which act as sentinels for capturing and sampling bloodborne and intraocular antigens. Large numbers of mast cells are present in the choroid of most species but are virtually absent from the anterior uvea in many laboratory animals. However, the human iris does contain mast cells. Small numbers of what are presumed to be trafficking lymphocytes are present in the uveal tract of normal eyes (McMenamin, 1997). The center aperture is the pupil. Through dilation and constriction, the pupil regulates the amount of light sent to the retina. The ciliary body is continuous with the iris and directly adjacent to the sclera. The ciliary processes, which produce aqueous humor, arise from the ciliary body. Fine suspensory ligaments of lens called the zonules of Zinn arise from ciliary processes. These ligaments connect the ciliary body to the lens (Davanger and Ringvold, 1977). The ciliary muscle is composed of radial, longitudinal, and circular fibers. The circular fibers help in contracting and relaxing, which in turn increases and decreases tension on the zonules, leading to lens accommodation (Hiraoka et al., 2010).

ROLE OF PROSTAGLANDINS IN THE OCULAR SYSTEM

Prostaglandins (PGs) are arachidonic acid (AA) metabolites that have receptors localized in a variety of ocular tissues and affect the physiology and pathophysiology of the ocular system (Fig. 5-1 and Table 5-1) (Hardy et al., 1994; Radi and Render, 2008). PGs can lower ocular pain threshold; disrupt the integrity of the retinal blood–aqueous barrier; increase the permeability of the blood–ocular barrier, increase or decrease intraocular pressure (IOP), produce miosis (constriction of the pupil of the eye), cause conjunctival hyperemia, increase retinal and corneal angiogenesis, exacerbate photophobia, be associated with a stinging or burning sensation, cause periocular hyperpigmentation, cause eyelash growth, and/or mediate ocular allergic reactions and pain responses (Kosaka et al., 1995; Damm et al., 2001; Schalmus, 2003; Wilkinson-Berke, 2004; Radi and Render, 2008; Hommer, 2010; Pirie et al., 2011). The IOP-lowering action of several established and potential antiglaucomatous drugs, including latanoprost (Kashiwagi and Tsukahara, 2003), brimonidine (Sponsel et al., 2002), epinephrine (Kaplan-Messas et al., 2003), and cannabinoids (Green et al., 2001), is mediated, at least in part, through the release of endogenous PGs. Decreased outflow of aqueous humor through the trabecular meshwork and Schlemm's canal characterizes primary open-angle glaucoma (OAG), which results in ocular hypertension. Latanoprost, a PG analog, has been used as an IOP agent for glaucoma and for the treatment of OAG in humans because of its ability to cause increased uveoscleral outflow (Camras, 1996; Camras et al.,

TABLE 5-1 Comparative Expression of Various Prostaglandins and their Receptors in the Eye

Ocular compartment	Species	PGs receptor type(s) and subtype(s)	References
Cornea, Epithelium	Pig	EP ₁ , EP ₂ , EP ₃	Zhao et al., 1995
Endothelium	Rabbit	PGE ₂	Joyce et al., 1995
	Pig	EP ₂ , EP ₃	Zhao et al., 1995; Zhao and Shichi, 1995
Sclera	Human	EP ₁ , EP ₂	Anthony et al., 2001
Lens, epithelium	Pig	EP ₃	Zhao et al., 1995
Iris Muscle	Human	PGE ₂ , PGF _{2α}	Matsuo and Cynader, 1992
	Pig	EP ₁	Zhao et al., 1995
Epithelium	Human	PGE ₂ , PGF _{2α}	Matsuo and Cynader, 1992
Ciliary body Epithelium	Pig	EP ₃	Asakura et al., 1992; Zhao et al., 1995
	Human	EP ₄	Crider and Sharif, 2001
Muscle	Mouse	PGE ₂ , EP ₁ , EP ₂ , EP ₃ , EP ₄	Takamatsu et al., 2000
	Monkey	PGE ₁ , PGE ₂	Yamaji et al., 2005
	Pig	EP ₂	Zhao et al., 1995
	Human	PGE ₂ , PGF _{2α}	Matsuo and Cynader, 1992; 1993
Trabecular meshwork	Human	EP ₂ , EP ₄	Crider and Sharif, 2001; Kamphuis et al., 2004
	Pig	EP ₂	Zhao et al., 1995
Retina	Human	PGE ₂ , PGF _{2α}	Matsuo and Cynader, 1992
	Pig	EP ₃	Zhao et al., 1995
Blood vessels	Pig	PGF _{2α}	Hardy et al., 1998
	Bovine	PGI ₂ , PGE ₂ , PGF _{2α}	Kulkarni and Payne, 1997
	Rabbit	PGF _{2α}	Poyer et al., 1992

Source: Reprinted with permission from Z. A. Radi and J.A. Render, *Ocular Pharmacology and Therapeutics*, 24(2), pp. 141–151. Copyright © 2008 Mary Ann Liebert, Inc. Publications. All rights reserved.

1996; Mishima et al., 1997; Noecker et al., 2003; Maihofner et al., 2001). Effects of PG analogs on IOP lowering in vivo were typically observed 4 to 24 h after treatment in beagle dogs and cynomolgus monkeys (Reitmair et al., 2010). Conjunctival hyperemia is a common side effect in patients with ocular hypertension given FP receptor agonists and PGs analog (Honrubia et al., 2009).

Different portions of the eye have different capacities to synthesize PGs (Table 5-1) (Kulkarni and Srinivasan, 1989; Radi and Render, 2008). For example, the cornea, lens, and retina have less capacity to synthesize COX products from AA than that of the conjunctiva and anterior uvea (Kulkarni and Srinivasan, 1989). Human retina has considerably less ability to metabolize AA into COX activity

(Kulkarni and Srinivasan, 1989). The anterior uvea of human, monkey, and rabbit can synthesize PGE₃ and PGD₃ (Kulkarni and Srinivasan, 1989). Conjunctiva and eyelid tissues of cynomolgus and rhesus monkeys can synthesize detectable amounts of COX products. In comparison, cynomolgus anterior uvea can synthesize a considerably smaller amount of COX products (Kulkarni et al., 1987). In the ciliary processes of pigs, PGs synthesis occurs in both nonpigmented and pigmented epithelial cells (Asakura et al., 1992). In humans, COX-2 is expressed constitutively in the nonpigmented secretory epithelium (NPE) of the ciliary body, but is lost completely in the NPE of patients with end-stage OAG (Maihöfner et al., 2001). In addition, significantly fewer PGE₂ levels were present in aqueous humor of patients with OAG than in cataract patients (Maihöfner et al., 2001). Certain PGs, such as PGF_{2α}, are specifically localized on the retinal blood vessels in the neonatal pig and along with PGI₂ and PGE₂ are synthesized by bovine retinal microvascular endothelial cells (Poyer et al., 1992; Kulkarni and Payne, 1997; Hardy et al., 1998).

In different mammalian species, there are significant differences in the responsiveness of the iris sphincters to the miotic effects, constriction of the pupil of the eye, of PGs (Miranda and Bito, 1989). In cats and dogs, the iris sphincter contracts in response to PGF_{2α}, but not in response to other PGs, at concentrations that can be expected to occur under *in vivo* physiological conditions. In both cats and dogs, PGF_{2α}, but none of the other PGs tested, yielded a dose-dependent full miosis when applied topically to intact eyes (Miranda and Bito, 1989). In contrast to the iris of cats, the bovine iris showed low sensitivity and low specificity and exhibited *in vitro* responses to high concentrations of several PGs (Miranda and Bito, 1989). In several other species (rabbits, rhesus and cynomolgus monkeys, baboons, humans) *in vivo* and *in vitro* studies showed that the iris sphincter does not exhibit similar miotic responses to any of the PGs that had been studied (Miranda and Bito, 1989). Therefore, these differences must be taken into consideration when comparing the effects of PGs on the iris sphincter across species.

Once synthesized, various PGs affect function by acting through specific receptors that are localized in various ocular tissues. The ciliary muscle is a well-documented center of PG receptor localization (Radi and Render, 2008). PGE₂ is produced by many cells of the body, including fibroblasts, macrophages, and dendritic cells. PGE₂ biological effects are mediated via four G-protein-coupled receptor subtypes (EP), which mediate stimulation of phosphoinositol turnover with elevation in intracellular calcium, activation of adenylyl cyclase activity resulting in elevation of intracellular cyclic AMP, or inhibition of adenylyl cyclase (Hinz et al., 2000). The capacity of ocular tissues to synthesize PGE₂ was initially determined on the basis of [¹⁴C]AA conversion *in vitro* and *in vivo* (Kulkarni et al., 1984; Bazan et al., 1985a; Preud'homme et al., 1985). Both the iris and the retina of the rabbit released PGE₂, PGF_{2α}, and thromboxane (TX) B₂ when incubated *in vitro*, and PGE₂ was the major COX product formed by each tissue (Preud'homme et al., 1985). The metabolism of radiolabeled AA in epithelium, stroma, and endothelium was studied in normal and cryogenically lesioned rabbit corneas (Bazan et al., 1985b). Two hours after injury, COX products in the epithelium increased, particularly PGF_{2α}. Prostaglandin levels in the stroma rose rapidly after injury and

remained elevated for 15 days. In the endothelium, increases in $\text{PGF}_{2\alpha}$ and PGE_2 were the most prominent effects of injury (Bazan et al., 1985b). Chronic or acute self-resolving inflammation was induced in mice by corneal suture or epithelial abrasion, respectively. Corneal levels of endogenous PGE_2 formation increased 4.3 and 6.6-fold after 2 and 4 days of suture-induced chronic inflammation, respectively, and remained elevated through day 7. The increase in endogenous PGE_2 formation correlated with pronounced neovascularization. In contrast, basal corneal levels of PGE_2 demonstrated no significant increase throughout the course of injury and wound healing during an acute, self-resolving epithelial abrasion (Liclican et al., 2010). PGE_2 has four receptor subtypes (EP_1 , EP_2 , EP_3 , and EP_4). In the ciliary muscle of mice, consistent EP_1 and EP_4 receptors of mRNA expression were present in the ciliary muscle, whereas EP_2 and EP_3 signals were not detected (Takamatsu et al., 2000). The gene regulatory networks engaged in mediating the physiological effects on EP_2 and EP_4 receptor stimulation were investigated using cultured human ciliary smooth muscle cells. The effects of EP_2 and EP_4 receptor stimulation on gene regulation were found to be generally very similar and mediated predominantly through the cAMP signaling pathway (Reitmair et al., 2010). Topical application of PGE_1 and PGE_2 attenuated ciliary muscle contraction in monkeys (Yamaji et al., 2005). In the human eye, receptors for both $\text{PGF}_{2\alpha}$ and PGE_2 are colocalized in the ciliary and iridal sphincter muscles (Matsuo and Cynader, 1992). EP_2 receptor is expressed in the iris sphincter muscle and ciliary muscle in pigs, while the EP_1 receptor is expressed in both the sphincter and dilator iris muscle (Zhao et al., 1995). In the human eye, the highest expression of EP_1 receptor mRNA and protein is found in the epithelia of the cornea, conjunctiva, lens, ciliary body, trabecular cells, iris vessels, and retinal ganglion cells (Schlötzer-Schrehardt et al., 2002). In addition, the expression of EP_1 mRNA receptors was found in human ciliary muscles, iris vasculature, and in the ganglion and inner and outer nuclear layers of human retina (Mukhopadhyay et al., 2001). Remodeling of the extracellular matrix (ECM) of the ciliary body involves matrix metalloproteinases (MMPs) which are released by ciliary smooth muscle cells. Some studies revealed that human ciliary smooth muscle cells can secrete MMP-1, MMP-2, MMP-3, and MMP-9 and that exposure to $\text{PGF}_{2\alpha}$ increased the production of all four MMPs (Weinreb et al., 1997). In pigs, EP_1 is found in the corneal epithelium and ciliary NPE (Abran et al., 1995; Zhao et al., 1995). In C57BL/6 [wild-type (WT)] mice or FP, EP_1 , EP_2 , and EP_3 receptor-deficient mice, the ocular hypotensive effects and changes of outflow after selective agonists of PGE_2 receptor subtype (EP_1 , EP_2 , EP_3 , and EP_4) treatment were investigated. The EP_2 agonist ONO-AE1-259-01 and EP_4 agonist ONO-AE1-329 significantly reduced IOP in a dose-dependent manner, whereas the EP_1 agonist ONO-DI-004 and EP_3 agonist ONO-AE-248 showed no effect. The reduction in IOP with ONO-AE1-259-01 was eliminated completely in EP_2 -knockout mice, whereas the reduction in IOP in other knockout mice was similar to that observed in wild-type mice. Thus, EP_2 and EP_4 receptors mediated IOP reduction in mice, whereas the contribution of EP_1 and EP_3 receptors was insignificant. In addition, the EP_2 and EP_4 receptor-mediated mechanisms of IOP reduction were different from those mediated by the FP receptor (Saeki et al., 2009).

EP₂ is associated with the corneal epithelium and endothelium, lens epithelium, and ciliary NPE (Matsuo and Cynader, 1993; Abran et al., 1995; Zhao and Shichi, 1995; Anthony et al., 2001; Crider and Sharif, 2001). EP₂ receptor agonists cause vasodilatation and disrupt the blood–aqueous barrier (Kitagawa et al., 2001; Bhattacharjee et al., 2002). In the human eye, EP₂ receptor mRNA and protein labeling was most prominent in the corneal epithelium and choriocapillaries (Schlötzer-Schrehardt et al., 2002). There are some regional differences in the intensity of immunofluorescence between EP receptor subtypes between human and mouse eye. In the human eye, immunoreactivity for EP₂ receptors in the conjunctiva and trabecular meshwork is stronger than that in the mouse eye (Biswas et al., 2004). EP₁ and EP₂ receptor localization in the anterior uvea of mice and humans is very similar to that seen in the pig (Zhao et al., 1995; Biswas et al., 2004). EP₂ is associated with the trabecular meshwork in humans and pigs (Zhao et al., 1995; Kamphuis et al., 2004). EP₁ and EP₂ receptors are also found in the scleral fibroblasts of humans (Anthony et al., 2001). The influence of PGE₂ on the expression of COX-2 in human NPE cells was studied. Data have shown that PGE₂ at physiologically relevant concentrations induced COX-2 expression via a mechanism involving EP₂ and EP₄ receptor activation and phosphorylation of the mitogen-activated protein kinases (MAPKs) p38 and p42/44 (Rösch et al., 2005). The long-term one-year effects of topical treatment with 0.1% EP₂ agonist AH13205 on the anterior eye segment was investigated in cynomolgus monkeys. In the ciliary muscle, there was a significant increase in optically empty spaces between muscle bundles in the anterior portion of the longitudinal and the reticular ciliary muscle compared with untreated and vehicle-treated control animals. Within these spaces, significantly more myelinated nerve fiber bundles were found in drug-treated than in normal control animals. The ciliary epithelium had a normal appearance (Richter et al., 2003). In another study in cynomolgus monkeys, after a one-year treatment with 0.1% butaprost, an EP₂ receptor agonist, the morphology of the ciliary muscle showed increased spaces between ciliary muscle bundles and the formation of new outflow channels (Nilsson et al., 2006).

In pigs, EP₃ is localized to the corneal epithelium and endothelium, the lens epithelium, and the pigmented ciliary epithelium, bipolar cell, horizontal cell, amacrine cell, ganglion cell, and Müller cells (Zhao et al., 1995). EP₃ is localized to all uveal tissues in pigs (Zhao and Shichi, 1995). In the human eye, EP₃ and EP₄ receptors mRNA and protein labeling were observed primarily in the corneal endothelium and keratocytes, trabecular cells, ciliary epithelium, and conjunctival and iridal stroma cells. In addition, EP₃ was found in retinal Müller cells (Schlötzer-Schrehardt et al., 2002). Localized receptors of EP₄ have been identified in the trabecular meshwork and ciliary nonpigmented epithelial cells in the human eye (Matsuo and Cynader 1993; Anthony et al., 2001; Crider and Sharif, 2001). EP₄ receptors mediate the disruption of the blood–aqueous barrier induced by EP receptor agonists and paracentesis (Bhattacharjee et al., 2002). In the human eye, PGF_{2 α} and PGE₂ receptors are expressed in the iris epithelium and retina (Matsuo and Cynader, 1992). In pigs, EP₃ is localized in the retinal photoreceptor (Zhao and Shichi, 1995). In newborn pigs, inhibition of COX-1 with valeryl salicylate caused increased density of PG receptors, EP₁, EP₃, and F_{2 α} in retinal vessels (Hardy et al.,

1998). In mice, EP₃ was constitutively expressed in conjunctival epithelium on the ocular surface (Ueta et al., 2009).

Besides the different areas of PGs receptor localization, there are also species differences in ocular anatomy and reactions of the eye to given exogenous PGs (Radi and Render, 2008). For example, the rabbit eye is most sensitive to exogenous PGs (e.g., PGF_{2α}) and the nonhuman primate eye is least sensitive (Bito, 1984; DeSantis and Sallee, 1989; Poyer et al., 1992). Exogenous PGF_{2α} and its analogs, PhXA85 and latanoprost, stimulated the formation of PGE₂, PGD₂, and PGF_{2α}, in iris and ciliary muscles isolated from cat, bovine, rabbit, dog, rhesus monkey, and human (Yousufzai et al., 1996).

In addition to their part in normal ocular physiology, PGs play a role in topical and intraocular injury and inflammation (Radi and Render, 2008). PGs are released into the aqueous humor in response to various intraocular conditions, such as paracentesis, mechanical or laser injury to the iris, and experimental immunogenic and nonimmunogenic ocular inflammation (Bhattacharjee et al., 1980). Following corneal surface injury, the production of PGs (PGI₂, PGF_{2α}, PGE₂, and PGD₂) by the corneal epithelium increases, and topical application of PGE₁ causes conjunctival changes that include vasodilatation (erythema), increased capillary permeability (chemosis), ocular discharge, decreased palpebral aperture, and occasional miosis (Eakins et al., 1972; Miller et al., 1973; Hall and Jaitly, 1977; Radi and Render, 2008). PGE₂ is synthesized by corneal endothelial cells, and its synthesis is increased in response to injury to the corneal endothelium of rabbits, and the amount in aqueous humor is increased following corneal wounding or inflammation in the anterior chamber (Joyce et al., 1995; Jumblatt, 1994; Jumblatt and Willer, 1996). Corneal regulation of EP expression during inflammatory or reparative response was investigated in a mouse model (Liclican et al., 2010). Chronic or acute self-resolving inflammation was induced in mice by corneal suture or epithelial abrasion, respectively. Interestingly, acute abrasion injury did not alter PGE₂ or EP levels. However, in chronic inflammation, the expression of COX-2, EP₂, and EP₄ was up-regulated and correlated with increased corneal PGE₂ levels and marked neovascularization. PGE₂ topical treatment, 100 ng applied three times a day for up to 7 days, exacerbated neutrophilic infiltration and the angiogenic response to chronic inflammation but did not affect wound healing or neutrophilic infiltration after epithelial abrasion. Exacerbated inflammatory neovascularization with PGE₂ treatment was independent of the vascular endothelial growth factor (VEGF) circuit but was associated with a significant induction of the eotaxin–CCR3 axis (Liclican et al., 2010). The expression of EP₃ protein was investigated in the conjunctiva of patients with various ocular surface diseases such as Stevens–Johnson syndrome (SJS), toxic epidermal necrolysis (TEN), chemical eye burns, Mooren’s ulcers, and ocular cicatricial pemphigoid (OCP) (Ueta et al., 2011). EP₃ was expressed in the conjunctival epithelium of patients with chemical eye burns and Mooren’s ulcer and in normal human conjunctival epithelium. However, it was markedly down-regulated in the conjunctival epithelium of SJS/TEN and OCP patients (Ueta et al., 2011). In an experimental allergic conjunctivitis (EAC) mouse model, PGE₂ acts on EP₃ in conjunctival epithelium and down-regulates the progression of EAC (Ueta et al., 2009). A selective EP₄ receptor agonist, 3,7-dithia PGE₁, and an isopropyl

ester prodrug reduced IOP in monkeys. A single dose of 3,7-dithia PGE₁ isopropyl ester at 0.01% or 0.1% decreased IOP in the glaucomatous monkey in the range 40 to 50% (Woodward et al., 2009). The nonclinical safety profile of a topically administered selective EP₄ receptor agonist, PF-04475270, was investigated in beagle dogs. Treatment with PF-04475270 in dogs significantly decreased the IOP by 5 to 6 mmHg when given 0.25 µg/eye or by 7 mmHg when given at ≥1 µg/eye. In addition, PF-04475270 induced corneal neovascularization at doses of ≥1.0 µg/eye and conjunctival hyperemia or red eye at doses of ≥0.25 µg/eye, and these findings were not reversible during the 1- or 4-week recovery period (Aguirre et al., 2009).

PGF_{2α} is a powerful ocular hypotensive agent in rabbits, cats, dogs, monkeys, and humans (Kerstetter et al., 1988; Hardy et al., 1998; Poyer et al., 1992; Sarchahi et al., 2012). The most frequent side effect observed during daily topical treatment with latanoprost, a PGF_{2α} analog, in dogs was miosis (Sarchahi et al., 2012). Central corneal thickness was decreased after topical treatment with latanoprost in patients with OAG (Sawada et al., 2012). High mRNA and protein expression, using immunohistochemistry and *in situ* hybridization, of PGF_{2α} receptor (FP) in cynomolgus monkey eye was found in the cornea, conjunctiva, and iridial epithelium, ciliary muscle, and ciliary processes. In the human eye, the highest expression of FP receptor protein was found in the corneal epithelium, in ciliary epithelium, in the circular portion of ciliary muscle, and in iris stromal and smooth muscle cells (Schlötzer-Schrehardt et al., 2002). Iridial and choroidal melanocytes, the retina, and the optic nerve expressed lower levels of both FP receptor message and protein (Ocklind et al., 1996). Human ciliary smooth muscle cells express functional FP receptors whose activation up-regulates the mRNA and protein expression levels of early growth response factor-1 and connective tissue growth factor, important transcriptional activators of downstream genes involved in tissue remodeling and angiogenesis (Hutchinson et al., 2010). Topical treatment with 2 µg of PGF_{2α} isopropyl ester twice daily for 5 days reduced IOP in cynomolgus monkeys by increasing uveoscleral outflow (Gabelt and Kaufman, 1989; Sagara et al., 1999). This increased uveoscleral outflow is thought to result from the dilatation of the intramuscular spaces of ciliary muscle bundles (Lütjen-Drecoll and Tamm, 1988; Yamaji et al., 2005). PGE₂ also reduced IOP when applied topically by the relaxation of the precontracted ciliary muscle (Takamatsu et al., 2000).

In male Wistar rats, intravenous infusions of prostacyclin (PGI₂) and PGE₂ dilated retinal blood vessels, increased fundus blood flow, and decreased systemic blood pressure in a dose-dependent manner. These vasodilatory effects of PGs on retinal arterioles were greater than those on retinal venules (Mori et al., 2007). Similarly, an EP₂ receptor agonist, ONO-AE1-259-01, dilated retinal blood vessels and increased fundus blood flow and decreased systemic blood pressure (Mori et al., 2007). In streptozotocin-induced diabetic rats, insulin-deficient diabetic rats had significant increases in retinal PGE₂ at two months of diabetes (Kern et al., 2007). Prostacyclin-stimulating factor (PSF) acts on vascular endothelial cells to stimulate the synthesis of PGI₂. PSF is associated primarily with retinal vessels (Hata et al., 2000). PGI₂ increased retinal blood flow (RBF) in control and diabetic rats. The early drop in RBF during the initial weeks after diabetes induction in

rats, as well as the later increase in RBF, both correlated with levels of retinal PSF. Thus, PSF can induce PGI₂, retinal vascular dilation, and increased RBF, and those alterations in retinal PSF expression may explain the biphasic changes in RBF observed in diabetes, at least in rats (Hata et al., 2000). The reduced blood flow may be associated with platelet thrombi in retinal capillaries of diabetic patients, a finding that may be prevented by antithrombotic drugs such as aspirin (The DAMAD Study Group, 1989; Boeri et al., 2001). The development of retinal hemorrhages and acellular capillaries in diabetic dogs was inhibited by aspirin (Kern and Engerman, 2001). In addition, aspirin decreased retinal vascular leakage in diabetic Long–Evans rats (Joussen et al., 2002). In rats with diabetic retinopathy, salicylates inhibited diabetes-induced loss of neuronal cells from the ganglion cell layer (Zheng et al., 2007). It has been suggested that nitric oxide synthase (NOS) and COX-2 work together to contribute to retinal cell death in diabetes and to the development of diabetic retinopathy and that inhibition of retinopathy by aminoguanidine or aspirin is due at least in part to inhibition of this NO/COX-2 axis (Du et al., 2004).

COX-1 EXPRESSION IN THE EYE UNDER NORMAL AND PATHOLOGICAL CONDITIONS

Normally, COX-1 is expressed in various anatomical locations in the eye (Figs. 5-3 to 5-5) (Radi and Render, 2008). This COX-1 expression is variable among different animal species (Table 5-2) (Radi and Render, 2008). The comparative cyclooxygenase product synthesis was investigated in albino rabbit, dog (puppy and adult), cat, cow, and human ocular tissues (Kulkarni et al., 1984). Albino

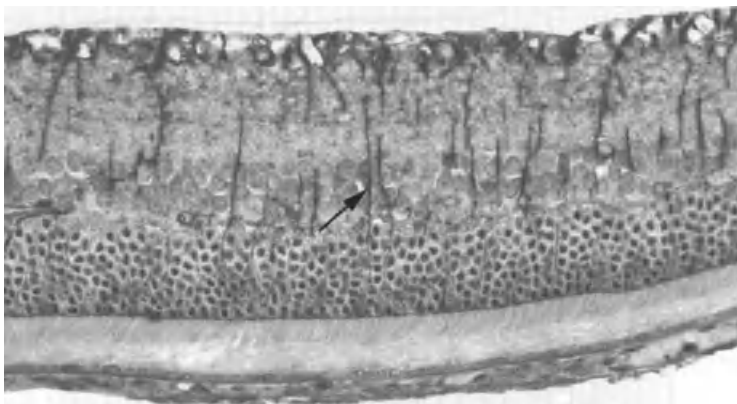


FIGURE 5-3 COX-1 expression in the normal retina of a rat. Note prominent expression of Müller cell processes (arrow). Immunohistochemical stain, original magnification $\times 40$. [Reprinted with permission from Z. A. Radi and J. A. Render, *Ocular Pharmacology and Therapeutics*, 24(2), pp. 141–151. Copyright © 2008 Mary Ann Liebert, Inc. Publications. All rights reserved.]

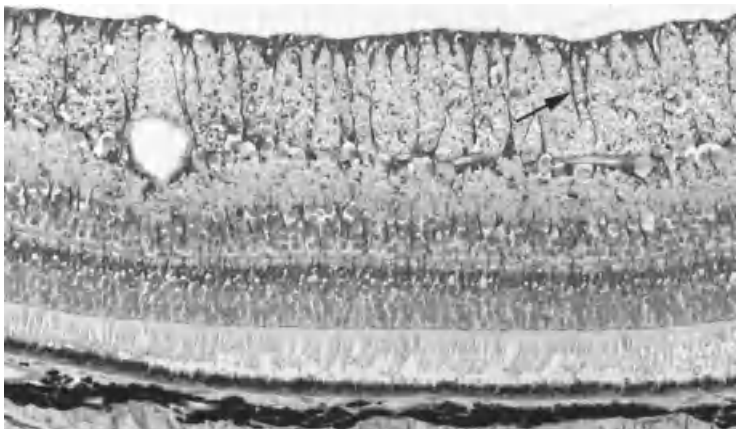


FIGURE 5-4 COX-1 expression in the normal retina of a monkey. Note prominent expression of Müller cell processes (arrow). Immunohistochemical stain, original magnification $\times 40$. [Reprinted with permission from Z. A. Radi and J. A. Render, *Ocular Pharmacology and Therapeutics*, 24(2), pp. 141–151. Copyright © 2008 Mary Ann Liebert, Inc. Publications. All rights reserved.]



FIGURE 5-5 COX-1 expression in the normal retina of a pig. Note prominent ganglion cell expression (arrow). Immunohistochemical stain, original magnification $\times 40$. [Reprinted with permission from Z. A. Radi and J. A. Render, *Ocular Pharmacology and Therapeutics*, 24(2), pp. 141–151. Copyright © 2008 Mary Ann Liebert, Inc. Publications. All rights reserved.]

rabbit conjunctiva synthesized a substantial amount (47%) of cyclooxygenase products, while cat and dog (puppy as well as adult) conjunctival tissues synthesized smaller but significant amounts of cyclooxygenase products (Kulkarni et al., 1984). In the anterior uvea, variable COX-1 expression exists among species (Radi and Render, 2008). Cyclooxygenase activity in the anterior uvea was greatest in the cat, followed by the albino rabbit, which was greater than that in the dog, followed by humans, and the least activity was noted in the cow. Interestingly, cow anterior uvea synthesized $\text{PGF}_{2\alpha}$ and 6-keto- $\text{PGF}_{1\alpha}$ (a stable metabolite of PGI_2), while human anterior uvea synthesized all cyclooxygenase products from 14-C-PGH₂ (Kulkarni et al., 1984). In New Zealand albino rabbits,

TABLE 5-2 Comparative COX-1 Expression in the Eye

Ocular compartment	Species	References
Conjunctiva	Cat, dog, rabbit	Kulkarni et al., 1984
Cornea	Rabbit	Amico et al., 2004; Miyamoto et al., 2004
Anterior uvea	Cat, dog, ox, human, rabbits	Kulkarni et al., 1984
Iris	Rabbit	Damm et al., 2001
Ciliary body, epithelium	Human	Maihöfner et al., 2001
Retina		
Ganglion cells	Human, mouse, pig, rat	Ju et al., 2002, personal communication
Astrocytes	Human	Ju et al., 2002
Microglia	Human, mouse, rat	Ju et al., 2002
Horizontal cells	Mouse	Ju et al., 2002
Photoreceptors	Mouse	Ju et al., 2002
Blood vessels	Human	Ju et al., 2002
Müller cell processes	Rat, monkey	Personal communication
Optic nerve, glial cells	Human	Neufeld et al., 1997

Source: Reprinted with permission from Z. A. Radi and J. A. Render *Ocular Pharmacology and Therapeutics*, 24(2), pp. 141–151. Copyright © 2008 Mary Ann Liebert, Inc. Publications. All rights reserved.

COX-1 is normally expressed, in mRNA and protein, throughout all layers of the cornea (and particularly in the endothelium) (Amico et al., 2004). This COX-1 expression was unaffected in all corneal tissues following corneal injury (Amico et al., 2004). In another study in albino rabbits, the COX-1 expression pattern in corneal cells after photorefractive keratectomy (PRK) and laser in situ keratomileusis (LASIK) procedures was studied. COX-1 protein was not detected immunohistochemically in corneal tissue during the healing intervals after both procedures (Miyamoto et al., 2004). Using real-time RT-PCR and Western blot analysis, the presence of COX-1 in freshly excised iris and ciliary body tissue from adult New Zealand white albino rabbits was demonstrated and NPE of the ciliary body did not show COX-1 immunoreactivity (Damm et al., 2001). In normal eyes of humans, ocular COX-1 expression was confined largely to the NPE of the ciliary body (Maihöfner et al., 2001). The expression of COX-1 in different retinal layers in various species was as follows: outer segments of photoreceptor cells (mouse), microglia (mouse, rat, human), astrocytes (human), horizontal cells (mouse), retinal ganglion cells (mouse, rat, human, and pig) (Fig. 5-5) (Radi and Render, 2008), amacrine cells (mouse, rat, human), and vascular cells. No COX-1 expression was present in the nerve fiber layer (human) and in Müller cell processes in rats and monkeys (Figs. 5-3 and 5-4) (Neufeld et al., 1997; Ju and Neufeld, 2002; Radi and Render, 2008). COX-1 was localized exclusively to the prelaminar and lamina cribrosa regions of the optic nerve head. No COX-1 staining was observed in the nerve fiber layer or the myelinated

optic nerve. COX-1 was associated with the astrocytes of the glial columns and the cribriform plates, but not with the endothelia lining the capillaries (Neufeld et al., 1997).

Ocular COX-1 expression may increase in some pathological conditions. In human eyes with congenital juvenile and angle-closure glaucoma, COX-1 expression remained unchanged in both the ciliary body, NPE, and in other sites of the eye (Maihöfner et al., 2001). In glaucoma in humans, more astrocytes stained with COX-1 than in normals, and staining was intensely perinuclear (Neufeld et al., 1997). COX-1 mRNA and protein expression were investigated in an induced conjunctivitis rat model. λ -Carrageenan (500 mg/eye) or bacterial lipopolysaccharide (LPS; 3 mg/eye) was injected into rat conjunctiva to induce conjunctivitis. COX-1 mRNA did not change by 24 hours after injection (Oka et al., 2004). COX-1 expression was studied in the cornea of mice with herpes simplex virus-1 (HSV-1) keratitis (Biswas et al., 2005). COX-1 mRNA was found to be expressed constitutively in naive corneas, and after HSV-1 infection no significant increase in the expression level was observed (Biswas et al., 2005). In dogs, COX-1 was expressed by ocular malignant melanomas (Pires et al., 2010). Using immunohistochemistry, COX-1 expression was evaluated in the cornea, eyelid, and third eyelid of healthy horses and those affected with squamous cell carcinoma (SCC). COX-1 was significantly greater in equine corneas with SCC than in control corneas. No significant differences in COX-1 immunoreactivity were detected in eyelid and third-eyelid SCC compared with site-matched control tissues (McInnis et al., 2007).

COX-2 EXPRESSION IN THE EYE UNDER NORMAL AND PATHOLOGICAL CONDITIONS

COX-2 expression is generally up-regulated during pathological conditions such as in ocular inflammation or injury (Table 5-3) (Ottino and Bazan, 2000a; Radi and Render, 2008). In an induced conjunctivitis rat model, COX-2 mRNA and protein expression were investigated. λ -Carrageenan (500 mg/eye) or bacterial lipopolysaccharide (LPS; 3 mg/eye) was injected into rat conjunctiva to induce conjunctivitis. In the carrageenan-injected model, COX-2 mRNA expression in the inflamed conjunctiva was significantly increased by 2 h and gradually increased until 24 h and COX-2 protein expression was increased markedly 4 h after injection of carrageenan. In the LPS-injected model, COX-2 mRNA expression was increased 1 h after injection, peaked at 2 h, and decreased at 4 h, and COX-2 protein expression increased 2 h after injection of LPS (Oka et al., 2004). In mice with herpes simplex virus-1 (HSV-1) keratitis, corneal COX-2 expression was evaluated (Biswas et al., 2005). Infected mice had higher COX-2 mRNA and PGE₂ protein levels at different days compared to naive cornea. The levels of COX-2 mRNA and PGE₂ protein were below the limit of detection in naive corneas (Biswas et al., 2005). It was found that IL-1 β induces COX-2 expression in mice cornea after ocular HSV-1 infection (Biswas et al., 2005). Thus, the likely source of COX-2, at least initially after HSV-1 infection, was corneal stromal fibroblasts stimulated by proinflammatory cytokines, such as IL-1 β , induced by HSV-1 replication (Biswas

TABLE 5-3 Comparative COX-2 Expression in the Eye Under Normal and Pathological Conditions

Ocular compartment	Species (pathological condition)	References
Conjunctiva	Mouse (keratitis), rat (inflammation)	Oka et al., 2004; Biswas et al., 2005
Cornea	Dog (glaucoma), rabbit (normal and after keratectomy)	Marshall et al., 2004; Sellers et al., 2004
Sclera	Dog (glaucoma)	Marshall et al., 2004
Anterior uvea	Rabbit (glaucoma)	Chang et al., 1997
Iris	Rabbit (normal)	Damm et al., 2001
Ciliary body	Dog (normal and glaucoma), human (normal), rabbit (normal)	Damm et al., 2001; Maihöfner et al., 2001; Marshall et al., 2004
Trabecular meshwork	Dog (glaucoma)	Marshall et al., 2004,
Retina	Newborn pig (normal), rat and pig (after ischemia)	Deji et al., 2001; Ju et al., 2002
Ganglion cells	Mouse (normal), pig (normal), rat (normal)	Ju et al., 2002, personal communication
Astrocytes	Mouse and rat (ischemic proliferative retinopathy) human (diabetic retinopathy)	Sennlaub et al., 2003
Amacrine cells	Mouse (normal), rat (normal)	Ju et al., 2002
Outer plexiform layer	Mouse (normal), human (normal), rat (normal)	Ju et al., 2002
Retinal pigmented epithelium	Rat (phagocytosis)	Ershov and Bazan, 1999
Optic nerve head	Human (glaucoma)	Neufeld et al., 1997

Source: Reprinted with permission from Z. A. Radi and J. A. Render, *Ocular Pharmacology and Therapeutics*, 24(2), pp. 141–151. Copyright © 2008 Mary Ann Liebert, Inc. Publications. All rights reserved.

et al., 2005). Chronic or acute self-resolving inflammation was induced in mice by corneal suture or epithelial abrasion, respectively. COX-2, EP₂, and EP₄ expression were up-regulated with chronic inflammation and correlated with increased corneal PGE₂ formation and marked neovascularization (Liclican et al., 2010). There is variable COX-2 expression across different species (Radi and Render, 2008). In dogs with keratitis, the most common inflammatory eye disease in dogs, and in glaucomatous eyes, COX-2 expression was observed in all corneal layers (epithelium, stromal cells, and endothelium) (Marshall et al., 2004; Sellers et al., 2004). COX-2 immunoreactivity was also noted in the stromal and epithelial cells of the iris and the stromal cells of the trabecular meshwork (Sellers et al., 2004). No COX-2 expression was present in the cornea of normal dogs (Sellers et al., 2004; Marshall et al., 2004). COX-2 is expressed strongly in stromal keratocytes of normal New Zealand rabbit corneas (Amico et al., 2004). In rabbits, COX-2 levels increase significantly after injury and, at least in the epithelium, COX-2 becomes the predominant COX isoform at an early stage of healing (Amico et al., 2004). The

COX-2 expression pattern in rabbit corneal cells after photorefractive keratectomy (PRK) was compared with laser in situ keratomileusis (LASIK) (Miyamoto et al., 2004). After PRK, the central and peripheral corneal epithelia COX-2 expression was up-regulated at three days; the central epithelium was positive at 4 weeks. Central and peripheral epithelia COX-2 levels were negative three months later. After LASIK, the central epithelium on the corneal flap had COX-2 up-regulated after 1 and 2 weeks and was negative at 4 weeks (Miyamoto et al., 2004). Keratocytes around the stromal incision between the flap and the stromal bed up-regulated COX-2 and returned to negative at 3 months. Increased expression of COX-2 occurred in the central uninjured epithelium and stromal keratocytes 3 to 14 days after a LASIK procedure in rabbits (Miyamoto et al., 2004). Ocular COX-2 expression appears to be regulated by glucocorticoids (Maihöfner et al., 2001).

COX-2 plays an important role in corneal healing by stimulating corneal neovascularization and angiogenesis that occurs after injury, trauma, infection, or surgery (Masferrer et al., 1999; Wilson et al., 2003; Wilkinson-Berka, 2004; Radi and Render, 2008). Several mediators, such as IL-1, nitric oxide (NO), VEGF, and TNF, contribute to the processes of corneal healing by inducing COX-2 (Bazan et al., 1985a; Wilson et al., 2003; Du et al., 2004; Wilkinson-Berka, 2004). The initial stages of corneal repair are mediated by PGs generated by COX-2 which influence the recruitment of inflammatory cells and the presence of edema and pain (Davies et al., 1984; Amico et al., 2004; Radi and Render, 2008).

In normal human eyes, COX-2 expression was confined primarily to the NPE of the ciliary body (Maihöfner et al., 2001). In normal dogs, only minimal COX-2 expression was noted in the ciliary epithelium (Marshall et al., 2004). COX-2 expression was lost completely in the nonpigmented ciliary epithelium of humans with end-stage primary open-angle glaucoma (Maihöfner et al., 2001). In dogs, COX-2 expression was observed in the ciliary body, trabecular meshwork of the filtration angle, angular aqueous plexus, and sclera of dogs with glaucoma (Marshall et al., 2004). COX-2 is present in the iris and ciliary body of normal rabbits, whereas no expression is present in the cornea or anterior chamber in normal dogs (Damm et al., 2001; Sellers et al., 2004). In rabbits, COX-2 was induced in the anterior uvea after surgery for glaucoma (Chang et al., 1997).

Normal expression of COX-2 in the retina is variable among species and is detectable in the retina of newborn pigs but not in the adult rat and monkey (Figs. 5-6 to 5-8) (Degi et al., 2001; Radi and Render, 2008). COX-2 is expressed in nerve processes of the outer plexiform layer (mouse and rat), certain amacrine cells (mouse and rat), retinal ganglion cells (mouse, rat, pig) (Fig. 5-8) (Radi and Render, 2008), and blood vessels (mouse), whereas in the human retina, COX-2 is reported only in nerve processes of the outer plexiform layer (Ju et al., 2002; Wilkinson-Berka et al., 2003). A recent study reported COX-2 expression in various normal human ocular locations (Wang et al., 2011). Moderate COX-2 expression was observed in the epithelial and endothelium cells of the cornea. Strong expression of COX-2 was found in the nonpigmented epithelial cells of the ciliary body. Moderate to strong COX-2 expression was observed in various layers of the retina, with the most abundant COX-2 expression being detected in the photoreceptor inner segment, the external limiting membrane, and the outer plexiform layer (Wang et al.,

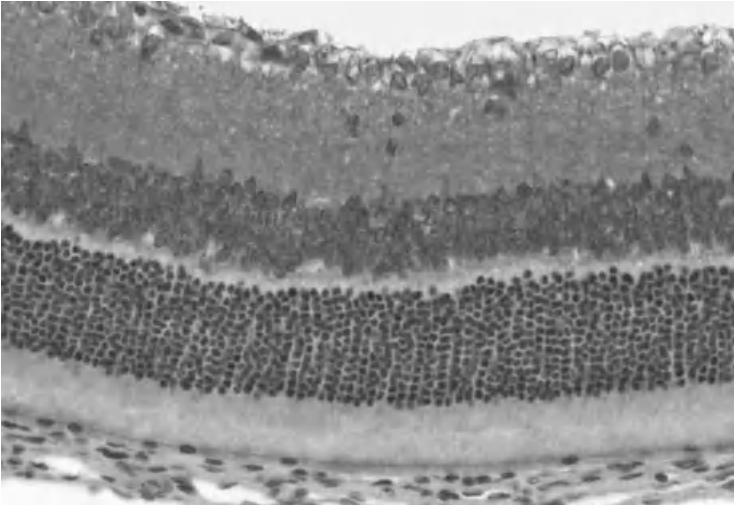


FIGURE 5-6 COX-2 expression in the normal retina of a rat. Immunohistochemical stain, original magnification $\times 40$. [Reprinted with permission from Z. A. Radi and J. A. Render, *Ocular Pharmacology and Therapeutics*, 24(2), pp. 141–151. Copyright © 2008 by Mary Ann Liebert, Inc. Publications. All rights reserved.]

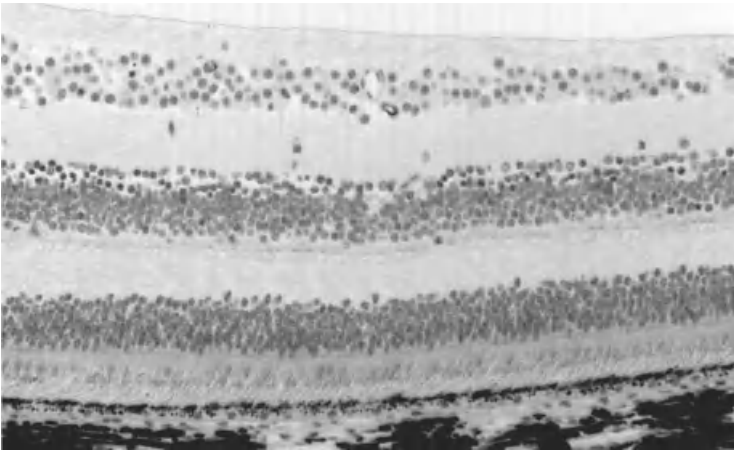


FIGURE 5-7 COX-2 expression in the normal retina of a monkey. Immunohistochemical stain, original magnification $\times 40$. [Reprinted with permission from Z. A. Radi and J. A. Render, *Ocular Pharmacology and Therapeutics*, 24(2), pp. 141–151. Copyright © 2008 Mary Ann Liebert, Inc. Publications. All rights reserved.]

2011). Following transient ischemia, increased COX-2 retinal expression was noted in the rat and pig (Degi et al., 2001; Ju et al., 2002). COX-2 is not expressed in the normal human optic nerve head, but a few COX-2-positive cells were found in the prelaminar, lamina cribrosa, and postlaminar regions of the glaucomatous optic nerves. Positive staining for COX-2 was not associated with microglia (Neufeld

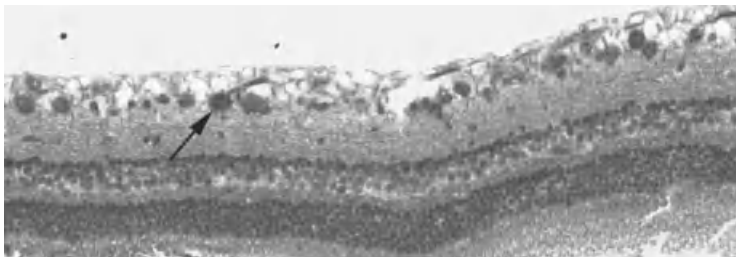


FIGURE 5-8 COX-2 expression in the normal retina of a pig. Note prominent ganglion cell expression (arrow). Immunohistochemical stain, original magnification $\times 40$. [Reprinted with permission from Z. A. Radi and J. A. Render, *Ocular Pharmacology and Therapeutics*, 24(2), pp. 141–151. Copyright © 2008 Mary Ann Liebert, Inc. Publications. All rights reserved.]

et al., 1997). An ocular condition called idiopathic epiretinal membrane (IERM) can be observed in the eye with no history of trauma, ocular inflammatory diseases, or any other type of ocular disease. Histologically, the IERM is composed of non-vascularized tissue growth along the inner limiting membrane (ILM) on the retinal surface (Kase et al., 2010). The number of COX-2-immunopositive cells was significantly higher in the IERM than that in the ILM (Kase et al., 2010). This suggests that COX-2 may play a potential role in the formation of avascular and vascularized epiretinal membranes in humans. In addition, epiretinal membranes which are formed in proliferative diabetic retinopathy (PDR) are composed primarily of neovascular stromal tissue (El-Asrar et al., 2008; Kase et al., 2010). Cytoplasmic immunoreactivity for COX-2 was detected in endothelial cells distributed in the PDR membranes (El-Asrar et al., 2008; Kase et al., 2010). COX-2 expression in retinal astrocytes was increased in human diabetic retinopathy and in mouse and rat models of ischemic proliferative retinopathy (Sennlaub et al., 2003). In a murine model of retinopathy of prematurity, equivalent COX-2 mRNA expression was observed in room air and after hyperoxia exposure at postnatal days 12 (P12), P14, and P17. Immunolocalization of COX-2 in the mouse retina was found to be similar to that in humans. In normoxic mice at P14, COX-2 protein was expressed significantly in retinal pigment epithelial cells in both the outer photoreceptor segment and the inner plexiform layer. In the posthyperoxia-exposed retinas, COX-2 expression was detected at P14 predominantly in astrocytes (Sennlaub et al., 2003). Phagocytosis of rod photoreceptor outer segments in rats was increased selectively with increased COX-2 expression in retinal pigmented epithelial cells (Ershov et al., 1999). Retinal COX-1 expression, on the other hand, did not change in diabetic rats (Fang et al., 1997).

COX-2 expression was investigated in various species and in various ocular neoplasms. In humans, COX-2 expression was lower in adenoma of nonpigmented ciliary body epithelium compared to the expression of the normal epithelium and negative in all medulloepithelioma cases of the nonpigmented ciliary body (Wang et al., 2011). No expression of COX-2 was noted in one case of retinoblastoma and decreased expression in other retinoblastoma cases compared to COX-2 expression

in the normal outer layers of retina (Wang et al., 2011). In another study, COX-2-positive immunoreactions were observed in 96% of retinoblastoma specimens from human patients (Karim et al., 2000). COX-2 expression was found in 58% of the human uveal melanoma cases (Figueiredo et al., 2003). Up-regulation of COX-2 expression appears to be associated with poor prognosis in uveal melanoma in humans (Cryan et al., 2008). In dogs, COX-2 expression was noted in ocular malignant melanoma (Paglia et al., 2009; Pires et al., 2010). In horses, ocular SCC and carcinoma in situ have significantly higher levels of COX-2 expression than that of normal control ocular tissue. However, the percentage of cells expressing positive immunohistochemical staining was consistently low (Smith et al., 2008).

EFFECTS OF COX-2 s-NSAIDs IN OPHTHALMOLOGY

During inflammatory tissue response, eicosanoids are thought to play a significant role in angiogenesis (Yamada et al., 1999). The ophthalmic uses of celecoxib mentioned in this chapter are investigational (for research purposes only) and are not within the labeled indications. The role of COX-2 in corneal angiogenic response was studied in a rat model. Angiogenesis was induced in the rat cornea by chemical cautery, and NS-398, a COX-2 s-NSAID, was applied topically three times daily for 4 days and neovascularization was quantitated (Yamada et al., 1999). COX-2 induction in cauterized rat corneas increased the level of eicosanoids, which resulted in corneal angiogenesis, and NS-398 significantly inhibited corneal neovascularization (Yamada et al., 1999). COX-2 and VEGF affect vascular permeability, and angiogenesis and can be induced by ocular tissue hypoxia and hyperglycemia (Bonazzi et al., 2000; Wilkinson-Berka, 2004). In addition, NO has been implicated in VEGF-mediated vascular permeability and angiogenesis (Wilkinson-Berka, 2004). In rabbit corneal epithelial cells, COX-2 mRNAs were increased by hypoxia (Bonazzi et al., 2000). In a rat model, COX-2 inhibition using SC-236 has been associated with attenuating angiogenesis and down-regulating VEGF and bFGF (Masferrer et al., 1999). Selective NSAIDs appear to have a great potential in inhibiting corneal angiogenesis and treating diabetic retinopathy and in intravitreal neovascularization associated with ischemic proliferative retinopathy in humans (Sennlaub et al., 2003). Diabetic persons are usually susceptible to diabetic retinopathy, which could lead to blindness due to retinal neovascularization, and ischemia is a common precursor to neovascularization in retinal diseases (Ayalasomayajula et al., 2004). The *ex vivo* effects of celecoxib on retinas from diabetic Sprague–Dawley rats were studied. Higher synthesis of PGE₂ was noted in diabetic rat retinas compared to normal rat retinas, and expression was elevated within a week of inducing diabetes in rats (Ayalasomayajula et al., 2004). In this *ex vivo* system, the rate of PGE₂ synthesis in diabetic rat retinas was inhibited significantly by celecoxib (1 μM), indicating the potential value of using celecoxib to treat diabetic retinopathy (Ayalasomayajula et al., 2004). Increased COX-2 expression leads to an increased production of PGs, which induce VEGF expression. This signaling pathway can effectively be blocked by administering celecoxib. In isolated

rat retinas, diabetes-induced PGE₂ expression was inhibited significantly by treatment with 1 μ M of celecoxib (Ayalasomayajula et al., 2004). Macular edema is the most common cause of visual impairment in diabetic patients leading to diabetic macular edema (DME). The important pathophysiology of DME is the loss of retinal capillary pericytes, resulting in increased vascular permeability (Ciulla et al., 2003). VEGF, a potent inducer of vascular permeability, is increased markedly in diabetic retina, DME, age-related macular degeneration (ARMD), and corneal neovascularization (Adamis et al., 1994; Aiello et al., 1994; Lopez et al., 1996; Cursiefen et al., 2000; Adamis, 2002). Bevacizumab, a humanized monoclonal antibody against VEGF, also binds and inhibits all the biologically active forms of VEGF (Presta et al., 1997). Bevacizumab has been used for intravitreal injection in patients with ARMD, DME, and iris neovascularization and was shown to provide beneficial effects in such patients (Haritoglou et al., 2006; Oshima et al., 2006; Yoganathan et al., 2006; Ozkiriş, 2009). Increased PGE₂ can lead to up-regulation of VEGF, which is responsible for the initiation of diabetic retinopathy (Cheng et al., 1998; Frank, 2004). Vascular hyperpermeability and neovascularization lead to vision loss in various ocular pathologies, such as diabetic retinopathy and ARMD (Castro et al., 2004). Histologically, there are vascular lesions in the early stages of diabetic retinopathy in both humans and animal models. These vascular lesions are characterized by the presence of saccular capillary microaneurysms, pericyte deficient capillaries, and obliterated and degenerate capillaries (Kern, 2007). These degenerate capillaries are not perfused, so increases in their frequency represent reductions in retinal perfusion. Thus, many of the defects that develop in retinas as a result of diabetes are consistent with a diabetes-induced inflammatory response. These inflammatory changes apparently are important in the pathogenesis of diabetic retinopathy, since inhibition of this inflammatory cascade at any of multiple steps can inhibit the early stages of diabetic retinopathy (notably, degeneration of retinal capillaries) in animal models. Findings of diabetes-induced inflammatory changes, generally, in the human eye also, are consistent with the postulate that inflammatory processes contribute to the development of diabetic retinopathy (Kern, 2007). Elevated VEGF expression is correlated with diabetic blood–retinal barrier breakdown and ischemia-related neovascularization in animal models and humans (Adamis, 2002). In a cynomolgus monkey model of experimental iris neovascularization, VEGF mRNA was increased in the aqueous fluid, and the aqueous VEGF mRNA levels changed synchronously and proportionally with the severity of neovascularization after retinal ischemia induced by laser occlusion of all branch retinal veins (Miller et al., 1994).

COX-2 s-NSAIDs (e.g., celecoxib, rofecoxib, deracoxib, valdecoxib, lumiracoxib, etoricoxib) spare COX-1 and inhibit COX-2. Retinopathy of prematurity (ROP) is a vascular biphasic disease of the eye unique to preterm infants (Heckmann, 2008). In the first phase of the disease, relative hyperoxia results in vaso-obliteration and vessel loss. The second phase is characterized by hypoxia-induced neovascularization, resulting in retinal detachment and blindness. Oxygen-dependent VEGF and oxygen-independent insulin-like growth factor (IGF-1) have been identified as important factors in the pathogenesis of ROP (Heckmann, 2008). In a mouse model of ROP, rofecoxib was given

intraperitoneally at 15 mg/kg body weight from postnatal day 12 (P12) to P17, and the effects on angiogenesis as measured by count blood vessel profiles (BVPs) in the inner retina (inner limiting membrane, ganglion cell layer, and inner plexiform layer) were evaluated (Wilkinson-Berka et al., 2003). Rofecoxib attenuated retinal angiogenesis that accompanied retinopathy of prematurity (Wilkinson-Berka et al., 2003). In a rabbit model of argon laser-induced iritis, the effects of COX-2 s-NSAIDs on hyaluronan responses were investigated. SC-236 and rofecoxib were administered orally at 6 and 1.5 mg/kg per day, respectively. Both COX-2 s-NSAIDs prolonged trauma-induced elevations of hyaluronan in the iris of rabbits (Koralewska-Makar et al., 2003). Celecoxib administered twice daily via oral gavage at 50 mg/kg for 7 days inhibited retinal VEGF expression and vascular leakage in streptozotocin-induced diabetic rat model (Ayalasomayajula and Kompella, 2003).

The ocular disease state can affect the ocular pharmacokinetics of drugs following topical and systemic delivery. For example, results from several studies in animal models showed that ocular inflammation can cause increased aqueous and vitreous levels of antibiotics following topical and systemic delivery (Ozturk et al., 2000; Yağci et al., 2007). These increased aqueous and vitreous levels are related to the alteration in blood-retinal and blood-aqueous barriers in the diseased ocular state (Cheruvu et al., 2009). The effect of diabetes and the resulting breakdown of the blood-retinal barrier on drug transscleral delivery are poorly understood. In addition, differences in pigmentation and the relationship to blood-retinal barrier breakdown between rat strains are also poorly understood. Thus, the effects of diabetes on the transscleral delivery of celecoxib and the relationship of difference in ocular pharmacokinetics were investigated using diabetic albino [Sprague-Dawley (SD)] and pigmented [brown Norway (BN)] rats. The transscleral retinal delivery of celecoxib was studied in albino (SD) and pigmented (BN) rats. Diabetes (two-month duration) resulted in higher blood-retinal barrier leakage in diabetic SD and BN rats than that in controls. Transscleral retinal and vitreal delivery of celecoxib, 3 mg/rat, was significantly higher in diabetic rats of both strains. Such an increase in retinal delivery of celecoxib due to diabetes (i.e., breakdown of the blood-retinal barrier) was higher in pigmented rats than in albino rats. Thus, higher delivery of celecoxib in diabetic animals compared to control animals can be attributed to the disruption of the blood-retinal barrier because of the disease state (i.e., diabetes) (Cheruvu et al., 2009). In a rat model of angiogenesis, corneal blood vessel formation was suppressed by celecoxib but not by the COX-1 inhibitor SC-560 (Masferrer et al., 2000). Celecoxib caused a substantial reduction in the number and length of sprouting capillaries and dose-dependently inhibited the angiogenic response with an ED₅₀ of 0.3 mg/kg per day, and with a maximal inhibitory activity of 80% at a dose of 30 mg/kg per day in rats (Masferrer et al., 2000). The COX-2 s-NSAID SC-236 given orally at a dose of 10 mg/kg per day (the treatment was started a day before corneal infection and continued until day 10 after infection) resulted in diminished angiogenic responses and significantly reduced levels of VEGF at 3 and 7 days after infection and milder herpetic stromal keratitis in mice (Biswas et al., 2005). These data strongly suggested that COX-2 s-NSAIDs have an antiangiogenic response. The numbers of corneas and ganglia

containing infectious herpes simplex virus type 1 were significantly lower in the celecoxib-treated mice than in the placebo-treated mice (Gebhardt et al., 2005). Therefore, it has been suggested that COX-2 s-NSAIDs can suppress hyperthermic stress-induced herpes viral reactivation in the nervous system (Gebhardt et al., 2005). The COX-2 s-NSAID SC-58236 prevented apoptotic cell death and was neuroprotective against loss of retinal ganglion cells after ischemia (Ju et al., 2003). The COX-2 s-NSAID NS-398 attenuated spontaneous and TNF α -induced increases in nonrapid eye movement sleep in rabbits (Yoshida et al., 2003).

In humans, cases of acute, reversible disturbances of vision associated with the use of celecoxib or rofecoxib were reported in the Intensive Medicines Monitoring Program in New Zealand (Coulter and Clark, 2004). These were identified from three different databases using strict selection criteria. Temporary blindness, visual field defect, scotoma, teichopsia, blurred vision, decreased vision, and abnormal vision were reported effects seen with the use of celecoxib and rofecoxib in New Zealand (Coulter and Clark, 2004). In the study celecoxib was used at doses that ranged from 100 to 400 mg/day for different indications, such as rheumatoid arthritis, osteoarthritis, knee surgery, back pain, gout, psoriatic arthropathy, or elbow pain. Rofecoxib in this study was used at doses that ranged from 12.5 to 50 mg/day for different indications, such as arthritis, shoulder pain, lower back pain, osteoarthritis, or pain in limb. The reactions had a mean onset time of 9.5 days and recovery occurred within 3 days following withdrawal of the drug. The reactions did not appear to be related to age, gender, dose, or indication for use. These reversible effects may be related to interference with retinal blood supply (Coulter and Clark, 2004). Vitreous floaters and conjunctival hemorrhage ocular adverse events have been reported, according to the celecoxib package insert. The route of administration could affect the drug availability into ocular tissues. For example, retinal availability of celecoxib was severalfold higher following periocular or subconjunctival administration compared to intraperitoneal or systemic administration (Ayalasomayajula and Kompella, 2004). The periocular effects of celecoxib–poly(lactide-*co*-glycolide) (PLGA) microparticles were tested using an ARPE-19 cell line (a spontaneously arising human retinal pigment epithelial cell line) and in a streptozotocin diabetic rat model (Amrite et al., 2006). The *in vitro* release of celecoxib from the PLGA particles was performed with dialysis membrane bag suspension of either plain celecoxib (20 μ g) or celecoxib–PLGA particles containing 20 μ g of celecoxib. Nanomolar concentrations of celecoxib reduced VEGF mRNA and VEGF protein secretion. Periocular celecoxib microparticles were shown to be useful sustained drug delivery systems for inhibiting diabetes-induced elevations in PGE₂, VEGF, and blood–retinal barrier leakage. The periocular celecoxib–PLGA microparticles were demonstrated to be safe and did not cause any damage to the retina (Amrite et al., 2006).

EFFECTS ns-NSAIDs IN OPHTHALMOLOGY

Topically applied ns-NSAIDs (e.g., diclofenac, flurbiprofen, suprofen, indomethacin) inhibit COX-1 and COX-2 and have been used in the management

of various ophthalmic conditions, such as seasonal allergic conjunctivitis, photophobia to manage pain after corneal refractive surgery, postoperative inflammation after cataract surgery, postoperative topical analgesia, prevention and treatment of cystoid macular edema (CME), maintenance of intraoperative mydriasis, and prophylaxis of surgical miosis (Frucht and Zauberman, 1984; Sakamoto et al., 1995; Gaynes and Fiseella, 2002; Schalnus, 2003; Takahashi et al., 2003; Radi and Render, 2008). Bromfenac, an ns-NSAID 0.09% ophthalmic solution, is used for the treatment of postoperative inflammation and reduction of ocular pain in subjects who have undergone cataract extraction (Stewart et al., 2007). Other ophthalmic conditions, such as diabetic retinopathy and AMD, may also be treated with ns-NSAIDs (Hariprasad et al., 2007). In veterinary medicine, systemic ns-NSAIDs (e.g., carprofen, flunixin meglumine) are used to treat uveal conditions (Giuliano, 2004). Acetylsalicylic acid, phenylbutazone, and flunixin meglumine have been the most commonly prescribed ns-NSAIDs for dogs, cats, and horses by veterinary ophthalmologists (Giuliano, 2004). Topically applied suspensions of diclofenac, flurbiprofen, and suprofen are effective in preventing blood–aqueous barrier disruption after paracentesis in dogs (Ward, 1996). Intravenous administration of flunixin meglumine significantly limited miosis and reduced the production of PGE₂ in the aqueous humor after acute inflammation induction in dogs (Millichamp et al., 1991). Tepoxalin was more effective than other ns-NSAIDs, carprofen or meloxicam, for controlling the production of PGE₂ in dogs with experimentally induced uveitis (Gilmour and Lehenbauer, 2009). In rabbits, intravenous administration of a COX-1 selective inhibitor, FR122047, inhibited the aqueous flare induced by PGE₂ (Abe et al., 2004). In dogs, topically applied flurbiprofen, an ns-NSAID, caused a decrease in aqueous outflow that was more marked in the inflamed eyes (Millichamp et al., 1991). In normal beagle dogs, the effects of topically applied flurbiprofen 0.03% and latanoprost 0.005%, alone or in combination, were studied (Pirie et al., 2011). Flurbiprofen resulted in a mean IOP elevation of 1.1 mmHg in the treated eye compared with the control eye. No effect on pupil size, conjunctival hyperemia, or aqueous flare was noted. Latanoprost resulted in a mean IOP reduction of 3.4 mmHg. Combined latanoprost and flurbiprofen resulted in a mean IOP reduction of 2.7 mmHg. Miosis was noted in the treated eyes during both latanoprost periods. Thus, concurrent administration of latanoprost and flurbiprofen resulted in a 20.41% reduction in the ocular hypotensive effect relative to latanoprost therapy alone (Pirie et al., 2011).

In diabetic beagle dogs, sulindac oral treatment with 10 mg/kg per day (this dose was based on previous studies using sulindac on diabetic animals) decreased retinal capillary basement membrane thickening and diabetic retinopathy (Gardiner et al., 2003). In nonhuman primates, continuous infusion of 25 µg/day of indomethacin via cannula that was implanted into the vitreous cavity for 14 days inhibited laser-induced subretinal neovascularization and reduced vascular leakage (Sakamoto et al., 1995). Topically applied indomethacin reduced uveitis in rabbits (Yamauchi et al., 1979) and markedly inhibited the breakdown of the blood–aqueous barrier after paracentesis or argon laser photocoagulation of the iris in rabbits (van Delft et al., 1987). When rat corneas with central epithelial abrasions were treated with indomethacin and flurbiprofen in organ culture, corneal

reepithelialization was not altered (Gupta et al., 1993). In newborn pigs, ibuprofen treatment at 30 mg/kg given intravenously reduced the basal concentrations of all prostanoids to nearly undetectable levels, prevented their changes during hypotension and hypertension, and enhanced retinal and choroidal blood flow autoregulation (Chemtob et al., 1991). Human infants treated with indomethacin have a lower incidence of retinopathy of prematurity (Gersony et al., 1983).

The systemic absorption of topically applied ophthalmic NSAIDs is generally minimal. However, systemic absorption may occur from mucosal surfaces of the nasolacrimal outflow system. Intraocular diclofenac and flurbiprofen concentrations in human aqueous humor were measured following topical application. Flurbiprofen at 0.03% and diclofenac at 0.1% after a single topical application reached peak aqueous concentrations of 60 and 82 ng/mL at 2.0 and 2.4 h, respectively (Ellis et al., 1994). Diclofenac concentration remained above 20 ng/mL for over 4 h and was detectable after 24 h. Flurbiprofen was undetectable after 7.25 h (Ellis et al., 1994). Topical ophthalmic ns-NSAIDs can lead to local irritations that result in transient burning, stinging, conjunctival hyperemia, and corneal anesthesia (Schalnus, 2003). Diclofenac has been associated with the development of corneal ulcers in patients after cataract surgery or photorefractive keratectomy (Price, 2000). Shimazaki et al. (1995) have reported the development of a postkeratoplasty persistent epithelial defect of the corneal epithelium with the use of diclofenac sodium. In addition, indolent corneal ulceration, perforation, and full-thickness corneal melt can be serious complications associated with the use of topical ns-NSAIDs (Gaynes and Fiscella, 2002; Mian et al., 2006; Isawi and Dhaliwal, 2007). Administration of 0.1% diclofenac sodium eye drops three times daily did not cause significant abnormalities in the corneal epithelial structure or function of patients who had undergone small-incision cataract surgery (Shimazaki et al., 1996).

Indomethacin when applied topically three times daily for 4 days inhibited corneal neovascularization in a rat model (Yamada et al., 1999). Etodolac given in a 5-mg/kg dose once daily for 7 or 14 days suppressed choroidal neovascularization in a mice model (Takahashi et al., 2004). Continuous infusion of indomethacin into the vitreous cavity reduces subretinal neovascularization in monkeys by reducing new blood vessel growth (Frucht and Zauberman, 1984; Sakamoto et al., 1995; Yamada et al., 1999). The topical ns-NSAID nepafenac inhibits choroidal neovascularization and ischemia-induced retinal neovascularization by decreasing production of VEGF in mice (Takahashi et al., 2003). Ketorolac 0.4% inhibited choroidal neovascularization by suppression of retinal VEGF in a rat model (Kim et al., 2010). Corneal neovascularization was induced by alkaline cautery in Sprague–Dawley rats and measured after 4 days. This cautery-induced corneal angiogenesis was partially inhibited by indomethacin, 3.5 or 7 mg/kg per day, and NS-398, 10 or 20 mg/kg per day. The COX-1 selective inhibitor SC-560 given at 10 or 20 mg/kg per day did not inhibit angiogenesis (Castro et al., 2004). In addition, both indomethacin and NS-398 suppressed cautery-induced VEGF protein increase in the cornea (Castro et al., 2004). The effectiveness of a topical 0.1% diclofenac and a topical steroidal drug (betamethasone 0.1%) in preventing CME and blood–aqueous barrier disruption after small-incision cataract surgery was examined in a multicenter prospective randomized comparison study.

Five weeks after surgery, the incidence of fluorescein angiographic CME was lower in the diclofenac group than in the betamethasone group (Asano et al., 2008).

CONCLUSIONS

The ocular anatomical and physiological interspecies differences are important to look at closely when considering the pathophysiological effects of COX inhibition on the ocular system. COX-1 is constitutively expressed in the ocular system, while COX-2 is usually up-regulated during various ophthalmic pathological conditions. In several experimental nonclinical models of different ocular diseases, s-NSAIDs have shown beneficial ophthalmic effects. Topically applied ns-NSAIDs have been used in the management of various ophthalmic conditions. The impact of ocular pathology on topically applied NSAIDs pharmacokinetic properties needs to be considered.

REFERENCES

- Abe T, Hayasaka Y, Zhang XY, Hayasaka S. Effects of intravenous administration of FR122047 (a selective cyclooxygenase 1 inhibitor) and FR188582 (a selective cyclooxygenase 2 inhibitor) on prostaglandin-E2-induced aqueous flare elevation in pigmented rabbits. *Ophthalmic Res* 2004;36:321–326.
- Abran D, Li DY, Varma DR, Chemtob S. Characterization and ontogeny of PGE2 and PGF2 alpha receptors on the retinal vasculature of the pig. *Prostaglandins* 1995;50:253–267.
- Adamis AP. Is diabetic retinopathy an inflammatory disease? *Br J Ophthalmol* 2002;86:363–365.
- Adamis AP, Miller JW, Bernal MT, D'Amico DJ, et al. Increased vascular endothelial growth factor levels in the vitreous of eyes with proliferative diabetic retinopathy. *Am J Ophthalmol* 1994;118:445–450.
- Aguirre SA, Huang W, Prasanna G, Jessen B. Corneal neovascularization and ocular irritancy responses in dogs following topical ocular administration of an EP4-prostaglandin E2 agonist. *Toxicol Pathol* 2009;37:911–920.
- Aiello LP, Avery RL, Arrigg PG, Keyt BA, et al. Vascular endothelial growth factor in ocular fluid of patients with diabetic retinopathy and other retinal disorders. *N Engl J Med* 1994;331:1480–1487.
- Amico C, Yakimov M, Catania MV, Giuffrida R, et al. Differential expression of cyclooxygenase-1 and cyclooxygenase-2 in the cornea during wound healing. *Tissue Cell* 2004;36:1–12.
- Amrite AC, Ayalasonmayajula SP, Cheruvu NP, Kompella UB. Single periocular injection of celecoxib–PLGA microparticles inhibits diabetes-induced elevations in retinal PGE2, VEGF, and vascular leakage. *Invest Ophthalmol Vis Sci* 2006;47:1149–1160.
- Anthony TL, Lindsey JD, Aihara M, Weinreb RN. Detection of prostaglandin EP(1), EP(2), and FP receptor subtypes in human sclera. *Invest Ophthalmol Vis Sci* 2001;42:3182–3186.
- Asakura T, Sano N, Shichi H. Prostaglandin synthesis and accumulation by porcine ciliary epithelium. *J Ocul Pharmacol* 1992;8:333–341.
- Asano S, Miyake K, Ota I, Sugita G, et al. Reducing angiographic cystoid macular edema and blood–aqueous barrier disruption after small-incision phacoemulsification and foldable intraocular lens implantation: multicenter prospective randomized comparison of topical diclofenac 0.1% and betamethasone 0.1%. *J Cataract Refract Surg* 2008;34:57–63.
- Ayalasonmayajula SP, Kompella UB. Celecoxib, a selective cyclooxygenase-2 inhibitor, inhibits retinal vascular endothelial growth factor expression and vascular leakage in a streptozotocin-induced diabetic rat model. *Eur J Pharmacol* 2003;458:283–289.

- Ayalasomayajula SP, Kompella UB. Retinal delivery of celecoxib is several-fold higher following subconjunctival administration compared to systemic administration. *Pharm Res* 2004;21:1797–1804.
- Ayalasomayajula SP, Amrite AC, Kompella UB. Inhibition of cyclooxygenase-2, but not cyclooxygenase-1, reduces prostaglandin E2 secretion from diabetic rat retinas. *Eur J Pharmacol* 2004;498:275–278.
- Bahn CF, Glassman RM, MacCallum DK, Lillie JH, et al. Postnatal development of corneal endothelium. *Invest Ophthalmol Vis Sci* 1986;27:44–51.
- Balazsi AG, Rootman J, Drance SM, Schulzer M, et al. The effect of age on the nerve fiber population of the human optic nerve. *Am J Ophthalmol* 1984;97:760–766.
- Bazan HE, Birkle DL, Beuerman RW, Bazan NG. Inflammation-induced stimulation of the synthesis of prostaglandins and lipoxygenase- reaction products in rabbit cornea. *Curr Eye Res* 1985a;4:175–179.
- Bazan HE, Birkle DL, Beuerman R, Bazan NG. Cryogenic lesion alters the metabolism of arachidonic acid in rabbit cornea layers. *Invest Ophthalmol Vis Sci* 1985b;26:474–480.
- Bazan NG., Allan G. Signal transduction and gene expression in the eye: a contemporary view of the pro-inflammatory, anti-inflammatory and modulatory roles of prostaglandins and other bioactive lipids. *Surv Ophthalmol* 1997;41 Suppl 2:S23–S34.
- Berry M, Ellingham RB, Corfield AP. Membrane-associated mucins in normal human conjunctiva. *Invest Ophthalmol Vis Sci* 2000;41:398–403.
- Bhattacharjee P. Prostaglandins and inflammatory reactions in the eye. *Methods Find Exp Clin Pharmacol* 1980;2:17–31.
- Bhattacharjee P, Mukhopadhyay P, Tilley SL, Koller BH, et al. Blood–aqueous barrier in prostaglandin EP₂ receptor knockout mice. *Ocular Immunol Inflammat* 2002;10:187–196.
- Biswas PS, Banerjee K, Kim B, Kinchington PR, et al. Role of inflammatory cytokine-induced cyclooxygenase 2 in the ocular immunopathologic disease. *J Virol* 2005;79:10589–10600.
- Biswas S, Bhattacharjee P, Paterson CA. Prostaglandin E2 receptor subtypes, EP1, EP2, EP3 and EP4 in human and mouse ocular tissues: a comparative immunohistochemical study. *Prostaglandins Leukot Essent Fatty Acids* 2004;71:277–288.
- Bito LZ. Species differences in the responses of the eye to irritation and trauma: a hypothesis of divergence in ocular defense mechanisms, and the choice of experimental animals for eye research. *Exp Eye Res* 1984;39:807–829.
- Boeri D, Maiello M, Lorenzi M. Increased prevalence of microthromboses in retinal capillaries of diabetic individuals. *Diabetes* 2001;50:1432–1439.
- Bonazzi A, Mastuyugin V, Mieyal PA, Dunn MW, et al. Regulation of cyclooxygenase-2 by hypoxia and peroxisome proliferators in the corneal epithelium. *J Biol Chem* 2000;275:2837–2844.
- Brusini P, Miani F, Tosoni C. Corneal thickness in glaucoma: An important parameter? *Acta Ophthalmol Scand Suppl* 2000;232:41–42.
- Camras CB. Comparison of latanoprost and timolol in patients with ocular hypertension and glaucoma: a six-month masked, multicenter trial in the United States. The United States Latanoprost Study Group. *Ophthalmology* 1996;103:138–147.
- Camras CB, Alm A, Watson P, Stjenschantz J. Latanoprost, a prostaglandin analog, for glaucoma therapy: efficacy and safety after 1 year of treatment in 198 patients. Latanoprost Study Groups. *Ophthalmology* 1996;103:1916–1924.
- Castro, MR, Lutz D, Edelman JL. Effect of COX inhibitors on VEGF-induced retinal vascular leakage and experimental corneal and choroidal neovascularization. *Exp Eye Res* 2004;79:275–285.
- Chemtob S, Beharry K, Rex J, Chatterjee T, et al. Ibuprofen enhances retinal and choroidal blood flow autoregulation in newborn piglets. *Invest Ophthalmol Vis Sci* 1991;32:1799–1807.
- Chang MS, Tsai JC, Yang R, DuBois RN, et al. Induction of rabbit cyclooxygenase 2 in the anterior uvea following glaucoma filtration surgery. *Curr Eye Res* 1997;16:1147–1151.
- Chen CH, Chen SC. Studies on soluble proteins of vitreous in experimental animals. *Exp Eye Res* 1981;32:381–388.
- Cheng T, Cao W, Wen R, Steinberg RH, et al. Prostaglandin E2 induces vascular endothelial growth factor and basic fibroblast growth factor mRNA expression in cultured rat Müller cells. *Invest Ophthalmol Vis Sci* 1998;39:581–591.
- Cheruvu NP, Amrite AC, Kompella UB. Effect of diabetes on transscleral delivery of celecoxib. *Pharm Res* 2009;26:404–414.

- Ciulla TA, Amador AG, Zinman B. Diabetic retinopathy and diabetic macular edema: pathophysiology, screening, and novel therapies. *Diabetes Care* 2003;26:2653–2664.
- Coulter DM, Clark DW. Disturbance of vision by COX-2 inhibitors. *Expert Opin Drug Saf* 2004;3:607–614.
- Crider JY, Sharif NA. Functional pharmacological evidence for EP2 and EP4 prostanoid receptors in immortalized human trabecular meshwork and non-pigmented ciliary epithelial cells. *J Ocul Pharmacol Ther* 2001;17:35–46.
- Cryan LM, Paraoan L, Hiscott P, Damato BE, et al. Expression of COX-2 and prognostic outcome in uveal melanoma. *Curr Eye Res* 2008;33:177–184.
- Curcio CA, Sloan KR, Kalina RE, Hendrickson AE. Human photoreceptor topography. *J Comp Neurol* 1990;292:497–523.
- Cursiefen C, Rummelt C, Kuchle M. Immunohistochemical localization of vascular endothelial growth factor, transforming growth factor alpha, and transforming growth factor beta1 in human corneas with neovascularization. *Cornea* 2000;19:526–533.
- Damm J, Rau T, Maihöfner C, Pahl A, et al. Constitutive expression and localization of COX-1 and COX-2 in rabbit iris and ciliary body. *Exp Eye Res* 2001;72:611–621.
- Davanger M, Ringvold A. The ciliary body and the suspension of the lens in a monkey (*Cercopithecus aethiops*): a scanning electron microscopic study. *Acta Ophthalmol (Copenh)* 1977;55:965–975.
- Davies P, Bailey PJ, Goldenberg MM, Ford-Hutchinson AW. The role of arachidonic acid oxygenation products in pain and inflammation. *Annu Rev Immunol* 1984;2:335–357.
- Dege R, Thore C, Bari F, Thrikawala N, et al. Ischemia increases prostaglandin H synthase-2 levels in retina and visual cortex in piglets. *Graefes Arch Clin Exp Ophthalmol* 2001;239:59–65.
- Denlinger JL, Eisner G, Balazs EA. Age-related changes in the vitreous and lens of rhesus monkeys (*Macaca mulatta*). *Exp Eye Res* 1980;31:67–79.
- DeSantis LL Jr, Sallee VL. Comparison of the effects of prostaglandins and their esters on blood–aqueous barrier integrity and intraocular pressure in rabbits. *Prog Clin Biol Res* 1989;312:379–386.
- Dimasi DP, Hewitt AW, Kagame K, Ruvama S, et al. Ethnic and mouse strain differences in central corneal thickness and association with pigmentation phenotype. *PLoS One* 2011;6:e22103.
- Du Y, Sarthy VP, Kern TS. Interaction between NO and COX pathways in retinal cells exposed to elevated glucose and retina of diabetic rats. *Am J Physiol Regul Integr Comp Physiol* 2004;287:R735–R741.
- Eakins KE, Whitelocke RA, Perkins ES, Bennett A, et al. Release of prostaglandins in ocular inflammation in the rabbit. *Nat New Biol* 1972;239:248–249.
- Edelman JL, Castro MR, Wen Y. Correlation of VEGF expression by leukocytes with the growth and regression of blood vessels in the rat cornea. *Invest Ophthalmol Vis Sci* 1999;40:1112–1123.
- Ehlers N, Hjortdal J. The cornea: epithelium and stroma. *Adv Organ Biol* 2005;10:83–111.
- El-Asrar AM, Missotten L, Geboes K. Expression of cyclo-oxygenase-2 and downstream enzymes in diabetic fibrovascular epiretinal membranes. *Br J Ophthalmol* 2008;92:1534–1539.
- Ellis PP, Pfoff, DS, Bloedow DC, Riegel M. Intraocular diclofenac and flurbiprofen concentrations in human aqueous humor following topical application. *J Ocul Pharmacol* 1994;10:677–682.
- Ershov AV, Bazan NG. Induction of cyclooxygenase-2 gene expression in retinal pigment epithelium cells by photoreceptor rod outer segment phagocytosis and growth factors. *J Neurosci Res* 1999;58:254–261.
- Fang C, Jiang Z, Tomlinson DR. Expression of constitutive cyclo-oxygenase (COX-1) in rats with streptozotocin-induced diabetes; effects of treatment with evening primrose oil or an aldose reductase inhibitor on COX-1 mRNA levels. *Prostaglandins Leukot Essent Fatty Acids* 1997;56:157–163.
- Figueiredo A, Caissie AL, Callejo SA, McLean IW, et al. Cyclooxygenase-2 expression in uveal melanoma: novel classification of mixed-cell-type tumours. *Can J Ophthalmol* 2003;38:352–356.
- Frank RN. Diabetic retinopathy. *N Engl J Med* 2004;350:48–58.
- Friedland BR, Maren TH. The role of carbonic anhydrase in lens ion transport and metabolism. *Ann NY Acad Sci* 1984;429:582–586.
- Frucht J, Zauberman H. Topical indomethacin effect on neovascularisation of the cornea and on prostaglandin E2 levels. *Br J Ophthalmol* 1984;68:656–659.

- Gabelt BT, Kaufman PL. Prostaglandin F2 alpha increases uveoscleral outflow in the cynomolgus monkey. *Exp Eye Res* 1989;49:389–402.
- Gardiner TA, Anderson HR, Degenhardt T, Thorpe SR, et al. Prevention of retinal capillary basement membrane thickening in diabetic dogs by a nonsteroidal anti-inflammatory drug. *Diabetologia* 2003;46:1269–1275.
- Gaynes BI, Fiscella R. Topical nonsteroidal anti-inflammatory drugs for ophthalmic use: a safety review. *Drug Saf* 2002;25:233–250.
- Gebhardt BM, Varnell ED, Kaufman HE. Inhibition of cyclooxygenase-2 synthesis suppresses herpes simplex virus type 1 reactivation. *J Ocul Pharmacol Ther* 2005;21:114–120.
- Gersony WM, Peckham GJ, Ellison RC, Miettinen OS, et al. Effects of indomethacin in premature infants with patent ductus arteriosus: results of a national collaborative study. *J Pediatr* 1983;102:895–906.
- Gherzeghiher T, Koss MC, Nordquist RE, Wilkinson CP. Analysis of vitreous and aqueous levels of hyaluronic acid: application of high-performance liquid chromatography. *Exp Eye Res* 1987;45:347–349.
- Giblin FJ. Glutathione: a vital lens antioxidant. *J Ocul Pharmacol Ther* 2000;16:121–135.
- Gilger BC, Wright JC, Whitley RD, McLaughlin SA. Corneal thickness measured by ultrasonic pachymetry in cats. *Am J Vet Res* 1993;54:228–230.
- Gilmour MA, Lehenbauer TW. Comparison of tepoxalin, carprofen, and meloxicam for reducing intraocular inflammation in dogs. *Am J Vet Res* 2009;70:902–907.
- Giuliano EA. Nonsteroidal anti-inflammatory drugs in veterinary ophthalmology. *Vet Clin North Am Small Anim Pract* 2004;34:707–723.
- Green K, Kearse EC, McIntyre OL. Interaction between Δ^9 -tetrahydrocannabinol and indomethacin. *Ophthalmic Res* 2001; 33:217–220.
- Gum GG, Gelatt KN, Samuelson DA. Maturation of the retina of the canine neonate as determined by electroretinography and histology. *Am J Vet Res* 1984;45:1166–1171.
- Gupta AG, Hirakata A, Proia AD. Effect of inhibitors of arachidonic acid metabolism on corneal reepithelialization in the rat. *Exp Eye Res* 1993;56:701–708.
- Hall DW, Jaitly KD. Inflammatory responses of the rabbit eye to prostaglandins. *Agents Actions Suppl* 1977;2:123–133.
- Hardy P, Abran D, Li DY, Fernandez H, et al. Free radicals in retinal and choroidal blood flow autoregulation in the piglet: interaction with prostaglandins. *Invest Ophthalmol Vis Sci* 1994;35:580–591.
- Hardy P, Bhattacharya M, Abran D, Peri KG, et al. Increases in retinovascular prostaglandin receptor functions by cyclooxygenase-1 and -2 inhibition. *Invest Ophthalmol Vis Sci* 1998;39:1888–1898.
- Hariprasad SM, Callanan D, Gainey S, He YG, et al. Cystoid and diabetic macular edema treated with nepafenac 0.1%. *J Ocul Pharmacol Ther* 2007;23:585–590.
- Haritoglou C, Kook D, Neubauer A, Wolf A, et al. Intravitreal bevacizumab (Avastin) therapy for persistent diffuse diabetic macular edema. *Retina* 2006;26:999–1005.
- Harocopos GJ, Shui YB, McKinnon M, Holekamp NM, et al. Importance of vitreous liquefaction in age-related cataract. *Invest Ophthalmol Vis Sci* 2004;45:77–85.
- Hata Y, Clermont A, Yamauchi T, Pierce EA, et al. Retinal expression, regulation, and functional bioactivity of prostacyclin-stimulating factor. *J Clin Invest* 2000;106:541–550.
- Head KA. Natural therapies for ocular disorders, part two: cataracts and glaucoma. *Altern Med Rev* 2001;6:141–166.
- Heckmann M. Pathogenesis of retinopathy of prematurity. *Ophthalmologe* 2008;105:1101–1107.
- Hinz B, Brune K, Pahl A. Cyclooxygenase-2 expression in lipopolysaccharide-stimulated human monocytes is modulated by cyclic AMP, prostaglandin E(2), and nonsteroidal anti-inflammatory drugs. *Biochem Biophys Res Commun* 2000;278:790–796.
- Hiraoka M, Inoue K, Ohtaka-Maruyama C, Ohsako S, et al. Intracapsular organization of ciliary zonules in monkey eyes. *Anat Rec (Hoboken)* 2010;293:1797–1804.
- Holland EJ, Mannis MJ. *Ocular Surface Disease: Medical and Surgical Management*. New York: Springer-Verlag, 2002.
- Hommer A. A review of preserved and preservative-free prostaglandin analogues for the treatment of open-angle glaucoma and ocular hypertension. *Drugs Today (Barc)* 2010;46:409–416.

- Honrubia F, García-Sánchez J, Polo V, de la Casa JM, et al. Conjunctival hyperaemia with the use of latanoprost versus other prostaglandin analogues in patients with ocular hypertension or glaucoma: a meta-analysis of randomised clinical trials. *Br J Ophthalmol* 2009;93:316–321.
- Hutchinson AJ, Coons SC, Chou CL, Xu W, et al. Induction of angiogenic immediate early genes by activation of FP prostanoid receptors in cultured human ciliary smooth muscle cells. *Curr Eye Res* 2010;35:408–418.
- Isawi H, Dhaliwal DK. Corneal melting and perforation in Stevens–Johnson syndrome following topical bromfenac use. *J Cataract Refract Surg* 2007;33:1644–1646.
- Joussen AM, Poulaki V, Mitsiades N, Kirchhof B, et al. Nonsteroidal anti-inflammatory drugs prevent early diabetic retinopathy via TNF-alpha suppression. *FASEB J* 2002;16:438–440.
- Joyce NC, Joyce SJ, Powell SM, Pierce EA, et al. EGF and PGE2: effects on corneal endothelial cell migration and monolayer spreading during wound repair in vitro. *Curr Eye Res* 1995;14:601–609.
- Ju WK, Neufeld AH. Cellular localization of cyclooxygenase-1 and cyclooxygenase-2 in the normal mouse, rat, and human retina. *J Comp Neurol* 2002;452:392–399.
- Ju WK, Kim KY, Neufeld AH. Increased activity of cyclooxygenase-2 signals early neurodegenerative events in the rat retina following transient ischemia. *Exp Eye Res* 2003;77:137–145.
- Jumblatt MM. Autocrine regulation of corneal endothelium by prostaglandin E2. *Invest Ophthalmol Vis Sci* 1994;35:2783–2790.
- Jumblatt MM, Willer SS. Corneal endothelial repair: regulation of prostaglandin E2 synthesis. *Invest Ophthalmol Vis Sci* 1996;37:1294–1301.
- Kamphuis W, Schneemann A, Shichi H, Broersma L, et al. Immunolocalization of prostanoid EP receptor isoforms in human trabecular meshwork. *Curr Eye Res* 2004;29:17–26.
- Kaplan-Messas A, Naveh N, Avni I, Marshall J. Ocular hypotensive effects of cholinergic and adrenergic drugs may be influenced by prostaglandins E₂ in the human and rabbit eye. *Eur J Ophthalmol* 2003;13:18–23.
- Karim MM, Hayashi Y, Inoue M, Imai Y, et al. COX-2 expression in retinoblastoma. *Am J Ophthalmol* 2000;129:398–401.
- Kase S, Saito W, Ohno S, Ishida S. Cyclo-oxygenase-2 expression in human idiopathic epiretinal membrane. *Retina* 2010;30:719–723.
- Kashiwagi K, Tsukahara S. Effect of non-steroidal anti-inflammatory ophthalmic solution on intraocular pressure reduction by latanoprost. *Br J Ophthalmol* 2003;87:297–301.
- Keeting PE, Lysz TW, Centra M, Fu SC. Prostaglandin biosynthesis in the rat lens. *Invest Ophthalmol Vis Sci* 1985;26:1083–1086.
- Kern TS. Contributions of inflammatory processes to the development of the early stages of diabetic retinopathy. *Exp Diabetes Res* 2007;2007:95103.
- Kern TS, Engerman RL. Pharmacological inhibition of diabetic retinopathy: aminoguanidine and aspirin. *Diabetes* 2001;50:1636–1642.
- Kern TS, Miller CM, Du Y, Zheng L, et al. Topical administration of nepafenac inhibits diabetes-induced retinal microvascular disease and underlying abnormalities of retinal metabolism and physiology. *Diabetes* 2007;56:373–379.
- Kersterter JR, Brubaker RF, Wilson SE, Kullerstrand LJ. Prostaglandin F2 alpha- 1-isopropylester lowers intraocular pressure without decreasing aqueous humor flow. *Am J Ophthalmol* 1988;105:30–34.
- Kevany BM, Palczewski K. Phagocytosis of retinal rod and cone photoreceptors. *Physiology (Bethesda)* 2010;25:8–15.
- Kim SJ, Toma HS, Barnett JM, Penn JS. Ketorolac inhibits choroidal neovascularization by suppression of retinal VEGF. *Exp Eye Res* 2010;91:537–543.
- Kitagawa K, Hayasaka S, Nagaki Y, Watanabe K. Effects of tetramethylpyrazine on prostaglandin E(2) and prostaglandin E(2) receptor agonist induced disruption of blood aqueous barrier in pigmented rabbits. *Jpn J Ophthalmol* 2001;45:227–232.
- Kleinberg TT, Tzekov RT, Stein L, Ravi N, Kaushal S. Vitreous substitutes: a comprehensive review. *Surv Ophthalmol* 2011;56:300–323.
- Knop E, Knop N, Millar T, Obata H, et al. The International Workshop on Meibomian Gland Dysfunction: Report of the Subcommittee on Anatomy, Physiology, and Pathophysiology of the Meibomian Gland. *Invest Ophthalmol Vis Sci* 2011;52:1938–1978.

- Koralewska-Makar A, Johnsson C, Bruun A, Stenevi U, et al. COX-2 inhibitors prolong trauma-induced elevations of iris hyaluronan. *J Ocul Pharmacol Ther* 2003;19:385–395.
- Kosaka T, Mishima HK, Kiuchi Y, Kataoka K. The effects of prostaglandins on the blood–ocular barrier. *Jpn J Ophthalmol* 1995;39:368–376.
- Kulkarni P, Payne S. Eicosanoids in bovine retinal microcirculation. *J Ocul Pharmacol Ther* 1997;13:139–149.
- Kulkarni PS, Srinivasan BD. Cyclooxygenase and lipoxygenase pathways in anterior uvea and conjunctiva. *Prog Clin Biol Res* 1989;312:39–52.
- Kulkarni PS, Fleisher L, Srinivasan BD. The synthesis of cyclooxygenase products in ocular tissues of various species. *Curr Eye Res* 1984;3:447–452.
- Kulkarni PS, Kaufman PL, Srinivasan BD. Cyclo-oxygenase and lipoxygenase pathways in cynomolgus and rhesus monkey conjunctiva, anterior uvea and eyelids. *Curr Eye Res* 1987;6:801–808.
- Lapuerta P, Schein SJ. A four-surface schematic eye of macaque monkey obtained by an optical method. *Vision Res* 1995;35:2245–2254.
- Lerman S. An experimental and clinical evaluation of lens transparency and aging. *J Gerontol* 1983;38:293–301.
- Licican EL, Nguyen V, Sullivan AB, Gronert K. Selective activation of the prostaglandin E2 circuit in chronic injury-induced pathologic angiogenesis. *Invest Ophthalmol Vis Sci* 2010;51:6311–6320.
- Lopez PF, Sippy BD, Lambert HM, Thach AB, et al. Transdifferentiated retinal pigment epithelial cells are immunoreactive for vascular endothelial growth factor in surgically excised age-related macular degeneration-related choroidal neovascular membranes. *Invest Ophthalmol Vis Sci* 1996;37:855–868.
- Los LI. The rabbit as an animal model for post-natal vitreous matrix differentiation and degeneration. *Eye (Lond)* 2008;22:1223–1232.
- Los LI, van Luyn MJ, Nieuwenhuis P. Organization of the rabbit vitreous body: lamellae, Cloquet's channel and a novel structure, the "alae canalis Cloqueti." *Exp Eye Res* 1999;69:343–350.
- Lütjen-Drecoll E, Tamm E. Morphological study of the anterior segment of cynomolgus monkey eyes following treatment with prostaglandin F2 alpha. *Exp Eye Res* 1988;47:761–769.
- Maihöfner C, Schlotzer-Schrehardt U, Guhring H, Zeilhofer HU, et al. Expression of cyclooxygenase-1 and -2 in normal and glaucomatous human eyes. *Invest Ophthalmol Vis Sci* 2001;42:2616–2624.
- Maloney SC, Fernandes BF, Castiglione E, Anteckka E, et al. Expression of cyclooxygenase-2 in choroidal neovascular membranes from age-related macular degeneration patients. *Retina* 2009;29:176–180.
- Manzanas LL, Pastor JC, Munoz R, Girbes T. Intraocular irrigating solutions and vitrectomy-related changes (in protein, lactic and ascorbic acid) in rabbit vitreous. *Ophthalmic Res* 1992;24:61–67.
- Marshall JL, Stanfield KM, Silverman L, Khan KN. Enhanced expression of cyclooxygenase-2 in glaucomatous dog eyes. *Vet Ophthalmol* 2004;7:59–62.
- Masferrer JL, Koki A, Seibert K. COX-2 inhibitors. A new class of antiangiogenic agents. *Ann NY Acad Sci* 1999;889:84–86.
- Masferrer JL, Leahy KM, Koki AT, Zweifel BS, et al. Antiangiogenic and antitumor activities of cyclooxygenase-2 inhibitors. *Cancer Res* 2000;60:1306–1311.
- Massof RW, Chang FW. A revision of the rat schematic eye. *Vision Res* 1972;12:793–796.
- Matsuo T, Cynader MS. Localisation of prostaglandin F2 alpha and E2 binding sites in the human eye. *Br J Ophthalmol* 1992;76:210–213.
- Matsuo T, Cynader MS. The EP2 receptor is the predominant prostanoid receptor in the human ciliary muscle. *Br J Ophthalmol* 1993;77:110–114.
- McInnis CL, Giuliano EA, Johnson PJ, Turk Jr. Immunohistochemical evaluation of cyclooxygenase expression in corneal squamous cell carcinoma in horses. *Am J Vet Res* 2007;68:165–170.
- McMenamin PG. The distribution of immune cells in the uveal tract of the normal eye. *Eye (Lond)* 1997;11:183–193.
- Merindano MD, Costa J, Canals M, Potau JM, et al. A comparative study of Bowman's layer in some mammals: relationships with other constituent corneal structures. *Eur J Anat* 2002;6:133–139.
- Mian SI, Gupta A, Pineda R 2nd. Corneal ulceration and perforation with ketorolac tromethamine (Acular) use after PRK. *Cornea* 2006;25:232–234.

- Miller JD, Eakins KE, Atwal M. The release of PGE₂-like activity into aqueous humor after paracentesis and its prevention by aspirin. *Invest Ophthalmol* 1973;12:939–942.
- Miller JW, Adamis AP, Shima DT, D'Amore PA, et al. Vascular endothelial growth factor/vascular permeability factor is temporally and spatially correlated with ocular angiogenesis in a primate model. *Am J Pathol* 1994;145:574–584.
- Millichamp NJ, Dziezyc J, Rohde BH, Chiou GC, et al. Acute effects of anti-inflammatory drugs on neodymium:yttrium aluminum garnet laser-induced uveitis in dogs. *Am J Vet Res* 1991;52:1279–1284.
- Miranda OC, Bito LZ. The putative and demonstrated mitotic effects of prostaglandins in mammals. *Prog Clin Biol Res* 1989;312:171–195.
- Mishima HK, Kiuchi Y, Takamatsu M, et al. Circadian intraocular pressure management with latanoprost: diurnal and nocturnal intraocular pressure reduction and increased uveoscleral outflow. *Surv Ophthalmol* 1997;41 Suppl 2:S139–S144.
- Miyamoto T, Saika S, Okada Y, Kawashima Y, et al. Expression of cyclooxygenase-2 in corneal cells after photorefractive keratectomy and laser in situ keratomileusis in rabbits. *J Cataract Refract Surg* 2004;30:2612–2617.
- Módis L Jr, Szalai E, Kertész K, Kemény-Beke A, et al. Evaluation of the corneal endothelium in patients with diabetes mellitus type I and II. *Histol Histopathol* 2010;25:1531–1537.
- Mori A, Saito M, Sakamoto K, Narita M, et al. Stimulation of prostanoid IP and EP(2) receptors dilates retinal arterioles and increases retinal and choroidal blood flow in rats. *Eur J Pharmacol* 2007;570:135–141.
- Mukhopadhyay M, Bian L, Bhattacharjee P, Paterson CA. Localization of EP1 and FP receptors in human ocular tissues by in situ hybridization. *Invest Ophthalmol Vis Sci* 2001;42:424–428.
- Mutti DO, Zadnik K, Murphy CJ. Naturally occurring vitreous chamber-based myopia in the Labrador retriever. *Invest Ophthalmol Vis Sci* 1999;40:1577–1584.
- Neufeld AH, Hernandez MR, Gonzalez M, Geller A. Cyclooxygenase-1 and cyclooxygenase-2 in the human optic nerve head. *Exp Eye Res* 1997;65:739–745.
- Nilsson SF, Drecoll E, Lütjen-Drecoll E, Toris CB, et al. The prostanoid EP2 receptor agonist butaprost increases uveoscleral outflow in the cynomolgus monkey. *Invest Ophthalmol Vis Sci* 2006;47:4042–4049.
- Noecker RS, Dirks MS, Choplin NT, Bernstein P, et al. A six-month randomized clinical trial comparing the intraocular pressure-lowering efficacy of bimatoprost and latanoprost in patients with ocular hypertension or glaucoma. *Am J Ophthalmol* 2003;135:55–63.
- Ocklind A, Lake S, Wentzel P, Nistér M, Stjernschantz J. Localization of the prostaglandin F₂ alpha receptor messenger RNA and protein in the cynomolgus monkey eye. *Invest Ophthalmol Vis Sci* 1996;37:716–726.
- Oka T, Shearer T, Azuma M. Involvement of cyclooxygenase-2 in rat models of conjunctivitis. *Curr Eye Res* 2004;29:27–34.
- Ollivier FJ, Brooks DE, Komaromy AM, Kallberg ME, et al. Corneal thickness and endothelial cell density measured by non-contact specular microscopy and pachymetry in rhesus macaques (*Macaca mulatta*) with laser-induced ocular hypertension. *Exp Eye Res* 2003;76:671–677.
- Oshima Y, Sakaguchi H, Gomi F, Tano Y. Regression of iris neovascularization after intravitreal injection of bevacizumab in patients with proliferative diabetic retinopathy. *Am J Ophthalmol* 2006;142:155–158.
- Ottino P, Bazan HEP. Cyclooxygenase-2 (COX-2) metabolites produced by platelet-activating factor (PAF) stimulation in corneal epithelial cells activate urokinase type plasminogen activator (uPA) and matrix metalloproteinases (MMP)-1 and 9. *Invest Ophthalmol Vis Sci* 2000;41:S906.
- Ozkiriş A. Intravitreal bevacizumab (Avastin) for primary treatment of diabetic macular oedema. *Eye (Lond)* 2009;23:616–620.
- Ozturk F, Kurt E, Inan U, Kortunay S, et al. The effects of prolonged acute use and inflammation on the ocular penetration of topical ciprofloxacin. *Int J Pharm* 2000;204:97–100.
- Packer O, Hendrickson AE, Curcio CA. Photoreceptor topography of the retina in the adult pigtail macaque (*Macaca nemestrina*). *J Comp Neurol* 1989;288:165–183.
- Paglia D, Dubielzig RR, Kado-Fong HK, Maggs DJ. Expression of cyclooxygenase-2 in canine uveal melanocytic neoplasms. *Am J Vet Res* 2009;70:1284–1290.

- Philipp W, Klima G, Miller K. Clinicopathological findings 11 months after implantation of a functioning aqueous-drainage silicone implant. *Graefes Arch Clin Exp Ophthalmol* 1990;228:481–486.
- Pires I, Garcia A, Prada J, Queiroga FL. COX-1 and COX-2 expression in canine cutaneous, oral and ocular melanocytic tumours. *J Comp Pathol* 2010;143:142–149.
- Pirie CG, Maranda LS, Pizzirani S. Effect of topical 0.03% flurbiprofen and 0.005% latanoprost, alone and in combination, on normal canine eyes. *Vet Ophthalmol* 2011;14:71–79.
- Plummer CE, Ramsey DT, Hauptman JG. Assessment of corneal thickness, intraocular pressure, optical corneal diameter, and axial globe dimensions in miniature horses. *Am J Vet Res* 2003;64:661–665.
- Poyer JF, Gabelt B, Kaufman PL. The effect of topical PGF2 alpha on uveoscleral outflow and outflow facility in the rabbit eye. *Exp Eye Res* 1992;54:277–283.
- Presta LG, Chen H, O'Connor SJ, Chisholm V, et al. Humanization of an antivascular endothelial growth factor monoclonal antibody for the therapy of solid tumors and other disorders. *Cancer Res* 1997;57:4593–4599.
- Preud'homme Y, Demolle D, Boeynaems JM. Metabolism of arachidonic acid in rabbit iris and retina. *Invest Ophthalmol Vis Sci* 1985;26:1336–1342.
- Price FW. New pieces for the puzzle: nonsteroidal anti-inflammatory drugs and corneal ulcers. *J Cataract Refract Surg* 2000;26:1263–1265.
- Radi ZA, Render JA. The pathophysiologic role of cyclo-oxygenases in the eye. *J Ocul Pharmacol Ther* 2008;24:141–151.
- Rasmussen CA, Kaufman PL. Primate glaucoma models. *Glaucoma* 2005;14:311–314.
- Reitmair A, Lambrecht NW, Yakubov I, Nieves A, et al. Prostaglandin E2 receptor subtype EP2- and EP4-regulated gene expression profiling in human ciliary smooth muscle cells. *Physiol Genomics* 2010;42:348–360.
- Richter M, Krauss AH, Woodward DF, Lütjen-Drecoll E. Morphological changes in the anterior eye segment after long-term treatment with different receptor selective prostaglandin agonists and a prostamide. *Invest Ophthalmol Vis Sci* 2003;44:4419–4426.
- Rösch S, Ramer R, Brune K, Hinz B. Prostaglandin E2 induces cyclooxygenase-2 expression in human non-pigmented ciliary epithelial cells through activation of p38 and p42/44 mitogen-activated protein kinases. *Biochem Biophys Res Commun* 2005;338:1171–1178.
- Rüfer F, Sander S, Klettner A, Frimpong-Boateng A, et al. Characterization of the thinnest point of the cornea compared with the central corneal thickness in normal subjects. *Cornea* 2009;28:177–180.
- Saeki T, Ota T, Aihara M, Araie M. Effects of prostanoid EP agonists on mouse intraocular pressure. *Invest Ophthalmol Vis Sci* 2009;50:2201–2208.
- Sagara T, Gatton DD, Lindsey JD, Gabelt BT, et al. Topical prostaglandin F2 alpha treatment reduces collagen types I, III, and IV in the monkey uveoscleral outflow pathway. *Arch Ophthalmol* 1999;117:794–801.
- Sakamoto T, Soriano D, Nassaralla J, Murphy TL, et al. Effect of intravitreal administration of indomethacin on experimental subretinal neovascularization in the subhuman primate. *Arch Ophthalmol* 1995;113:222–226.
- Sanchez RM, Dunkelberger GR, Quigley HA. The number and diameter distribution of axons in the monkey optic nerve. *Invest Ophthalmol Vis Sci* 1986;27:1342–1350.
- Sarchahi AA, Abbasi N, Gholipour MA. Effects of an unfixed combination of latanoprost and pilocarpine on the intraocular pressure and pupil size of normal dogs. *Vet Ophthalmol* 2012;15 Suppl 1:64–70.
- Sawada A, Yamamoto T, Takatsuka N. Randomized crossover study of latanoprost and travoprost in eyes with open-angle glaucoma. *Graefes Arch Clin Exp Ophthalmol* 2012;250:123–129.
- Schalnus R. Topical nonsteroidal anti-inflammatory therapy in ophthalmology. *Ophthalmologica* 2003;217:89–98.
- Schlötzer-Schrehardt U, Zenkel M, Nüsing RM. Expression and localization of FP and EP prostanoid receptor subtypes in human ocular tissues. *Invest Ophthalmol Vis Sci* 2002;43:1475–1487.
- Sebag J, Balazs EA. Morphology and ultrastructure of human vitreous fibers. *Invest Ophthalmol Vis Sci* 1989;30:1867–1871.
- Sellers RS, Silverman L, Khan KN. Cyclooxygenase-2 expression in the cornea of dogs with keratitis. *Vet Pathol* 2004;41:116–121.

- Sennlaub F, Valamanesh F, Vazquez-Tello A, El-Asrar AM, et al. Cyclooxygenase-2 in human and experimental ischemic proliferative retinopathy. *Circulation* 2003;108:198–204.
- Shimazaki J, Saito H, Yang HY, Toda I, et al. Persistent epithelial defect following penetrating keratoplasty: an adverse effect of diclofenac eyedrops. *Cornea* 1995;14:623–627.
- Shimazaki J, Fujishima H, Yagi Y, Tsubota K, et al. Effects of diclofenac eye drops on corneal epithelial structure and function after small-incision cataract surgery. *Ophthalmology* 1996;103:50–57.
- Smith KM, Scase TJ, Miller JL, Donaldson D, et al. Expression of cyclooxygenase-2 by equine ocular and adnexal squamous cell carcinomas. *Vet Ophthalmol* 2008;11:8–14.
- Sponsel WE, Paris G, Trigo Y, Pena M, et al. Latanoprost and brimonidine: therapeutic and physiologic assessment before and after oral nonsteroidal anti-inflammatory therapy. *Am J Ophthalmol* 2002;133:11–18.
- Steven P, Gebert A. Conjunctiva-associated lymphoid tissue: current knowledge, animal models and experimental prospects. *Ophthalmic Res* 2009;42:2–8.
- Stewart RH, Grillone LR, Shiffman ML, Donnenfeld ED, et al. The systemic safety of bromfenac ophthalmic solution 0.09%. *J Ocul Pharmacol Ther* 2007;23:601–612.
- Streilein JW, Cousins SW. Aqueous humor factors and their effect on the immune response in the anterior chamber. *Curr Eye Res* 1990;9 Suppl: 175–182.
- Szél A, Röhlich P, Caffé AR, van Veen T. Distribution of cone photoreceptors in the mammalian retina. *Microsc Res Tech* 1996;35:445–462.
- Takahashi K, Saishin Y, Saishin Y, Mori K, et al. Topical nepafenac inhibits ocular neovascularization. *Invest Ophthalmol Vis Sci* 2003;44:409–415.
- Takahashi H, Yanagi Y, Tamaki Y, Uchida S, et al. COX-2-selective inhibitor, etodolac, suppresses choroidal neovascularization in a mice model. *Biochem Biophys Res Commun* 2004;325:461–466.
- Takamatsu M, Hotehama Y, Goh Y, Mishima HK. Localization of prostaglandin E receptor subtypes in the ciliary body of mouse eye. *Exp Eye Res* 2000;70:623–628.
- Taylor AW, Yee DG. Somatostatin is an immunosuppressive factor in aqueous humor. *Invest Ophthalmol Vis Sci* 2003;44:2644–2649.
- Taylor AW, Streilein JW, Cousins SW. Immunoreactive vasoactive intestinal peptide contributes to the immunosuppressive activity of normal aqueous humor. *J Immunol* 1994;153:1080–1086.
- The DAMAD Study Group. Effect of aspirin alone and aspirin plus dipyridamole in early diabetic retinopathy: a multicenter randomized controlled clinical trial. *Diabetes* 1989;38:491–498.
- Thomas MA, O'Grady GE, Swartz SL. Prostaglandin levels in human vitreous. *Br J Ophthalmol* 1985;69:275–279.
- Tseng SH, Tang MJ. Na,K-ATPase in lens epithelia from patients with senile cataracts. *J Formos Med Assoc* 1999;98:627–632.
- Tuft SJ, Williams KA, Coster DJ. Endothelial repair in the rat cornea. *Invest Ophthalmol Vis Sci* 1986;27:1199–1204.
- Ueta M, Matsuoka T, Narumiya S, Kinoshita S. Prostaglandin E receptor subtype EP3 in conjunctival epithelium regulates late-phase reaction of experimental allergic conjunctivitis. *J Allergy Clin Immunol* 2009;123:466–471.
- Ueta M, Sotozono C, Yokoi N, Inatomi T, et al. Prostaglandin E receptor subtype EP3 expression in human conjunctival epithelium and its changes in various ocular surface disorders. *PLoS One* 2011;6:e25209.
- Vakkur GJ, Bishop PO. The schematic eye in the cat. *Vision Res* 1963;61:357–381.
- van Delft JL, van Haeringen NJ, Glasius E, Barthen ER, et al. Comparison of the effects of corticosteroids and indomethacin on the response of the blood–aqueous barrier to injury. *Curr Eye Res* 1987;6:419–425.
- Ventura AC, Böhnke M, Mojon DS. Central corneal thickness measurements in patients with normal tension glaucoma, primary open angle glaucoma, pseudoexfoliation glaucoma, or ocular hypertension. *Br J Ophthalmol* 2001;85:792–795.

- Vogel M. Postnatal development of the cat's retina: a concept of maturation obtained by qualitative and quantitative examinations. *Albrecht Von Graefes Arch Klin Exp Ophthalmol* 1978;208:93–107.
- Wang J, Wu Y, Heegaard S, Kolko M. Cyclooxygenase-2 expression in the normal human eye and its expression pattern in selected eye tumours. *Acta Ophthalmol* 2011;89:681–685.
- Ward DA. Comparative efficacy of topically applied flurbiprofen, diclofenac, tolmetin, and suprofen for the treatment of experimentally induced blood–aqueous barrier disruption in dogs. *Am J Vet Res* 1996;57:875–878.
- Weber H, Landwehr G, Kilp H, Neubauer H. The mechanical properties of the vitreous of pig and human donor eyes. *Ophthalmic Res* 1982;14:335–343.
- Weinreb RN, Kashiwagi K, Kashiwagi F, Tsukahara S, et al. Prostaglandins increase matrix metalloproteinase release from human ciliary smooth muscle cells. *Invest Ophthalmol Vis Sci* 1997;38:2772–2780.
- Wen Y, Bekhor I. Levels of expression of hexokinase, aldose reductase and sorbitol dehydrogenase genes in lens of mouse and rat. *Curr Eye Res* 1993;12:323–332.
- Wilkinson-Berka JL. Vasoactive factors and diabetic retinopathy: vascular endothelial growth factor, cyclooxygenase-2 and nitric oxide. *Curr Pharm Des* 2004;10:3331–3348.
- Wilkinson-Berka JL, Alousis NS, Kelly DJ, Gilbert RE, et al. COX-2 inhibition and retinal angiogenesis in a mouse model of retinopathy of prematurity. *Invest Ophthalmol Vis Sci* 2003;44:974–979.
- Willoughby CE, Ponzin D, Ferrari S, Lobo A, et al. Anatomy and physiology of the human eye: effects of mucopolysaccharidosis disease on structure and function: a review. *Clin Exp Ophthalmol* 2010;38:2–11.
- Wilson SE, Netto M, Ambrosio R Jr. Corneal cells: chatty in development, homeostasis, wound healing, and disease. *Am J Ophthalmol* 2003;136:530–536.
- Woodward DF, Nilsson SFE, Toris CB, Kharlamb AB, et al. Prostanoid EP4 receptor stimulation produces ocular hypotension by a mechanism that does not appear to involve uveoscleral outflow. *Invest Ophthalmol Vis Sci* 2009;50:3320–3328.
- Xu KP, Riggs A, Ding Y, Yu FS. Role of ErbB2 in corneal epithelial wound healing. *Invest Ophthalmol Vis Sci* 2004;45:4277–4283.
- Yagci R, Ofly Y, Dincel A, Kaya E, et al. Penetration of second-, third-, and fourth-generation topical fluoroquinolone into aqueous and vitreous humour in a rabbit endophthalmitis model. *Eye* 2007;21:990–994.
- Yamada M, Kawai M, Kawai Y, Mashima Y. The effect of selective cyclooxygenase-2 inhibitor on corneal angiogenesis in the rat. *Curr Eye Res* 1999;19:300–304.
- Yamaji K, Yoshitomi T, Ishikawa H, Usui S. Prostaglandins E1 and E2, but not F2 alpha or latanoprost, inhibit monkey ciliary muscle contraction. *Curr Eye Res* 2005;30:661–665.
- Yamauchi H, Iso T, Iwao J, Iwata H. The role of prostaglandins in experimental ocular inflammations. *Agents Actions* 1979;9:280–283.
- Yoganathan P, Deramo VA, Lai JC, Tibrewala RK, et al. Visual improvement following intravitreal bevacizumab (Avastin) in exudative age-related macular degeneration. *Retina* 2006;26:994–998.
- Yoshida H, Kubota T, Krueger JM. A cyclooxygenase-2 inhibitor attenuates spontaneous and TNF-alpha-induced non-rapid eye movement sleep in rabbits. *Am J Physiol Regul Integr Comp Physiol* 2003;285:R99–R109.
- Yousufzai SY, Ye Z, Abdel-Latif AA. Prostaglandin F2 alpha and its analogs induce release of endogenous prostaglandins in iris and ciliary muscles isolated from cat and other mammalian species. *Exp Eye Res* 1996;63:305–310.
- Yu FS, Yin J, Xu K, Huang J. Growth factors and corneal epithelial wound healing. *Brain Res Bull* 2010;81:229–235.
- Zeiss CJ. Animals as models of age-related macular degeneration: an imperfect measure of the truth. *Vet Pathol* 2010;47:396–413.
- Zhao C, Shichi H. Immunocytochemical localization of prostaglandin E2 receptor subtypes in porcine ocular tissues: II. Nonuveal tissues. *J Ocul Pharmacol Ther* 1995;11:437–445.
- Zhao C, Fujimoto N, Shichi H. Immunocytochemical localization of prostaglandin E2 receptor subtypes in porcine ocular tissues: I. Uveal tissues. *J Ocul Pharmacol Ther* 1995;11:421–435.

- Zheng L, Howell SJ, Hatala DA, Huang K, et al. Salicylate-based anti-inflammatory drugs inhibit the early lesion of diabetic retinopathy. *Diabetes* 2007;56:337–345.
- Zhou R, Horai R, Mattapallil MJ, Caspi RR. A new look at immune privilege of the eye: dual role for the vision-related molecule retinoic acid. *J Immunol* 2011;187:4170–4177.
- Zhou X, Wang W, Lu F, Hu S, et al. A comparative gene expression profile of the whole eye from human, mouse, and guinea pig. *Mol Vis* 2007;13:2214–2221.

RESPIRATORY SYSTEM

INTRODUCTION

Respiratory tissues respond to physiological and pathophysiological stimuli via activation of phospholipases and subsequent release of biologically active metabolites such as prostaglandins (PGs) from membrane phospholipids (Radi and Ackermann, 2011). PGs have receptors localized in a variety of respiratory tissues and affect its physiology and pathophysiology (Rolin et al., 2006). Cyclooxygenase isoenzymes (COX-1 and COX-2) catalyze the conversion of arachidonic acids (AA) to PGs (Radi and Ackermann, 2011). The COX-1 isoenzyme is expressed in a variety of respiratory tissues, and this expression is variable among different animal species (Radi and Ostroski, 2007; Radi and Ackermann, 2011). Prostanoids, generated by COX, are present in high concentrations during various pulmonary disease conditions (Jackson et al., 1993; Fulkerson et al., 1996; Vigano et al., 1998). COX-2 selective nonsteroidal anti-inflammatory drugs (COX-2 s-NSAIDs) and nonselective nonsteroidal anti-inflammatory drugs (ns-NSAIDs) inhibit COX isoenzymes. In this chapter we discuss the expression of COX-1 and COX-2 in the respiratory system, the role of prostaglandins and COX in respiratory physiology and pathophysiology, and the effects of COX-2 s-NSAIDs and ns-NSAIDs in pulmonary conditions.

COMPARATIVE PHYSIOLOGICAL AND ANATOMICAL ASPECTS OF THE RESPIRATORY SYSTEM

Understanding the comparative physiological and anatomical aspects of the respiratory system is important for an understanding of the pathophysiological consequences of COX inhibition on this system. The lungs are the principal structures of the respiratory system. The respiratory system has conductive and transitional systems (Mead, 1961). The conductive system includes nasal cavity, pharynx, larynx, trachea, and bronchi. Conducting airways are lined by pseudostratified ciliated epithelium that transports the air–surface liquid (ASL) toward the pharynx or nares (Ackermann et al., 2010). ASL is produced by secretion products from goblet cells and submucosal glands. Within the ASL are mucins as well as antimicrobial proteins (e.g., lysozyme, lactoferrin, surfactant proteins A and D, SLPI, PLUNC, and

others); and antimicrobial peptides (defensins and RNAase 7), which are produced by ciliated epithelial cells. The oxidative defense system (ODS) is composed of lactoperoxidase (LPO) produced by submucosal glands, dual function oxidases 1 and 2 (Duox1 and Duox2) produced by epithelia, and thiocyanate (SCN^-) transport proteins produced by epithelia. Duox1 and 2 produce hydrogen peroxide (H_2O_2), which, in the presence of SCN^- , is converted to OSCN^- , which has potent antimicrobial activity (Ackermann et al., 2010). The transitional system is composed of bronchioles and an alveolar gas exchange system (Mead, 1961; Massaro and Massaro, 1996). The lung alveolar system is the largest surface of the human body that is exposed to the environment, covering up to approximately 120 m^2 (Johnson et al., 2006). Thus, these systems are susceptible to injury after exposure to microbes and toxicants. The primary functions of the respiratory system are gas exchange, maintaining acid–base balance, olfaction, and protection against noxious agents (Haschek et al., 2009). Gas exchange is the main function of the pulmonary system, and this involves three processes: ventilation, perfusion, and diffusion of gases across the air–blood barrier (Haschek et al., 2009). In the alveolar zone, O_2 and CO_2 move across the air–blood barrier via diffusion. Ventilation brings O_2 to the alveoli and removes CO_2 . A respiratory cycle consists of an inspiratory phase followed by an expiratory phase.

Many interspecies differences exist in the respiratory system. Extensive bronchioles are present in dogs, cats, and rhesus monkeys, while minimal bronchioles are present in humans, rats, mice, horses, and pigs (Haschek et al., 2009). The pleura, the cellular layer that envelopes the lung surface, of rats, mice, dogs, cats, and rhesus monkeys are thin, and are thick in humans, horses and pigs (Haschek et al., 2009). Cattle have a relatively long tracheobronchial tree which increases the amount of dead space volume in comparison to dogs, pigs, and horses (Ackermann et al., 2010). Increased dead space affects the amount of fresh oxygen that can be delivered to the lung and increases the risk of alveolar hypoventilation with partial obstruction (Ackermann et al., 2010). Anatomical and physiological features of the respiratory system that predispose cattle to respiratory infections include the fact that: (1) cattle have a relatively increased area of dead space and also have a right tracheal bronchus; (2) their lungs have interlobular septae with limited interdependence, increased resistance, and decreased compliance; and (3) collateral ventilation is reduced due to a lack of (a) bronchoalveolar communication (channels of Lambert), (b) alveolar pores (pores of Kohn), and (c) interbronchiolar connections (channels of Martin). Due to the lack of collateral ventilation, atelectasis occurs readily and these areas of lung remain consolidated and lack functional gaseous exchange. Regions of atelectasis are also under hypoxic vasoconstriction whereby arterioles shunt blood flow away from these areas to better perfuse regions with adequate gaseous exchange (Ackermann et al., 2010). Thus, these anatomical and physiological conditions increase the demands for protective immune responses. The nasal turbinates or scrolls are relatively simple in humans and nonhuman primates, a double scroll is present in rodents, and a complex membranous branched scroll is present in dogs (Haschek et al., 2009).

There are approximately 40 cell types in the respiratory system (Haschek et al., 2009). Highly differentiated type I alveolar epithelial cells that do not divide

line approximately 90 to 95% of the alveolar surfaces. These cells prevent the leakage of fluid across the alveolar wall (Haschek et al., 2009). Type II alveolar cuboidal epithelial cells, which cover approximately 2 to 4% of the internal surface of the lung, synthesize and secrete pulmonary surfactants and are involved in the reepithelialization process after lung injury (Johnson et al., 2006; Haschek et al., 2009). Surfactants protect alveolar walls and enhance phagocytosis. Surfactant reduces alveolar surface tension at low lung volume, thereby reducing the work of breathing and preventing lung collapse. The surface tension-reducing function of surfactant stems from the interaction of phospholipid, neutral lipid, and two hydrophobic proteins, surfactant protein (SP)-B and SP-C. In addition, surfactant plays a key role in innate immunity (Mulugeta and Beers, 2006). Surfactant protein C (SP-C), a highly hydrophobic protein found in pulmonary surfactant, is synthesized exclusively in alveolar type II pneumocytes as a 21-kDa integral membrane precursor protein (Mulugeta and Beers, 2006). SP-C enhances the adsorption and spreading of phospholipids at the air–liquid interface thereby promoting the surface tension–lowering properties of surfactant and probably playing a fundamental role in pulmonary immunology both during acute lung infection and during chronic lung disease (Mulugeta and Beers, 2006). SP-C participates in the pulmonary host defense system through direct interaction with infectious agents and pattern recognition molecules (e.g., CD14) (Mulugeta and Beers, 2006). Surfactant protein-A (SP-A) production by lung epithelia increases markedly in fetal lung near term and thus roughly delineates the level of lung maturation at birth. SP-A production can also be increased with viral pneumonia and enter the pulmonary lymphatic vessels, where it is carried by the thoracic duct to the systemic blood circulation. Thus, serum SP-A measurement has the potential to be a marker of respiratory tract maturation and pneumonia severity (Ackermann et al., 2010).

Shortly before birth the fetal lung converts from fluid secretion to fluid reabsorption. Efficient gas exchange after birth depends on regulation of the amount of fluid in the thin (average, 0.2 μm) liquid layer lining the alveolar epithelium (Bastacky et al., 1995). The alveolar epithelium is the major site of Na^+ transport and fluid absorption in the adult lung (Johnson et al., 2006). Type I pneumocytes contain several types of cation channels (e.g., K^+ channels) and at least one type of anion channel [e.g., cystic fibrosis transmembrane regulator (CFTR)]. There is no evidence that type II pneumocytes contain K^+ or cyclic nucleotide-gated (CNG) channels (Johnson et al., 2006). Sodium ion transport occurs across the entire alveolar epithelium (type I and II pneumocytes) rather than only at specialized anatomical locations (i.e., across type II pneumocytes). Sodium ion is absorbed from the apical surface of both type I and II pneumocytes via epithelial Na^+ channels (ENaC) and CNG channels and transported into the interstitial space by Na^+ , K^+ -ATPase. K^+ may be transported via K^+ channels located on the apical surface of type II pneumocytes cells or through basolateral K^+ channels in type II pneumocytes (Johnson et al., 2006). If net ion transport is from the apical surface to the interstitium, an osmotic gradient would be created that would direct water transport either through aquaporins or by diffusion. Electroneutrality is conserved with Cl^- movement via CFTR in both type I and II pneumocyte cells (Johnson et al., 2006).

Located within the alveolar interstitium are alveolar macrophages. Pulmonary intravascular macrophages (PIMs), fixed macrophages that reside within pulmonary capillaries and have specialized junctional complexes, are present in cattle, pigs, horses, and cats and absent in nonhuman primates, dogs, and rodents (Longworth, 1997; Brain et al., 1999; Haschek et al., 2009). While one study demonstrated the presence of PIMs in human lung (Dehring and Wismar, 1989), a morphometric study of human lung did not show macrophages or macrophage-like cells in the pulmonary capillaries (Zeltner et al., 1987). There are marked species differences in PIMs' contribution to the mononuclear phagocytic system. Ruminants, pigs, and cats have extensive resident PIMs that avidly remove circulating particles from the blood, whereas rodents, monkeys, and chickens do not (Brain et al., 1999). In rodents, monkeys, and chickens, the removal of pulmonary particles is done primarily by monocytes and neutrophils (Brain et al., 1999). PIMs are large (20 to 80 μm in diameter) mature macrophages that are attached to the pulmonary capillary endothelium and have characteristic morphological features of differentiated macrophages (Brain et al., 1999). PIMs are involved in phagocytosis and removal of endotoxin and particles from the circulation. PIMs may play a role in normal removal of effete erythrocytes or fibrin and cell debris during inflammation (Brain et al., 1999). Rats and rabbits are quite resistant to endotoxin-induced acute lung injury, but sheep, goats, and pigs have commonly been used as animal models of acute lung injury. The increased sensitivity of sheep, goats, and pigs to endotoxin is probably due to the presence of abundant PIMs (Brain et al., 1999). In a study of freshly prepared PIMs (obtained from pigs) that were stimulated *in vitro* with LPS (10 $\mu\text{g}/\text{mL}$), COX-2 expression was investigated. Results showed that LPS resulted in the up-regulation of the expression of COX-2 in the PIMs (Chen et al., 2003). In many species, activation of macrophages occurs in a classical, proinflammatory/cell-mediated Th1-type response induced by interferon gamma and TNF, an alternative Th2-type response induced by IL-4, and an anti-inflammatory regulatory response induced by IL-10 (Ackermann et al., 2010). In cattle; however, the Th1/Th2 paradigm is not as clearly distinct functionally as in other species. Despite this, alveolar and PIMs of the bovine do function in the generation of cell-mediated, humoral, and regulatory (inhibitory) responses. In allergic (Th2-type) conditions, eosinophilic and mast cell infiltration occurs with release of granule content. Once established, inhaled antigen can cross-link IgE receptors on mast cells and basophils, resulting in cellular activation (Ackermann et al., 2010).

Bronchiolar nonciliated Clara cells are involved in the detoxification of xenobiotics. Clara cells also produce CC10, an immunomodulatory protein, and express cytochrome P450 enzymes that biometabolize toxins. After pulmonary injury, type II and Clara cells proliferate and replace damaged cells (Ackermann et al., 2010). Clara cells' morphological characteristics are abundance of agranular endoplasmic reticulum (AER) and numerous membrane-bound ovoid granules. There is considerable interspecies (adult male rabbits, guinea pigs, rats, hamsters, and mice) variation in abundance, size, and morphology of the granules, in abundance and distribution of AER, and in mitochondrial morphology. Granules were most abundant in the rat and least in the hamster, largest in the hamster, and of uniform

electron density except in the guinea pig (Plopper et al., 1980). Another pulmonary cell type located within the interstitium is the fibroblast, which produces matrix components, enzymes, and PGs and is involved in pulmonary fibrosis (Haschek et al., 2009). Both the sympathetic and parasympathetic nervous systems provide innervations to the pulmonary system, including bronchial smooth muscle, blood vessel, submucosal glands, and lymphatics (Haschek et al., 2009). Of the immunological compartments of the respiratory system that participate in the humoral immunity of the pulmonary system is mucosa-associated lymphoid tissue (MALT). MALT has IgA as the predominant class of opsinizing antibodies that phagocytose and eliminate inhaled particles (Haschek et al., 2009).

Pulmonary epithelial cells play an important role in airway homeostasis, represent the first line of defense in infection, and perform many important biological functions (Takizawa, 1998; Holgate et al., 2009; Holgate, 2011). Epithelial cells are central to respiratory system sensing of the external environment (Ackermann et al., 2010). Most particulate matter and microbial agents are removed from the inhaled air in the nares, nasal conchae, and trachea, leaving the deeper lung sterile and relatively free of particulate material. Once through the ASL, these substances, along with mists, vapors, and gases, can bind the lung epithelia and trigger activation, cell injury, metaplasia, or cell death. Microbial agents produce a number of conserved molecular patterns, termed pathogen-associated molecular patterns (PAMPs), which include substances such as teichoic acid from gram-positive bacteria, lipopolysaccharide (LPS) from gram-negative bacteria, cytokine-phosphate-guanine (CpG) DNA, single- and double-stranded RNA (dsRNA), flaggellin, fungal zymosan, and lipopeptides from mycobacteria (Ackermann et al., 2010). Bronchial epithelial cells are known to have an integral role in the airway defense mechanism via the mucociliary system as well as mechanical barriers (Radi and Ackermann, 2011). In addition, bronchial epithelial cells produce and release biologically active compounds, including lipid mediators, growth factors, and a variety of cytokines important in the pathogenesis of airway disorders (Brannon et al., 1998; Takizawa, 2005). Neutrophils, alveolar and PIMs, α/β T (CD4 and CD8) cells and γ/δ T cells, along with B, NK, and dendritic cells, are effector cells present along the respiratory tree for induction of adaptive immune responses (Ackermann et al., 2010). With inflammation, neutrophils and macrophages are present in the alveolar lumen, bronchioles, and airways. Other pulmonary immune responses include pattern recognition receptors as well as cytokine, interferon, and chemokine responses (Ackermann et al., 2010). Of special interest in cattle are γ/δ T-cells because newborn calves have an unusually high number of circulating γ/δ T-cells and also because in ruminants these cells express WC1 antigen (Ackermann et al., 2010). γ/δ T-cells account for 60% of the peripheral blood mononuclear cells in young calves. WC1⁺ γ/δ T-cells are considered an inflammatory population, whereas CD1⁻ γ/δ T-cells are regulatory with myeloid cell features (Ackermann et al., 2010). In genetically susceptible human patients with asthma, an impaired epithelial barrier function renders the airways vulnerable to early viral infection, and this in turn provides the stimulus to prime immature dendritic cells toward directing a Th2 response and local allergen sensitization. Continued epithelial susceptibility to environmental insults such as viral, allergen, and pollutant exposure and impaired

repair responses leads to asthma persistence and provides a mediator and growth factor microenvironment that leads to the persistence of inflammation and airway wall remodeling. Increased deposition of matrix in the epithelial lamina reticularis provides evidence for ongoing epithelial barrier dysfunction, while physical distortion of the epithelium consequent upon repeated bronchoconstriction provides additional stimuli for remodeling (Holgate, 2011).

Immune-mediated hypersensitivity diseases or allergies are common respiratory diseases, with type I (immediate hypersensitivity) and type III (Arthus type) being most common in the pulmonary system (Haschek et al., 2009). Pathologic manifestations of rhinitis and asthma can be the result of type I hypersensitivity, while extrinsic allergic alveolitis results from type III hypersensitivity and is related to antigen antibody deposition in the lung with complement activation (Haschek et al., 2009). Several factors, including gender, age, genetics, nutrition, smoking status, and preexisting pulmonary disease, can affect respiratory system response to injury (Haschek et al., 2009). Pathologically, asthma is a chronic airway inflammatory disease dominated by a Th2-type pattern and can be divided into intrinsic (idiosyncratic) or extrinsic disease (Haschek et al., 2009). Antigen-presenting cells such as airway dendritic cells (DCs) play a critical role in initiating and regulating early inflammatory events and mounting the adaptive immune response (Holgate et al., 2009; Holgate, 2011). Tracheal epithelial cells secrete soluble factors that down-regulate TNF α and IL-12p40 secretion by bone marrow-derived DCs but up-regulate IL-10 and arginase-1. Airway tracheal epithelial cells constitutively release PGE₂. Blocking the synthesis of PGs within airway epithelial cells relieved DCs from inhibition (Schmidt et al., 2011). The airway epithelium is crucial to both the origins and progression of asthma as well as playing a key role in asthma exacerbations (Holgate et al., 2009). The physical and functional barriers of the airway epithelium are both defective in asthma, with disrupted tight junctions, reduced antioxidant activity, and impaired innate immunity. Damage to the epithelium results in augmented expression of epidermal growth factor (EGF) receptors, but because of the reduced ability of signaling through these to repair the epithelium through “primary intention” in response to the levels of EGFR ligands available, the epithelium enters into “frustrated repair (or repair by secondary intention),” leading to enhanced profibrotic growth factor release and a tendency toward epithelial–mesenchymal transition (Holgate et al., 2009). Thus, the defect in epithelial tight junction assembly in asthma may be the result of EGFR signaling and may represent another feature of the chronic wound process (Holgate et al., 2009).

ROLE OF PROSTAGLANDINS IN THE RESPIRATORY SYSTEM

Prostaglandins have been implicated in lung pathophysiology (Radi and Ackermann, 2011). PGs are synthesized from arachidonic acid (AA) by enzymatic reactions such as cyclooxygenases (COXs), specifically COX-1 and COX-2 (Radi and Ackermann, 2011). COX-1 is generally found in most normal body tissues

and is involved in pulmonary physiological processes. COX-2 is expressed in normal tissues at very low levels and is highly induced by proinflammatory mediators in the setting of inflammation (Radi, 2009). PGs mediate various pulmonary functions (i.e., vascular vasodilatation during the perinatal, late fetal, and early postnatal periods) (Brannon et al., 1998; Lassus et al., 2000). The increased PG synthesis that occurs during gestation and in the newborn may modulate surfactant synthesis during the late fetal and early newborn periods (Pace-Asciak, 1977; Powell and Solomon, 1978; Acarregui et al., 1990). Microsomal fraction of sheep lung possesses active prostaglandin synthase, prostacyclin synthase, and thromboxane synthase activities (Tai et al., 1978). Fetal sheep lung homogenates from all ages (40 days to term) formed both PGE₂ and PGF_{2α} (Pace-Asciak, 1977). PGF_{2α} was formed in the lung to a greater extent than PGE₂ by day 40. PGE₂ increased with increasing age until at term, at which time the ratio of both prostaglandins approached unity (Pace-Asciak, 1977). Total prostaglandin biosynthesis (E₂ and F_{2α}) rose gradually with age (approximately a threefold increase between day 40 and term). Prostaglandin catabolic activity rose sharply at day 90 (approximately threefold), with a maximum around day 110 (approximately four fold), decreasing to day 40 levels by term (day 143) (Pace-Asciak, 1977). Fetal nonhuman primate, baboon, and lung EP receptor expression was investigated. The mRNA levels, protein localization, and abundance of all four PGE₂ receptors by real-time polymerase chain reaction (PCR), immunohistochemistry, and Western blot were studied. EP receptors were widely distributed in bronchiolar epithelium, bronchiolar smooth muscle, and endothelium and media of blood vessels, but not in alveoli (Schmitz et al., 2007). The role of PGs on SP-A gene expression in human fetal lung was studied in vitro (Acarregui et al., 1990). Dexamethasone resulted in a marked decrease in the levels of the PGE₂ and PGF_{2α}, the prostacyclin metabolite, 6-keto-PGF_{1α}, and the thromboxane A₂ metabolite, thromboxane B₂ (TXB₂). Indomethacin caused a pronounced decrease in the levels of these PGs and had a marked ability to reduce SP-A mRNA levels in human fetal lung in vitro (Acarregui et al., 1990). Indomethacin effects were associated with a 73% reduction in cAMP formation and were prevented by simultaneous incubation with dibutyryl cAMP or with PGE₂. PGE₂ markedly increased cAMP formation by the human fetal lung tissue incubated in the absence or presence of indomethacin. The effects of dexamethasone and indomethacin were also observed on two morphological indices of lung differentiation: alveolar luminal volume density and lamellar body volume density. PGE₂ significantly increased the luminal volume density of human fetal lung explants (Acarregui et al., 1990). Levels of various PGs were studied in fetal and adult bovine and rabbit lung homogenates. Adult bovine lungs were very active in converting AA (100 μg/g tissue) to both PGE₂ (10.7 μg/g tissue) and TXB₂ (6.2 μg/g tissue) (Powell and Solomon, 1978). Smaller amounts of PGF_{2α} (0.9 μg/g) and 6-oxo-PGF_{1α} were formed. Fetal bovine lungs during the third trimester of pregnancy were active in converting AA to PGE₂, but formed very little TXB₂, PGF_{2α}, or 6-oxo-PGF_{1α}. Rabbit lung homogenates converted AA (100 μg/g) mainly to PGE₂, both before and after birth. The amount of PGE₂ formed increased during gestation to a maximum of about 6 μg/g of tissue at 28 days of gestation. It then decreased to a minimum (1.5 μg/g), which was observed

8 days after birth, followed by an increase to about 4 $\mu\text{g/g}$ in older rabbits (Powell and Solomon, 1978).

PGs regulate vascular tone (Holtzman, 1991). High arterial blood circulating levels of prostacyclin (PGI_2) are present in humans and cats (Gryglewski, 1980). In the lungs, generation of PGI_2 can be increased by angiotensin II, bradykinin, and AA, provided that low concentrations of these substances are infused into the pulmonary artery. Air pulmonary emboli and mechanical hyperventilation stimulate the lungs to generate more prostacyclin. Respiratory stimulants such as lobeline or almitrine are also effective PGI_2 releasers from the lung. It is proposed that this para-endocrine function of the lung protects coronary and cerebral arteries against thrombosis and atherosclerosis (Gryglewski, 1980). To test whether vasodilator PGI_2 was synthesized by the lungs in response to vasoconstriction, vasoconstriction induced by angiotensin II in isolated rat lungs before and after inhibition of PG synthetase was studied (Voelkel et al., 1981). It was found that 6-keto- $\text{PGF}_{1\alpha}$ was the major AA metabolite released during pulmonary vasoconstriction. Thus, PGI_2 is produced by the lungs in response to vasoconstriction. Hypoxia by itself seems not to be the adequate stimulus for enhanced lung PGI_2 formation (Voelkel et al., 1981). Up-regulation of COX-2 in the lung has been demonstrated in a hypertensive mouse model that expresses the human renin and angiotensinogen genes (Radi and Ostoroski, 2007). Inhaled PGI_2 analogs have been proposed for the treatment of pulmonary hypertension (Gessler et al., 2011). Inhaled treprostinil sodium, a prostacyclin analog, is the most recent agent to receive U.S. Food and Drug Administration (FDA) approval for the treatment of pulmonary arterial hypertension (Ferrantino and White, 2011).

The effects of acetylcholine (ACh), a pulmonary vasodilator, infusion on pulmonary perfusion pressure, vascular responsiveness, and lung PGI_2 production were investigated (Feddersen et al., 1986a). The prolonged effect of depression of subsequent hypoxic and angiotensin II-induced vasoconstrictions, but not the immediate vasoconstriction response of ACh, was associated with an increase in perfusate 6-keto- $\text{PGF}_{1\alpha}$ concentration. The ACh-stimulated increase in 6-keto- $\text{PGF}_{1\alpha}$ production was inhibited by meclofenamate, an ns-NSAID. Thus, in isolated rat lungs ACh caused immediate vasodilation and prolonged time-dependent depression of vascular responsiveness (Feddersen et al., 1986a). Another study tested whether diminished ACh vasodilation would result from damage of lung vascular endothelium and whether this response could be used as an indication of endothelial injury in a rat model (Feddersen et al., 1986b). No difference between the prolonged depression of vascular responsiveness to hypoxia or angiotensin II and pulmonary vascular responses to ACh were found (Feddersen et al., 1986b). In isolated rat lung perfused with a cell- and protein-free physiological salt solution, the effects of AA on pulmonary vasodilation were studied (Feddersen et al., 1990). When pulmonary vascular tone was elevated by hypoxia, bolus injection of a large dose of AA (75 μg) caused transient vasoconstriction followed by vasodilation. Dosages of less than 7.5 μg of AA caused vasodilation only when injected during hypoxic vasoconstriction and with subsequent blunting of either angiotensin II- or hypoxia-induced pulmonary vasoconstriction. Only the higher doses of AA (7.5 and 75 μg), but not the lower doses (7.5 to 750 ng), caused increases in

effluent 6-keto-PGF_{1α}, TXB₂, and PGE₂ and PGF_{1α}, with 6-keto-PGF_{1α} being the major PG product (Feddersen et al., 1990). The effects of PGI₂ on pulmonary function were investigated in a swine model of septic shock. PGI₂ did not mediate blood gas changes, alter pulmonary hemodynamics, or lead to platelet abnormalities in this porcine septic shock model. Antiprostacyclin antibody infusion did not change the pulmonary hypertension and hypoxemia, and infusion of PGI₂ to pathophysiological blood concentrations did not reproduce such changes (Tran et al., 2001). Inhalation of PGI₂ (28 ng/kg per minute) over a period of 8 h in healthy lambs does not produce major side effects or acute pulmonary toxicity (Habler et al., 1996).

PGs are released during various pulmonary pathological conditions (Fulkeron et al., 1996; Vigano et al., 1998; Profita et al., 2003; Rolin et al., 2006; Radi and Ackermann, 2011). Tumor necrosis factor alpha (TNFα) has been proposed as a mediator of endotoxin-induced lung injury. TNFα induces rapid release of TXA₂, PGE₂, and PGI₂ (Wheeler et al., 1992). TNFα contributes to the pathophysiology of adult respiratory distress syndrome (ARDS) (Arias-Diaz et al., 1994). Aerosolized prostacyclin improved oxygenation in children with acute lung injury (Dahlem et al., 2004). The pulmonary effects of PGE₁ in a 30-ng/kg dose were studied in severely ill surgical patients with ARDS. PGE₁ markedly decreased pulmonary artery pressure, pulmonary and systemic vascular resistance indices, and venous pressures while increasing cardiac output, arterial PO₂, oxygen delivery, and oxygen consumption (Shoemaker and Appel, 1986). In another study, the physiological and side effects of PGE₁ were investigated in patients with ARDS who did not have significant renal or hepatic dysfunction. These patients were given PGE₁ by continuous central venous infusion (30 ng/kg per minute). PGE₁ caused significant systemic vasodilation and possibly decreased intrapulmonary polymorphonuclear leukocyte sequestration. However, PGE₁ did not influence multiple-system organ failure or mortality of patients with ARDS without renal or hepatic dysfunction (Russell et al., 1990). The safety and efficacy of an intravenous liposomal dispersion of PGE₁ for the treatment of patients with ARDS was studied in a randomized prospective multicenter double-blind placebo-controlled phase III clinical trial. PGE₁ accelerated improvement in indexes of oxygenation but did not decrease the duration of mechanical ventilation and did not improve 28-day survival (Abraham et al., 1999).

Mucus production is a primary feature of bronchial asthma (Izuhara et al., 2009). Goblet cells are major mucus-producing cells, and goblet cell hyperplasia (GCH) is one feature of airway remodeling, defined as airway structural changes. Th2-type cells play critical roles in this remodeling process, and among Th2-type cytokines, interleukin-13 (IL-13) in particular is a central mediator for GCH (Izuhara et al., 2009). Mouse calcium-activated chloride channel-3 (mCLCA-3; gob-5)/human CLCA-1 acts as a downstream molecule of Th2 cytokines, IL-4/IL-9/IL-13 signals, playing an important role in mucus production (Izuhara et al., 2009). Pendrin, an anion transporter, is induced by IL-13 and causes mucus production in airway epithelial cells (Izuhara et al., 2009). PGs have been shown to play a role in bronchial mucus secretion (Tamaoki et al., 1992). Emerging data strongly

suggest that PGs collaborate with cytokines and critically regulate T-cell proliferation, differentiation, and functions (Sakata et al., 2010). PGE₂ facilitated Th1 cell differentiation and Th17 cell expansion in collaboration with IL-12 and IL-23, respectively, and these PGE₂ actions contributed to the development of immune diseases mediated by these Th subsets (Sakata et al., 2010). Furthermore, studies using receptor-deficient mice have revealed that PGD₂ and PGI₂ contributed to regulation of immune diseases of the Th2 type, such as allergic asthma (Sakata et al., 2010). In a sensitized BALB/c mouse model of asthma, treatment with a PGD₂ receptor (DP1) agonist or DP1 agonist-treated DCs resulted in an increase in Foxp3⁺ CD4⁺ regulatory T cells that suppressed inflammation in an IL-10-dependent way. These effects of DP1 agonist on DCs were mediated by cAMP-dependent protein kinase A. In addition, activation of DP1 by an endogenous ligand inhibited airway inflammation. Triggering DP1 on DCs is an important mechanism that induced regulatory T cells and controlled the extent of airway inflammation (Hammad et al., 2007). Selective DP1 agonists that exploit the full anti-inflammatory effect on airway DCs could be a potential asthma therapeutic strategy. Thus, there are emerging roles for PGs in T cell-mediated immunity and immune diseases of the respiratory system.

PGE₂ is largely produced by epithelial and airway smooth muscle cells, but all cells in the airways have the capacity to release prostanoids (Montuschi and Barnes, 2002). PGE₂ has bronchoprotective and inhibitory effects on inflammatory cells at concentrations known to occur in the airways (Pavord and Tattersfield, 1995). Marked increases in PGE₂ synthesis and up-regulation of COX-2 have been reported in acid-induced epithelial injury (Bonnans et al., 2006). Cystic fibrosis (CF) is one of the most common autosomal recessive diseases among Caucasians caused by a mutation in the CF transmembrane conductance regulator (CFTR) gene. CFTR has been reported to be a negative regulator of PGE₂-mediated inflammatory response, a defect of which may result in excessive activation of NFκB, leading to overproduction of PGE₂ as seen in inflammatory CF tissues (Chen et al., 2012). The effects of inhaled PGE₂ on allergen-induced airway responses and inflammation were investigated in patients with mild asthma. Inhaled PGE₂ attenuated allergen-induced airway responses, hyperresponsiveness, and inflammation when given immediately before inhaled allergen (Gauvreau et al., 1999). The effect of inhaled PGE₂ on allergen-induced asthma was examined in a double-blind crossover study of eight subjects with asthma. Subjects in study 1 inhaled 100 μg of PGE₂ 5 min before a normal saline challenge, and FEV1 and bronchial reactivity to methacholine was measured at intervals for 7 h. In study 2, which had a similar design, subjects inhaled the same dose of PGE₂ or placebo followed by a dose of allergen previously shown to cause a fall in FEV1 of 20% or more. PGE₂ inhibited early and late response to allergen (Pavord et al., 1993). PGE₂ was a bronchodilator in healthy subjects but caused either dilation or constriction (the direction of the change in specific airway conductance being consistent for each subject) in asthmatics (Mathé and Hedqvist, 1975). Impaired production of PGE₂ has been proposed to contribute to the pathogenesis of asthma (Pavord and Tattersfield, 1995). PGE₂-like immunoreactivity was measurable in exhaled breath condensate (EBC) in healthy subjects and patients with asthma (Montuschi and Barnes, 2002).

PGE₂ inhibits fibroblast proliferation and collagen production. PGE₂ synthesis by fibroblasts is induced by profibrotic mediators, including transforming growth factor beta (TGFβ) (Keerthisingam et al., 2001). Cyclooxygenase-2 deficiency resulted in loss of the antiproliferative response to TGFβ in human fibrotic lung fibroblasts and promoted bleomycin-induced pulmonary fibrosis in mice (Keerthisingam et al., 2001). Dysregulation of the PGE₂ synthesis–response axis has been identified in human pulmonary fibrotic diseases and implicated in the pathogenesis of animal models of lung parenchymal fibrosis (Wilborn et al., 1995a; Stumm et al., 2011). Reduced expression of COX-2 and PGE₂ in fibroblasts from patients with idiopathic pulmonary fibrosis (IPF) is one factor that promotes fibroblast survival in the fibrotic lung (Maher et al., 2010). IPF is a lung disease that is characterized by excessive proliferation of fibroblasts. Down-regulation of PGE receptor 2 gene (PTGER2) and consequent PGE₂ resistance are both mediated by DNA hypermethylation. Increased Akt signal transduction is a novel mechanism that promotes DNA hypermethylation during pulmonary fibrogenesis in humans and mice (Huang et al., 2010).

There is a homeostatic balance within the lung that requires crosstalk between alveolar epithelial cells, fibroblasts, and inflammatory cells (Bozyk and Moore, 2011). Alveolar epithelial cells produce PGE₂, which limits fibroproliferation and promotes appropriate alveolar epithelial repair. In the normal lung, PGE₂ signals via EP₂ receptor-mediated increases in cAMP that induce fibroblast apoptosis and limit myofibroblast transformation, proliferation, and collagen secretion (Bozyk and Moore, 2011). In pulmonary fibrosis, the homeostatic balance is altered and PGE₂ production becomes limited via inflammatory mediators and epigenetic silencing of the COX-2 promoter (Bozyk and Moore, 2011). Furthermore, fibrotic fibroblasts lose EP₂ receptor expression and may lose expression of the downstream effectors protein kinase A (PKA) and phospho-cAMP response element binding (CREB) (Bozyk and Moore, 2011). Fibrosis is a male-predominant disease, and at least one study has suggested that male gender is associated with reduced EP₂ and EP₄ levels and reduced PGE₂ production in splenic macrophages after trauma (Stapleton et al., 2004). PGE inhalation therapy may be the best option for patients with lung fibrosis, but nebulization of PGE₂ or EP₂ agonists is not practical (Bozyk and Moore, 2011).

Aerosolized PGE₂ prevented experimentally induced airway response to allergen challenge in asthmatics (Herrerias et al., 2009). The effects of PGE₂ on airway inflammation were investigated in a house dust mite–sensitive mouse (HDM) model, a model that reproduces the spontaneous exposure of allergic asthma patients to aeroallergens (Herrerias et al., 2009). Exogenous PGE₂ reduced by half eosinophilic infiltration in HDM-sensitized mice and led to a strong reduction in airway Th2 cytokine expression (Herrerias et al., 2009). The EP₃ receptor has been identified to mediate PGE₂-induced depolarization of sensory nerves in humans, mice, and guinea pigs. Thus, PGE₂ mediates coughs via the EP₃ receptor (Maher et al., 2009). The receptor involved in PGE₂-induced relaxation in guinea pig, murine, monkey, rat, and human airways was studied *in vitro*. It was found that EP₂ receptor mediates PGE₂-induced relaxation of guinea pig, murine and monkey trachea and that the EP₄ receptor mediates PGE₂-induced

relaxation of the rat trachea. Thus, EP₄ receptor was proposed as a new target for bronchodilator therapy (Buckley et al., 2011).

Chronic obstructive pulmonary disease (COPD) is a slowly progressive, chronic, and complex airway disease involving several types of inflammatory cells (e.g., alveolar macrophages, dendritic cells, neutrophils, T-lymphocytes) and mediators. A major cell type in COPD pathophysiology is alveolar macrophages. Some of the major stimuli that activate macrophages are bacterial endotoxin and proinflammatory cytokines such as IL-1 β and TNF α (Murugan and Peck, 2009). Thus, alveolar macrophage plays a role in pulmonary defense (Wilborn et al., 1995b; Radi et al., 2010; Radi and Ackermann, 2011). Alveolar macrophages have the capacity to generate PGs. Alveolar macrophages secrete PGE₂ and may contribute to the increased PGE₂ in the exhaled breath of COPD patients (Montuschi et al., 2003). There is increased COX-2 expression in alveolar macrophages from patients with COPD compared to normal control subjects (Taha et al., 2000). TXA₂ biosynthesis is enhanced in patients with COPD and may be influenced by arterial oxygen tension changes (Davi et al., 1997).

PGs are involved in surfactant homeostasis (Oyarzun and Clements, 1978; Arias-Diaz et al., 1994; Wilborn et al., 1995b). In vitro PGE₂ induces surfactant production via EP₁ and cyclic adenosine monophosphate (cAMP)-coupled EP₂ and EP₄ receptors (Schmitz et al., 2007). Human fetal lung in vitro secretes into the culture medium relatively large amounts of PGE₂ and PGF_{2 α} and of the PGI₂ and TXA₂ metabolites (Mendelson et al., 1991). In addition, indomethacin, an ns-NSAID, markedly inhibited SP-A gene expression and cAMP formation by human fetal lung in culture. Furthermore, the inhibitory effect of indomethacin on SP-A gene expression can be prevented by simultaneous incubation with either PGE₂ (Mendelson et al., 1991). It has been shown that PGE₁, PGE₂, and PGF_{2 α} are involved in controlling alveolar surfactant during increased minute ventilation in rabbit lung (Oyarzun and Clements, 1978).

The kinetics of PGE₂ production and the expression of COX enzymes during the course of experimental pulmonary tuberculosis was studied in a BALB/c mouse model infected via the trachea with *Mycobacterium tuberculosis* (Rangel Moreno et al., 2002). The PGE₂ quantification in lung homogenates showed stable low concentrations during the first month of infection, followed by a significant twofold increase at day 60 and a fourfold increase at day 90 postinfection compared to day 28 of infection. These results correlated with the kinetics of the gene expression of COX-1, COX-2, and PGE synthase, which showed a progressive increase that reached a peak at day 90 of infection. Moreover, the expression of IL-17 was detected only during the advanced phase of infection. Macrophages were the cells that most commonly expressed COX-2, PG synthase, and PGE₂. At the beginning of the infection, days 1 and 3, these macrophages showed the morphological features of activated macrophages (large cells with abundant and compact cytoplasm) and were located in the alveolar–capillary interstitium, where they constituted 20 \pm 7% of the total inflammatory cells. Granulomas started to form after 2 weeks of infection. These granulomas had activated macrophages with immunoreactivity to COX-2 and PGE, but during the entire course of the infection they were maintained at a stable percentage from 13 to 16 \pm 7%. In contrast, macrophages embedded in

the pneumonic areas which showed positive immunostaining to PGE₂ and COX-2 showed vacuolated cytoplasm, and corresponded to the $17 \pm 5\%$ and $25 \pm 6\%$ of the total inflammatory cells at days 60 and 90, respectively. Considering that these pneumonic areas increased progressively during infection, it was evident that these vacuolated cells were the most important source of PGE₂ during the advanced phase of the infection. In addition, these pneumonic areas also showed COX-1 immunostained cells, but they were monocytes located in the alveolar–capillary interstitium. Thus, PGE₂ contributed significantly to the pathogenesis of pulmonary tuberculosis, and high PGE₂ concentrations during the late phase of the disease contribute to down-regulate cell-mediated immunity, permitting disease progression (Rangel Moreno et al., 2002).

Pulmonary epithelial cells play an integral role in airway homeostasis, perform numerous biological functions, and represent the first line of defense against infection (Takizawa, 1998). The bovine lung anatomical and physiological features predispose cattle to various respiratory infections (Ackermann et al., 2010). Parainfluenza virus (PI) and bovine respiratory syncytial virus (RSV) are major pulmonary pathogens of cattle, which all produce some type of PAMP, recognized by epithelia, alveolar macrophages, and intravascular macrophages (Ackermann et al., 2010). In addition, both RSV and PI are pathogens of human infants and perinatal lambs (Radi et al., 2010; Radi and Ackermann, 2011). RSV and PI are leading viral causes of respiratory disease in infants in their first year of life and cause morbidity and mortality in transplant patients and older adults (Hall, 2001; Thompson et al., 2003; Radi and Ackermann, 2011). Bovine and ovine strains of both RSV and paramyxoviruses have high homology to human strains and induce identical pulmonary lesions (Cutlip and Lehmkuhl, 1979; Lehmkuhl and Cutlip, 1983; Hall, 2001; Grubor et al., 2004; Meyerholz et al., 2004; Johnson et al., 2007; Radi, 2009; Radi et al., 2010). Several proinflammatory cytokines and chemokines can be detected in patients with RSV and PI infection (Bonville et al., 1999; Hornsleth et al., 2001; Graham et al., 2002; Bennett et al., 2007). Increased levels of PGE₂ in the plasma or endotracheal aspirates has been demonstrated in animals and infants infected with RSV (Gershwin et al., 1989; Sznajder et al., 2004). Infection of a human alveolar epithelial transformed cell line (A549 cells) with live RSV substantially increased production of PGE₂ (Bryan et al., 2005). In addition, RSV induced PGE₂ production in human alveolar type II-like epithelial cells (Liu et al., 2005).

Mast cell–derived PGD₂ is one of the essential modulators of eosinophilic airway inflammation in asthma and allergic rhinitis (Shiraishi et al., 2005; Uller et al., 2007). Chemoattractant receptor homologous molecule expressed on Th2 cells (CRTh2), a high-affinity receptor for PGD₂, mediates trafficking of Th2-cells, mast cells, and eosinophils to inflammatory sites, and has been proposed as a target for treatment of allergic airway diseases (Uller et al., 2007). The anti-allergic efficacy of a highly selective small-molecule CRTh2 antagonist has been demonstrated in a mouse asthma model (Uller et al., 2007). Matsuoka et al. (2000) demonstrated that PGD₂ plays a key role in allergic asthma by using mice deficient in the prostanoid DP receptor. Sensitization and aerosol challenge with ovalbumin of the homozygous mutant (DP^{-/-}) mice induced increases in the serum

concentration of immunoglobulin E (IgE) similar to those in wild-type mice. However, the concentrations of Th2 cytokines and the extent of lymphocyte accumulation in the lung of OVA-challenged DP^{-/-} mice were greatly reduced compared with those in wild-type animals. In addition, DP^{-/-} mice had only marginal infiltration of eosinophils and failed to develop airway hyperreactivity. Thus, PGD₂ functions as a mast cell-derived mediator to trigger asthmatic responses. PGD₂ overproduction has been demonstrated in patients with ARDS and acute extrinsic allergic alveolitis (Higashi et al., 2005).

COX-1 EXPRESSION IN THE RESPIRATORY SYSTEM UNDER NORMAL AND PATHOLOGICAL CONDITIONS

Normally, COX-1 is expressed in many tissues throughout the body, including the lung (Figs. 6-1 and 6-2A) (Radi et al., 2010; Radi and Ackermann, 2011). COX-1 isoenzyme is expressed in a variety of respiratory tissues, and this expression is variable among different animal species. In ovine lungs, COX-1 is the main isoform that is expressed in endothelial cells and airway epithelium and is involved in vasodilatation, bronchodilation, and surfactant synthesis (Brannon et al., 1998). The ontogeny of COX-1 expression was investigated in the ovine lungs at time points of ontologic development that include preterm, term, and after birth (of full-gestation lambs) (Table 6-1) (Radi and Ackermann, 2011). Moderate to strong COX-1 expression was present in all pulmonary microanatomic locations from preterm, full-term, and postnatal lambs, with the exception of bronchial and bronchiolar epithelial cells, which had minimal expression (Radi and Ackermann, 2011). Other studies in the ovine lung have showed the lack of significant changes in COX-1 expression between the fetal preterm to term (125 to 135 days of gestation) and postnatal (7 days old) (Brannon et al., 1998). A significant maturational increase in COX-1 expression was demonstrated in the airway epithelium only in the postnatal lung of lambs that were 1 to 4 months old (Brannon et al., 1998). In neonatal lambs, COX-1 expression in alveolar macrophages was noted (Wilborn et al., 1995b; Radi and Ackermann, 2011). Thus, COX-1 is expressed constitutively in the lungs from preterm, full-term, and after-birth lambs in various microanatomical pulmonary locations, and there is differential expression of COX-1 in the developing lung (Radi and Ackermann, 2011).

COX-1 expression in vascular endothelium and alveolar epithelial cells has been shown in nonhuman primates and ovine lung (Khan et al., 2000; Radi and Ackermann, 2011). In lungs from adult rats and normal adult humans, COX-1 was expressed in bronchiolar epithelium, bronchiolar smooth muscle, alveolar macrophages, endothelial cells, and vascular smooth muscle cells (Brannon et al., 1994, 1998; Ermert et al., 1998; Hasturk et al., 2002; Radi and Ackermann, 2011). COX-1 was present in vascular endothelium and alveolar epithelial cells in the nonhuman primate (Khan et al., 2000). In lungs of normal mice, positive immunohistochemical COX-1 staining was observed in the bronchiolar epithelium (Clara cells), in the smooth muscle underlying the bronchiolar epithelium, in alveolar macrophages, and in the alveolar epithelium (Bauer et al., 2000). Another study

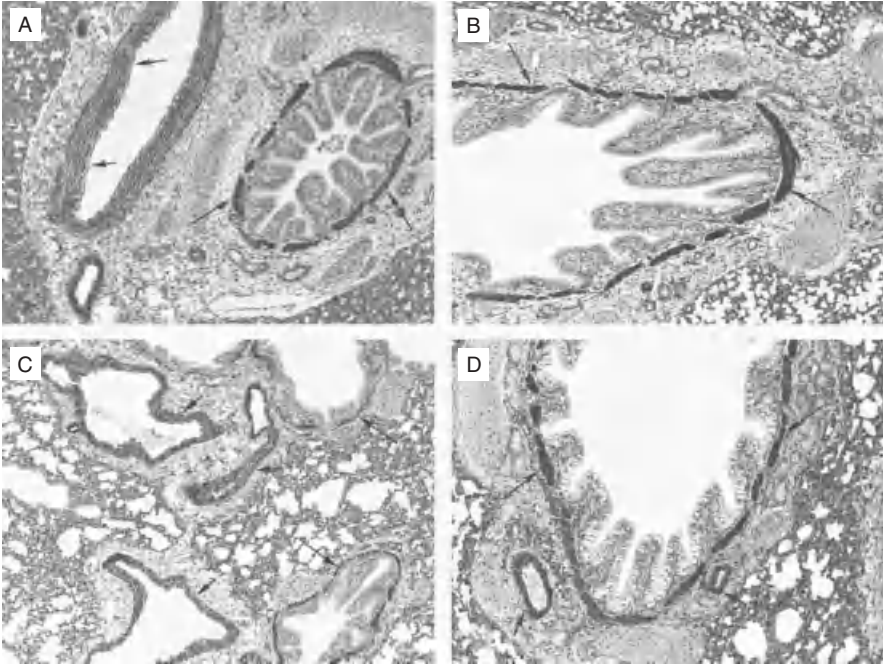


FIGURE 6-1 (A) COX-1 expression in the lung from a preterm lamb at 115 days of gestation. Strong expression in bronchial smooth muscle cells (long arrows) and vascular smooth muscle and endothelial cells (short arrows). (B) COX-1 expression in the lung from a preterm lamb at 130 days of gestation. Strong expression in bronchial smooth muscle cells (long arrows) and moderate expression in alveolar septa (short arrows). (C) COX-1 expression in the lung from a term lamb at 145 days of gestation. Strong expression in bronchial smooth muscle cells (long arrows) and vascular smooth muscle cells (short arrows). (D) COX-1 expression in the lung from a postnatal lamb. Strong expression in bronchial smooth muscle cells (long arrows) and vascular smooth muscle cells (short arrows). Immunohistochemical stain, original magnification 10 \times . (From Z. A. Radi and M. R. Ackermann, *Pathophysiology*, 18, pp. 215–219. Copyright © 2011 Elsevier Ireland Ltd. All rights reserved.)

investigated the role of COX-1 in the lung using tissue from genetically modified mice lacking functional COX-1 (COX-1^{-/-}). Bronchi from wild-type mice contained predominantly COX-1 immunoreactivity, while bronchi from COX-1^{-/-} mice were hyperresponsive to bronchoconstrictors (Harrington et al., 2008). Thus, COX-1 was shown to be the functional isoform present in the airway with regard to bronchoconstriction.

In normal human lung, strong COX-1 immunostaining was noted in airway (bronchial) epithelial cells and in endothelial cells of pulmonary vessels (Ermer et al., 2003). Other studies have demonstrated COX-1 expression in various pulmonary microanatomical locations in normal human lungs (Hasturk et al., 2002). The allele frequencies of 20 polymorphisms in the promoter and coding region of the COX-1 gene was studied in random Australian Caucasian subjects, and four common polymorphisms were studied further in relation to asthma and atopy. This

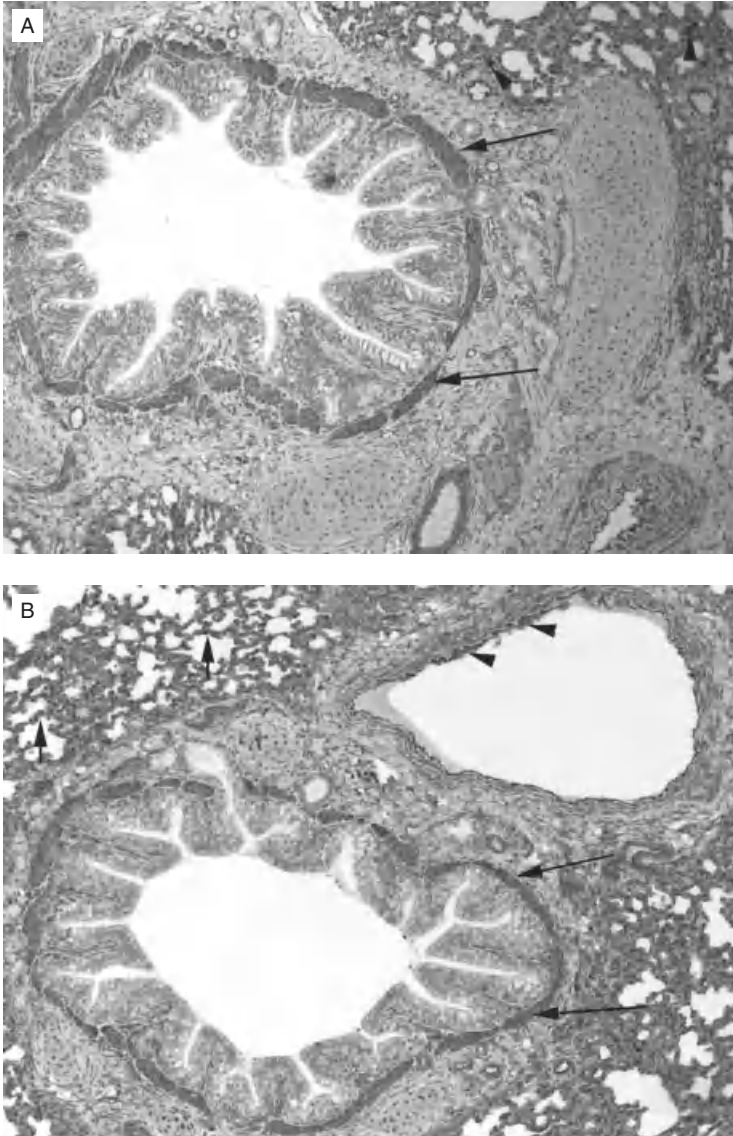


FIGURE 6-2 (A) COX-1 expression in the lung from a control lamb. Strong expression in bronchial smooth muscle cells (long arrows) and macrophages (arrowheads) can be seen (immunohistochemical stain, original magnification 10 \times). (B) COX-1 expression in the lung from a RSV-infected lamb. Strong expression in bronchial smooth muscle cells (long arrows), alveolar septa (short arrows), and vascular endothelial cells (arrowheads) can be seen (immunohistochemical stain, original magnification 10 \times). (C) COX-1 expression in the lung from a PI3-infected lamb. Strong expression in bronchial and bronchiolar smooth muscle cells (long arrows) and vascular endothelial cells (arrowheads) can be seen (immunohistochemical stain, original magnification 10 \times). (From Z. A. Radi, D. K. Meyerholz and M. R. Ackermann, *Viral Immunology*, 23, pp. 43–48. Copyright © 2010 Mary Ann Liebert, Inc. Publications. All rights reserved.)

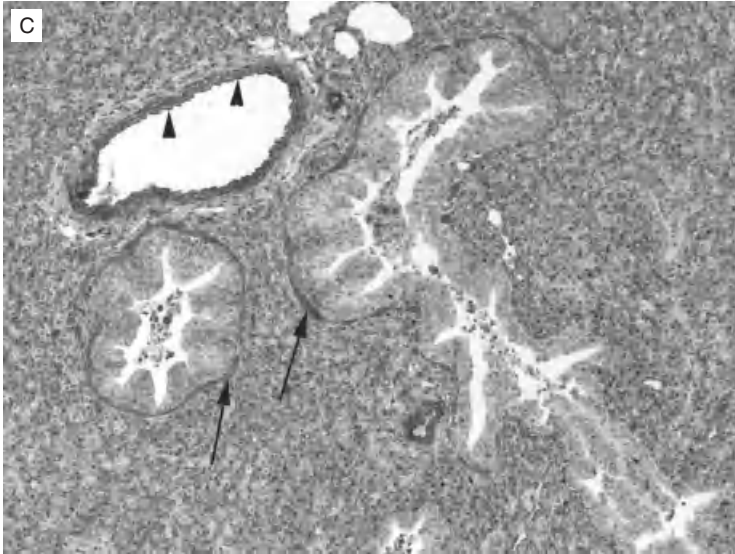


FIGURE 6-2 (Continued)

TABLE 6-1 Ontogeny of Pulmonary COX-1 Expression and Distribution^a

Pulmonary compartment	Preterm		Term 145 days	Postnatal 15 days
	115 days	130 days		
Alveolar septa	+++	+++	+++	+++
Bronchial epithelium	+	+	+	+
Bronchial SMC	++++	++++	++++	++++
Bronchiolar epithelium	+	+	+	+
Bronchiolar SMC	++++	++++	++++	++++
Alveolar macrophages	+++	+++	+++	+++
Vascular EC	++++	++++	++++	++++
Vascular SMC	++++	++++	++++	++++

Source: From Z. A. Radi and M. R. Ackermann, *Pathophysiology*, 18, pp. 215–219. Copyright © 2011 Elsevier Ireland Ltd. All rights reserved.

^a+, minimal staining; ++, mild staining; +++, moderate staining; +++++, strong staining; EC, endothelial cells; SMC, smooth muscle cells.

study did not find any associations of any of the four individual polymorphisms or their haplotypes with asthma or asthma severity, suggesting that despite their potential functional importance, these promoter and coding region polymorphisms in the COX-1 gene are unlikely to play a role in asthma. However, the results from the study did indicate that the c.22TT genotype may confer a small protective effect against atopy (Shi et al., 2005). COX-1 expression in cultured airway tissue from “aspirin-sensitive” and control patients was investigated. It was shown that despite

detectable levels of COX-2, COX-1 was functionally predominant in the airways (Harrington et al., 2008). The expression of COX-1 and COX-2 has been studied in the bronchial mucosa of 10 normal and 18 asthmatic subjects, 11 of whom had aspirin-sensitive asthma (ASA) and seven had non-aspirin-sensitive asthma (NASA). Significant increase in the epithelial and submucosal cellular expression of COX-2, but not of COX-1, was noted in asthmatic patients. There was no significant difference in the total number of cells staining for either COX-1 or COX-2 between subjects with ASA and NASA, but the number and percentage of mast cells that expressed COX-2 was increased significantly in individuals with ASA (Sousa et al., 1997). Thus, both isoforms of COX are present in the airways of patients with aspirin-sensitive asthma.

Some studies have demonstrated increased COX-1 in pulmonary neoplastic and nonneoplastic conditions. COX-1 was highly expressed in lung tumor epithelial cell hyperplasias and adenomas in mice (Bauer et al., 2000). COX-1 expression was investigated in human non-small-cell lung cancer (NSLC) (Ermer et al., 2003). Only 4 of 15 adenocarcinomas and the chondrohamartomas showed a moderate COX-1 immunostaining intensity. No COX-1 expression was noted in squamous cell carcinomas and in vascular smooth muscle cells or endothelial cells of pulmonary vessels located within the tumor or adjacent to the tumor (Ermer et al., 2003). COX-1 mRNA expression in NSLC via *in situ* hybridization was absent or below the level of detection. COX-1 immunohistochemistry demonstrated uniform faint cytoplasmic staining in tumor cells and stromal inflammatory cells (Watkins et al., 1999). The COX biosynthetic pathway may act synergistically and enhance tumor angiogenesis, the expression of angiogenic factors, and metastases in patients with small cell lung cancer (Yoshimoto et al., 2005). COX-1 mRNA levels were significantly higher in the lung parenchyma of COPD patients than in control subjects (Roca-Ferrer et al., 2011). COX-1 expression was examined in nasal biopsies from patients with allergic rhinitis (AR), seasonal AR (SAR), and perennial AR (PAR). No significant differences were noted in the lamina propria in immunostaining for COX-1. Within the epithelium, increased expression of COX-1 was observed in PAR and SAR biopsies and was associated with more intraepithelial mast cells in groups (Westergren et al., 2009). COX-1 mRNA expression was investigated in an ovalbumin-sensitized and ovalbumin-challenged guineapig lung model. The levels of COX-1 mRNA remained unchanged (Oguma et al., 2002). COX-1 expression in bronchiolar epithelial cells was significantly lower in IPF and sarcoidosis than in controls (Petkova et al., 2003). Increased COX expression has been demonstrated in various viral infections (Fig. 6-2B and C) (Steer and Corbett, 2003; Radi et al., 2010). Therefore, prostanoids are important mediators in both normal and disease pulmonary functions (Radi and Ackermann, 2011). In a study in a neonatal lamb model of viral infection, all microanatomical locations in control, RSV, and PI3-infected lungs had some degree of COX-1 expression (Table 6-2) (Radi et al., 2010). A slightly higher COX-1 expression was present in bronchial and bronchiolar epithelial cells from RSV-infected lungs compared to controls of PI3-infected lungs (Radi et al., 2010). Thus, COX-1 expression is not altered after RSV or PI3 pulmonary infection (Radi et al., 2010).

TABLE 6-2 Pulmonary Cellular Expression of COX-1 Following RSV and PI3 Infection^a

Pulmonary compartment	Control	RSV	PI3
Alveolar septa	+++	++++	+++
Bronchial epithelium	+	++	+
Bronchial SMC	++++	++++	++++
Bronchiolar epithelium	+	++	+
Bronchiolar SMC	++++	++++	++++
Macrophages	++++	++++	++++
Vascular EC	++++	++++	++++
Vascular SMC	++++	++++	++++

Source: From Z. A. Radi, D. K. Meyerholz, and M. R. Ackermann, *Viral Immunology*, 23, pp. 43–48. Copyright © 2010 Mary Ann Liebert, Inc. Publications. All rights reserved.

^a+, minimal expression; ++, mild expression; +++, moderate expression; +++++, strong expression; EC, endothelial cells; SMC, smooth muscle cells.

COX-2 EXPRESSION IN THE RESPIRATORY SYSTEM UNDER NORMAL AND PATHOLOGICAL CONDITIONS

The COX-2 isoenzyme is not generally expressed in normal respiratory tissues, but is up-regulated during pathological conditions (Fig. 6-3) (Radi and Ackermann, 2011). Airway epithelium forms a continuous barrier that limits the access of luminal substances to the systemic circulation (Wallace, 2006; Radi and Ackermann, 2011). In a human airway epithelial cell culture system, COX-2 induction was observed in the setting of inflammatory cytokine stimulation (Watkins et al., 1997). No COX-2 expression was present in lungs of preterm lambs (Radi and Ackermann, 2011). The lack of inducible COX-2 expression in the lung of preterm lambs may be attributed to the sterility of the fetal environment (Radi and Ackermann, 2011). However, minimal COX-2 expression was present in bronchial and bronchiolar epithelial cells and the alveolar septa and macrophages 15 days postnatally in the ovine lung (Table 6-3) (Radi and Ackermann, 2011). Other studies noted low levels of COX-2 in untreated human airway epithelial cells in culture (Mitchell et al., 1994). In vitro studies using cultured human bronchial epithelial cells have demonstrated that these cells express COX-2 constitutively (Asano et al., 1996). The biological significance of COX-2 expression in airway epithelia in term and 15-day-old lambs may be related to pulmonary epithelial cells direct regulatory function via an action of cytokines released from alveolar macrophages on specific epithelial cell receptors (Radi and Ackermann, 2011). Airway epithelial cells express a number of cytokines (e.g., IL-1 β) that are known to induce COX-2 (Devalia and Davies, 1993). Thus, epithelial cells may generate such cytokines, which then act in an autocrine fashion, leading to COX-2 expression up-regulation (Devalia and Davies, 1993). In human fetal lung, COX-2 is present in the perinatal

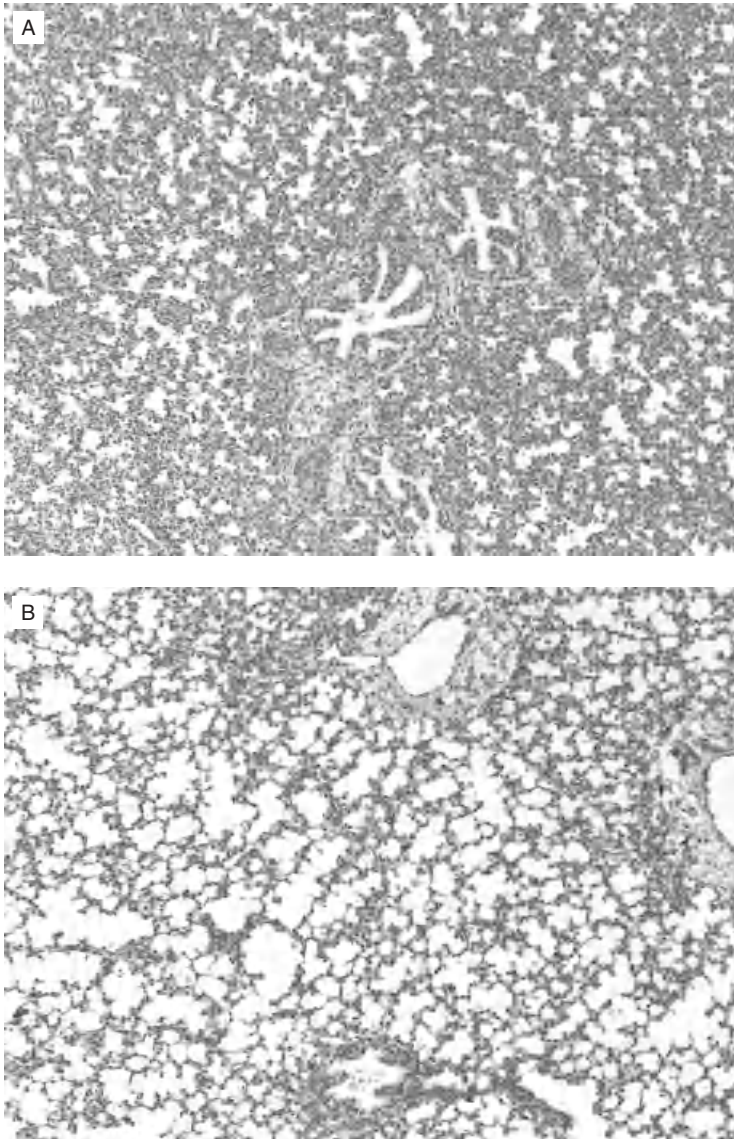


FIGURE 6-3 (A) COX-2 expression in the lung from a preterm lamb at 115 days of gestation. No expression in any pulmonary microanatomic location. (B) COX-2 expression in the lung from a preterm lamb at 130 days of gestation. No expression in any pulmonary microanatomic location. (C) COX-2 expression in the lung from a term lamb at 145 days of gestation. Mild expression in bronchial (long arrows) and bronchiolar (short arrows) epithelial cells. (D) COX-2 expression in the lung from a postnatal lamb. Mild expression in bronchial and bronchiolar epithelial cells (long arrows). Immunohistochemical stain, original magnification 10 \times . (From Z. A. Radi and M. R. Ackermann, *Pathophysiology*, 18, pp. 215–219. Copyright © 2011 Elsevier Ireland Ltd. All rights reserved.)

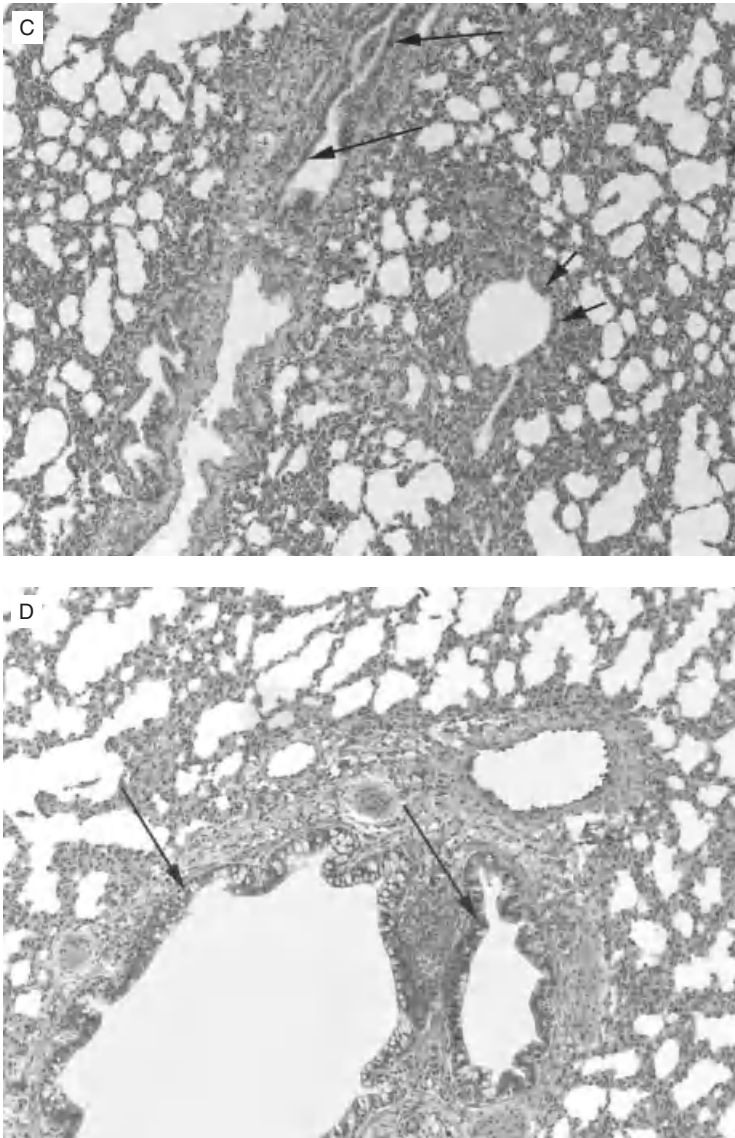


FIGURE 6-3 (Continued)

lung of neonates from the gestational age of 16 weeks to term (Lassus et al., 2000). COX-2 staining was found exclusively in the alveolar and bronchial epithelial cells, with none in the interstitium, inflammatory cells, or endothelium. Bronchial staining was localized in ciliated epithelial cells. Alveolar staining was seen in cells resembling type II pneumocytes and in most of the cells lining the alveolar epithelium. In preterm infants, alveolar staining was most intense in areas with hyaline membranes. In term infants, the pattern of alveolar staining was similar to that

TABLE 6-3 Ontogeny of Pulmonary COX-2 Expression and Distribution^a

Pulmonary compartment	Preterm		Term	Postnatal
	115 days	130 days	145 days	15 days
Alveolar septa	—	—	—	—
Bronchial epithelium	—	—	+ / + +	+ / + +
Bronchial SMC	—	—	—	—
Bronchiolar epithelium	—	—	+ / + +	+ / + +
Bronchiolar SMC	—	—	—	—
Alveolar macrophages	—	—	—	++
Vascular EC	—	—	—	—
Vascular SMC	—	—	—	—

Source: From Z. A. Radi and M. R. Ackermann, *Pathophysiology*, 18, pp. 215–219. Copyright © 2011 Elsevier Ireland Ltd. All rights reserved.

^a —, no staining; +, minimal staining; ++, mild staining; EC, endothelial cells; SMC, smooth muscle cells.

seen in preterm infants, but with a lower proportion of positive cells (Lassus et al., 2000). In bronchopulmonary dysplasia (BPD), no staining appeared in alveolar epithelial cells. In three cases with BPD and with clinically and microscopically verified pneumonic infection at the time of death, alveolar staining showed a pattern similar to that in preterm infants. In some samples, an infiltration of granulocytes was apparent, and in these cells an occasional positivity was observable (Lassus et al., 2000).

In lungs of adult normal subjects, COX-2 expression was found in bronchial epithelium (Demoly et al., 1997). Bronchial epithelial cells play an integral role in the airway defense mechanism via the mucociliary system, as well as mechanical barriers (Radi et al., 2010). In addition, bronchial epithelial cells produce and release biologically active compounds, including lipid mediators, growth factors, and a variety of cytokines important in the pathogenesis of airway disorders (Takizawa, 2005; Radi et al., 2010). Some in vitro studies have demonstrated that cultured human bronchial epithelial cells express COX-2 constitutively (Asano et al., 1996). Pulmonary vascular endothelial cells lacked COX-2 expression under basal conditions in humans and lambs (Jackson et al., 1993; Radi and Ackermann, 2011).

RSV, PI1, and PI3 cause respiratory infection and hospitalization in young children and animals (Hall, 2001; Radi et al., 2010). Marked increase in COX-2 expression was noted in pulmonary bronchial and bronchiolar epithelium and macrophages following RSV or PI3 infection in a study in neonatal lambs (Fig. 6-4 and Table 6-4) (Radi et al., 2010). Minimal COX-2 expression was present in macrophages and bronchial and bronchiolar epithelial cells from control animals, but was increased in RSV and in a PI3-infected neonatal lamb model (Radi et al., 2010). In an experimental mouse model of acute lung, significant induction of COX-2 expression was observed after injury (Fukunaga et al., 2005). It has been shown using in vitro human alveolar type II-like epithelial cells that RSV infection

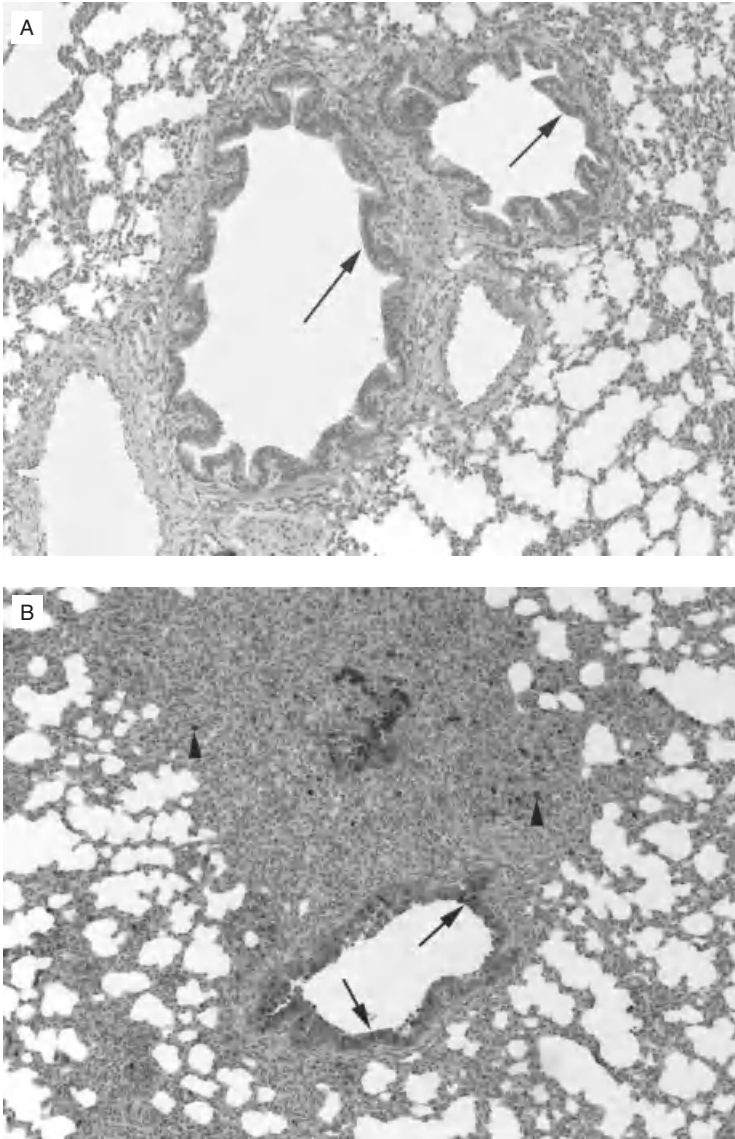


FIGURE 6-4 (A) COX-2 expression in the lung from a control lamb. Minimal expression in bronchial and bronchiolar epithelial cells (long arrows) can be seen (immunohistochemical stain, original magnification 10 \times). (B) COX-2 expression in the lung from an RSV-infected lamb. Strong expression in bronchiolar epithelial cells (long arrows) and macrophages (arrowheads) can be seen (immunohistochemical stain, original magnification 10 \times). (C) COX-2 expression in the lung from a PI3-infected lamb. Strong expression in bronchial epithelial cells (long arrows) and macrophages (arrowheads) can be seen (immunohistochemical stain, original magnification 10 \times). (From Z. A. Radi, D. K. Meyerholz, and M. R. Ackermann, *Viral Immunology*, 23, pp. 43–48. Copyright © 2010 Mary Ann Liebert, Inc. Publications. All rights reserved.)



FIGURE 6-4 (Continued)

TABLE 6-4 Pulmonary Cellular Expression of COX-2 Following RSV and PI3 Infection^a

Pulmonary compartment	Control	RSV	PI3
Alveolar septa	—	—	—
Bronchial epithelium	+	+++ /++++	++++
Bronchial SMC	—	—	—
Bronchiolar epithelium	+	+++ /++++	+++ /++++
Bronchiolar SMC	—	—	—
Macrophages	+	++++	++++
Vascular EC	—	—	—
Vascular SMC	—	—	—

Source: From Z. A. Radi, D. K. Meyerholz, and M. R. Ackermann, *Viral Immunology*, 23, pp. 43–48. Copyright © 2010 Mary Ann Liebert, Inc. Publications. All rights reserved.

^a—, no staining; +, minimal expression; ++, mild expression; +++, moderate expression; +++++, strong expression; EC, endothelial cells; SMC, smooth muscle cells.

induces a time-dependent increase in COX-2 expression, is a potent inducer of PGE₂, and that viral replication is required for PGE₂ secretion (Liu et al., 2005). The cotton rat is a powerful model for studying RSV infection in vivo (Richardson et al., 2005). In a cotton rat model, increased COX-2 protein expression was noted 1 day post-RSV virus infection and persisted on day 2. Thus, RSV induced

COX-2 mRNA expression in lungs of infected cotton rats. Lung epithelial cells and macrophages (peritoneal and bronchioalveolar) are potential sources of COX-2 and PG during infection with RSV (Richardson et al., 2005). COX-2 was immunoprecipitated in all infected animals during the first 7 days postinfection with RSV. There were two peaks of immunoreactive COX-2. The first was detected as early as 6 h postinfection, which decreased slightly after 12 h, but it remained detectable throughout day 3 postinfection (Richardson et al., 2005). A second peak was seen on day 5 postinfection and correlated with the peak of lung pathology during primary RSV infection in cotton rats. Thus, COX-2 is strongly induced *in vivo* during primary RSV infection in the lung (Richardson et al., 2005; Radi et al., 2010).

Alveolar macrophages are a major source of PGE₂ (Hempel et al., 1994). Marked increase in COX-2 expression in macrophages occurred after RSV infection (Richardson et al., 2005; Radi et al., 2010). Human cord blood-derived macrophages and dendritic cells have been shown to secrete PGE₂ following exposure to RSV (Bartz et al., 2002). Increased COX-2 levels in macrophages have been demonstrated in humans after rhinovirus infection (Seymour et al., 2002). Macrophages are postulated to be the primary cell type expressing COX-2 at sites of inflammation (Seibert et al., 1994). In a mouse model of oxygen-induced ARDS, COX-2 was expressed in alveolar macrophages (Adawi et al., 1998). Thus, COX-2 expression is up-regulated in bronchiolar and bronchial epithelial cells and macrophages after RSV and PI3 infection, and pulmonary epithelia along with macrophages are important microanatomical compartments regulating host inflammatory response during viral infection (Radi et al., 2010).

COX-2 and vascular endothelial growth factor (VEGF) affect vascular permeability and angiogenesis and may be induced by hyperglycemia and tissue hypoxia (Wilkinson-Berka, 2004). COX-2 inhibition has been associated with attenuating angiogenesis and down-regulating VEGF and bFGF (Masferrer et al., 1999). In inflamed tissues, eicosanoids are thought to play a significant role in angiogenesis (Yamada et al., 1999). Total COX-2 mRNA expression in cancer cells and surrounding stromal cells correlated strongly and positively with VEGF mRNA expression, intratumoral microvessel counts, and adverse prognosis in NSCLC patients (Yuan et al., 2005).

COX-2 expression in pulmonary neoplasia is variable depending on the type and grade of the tumor. The expression of COX-2 mRNA and protein was studied in human lung adenocarcinoma, squamous cell carcinoma, and small cell lung cancer (Wolff et al., 1998). Ninety percent of lung tumors (e.g., squamous cell carcinomas and adenocarcinomas) expressed COX-2 at a moderate to strong level, which was significantly different from the negligible expression in distant nonneoplastic epithelium (Soslow et al., 2000). COX-2 mRNA steady-state levels were high in well-differentiated adenocarcinoma samples but low in poorly differentiated adenocarcinoma, squamous cell carcinoma, and small cell lung cancer. Immunohistochemistry showed COX-2 staining in 19 of 21 adenocarcinomas. However, well-differentiated adenocarcinomas had more COX-2 staining than did poorly differentiated adenocarcinomas. Expression of the COX-2 protein was also seen in all 11 squamous cell carcinomas studied, although the level of staining seemed to be less than that in the adenocarcinomas. Small cell lung cancer specimens stained with

a relatively weak intensity (Wolff et al., 1998). There were no differences in the COX-2 mRNA levels between squamous carcinoma and adenocarcinoma. COX-2 protein levels were significantly higher in tumors than in lung parenchyma and airways. COX-2 protein levels were higher in adenocarcinoma than in squamous carcinoma (Roca-Ferrer et al., 2011). HuR is an mRNA-binding protein that binds to labile transcripts containing AU-rich elements, such as mRNAs for protooncogenes, cytokines, and cytokine-response genes. Cytoplasmic HuR expression was associated with COX-2 expression in pulmonary squamous cell carcinomas. Thus, COX-2 could be a potential target of the mRNA-stabilizing activity of cytoplasmic HuR, resulting in COX-2 overexpression. Increased COX-2 expression is associated with active conversion of survivin from nuclear to cytoplasmic, and low expression of nuclear survivin, which contributes to the antiapoptotic effect and overproliferation of pulmonary squamous cell carcinomas (Kim et al., 2011). In another study, increased COX-2 expression occurred frequently in human lung cancers and specifically in adenocarcinomas (Hida et al., 1998). Scattered weak COX-2 reactivity was seen in normal airway epithelial cells, and markedly up-regulated COX-2 expression was detected in about one-third of atypical adenomatous hyperplasias and carcinoma in situ specimens, and a significant increase in COX-2 expression was observed in 70% of invasive adenocarcinoma cases (Hida et al., 1998).

COX-2 expression in bronchiolar epithelial cells was significantly lower in IPF and sarcoidosis than in controls. No significant difference was found in COX-2 expression between macrophages in IPF and control sections, but COX-2 was reduced in macrophages in sarcoidosis compared with controls (Petkova et al., 2003). Atypical alveolar epithelium, which associates with asbestosis and idiopathic fibrosing alveolitis and is considered to be a precursor lesion for lung cancer, expressed the COX-2 protein (Wolff et al., 1998). In the lung parenchyma of COPD patients, COX-2 mRNA levels were increased significantly compared with those of control subjects (Roca-Ferrer et al., 2011). COX-2 expression was examined in nasal biopsies from patients with allergic rhinitis (AR), seasonal AR (SAR), and perennial AR (PAR). No significant differences in the lamina propria in immunostaining for COX-2 were noted among groups (Westergren et al., 2009). A significant increase in the epithelial and submucosal cellular expression of COX-2 has been reported in asthmatic patients (Sousa et al., 1997). The 72-h kinetics of COX-2 mRNA expression was investigated in an ovalbumin-sensitized and ovalbumin-challenged guinea pig lung model. The sensitized animals showed a robust and transient induction of COX-2 mRNA expression within 1 h after ovalbumin challenge (Oguma et al., 2002). In a human CF bronchial epithelia cell line, increased COX-2 expression and overproduction of PGE₂ were noted (Chen et al., 2012).

EFFECTS OF COX-2 s-NSAIDs ON THE RESPIRATORY SYSTEM

Because of the role COX-2 plays in the pathophysiology of several pulmonary tumors, COX-2 s-NSAIDs have been proposed as potential therapeutic agents.

Lung tumor prevention with NSAIDs involves both the induction of apoptosis and the inhibition of COX-2 expression (Yao et al., 2000). COX-2 was characterized in several human epithelial cancers. COX-2 was detected in 85% of the hyperproliferating, dysplastic, and neoplastic epithelial cells and in the existing and angiogenic vasculature within and adjacent to hyperplastic/neoplastic lesions (Koki et al., 2002). This implied COX-2 may play an important role during premalignant hyperproliferation as well as the later stages of invasive carcinoma and metastasis in various human epithelial cancers (Koki et al., 2002). PGE₂ production by A549 non-small-cell lung cancer (NSCLC) cells was elevated up to 50-fold in response to IL-1 β . Reversal of IL-1 β -induced PGE₂ production in A549 cells was achieved by specific pharmacological or antisense oligonucleotide inhibition of COX-2 activity or expression. In contrast, specific COX-1 inhibition was not effective (Huang et al., 1998). The role of host-derived COX-1 and COX-2 in tumor growth was investigated using grafted Lewis lung carcinoma (LLC) cells into either wild-type (WT), COX-1^{-/-}, or COX-2^{-/-} C57BL/6 mice (Williams et al., 2000). LLC cells grown rapidly as solid tumors when implanted in C57BL/6 mice. Tumor growth was markedly attenuated in COX-2^{-/-} but not in COX-1^{-/-} or WT mice. Treatment of WT C57BL/6 mice bearing LLC tumors with celecoxib also reduced tumor growth. A decrease in vascular density was observed in tumors grown in COX-2^{-/-} mice compared with those in WT mice. In addition, COX-2^{-/-} mouse fibroblasts had a 94% reduction in their ability to produce the proangiogenic factor VEGF. Furthermore, treatment of WT mouse fibroblasts with the s-NSAID SC-58635 reduced VEGF production by 92% (Williams et al., 2000). Thus, inhibition of the COX-2/VEGF-dependent pathway is effective in tumor-associated angiogenesis, tumor growth, and metastasis (Yoshida et al., 2003).

Nimesulide inhibited proliferation of NSCLC cell lines *in vitro* in a dose-dependent manner, in part by inducing apoptosis even at clinically achievable low concentrations (Hida et al., 2000). In another experiment using NSCLC cell lines, celecoxib treatment decreased cell survival, activated caspase cascades, and increased DNA fragmentation. In addition, celecoxib treatment induced the expression of death receptors, particularly that of DR5. Thus, induction of apoptosis using celecoxib in human NSCLC is through the extrinsic death receptor pathway (Liu et al., 2004). The molecular effects of a derivative of celecoxib, 2,5-dimethylcelecoxib (DMC), on NSCLC cells were investigated. DMC sensitizes human NSCLC cells to tumor necrosis factor-related apoptosis-inducing ligand (TRAIL)-induced apoptosis via induction of DR5 and down-regulation of cellular FLICE-inhibitory protein (c-FLIP) (Chen et al., 2007). Rofecoxib, a COX-2 s-NSAID, significantly attenuated growth of murine Lewis lung carcinoma cells (3LL) *in vitro*. It caused considerable dose- and time-dependent inhibition of proliferation in cancerous cells and, similarly, induced dose-dependent apoptosis (Qadri et al., 2002). There is compelling experimental evidence that s-NSAIDs have potential for the chemoprevention of lung cancers. Molecular studies revealed that COX-2 overexpression is a prominent feature of premalignant and malignant neoplasms (Harris, 2009). Evidence is accumulating that carcinogenesis often evolves as a progressive series of highly specific cellular and molecular changes in response

to induction of constitutive overexpression of COX-2 and the PG cascade in the “inflammogenesis of cancer” (Harris, 2009). Lung adenocarcinoma cell line growth was inhibited *in vitro* by JTE-522, a COX-2 s-NSAID, as a single or adjunct agent of conventional anticancer drugs (e.g., docetaxel, vinorelbine). In addition, the combined use of JTE-522 with conventional anticancer drugs was shown to exhibit significant enhancement in treatment efficacy using an *in vivo* athymic nude mouse model with xenografted lung adenocarcinoma cells (Hida et al., 2002). NS-398, a COX-2 s-NSAID, inhibited tumor multiplicity and returned plasma PGE₂ to basal levels observed in untreated mice in a A/J female mouse model of lung tumorigenesis (Rioux and Castonguay, 1998).

The effects of COX-2 s-NSAID celecoxib or rofecoxib use on lung cancer were studied in a case–control study. Use of either drug for more than one year produced a significant reduction (60%) in the risk of lung cancer (Harris et al., 2007). The effects of celecoxib on lung cancer prevention were investigated in a randomized double-blind placebo-controlled trial (Mao et al., 2011). Former-smoker subjects (age ≥ 45 , ≥ 30 pack-years of smoking, ≥ 1 year of sustained abstinence from smoking) received celecoxib (400 mg by mouth twice daily). The impact of celecoxib on cellular and molecular events associated with lung cancer pathogenesis was assessed. The primary endpoint was the bronchial Ki-67 labeling index (Ki-67 LI) after six months of treatment. Decreased Ki-67 LI correlated with a reduction and/or resolution of lung nodules on computed tomography. Celecoxib significantly reduced plasma C-reactive protein and IL-6 mRNA and protein and increased 15(*S*)-hydroxyeicosatetraenoic acid levels in bronchoalveolar lavage samples (Mao et al., 2011). In another study, celecoxib decreased Ki-67 labeling by 3.85% in former smokers and by 1.10% in current smokers. This was a significantly greater reduction than that seen with placebo after adjusting for metaplasia and smoking status. Celecoxib (400 mg twice daily) was biologically active in the bronchial epithelium of current and former smokers (Kim et al., 2010). In a study of populations of patients with advanced NSCLC, the addition of celecoxib (400 mg twice daily) to docetaxel did not seem to improve the outcome compared with the single agent docetaxel (Gadgeel et al., 2008). However, in another study in patients with stage IIIb/IV NSCLC who had pathological confirmation and no prior chemotherapy, the effect of celecoxib was evaluated. Treatment consisted of docetaxel and carboplatin every 3 weeks for five cycles. Patients were randomly assigned to receive celecoxib 400 mg twice daily. It was found that in advanced NSCLC, celecoxib does not improve survival (Groen et al., 2011).

The role of COX-2 in pulmonary inflammation was investigated. Allergen-induced pulmonary inflammation and airway hyperresponsiveness were studied in WT mice and in COX-1^{-/-} and COX-2^{-/-} mice. After allergen exposure, immunized WT mice had mild pulmonary inflammation, mostly in the perivascular/peribronchial regions, characterized by the presence of lymphoid aggregates, focal areas of consolidation with mononuclear and polymorphonuclear leukocytes, occasional large eosinophilic alveolar macrophages, and rare multinucleated giant cells (Gavett et al., 1999). In contrast, lungs from allergic COX-1^{-/-} mice had severe inflammation that not only involved perivascular and peribronchial regions, but also extended into the airspace. Lymphoid aggregates were identifiable

around most blood vessels and bronchi and often involved the smallest vessels. Airway epithelium was thickened, alveoli contained large numbers of large eosinophilic macrophages and eosinophils, and multinucleated giant cells were numerous (Gavett et al., 1999). Lungs from allergic COX-2^{-/-} mice had pulmonary inflammation that was less intense than that in allergic COX-1^{-/-} mice but more severe than that in allergic WT mice. Compared with allergic COX-1^{-/-} mice, the inflammation observed in allergic COX-2^{-/-} mice was more focal and confined primarily to interstitial regions surrounding vessels and bronchi. Allergic COX-2^{-/-} mice showed loss of fine alveolar septae in comparison with allergic WT mice, and remaining septae were thickened. These alterations in parenchymal alveolar structure were comparable to those observed in allergic COX-1^{-/-} mice. Airway mucus production was more pronounced in allergic COX-1^{-/-} and COX-2^{-/-} mice than in allergic WT or nonimmunized mice of any genotype. Both allergic COX-1^{-/-} and COX-2^{-/-} mice exhibited decreased baseline respiratory system compliance, whereas only allergic COX-1^{-/-} mice showed increased baseline resistance and responsiveness to methacholine (Gavett et al., 1999). COX inhibition during allergic sensitization with ovalbumin in a murine model leads to an increase in type 2 cytokines (i.e., IL-5 and IL-13) (Peeble et al., 2002). In a BALB/c mouse model, COX inhibition with either a COX-1 (SC-58560) or a COX-2 (SC-58236) inhibitor during allergen sensitization augmented production of IL-13, increased lung eosinophilia, and increased airway hyperresponsiveness (Peeble et al., 2002). In this experiment, the mice were exposed to aerosols of 1% ovalbumin on days 14 through 21 for 40 min each day. Methacholine challenges were performed on day 22 (Peeble et al., 2002). In an experiment in ovalbumin-sensitized and ovalbumin-challenged male Hartley guinea pig model, the effects of NS-398 and JTE-522 administration on pulmonary allergic inflammation during airway challenge were investigated (Oguma et al., 2002). COX-2 s-NSAID treatment did not modify the enhanced airway responsiveness to histamine observed after allergen sensitization and challenge, but it did significantly reduce the number of eosinophils and neutrophils in bronchoalveolar lavage fluid (Oguma et al., 2002). In an experimental dog model of acute lung injury (ALI), the effects of SC-236, a COX-2 s-NSAID, on pulmonary perfusion pattern were evaluated. ALI was induced using oleic acid (OA), and SC-236 was given 50 min before OA. SC-236 prevented the loss of perfusion redistribution associated with endotoxin (Gust et al., 1999).

Treatment for 1 week with oral celecoxib (200 mg twice daily) did not affect bronchial responsiveness in asthmatic patients (Dicpinigaitis, 2001). Aspirin-exacerbated respiratory disease (AERD) is a distinct clinical entity that is characterized by aspirin-induced respiratory reactions, asthma, nasal polyposis, and chronic hyperplastic eosinophilic sinusitis (CHES) (Stevenson and Szczeklik, 2006). Etoricoxib was well tolerated, without any signs of immediate or delayed hypersensitivity in aspirin and NSAID-induced asthmatic patients (El Miedany et al., 2006). Rofecoxib (25 mg) was well tolerated and basal FEV1 remained unchanged during the period of observation in patients with aspirin-induced asthma (Micheletto et al., 2006).

EFFECTS OF ns-NSAIDs ON THE RESPIRATORY SYSTEM

The effects of indomethacin on endothelial dysfunction during lipopolysaccharide (LPS)-induced sepsis were investigated in an isolated rat lung model. Rats were administered intraperitoneally indomethacin at 5 or 10 mg/kg. Three hours later the rats were anesthetized, the lungs were isolated, and pulmonary vasoreactivity was assessed with bradykinin or receptor-independent hypoxic pulmonary vasoconstriction. Indomethacin significantly attenuated bradykinin-induced vasoconstriction in septic isolated rat lungs (Fischer et al., 2000). In an adult New Zealand white rabbit smoke inhalation model, the effect of ibuprofen on extravascular lung water accumulation was studied. Rabbits were anaesthetized and intubated, and each ibuprofen-treated animal received a dose of 50 mg/kg either intraperitoneally or intravenously. Peak carboxyhemoglobin levels as well as CO half-lives were not significantly different between ibuprofen-treated groups and the controls. However, ibuprofen treatment resulted in significantly decreased lung water. Thus, ibuprofen promoted an early reduction in lung water accumulation (Stewart et al., 1990). The effects of ibuprofen (35 mg/kg orally twice daily) on chronic *Pseudomonas* endobronchial infection and inflammation were investigated in a rat model. The area of lung inflammation 14 days after animal inoculation with *Pseudomonas* was significantly less in animals treated with ibuprofen than in animals given placebo. Ibuprofen did not increase the pulmonary burden of *Pseudomonas*, and the ibuprofen-treated infected animals gained weight better than did placebo-treated controls (Konstan et al., 1990). The postnatal pulmonary effects of diclofenac sodium were studied in the rat offspring treated with diclofenac sodium during pregnancy. Pregnant female rats were given diclofenac sodium at 1 mg/kg, which was injected intraperitoneally during gestational days 5 to 19. Histopathological examination of the lung tissues of 4- and 20-week-old rats revealed no significant differences between males and females in both the control and diclofenac sodium-treated rats (Ragbetli et al., 2011).

Ingestion of aspirin can result in a spectrum of upper and/or lower respiratory reactions, to include rhinitis, conjunctivitis, laryngospasm, and bronchospasm (Lee and Stevenson, 2011). Aspirin and other ns-NSAIDs that inhibit COX-1 induce unique nonallergic reactions, consisting of attacks of rhinitis and asthma. These hypersensitivity reactions occur in a subset of asthmatic subjects (Stevenson and Szczeklik, 2006). Samter and Beers first described a clinical syndrome known as Samter's triad, which includes asthma, aspirin sensitivity, and nasal polyps (Zeitzi, 1988). Symptoms can occur within minutes to hours after aspirin ingestion and include angioedema, facial flushing, and conjunctivitis. Aspirin- and ns-NSAID-induced bronchospasm has been reported (Lee and Stevenson, 2011; Sun and Pei, 2011). Aspirin-exacerbated respiratory disease (AERD) is a clinical tetrad of nasal polyps, chronic hypertrophic eosinophilic sinusitis, asthma, and sensitivity to aspirin and other NSAIDs (Lee and Stevenson, 2011). AERD has been described as Samter's triad. AERD affects 0.3 to 0.9% of the general population, but the prevalence rises to 10 to 20% of asthmatics and up to 30 to 40% in those asthmatics with

nasal polyposis (Lee and Stevenson, 2011). AERD is more commonly reported in females. Nasal ketorolac administration has been shown to be a reasonably accurate and safe method for diagnosing AERD (White et al., 2006). Alteration in the function of PGE₂ receptors (particularly EP₂) might contribute to the inability of PGE₂ to sustain the blockade. From mast cells, PGD₂ is oversynthesized, and histamine and tryptase are released during reactions (Stevenson and Szczeklik, 2006). Short term treatment with ibuprofen reduced PGE₂ concentrations in EBC in patients with COPD (Montuschi et al., 2005). Ibuprofen decreased exhaled PGE₂ concentrations in patients with stable COPD (Montuschi et al., 2001).

Although this is not an approved indication, ibuprofen has been shown in some clinical trials to slow progression of lung disease in patients with cystic fibrosis (CF), particularly in children and adolescents with mild to moderate disease. The use of ibuprofen in over 1000 children followed by the CF Foundation Patient Registry supported the finding that ibuprofen therapy slowed disease progression as measured by forced expiratory volume (FEV₁) (Konstan et al., 2007). In a two-year multicenter double-blind placebo-controlled trial conducted in 12 Canadian centers, a total of 142 patients age 6 to 18 years with mild CF disease were randomized to receive high-dose ibuprofen (20 to 30 mg/kg twice daily, adjusted to a peak serum concentration of 50 to 100 µg/mL). Those patients in the high-dose ibuprofen group exhibited a significant reduction in the rate of decline of forced vital capacity percent predicted, but not forced expiratory volume in 1 min % (Lands et al., 2007). In a retrospective study, pulmonary function decline and hospitalization rates were compared among 51 children and adolescents treated with ibuprofen versus 39 untreated patients. The medical records of all patients, ages 5 to 18 years, were followed at the CF center from 1995 to 2002. Pulmonary function decline and hospitalization rates for each group were compared, examining both intent to treat and patients who continued therapy for at least four years. No differences in either outcome measure were observed in the intent-to-treat group or those who completed at least four years of therapy. Neither use of high-dose ibuprofen nor its cessation resulted in a significant change in the rate of decline in pulmonary function or influenced hospitalization rates. Matching based on age, gender, pancreatic sufficiency status, pretreatment FEV₁, and *Pseudomonas* status failed to show differences in FEV₁ decline between the treated and untreated groups. A confounding factor in this retrospective study was the high and disproportionate use of systemic corticosteroids among these patients (Fennell et al., 2007).

CONCLUSIONS

There are important anatomical and physiological interspecies differences in the respiratory system that can affect the pathophysiological effects noted after COX inhibition. The normal ontogeny of COX-1 and COX-2 expression varies across species during pulmonary development and in pathological conditions that affect the lung. In experimental nonclinical studies, NSAIDs have shown some potential for the chemoprevention of some lung cancers.

REFERENCES

- Abraham E, Baughman R, Fletcher E, Heard S, et al. Liposomal prostaglandin E1 (TLC C-53) in acute respiratory distress syndrome: a controlled, randomized, double-blind, multicenter clinical trial. TLC C-53 ARDS Study Group. *Crit Care Med* 1999;27:1478–1485.
- Acarregui MJ, Snyder JM, Mitchell MD, Mendelson CR. Prostaglandins regulate surfactant protein A (SP-A) gene expression in human fetal lung in vitro. *Endocrinology* 1990;127:1105–1113.
- Ackermann MR, Derscheid R, Roth JA. Innate immunology of bovine respiratory disease. *Vet Clin North Am Food Anim Pract* 2010;26:215–228.
- Adawi A, Zhang Y, Baggs R, Finkelstein J, et al. Disruption of the CD40–CD40 ligand system prevents an oxygen-induced respiratory distress syndrome. *Am J Pathol* 1998;152:651–657.
- Arias-Diaz J, Vara E, Garcia C, Balibrea JL. Tumor necrosis factor-alpha-induced inhibition of phosphatidylcholine synthesis by human type II pneumocytes is partially mediated by prostaglandins. *J Clin Invest* 1994;94:244–250.
- Asano K, Lilly CM, Drazen JM. Prostaglandin G/H synthase-2 is the constitutive and dominant isoform in cultured human lung epithelial cells. *Am J Physiol* 1996;271:L126–L131.
- Bartz H, Buning-Pfaue F, Turkel O, Schauer U. Respiratory syncytial virus induces prostaglandin E2, IL-10 and IL-11 generation in antigen presenting cells. *Clin Exp Immunol* 2002;129:438–445.
- Bastacky J, Lee CY, Goerke J, Koushafar H, et al. Alveolar lining layer is thin and continuous: low-temperature scanning electron microscopy of rat lung. *J Appl Physiol* 1995;79:1615–1628.
- Bauer AK, Dwyer-Nield LD, Malkinson AM. High cyclooxygenase 1 (COX-1) and cyclooxygenase 2 (COX-2) contents in mouse lung tumors. *Carcinogenesis* 2000;21:543–550.
- Bennett BL, Garofalo RP, Cron SG, Hosakote YM, et al. Immunopathogenesis of respiratory syncytial virus bronchiolitis. *J Infect Dis* 2007;195:1532–1540.
- Bonnans C, Fukunaga K, Levy MA, Levy BD. Lipoxin A4 regulates bronchial epithelial cell responses to acid injury. *Am J Pathol* 2006;168:1064–1072.
- Bonville CA, Rosenberg HF, Domachowski JB. Macrophage inflammatory protein-1alpha and RANTES are present in nasal secretions during ongoing upper respiratory tract infection. *Pediatr Allergy Immunol* 1999;10:39–44.
- Bozyk PD, Moore BB. Prostaglandin E2 and the pathogenesis of pulmonary fibrosis. *Am J Respir Cell Mol Biol* 2011;45:445–452.
- Brain JD, Molina RM, DeCamp MM, Warner AE. Pulmonary intravascular macrophages: their contribution to the mononuclear phagocyte system in 13 species. *Am J Physiol* 1999;276:L146–L154.
- Brannon TS, North AJ, Wells LB, Shaul PW. Prostacyclin synthesis in ovine pulmonary artery is developmentally regulated by changes in cyclooxygenase-1 gene expression. *J Clin Invest* 1994;93:2230–2235.
- Brannon TS, MacRitchie AN, Jaramillo MA, Sherman TS, et al. Ontogeny of cyclooxygenase-1 and cyclooxygenase-2 gene expression in ovine lung. *Am J Physiol* 1998;274:L66–L71.
- Bryan DL, Hart P, Forsyth K, Gibson R. Modulation of respiratory syncytial virus-induced prostaglandin E2 production by n-3 long-chain polyunsaturated fatty acids in human respiratory epithelium. *Lipids* 2005;40:1007–1011.
- Buckley J, Birrell MA, Maher SA, Nials AT, et al. EP4 receptor as a new target for bronchodilator therapy. *Thorax* 2011;66:1029–1035.
- Chen J, Jiang XH, Chen H, Guo JH, et al. CFTR negatively regulates cyclooxygenase-2- PGE(2) positive feedback loop in inflammation. *J Cell Physiol* 2012;227:2759–2766.
- Chen S, Liu X, Yue P, Schönthal AH, et al. CCAAT/enhancer binding protein homologous protein-dependent death receptor 5 induction and ubiquitin/proteasome-mediated cellular FLICE-inhibitory protein down-regulation contribute to enhancement of tumor necrosis factor-related apoptosis-inducing ligand-induced apoptosis by dimethyl-celecoxib in human non small-cell lung cancer cells. *Mol Pharmacol* 2007;72:1269–1279.
- Chen ZT, Li SL, Cai EQ, Wu WL, et al. LPS induces pulmonary intravascular macrophages producing inflammatory mediators via activating NF-kappaB. *J Cell Biochem* 2003;89:1206–1214.
- Cutlip RC, Lehmkuhl HD. Lesions in lambs experimentally infected with bovine respiratory syncytial virus. *Am J Vet Res* 1979;40:1479–1482.

- Dahlem P, van Aalderen WM, de Neef M, Dijkgraaf MG, et al. Randomized controlled trial of aerosolized prostacyclin therapy in children with acute lung injury. *Crit Care Med* 2004;32:1055–1060.
- Davi G, Basili S, Vieri M, Cipollone F, et al. Enhanced thromboxane biosynthesis in patients with chronic obstructive pulmonary disease. The Chronic Obstructive Bronchitis and Haemostasis Study Group. *Am J Respir Crit Care Med* 1997;156:1794–1799.
- Dehring DJ, Wismar BL. Intravascular macrophages in pulmonary capillaries of humans. *Am Rev Respir Dis* 1989;139:1027–1029.
- Demoly P, Jaffuel D, Lequeux N, Weksler B, et al. Prostaglandin H synthase 1 and 2 immunoreactivities in the bronchial mucosa of asthmatics. *Am J Respir Crit Care Med* 1997;155:670–675.
- Devalia JL, Davies RJ. Airway epithelial cells and mediators of inflammation. *Respir Med* 1993;87:405–408.
- Dicpinigaitis PV. Effect of the cyclooxygenase-2 inhibitor celecoxib on bronchial responsiveness and cough reflex sensitivity in asthmatics. *Pulm Pharmacol Ther* 2001;14:93–97.
- El Miedany Y, Youssef S, Ahmed I, El Gaafary M. Safety of etoricoxib, a specific cyclooxygenase-2 inhibitor, in asthmatic patients with aspirin-exacerbated respiratory disease. *Ann Allergy Asthma Immunol* 2006;97:105–109.
- Ermert L, Ermert M, Goppelt-Struebe M, Walrath D, et al. Cyclooxygenase isoenzyme localization and mRNA expression in rat lungs. *Am J Respir Cell Mol Biol* 1998;18:479–488.
- Ermert L, Dierkes C, Ermert M. Immunohistochemical expression of cyclooxygenase isoenzymes and downstream enzymes in human lung tumors. *Clin Cancer Res* 2003;9:1604–1610.
- Fedderson CO, Mathias MM, McMurtry IF, Voelkel NF. Acetylcholine induces vasodilation and prostacyclin synthesis in rat lungs. *Prostaglandins* 1986a;31:973–987.
- Fedderson CO, McMurtry IF, Henson P, Voelkel NF. Acetylcholine-induced pulmonary vasodilation in lung vascular injury. *Am Rev Respir Dis* 1986b;133:197–204.
- Fedderson CO, Chang S, Czartalomna J, Voelkel NF. Arachidonic acid causes cyclooxygenase-dependent and -independent pulmonary vasodilation. *J Appl Physiol* 1990;68:1799–1808.
- Fennell PB, Quante J, Wilson K, Boyle M, et al. Use of high-dose ibuprofen in a pediatric cystic fibrosis center. *J Cyst Fibros* 2007;6:153–158.
- Ferrantino M, White RJ. Inhaled treprostinil sodium for the treatment of pulmonary arterial hypertension. *Expert Opin Pharmacother* 2011;12:2583–2593.
- Fischer LG, Hollmann MW, Horstman DJ, Rich GF. Cyclooxygenase inhibitors attenuate bradykinin-induced vasoconstriction in septic isolated rat lungs. *Anesth Analg* 2000;90:625–631.
- Fukunaga K, Kohli P, Bonnans C, Fredenburgh LE, et al. Cyclooxygenase 2 plays a pivotal role in the resolution of acute lung injury. *J Immunol* 2005;174:5033–5039.
- Fulkerson WJ, MacIntyre N, Stamler J, Crapo JD. Pathogenesis and treatment of the adult respiratory distress syndrome. *Arch Intern Med* 1996;156:29–38.
- Gadgeel SM, Wozniak A, Ruckdeschel JC, Heilbrun LK, et al. Phase II study of docetaxel and celecoxib, a cyclooxygenase-2 inhibitor, in elderly or poor performance status (PS2) patients with advanced non-small cell lung cancer. *J Thorac Oncol* 2008;3:1293–1300.
- Gauvreau GM, Watson RM, O'Byrne PM. Protective effects of inhaled PGE2 on allergen-induced airway responses and airway inflammation. *Am J Respir Crit Care Med* 1999;159:31–36.
- Gavett SH, Madison SL, Chulada PC, Scarborough PE, et al. Allergic lung responses are increased in prostaglandin H synthase-deficient mice. *J Clin Invest* 1999;104:721–732.
- Gershwin LJ, Giri SN, Stewart RS, Chen J. Prostaglandin and thromboxane concentrations in plasma and lung lavage fluids during sequential infection of vaccinated and nonvaccinated calves with bovine respiratory syncytial virus. *Am J Vet Res* 1989;50:1254–1262.
- Gessler T, Seeger W, Schmehl T. The potential for inhaled treprostinil in the treatment of pulmonary arterial hypertension. *Ther Adv Respir Dis* 2011;5:195–206.
- Graham BS, Rutigliano JA, Johnson TR. Respiratory syncytial virus immunobiology and pathogenesis. *Virology* 2002;297:1–7.
- Groen HJ, Sietsma H, Vincent A, Hochstenbag MM, et al. Randomized, placebo-controlled phase III study of docetaxel plus carboplatin with celecoxib and cyclooxygenase-2 expression as a biomarker for patients with advanced non-small-cell lung cancer: the NVALT-4 study. *J Clin Oncol* 2011;29:4320–4326.

- Grubor B, Gallup JM, Meyerholz DK, Crouch E, et al. Enhanced surfactant protein and defensin mRNA levels and reduced viral replication during paramyxoviral pneumonia in neonatal lambs. *Clin Diag Lab Immunol* 2004;11:599–607.
- Gryglewski RJ. The lung as a generator of prostacyclin. *Ciba Found Symp* 1980;78:147–164.
- Gust R, Kozlowski JK, Stephenson AH, Schuster DP. Role of cyclooxygenase-2 in oleic acid–induced acute lung injury. *Am J Respir Crit Care Med* 1999;160:1165–1170.
- Habler O, Kleen M, Zwissler B, Pusch R, et al. Inhalation of prostacyclin (PGI₂) for 8 hours does not produce signs of acute pulmonary toxicity in healthy lambs. *Intensive Care Med* 1996;22:426–433.
- Hall CB. Respiratory syncytial virus and parainfluenza virus. *N Engl J Med* 2001;344:1917–1928.
- Hammad H, Kool M, Soullié T, Narumiya S, et al. Activation of the D prostanoid 1 receptor suppresses asthma by modulation of lung dendritic cell function and induction of regulatory T cells. *J Exp Med* 2007;204:357–367.
- Harrington LS, Lucas R, McMaster SK, Moreno L, et al. COX-1, and not COX-2 activity, regulates airway function: relevance to aspirin-sensitive asthma. *FASEB J* 2008;22:4005–4010.
- Harris RE. Cyclooxygenase-2 (COX-2) blockade in the chemoprevention of cancers of the colon, breast, prostate, and lung. *Inflammopharmacology* 2009;17:55–67.
- Harris RE, Beebe-Donk J, Alshafie GA. Reduced risk of human lung cancer by selective cyclooxygenase 2 (COX-2) blockade: results of a case–control study. *Int J Biol Sci* 2007;3:328–334.
- Haschek WM, Rousseaux CG, Wallig MA (editors). Chapter 6: Respiratory system. In: *Fundamentals of Toxicologic Pathology*. Elsevier Science Publishing Inc. 2009, pp. 93–133.
- Hasturk S, Kemp B, Kalapurakal SK, Kurie JM, et al. Expression of cyclooxygenase-1 and cyclooxygenase-2 in bronchial epithelium and nonsmall cell lung carcinoma. *Cancer* 2002;94:1023–1031.
- Hempel SL, Monick MM, Hunninghake GW. Lipopolysaccharide induces prostaglandin H synthase-2 protein and mRNA in human alveolar macrophages and blood monocytes. *J Clin Invest* 1994;93:391–396.
- Herrerias A, Torres R, Serra M, Marco A, et al. Subcutaneous prostaglandin E₂ restrains airway mast cell activity in vivo and reduces lung eosinophilia and Th₂ cytokine overproduction in house dust mite–sensitive mice. *Int Arch Allergy Immunol* 2009;149:323–332.
- Hida T, Yatabe Y, Achiwa H, Muramatsu H, et al. Increased expression of cyclooxygenase 2 occurs frequently in human lung cancers, specifically in adenocarcinomas. *Cancer Res* 1998;58:3761–3764.
- Hida T, Kozaki K, Muramatsu H, Masuda A, et al. Cyclooxygenase-2 inhibitor induces apoptosis and enhances cytotoxicity of various anticancer agents in non-small cell lung cancer cell lines. *Clin Cancer Res* 2000;6:2006–2011.
- Hida T, Kozaki K, Ito H, Miyaishi O, et al. Significant growth inhibition of human lung cancer cells both in vitro and in vivo by the combined use of a selective cyclooxygenase 2 inhibitor, JTE-522, and conventional anticancer agents. *Clin Cancer Res* 2002;8:2443–2447.
- Higashi A, Higashi N, Tsuburai T, Takeuchi Y, et al. Involvement of eicosanoids and surfactant protein D in extrinsic allergic alveolitis. *Eur Respir J* 2005;26:1069–1073.
- Holgate ST. The sentinel role of the airway epithelium in asthma pathogenesis. *Immunol Rev* 2011;242:205–219.
- Holgate ST, Roberts G, Arshad HS, Howarth PH, et al. The role of the airway epithelium and its interaction with environmental factors in asthma pathogenesis. *Proc Am Thorac Soc* 2009;6:655–659.
- Holtzman MJ. Arachidonic acid metabolism: implications of biological chemistry for lung function and disease. *Am Rev Respir Dis* 1991;143:188–203.
- Hornsleth A, Loland L, Larsen LB. Cytokines and chemokines in respiratory secretion and severity of disease in infants with respiratory syncytial virus (RSV) infection: cytokines and chemokines in respiratory secretion and severity of disease in infants with respiratory syncytial virus (RSV) infection. *J Clin Virol* 2001;21:163–170.
- Huang M, Stolina M, Sharma S, Mao JT, et al. Non-small cell lung cancer cyclooxygenase-2-dependent regulation of cytokine balance in lymphocytes and macrophages: up-regulation of interleukin 10 and down-regulation of interleukin 12 production. *Cancer Res* 1998;58:1208–1226.
- Huang SK, Fisher AS, Scruggs AM, White ES, et al. Hypermethylation of PTGER2 confers prostaglandin E₂ resistance in fibrotic fibroblasts from humans and mice. *Am J Pathol* 2010;177:2245–2255.

- Izuhara K, Ohta S, Shiraishi H, Suzuki S, et al. The mechanism of mucus production in bronchial asthma. *Curr Med Chem* 2009;16:2867–2875.
- Jackson BA, Goldstein RH, Roy R, Cozzani M, et al. Effects of transforming growth factor beta and interleukin-1 beta on expression of cyclooxygenase 1 and 2 and phospholipase A2 mRNA in lung fibroblasts and endothelial cells in culture. *Biochem Biophys Res Commun* 1993;197:1465–1474.
- Johnson JE, Gonzales RA, Olson SJ, Wright PF, et al. The histopathology of fatal untreated human respiratory syncytial virus infection. *Mod Pathol* 2007;20:108–119.
- Johnson MD, Bao HF, Helms MN, Chen XJ, et al. Functional ion channels in pulmonary alveolar type I cells support a role for type I cells in lung ion transport. *Proc Natl Acad Sci USA* 2006;103:4964–4969.
- Keerthisingam CB, Jenkins RG, Harrison NK, Hernandez-Rodriguez NA, et al. Cyclooxygenase-2 deficiency results in a loss of the anti-proliferative response to transforming growth factor-beta in human fibrotic lung fibroblasts and promotes bleomycin-induced pulmonary fibrosis in mice. *Am J Pathol* 2001;158:1411–1422.
- Khan KN, Stanfield K, Trajkovic D, Harris RK. Cyclooxygenase-2 expression in inflammatory lung lesions of nonhuman primates. *Vet Pathol* 2000;37:512–516.
- Kim ES, Hong WK, Lee JJ, Mao L, et al. Biological activity of celecoxib in the bronchial epithelium of current and former smokers. *Cancer Prev Res (Phila)* 2010;3:148–159.
- Kim GY, Lim SJ, Kim YW. Expression of HuR, COX-2, and survivin in lung cancers; cytoplasmic HuR stabilizes cyclooxygenase-2 in squamous cell carcinomas. *Mod Pathol* 2011;24:1336–1347.
- Koki AT, Khan NK, Woerner BM, Seibert K, et al. Characterization of cyclooxygenase-2 (COX-2) during tumorigenesis in human epithelial cancers: evidence for potential clinical utility of COX-2 inhibitors in epithelial cancers. *Prostaglandins Leukot Essent Fatty Acids* 2002;66:13–18.
- Konstan MW, Vargo KM, Davis PB. Ibuprofen attenuates the inflammatory response to *Pseudomonas aeruginosa* in a rat model of chronic pulmonary infection: implications for antiinflammatory therapy in cystic fibrosis. *Am Rev Respir Dis* 1990;141:186–192.
- Konstan MW, Schluchter MD, Xue W, Davis PB. Clinical use of ibuprofen is associated with slower FEV₁ decline in children with cystic fibrosis. *Am J Respir Crit Care Med* 2007;176:1084–1089.
- Lands LC, Milner R, Cantin AM, Manson D, et al. High-dose ibuprofen in cystic fibrosis: Canadian safety and effectiveness trial. *J Pediatr* 2007;151:249–254.
- Lassus P, Wolff H, Andersson S. Cyclooxygenase-2 in human perinatal lung. *Pediatr Res* 2000;47:602–605.
- Lee RU, Stevenson DD. Aspirin-exacerbated respiratory disease: evaluation and management. *Allergy Asthma Immunol Res* 2011;3:3–10.
- Lehmkuhl HD, Cutlip RC. Experimental parainfluenza type 3 infection in young lambs: clinical, microbiological, and serological response. *Vet Microbiol* 1983;8:437–442.
- Liu T, Zaman W, Kaphalia BS, Ansari GA, et al. RSV-induced prostaglandin E2 production occurs via cPLA2 activation: role in viral replication. *Virology* 2005;343:12–24.
- Liu X, Yue P, Zhou Z, Khuri FR, et al. Death receptor regulation and celecoxib-induced apoptosis in human lung cancer cells. *J Natl Cancer Inst* 2004;96:1769–1780.
- Longworth KE. The comparative biology of pulmonary intravascular macrophages. *Front Biosci* 1997;2:d232–d241.
- Maher SA, Birrell MA, Belvisi MG. Prostaglandin E2 mediates cough via the EP3 receptor: implications for future disease therapy. *Am J Respir Crit Care Med* 2009;180:923–928.
- Maher TM, Evans IC, Bottoms SE, Mercer PF, et al. Diminished prostaglandin E2 contributes to the apoptosis paradox in idiopathic pulmonary fibrosis. *Am J Respir Crit Care Med* 2010;182:73–82.
- Mao JT, Roth MD, Fishbein MC, Aberle DR, et al. Lung cancer chemoprevention with celecoxib in former smokers. *Cancer Prev Res (Phila)* 2011;4:984–993.
- Masferrer JL, Koki A, Seibert K. COX-2 inhibitors: a new class of antiangiogenic agents. *Ann NY Acad Sci* 1999;889:84–86.
- Massaro GD, Massaro D. Formation of pulmonary alveoli and gas-exchange surface area: quantitation and regulation. *Annu Rev Physiol* 1996;58:73–92.
- Mathé AA, Hedqvist P. Effect of prostaglandins F2 alpha and E2 on airway conductance in healthy subjects and asthmatic patients. *Am Rev Respir Dis* 1975;111:313–320.

- Matsuoka T, Hirata H, Tanaka Y, Takahashi Y, et al. Prostaglandin D2 as a mediator of allergic asthma. *Science* 2000;287:2013–2017.
- Mead J. Mechanical properties of lungs. *Physiol Rev* 1961;41:281–330.
- Mendelson CR, Acarregui MJ, Odom MJ, Boggaram V. Developmental and hormonal regulation of surfactant protein A (SP-A) gene expression in fetal lung. *J Dev Physiol* 1991;15:61–69.
- Meyerholz DK, Grubor B, Fach SJ, Sacco RE, et al. Reduced clearance of respiratory syncytial virus in a preterm lamb model. *Microbes Infect* 2004;6:1312–1319.
- Micheletto C, Tognella S, Guerriero M, Dal Negro R. Nasal and bronchial tolerability of Rofecoxib in patients with aspirin induced asthma. *Eur Ann Allergy Clin Immunol* 2006;38:10–14.
- Mitchell JA, Belvisi MG, Akarasereonot P, Robbins RA, et al. Induction of cyclo-oxygenase-2 by cytokines in human pulmonary epithelial cells: regulation by dexamethasone. *Br J Pharmacol* 1994;113:1008–1014.
- Montuschi P, Barnes PJ. Exhaled leukotrienes and prostaglandins in asthma. *J Allergy Clin Immunol* 2002;109:615–620.
- Montuschi P, Ciabattini G, Kharitonov SA, et al. Non selective cyclo-oxygenase inhibition decreases exhaled prostaglandin E₂ in patients with chronic obstructive pulmonary disease. *Am J Respir Crit Care Med* 2001;163:A908.
- Montuschi P, Kharitonov SA, Ciabattini G, Barnes PJ. Exhaled leukotrienes and prostaglandins in COPD. *Thorax* 2003;58:585–588.
- Montuschi P, Macagno F, Parente P, Valente S, et al. Effects of cyclo-oxygenase inhibition on exhaled eicosanoids in patients with COPD. *Thorax* 2005;60:827–833.
- Mulugeta S, Beers MF. Surfactant protein C: its unique properties and emerging immunomodulatory role in the lung. *Microbes Infect* 2006;8:2317–2323.
- Murugan V, Peck MJ. Signal transduction pathways linking the activation of alveolar macrophages with the recruitment of neutrophils to lungs in chronic obstructive pulmonary disease. *Exp Lung Res* 2009;35:439–485.
- Oguma T, Asano K, Shiomi T, Fukunaga K, et al. Cyclooxygenase-2 expression during allergic inflammation in guinea-pig lungs. *Am J Respir Crit Care Med* 2002;165:382–386.
- Oyarzun MJ, Clements JA. Control of lung surfactant by ventilation, adrenergic mediators, and prostaglandins in the rabbit. *Am Rev Respir Dis* 1978;117:879–891.
- Pace-Asciak CR. Prostaglandin biosynthesis and catabolism in the developing fetal sheep lung. *Prostaglandins* 1977;13:649–660.
- Pavord ID, Tattersfield AE. Bronchoprotective role for endogenous prostaglandin E₂. *Lancet* 1995;345:436–438.
- Pavord ID, Wong CS, Williams J, Tattersfield AE. Effect of inhaled prostaglandin E₂ on allergen-induced asthma. *Am Rev Respir Dis* 1993;148:87–90.
- Peebles RS Jr, Hashimoto K, Morrow JD, Dworski R, et al. Selective cyclooxygenase-1 and -2 inhibitors each increase allergic inflammation and airway hyperresponsiveness in mice. *Am J Respir Crit Care Med* 2002;165:1154–1160.
- Petkova DK, Clelland CA, Ronan JE, Lewis S, Knox AJ. Reduced expression of cyclooxygenase (COX) in idiopathic pulmonary fibrosis and sarcoidosis. *Histopathology* 2003;43:381–386.
- Plopper CG, Mariassy AT, Hill LH. Ultrastructure of the nonciliated bronchiolar epithelial (Clara) cell of mammalian lung: I. A comparison of rabbit, guinea pig, rat, hamster, and mouse. *Exp Lung Res* 1980;1:139–154.
- Powell WS, Solomon S. Biosynthesis of prostaglandins and thromboxane B₂ by fetal lung homogenates. *Prostaglandins* 1978;15:351–364.
- Profita M, Sala A, Bonanno A, Riccobono I, et al. Increased prostaglandin E₂ concentrations and cyclooxygenase-2 expression in asthmatic subjects with sputum eosinophilia. *J Allergy Clin Immunol* 2003;112:709–716.
- Qadri SS, Wang JH, Redmond KC, O'Donnell AF, et al. The role of COX-2 inhibitors in lung cancer. *Ann Thorac Surg* 2002;74:1648–1652.
- Radi ZA. Pathophysiology of cyclooxygenase inhibition in animal models. *Toxicol Pathol* 2009;37:34–46.
- Radi ZA, Ackermann MR. Ontogeny of pulmonary cyclooxygenase-1 (COX-1) and -2 (COX-2). *Pathophysiology* 2011;18:215–219.

- Radi ZA, Ostroski O, Pulmonary and cardiorenal cyclooxygenase-1 (COX- 1), -2 (COX-2), and microsomal prostaglandin E synthase-1 (mPGES-1) and -2 (mPGES-2) expression in a hypertension model. *Mediators Inflamm* 2007;2007:85091.
- Radi ZA, Meyerholz DK, Ackermann MR. Pulmonary cyclooxygenase-1 (COX-1) and -2 (COX-2) cellular expression and distribution following respiratory syncytial virus and parainfluenza virus infection. *Viral Immunol* 2010;23:43–48.
- Ragbetli C, Ilhan F, Aydinlioğlu A, Kara M, et al. A histological investigation concerning the effects of diclofenac sodium to the lung in 4- and 20-week-old rats treated prenatally. *J Matern Fetal Neonatal Med* 2011;24:208–212.
- Rangel Moreno J, Estrada García I, De La Luz García Hernández M, et al. The role of prostaglandin E2 in the immunopathogenesis of experimental pulmonary tuberculosis. *Immunology* 2002;106:257–266.
- Richardson JY, Ottolini MG, Pletneva L, et al. Respiratory syncytial virus (RSV) infection induces cyclooxygenase 2: a potential target for RSV therapy. *J Immunol* 2005;174:4356–4364.
- Rioux N, Castonguay A. Prevention of NNK-induced lung tumorigenesis in A/J mice by acetylsalicylic acid and NS-398. *Cancer Res* 1998;58:5354–5360.
- Roca-Ferrer J, Pujols L, Agusti C, Xaubet A, et al. Cyclooxygenase-2 levels are increased in the lung tissue and bronchial tumors of patients with chronic obstructive pulmonary disease. *Arch Bronconeumol* 2011;47:584–589.
- Rolin S, Masereel B, Dogne JM. Prostanoids as pharmacological targets in COPD and asthma. *Eur J Pharmacol* 2006;533:89–100.
- Russell JA, Ronco JJ, Dodek PM. Physiologic effects and side effects of prostaglandin E1 in the adult respiratory distress syndrome. *Chest* 1990;97:684–692.
- Sakata D, Yao C, Narumiya S. Emerging roles of prostanoids in T cell-mediated immunity. *IUBMB Life* 2010;62:591–596.
- Schmidt LM, Belvisi MG, Bode KA, Bauer J, et al. Bronchial epithelial cell-derived prostaglandin E2 dampens the reactivity of dendritic cells. *J Immunol* 2011;186:2095–2105.
- Schmitz T, Cox LA, Li C, Levine BA, et al. Prostaglandin E2 receptor expression in fetal baboon lung at 0.7 gestation after betamethasone exposure. *Pediatr Res* 2007;61:421–426.
- Seibert K, Zhang Y, Leahy K, Hauser S, et al. Pharmacological and biochemical demonstration of the role of cyclooxygenase 2 in inflammation and pain. *Proc Natl Acad Sci USA* 1994;91:12013–12017.
- Seymour ML, Gilby N, Bardin PG, et al. Rhinovirus infection increases 5-lipoxygenase and cyclooxygenase-2 in bronchial biopsy specimens from nonatopic subjects. *J Infect Dis* 2002;185:540–544.
- Shi J, Misso NL, Duffy DL, Bradley B, et al. Cyclooxygenase-1 gene polymorphisms in patients with different asthma phenotypes and atopy. *Eur Respir J* 2005;26:249–256.
- Shiraishi Y, Shiraishi Y, Asano K, Nakajima T, et al. Prostaglandin D2-induced eosinophilic airway inflammation is mediated by CRTH2 receptor. *J Pharmacol Exp Ther* 2005;312:954–960.
- Shoemaker WC, Appel PL. Effects of prostaglandin E1 in adult respiratory distress syndrome. *Surgery* 1986;99:275–283.
- Soslow RA, Dannenberg AJ, Rush D, Woerner BM, et al. COX-2 is expressed in human pulmonary, colonic, and mammary tumors. *Cancer* 2000;89:2637–2645.
- Sousa A, Pfister R, Christie PE, Lane SJ, et al. Enhanced expression of cyclooxygenase isoenzyme 2 (COX-2) in asthmatic airways and its cellular distribution in aspirin-sensitive asthma. *Thorax* 1997;52:940–945.
- Stapleton PP, Strong VE, Freeman TA, Winter J, et al. Gender affects macrophage cytokine and prostaglandin E2 production and PGE2 receptor expression after trauma. *J Surg Res* 2004;122:1–127.
- Steer SA, Corbett JA. The role and regulation of COX-2 during viral infection. *Viral Immunol* 2003;16:447–460.
- Stevenson DD, Szczeklik A. Clinical and pathologic perspectives on aspirin sensitivity and asthma. *J Allergy Clin Immunol* 2006;118:773–786.
- Stewart RJ, Yamaguchi KT, Knost PM, Mason SW, et al. Effects of ibuprofen on pulmonary oedema in an animal smoke inhalation model. *Burns* 1990;16:409–413.

- Stumm CL, Wettlaufer SH, Jancar S, Peters-Golden M. Airway remodeling in murine asthma correlates with a defect in PGE2 synthesis by lung fibroblasts. *Am J Physiol Lung Cell Mol Physiol* 2011;301:L636–L644.
- Sun W, Pei L. Flurbiprofen axetil, nasal polyps, and status asthmaticus: an unusual case report. *J Asthma* 2011;48:647–649.
- Sznajder Y, Westcott JY, Wenzel SE, Mazer B, et al. Airway eicosanoids in acute severe respiratory syncytial virus bronchiolitis. *J Pediatr* 2004;145:115–118.
- Taha R, Olivenstein R, Utsumi T, Ernst P, et al. Prostaglandin H synthase 2 expression in airway cells from patients with asthma and chronic obstructive pulmonary disease. *Am J Respir Crit Care Med* 2000;161:636–640.
- Tai HH, Yuan B, Wu AT. Transformation of arachidonate into 6-oxoprostaglandin F1 alpha, thromboxane B2 and prostaglandin E2 by sheep lung microsomal fraction. *Biochem J* 1978;170:441–444.
- Takizawa H. Airway epithelial cells as regulators of airway inflammation. *Int J Mol Med* 1998;1:367–378.
- Takizawa H. Bronchial epithelial cells in allergic reactions. *Curr Drug Targets Inflamm Allergy* 2005;4:305–311.
- Tamaoki J, Chiyotani A, Kobayashi K, Sakai N, et al. Effect of indomethacin on bronchorrhea in patients with chronic bronchitis, diffuse panbronchiolitis, or bronchiectasis. *Am Rev Respir Dis* 1992;145:548–552.
- Thompson WW, Shay DK, Weintraub E, Brammer L, et al. Mortality associated with influenza and respiratory syncytial virus in the United States. *J Am Med Assoc* 2003;289:179–186.
- Tran HS, Quinn JV, Puc MM, Woolley DS, et al. Prostacyclin is neither sufficient alone nor necessary to cause pulmonary dysfunction: results from infusions of prostacyclin and antiprostacyclin antibody in porcine septic shock. *Crit Care Med* 2001;29:1445–1451.
- Uller L, Mathiesen JM, Alenmyr L, Korsgren M, et al. Antagonism of the prostaglandin D2 receptor CRTH2 attenuates asthma pathology in mouse eosinophilic airway inflammation. *Respir Res* 2007;8:16.
- Vigano T, Toia A, Crivellari MT, Galli G, et al. Prostaglandin synthetase inhibition and formation of lipoxygenase products in immunologically challenged normal human lung parenchyma. *Eicosanoids* 1998;1:73–77.
- Voelkel NF, Gerber JG, McMurtry IF, Nies AS, et al. Release of vasodilator prostaglandin, PGI2, from isolated rat lung during vasoconstriction. *Circ Res* 1981;48:207–213.
- Wallace JL. Commonality of defensive roles of COX-2 in the lung and gut. *Am J Pathol* 2006;168:1060–1063.
- Watkins DN, Garlepp MJ, Thompson PJ. Regulation of the inducible cyclooxygenase pathway in human cultured airway epithelial (A549) cells by nitric oxide. *Br J Pharmacol* 1997;121:1482–1488.
- Watkins DN, Lenzo JC, Segal A, Garlepp MJ, et al. Expression and localization of cyclo-oxygenase isoforms in non-small cell lung cancer. *Eur Respir J* 1999;14:412–418.
- Westergren VS, Wilson SJ, Penrose JF, Howarth PH, et al. Nasal mucosal expression of the leukotriene and prostanoid pathways in seasonal and perennial allergic rhinitis. *Clin Exp Allergy* 2009;39:820–828.
- Wheeler AP, Hardie WD, Bernard GR. The role of cyclooxygenase products in lung injury induced by tumor necrosis factor in sheep. *Am Rev Respir Dis* 1992;145:632–639.
- White A, Bigby T, Stevenson D. Intranasal ketorolac challenge for the diagnosis of aspirin-exacerbated respiratory disease. *Ann Allergy Asthma Immunol* 2006;97:190–195.
- Wilborn J, Crofford LJ, Burdick MD, Kunkel SL, et al. Cultured lung fibroblasts isolated from patients with idiopathic pulmonary fibrosis have a diminished capacity to synthesize prostaglandin E2 and to express cyclooxygenase-2. *J Clin Invest* 1995a;95:1861–1868.
- Wilborn J, DeWitt DL, Peters-Golden M. Expression and role of cyclooxygenase isoforms in alveolar and peritoneal macrophages. *Am J Physiol* 1995b;268:L294–L301.
- Wilkinson-Berka JL. Vasoactive factors and diabetic retinopathy: vascular endothelial growth factor, cyclooxygenase-2 and nitric oxide. *Curr Pharm Des* 2004;10:3331–3348.
- Williams CS, Tsujii M, Reese J, Dey SK, et al. Host cyclooxygenase-2 modulates carcinoma growth. *J Clin Invest* 2000;105:1589–1594.

- Wolff H, Saukkonen K, Anttila S, Karjalainen A, et al. Expression of cyclooxygenase-2 in human lung carcinoma. *Cancer Res* 1998;58:4997–5001.
- Yamada M, Kawai M, Kawai Y, Mashima Y. The effect of selective cyclooxygenase-2 inhibitor on corneal angiogenesis in the rat. *Curr Eye Res* 1999;19:300–304.
- Yao R, Rioux N, Castonguay A, You M. Inhibition of COX-2 and induction of apoptosis: two determinants of nonsteroidal anti-inflammatory drugs' chemopreventive efficacies in mouse lung tumorigenesis. *Exp Lung Res* 2000;26:731–742.
- Yoshida S, Amano H, Hayashi I, Kitasato H, et al. COX-2/VEGF-dependent facilitation of tumor-associated angiogenesis and tumor growth in vivo. *Lab Invest* 2003;83:1385–1394.
- Yoshimoto A, Kasahara K, Kawashima A, Fujimura M, et al. Characterization of the prostaglandin biosynthetic pathway in non-small cell lung cancer: a comparison with small cell lung cancer and correlation with angiogenesis, angiogenic factors and metastases. *Oncol Rep* 2005;13:1049–1057.
- Yuan A, Yu CJ, Shun CT, Luh KT, et al. Total cyclooxygenase-2 mRNA levels correlate with vascular endothelial growth factor mRNA levels, tumor angiogenesis and prognosis in non-small cell lung cancer patients. *Int J Cancer* 2005;115:545–555.
- Zeitl HJ. Bronchial asthma, nasal polyps, and aspirin sensitivity: Samter's syndrome. *Clin Chest Med* 1988;9:567–576.
- Zeltner TB, Caduff JH, Gehr P, Pfenninger J, et al. The postnatal development and growth of the human lung: I. Morphometry. *Respir Physiol* 1987;67:247–267.

CURRENT RESEARCH STRATEGIES FOR DESIGNING SAFER NSAIDs

NITRIC OXIDE–RELEASING NSAIDs

The nitric oxide (NO) synthase system has roles in gastrointestinal (GI) inflammation and mucosal defense (Nishio et al., 2006). NO released from vascular epithelium, epithelial cells of GI tract, and sensory nerves can influence many of the same components of mucosal defense as do prostaglandins (PGs) (Pajdo et al., 2011). A novel class of nitric oxide–releasing NSAID (NO-NSAID) derivatives has been described which exert similar anti-inflammatory activities in experimental animals but produce significantly less GI injury than the parent NSAID from which they are derived (Wallace et al., 1994; Elliott et al., 1995; Davies et al., 1997; Coruzzi et al., 2002; Stefano and Distrutti, 2007). A Wistar rat model of GI injury used to determine if a nitroxybutyl ester derivative of naproxen was less ulcerogenic to the GI tract than was its parent ns-NSAID, naproxen (Davies et al., 1997). In the acute gastric damage model, rats were given oral doses of naproxen at 40 or 80 mg/kg or equimolar doses of NO-naproxen at 58 or 116 mg/kg and were euthanized 3 h after dosing (Davies et al., 1997). Extensive gastric hemorrhage and ulceration were noted in the naproxen-dosed rats, whereas the stomachs from the NO-naproxen-dosed rats were similar to those of controls. In the small intestinal damage model, rats were given oral twice-daily doses of naproxen at 20 mg/kg or equimolar doses of NO-naproxen at 29 mg/kg for 1 week. At the end of this dosing period, the doses of naproxen and NO-naproxen were increased to 30 and 44 mg/kg and dosing continued for 7 days. At the end of the second week, the doses of naproxen and NO-naproxen were increased to 45 and 66 mg/kg; however, the rats dosed with the 45 mg/kg naproxen became moribund by day 3 of further dosing, and animals were euthanized on day 18 (Davies et al., 1997). Rats dosed with naproxen had penetrating intestinal ulcers, whereas rats dosed with NO-naproxen did not have intestinal ulcers (Davies et al., 1997). AZD3582 [4-(nitro-oxy)butyl-(2*S*)-2-(6-methoxy-2-naphthyl)propanoate] is the first cyclooxygenase (COX) inhibiting nitric oxide donator (CINOD) to be studied in large clinical trials. AZD3582 donates

NO and inhibits both COX-1 and COX-2 (Lohmander et al., 2005). The GI safety and efficacy of AZD3582 were studied in patients with hip or knee osteoarthritis (OA). AZD3582 was given at 750 mg twice daily and naproxen at 500 mg twice daily in a double-blind study. The primary endpoint was the 6-week incidence of endoscopic gastroduodenal ulcers (diameter ≥ 3 mm). Compared with baseline, significantly fewer ulcers and erosions developed in stomach and stomach–duodenum combined, and fewer erosions developed in stomach, duodenum, and both combined on AZD3582 than on naproxen. The GI symptom rating scale (GSRS) reflux and abdominal pain subscale scores were lower for AZD3582 than for naproxen and AZD3582 was as effective as naproxen (Lohmander et al., 2005). In another clinical study, the efficacy, safety, and tolerability of AZD3582 were compared with that of rofecoxib, naproxen, and placebo in patients with knee OA. Patients who experienced increased pain on withdrawal of analgesia were randomized to receive AZD3582 125, 375, or 750 mg twice a day; rofecoxib 25 mg once a day; naproxen 500 mg twice a day; or placebo for 6 weeks. AZD3582 375 and 750 mg twice a day were superior to placebo and as effective as rofecoxib 25 mg/day in treating the signs and symptoms of knee OA (Schnitzer et al., 2005). AZD3582 has been the first, and so far the only, CINOD investigated extensively in clinical trials. Despite its promising profile, approval of this drug was recently rejected by the U.S. Food and Drug Administration because of the lack of long-term controlled studies (Fiorucci and Santucci, 2011).

The pathogenesis of nitric oxide GI tract protective effects is related to (1) decreased leukocyte activation and infiltration, (2) decreased reactive oxygen species formation, (3) maintenance of GI blood flow, (4) increased GI mucus gel thickness, and (5) modulation of intestinal permeability (Brown et al., 1992; Davies et al., 1997; Fiorucci and Antonelli, 2006). In experimental models, NO-releasing aspirin derivative effects included inhibition of leukocyte adherence, preservation of blood flow during ischemic events, more potent inhibition of platelet aggregation, reduction of blood pressure in hypertension, and inhibition of vascular smooth muscle proliferation (Wallace et al., 2002). In general, NO-releasing aspirin derivatives are more potent anti-inflammatory and antithrombotic agents than is the parent drug (Wallace et al., 2002). NO-aspirin can be metabolized by esterases (primarily in the liver and in plasma) to yield the parent drug plus the spacer attached to the NO-releasing moiety. Subsequent metabolism of the latter leads to the liberation of NO, which can occur many hours after oral administration of the drug (Wallace et al., 2002). Lipoxins were recently considered as another group of lipid mediators that can protect the stomach similarly to NO donors (Pajdo et al., 2011). Aspirin-triggered lipoxin synthesis via COX-2 acts to reduce the severity of GI damage induced by NSAIDs. Lipoxin analogs may prove to be useful for preventing mucosal injury and for modulating mucosal inflammation (Pajdo et al., 2011). NO-releasing derivatives of NSAIDs offer great potential as GI-sparing and antithrombotic drugs with reduced toxicities (Wallace et al., 1999). NCX-4016 is a NO-releasing derivative of aspirin with antiplatelet activity. The effect of NCX-4016 on GI mucosa and platelet functions was evaluated in healthy human volunteers (Fiorucci et al., 2003). Forty healthy subjects were randomly allocated to receive 7 days of treatment with NCX-4016 (400 and 800 mg twice daily)

or equimolar doses of aspirin (200 and 420 mg twice daily). Upper endoscopies were performed before and at the end of the treatment period, and GI lesions were graded. Basal and posttreatment platelet aggregation in response to arachidonic acid (AA) and serum thromboxane (TX) B₂ (TXB) and AA-stimulated platelet TXB₂ production were investigated. NCX-4016 was virtually devoid of gastric and duodenal toxicity and inhibited AA-induced platelet aggregation as well as serum TXB₂ and platelet TXB₂ generation induced by AA to the same extent as aspirin (Fiorucci et al., 2003). Therefore, several NSAIDs, such as aspirin, naproxan, diclofenac, ketoprofen, and ibuprofen, have been coupled to a nitroxybutyl or a nitrosothiol NO moiety to generate new chemical entities (Fiorucci and Antonelli, 2006; Stefano and Distrutti, 2007; Fiorucci and Santucci, 2011; Pajdo et al., 2011). The design and synthesis of hybrid aspirin, ibuprofen, and indomethacin derivatives coupled with novel NO-donating prodrugs have been described (Abdellatif et al., 2009).

HYDROGEN SULFIDE–RELEASING NSAIDs

H₂S plays a significant role in regulating gastric mucosal blood flow and is involved in the maintenance of gastric mucosal integrity in experimental rodent models exposed to NSAIDs (Fiorucci et al., 2006). Aspirin given at 30 mg/kg orally induced extensive gastric damage in the rat stomach, and this was accompanied by infiltration of granulocytes into gastric tissue and increased expression of TNF α mRNA (Fiorucci et al., 2006). Pretreatment with an H₂S donor (NaHS; 100 μ mol/kg) reduced gastric damage and inflammation (Fiorucci et al., 2006). Deficiencies of H₂S synthesis may contribute to the pathogenesis of several gastrointestinal disorders (Fiorucci et al., 2006). In addition, H₂S have an overlapping actions with NO and PGs in terms of modulating mucosal defense and resolution of inflammation (Wallace, 2010). The GI safety and anti-inflammatory effects of a novel “HS-NSAID” (ATB-337) that consists of diclofenac linked to a H₂S-releasing moiety was evaluated in Wistar rats (Wallace et al., 2007). Rats were dosed orally with diclofenac (10, 27, and 50 μ mol/kg) or ATB-337 (equimolar doses), and 3 h later the rats were killed for blind assessment of gastric damage (Wallace et al., 2007). Oral administration of diclofenac resulted in the development of dose-related hemorrhagic erosions in the rat stomach. In contrast, oral administration of ATB-337 at doses equimolar to those of diclofenac did not produce any hemorrhagic erosions (Wallace et al., 2007). Thus, H₂S-NSAIDs are a potential new class of anti-inflammatory and analgesic agents with the potential to spare the GI and cardiovascular system (Fiorucci and Santucci, 2011).

NSAIDs ASSOCIATED WITH ZWITTERIONIC PHOSPHOLIPIDS

Zwitterionic are neutral compounds with a positive and a negative electrical charge at different locations. The lipid bilayer bending modulus, characterized by thermal

undulations, is often affected by the presence of membrane active molecules (Boggara et al., 2010). The intercalation of phospholipid bilayers with small molecules is expected to lead to significant changes in the mechanical properties of the lipid bilayer and is typically quantified by the bilayer bending modulus (Boggara et al., 2010). In addition, properties such as headgroup charges, hydration, and bilayer thickness play a role in bilayer mechanical properties (Boggara et al., 2010). NSAIDs are known to have strong interactions with lipid membranes (Boggara and Krishnamoorti, 2010). The effect of ibuprofen, an ns-NSAID, on the radius of small unilamellar vesicles of 1,2-dimyristoyl-*sn*-glycero-3-phosphatidylcholine (DMPC) and their bilayer structure was studied as a function of pH (ranging from 2 to 8) and drug-to-lipid mole ratio (Boggara and Krishnamoorti, 2010). Ibuprofen was found to affect the bilayer structure significantly at all pH values, whatever the charge state of the drug. At low pH values, the ibuprofen reduced the bilayer thickness, induced fluidlike behavior, and changed headgroup hydration (Boggara and Krishnamoorti, 2010). In another study, the effect of ibuprofen on the bending modulus of phospholipid membranes was studied as a function of pH and temperature. Ibuprofen was found to lower the bending modulus at all pH values (Boggara et al., 2010). Salicylic acid and related NSAIDs may alter the stability of membranes, inducing the formation of unstable pores that may lead to back-diffusion of luminal acid and membrane rupture, which explains the associated GI mucosal damage (Lichtenberger et al., 2006). Thus, interactions between NSAIDs and the lipid membrane and the protonation and deprotonation of NSAIDs with pH can affect the incorporation of NSAIDs into the lipid membrane and alter the mechanical properties of the membrane (Boggara et al., 2010). It has been proposed that direct interactions of ns-NSAIDs with zwitterionic phospholipids (i.e., GI tract lining) are responsible for GI toxicity (Lichtenberger et al., 2001). Therefore, combining NSAIDs with zwitterionic phospholipids could be a strategy to prevent the interaction of hydrophobic portion of cells with NSAID drugs, which may help in reducing toxicity. For example, the potential of omeprazole, a proton pump inhibitor, to interfere with the bioavailability of aspirin administered to rats either alone or complexed with the zwitterionic phospholipid dipalmitoylphosphatidylcholine (DPPC) was investigated (Girud et al., 1997). DPPC increased the lipid solubility and gastric permeability of NSAIDs. Combination of acetylsalicylic acid and DPPC retained analgesic and anti-inflammatory effects while causing significantly less GI damage (Girud et al., 1997). Preassociating a number of NSAIDs with exogenous zwitterionic phospholipids prevented an increase in the surface wettability of the mucus gel layer and protected rats against the GI side effects of NSAIDs while enhancing their lipid permeability and antipyretic and anti-inflammatory activity (Lichtenberger et al., 1995). Thus, the GI toxicity of NSAIDs can be reduced markedly when the drug is chemically preassociated with a zwitterionic phospholipid such as DPPC before intragastric administration (Lichtenberger et al., 1996). Aspirin's gastric toxicity is dependent, in part, on its ability to attenuate the stomach's surface hydrophobic barrier. This adverse drug effect can be circumvented by the administration of phosphatidylcholine (PC)-associated aspirin to maintain the stomach's hydrophobic properties (Lichtenberger et al.,

2007). Lipid-based PC-NSAID formulations that are showing encouraging preclinical and clinical observations are being validated for their GI safety and therapeutic efficacy and constitute a novel strategy to reduce GI toxicity (Lichtenberger et al., 2009).

CHIRAL NSAIDs

Left and right hands are similar but are mirror images of each other. This phenomenon of chemical “handedness” is called chirality, from *cheiro*, Greek for “hand” (Sweetman, 2003). A chiral molecule is one that lacks an internal plane of symmetry and thus has a nonsuperimposable mirror image. The opposing pairs of isomers are referred to collectively as enantiomers from the Greek *enantios*, meaning “opposite” (Sweetman, 2003). The conversion of the *R* to the *S* enantiomer is extensive in some rodents, such as rats and mice, and in monkeys, but is low in guinea pigs, rabbits, gerbils, and humans. In mice, the *R* enantiomer of ketoprofen undergoes about 60% partial unidirectional metabolic inversion to the corresponding *S* enantiomer. This is carried out by a stereoselective microsomal or mitochondrial acyl-CoA synthetase (Sweetman, 2003). The *R*-to-*S* conversion also occurs with flurbiprofen, although only to the extent of about 25%. The *R* isomer of ketoprofen has no NSAID activity, highlighting the importance of the three-dimensional structure in cyclooxygenase inhibition (Sweetman, 2003). It is thought that the inhibitory effect of chiral NSAIDs on the synthesis of PGs and hence their efficacy and toxicity are due primarily to the *S* enantiomer, although the other isomer is safer (Davies et al., 1996). The effects of three NSAIDs (flurbiprofen, ibuprofen, and ketoprofen) on small intestinal permeability were investigated in rats. Single doses of each NSAID were administered orally as either the racemate or the *R* or *S* enantiomer, the enantiomer dose being half that of the racemate. Each treatment caused a significant increase in intestinal permeability above that seen in untreated rats. The *R* enantiomers of all three NSAIDs increased small intestinal permeability significantly above baseline. *S*-Flurbiprofen, used at one-half the dose of the racemate, increased permeability to a magnitude similar to that of the racemate (Davies et al., 1996). Some experiments in animals show that the *S* isoform leads to GI mucosal damage, whereas *R* has substantially less propensity to do so. The intestinal ulcerogenic effects of single oral doses of *S*-ketoprofen were compared with racemic ketoprofen in the small intestine and cecum of rats (Cabr e et al., 1998). *S*-Ketoprofen had no significant ulcerogenic effect at 10 or 20 mg/kg. However, racemic ketoprofen was clearly ulcerogenic in the small intestine and cecum at 40 mg. *R*-Ketoprofen at 20 mg/kg does not show any effect in the cecum and only limited ulcerogenesis in the small intestine: The ulcerogenic action of racemic ketoprofen can be interpreted as a synergism between *S*- and *R*-ketoprofen (Cabr e et al., 1998). The stereoselective inhibition of COX-2 by chiral NSAIDs, ketoprofen, flurbiprofen, and ketorolac has been investigated (Carbaza et al., 1996). It was found that chiral NSAIDs inhibited, with comparable stereoselectivity, both COX-2 and COX-1 isoenzymes, and that the inhibition of COX-2 observed previously for racemic NSAIDs should be attributed almost exclusively

to their *S*-enantiomers (Carbaza et al., 1996). The comparative pathogenesis of intestinal injury induced by racemic ketoprofen and its enantiomers was evaluated in re-fed rats. Racemic ketoprofen and *R*-ketoprofen dose-dependently caused similar and multiple lesions in the mid-jejunum significantly higher than those observed with *S*-ketoprofen (Nieto et al., 2002).

TREFOIL PEPTIDES

Trefoil peptides are a family of cysteine-containing protective peptides normally secreted in the GI tract. Trefoil peptides are expressed aberrantly by a wide range of human GI inflammatory conditions. They impart protection from injury to the GI mucosa by possible interaction with mucin glycoproteins. Trefoil peptides influence epithelial cell migration and mucosal restitution following injury (Longman et al., 1999). Trefoil peptides have been implicated in the formation of new blood vessels during normal and pathophysiological processes linked to wound healing, inflammation, and cancer progression in the digestive mucosa and other human solid tumors associated with aberrant expression of trefoil peptides (Rodrigues et al., 2003). Mice lacking the intestinal trefoil factor had impaired mucosal healing and died from extensive colitis after oral administration of dextran sulfate sodium (Mashimo et al., 1995). In a rat model, gastric injury was induced by either intragastric absolute ethanol or subcutaneous indomethacin at 20 mg/kg. Rat intestinal trefoil factor (ITF) was administered at different doses and time points before or after injury. ITF markedly protected against both ethanol- and indomethacin-induced gastric injury when given up to 2 h before injury. ITF did not alter gastric pH (Babyatsky et al., 1996). Trefoil peptide (TFF) is expressed in normal epithelium of the stomach, and expression is lost in gastric adenocarcinomas. The antral and pyloric gastric mucosa of TFF-null mice was dysfunctional and exhibited severe hyperplasia and dysplasia. All homozygous mutant mice developed antropyloric adenoma, and 30% developed multifocal intraepithelial or intramucosal carcinomas (Lefebvre et al., 1996). The GI tract COX-2 expression and the effects of celecoxib on gastric adenoma were studied in TFF1-deficient mice (Saukkonen et al., 2003). Strong COX-2 mRNA and protein expression were noted in the pyloric adenomas of the TFF1^{-/-} mice. Nonneoplastic GI tissues of wild-type or TFF1^{-/-} mice expressed low or undetectable levels of COX-2. Chronic oral administration of celecoxib (1600 ppm for three months) caused ulceration and inflammation of the adenoma, but not of the nonneoplastic GI tissue, in all TFF1^{-/-} mice treated. All untreated TFF1^{-/-} mice had an adenoma, but none demonstrated the combination of ulceration and inflammation. Thus, COX-2 is expressed in gastric adenomas of TFF1^{-/-} mice, and s-NSAIDs disturb the integrity of the adenoma by promoting ulceration and inflammation (Saukkonen et al., 2003).

NOVEL MECHANISM OF ACTION NSIADS

An alternative and novel pathway of AA metabolism is the leukotriene pathway. Inhibition of 5-lipoxygenase (5-LOX) inhibits the synthesis of leukotrienes

(Radmark, 2000). A balanced inhibition of both the COX and LOX pathways may provide superior anti-inflammatory effects and reduce the adverse side effects associated with NSAID use (Fiorucci et al., 2001). Thus, developing NSAID compounds with a novel mechanism of action and an improved safety profile compared to standard NSAIDs is one strategy that has been considered (Laufer, 2001; Tries et al., 2002b). Compounds designed to block both COX and 5-lipoxygenase (5-LOX) were evaluated in animal models and have shown to have anti-inflammatory and antipyretic activity with a better GI safety profile (Hidaka et al., 1984; Wong et al., 1992; Argentieri et al., 1994). The use of these compounds was stopped due to their liver toxicity. However, the liver toxicity was not related to the pharmacological mode of action of inhibiting COX and 5-LOX, but to common structural features of the molecules (Laufer, 2001). These compounds are redox-active and all have a di-*tert*-butyl moiety or are hydroxamic acids. Both COX and 5-LOX are redox enzymes containing an iron ion at the active site. Therefore, redox active compounds and iron chelators, such as hydroxamic acids, interfere with both enzymes, and they also interfere with other enzyme systems in the liver, leading to hepatotoxicity (Laufer, 2001). A competitive COX-1, COX-2, and 5-LOX inhibitor with a nonredox substrate named ML3000 ([2,2-dimethyl-6-(4-chlorophenyl)-7-phenyl-2,3-dihydro-1*H*-pyrrolizine-5-yl]acetic acid) was discovered and designed (Laufer, 2001). ML3000 (also called licofelone) has analgesic, anti-inflammatory, antipyretic, antiplatelet, and antibronchoconstrictive activity, and minimal GI side effects (Laufer, 2001; Tries et al., 2002a). The tolerability of licofelone, assessed by gastro- and duodenoscopy, was tested in a randomized trial in healthy volunteers who received licofelone 200 mg (twice daily) licofelone 400 mg (twice daily), or naproxen 500 mg (twice daily) for 4 weeks (Bias et al., 2004). Licofelone was associated with significantly superior gastric tolerability and a lower incidence of ulcers than was naproxen (Bias et al., 2004). Licofelone (200 mg twice a day) and naproxen (500 mg twice a day) were equally effective in reducing osteoarthritis (OA) symptoms; however, licofelone significantly reduced cartilage volume loss over time in patients with knee OA (Raynauld et al., 2009). Licofelone phase III clinical trials have been completed in OA patients. Tepoxalin [5-(4-chlorophenyl)-*N*-hydroxy-1-(4-methoxyphenyl)-*N*-methyl-1*H*-pyrazole-3-propanamide] is an orally active anti-inflammatory agent which inhibits both COX and 5-LOX activities. The oral toxicity profile of tepoxalin (Zubrin) was evaluated in 1- and 6-month rat (up to 50 mg/kg per day) and dog (up to 150 mg/kg, twice daily) studies (Knight et al., 1996). Analgesic nephropathy syndrome (i.e., papillary edema or necrosis, cortical tubular dilatation) was seen at ≥ 15 mg/kg. Gastrointestinal erosions and ulcers were seen in female rats given 40 mg/kg per day for six months. Small pyloric ulcerations were seen in dogs in doses of 100 and 300 mg/kg per day up to six months. The no-effect doses in rats were 5 mg/kg per day and in dogs were 20 mg/kg per day (Knight et al., 1996). Zubrin is approved for the treatment of OA in dogs. Structure-based virtual screening has been used to identify thiazolidinones ring scaffolds as dual COX/LOX inhibitors (Geronikaki et al., 2008).

mPGES-1 INHIBITORS

Microsomal PGE synthase-1 (mPGES-1) is a member of the membrane-associated proteins involved in the eicosanoid and glutathione metabolism (MAPEG) superfamily with the ability to catalyze the conversion of PGH₂ to PGE₂ (Jakobsson et al., 1999). mPGES-1-deficient mice (mPGES-1^{-/-}) are viable and fertile, develop normally compared with wild-type controls, and could not be distinguished from wild-type controls in their general behavior, appearance, body weight, or various tissue histological or hematological parameters (Trebino et al., 2003). In addition, mPGES-1^{-/-} mice displayed a marked reduction in inflammatory responses compared with mPGES-1^{+/+} mice. Edema formation in antigen- or saline-injected mPGES-1^{-/-} mice was similar to that of saline-injected mPGES-1^{+/+} mice (Trebino et al., 2003). mPGES-1^{-/-} mice displayed significant reduction in severity and incidence of collagen-induced arthritis disease compared with wild-type controls (Trebino et al., 2003). Disruption of mPGES-1 retarded atherogenesis and did not affect blood pressure in mPGES-1^{-/-} mice, which were crossed into a low-density lipoprotein receptor knockout (LDLR^{-/-}) mouse model (Wang et al., 2006). The effects of genetic mPGES-1 loss on myocardial damage after coronary occlusion were studied in mPGES-1^{-/-} mice (Wu et al., 2009). Reduced myocardial damage was noted in mice lacking mPGES-1 (Wu et al., 2009). Genetic deletion of mPGES-1 suppressed intestinal tumorigenesis in an *Apc*^{Δ14/+} mouse model (Nakanishi et al., 2008). Reduced size and numbers of preneoplastic aberrant crypt foci (ACF) were observed in this *Apc*^{Δ14/+} mouse model after treatment with the colon carcinogen azoxymethane (Nakanishi et al., 2008). Thus, mPGES-1 inhibitors are attractive therapeutic targets for the treatment of inflammatory pain and as chemotherapeutic agents. The effects of a novel and selective mPGES-1 inhibitor, MF63 [2-(6-chloro-1*H*-phenanthro-[9,10-*d*]imidazol-2-yl)isophthalonitrile], were tested in animal models of inflammation (Xu et al., 2008). MF63 did not cause GI side effects that can be seen with NSAIDs, such as mucosal erosions in knockout mice or non-human primates, although it markedly inhibited PGE₂ synthesis (Xu et al., 2008). Ring templates, including fatty acid derivatives, have been developed as mPGES-1 and dual mPGES-1/5-LOX inhibitors (Friesen and Mancini, 2008). Pirinixic acid derivatives is a novel class of dual mPGES-1/5-LO inhibitors with a promising pharmacological profile and a potential for therapeutic use (Koeberle et al., 2008).

REFERENCES

- Abdellatif KR, Chowdhury MA, Dong Y, Das D, et al. Dinitroglyceryl and diazen-1-ium-1,2-diolated nitric oxide donor ester prodrugs of aspirin, indomethacin and ibuprofen: synthesis, biological evaluation and nitric oxide release studies. *Bioorg Med Chem Lett* 2009;19:3014–3018.
- Argentieri DC, Ritchie DM, Ferro MP, Kirchner T, et al. Tepoxalin: a dual cyclooxygenase/5-lipoxygenase inhibitor of arachidonic acid metabolism with potent anti-inflammatory activity and a favorable gastrointestinal profile. *J Pharmacol Exp Ther* 1994;271:1399–1408.
- Babyatsky MW, deBeaumont M, Thim L, Podolsky DK. Oral trefoil peptides protect against ethanol- and indomethacin-induced gastric injury in rats. *Gastroenterology* 1996;110:489–497.

- Bias P, Buchner A, Klessler B, Laufer S. The gastrointestinal tolerability of the LOX/COX inhibitor, licofelone, is similar to placebo and superior to naproxen therapy in healthy volunteers: results from a randomized, controlled trial. *Am J Gastroenterol* 2004;99:611–618.
- Boggara MB, Faraone A, Krishnamoorti R. Effect of pH and ibuprofen on the phospholipid bilayer bending modulus. *J Phys Chem B* 2010;114:8061–8066.
- Boggara MB, Krishnamoorti R. Small-angle neutron scattering studies of phospholipid–NSAID adducts. *Langmuir* 2010;26:5734–5745.
- Brown JF, Hanson PJ, Whittle BJ. Nitric oxide donors increase mucus gel thickness in rat stomach. *Eur J Pharmacol* 1992;223:103–104.
- Cabr e F, Fern andez F, Zapatero MI, Ara no A, et al. Intestinal ulcerogenic effect of S(+)- ketoprofen in the rat. *J Clin Pharmacol* 1998;38:27S–32S.
- Carbaza A, Cabr e F, Rotten E, G omez M, et al. Stereoselective inhibition of cyclooxygenase by chiral nonsteroidal antiinflammatory drugs. *J Clin Pharmacol* 1996; 505–512.
- Coruzzi G, Coppelli G, Spaggiari S, Cavestro GM, et al. Gastroprotective effects of amtolmetin guacyl: a new non-steroidal anti-inflammatory drug that activates inducible gastric nitric oxide synthase. *Dig Liver Dis* 2002;34:403–410.
- Davies NM, Wright MR, Russell AS, Jamali F. Effect of the enantiomers of flurbiprofen, ibuprofen, and ketoprofen on intestinal permeability. *J Pharm Sci* 1996;85:1170–1173.
- Davies NM, Seth AG, Appley, McKnight W, et al. No-naproxan vs. naproxan: ulcerogenic, analgesic and anti-inflammatory effects. *Alim Pharmacol Ther* 1997;11:69–79.
- Elliott SN, McKnight W, Cirino G, Wallace JL. A nitric oxide-releasing nonsteroidal anti-inflammatory drug accelerates gastric ulcer healing in rats. *Gastroenterology* 1995;109:524–530.
- Fiorucci F, Distrutti E, Cirino G, Wallace JL. The emerging roles of hydrogen sulphide in the gastrointestinal tract and liver. *Gastroenterology* 2006;131:259–271.
- Fiorucci S, Antonelli E. NO-NSAIDs: from inflammatory mediators to clinical readouts. *Inflamm Allergy Drug Targets* 2006;5:121–131.
- Fiorucci S, Santucci L. Hydrogen sulfide-based therapies: focus on H₂S releasing NSAIDs. *Inflamm Allergy Drug Targets* 2011;10:133–140.
- Fiorucci S, Meli R, Bucci M, Cirino G. Dual inhibitors of cyclooxygenase and 5-lipoxygenase: a new avenue in anti-inflammatory therapy? *Biochem Pharmacol* 2001;62:1433–1438.
- Fiorucci S, Santucci L, Gresele P, Faccino RM, et al. Gastrointestinal safety of NO- aspirin (NCX-4016) in healthy human volunteers: a proof of concept endoscopic study. *Gastroenterology* 2003;124: 600–607.
- Friesen RW, Mancini JA. Microsomal prostaglandin E₂ synthase-1 (mPGES-1): a novel anti-inflammatory therapeutic target. *J Med Chem* 2008;51:4059–4067.
- Geronikaki AA, Lagunin AA, Hadjipavlou-Litina DI, Eleftheriou PT, et al. Computer-aided discovery of anti-inflammatory thiazolidinones with dual cyclooxygenase/lipoxygenase inhibition. *J Med Chem* 2008;51:1601–1609.
- Giraud MN, Sandujask, Felder TB, Illich PA, et al. The effect of omeprazole on the bioavailability of unmodified and phospholipid complexed aspirin in rats. *Alimert Pharmacol Ther* 1997;11:899–906.
- Hidaka T, Hosoe K, Ariki Y, Takeo K, et al. Pharmacological properties of a new anti-inflammatory compound, alpha-(3,5-di-*tert*-butyl-4-hydroxybenzylidene)-gamma-butyrolactone (KME-4), and its inhibitory effects on prostaglandin synthetase and 5-lipoxygenase. *Jpn J Pharmacol* 1984;36:77–85.
- Jakobsson PJ, Thoren S, Morgenstern R, Samuelsson B. Identification of human prostaglandin E synthase: a microsomal, glutathione-dependent, inducible enzyme, constituting a potential novel drug target. *Proc Natl Acad Sci USA* 1999;96:7220–7225.
- Knight EV, Kimball JP, Keenan CM, Smith IL, et al. Preclinical toxicity evaluation of tepoxalin, a dual inhibitor of cyclooxygenase and 5-lipoxygenase, in Sprague–Dawley rats and beagle dogs. *Fundam Appl Toxicol* 1996;33:38–48.
- Koeberle A, Zettl H, Greiner C, Wurglics M, et al. Pirinixic acid derivatives as novel dual inhibitors of microsomal prostaglandin E₂ synthase-1 and 5-lipoxygenase. *J Med Chem* 2008;51:8068–8076.
- Laufer S. Discovery and development of ML3000. *Inflammopharmacology* 2001;1:101–112.
- Lefebvre O, Chenard MP, Masson R, Linares J, et al. Gastric mucosa abnormalities and tumorigenesis in mice lacking the p52 trefoil protein. *Science* 1996;274:259–262.

- Lichtenberger LM, Wang ZM, Romero JJ, Ulloa C, et al. Non-steroidal anti-inflammatory drugs (NSAIDs) associate with zwitterionic phospholipids: insight into the mechanism and reversal of NSAID-induced gastrointestinal injury. *Nat Med* 1995;1:154–158.
- Lichtenberger LM, Ulloa C, Vanous AL, Romero JJ, et al. Zwitterionic phospholipids enhance aspirin's therapeutic activity, as demonstrated in rodent model systems. *J Pharmacol Exp Ther* 1996;277:1221–1227.
- Lichtenberger LM, Romero JJ, de Ruijter WM, Behbod F, et al. Phosphatidylcholine association increases the anti-inflammatory and analgesic activity of ibuprofen in acute and chronic rodent models of joint inflammation: relationship to alterations in bioavailability and cyclooxygenase-inhibitory potency. *J Pharmacol Exp Ther* 2001;298:279–287.
- Lichtenberger LM, Zhou Y, Dial EJ, Raphael RM. NSAID injury to the gastrointestinal tract: evidence that NSAIDs interact with phospholipids to weaken the hydrophobic surface barrier and induce the formation of unstable pores in membranes. *J Pharm Pharmacol* 2006;58:1421–1428.
- Lichtenberger LM, Romero JJ, Dial EJ. Surface phospholipids in gastric injury and protection when a selective cyclooxygenase-2 inhibitor (Coxib) is used in combination with aspirin. *Br J Pharmacol* 2007;150:913–919.
- Lichtenberger LM, Barron M, Marathi U. Association of phosphatidylcholine and NSAIDs as a novel strategy to reduce gastrointestinal toxicity. *Drugs Today (Barc)* 2009;45:877–890.
- Lohmander LS, McKeith D, Svensson O, Malmenäs M, et al. A randomised, placebo controlled, comparative trial of the gastrointestinal safety and efficacy of AZD3582 versus naproxen in osteoarthritis. *Ann Rheum Dis* 2005;64:449–456.
- Longman RJ, Thomas MG, Poulsom R. Trefoil peptides and surgical disease. *Br J Surg* 1999;86:740–748.
- Mashimo HM, Wu DC, Podolasky DK, Fishman MC. Impaired defenses of intestinal mucosa in mice lacking in intestinal foil peptides. *Science* 1995;274:262–265.
- Nakanishi M, Montrose DC, Clark P, Nambiar PR, et al. Genetic deletion of mPGES-1 suppresses intestinal tumorigenesis. *Cancer Res* 2008;68:3251–3259.
- Nieto AI, Cabré F, Moreno FJ, Alarcón de la Lastra C. Mechanisms involved in the attenuation of intestinal toxicity induced by (S)-(+)-ketoprofen in re-fed rats. *Dig Dis Sci* 2002;47:905–913.
- Nishio H, Hayashi Y, Terashima S, Takeuchi K. Role of endogenous nitric oxide in mucosal defense of inflamed rat stomach following iodoacetamide treatment. *Life Sci* 2006;79:1523–1530.
- Pajdo R, Brzozowski T, Szlachcic A, Konturek PC, et al. Lipoxins, the novel mediators of gastroprotection and gastric adaptation to ulcerogenic action of aspirin. *Curr Pharm Des* 2011;17:1541–1551.
- Radmark OP. The molecular biology and regulation of 5-lipoxygenase. *Am J Respir Crit Care Med* 2000;161:S11–S15.
- Raynauld JP, Martel-Pelletier J, Bias P, Laufer S, et al. Protective effects of licofelone, a 5-lipoxygenase and cyclo-oxygenase inhibitor, versus naproxen on cartilage loss in knee osteoarthritis: a first multi-centre clinical trial using quantitative MRI. *Ann Rheum Dis* 2009;68:938–947.
- Rodrigues S, Van Aken E, Van Bocxlaer S, Attoub S, et al. Trefoil peptides as proangiogenic factors in vivo and in vitro: implication of cyclooxygenase-2 and EGF receptor signaling. *FASEB J* 2003;17:7–16.
- Saukkonen K, Tomasetto C, Narko K, Rio MC, et al. Cyclooxygenase-2 expression and effect of celecoxib in gastric adenomas of trefoil factor 1-deficient mice. *Cancer Res* 2003;63:3032–3036.
- Schnitzer TJ, Kivitz AJ, Lipetz RS, Sanders N, et al. Comparison of the COX-inhibiting nitric oxide donator AZD3582 and rofecoxib in treating the signs and symptoms of osteoarthritis of the knee. *Arthritis Rheum* 2005;53:827–837.
- Stefano F, Distrutti E. Cyclo-oxygenase (COX) inhibiting nitric oxide donating (CINODs) drugs: a review of their current status. *Curr Top Med Chem* 2007;7:277–282.
- Sweetman BJ. Development and use of the quick acting chiral NSAID dexketoprofen trometamol (keral). *Acute Pain* 2003;4:109–115.
- Trebino CE, Stock JL, Gibbons CP, Naiman BM, et al. Impaired inflammatory and pain responses in mice lacking an inducible prostaglandin E synthase. *Proc Natl Acad Sci USA* 2003;100:9044–9049.
- Tries S, Laufer S, Radziwon P, Breddin HK. Antithrombotic and platelet function inhibiting effects of ML3000, a new antiinflammatory drug with Cox/5-LOX inhibitory activity. *Inflamm Res* 2002a;51:129–134.

- Tries S, Neuper TW, Laufer S. The mechanism of action of new compound ML3000 (locofelone): inhibition of 5-LO COX-1, and COX-2. *Inflamm Res* 2002b;51:135–43.
- Wallace JL. Physiological and pathophysiological roles of hydrogen sulfide in the gastrointestinal tract. *Antioxid Redox Signal* 2010;12:1125–1133.
- Wallace JL, Reuter B, Cicala C, McKnight W, et al. A diclofenac derivative without ulcerogenic properties. *Eur J Pharmacol* 1994;257:249–255.
- Wallace JL, Del Soldato P, Cirino G, Muscará MN. Nitric oxide-releasing NSAIDs: GI- safe antithrombotics. *IDrugs* 1999;2:321–326.
- Wallace JL, Ignarro LJ, Fiorucci S. Potential cardioprotective actions of no-releasing aspirin. *Nat Rev Drug Discov* 2002;1:375–382.
- Wallace JL, Caliendo G, Santagada V, Cirino G, et al. Gastrointestinal safety and anti-inflammatory effects of a hydrogen sulphide-releasing diclofenac derivative in the rat. *Gastroenterology* 2007;132:261–271.
- Wang M, Zukas AM, Hui Y, Ricciotti E, et al. Deletion of microsomal prostaglandin E synthase-1 augments prostacyclin and retards atherogenesis. *Proc Natl Acad Sci USA* 2006;103:14507–14512.
- Wong S, Lee SJ, Frierson MR 3rd, Proch J, et al. Antiarthritic profile of BF-389: a novel anti-inflammatory agent with low ulcerogenic liability. *Agents Actions* 1992;37:90–98.
- Wu D, Mennerich D, Arndt K, Sugiyama K, et al. Comparison of microsomal prostaglandin E synthase-1 deletion and COX-2 inhibition in acute cardiac ischemia in mice. *Prostaglandins Other Lipid Mediat* 2009;90:21–25.
- Xu D, Rowland SE, Clark P, Giroux A, et al. MF63 [2-(6-chloro-1*H*-phenanthro[9,10-*d*]imidazol-2-yl)-isophthalonitrile], a selective microsomal prostaglandin E synthase-1 inhibitor, relieves pyresis and pain in preclinical models of inflammation. *J Pharmacol Exp Ther* 2008;326:754–763.

INDEX

- Absorption, 50
ACE, 136, 187
Acetic acid, 16
Acetylsalicylic acid, 2
Ach, 277
Active transport, 50
Adenomatous polyps, 15
Adhesion molecules, GI, 49
ADVANTAGE, 32
Advil, 17
Age, skeleton, 75
Age-related macular degeneration, 236
Aging, GI, 43
Airway epithelium, 282
Alarmin, 232
Aleve, 19
Allergen-induced inflammation, 297
Allergic alveolitis, 275
Alveolar macrophages, 273
Aminonicotinic acid, 16
Analgesic nephropathy, 159
Anatomical differences
 bone, 72
 GI, 40
Ang II, 187
Angiogenesis, 255
Animal models, cardiovascular, 189
Anterior chamber, 233
Anthranilic acid, 16, 30
Apo E, 215
Apolipoprotein, 190
APPROVe, 209
Arachidonic acid, 2
Arylpropionic acid, 16
Aspirin, 1, 29
Aspirin-exacerbated respiratory disease, 299
Asthma, 280
AT1 receptors, 187
ATB-337, 311
Atherosclerosis, 191, 215
Atropine, 186
AZD3582, 310
Banamine, 26
Bicarbonate secretion, 43
Biotransformation, 42
Blood flow, 183, 211
 gut, 40
Blood pressure, 183, 184, 211
BMP, 90
Bone, 72
Bone morphogenic proteins, 78
Bone remodeling, 74
Bradycardia, 186
Bradykinin, 139
Calcium, 187
Callus, 86
Carboxylic acid, 139
Cardiac troponin, 183
Cardiovascular system, 180
Carprofen, 20
Cataflam, 26
Cataract, 234
CD2AP, 133
Cecum, 13
CETP, 190
Chiral NSAIDs, 313
Choroid, 238
Ciliary body, 238
CINOD, 309
Clara cells, 273
CLASS, 34, 210
Cloquet's canal, 235
Colitis, 14, 28
Collagen, 230

- Collagen-induced arthritis, 79, 109
- Colon, 13
- Conduction system, 183
- Conjunctivitis, 243
- COPD, 281
- Cornea, 230
- Coronary artery, 211
- COX-1
 - cardiac, 192, 194
 - GI, 30
 - ocular, 245
 - respiratory, 283
- COX-2
 - cardiac, 194
 - GI, 31, 32
 - ocular, 248
 - respiratory, 288
- COX-3, 6
- Cystic fibrosis, 279
- Cytochrome P450, 54

- Deracoxib, 35
- Deramaxx, 35
- Diabetic, 257
- Diarrhea, 46
- Diclofenac, 26
- Digestive process, 44
- Dopamine, 137
- Duodenum, 13
- DuP697, 8

- Enantiomers, 313
- Endophthalmitis, 234
- Endothelium, 211
- Enolic acid, 16
- Enterobacteria, 52
- Enterohepatic recirculation, 41
- Epiphysis, 72
- Expression
 - bone, 91
 - cardiovascular, 192
 - GI, 13
 - renal, 149
- Eye, 228

- Fenoprofen, 21
- FGFR-3, 87
- Firocoxib, 36
- Flunixin meglumine, 26
- Fluriprofen, 21

- Frank-Starling law, 186
- Function, renal, 129

- Gamma delta cells, 274
- Gastric gland, 48
- Gastritis, 14, 22
- Gastrointestinal, 11
- GFR, 132
- GI motility, 46
- Glomerular basement membrane, 135
- Glomeruli, 132
- Glomerulogenesis, 161
- Glomerulonephritis, 137, 143
- Glucuronidation, 42
- Growth plate, 74
- Gut blood flow, 40

- HDL, 190
- Healing
 - bone, 77, 85
 - GI, 48
 - ligament, 112
 - tendon, 112
- Heart, 181
- Heart rate, 186
- Helicobacter, 14
- Hemorrhage, 39, 44
- Historical, 1
- Hydrogen sulfide-releasing NSAIDs, 311
- Hyperkalemia, 156
- Hypersensitivity, lung, 275
- Hypertension, 184
- Hypertrophy, 184
- Hyporeninemic hypoaldosteronism, 157

- IBD, 28
- Ibuprofen, 17, 97
- IL-13, 278
- Ileum, 13
- Indomethacin, 23
- Intestinal absorption, 50
- IOP, 238
- IP, cardiac, 199
- Iritis, 255
- Ischemia/reperfusion, 198, 201
- Ischemic preconditioning, 207

- Jejunum, 13

- Keratitis, 248
- Ketoprofen, 20

- Kidney, 127
 Laminitis, 27
 Laplace law, 187
 LASIK, 247
 LDL, 190
 Lens, 233
 Ligament, 72, 112
 Loop of Henle, 131
 Low-density lipoprotein receptor-related protein 5, 76
 5-LOX, 314
 Lung, 270

 Macrophages, 273
 Macula Densa, 136
 MAPK, 57, 242
 Mastitis, 21
 M-CSF, 80
 Mechanisms, GI, 38
 MEDAL, 34
 Mesangium, 135
 Metabolism, GI, 54
 MI, 195, 201, 203
 Mitochondria, 56
 MMPs, 193
 Motility, GI, 46, 52
 Motrin, 17
 mPGES-1 inhibitors, 316
 MUCOSA, 45
 injury, 46
 Mucosal defense, 44
 Muscarinic, 186
 MyD88, 55
 Myenteric neurons, 52
 Myocarditis, 188
 Myocardium, 182

 Nabumetone, 26
 Naproxen, 19
 Natriuretic peptides, 188
 NCX-4016, 310
 Nephrin, 133
 Nephritis, 137, 154
 Nephron, 130, 131
 Nicotinic, 186
 Nimesulide, 164
 Nitric oxide-releasing NSAID, 309
 Nonhuman primate, 191
 Norepinephrine, 186

 NS-398, 37
 NSCLC, 296

 Ocular system, 228
 Ontogeny, 286
 Optic nerve, 237
 Organic cation transporters, 138
 Osteoarthritis, 84, 98
 Osteoblast, 92
 Osteoclast, 92
 Osteocyte, 92
 Osteomyelitis, 82
 Osteopetrosis, 80
 Osteoprotegerin, 78
 Oxidation, 22
 Ox-LDL, 214

 Parasympathetic, 186
 Passive diffusion, 50
 Patent ductus arteriosus, 160
 Pathophysiology
 GI, 38
 renal, 128
 Pericardium, 182
 PGD₂, renal, 145
 PGF₂, ocular, 244
 PGI₂
 cardiovascular, 197
 renal, 144
 pH, GI, 50
 Pharmacokinetics, 40, 138, 255
 Phenylbutazone, 26, 98
 Phosphatidylcholine, 53
 Photoreceptors, 236
 Physiology, renal, 129
 PI3, 291
 Pig, 191
 PIMs, 273
 Piroxicam, 22, 98
 Podocyte, 133
 Pores of Kohn, 271
 Potency, 39
 PPAR, 56
 Previcox, 36
 Primary open-angle glaucoma, 238
 Prostaglandins, 2
 cardiovascular, 196
 ocular, 238
 pulmonary, 275
 renal, 140, 141

- Prostaglandins (*Continued*)
skeleton, 78
Protein kinase A, 280
Proteinuria, 132
Proximal tubule, 137
PTH, 88
Pyrazoles, 16
- RA, 11
RAAS, 136, 187
RANKL, 79
Remodeling, bone, 86
Renal papillary necrosis, 159
Renal system, 127
Resorption, 88
Respiratory system, 270
Retina, 235
Rhythmicity, 182
Rimadyl, 20
Robenacoxib, 36
RPE, 235
RSV, 283
- Salicylates, 1
Salicylic acid, 16, 28
Salt sensitive, 213
SHR model, 190
Skeleton, 72
Small intestine, 15
Species differences, GI, 39
Stomach, 11, 40
Stress, 43
Stress-related mucosal disease, 43
Stroke volume, 184
- Sulfonamide, 166
Sulindac, 26
Surfactant, 272
Sympathetic, 186
- Tachycardia, 186
Tendon, 72, 112
Th17, 279
Thrombosis, cardiac, 209
TLR, GI, 54
TP, cardiac, 196
Transporters, renal, 138
Trefol peptides, 314
TXA₂, renal, 143
Type II pneumocyte, 272
- UDP-glucuronosyltransferase, 42
Ulcer, 16, 243
Upper GI, 15
Uveal tract, 238
Uveitis, 257
- Valve, heart, 182
VEGF, 133, 253
VIGOR, 32
Vioxx, 32
Vision, 234
Vitreous humor, 234
Voltarin, 26
- Wolff's law, 74
- Zubrin, 315
Zwitterionic, 311